AN EVALUATION OF THE USE OF FE-TI OXIDE GEOCHEMISTRY AND ENVIRONMENTAL MAGNETISM AS SEDIMENTARY PROVENANCE INDICATORS IN THE RIVER EDEN CATCHMENT, SCOTLAND

Edurne Martinez

A Thesis Submitted for the Degree of PhD
at the
University of St Andrews

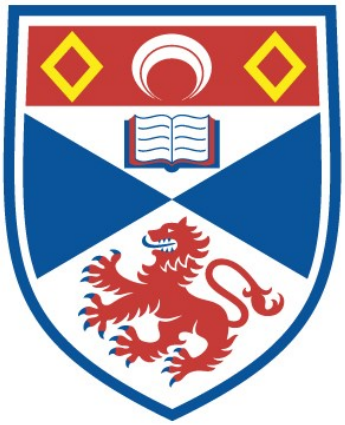

1998

An evaluation of the use of Fe-Ti oxide geochemistry and environmental magnetism as sedimentary provenance indicators in the River Eden catchment, Scotland

Edurne Martínez

This thesis is submitted to the Department of Geosciences
of the University of St. Andrews for the Degree of Doctor of Philosophy

March 1998

ProQuest LLC.
789 East Eisenhower Parkway
P.O. Box 1346
Ann Arbor, MI 48106 – 1346

(i) I, Edurne Martínez, hereby certify that this thesis, which is approximately 68,000 words in length, has been written by me, that is the record of work carried out by me and that it has not been submitted in any previous application for a higher degree.

date signature of the candidate

18 March 1998

(ii) I was admitted as a research student in October 1994 and as a candidate for the degree of Ph.D. in March 1998; the higher study for which this is a record was carried out in the University of St. Andrews between 1994 and 1998.

date signature of the candidate

18 March 1998

(iii) I hereby certify that the candidate has fulfilled the conditions of the Resolution and Regulations appropriated for the degree of Ph.D. in the University of St. Andrews and that the candidate is qualified to submit this thesis in application for that degree.

date signature of the supervisor

18 March 1998

In submitting this thesis to the University of St. Andrews I understand that I am giving permission for it to be made available for use in accordance with the regulations of the University Library for the time being in force, subject to any copyright vested in the work not being affected thereby. I also understand that the title and abstract will be published, and that a copy of the work may be made and supplied to any bona fide library or research worker.

date signature of the candidate

18 March 1998

Abstract

The potential of geochemical and magnetic measurements in sedimentary provenance studies is evaluated in the River Eden catchment (Scotland), where three principal rock types (basalts, andesites and sedimentary rocks) are petrogenetically, temporally and spatially distinct. The northern part of the catchment, occupied by Lower Devonian andesitic rocks, is separated from the southern part of the catchment, occupied by Upper Carboniferous basaltic rocks, by a valley underlain by more erodable Upper Devonian sandstones. All rock types are partially covered by Quaternary glacial till. These four well distinguished potential sediment sources were expected to robustly fingerprint the source components of the stream sediment transported by the fluvial system defining the River Eden catchment.

Mineral composition analysis together with magnetic measurements have enabled the characterisation, differentiation and, therefore, the classification of different groups within all potential sources (rocks and till) in terms of concentration, composition and grain size of Fe-Ti oxides. Stream sediment samples were also characterised using the same approaches. Raw data are analysed and interpreted graphically by scattergrams, and statistically by correlation coefficients, analysis of variance and simultaneous R- and Q-mode factor analysis. A comparison of both source and sediment characteristics is assisted principally by discriminant function analysis which leads to a qualitative estimation of each source contribution to the sediment. Linear programming is then applied in order to model quantitatively the provenance of stream sediment samples.

Magnetite is found to be the best provenance indicator in the study area. Basalts have higher concentrations, Ti-content and grain size of magnetite than andesites. Till shows a wide variability in magnetite composition, its concentration being close to the that of the andesites, whereas the sedimentary rocks are characterised by the scarcity or absence of magnetite. Oxidation of magnetite, eventually to hematite, is found to occur during rock crystallisation, and alteration under aerial conditions. However, during fluvial transport magnetite transforms to sphene. Despite the chemical alteration of magnetite, an environmentally-consistent qualitative provenance model is derived in this study. The sediment transported by each Eden tributary is found to be mineralogically unique as a result not only of mineralogical differences but also of the mixing proportions of the constituting sources. Although, tributary inputs are recognised downstream the River Eden course, sediment characteristics in the main course tend to be homogenised during

transport. Even when magnetic parameters are more discriminating than magnetite composition, the intra-source magnetic variability and principally the magnetic interdependence of the sediment sources significantly hinder successful modelling of mixtures using linear programming methodology. More complex statistical methods and/or more discriminating and independent variables are required to achieve a complete quantitative model of the stream sediment provenance over the whole River Eden catchment.

Acknowledgements

I would like to acknowledge, gratefully and sincerely, to all those who have accompanied me during the long and hard time of this thesis.

I thank to my supervisors for all their suggestions, the patient correction of the manuscript, and their strength and entertainment during field work. In special, I thank: to Dr. W. E. Stephens for his time, for his always so positive and enthusiastic comments and his continuous encouragement; to Dr. R. W. Duck for putting so much effort in improving the text; and to Dr. J. Walden for introducing me in the exciting magnetic and statistical worlds.

I would also like to thank the 'labsters' Angus, Donald and Andy for their technical assistance with XRF and XRD, with probe, and with rock thin sections' preparation, respectively, as well as for their constant support. Thanks to Cheesy Peas for the supertime when going for picnics around Fife!

Special thanks go to Luis for listening (very patiently!) and for reading (without falling asleep) the manuscript. Thanks to my friends Silke and Sabine for their understanding and for crying with me.

I would like to dedicate this thesis to my parents without whom I would have never made it.

This project has been funded for four years by the Programa de Formación de Investigadores del Departamento de Educación, Universidades e Investigación del Gobierno Vasco which is gratefully acknowledged.

Para aita y ama

Contents

List of Appendices

1. Introduction

An understanding of sediment origin is critical in the study of clastic depositional systems. The determination of sedimentary provenance places important constraints on transport, dispersal and depositional patterns, leading to an evaluation of the environmental, tectonic and human inputs on both local and regional scales.

Diverse approaches are traditionally applied in constraining sediment origin, all of which are commonly based on the mineralogical composition of the sediment: from whole-sediment characteristic determinations, including chemical and mineral distribution analyses, to the study of a unique mineral species found in the sediment. Nevertheless, whatever the approach, it must be based on tracing a sediment characteristic directly inherited from its source and which remains unchanged with respect to the physical (abrasion) and chemical (weathering) attacks suffered since the sediment formation, during transport, and after deposition (diagenesis), to record source fingerprints in the sediment.

Heavy minerals are found to be ideal as provenance indicators because of their high chemical and mechanical resistance. The constituents vary due mainly to differential weathering, hydraulic sorting, and dissimilar dissolution during diagenesis. However, chemical and morphological (internal texture, shape and size) characteristics of single mineral species result from a complex combination of the activities of the elements present, other co-precipitating phases, temperature, cooling rate, growth rate, nucleation density, oxygen fugacity, etc., during the crystallisation of parent igneous rocks. Therefore, both composition and morphology of a single heavy mineral species contribute to the evaluation of source lithologies.

Magnetism, compared with geochemistry, is a more recent technique applied to environmental studies. Magnetic measurements provide valuable information about concentration, composition, and grain size of magnetic minerals found in sediments and source materials. The commonest magnetic minerals in nature are the iron oxides (mainly magnetite and hematite) and iron hydroxides (mainly goethite). Thus, the combination of geochemical and magnetic methods has the potential to provide a more detailed characterisation of these minerals, increasing their potential as sedimentary provenance indicators.

The amount and variety of data required in any sedimentary provenance study necessitates the application of statistical analysis of the data. Simple plots using raw data and/or ratios, as well as the results of statistical analyses, such as factor analysis and discriminant function analysis, assist the characterisation and differentiation of source groups and sediment samples by establishing the interrelationships existing between the variables within each group or sample. Subsequently, the results obtained serve as the basis for establishing quantitative criteria for determining the provenance of the sediment by studying the interrelationship between sources and sediment using linear programming. The success of a provenance model, derived by statistical analysis of the variables, is directly dependent on the initial differentiation of the sources, the immutability of geochemical and magnetic parameters during geological processes and the interdependence of the variables.

All these analytical and statistical approaches have been used in this study to determine the provenance and dispersal of the sediment transported by the fluvial system of the River Eden, Scotland.

1.1. Choice of study area

The River Eden catchment is located in the northern part of the Scottish region of Fife (Figure 1.1). Three areas are clearly distinguished in the catchment on the basis of different types of rocks which appear separated temporally and spatially (Figure 2.1), namely: (1) Lower Devonian lavas, mainly consisting of andesitic rocks, in the northern part of the catchment, (2) Carboniferous sedimentary and intrusive igneous rocks (mainly dolerites) in the southern part of the catchment, and (3) Upper Devonian sandstones occupying the central valley in which the main River Eden course flows. All these materials appear covered by Quaternary deposits consisting mainly of glacial till which is variable in thickness. Due to the greater resistance to erosion of igneous rocks compared with sedimentary rocks, the northern and southern areas of the catchment are characterised by high ground with peak altitudes of 285 m at Norman's Law (NO 3306 7203) and 424 m at East Lomond (NO 3245 7058), in the north and south respectively. This topographic distribution conditions the hydrological courses. Thus, northern tributaries flowing over Lower Devonian andesitic rocks and southern tributaries flowing mainly over Carboniferous basaltic rocks join the main River Eden course flowing over Upper Devonian sedimentary rocks where sediment of different provenance is mixed

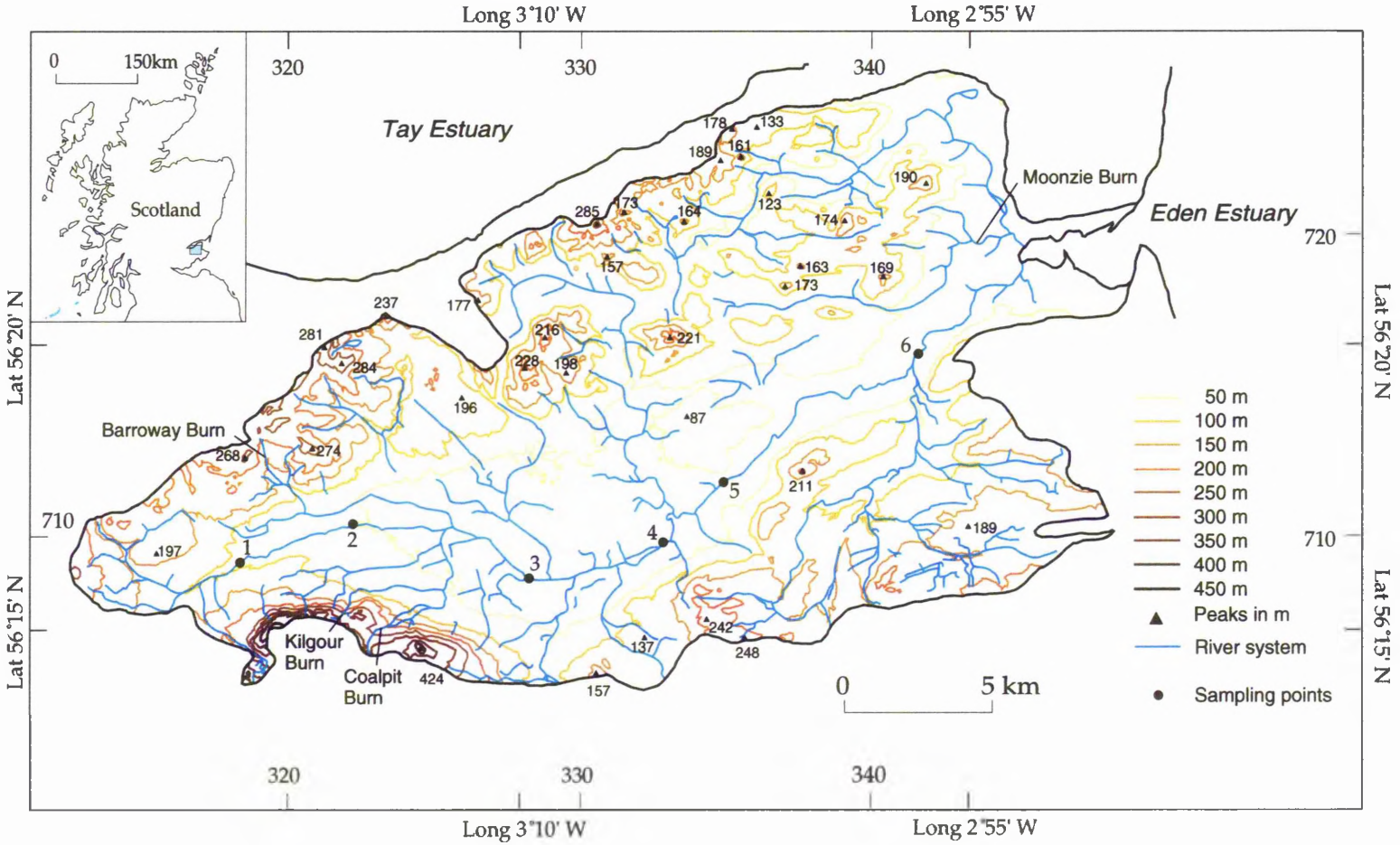

Figure 1.1. River Eden catchment (based on Ordnance Survey 1:50 000 sheets 58 and 59).
The relationship between topography and river course, including sampling points along the River Eden, is shown.

(Figure 1.1), and this near perfect differentiation of sources influenced the choice of the study area.

The igneous rock outcrops present in the Eden catchment are expected to be rich in Fe-bearing minerals (e.g. Fe-Ti oxides) which show chemical and morphological differences associated with different petrogenetic conditions. Sedimentary rocks, on the other hand, are expected to be poorer in such minerals. Glacial till, deposited in the topographically lower areas of the catchment (Figure 2.2), would be clearly differentiated mineralogically as being a sedimentary deposit derived from markedly different materials (principally igneous and metamorphic rocks from the Scottish Highlands) (Chapter 2).

The River Eden catchment is thus found to be an ideal area in which to test provenance models based on magnetic minerals using both geochemical and magnetic approaches to source characterisation.

1.2. Aims of thesis

This study has the following principal aims:

1. The detailed characterisation of rocks, till and stream sediments present in the River Eden catchment on the basis of chemical composition, internal texture, grain size and concentration of magnetic minerals.

2. The evaluation of chemical and physical changes suffered by magnetic minerals (mainly magnetite) by weathering and abrasion during sediment formation and fluvial transport.

3. The qualitative and/or quantitative estimation of the provenance of sediments in the River Eden, with particular interest in the relative contribution of each potential source to the sediment.

4. The testing of the reliability of both geochemical and magnetic measurements as provenance indicators.

5. The testing of the applicability of statistical methods to environmental studies of sedimentary provenance.

1.3. Structure of thesis

The thesis is organised as follows, closely following the actual sequence involved in the study:

1. *Literature review*. A detailed literature review (Chapter 2) was carried out in order to recognise the materials present in the study area, including the rocks and Quaternary deposits, in particular to identify potential sediment sources, and also to survey the various methods and approaches used by previous authors in the studies with similar objectives. On the basis of the information acquired by this initial research, four main potential source groups were distinguished: Carboniferous basalts, Lower Devonian andesites, Upper Devonian sedimentary rocks and glacial till, as these are volumetrically the most important materials in the River Eden catchment. Also, magnetite and ilmenite were identified as potential sedimentary provenance indicators.

2. *Sampling*. Samples of rocks and till were collected in the catchment at points conditioned by the outcrops found in the study area. Also sediment samples were collected along four selected tributaries and the main channel of the River Eden (Chapter 3). Two tributaries draining the northern part of the catchment and two tributaries draining the southern part of the catchment were chosen as the sediment transported by them is known to derive from a restricted number of known sources. This serves as the basis of setting up quantitative criteria for determining sediment provenance and, at the same time, permits evaluation of the local fluvial dynamics on sediment transport.

Additionally, dolerite samples found to be weathered under subaerial and subaqueous conditions were also collected in order to investigate the compositional changes suffered by their Fe-Ti oxide minerals during weathering.

3. *Laboratory analysis*. The mineral assemblages, as well as the chemical and textural characteristics of each single mineral species constituting a rock are related to the magmatic crystallisation condition. Hence, a characterisation of the source groups mentioned above was performed using both geochemical and magnetic measurements with the aim of detecting any Fe-Ti oxide mineralogical variations between and within the groups. Such variations assist in the recognition and classification of the potential sediment sources present in the catchment. The analytical approaches include: (1) X-ray fluorescence of whole-igneous rock samples to determine their major and trace element composition, (2) X-ray

diffractometry in order to identify the heavy mineral fraction of the source materials (rocks and till), and (3) magnetic parameters, consisting of magnetic susceptibility, anhysteretic remanent magnetisation, and isothermal remanent magnetisation, measured in igneous and sedimentary rocks and glacial till samples which provide a detailed characterisation of the sediment sources in terms of their magnetic mineral concentration, composition and grain size. All these analytical methods are described in detail in Chapter 3. As ilmenite and magnetite were selected as provenance indicators an analysis of the composition and texture of the Fe-Ti oxide minerals was performed using electron probe microanalysis and backscattered imaging (Chapter 3), respectively.

Bulk sediment samples and subsamples resulting from sieving bulk sediment samples were also analysed using many of the techniques described above (with the exception of X-ray fluorescence) in order to characterise the concentrations, compositions and grain sizes of their constituent magnetic minerals.

4. *Interpretation of analytical results*. Scattergrams of raw data and of the results from multivariate statistical analyses, such as simultaneous R- and Q-mode factor analysis, were used to assist in the interpretation of the analytical results by establishing the interrelationships between the variables which may lead to the identification and classification of sediment sources, and also to mineralogical characterisation of the sediment samples. Subsequently, and together with discriminant function analysis, the interrelationships between sources and sediment were established, allowing a qualitative estimation of the sedimentary provenance. The interpretation of the results provides a framework for a quantitative provenance model.

5. *Modelling*. Various statistical models were derived, the most important being based on linear programming. This technique can be configured to provide a quantitative estimate of the relative contribution of each source to the sediment. Models performed using magnetite composition and/or magnetic measurements are evaluated. The efficiency of the linear programming results was tested by modelling sediment samples considering the River Eden tributaries as sources.

2. Literature review

Many authors have established the provenance of sediments using different approaches. In this project, two main data sets will be used to fingerprint where the sediments transported by the River Eden and its tributaries come from; one obtained by a geochemical approach and the other one resulting from magnetic measurements of potential source materials and sediments derived from them. In this chapter, the way in which both methods have been applied by previous authors is outlined, and the geological setting of the study area is also described.

2.1. Fe-Ti oxides as sedimentary provenance indicators

Sediments are made up of mixtures of minerals and rock fragments which were previously components of older rocks. Consequently, sediments and their source rocks are mineralogically related. However, an accurate mineral characterisation of both materials is required in order to compare and establish the precise relationship between them. Heavy minerals play a major role in provenance studies because of their high chemical stability. The distribution of heavy minerals in sediments, however, becomes changed relative to those of their parent rocks by processes of differential weathering, hydraulic sorting and diagenesis. In consequence, identification of provenance from heavy mineral assemblages is often problematic and may lead to erroneous conclusions (Basu and Molinaroli, 1991; Morton, 1991). The chemical composition and petrographic properties (morphology, internal structure, and other crystallographic properties) of a single mineral species are related to the conditions under which the parental rocks were formed. Thus, mineralogical relationships between sediments and their source materials may be identified by the combined analyses of both chemical and petrographic characteristics of one or more single mineral species. This approach has been successfully applied using such diverse minerals as, **tourmaline** (e.g. Henry and Dutrow, 1992; Henry *et al.*, 1994), **garnet** (e.g. Haughton and Farrow, 1989; Morton, 1987), **pyroxene** (e.g. Cawood, 1983), **chromite** (e.g. Hiscott, 1978), **zircon** (e.g. Owen, 1987), **ilmenite** (e.g. Darby and Tsang, 1987; Basu and Molinaroli, 1989 and 1991; Grigsby, 1992), and **magnetite** (e.g. Basu and Molinaroli, 1989 and 1991; Grigsby, 1990; Razjigaeva and Naumova, 1992). All

these studies show how useful and reliable heavy minerals are as sedimentary provenance indicators.

As will be seen in subsequent chapters, Fe-Ti oxides are used here as sediment source fingerprints. Basu and Molinaroli (1989 and 1991) evaluated the variability of ilmenite composition as a discriminator of source rocks. They differentiated ilmenite grains from igneous and metamorphic rocks on the basis of their compositional variability, texture and grain size. Then, they performed discriminant function analysis to examine the variability of six oxides components (Mg, Al, Ti, Cr, Mn, Fe), and of the number, directions and widths of 'exsolution' lamellae in detrital ilmenite, in ascertaining the reliability of all these variables in provenance determination. They found that discriminant analysis of all chemical and petrographic variables taken together provides an efficient identification of provenance with more than 95% correct determinations. However, although lamellae width and intergrowth patterns of the Fe-Ti oxides are strongly suggestive of provenance, no single character alone is diagnostic of provenance. On the basis of these results, they modelled quantitatively the provenance of sediments. Nevertheless, these authors also noted that a definitive generalisation is not warranted as the success with the statistical analysis could be more apparent than real. It is suggested that a high degree of diagenetic alteration may obliterate all the observed differential features of the sediments, even when they show that weathering and diagenesis do not always obliterate all petrographic indicators of provenance.

A similar approach was adopted by Darby and Tsang (1986) in order to differentiate drainage basins on the basis of ilmenite composition. These authors tried to estimate the downstream compositional variation of ilmenite grains transported by rivers, and whether the changes are due to tributary input or to selective removal of one or more elements (either due to leaching or destruction of exsolved mineral phases by weathering). They found that, although non-opaque heavy minerals change in abundance and type downstream due to tributary input, the overall detrital ilmenite composition remains virtually unchanged along the major river courses, despite addition of ilmenite of quite different composition from tributaries. Also, the chemical composition of ilmenite grains was found to vary between adjacent drainage basins which erode similar rock types. The difference in the proportions of the source rocks in each basin was suggested as the most probable explanation. On the other hand, composition of ilmenite appeared to be insensitive to ilmenite grain type (twinning, inclusions, and leucoxene rims) and weathering effects (primarily leucoxene rims and removal of hematite lamellae). Basu and Molinaroli

(1989), Darby and Tsang (1986) thus concluded that the composition of surviving ilmenite grains should provide a reliable indicator of provenance.

Grigsby (1990 and 1991) used both magnetite and ilmenite as sedimentary provenance indicators. This author stated that it is necessary to determine the collective significance of the full set of variables through discriminant function analysis before the value of those variables in fingerprinting detrital ilmenite and magnetite can be fully assessed. He successfully discriminated mafic and felsic igneous parent rocks on the basis of their differences in ilmenite chemical composition. On the other hand, he found petrographic differences in detrital magnetite grains from different parent rock types, concluding that most information about the source rocks can be obtained by studying homogeneous detrital magnetic grains, grains with magnetite-ilmenite intergrowths (trellis- and composite types), and grains with exsolved pleonaste or ulvospinel. Therefore, textural differences observed in magnetite and ilmenite grains discriminate successfully magnetite coming from felsic and mafic plutonic and volcanic, intermediate volcanic, and metamorphosed mafic and ultramafic parent rocks.

2.2. Provenance studies using magnetic measurements

Sediments derived from different sources within a catchment area will become mixed during the complex processes of erosion, transport and deposition. Stott (1986) has suggested that certain magnetic properties (magnetic susceptibility and isothermal remanent magnetisation) of the resulting mixtures of sediments are dependent on the original characteristics of the source materials and the relative proportions of each source material in the mixture. Consequently, such magnetic properties may then be considered as sedimentary provenance indicators.

Several authors have applied combined magnetic measurements to trace provenance; e.g. Yu and Oldfield (1989 and 1993) trace the source of sediments from the Rhode River (USA), and from a dried-out reservoir in Níjar (Spain) respectively, by measuring magnetic susceptibility, anhysteretic remanent magnetisation and isothermal remanent magnetisation. A similar approach has been used by Stober and Thompson (1979) who determined the major source of ferrimagnetic minerals in sediments of five Finnish lakes by measuring magnetic susceptibility, isothermal remanent magnetisation and coercivity of remanence (see Chapter 3 for explanation of these magnetic properties).

Two different approaches can be distinguished in previous studies: the first consists of a comparison between naturally contrasting magnetic properties of sediments and their potential source materials (e.g. Oldfield *et al.*, 1979; Walling *et al.*, 1979; Bradshaw and Thompson, 1985; Oldfield *et al.*, 1985; Andrews and Jennings, 1987). The second involves the identification of sediment source components by using simulated mixing tests (e.g. Stott, 1986; Thompson, 1986; Yu and Oldfield, 1989). The use of diverse statistical methods, such as cluster analysis, principal component and factor analysis, lead to a classification of the source materials on the basis of their magnetic properties. All these statistical analysis, together with scattergrams, provide a qualitative interpretation of sediment provenance (e.g. Walden *et al.*, 1992a; Walden *et al.*, 1996). Whereas, multivariate linear modelling leads to the establishment of quantitative linkages between sediments and sources (e.g. Thompson, 1986; Yu and Oldfield, 1989; Yu and Oldfield, 1993; Lees, 1994; Walden *et al.*, 1997).

It has been found that magnetic properties of unconsolidated deposits are strongly particle size-dependent (Yu and Oldfield, 1993). In provenance studies, a detailed magnetic characterisation of sources and sediments on a particle size-related basis is therefore necessary, whatever the approach used, in order to prevent coincidental or invalid sediment source identification (Oldfield *et al.*, 1985). Differences in magnetic measurements due to particle size can be the result of:

- different concentrations or relative proportions of magnetic minerals produced by mechanical sorting associated with the energy of the transport medium (Stober and Thompson, 1979; Thompson and Morton, 1979; Björck *et al.*, 1982; Dearing *et al.*, 1985); and /or

- variations in magnetite grain size with particle size. These were found by Oldfield and Yu (1994) to be a complex relationship which cannot be explained solely by the high density of magnetite (5.25 g /cm^3).

These studies demonstrate the suitability, both qualitatively and quantitatively, of magnetic susceptibility, anhysteretic remanent magnetisation, isothermal remanent magnetisation and coercivity of remanence as sedimentary provenance indicators. However, as noted by Oldfield (1991), the complexity and unfamiliarity of many natural magnetic assemblages, coupled with the very versatility and sensitivity of the measurements, can often limit the interpretations. The use of other techniques, such as X-ray diffractometry (XRD), scanning and transmission electron microscopy, Mössbauer resonance and pollen analyses, in a

limited and selective way can help to develop possible explanations for the magnetic variations observed in many cases.

2.3. Solid geology of the River Eden catchment

Three areas, with a general north-east to south-west trend, can be distinguished in the catchment of the River Eden: a northern area, consisting principally of Lower Devonian lavas, a central area, underlain by sedimentary sequences of Upper Devonian age, and a southern area of Lower Carboniferous sedimentary units with Upper Carboniferous intrusions consisting principally of olivine-dolerite and quartz-dolerite sills (Figure 2.1).

The Devonian rocks are entirely non-marine and are characterised by the facies known in Britain as the Old Red Sandstone. Lower and Upper divisions are distinguished, separated by a marked unconformity, whilst Carboniferous deposits rest conformably on the Upper Old Red Sandstone.

Detailed geological studies of different parts of the study area have been carried out by several workers. The Lower Devonian deposits have been widely described by Armstrong *et al.* (1985), whilst the Upper Devonian has been studied in detail by Chisholm and Dean (1974). In addition, Forsyth and Chisholm (1977) provide extensive information about the Carboniferous deposits of the study area. The geology of the catchment of the River Eden, as described below, is thus principally based on the information provided by all these authors.

2.3.1. Lower Devonian

The Lower Devonian rocks of the Midland Valley of Scotland in general consist mainly of sandstones and conglomerates. In the study area, however, sedimentary rocks of Lower Devonian age are scarce. They consist of cross-bedded sandstones (Garvock Group), which contain clasts of metamorphic and igneous rocks and also pebbles of limestone, mudstone and siltstone, probably representing the deposits of a powerful, braided river system. The major part of the Lower Devonian in the area is dominantly of volcanic rocks (Ochil Volcanic Formation), being built up of agglomerate and lava, with occasional intercalations of tuffs and volcanic conglomerates (see Figure 2.1) (Geikie, 1900).

The lavas consist principally of varieties of andesite and basalt, with some flows of trachyandesite, reaching their maximum development of at least 2400 m in

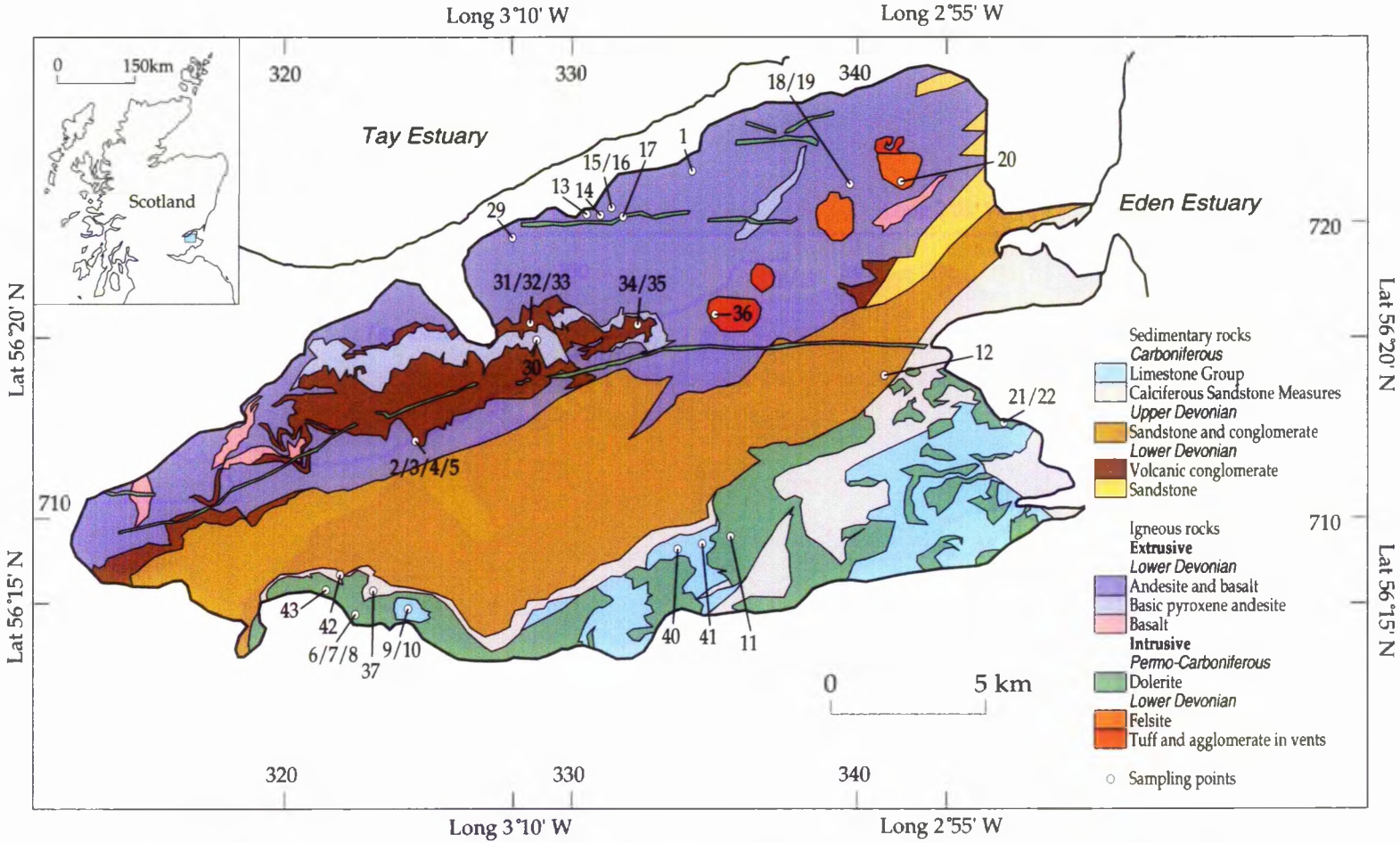

Figure 2.1. Solid geology of the River Eden catchment (based on BGS 1:50 000 solid geology sheets 40, 41, 48E, 48W and 49), showing locations of rock samples.

thickness to the north-west of Cupar (NO 3375 7145). They are characterised by the presence of amygdales, mainly filled with calcite, quartz and chloritic minerals in their upper parts, and also by autobrecciation processes which can affect the whole thickness of a lava flow. Erupted mainly subaerially onto the alluvial plains of a major river system, these lavas probably built successive, upstanding volcanic terrains which were periodically overlapped by fluvial sediments derived from the north. Thus sediments invaded the lavas and infilled fissures and cavities within them. The youngest lava flows tend to persist farthest, suggesting a migration to the north-east of the main focus of volcanic activity. It is unclear whether the lavas were derived from a single large centre, possibly situated to the south of the present outcrop, or were extruded, perhaps from fissures, at a number of localities.

Basic pyroxene-andesites predominate over all other lava types. However, only those which contain abundant large (greater than 3 mm) feldspar phenocrysts are differentiated on the map (see Figure 2.1). The rocks classed as andesites are mainly basic, non-feldsparphyric, pyroxene-andesites but also include hypersthene-andesites, and basalts which differ from andesites in having a silica content lower than 53 per cent and higher proportion of olivine pseudomorphs. A series of basalt flows about 100 m thick has been, however, traced (see Figure 2.1), the lowest flows being markedly olivine-phyric and the upper flows being feldsparphyric .

Tuff and agglomerate occur within vents (see Figure 2.1), containing blocks of various lava types of all sizes. They are possibly altered volcaniclastic sediments in the metamorphic aureoles of concealed intrusions. Volcanic conglomerates are generally coarse-grained, with angular to well-rounded blocks mainly of basic lava, and some acid pebbles, constituting lava debris.

In addition to the extrusive deposits, numerous minor intrusions which cut both the lavas and the sediments occur. They are chemically similar to the lavas, and are considered to be broadly contemporaneous. The minor intrusions vary in size and form from thin, near vertical dykes to sills and veins, through bosses. The largest intrusion is a fine-grained rhyolitic felsite (see Figure 2.1) which is probably a laccolith. Other acid intrusions are small bodies of similar composition classed as 'felsic alkaline rocks' which form a group of small dykes and sills in the area between Dunbog (NO 3285 7178) and Balmerino (NO 3358 7248). At Forret Hill (NO 3387 7200) a boss of microgranodiorite is exposed which is chemically equivalent to the trachyandesite lavas.

The lavas and their associated minor intrusions as a whole constitute a volcanic province of calc-alkaline affinity and the volcanic activity was apparently

related to subduction associated with the closure of the Iapetus Ocean (Thirlwall, 1981).

During the Middle Devonian, the Lower Devonian rocks were deformed, giving rise to a series of major north-east-trending fold structures. The studied area is situated on the south-east limb of the Sidlaw Anticline. As the lavas were much more competent than the sedimentary rocks they developed many faults, of north-west to south-east trend, as a result of the deformation process. Subsequent uplift permitted deep erosion of the deformed Lower Devonian rocks, onto which the Upper Devonian formations were unconformably deposited.

2.3.2. Upper Devonian

The central part of the study area consists of sedimentary rocks which rest unconformably on the Lower Devonian lavas (Geikie, 1900; Chisholm and Dean, 1974). These are clearly of Upper Devonian age from the evidence of fossils (Geikie, 1900; Armstrong *et al.*, 1985). These rocks are mainly sandstones (Chisholm and Dean, 1974), although marls and conglomerates are also present (Geikie, 1900); six formations being recognised by Chisholm and Dean (1974) (see Figure 2.1 in Chisholm and Dean, 1974, p. 2).

The oldest deposits consist of cross-bedded sandstones containing pebbles of lava derived from Lower Devonian sources and metamorphic clasts derived from the Highland terrains. The presence of intraformational mudstone clasts (Burnside Formation) is indicative of deposition mainly in the channels of a river flowing eastwards (Armstrong *et al.*, 1985). In the later deposits of this phase of deposition, however, only intraformational pebbles are present (Glenvale Formation). A second phase of deposition produced a distinctive group of sandstones (Knox Pulpit Formation in the Lomond Hills area, and Kemback Formation in the Stratheden area), weakly cemented and variable in grain size (mainly Knox Pulpit Formation), which were deposited by currents flowing mainly towards the west. However, alternating east-west, perhaps tidal, flows are also evident on the basis of sedimentary structures. These deposits are interpreted as shallow marine by Chisholm and Dean (1974), although contributions from fluvial and particularly aeolian processes cannot be ruled out. In the Dura Den area, the environmental change from the first to the second phase of deposition took place gradually, the Dura Den Formation thus being differentiated. This formation is characterised by its abundant fish remains, and consists of siltstones which alternate irregularly with fine- and very fine-grained sandstones.

After a marine transgression, fluvial conditions were re-established, and currents flowing eastwards deposited mainly sandstones (Kinnesswood Formation). These contain mudstone bands, nodular and concretionary dolomite ('cornstone'), and "Highland" pebbles, apparently indicating an uplift in the source areas accompanying the regression. This latter formation thins progressively along the strike north-eastwards from the Lomond Hills to the Pitlessie area (see Figure 2.1 in Chisholm and Dean, 1974, p. 2), where it apparently disappears.

2.3.3. Lower Carboniferous

The Lower Carboniferous deposits rest conformably on the Upper Old Red Sandstone rocks. During Lower Carboniferous times a succession of cyclic sequences of sandstones, siltstones and mudstones with subordinate coal and marine carbonate rocks, was deposited. The earliest deposits (Calciferous Sandstone Measures) consist principally of sandstones. Limestones, consisting of bedded, nodular and conglomeratic dolomite and siderite, are scarce. The clastic units are interpreted as having been laid down in a delta by rivers flowing southwards, and the carbonates, which are believed to be of marine origin, were deposited during periods of reduced supply of fluvial sediments. With time, marine conditions became more widespread and persistent, and greater amounts of mudstones and marine limestone were laid down in shallow seas with richer faunas (Lower Limestone Group). The cyclic pattern of sedimentation continued, however, and thick coal seams are the product of prolonged periods of emergence of the delta during which vegetation flourished on the delta tops.

2.3.4. Upper Carboniferous

At the beginning of the Upper Carboniferous the marine influence became less and coal-bearing sedimentary cycles predominated (Limestone Coal Group), each cycle consisting of an ascending sequence of coal, mudstone, siltstone, sandstone and seatearth. The delta top was periodically eroded by powerful tributaries which laid down coarse fluvial sandstones.

Above the Limestone Coal Group deposits, sequences of sandstones, mudstones, siltstones, limestones and coal seams continued to be deposited, in association with a major volcanic event which resulted in thick accumulations of tuffs and volcanic detritus. However, these latter deposits are not all represented in the study area as a major intrusion, a sill of olivine-dolerite, was emplaced at the end of Upper Carboniferous times, intruding the earlier sedimentary rocks of the Upper Carboniferous.

The Carboniferous sedimentary units have been gently folded and faulted along north-easterly, north-westerly and east-west trends, both folding and faulting being accompanied by uplift and erosion. The age of the complex sill of olivine-dolerite present in the area is uncertain, its relationship to the faulting being unclear. It is likely that this intrusion is related to the volcanism that occurred during the later part of the Upper Carboniferous.

A detailed study of the emplacement of this sill was made by Francis and Walker (1987) and Walker and Francis (1987) in adjoining areas.

The sill-complex, of olivine-dolerite and allied rock types, consists principally of ophitic and non-ophitic olivine-dolerite which are composed mostly of labradorite, with augite, olivine, analcime and biotite also present. The principal accessory minerals are iron oxides and apatite. Olivine-basalts, composed mainly of labradorite, olivine and augite; and analcime-basanite, consisting mostly of augite and olivine (altered to serpentine), are also present in the study area as part of the sill.

Quartz-dolerite and tholeiitic intrusions were mainly emplaced after faulting, being late Carboniferous or early Permian in age. However, their age-relationship to the olivine-dolerite sill-complex remains unknown. They include both dykes and sills which occupy geographically separate areas: the dykes in the north, following a general east-west orientation, and the sills in the south. Both the quartz-dolerites and tholeiites consist principally of labradorite, augite and hypersthene, with occasional pigeonite, Fe-Ti oxides and a quartz-feldspathic or glassy residuum, with accessory apatite, pyrite and secondary amphibole and biotite (Armstrong *et al.*, 1985). They are differentiated mainly by their mesostasis which comprises glass or devitrification products in the tholeiites and micropegmatitic intergrowths of quartz and alkali-feldspar in the quartz-dolerites. Many of the tholeiite dykes are texturally similar to the quartz-dolerites and grade into the latter.

Both petrographical evidence and their close spatial association indicate a genetic connection between quartz-dolerite and tholeiite, both being crystallised from high Fe-Ti tholeiitic mantle-derived magmas which are associated with active lithospheric spreading areas (Armstrong *et al.*, 1985). A detailed geochemical study of the quartz-dolerite dykes of Scotland has been carried out by MacDonald *et al.* (1981).

Some volcanic necks also cut the Upper Carboniferous strata. They consist mainly of pyroclastic rocks composed of Carboniferous sedimentary and basaltic

material, in proportions ranging widely from almost entirely sedimentary- to almost entirely basaltic-derived. In the latter case, the rocks of necks range from mafic olivine-basalt to monchiquite in character.

A late-Carboniferous, north-south extension opened the tension fractures occupied by the east-west quartz-dolerite dykes, and produced the subsidence of the Upper Devonian and Carboniferous strata between faults of east-west and north-east south-west trend.

2.4. Quaternary deposits in the River Eden catchment

The Quaternary deposits and their distributions in the Eden catchment are shown in Figure 2.2. These are mainly glacial deposits; till, glacial meltwater deposits, late-glacial and post-glacial marine deposits. All of these deposits are attributed to a glaciation of Devensian age which culminated about 18000 years ago (BGS Sheet 48 E drift edition). This was a period of powerful erosion, in which the uplands were moulded and earlier sediments were removed from the lowlands as the glaciers, formed and expanded from the Highlands, flowed eastwards across Scotland (Boulton *et al.*, 1991).

Till is the most widely distributed glacial deposit, comprising material transported by the ice and laid down, either at the base of the moving ice sheet or lowered as the ice melted, over almost the whole of the area (BGS Sheet 48 E drift edition). It is commonly 3 to 5 m in thickness, although thinner or absent on many hilltops (BGS Sheet 48 E drift edition). It consists of a variety of stony and sandy clays (Forsyth and Chisholm, 1977) whose composition and texture are indicative of a mainly local derivation. A small proportion of the clasts were derived from greater distances constituting erratics of Highland metamorphic rocks and igneous rocks from the Ochil and Sidlaw Hills. Till colour varies from grey to red depending on the materials from which it was formed - shales, coals and fine clays, or sandstones, respectively (Geikie, 1900). A detailed analysis of heavy mineral assemblages in stream sediments of the glaciated Glen Artney and Glen Lednock, Perthshire, has been carried out by Abdalla and Whyte (1979).

In the late Devensian, glaciers started to retreat and melt waters resulted from ice wastage. Fluvioglacial sand and gravel deposits were deposited by such melt waters at and near the margins of melting ice (Forsyth and Chisholm, 1977). The

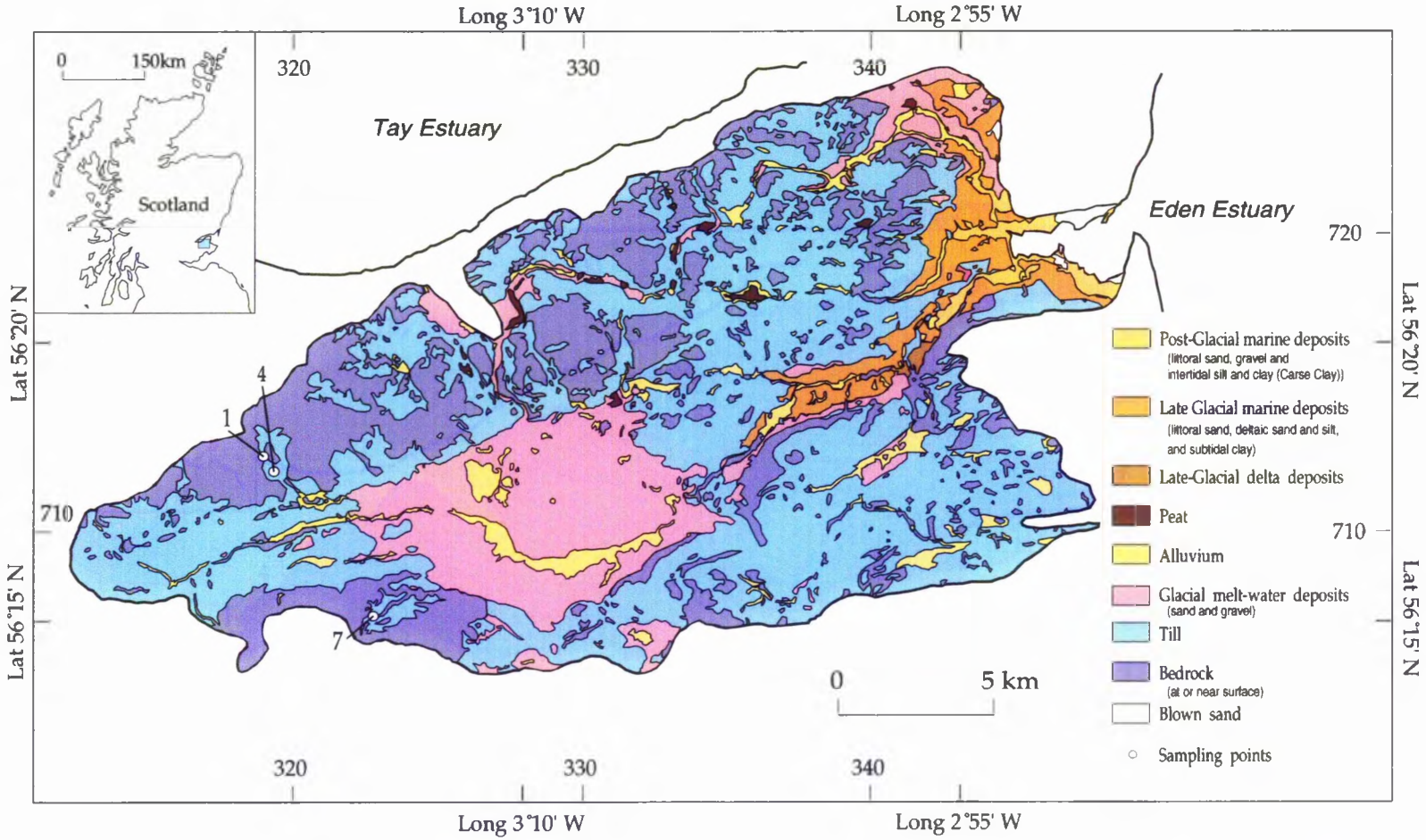

Figure 2.2. Quaternay deposits in the River Eden catchment (based on BGS 1:50 000 drift geology sheets 40, 41, 48E, 48W and 49), showing locations of till samples: 1 (Till BB1), 4 (Till BB4), 7 (Till CB7).

later parts of these fluvioglacial deposits were laid down in a delta prograding into the late-Glacial sea (Laxton and Ross, 1981).

Ice melting lead to an eustatic rise in sea level due to the increased volume of ocean water. At the same time isostatic rise of the land took place due to the removal of the weight of the ice. As a consequence of both processes, changes in relative sea level took place during and after deglaciation (Laxton and Ross, 1981). Successive laminated clays and silts of intertidal to subtidal origin, coarser littoral deposits (gravels) associated with raised beaches, and deltaic deposits were laid down (Armstrong *et al.*, 1985) and then raised above sea level as isostatic uplift generally outpaced eustatic sea level rise (BGS Sheet 48 E drift edition).

After deglaciation, a post-Glacial marine transgression (Flandrian Transgression) took place as eustatic sea level rise was then faster than isostatic uplift. The resulting depositional sequence, which was laid down on a peat bed (Sub-Carse Peat) formed during the marine withdrawal which preceded the transgression, principally comprises silts and clays ('Carse Clay') in estuarine areas. By contrast, in exposed coastal areas the deposits of the transgression consist mainly of sand (Chisholm, 1971). This last post-Glacial transgression culminated about 6500 years ago (Laxton and Ross, 1981) and, after that, isostatic recovery occurred until the present sea level was reached. Such rise of the land was accompanied by incision of streams and by erosion of the sequences deposited during post-Glacial transgression. Thus both post-Glacial marine and estuarine deposits were eroded to form a partly dissected platform, known as the post-Glacial raised beach, with a surface reworked into wind blown dunes (Chisholm, 1971). However, relatively little deposition of sediments occurred (Chisholm, 1971); being represented mainly by fluvial deposits of gravel, sand and silt along the courses of rivers and streams, and silt and mud, commonly peaty, at the site of former lochs (Armstrong *et al.*, 1985).

3. Methodology

In order to obtain the necessary data for this study, samples of rocks, glacial till and stream sediments were collected in the River Eden catchment. They were, firstly, analysed in the laboratory using two different analytical approaches which involved chemical measurements by X-ray fluorescence, X-ray diffraction and electron probe microanalyses, and magnetic measurements of magnetic susceptibility, anhysteretic remanent magnetisation and isothermal remanent magnetisation. Sample preparation and operating conditions during analysis are described in Appendix 1.

The subsequent interpretation of the data, obtained from all these analytical methods, was assisted using bivariate scattergrams and statistical analysis. Four main statistical approaches were used, correlation coefficients, analysis of variance (ANOVA), simultaneous R- and Q- mode factor analysis and discriminant analysis. Both ANOVA and factor analysis were performed by a statistical package called MINITAB whilst correlation coefficient and discriminant functions were calculated using SPSS statistical package. These statistical analyses led to a classification of all the potential sediment sources present in the study area on the basis of their mineralogy. Such a classification was then used in attempting to model qualitatively (mainly by discriminant analysis), and quantitatively using linear programming, the provenance of the stream sediments.

3.1. Field sampling

The lithologies present in the study area, their relative abundance and the location of the outcrop were reviewed in Sections 2.3 and 2.4. Therefore, sample sites were determined according to a strategy of regional sampling coupled with the detailed analysis of specific tributaries. Samples of both source material, including rocks and glacial till, and sediments transported by the River Eden and its tributaries were collected.

3.1.1. Regional geology

The outcrop in the area is limited to hill tops and small quarries, the locations of which are detailed in Forsyth and Chisholm (1977). Representative samples of the volumetrically most important rocks, i.e. those principally contributing to sediment formation, were collected from the study catchment using the published information on outcrop distribution as a guide to site selection. Rock types included andesites, dolerites, felsites, tuff and agglomerates in vents, volcanic conglomerates, sandstones, and limestones. All rock sampling points are shown in Figure 2.1. Rock samples in this thesis are labelled as 'em', followed by a number. However, in Figure 2.1 the prefix 'em' has been omitted for easier reading.

The samples collected, and described in Table 3.1, are:

* Fourteen samples of **andesite**: em1, em2, em3, em4, em5, em13, em14, em15, em16, em18, em19, em29, em30 and em34.

* Six samples of **dolerite**: em8, em11, em17, em21, em22 and em43.

* Three samples of **volcanic conglomerate**: em31, em33, and em35.

* One sample of **felsite**: em20.

* One sample of **tuff and agglomerate in vents**: em36.

* Two samples of **sandstone**: em12 and em42.

* One sample of **limestone**: em41.

3.1.2. Weathered rock samples

Mechanical disintegration of rocks reduces them to small fragments and even individual mineral particles. However, chemical decomposition (weathering) produces mineralogical changes in the resultant sediments.

At Craigmead Quarry (NO 3230 7058), the Carboniferous quartz-dolerite sill exhibits various stages of chemical weathering (spheroidal or onion-skin texture) providing an opportunity to study progressive degradation of the rock. The samples collected included: a fresh dolerite sample (em8), a weathered sample showing an orange colour (em27), a sample of weathered rim (em25), five weathered layers (em24/1, em24/2, em24/3, em24/4, em24/5) (Figure 3.1) from the rim to the fresh central part of the rock (core stone), a sample constituted by several weathered layers

mixed (em23), and a sample of the soil resulting from the total disintegration and decomposition of the rock (em28).

Table 3.1. List of rock samples collected for the present study, including their classification, age and location.

Sample	Rock type	Age	Location
em1	Andesite	Lower Devonian	NO 3341 7214
em2	Andesite	Lower Devonian	NO 3249 7120
em3	Andesite	Lower Devonian	NO 3249 7120
em4	Andesite	Lower Devonian	NO 3249 7120
em5	Andesite	Lower Devonian	NO 3249 7120
em8	Qz-dolerite	Permo-Carboniferous	NO 3230 7058
em11	Qz-dolerite	Permo-Carboniferous	NO 3365 7096
em12	Sandstone	Upper Devonian	NO 3417 7147
em13	Andesite	Lower Devonian	NO 3306 7203
em14	Andesite	Lower Devonian	NO 3308 7202
em15	Andesite	Lower Devonian	NO 3312 7201
em16	Andesite	Lower Devonian	NO 3312 7200
em17	Qz-dolerite	Permo-Carboniferous	NO 3316 7199
em18	Andesite	Lower Devonian	NO 3398 7218
em19	Andesite	Lower Devonian	NO 3398 7218
em20	Felsite	Lower Devonian	NO 3417 7214
em21	Olivine-dolerite	Permo-Carboniferous	NO 3458 7133
em22	Olivine-dolerite	Permo-Carboniferous	NO 3458 7133
em29	Hypersthene-andesite	Lower Devonian	NO 3280 7194
em30	Basic pyroxene-andesite	Lower Devonian	NO 3290 7165
em31	Volcanic conglomerate	Lower Devonian	NO 3290 7166
em33	Volcanic conglomerate	Lower Devonian	NO 3290 7166
em34	Basic pyroxene-andesite	Lower Devonian	NO 3329 7166
em35	Volcanic conglomerate	Lower Devonian	NO 3329 7166
em36	Tuff and agglomerate	Lower Devonian	NO 3353 7171
em41	Limestone	Lower Carboniferous	NO 3355 7088
em42	Sandstone	Upper Devonian	NO 3220 7075
em43	Qz-dolerite	Permo-Carboniferous	NO 3219 7072

At a second locality, on the shore zone of an artificial reservoir, Holl Reservoir (NO 3225 7037), rocks belonging to the same quartz-dolerite sill present in the study area are known to have been submerged since 1901, when the reservoir was constructed (Duck and McManus, 1990). Two samples were collected: one from under the water (em39) and the second from above the water level (em38), in order empirically to compare the changes in the same rock type under subaqueous and subaerial recent weathering conditions.

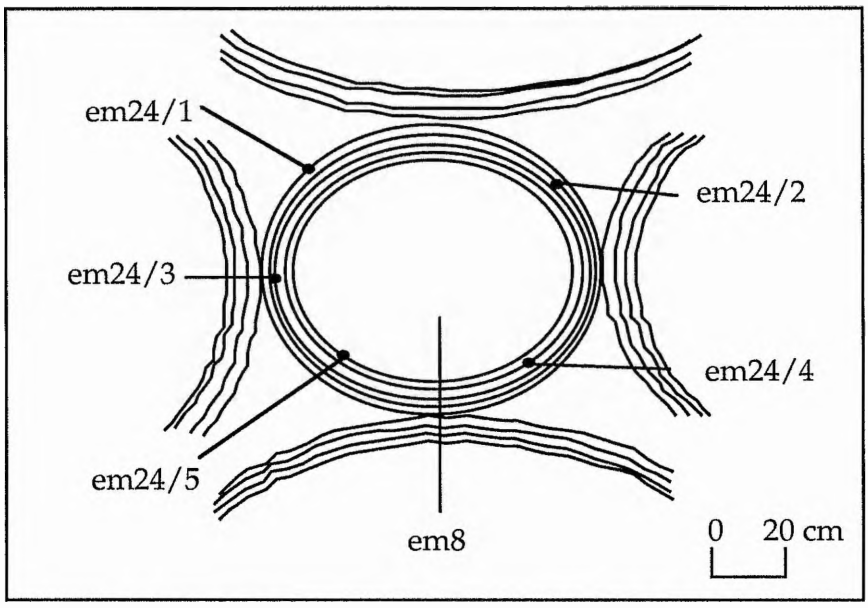

Figure 3.1. Sketch showing the sampling in a dolerite exhibiting onion-skin texture.

3.1.3. Glacial till

Glacial till deposit exposure is restricted in the River Eden catchment. For this reason, till samples were collected along stream courses and their number was limited. Sampling points are shown in Figure 2.2 and, as with the rock sampling points, they are simply indicated by a number. Restricted exposure of till limited the number of samples collected which are: Till BB1 (NO 3190 7118) and Till BB4 (NO 3200 7122), collected along the Barroway Burn course (Figure 1.1), and Till CB7 (NO 3231 7066) from the Coalpit Burn.

3.1.4. Stream sediments

Four small streams in the study area were initially selected for sediment sampling; two in the northern part of the catchment (Barroway Burn and Moonzie Burn) flowing through Lower Devonian rocks, and two in the southern part of the catchment (Kilgour Burn and Coalpit Burn) which flow through Carboniferous rocks (see Figure 1.1). Sediments in these small streams are mainly the product of disintegration and decomposition of andesite (northern streams) and dolerite (southern streams). Therefore, a study of stream sediments should help to understand the chemical and physical changes that the various minerals suffer during the processes of weathering and erosion from the andesites and dolerites, the two main sediment sources in the study area. At the same time, this study would also lead to estimate the contribution of other materials (e.g. glacial till) to the sediments.

This characterisation of the sediments derived from the two main source rocks was carried out in order to understand and model the provenance of sediments transported by the River Eden, which constitute mixtures of materials derived from different sources.

The stream sediment samples collected were:

* Seven samples from the Barroway Burn (see Figure 3.2a), labelled as BB followed by a number.

* Four samples from the Moonzie Burn (see Figure 3.2b), labelled as MB followed by a number.

* Six samples from the Kilgour Burn (see Figure 3.3a), labelled as KB followed by a number.

* Eight samples from the Coalpit Burn (see Figure 3.3b), labelled as CB followed by a number.

All these samples are of bedload transported sediments (i.e. sands and coarser grades), sampled along the stream channel wherever a change in slope and/or source material (mainly rocks, but also glacial till) was seen.

In the River Eden, six sediment samples were collected (labelled as RE followed by a number) from locations shown in Figure 1.1.

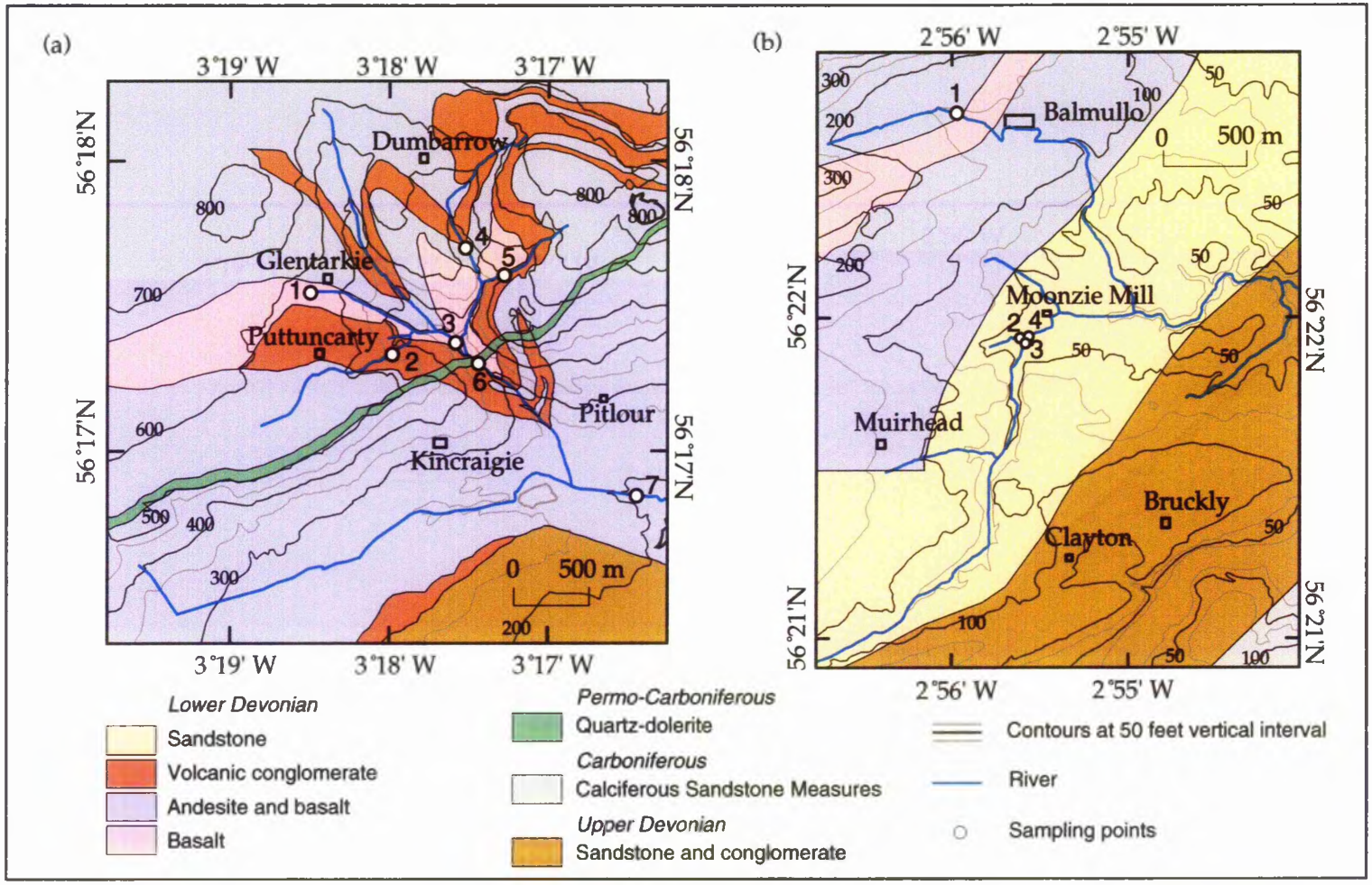

Figure 3.2. Sampling points of sediments along two tributaries located in the northern part of the River Eden catchment: (a) Barroway Burn and (b) Moonzie Burn. Geology based on BGS 1:50 000 solid geology 48E and 49 sheets, and topography based on Ordnance Survey 1:10 000 sheets NO 42 SW, NO 41 NW, NO 11 SE and NO 21 SW.

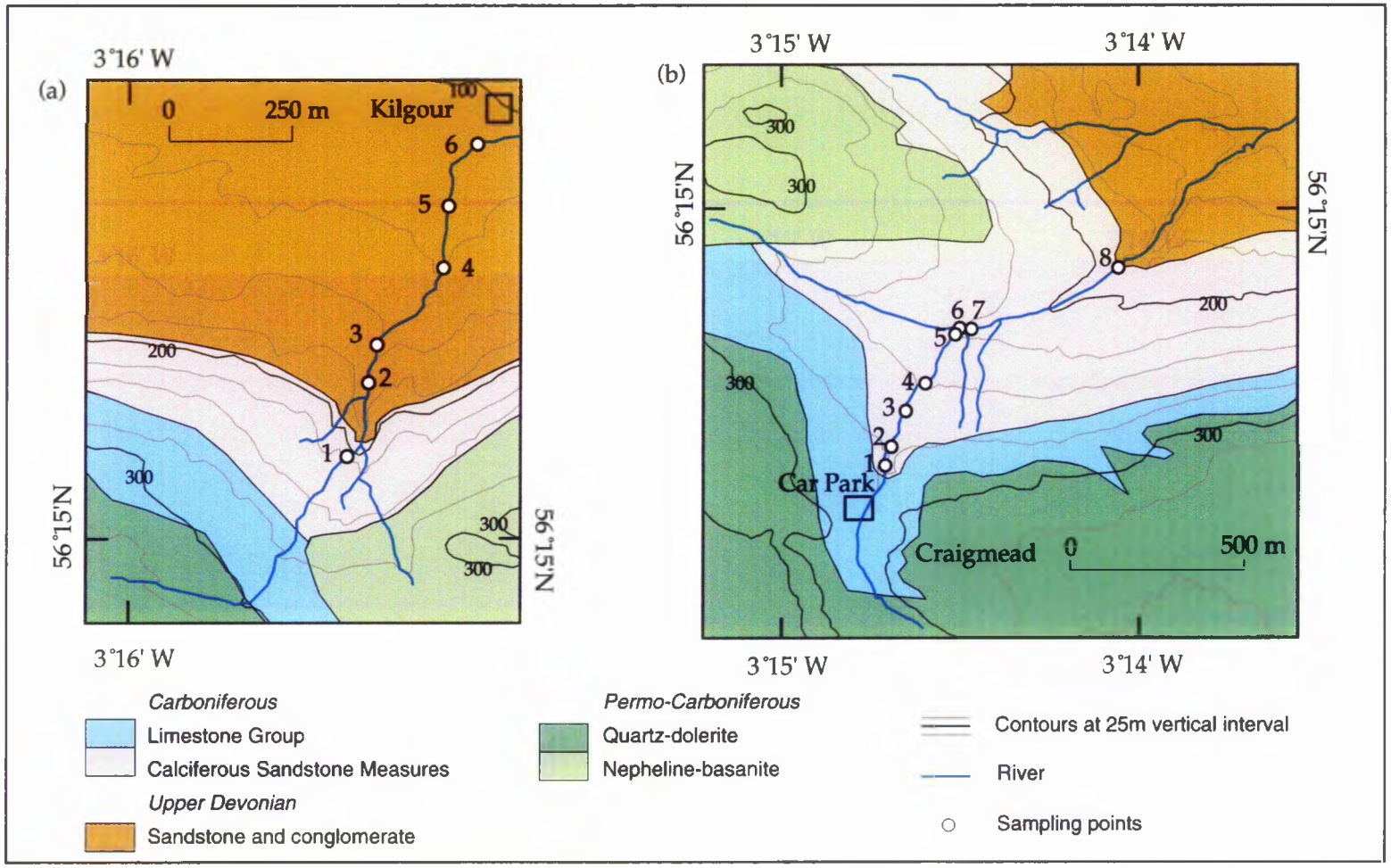

Figure 3.3. Sampling points of sediments along two tributaries located in the southern part of the Eden catchment: (a) Kilgour Burn and (b) Coalpit Burn. Geology based on BGS 1:50 000 solid geology sheets 40 and 41, and topography based on Ordnance Survey 1:10 000 sheets NO 20 NW.

3.2. Characterisation of rock composition

Chemical analysis of rock samples allows a full characterisation of the rock's composition both in terms of essential constituents (major oxides) and trace elements.

In this study, chemical characterisation of the igneous rocks (including volcanic conglomerates) was made as a first step to distinguish the compositional range of potential sediment sources. The concentrations of major and trace elements in the samples were measured using a Philips 1050/20 X-ray fluorescence spectrometer. The major elements analysed were Si, Ti, Al, Fe, Mn, Mg, Ca, Na, K and P, quoted as weight percentage oxides. The trace elements analysed were Nb, Zr, Y, Sr, U, Rb, Th, Pb, Ga, Zn, Cu, Ni, Cr, Ce, Sc, V, Ba and La, quoted in ppm.

3.3. Characterisation of mineralogy

Once all rocks present in the study area had been identified and distinguished as potential sediment sources, the heavy minerals were then identified using X-ray diffractometry, as these minerals are often the most suitable for sedimentary provenance studies (see Chapter 2). Fe-Ti oxides were chosen in the present study as provenance indicators because initial analyses determined their presence in all igneous rocks of the catchment and their absence in the sedimentary rocks. This makes possible the combined use of chemical and textural analyses of these Fe-Ti minerals, together with the magnetic properties of the rocks and sediments which contain them, as provenance indicators.

The chemical and textural analyses of the Fe-Ti oxides were carried out using a JEOL JCXA-733 Superprobe. Optical microscope identification of the different Fe-Ti oxides and their internal texture was often very difficult due to the small size of the grains (< 100 μm). In contrast, backscattered electron images (BSE) were invaluable in detecting chemical variability in individual mineral grains, and provided important information about the inter-relation of different mineral species.

Electron probe microanalysis was carried out for nine elements (Si, Ti, Al, Fe, Mn, Mg, Ca, Na and K) as oxides on grains of magnetite and ilmenite in a thin section of each igneous rock sample and some selected till and stream sediment samples. In all minerals Fe was analysed as FeO and recalculated to weight percent Fe_2O_3 and FeO following the procedure of Droop (1987).

3.4. Characterisation of magnetic properties

This section provides a detailed introduction to the magnetic properties measured and their underlying controls in order to settle the information required to understand the terminology and interpretations described in subsequent chapters. Most of the information has been gleaned from O'Reilly (1984), Thompson and Oldfield (1986), Jiles (1991), and Dearing (1994). The instruments used to obtain magnetic data are described in Appendix 1, together with sample preparation and measurement procedures.

3.4.1. Environmental magnetism

The magnetism of natural materials is produced by the movement of the electrons in their constituent atoms. Within an atom the electrons move describing two different movements: an orbital rotation around the central nucleus and, at the same time, a spin motion about their own axes. As electrons are electrically charged each of these movements generates an electric current which results in a magnetic moment. However, the electron spin magnetic moment dominates the magnetic behaviour shown by all substances as the alignment of all electron spin magnetic moments in an atom determines the magnetic moment of such atom. Atoms in which all electrons have paired spins have no net magnetic moment while those having one or more unpaired electron spins do have net magnetic moment and behave like permanent magnetic dipoles. The nature of the atomic magnetic moments alignment in a material will then determine the degree of the magnetic behaviour shown by such material.

3.4.1.1. Magnetic behaviour

Five main types of magnetic behaviour have been described which are, in order of increasing strength: diamagnetism, paramagnetism, antiferromagnetism, ferrimagnetism and ferromagnetism. They are summarised in Table 3.2, and described below.

Diamagnetism

Substances (such as quartz, feldspar, calcite and water) in which all atoms have paired electron spins, and therefore no net atomic magnetic moments, have no magnetic moment. When in a magnetic field such substances acquire a very weak magnetisation which opposes the applied field and is due to the interaction of the magnetic field with the orbital electron magnetic moments. This temperature

independent magnetisation is lost as soon as the applied magnetic field is removed. Substances showing such magnetic behaviour are termed diamagnetic.

Paramagnetism

Paramagnetic materials (such as olivine, pyroxene, garnet, biotite, Fe and Mn carbonates) contain atoms which possess a permanent magnetic moment. However, these atomic magnetic moments are randomly aligned due to thermal energy being greater than the interactions between atomic magnetic moments. This results in materials having no magnetic moment as atomic moments cancel each other. When in a magnetic field the atomic magnetic dipoles align themselves slightly parallel with the direction of the applied field; a weak positive magnetisation then being caused which is lost as soon as the magnetic field is removed. Therefore, paramagnetism is a function not only of the applied magnetic field but also of the absolute temperature, as the magnetic moment depends on the balance between thermal agitation and magnetic ordering.

Antiferromagnetism, Ferrimagnetism and Ferromagnetism

In materials exhibiting any of these behaviours, below a critical temperature (Curie temperature for ferri- and ferromagnetic materials, and Néel temperature for antiferromagnetic materials) which is characteristic of each material, powerful magnetic interactions between adjacent atoms cause the atomic moments to remain aligned despite the continual disturbance of thermal agitation. Therefore, below such a temperature, these materials carry a strong remanent magnetisation while above it, they behave as paramagnetic materials because the thermal energy breaks down the ordering of the spin magnetic moment of electrons by exchange energy.

When in a magnetic field, these materials acquire a positive magnetisation which exists even in the absence of a magnetic field, and so is referred to as remanent magnetisation. However, the intensity of such magnetisation varies among these three magnetic behaviours due to differences in the sense of coupling of adjacent atomic magnetic moments. Such sense of coupling depends on the first transition series element involved (particularly Fe and Mn) and on crystal structure (Thompson and Oldfield, 1986). In ferromagnetic materials the coupling is parallel, while in both ferri- and antiferromagnetic materials coupling is parallel within layers of atomic magnetic moments, but antiparallel between them (Table 3.2). On the other hand, in ferrimagnetic materials (e.g. magnetite) such layers are of unequal magnetic moment, i.e. the sum of the moments pointing in one direction exceeds that in the opposite direction, leading to net magnetisation. This fact may be due to different

Table 3.2. Magnetic behaviour of natural materials, showing alignment of the atomic magnetic moments (represented by arrows), the net magnetic moment of the material (O if the material have no magnetic moment), and the induced magnetisation when in a magnetic field.

Magnetic Behaviour	Atomic Magnetic Moment Alignment	Net Magnetic Moment	Induced Magnetisation	Substances
Diamagnetism	No permanent atomic magnetic moment	O	Very weak and negative No remanence acquired	Water, organic matter, quartz, feldspar, calcite
Paramagnetism	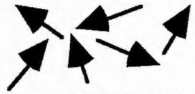	O	Very weak and positive No remanence acquired	Fe and Mn carbonates, olivine, pyroxene, garnet, biotite
Antiferromagnetism	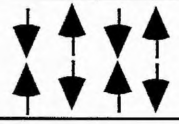	O	Weak and positive Remanence acquired	Hematite
Canted Antiferromagnetism			Weak and positive Remanence acquired	Hematite, goethite
Ferrimagnetism	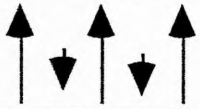		Strong and positive Remanence acquired	Magnetite, maghemite
Ferromagnetism			Strong and positive Remanence acquired	Transition metals (Fe, Mn, Co, Ni)

ionic populations or to crystallographic dissimilarities (Thompson and Oldfield, 1986). In antiferromagnetic materials such layers are of identical magnetic moment, and so the net magnetisation is zero.

In natural environments, ferromagnetic materials are hardly found, and imperfect antiferromagnetic forms are often seen as a result of heterogeneities (due to impurities or lattice defects) or not precisely antiparallel spin directions (spin canting) (e.g. hematite and goethite) which arises from a slight modification of the true antiferromagnetic antiparallelism. These imperfect forms represent parasitic ferromagnetism and lead to a small residual spontaneous magnetisation. Therefore, ferrimagnetic materials will often dominate much of the magnetic information gained from bulk sample measurements, even when present in very small concentrations (Dearing *et al.*, 1985).

3.4.1.2. Magnetic domains

In strongly magnetic materials (antiferromagnetic, ferrimagnetic and ferromagnetic), in the absence of an applied magnetic field, the atoms tend to group themselves into regions of similar direction of magnetisation, in order to reduce the overall free energy associated with the magnetic ordering (Putnis, 1992). These regions are termed magnetic domains, and neighbouring domains can be magnetised in different directions.

The total free energy in a material results from the sum of the energy derived from three main effects: magnetocrystalline anisotropy, magnetostatic effect and magnetostriction. The magnetocrystalline anisotropy depends on the crystal structure as energy is lower if the magnetic moment is in a particular crystallographic direction (easy direction of magnetisation). The magnetostatic effect is due to the presence of magnetic dipoles at a free surface or a domain boundary which interact between them generating an energy. This energy depends on the shape of the crystal and on the distribution of magnetic domains within it, being reduced by aligning the moments in each domain in opposite directions. The magnetostriction is the elastic strain energy which results from a slight change in shape of magnetic materials when they are magnetised (Putnis, 1992).

Magnetic domains are bounded by domain walls across which the direction of magnetisation changes gradually from one domain to the next one.

Three main domain behaviours are distinguished: multidomain behaviour (MD), single domain behaviour (SD) and superparamagnetism (SP). They are grain

size-dependent as increasing size of magnetic grain favours domain walls formation to reduce magnetostatic energy and increase exchange energy.

Multidomain behaviour

If the decrease in magnetostatic energy is greater than the energy needed to form magnetic domain walls, then multidomain specimens will arise. When in a magnetic field, domains magnetisation tends to align into the direction of the applied field. Domains with magnetisation in the direction of the applied field will then grow at the expense of other domains. Initial changes will be reversible. However, in stronger fields domain walls will reach a new equilibrium making changes permanent and causing, in this way, a remanent magnetisation. Saturation is obtained when all domains' magnetisation are aligned in the applied field direction.

Small multidomain grains, called pseudo-single domain grains (PSD), have intermediate magnetic properties between SD and large MD grains (Clark, 1983).

Single domain behaviour

In the case of single domain grains, the alignment of the domain magnetisation may require very strong magnetic fields as it may be oriented in the opposite direction to the magnetic field. They are more difficult to magnetise, compared to multidomain grains, but their magnetic remanence is much higher and more stable.

Superparamagnetism

Superparamagnetism occurs when single domain grains are so small that thermal energy, at room temperature, destroys the magnetisation induced by a magnetic field impeding a stable remanent magnetisation.

Superparamagnetic grains behave as stable single domain (SSD) grains at certain 'blocking' frequencies (see ***Magnetic Susceptibility***) or low 'blocking' temperatures, the magnitude of which depends on the grain volume.

As already mentioned, domain behaviour depends on grain size, but also on shape (see Figure 3.4) and on the chemistry of the magnetic grain, as the critical grain size bounding each domain behaviour differs from one mineral species to another. Several authors have tried to establish the critical grain size, principally for magnetite (see Table 3.3).

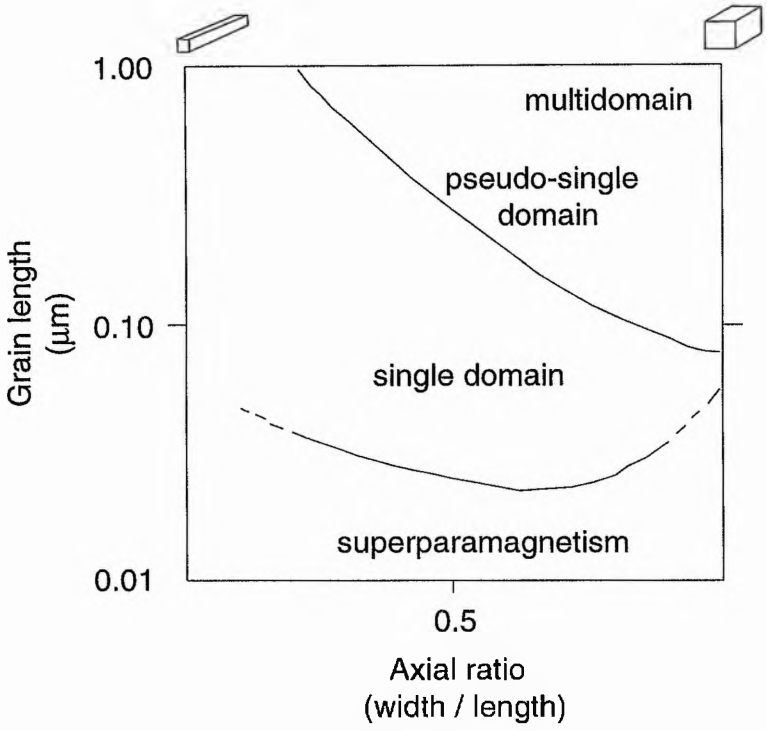

Figure 3.4. Domain behaviour of magnetite grains as a function of their shape (after Butler and Banerjee, 1975).

Table 3.3. Critical grain size between domain behaviours in magnetite.

Author	MD-PSD boundary	PSD-SSD boundary	SSD-SP boundary
Day *et al.* (1977)	20-10 μm		
Banerjee (1981)	40 μm	1 μm	
King *et al.* (1982)	20-10 μm	~0.1 μm	
Clark (1983)	20-15 μm	0.06 μm	
Maher (1988)	20-10 μm		~0.035 μm
Yu and Oldfield (1993)			~0.02 μm

The two main magnetic grain-size boundaries are (1) the division between SP grains and small SSD grains, which occurs, at room temperature, in magnetite grains of around 0.03 μm; and (2) the division between MD and SSD grains which is

difficult to estimate (Thompson and Oldfield, 1986). Hematite is found to have a much larger MD-SSD transition size (1000 μm) than magnetite, mainly due to its lower saturation magnetisation. This large critical size ensures that most natural hematite grains show single domain behaviour (Thompson and Oldfield, 1986).

3.4.1.3. Summary

In summary, the magnetic properties of a single grain depend on (a) its chemical composition which characterises its magnetic behaviour, (b) its size which characterises its domain behaviour, and (c) its crystallographic properties (morphology, internal structure) which characterises its magnetic anisotropy.

In natural environments, rocks and sediments are mixtures of different grains. In consequence, the magnetic properties of these natural materials result from the combination of the magnetic characteristics of each grain present in the mixture. Their relative concentration and interaction of the grains will control the overall magnetic behaviour of the material. In addition, rocks and sediments also show magnetic anisotropy because of the non-random distribution of constituent minerals.

3.4.2. Magnetic Properties

Several magnetic properties have been measured in the present research in order to characterise rocks and sediments in terms of mineral composition, concentration and grain size. All of these properties are derived from placing the sample in magnetic fields of different intensities. They are, in order of increasing intensity of the applied magnetic field, magnetic susceptibility, anhysteretic remanence magnetisation and isothermal remanent magnetisation. In Table 3.4 the magnetic properties of different types of magnetic materials are summarised.

Magnetic Susceptibility

Magnetic susceptibility is a measure of the ease with which a material can be magnetised. Within a small magnetic field (< 1mT) the material acquires a weak magnetisation which is lost as soon as the field is removed.

Ferrimagnetic grains often dominate the magnetic susceptibility measurements as antiferromagnetic and paramagnetic grains exhibit lower magnetic susceptibility values, and diamagnetic grains give weak and negative values. However, when ferrimagnetic grains are scarce, antiferromagnetic, paramagnetic, and even diamagnetic grains, can make substantial contributions to susceptibility. The concentration of the magnetically strongest grains present in the studied sample

Table 3.4. Domain behaviour: MD = multidomain, SSD = stable single domain, SP = superparamagnetism, and magnetic properties: χ = magnetic susceptibility (at low frequency (χ_{lf}) and at high frequency (χ_{hf})), χ_{ARM} = susceptibility of anhysteretic remanent magnetisation, IRM = isothermal remanent magnetisation, SIRM = saturation isothermal remanent magnetisation, $(Bo)_{CR}$ = coercivity of remanence, of natural magnetic minerals (see text and Appendix 2 for explanation).

Magnetic Behaviour	Domain Behaviour	Magnetic Susceptibility	χ_{ARM}	IRM	$(Bo)_{CR}$	SIRM/ARM
Diamagnetism		$\chi_{Dia} < 0$	0	0	0	
Paramagnetism		$0 < \chi_{Para} < \chi_{Anti}$	0	0	0	
Canted Antiferromagnetism	MD SSD	$\chi_{Anti} < \chi_{Ferri}$ $\chi_{MD} \sim \chi_{SSD}$		High Hard IRM values	> -100 mT	
Ferrimagnetism	MD	$(\chi_{lf})_{MD} \sim (\chi_{lf})_{SSD}$		High Soft IRM values		MD > 100
	SSD	$<< (\chi_{lf})_{SP}$	SSD >>> MD	$(SIRM)_{SSD} > (SIRM)_{MD}$	MD < SSD < -100 mT	SSD < 30
	SP	$(\chi_{lf})_{SP} > (\chi_{hf})_{SP}$	$(\chi_{ARM})_{SP} = 0$	$(SIRM)_{SP} = 0$		

is the main factor controlling susceptibility values, although mineral composition, crystal size and crystal shape (in order of decreasing importance) also contribute (Dearing, 1994).

A dual frequency Bartington MS2 susceptibility meter (see Appendix 1) has been used. The measurement of susceptibility at a low frequency (χ_{lf}) of 0.46 kHz and at a high frequency (χ_{hf}) of 4.6 kHz allows to detect the presence of SP grains and also to estimate their concentration. This is because at low frequency, SP grains close to the boundary with SD grains contribute fully to susceptibility, whilst at high frequency the domain boundary between SP and SD grains is shifted to smaller grains, and consequently, SP grains close to such a boundary behave like SD grains with a lower susceptibility value. Thus, the higher the percentage frequency-dependent susceptibility ($\chi_{fd\%}$), the higher the content of SP grains (Dearing, 1994).

Anhysteretic Remanent Magnetisation

The anhysteretic remanent magnetisation (ARM) is the magnetisation acquired by a material after being in a strong alternating magnetic field which is smoothly decreased to zero in the presence of a small steady field.

Magnetisation increases in strength with the application of either a stronger steady field or a stronger alternating field until saturation is reached. A linear change in remanence with field strength is found for steady fields with magnitudes similar to the Earth's field (of the order of 0.04 mT). This linear rate of change is referred to as the susceptibility of anhysteretic remanence (χ_{ARM}).

The ARM shows more complicated variations with grain size than isothermal remanent magnetisation and it is significantly reduced by grain interactions. However, for most natural samples, χ_{ARM} is highly selective of true SSD ferrimagnetic grains in the 0.02 to 0.4 μm range as ferrimagnetic grains with sizes both above and below this range show lower χ_{ARM} values. Therefore, in most cases, this parameter will be proportional to the concentration of SSD ferrimagnetic minerals in the sample. Of course, as the parameter is concentration-dependent, similar bulk values might be produced by high concentration of relatively coarse (MD) magnetite or by much lower concentrations of finer (SSD) magnetite grains (Maher, 1988).

Isothermal Remanent Magnetisation

As mentioned earlier, strongly magnetic materials (antiferro-, ferri- and ferromagnetic materials), within a magnetic field, acquire a magnetisation which

remains in those materials after the field is removed. Such magnetisation is called isothermal remanent magnetisation (IRM). It is characteristic of a given temperature, and its magnitude depends on both the strength of the applied field and the magnetic properties of the material. The field at which saturation of remanent magnetisation (SIRM) is reached by a material depends on its composition and microstructure (e.g. grain size). Thus, this measure leads to an estimation of the content of magnetic minerals and their grain size, being influenced mainly by magnetite and hematite, and single-domain grains rather than large multidomain grains.

Thompson (1986) defined both magnetite and hematite fields (Figure 3.5) by plotting the idealised, empirically derived, normalised isothermal remanent magnetisation (IRM/SIRM) acquired for magnetite and hematite of different grain sizes as sets of curves. The use of these fields may then assist in recognising the presence of ferrimagnetic (magnetite) and/or canted-antiferromagnetic minerals, and in estimating approximately magnetic grain size (see Chapter 4).

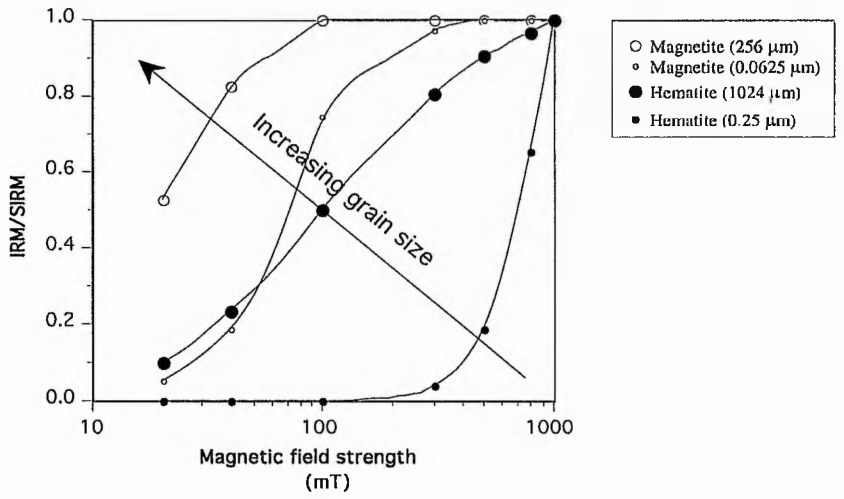

Figure 3.5. Empirically derived, idealised normalised acquisition of isothermal remanent magnetisation (IRM/SIRM) curves for magnetite of grain diameters 0.0625 and 256 μm, and for hematite of grain diameters 0.25 and 1024 μm (after Thompson, 1986).

From all these magnetic properties, several magnetic parameters have been obtained which are used in the following chapters to characterise the rocks and sediments of the study area, and as fingerprints of sedimentary provenance. Such magnetic parameters, including their interpretation, are described in Appendix 2.

3.5. Statistical analysis

The rationale and basic procedures of the various statistical analyses used in this study are presented below, noting that a more detailed description may be found in many text books (e.g. Le Maitre, 1982 and Davis, 1986).

Both correlation coefficients and analyses of variance provide a general estimation of the potentially different sediment sources present in the study area, and also of the measured parameters which mostly differentiate those sources. These are computed before the more complex, discriminant analysis and factor analysis, as these two latter methods not only help in the understanding of the data inter-relationship (Chapter 4) but also allow sample classification. The multivariate statistical analysis of the data leads to a qualitative modelling of sediment provenance, and also provides the basis for quantitative modelling (Chapter 5).

3.5.1. Correlation coefficient

The correlation coefficient is the simplest statistical measure of the linear relationship between two variables. When considering a bivariate frequency distribution, the means and the standard deviations of both variables will be insufficient to define it, and a parameter called covariance is required. Covariance is the sum of the products of the standard deviations from the means of the two variables divided by n (= number of measurements) -1. If both variables are the same, the covariance simply becomes the variance of the variable. Covariance may then equal but cannot exceed the product of the standard deviations of its variables. This is a difficult measure to interpret as the variables are measured in different units. For this reason, in order to estimate the degree of interrelation between variables in a manner not influenced by measurement units, the correlation coefficient is used instead.

Correlation coefficient (r) is the ratio of the covariance of two variables to the product of their standard deviations. It will therefore range from +1 to -1. A correlation of +1 indicates a perfect direct relationship between the two variables, whereas a correlation of -1 shows that one variable changes inversely with relation to the other, i.e. a perfect indirect relationship. Between the two extremes there is a spectrum of less-than-perfect relationships. The closer the correlation coefficient is to 0, the weaker the correlation. However, a correlation coefficient of zero implies only that there is no linear relationship between the variables, other types of relationship (e.g. curvilinear) may exist between them. The correlation coefficient is,

therefore, used to examine the strength of the linear relationship between variables in terms of their variation, and is unsuitable for detecting any other kind of relationship between them.

It is possible that a high correlation coefficient results by chance when using relatively small samples sizes. The larger the sample size, the more confidence can be placed in the result. Therefore, the significance of r must be estimated. This is done from a t-value which tests a null hypothesis that considers the correlation coefficient between two variables to be zero. The alternative hypothesis is that r is different from zero. If the t-value calculated exceeds the tabulated value for n-2 degrees of freedom, the null hypothesis is rejected, suggesting that there is a linear relationship between the variables. However, although r can be significant it may be influenced by a third unknown variable. Also, some correlations between variables do not reflect the relationships between them, but are induced by an operation or transformation that has been performed on the variables.

Two correlation coefficients are commonly used, Pearson's product moment correlation coefficient, and Spearman's rank correlation coefficient. The main limitations of Pearson's correlation coefficient are that interval scale data are required and it is not suitable for ordinal or nominal data forms. This is a parametric statistical analysis, which assumes that both variables are normally distributed. In addition, it assumes that the relationship between the variables is both consistent in direction (either raising or falling) and linear.

On the other hand, Spearman's rank correlation coefficient is a non-parametric statistical analysis and so it may be used for non-normally distributed variables avoiding possible relationships to be induced by transforms of the original data in order to normalise them. This correlation coefficient is also suitable not only for interval but also for ordinal data. Its main limitation is that, even though it does not assume that the relationship between the variables is linear, it does assume that such relationship is consistent in direction. The significance of Pearson's product moment correlation coefficient in all cases, and Spearman's rank correlation coefficient for large sample sizes (> 100 measurements) is tested using the t-test as described above. However, Spearman's rank correlation coefficient, for samples of less than 100 measurements, may be tested comparing the calculated r-value directly with the tabulated r-value for n (= number of measurements) degrees of freedom in the same way as has been described for the t-value.

3.5.2. Analysis of variance (ANOVA)

Analysis of variance (ANOVA) tests for both differences in means and in variances amongst more than two populations simultaneously. This statistical analysis includes several methods. The one-way classification method is the simplest and it is most appropriate when comparing populations using a unique variable. This method assumes that the variances are similar. The null hypothesis, therefore, is that the means of the populations from which the samples are drawn are all equal. The alternative hypothesis is that the null hypothesis is not true, that is that the means of the populations are not all equal, as ANOVA does not indicate which means of the populations are different.

One-way analysis of variance, firstly, estimates the population variance in two different ways and, then, compares the results with a variance ratio or *F*-test. A first estimate consists of calculating the variance of the means of each group and is called the mean square between groups. The other is a pooled estimate, called the within groups mean square. A third estimate can also be made by calculating the variance of all the observations as if they had come from one population. This is usually reported as a check, as this total sum of squares and degrees of freedom is equal to the sum of the between and within sum of squares and degrees of freedom, respectively (Le Maitre, 1982). When the ratio of the between groups to the within groups mean square (*F*-ratio) exceeds the critical value of *F* for *m* (= number of groups)-1 and *N* (= total number of observations)-*m* degrees of freedom, the null hypothesis is rejected.

A one-way analysis of variance is performed for diverse data sets obtained from the analytical approaches described above, principally in order to distinguish all the potential sediment sources present in the study area. ANOVA assumes that the data are normally distributed and have similar variances, and also that the observations are independent. Data will then be normalised, if necessary, before performing the analysis of variance. MINITAB will display (as can be seen in Appendix 5) sum of squares (SS), degrees of freedom (DF) and variance or mean square (MS) between and within the considered groups. It also shows the *F*-ratio and the p-value which is the probability of obtaining this result by sampling variation. The number of samples (*N*), the mean and the standard deviation for each group are also presented and then the groups are compared with each other on the basis of the pooled standard deviation.

The Mood's median test is a nonparametric alternative to one-way analysis of variance. It tests the null hypothesis that all groups have the same median. The test

assumes that the data are independent random samples from distributions having the same shape. If there are only 2 factor levels, then a 95% two sample confidence interval for the difference between the two population medians is displayed. In this case, the chi-square value will test the significance of the results in a similar way as the *F*-ratio does in one-way ANOVA, the null hypothesis being rejected when the chi-square value is lower than the critical chi-square value for *m* (= number of groups)-1 degrees of freedom.

3.5.3. Factor analysis

Factor analysis helps to determine how sample sets respond to groups of variables simultaneously by revealing a simple underlying structure within a set of multivariate observations (Davis, 1986). Factor methods are divided into R-mode and Q-mode techniques. The R-mode refers to the relationships between variables whereas the Q-mode is concerned with the relationships between samples. Both techniques involve the extraction of eigenvalues and eigenvectors from a covariance or correlation matrix for R-mode, and from a matrix of similarities between all possible pairs of objects for Q-mode. The eigenvalues calculated from a standardised variance-covariance (or correlation) matrix ensures that all variables are weighted equally, and also allows the conversion of the eigenvectors into factors by multiplying each element in a normalised eigenvector by its own eigenvalue. The resultant factors (factor loadings) are vectors whose lengths are proportional to the variation they represent. Factor loadings for both the variables and the samples will therefore allow their positions to be plotted in relation to any two of the new factors as a simple scatter diagram. Variables that plot close to each other are generally correlated whilst samples in close proximity can be interpreted as being most similar in terms of their values of all the original variables (Walden and Smith, 1995).

After the initial factor loadings are determined they are usually rotated, in order to get absolute magnitudes which are either as small or as large as possible, so that they may be more easily interpreted. However, Temple (1978) points out that there is no reason to regard such easily interpretable positions as having any special scientific significance. He also emphasises that the simplest axes on which to plot both individuals and variables are provided by the eigenvectors of the covariance or correlation matrix.

The data used in a simultaneous R- and Q-mode factor analysis should be multivariate normally distributed, and the number of samples larger than the number of variables. However, moderate departures from these assumptions are not considered to be critical (Walden *et al.*, 1992b).

Simultaneous R- and Q-mode factor analysis for both chemical and magnetic data sets obtained in this study was performed following the procedure of Walden and Smith (1995) which involves a range of basic algebraic operations on the original raw data matrix. This method does not use factor rotation techniques, thereby avoiding Temple's (1978) criticism of the application of factor analysis in geology and making the method mathematically simple. Two main limitations are mentioned by Walden and Smith (1995), one on the use of any geochemical or mineralogical data set in establishing sediment correlation or source linkages, and the second refers to the fact that this is a mathematical rather than statistical technique. These limitations enable the method to quantify the effects of different processes on the mineralogical characteristics of the sediments during their transport (e.g. particle abrasion, chemical weathering or dilution of their magnetic properties), and also the relative proportions of each source.

The data are firstly stored in a matrix of n samples (rows) by m variables (columns) format and then standardised, in order to obtain the matrices from which eigenvalues and eigenvectors are extracted. Two short macros, labelled as RQ.MTB and STANDARD.MTB (Appendix 3), assist in the standardisation of the original data and also in all subsequent algebraic operations necessary to obtain both variable and sample factor loadings.

The program will finally display the eigenvalues which will be used to compute the percentage of the total variation in the original data set explained by the new underlying factors. Both the R-mode and the Q-mode factor loadings matrices will be stored in a continuous sequence of columns in the MINITAB worksheet and the two main variable and sample factor loadings, i.e. those with greater eigenvalues, will be plotted.

3.5.4. Discriminant function analysis

Discriminant function analysis highlights the variation between groups of data. This method does not classify the samples but it relies on prior knowledge of the different sample groups existing. It consists of finding a transform which gives the minimum ratio of the difference between the group multivariate means to the multivariate variance within the groups (Figure 3.6a). Such a transform involves sums of squares and product matrices (Davis, 1986).

Linear functions result from the analysis along which the groups have the greatest separation at the same time as the least inflation. These discriminant functions or eigenvectors represent directions in space which successively separate

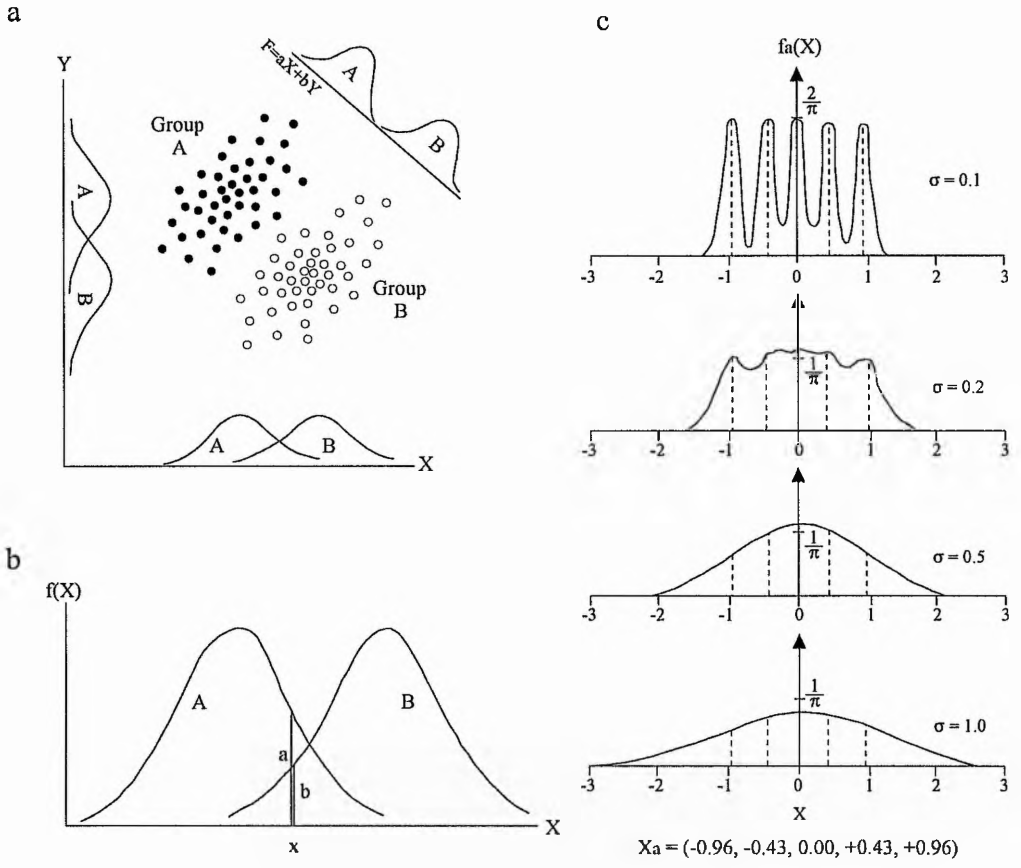

Figure 3.6. Discriminant function analysis (Le Maitre, 1982). a) The geometric interpretation of discriminant analysis using two groups A and B. The single discriminant function defines the normal to the plane that best separates the two groups, reducing the dimensionality by replacing the two original variables, X and Y. b) Classification of an unknown sample, x, to one of two groups, A and B, using discriminant functions. The sample is considered to belong to that group for which the value of the function ((a) for group A and (b) for group B) is the greater. c) The smoothing parameter, σ, in the empirical discriminant function can affect the shape of the function (after Pearce, 1976).

the groups from each other by decreasing amounts (Le Maitre, 1982), their location depending on the dispersion matrices of the groups. The groups must have equal dispersion matrices, in other words, the same probability contour shape and orientation, in order to avoid that the surface which best separates the groups becomes curved. As in factor analysis, each eigenvector is associated with an eigenvalue. However, in discriminant analysis, although the eigenvectors are uncorrelated with each other, they are only perpendicular when the variables are also uncorrelated. Each linear discriminant function transforms an original set of measurements on a sample into a single discriminant score which represents the

sample's position along a line defined by the linear discriminant function. It is then possible to produce a plot, showing the distribution of the groups in the discriminant space, by projecting the original data onto the successive discriminant functions. This also allows the allocation of new samples of unknown origin to one of the groups.

The main limitation of this statistical method is that it forces samples into defined groups and so it can lead one to think that the sources are better discriminated and have less variation than exists in reality.

Because it is a statistical method, tests of significance can be applied to the discriminant analysis results. On the one hand, the differences between the group means will indicate how easily the groups can be separated. The group means being very close together will make it difficult to separate the groups, especially if such groups have very large variances. However, those groups having well separated means and low dispersion around the mean will be easily discriminated. On the other hand, the significance of the resulting discriminant functions can also be tested. Both approaches will become equivalent when only one discriminant function results from the analysis.

A multivariate extension of the analysis of variance (ANOVA) based on Wilks' Lambda is traditionally used to estimate the separation of the group means. The procedure is similar to that for the one-variable case, except that the components of variation are presented as matrices. Wilks' Lambda is related to the F-ratio in a simple way, as described by Le Maitre (1982), and the critical value of F will determine the significance of the difference between the group means. Furthermore, a chi-square test will determine the significance or amount of discrimination contained in the discriminant functions.

Once the different groups have been discriminated, a second objective of the discriminant analysis is to classify unknown samples into one of the pre-defined groups. Bayes's Decision Rule is the most usual method used, being based on calculating the value of the probability density function for each group. Two different numerical methods are described by Pearce (1976). Firstly, unknown samples can be classified using normal distribution functions by assigning them to that group with the largest value of the probability of density (Figure 3.6b). Secondly, empirical discriminant functions are used for non-normally distributed data. These functions are determined by using only a part of the available data while the remaining data are used to optimise the shape of the functions in order to minimise the number of misclassifications (Figure 3.6c). The success rate of each

method can then be evaluated by classifying samples of known groups and counting the correct classifications.

Discriminant analysis was performed for both chemical and magnetic data of rocks using the SPSS statistical package. The number of samples must be larger than the number of variables, and the latter should not be strongly correlated. The number of discriminant functions obtained is the smaller of the number of groups menus 1 and the number of variables (Le Maitre, 1982). A set of eigenvectors, which correspond to the coefficients of the original variables in the discriminant functions, is received as output. Eigenvalues, percentage of variance and significance of each discriminant function, as well as the summary of misclassified observations, are also displayed.

3.6. Linear programming model

Linear programming has been used to determine the source component proportions of the sediments. The basic mathematical formulation of the unmixing model used here follows Thompson (1986). He applies, successfully, a standard linear algebraic method called SIMPLEX to mixtures of source materials and mixtures of magnetic crystals on the basis of magnetic parameters, as mentioned in Chapter 2.

Any numerical linear unmixing model requires that the parameters considered in the modelling are linearly additive. This means that knowing the values of one or more specific parameters for each different source material involved, and also the proportions in which such sources are mixed, then the value of the considered parameters for the mixture will be equal to the sum of the proportions of the values of such parameters corresponding to each source material. Therefore, if b_j (j = 1, 2, ..., n) are n independent magnetic measurements of a mixture (or sediment sample) composed of m distinct sources, and a_{ij} (i = 1, 2, ..., m) are the corresponding variables measured on the i-th source material, in a linear model the value of the measurement of the mixture is a linear combination of the values for the individual sources:

$$b_j = \sum_{i=1}^{m} x_i a_{ij} \qquad \text{(Equation 3.1)}$$

Given the values of b_j and a_{ij}, this relationship provides a system of n simultaneous linear equations for the unknown proportions x_i. When the number of

variables (n) is greater than the number of potential sources (m), then a least squares solution to the n equations can be found; i.e. the calculated unknown proportions of the source materials (x_i) will be those which distribute the residuals to each equation according to Gauss's law of error and minimise the length of the residual vector ($r = (b_j - \sum x_i a_{ij})$) (Thompson, 1986).

The model essentially carries out an iterative search to discover the optimum combination of the source materials which minimises the difference between the values of the variables measured on the mixtures and the values obtained mathematically from mixing of the sources. The values of x_i are not all independent and, therefore, in order to perform the model, source proportions must be positive ($x_i \geq 0$) and their sum must be unity ($\sum x_i = 1$). This means that a constrained optimisation approach needs to be applied. On the other hand, difficulties may occur when the variables used in the model vary by orders of magnitude, as those variables with large values may dominate the model. Weighting certain variables can overcome this problem.

Thompson's (1986) SIMPLEX method is based on the method of Nedler and Mead (1965). SIMPLEX presents several advantages such as: divergence being impossible, no knowledge of the first derivatives of the response surface being required, contour conditions and equations of conditions being easily added as necessary, and the criterion to judge the quality of fit of the model and data being easily adjusted. The only additional information necessary to use this method is an initial guess of each model parameter (n values), the maximum error allowed (typically 10^{-5}) and the maximum number of iterations (very roughly around $20\ n^2$).

Two approaches are considered to estimate the errors associated with the fitting calculations. One consists of investigating the range of variation of the model parameters. The goodness of fit is quantified by a chi-squared test, and the range of permitted variation found out by a grid search, contour tracing algorithm, or random Monte Carlo search strategy. A second approach (sensitivity analysis) consists of processing simulated data sets which are obtained by adding pseudo-random errors drawn from a normal distribution with 0 mean and the same variance as the residuals from the best fitting model. The calculated variation in model parameters then provides an estimation of the errors associated to the fitting of the original data. The objective function to be minimised is the sum of the relative errors:

$$f(x_i) = E_j/b_j \text{ where } E_j = | b_j - \sum x_i a_{ij} | \qquad \text{(Equation 3.2)}$$

The model was run in a Microsoft Excel spreadsheet using the Solver 'add in' component. The analytical data resulting from measuring diverse parameters on both all potential source materials and sediment samples to be 'unmixed' are included together with the initial starting proportions of each source from which the optimisation routine will move to find the best solution.

Although the minimum difference between the modelled and the original values of the variables measured on the mixtures is estimated by minimising

$$\sum_{j=1}^{n} \left(\sum_{i=1}^{m} a_{ij} x_i - b_j \right)^2 = \sum_{j=1}^{n} (s_j - b_j)^2 \qquad \text{(Equation 3.3)}$$

where $s_j = \sum_{i=1}^{m} a_{ij} x_i$, is the modelled value of the j variable in the simulated version of the natural sample, the equation

$$\sum_{j=1}^{n} \{((b_j - s_j) / s_j) * 100\}^2 \qquad \text{(Equation 3.4)}$$

is preferred. The reason for this is that, as mentioned above, differences in the absolute scales by which variables are measured may lead to some variables exerting greater control on the model than others. The latter equation weights the variables by expressing the differences between modelled and measured values as a percentage of the modelled value.

4. Results

The data obtained from both chemical and magnetic measurements, as described in the previous Chapter 3, are presented in this chapter for rocks, glacial till and stream sediments. The interpretations and the interrelationships of the chemical and magnetic results from each group of materials are principally established using both bivariate scattergrams and simultaneous R- and Q-mode factor analysis (see Chapter 3 for details). The use of graphical and statistical analysis leads to a precise mineral characterisation of the three groups of materials under study, and it also highlights the presence of any subgroup; in other words, the interpretation of the results will reflect different sediment source materials on the basis of their mineralogy. Detailed tables showing all analytical results are included in Appendix 4.

4.1. Chemical and mineralogical characterisation of the rocks

The whole-rock chemistry of the igneous rocks and the magnetic properties of both igneous and sedimentary rocks were analysed in order to obtain an accurate classification and mineral characterisation of all the source rocks present in the River Eden catchment. Electron probe microanalyses were performed only for thin sections of the igneous rocks as initial X-ray diffractometry analyses indicated the presence of important concentrations of Fe-Ti oxides, whilst such minerals were present in insignificant amounts in the sedimentary rocks (Chapter 3).

4.1.1. Whole-rock chemical composition of the igneous rocks

The igneous rocks present in the study area, which include dolerites, andesites and some other minor intrusions (see Chapter 2), were classified, initially, on the basis of their major oxides content using a K_2O versus SiO_2 diagram (Figure 4.1). This diagram illustrates the chemical homogeneity of the dolerites, in contrast with the range of variation in both K_2O and SiO_2 contents shown by the andesites, which are classified in order of increasing acidity (SiO_2 content) as: basaltic andesites, andesites, dacite-rhyolites. A chemical classification of these igneous rocks is preferred over the mineralogical classification typically used in geological maps (see Chapter 2) as many of these rocks are fine grained and somewhat altered.

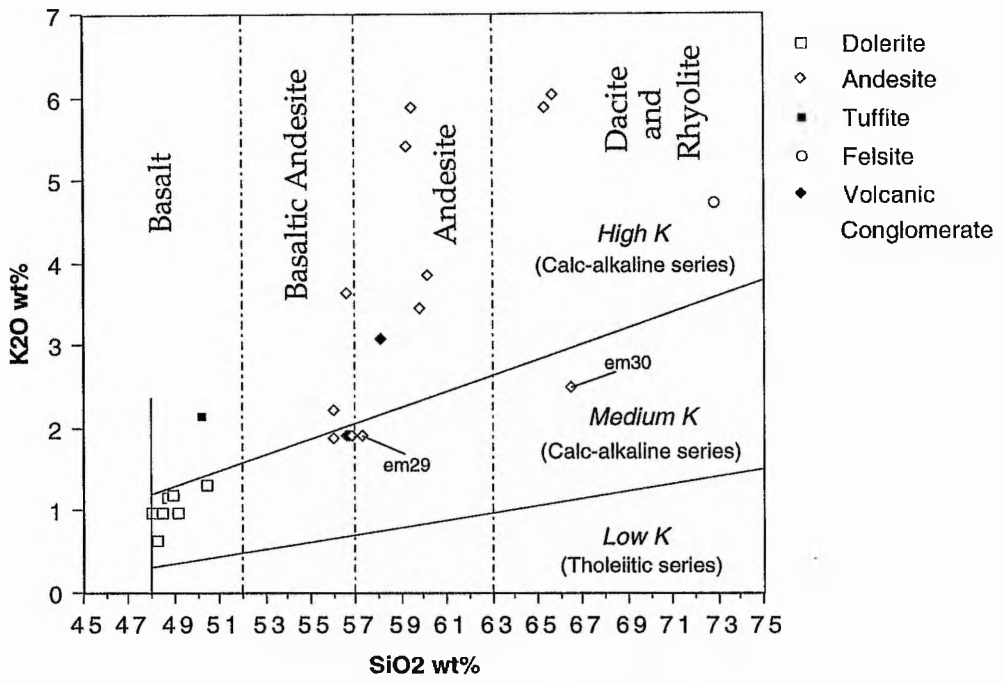

Figure 4.1. Chemical classification of the igneous rocks present in the Eden catchment using a K_2O versus SiO_2 diagram (Peccerillo and Taylor, 1976). The subdivisions of Le Maitre *et al.* (1989) in italics, and of Rickwood (1989) in brackets are also shown.

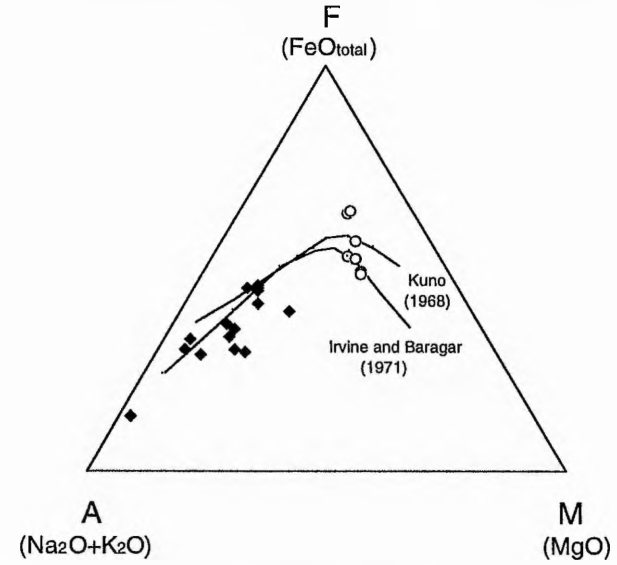

Figure 4.2. An AFM diagram for dolerites (circles) and andesites (diamonds) showing the boundary between the calc-alkaline field and the tholeiitic field, after Kuno (1968) and Irvine and Baragar (1971) (from Rollinson, 1993).

Even when it is not relevant to the present study, the whole-rock chemistry also gives valuable information about petrogenesis and the tectonic setting in which these igneous rocks were formed. Figure 4.1 shows how the andesites have a calc-alkaline affinity with relatively high K contents. This concurs with the findings of other geochemical studies of similar rocks in this region (e.g. Gandy, 1975; Thirlwall, 1981 and 1983). In an AFM diagram (Figure 4.2) they plot at the boundary between the calc-alkaline and the tholeiitic series. A comparison with the analyses of Macdonald *et al.* (1981), who also studied similar dolerites from all over Scotland, shows agreement with the present results.

Statistical analysis of the whole-rock chemistry leads to the identification of those elements measured in the rock samples which most efficiently discriminate them into groups. Firstly, correlation coefficients are calculated to determine any linear relationship between all major and trace elements. Data are not normally distributed and so Spearman's rank correlation coefficients are calculated in order to avoid correlations induced by any operation or transformation performed on the variables (Chapter 3). Subsequently, Mood's median test is performed which highlights those elements which best separate the rock groups distinguished from Figure 4.1. The results of all these statistical analyses are given in Appendix 5, and they assist in the chemical classification of the rock samples using a minimum number of variables. It is found that major elements are the most effective in distinguishing the rock groups, with SiO_2, Al_2O_3 and Na_2O having the greatest chi-square values and the lowest p-values (Table 4.1) and so being the best discriminant variables. Within the trace elements, Ce, Sc and V are also found to be highly discriminant.

A simultaneous R- and Q-mode factor analysis, performed for all major and trace elements analysed in the rocks (Figure 4.3), stresses the chemical difference between basalts, basaltic andesites, andesites and dacite-rhyolites. As was mentioned in Chapter 3, this multivariate statistical analysis allows one to judge more clearly the relationship within and between the variables and the samples. Those variables that plot close to each other are generally positively correlated whilst variables plotting opposite with respect to the origin will be negatively correlated. On the other hand, samples in close proximity are interpreted as being most similar in terms of their values for all the original variables, such values being greater the closer the samples to the variables. The position of the original variables with respect to the two factors plotted in Figure 4.3, which explain most of the variability of all the 28 variables considered (67.13%), shows that Factor 1 is dominated by those major elements (mainly Si, Ca, Fe, Ti, Mg) whose concentration is a direct function of the

differentiation processes of the magma. The negative correlation between Si and Fe, Ti and Mg, indicating an increase in the Si content towards more differentiated rocks while there is a decrease in mafic minerals reflected in Fe, Ti and Mg (Figure 4.3). Therefore, Factor 1 differentiates rock samples on the basis of their acidity. On the other hand, Factor 2 seems to be dominated by trace elements and also some major elements (e.g. Na, Sr) which are compatible with plagioclase. This factor controls the chemical variability within the rock groups and could be indicating differences in the plagioclase content of the rock samples under study.

Table 4.1. Major and trace elements analysed in whole-rock samples found by Mood's median test to contribute most to the discrimination of the four igneous rock groups distinguished in the River Eden catchment on the basis of their chemical composition: basalts, basaltic andesites, andesites, and dacite-rhyolites. Critical value of chi-square with 3 degrees of freedom is 11.30 at the 99% confidence level.

Variable	Degrees of freedom	Chi-square	p-value
SiO_2	3	17.14	0.001
Al_2O_3	3	17.57	0.001
MnO	3	15.02	0.002
MgO	3	13.49	0.004
CaO	3	13.94	0.003
Na_2O	3	17.80	0.001
Zr	3	14.29	0.003
Rb	3	13.87	0.003
Th	3	13.94	0.003
Ni	3	14.14	0.003
Cr	3	14.14	0.003
Ce	3	17.57	0.001
Sc	3	17.14	0.001
V	3	17.14	0.001

Figures 4.1 and 4.3 show similar groupings of the rock samples, on the basis of their chemical compositions. However, sample em29, which has been classified as an andesite with medium K content in Figure 4.1, is chemically similar to the basaltic andesites. On the other hand, sample em30 classified as a dacite with medium K content appears in Figure 4.3 close to the field of the andesites with high K content. This shows how a multivariate analysis of the data leads to slightly different classification of samples than conventional diagrams.

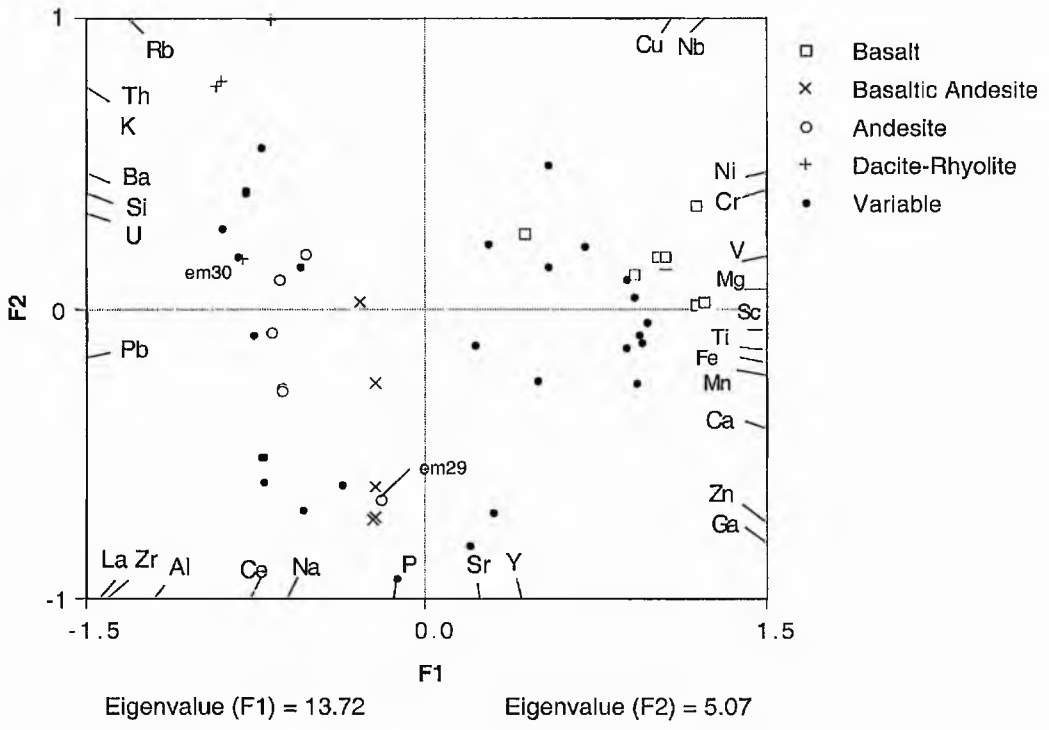

Figure 4.3. A simultaneous R- and Q-mode factor analysis of both major and trace elements constituting the principal igneous rocks present in the Eden catchment. Factor 1 (F1) and Factor 2 (F2) combined explain 67.13% of the variability in the 28 original variables.

4.1.2. Fe-Ti oxides in the igneous rocks

Data from electron probe microanalysis of magnetite and ilmenite grains from igneous rock samples were first plotted as a FeO-Fe_2O_3-TiO_2 ternary diagram (Figure 4.4) in order to determine the compositional range of the Fe-Ti oxides under study. In all rock samples magnetite is enriched in Ti (titanomagnetite), each sample showing variations in the proportions of the ulvospinel (Fe_2TiO_4) and magnetite (Fe_2O_3) phases which span from approximately 12% to 50% of the whole range. Despite this variability it is seen that in each rock sample magnetite appears clearly enriched in either the ulvospinel phase (> 50% ulvospinel) or in the magnetite phase (> 50% magnetite) with the exception of the volcanic conglomerate samples (em31, em33 and em35) (Table 4.2), since they are composed of fragments of different rocks. Thus a difference in the chemistry of the magnetite is found between the various rock samples.

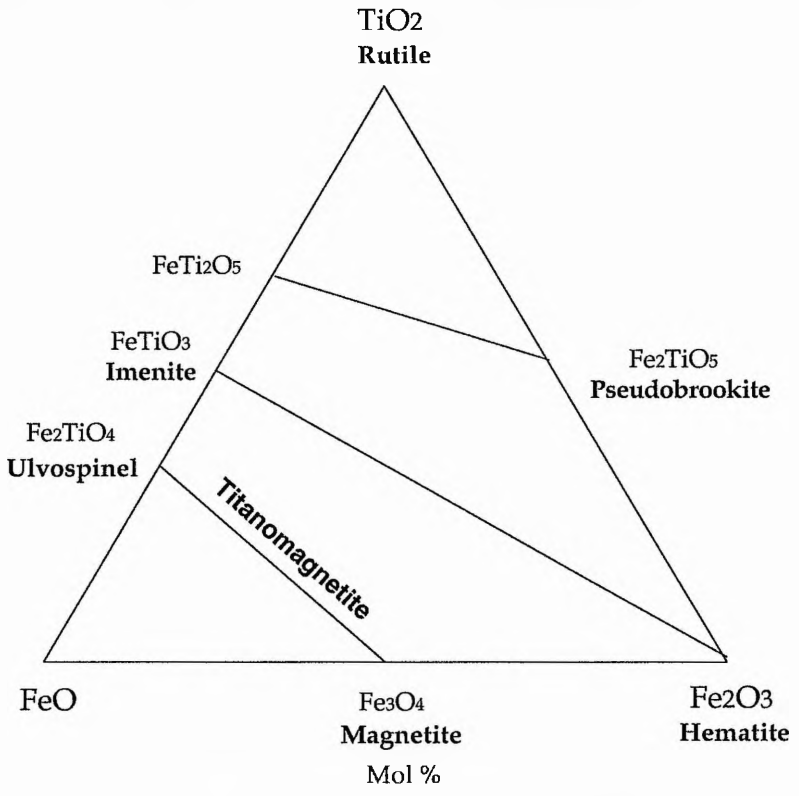

Figure 4.4. The system FeO-Fe_2O_3-TiO_2 showing the major high temperature solid solution series magnetite-ulvospinel, hematite-ilmenite, and pseudobrookite-$FeTi_2O_5$ plotted on a mol per cent basis.

In order to compare all different rocks, a simultaneous R- and Q-mode factor analysis of magnetite composition was made using the mean values of the eight principal elements (Table 4.3) measured in all magnetite grains in each rock sample. The two factors which most explain the variability of the titanomagnetite composition between and within the rock samples (66.16%) are plotted in Figure 4.5. Factor 1 is dominated by the three main elements (Ti, Fe^{2+} and Fe^{3+}) constituting the titanomagnetite chemistry, and therefore this factor will indicate differences in the relative proportions of ulvospinel and magnetite in the titanomagnetite grains. Factor 2 is dominated by the minor elements analysed in the titanomagnetite, showing a positive correlation between Ca and Si which are negatively correlated with Mn, Mg and Al. Samples appear widely spread by both factors and, even when most basalt samples are seen to have magnetite enriched in the ulvospinel phase, there is not a clear differentiation of the rock groups, previously distinguished on the basis of their whole-rock chemistry, with respect to their titanomagnetite chemistry. A discrimination of the source rocks on the basis of their Fe-Ti mineralogy is, therefore, difficult as the variability between rock groups is found to be small.

Table 4.2. Compositional range of magnetite and ilmenite in terms of mol per cent of ulvospinel (Fe_2TiO_4) and ilmenite ($FeTiO_3$) phases respectively. (1): Basalt, (2): Basaltic andesite, (3): Andesite, (4): Dacite-rhyolite.

Sample	Range in mol % Ulvospinel	Range in mol % Ilmenite
em8 (1)	35.54 - 77.19	94.08 - 100.00
em11 (1)	-	90.17 - 100.00
em17 (1)	0.13 - 42.87	-
em21 (1)	69.87 - 82.64	92.78 - 99.29
em22 (1)	47.06 - 100.00	87.38 - 100.00
em38 (1)	43.11 - 62.18	94.11 - 95.99
em39 (1)	25.48 - 57.20	88.70 - 90.30
em43 (1)	61.15 - 77.69	-
em36 (1)	4.28 - 24.72	-
em1 (2)	3.52 - 52.59	92.04 - 100.00
em13 (2)	51.49 - 91.64	96.49 - 100.00
em14 (2)	4.40 - 63.24	66.97 - 100.00
em15 (2)	28.37 - 49.77	91.48 - 95.06
em16 (2)	5.95 - 84.32	63.66 - 100.00
em29 (2)	40.02 - 78.97	60.33 - 96.48
em34 (2)	4.87 - 55.30	67.08 - 100.00
em2 (3)	8.45 - 45.92	81.71 - 90.90
em3 (3)	3.88 - 26.60	-
em4 (3)	6.38 - 8.92	-
em5 (3)	1.07 - 65.47	100.00
em31 (3)	6.88 - 63.65	79.48 - 100.00
em33 (3)	14.63 - 57.69	72.01
em35 (3)	5.37 - 100	-
em18 (4)	11.53 - 93.69	69.30 - 100.00
em19 (4)	1.48 - 70.49	92.90 - 100.00
em20 (4)	8.67 - 13.04	-
em30 (4)	1.92 - 51.59	97.38 - 100.00

On the other hand, ilmenite grains show a homogeneous chemistry in terms of the weight percentage TiO_2, FeO and Fe_2O_3 both within and between samples. Most of the analysed grains are composed of pure ilmenite ($FeTiO_3$) and only few have some Fe_2O_3 (< 30%) indicating some solid solution to hematite (Table 4.2).

Backscattered electron images help the recognition of the textural relationships between magnetite and ilmenite. Three main types of grains are observed: homogeneous, composite and trellis (as described by Grigsby, 1990; and Haggerty, 1991) (Plate 4.1). A textural count and also an estimation of the mean grain size of magnetite was made in few representative samples (Table 4.4).

Table 4.3. Mean values of eight principal elements (as weight per cent oxides) analysed in magnetite grains of the igneous rocks sampled in the Eden catchment. And the relative proportion of magnetite and ulvospinel phases calculated from these mean titanomagnetite compositions for each rock sample. (1): Basalt, (2): Basaltic andesite, (3): Andesite, (4): Dacite-rhyolite. Note that Na_2O and K_2O percentages have not been included as they are trace.

Sample	SiO_2	TiO_2	Al_2O_3	Fe_2O_3	FeO	MnO	MgO	CaO	mol % Magnetite	mol % Ulvospinel
em8 (1)	0.40	17.7	1.40	28.74	46.52	0.47	0.04	0.08	44.85	55.15
em17 (1)	1.67	0.97	0.60	55.21	34.13	0.21	0.44	0.25	96.60	3.40
em21 (1)	0.42	25.54	0.34	15.32	52.08	1.59	0.13	0.10	23.10	76.90
em22 (1)	0.36	22.61	0.62	19.23	46.99	1.34	0.21	0.05	29.88	70.12
em38 (1)	1.00	15.90	0.76	29.56	44.12	0.64	0.03	0.47	48.23	51.77
em39 (1)	2.14	13.54	0.83	32.70	41.75	0.70	0.06	0.53	54.74	45.26
em43 (1)	0.41	21.84	1.96	21.23	47.64	1.04	1.22	0.21	32.75	67.25
em36 (1)	0.29	4.53	0.26	54.10	31.83	0.09	0.46	0.37	85.67	14.33
em1 (2)	0.34	9.85	0.74	46.82	38.43	0.47	0.42	0.05	70.42	29.58
em13 (2)	0.58	25.28	0.51	15.90	52.76	1.38	0.31	0.09	23.96	76.04
em14 (2)	0.31	11.98	0.80	41.27	39.91	0.59	0.40	0.06	63.31	36.69
em15 (2)	0.30	11.69	1.05	40.64	39.52	0.81	0.18	0.10	63.51	36.49
em16 (2)	0.33	18.89	0.63	25.60	45.22	0.50	0.85	0.08	40.43	59.57
em29 (2)	0.38	17.13	0.94	29.54	43.49	2.27	0.10	0.08	46.34	53.66
em34 (2)	0.36	8.82	1.84	44.20	33.11	0.22	2.64	0.04	71.52	28.48
em2 (3)	0.77	8.26	1.29	47.48	38.13	0.38	0.30	0.07	74.22	25.78
em3 (3)	1.51	3.03	0.66	56.21	34.26	0.37	0.27	0.16	90.28	9.72
em4 (3)	1.21	2.37	1.78	57.20	32.74	0.43	0.43	0.10	92.36	7.64
em5 (3)	0.98	2.36	1.33	51.95	33.80	0.37	0.36	0.25	91.68	8.32
em31 (3)	0.47	10.12	2.09	39.73	35.53	0.77	0.99	0.08	66.29	33.71
em33 (3)	0.59	11.93	1.29	36.28	37.97	1.52	0.48	0.04	60.37	39.63
em35 (3)	1.34	11.71	1.79	34.33	39.21	0.34	1.16	0.06	59.49	40.51
em18 (4)	0.42	9.02	0.59	39.45	36.76	0.48	0.14	0.09	68.66	31.34
em19 (4)	0.68	8.08	0.70	45.65	36.38	0.24	0.15	0.08	73.89	26.11
em20 (4)	0.34	3.51	1.57	54.64	24.38	6.32	1.20	0.02	88.62	11.38
em30 (4)	1.06	6.78	0.66	46.55	34.73	0.52	0.11	0.20	77.48	22.52

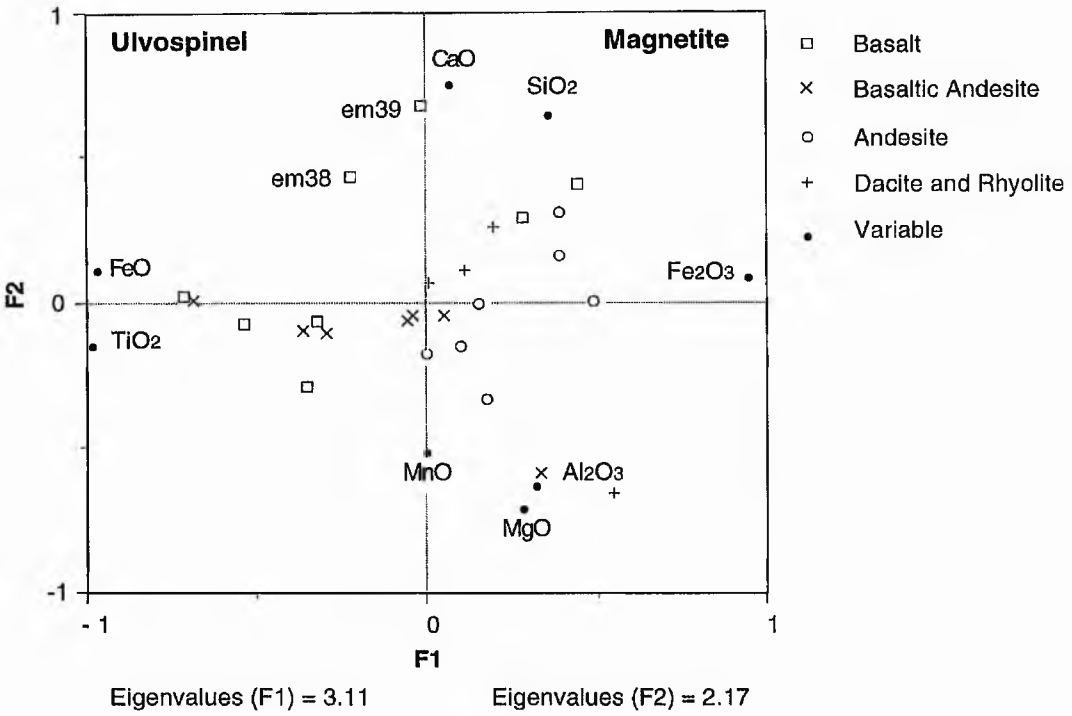

Figure 4.5. A simultaneous R- and Q-mode factor analysis of the mean composition of all grains of titanomagnetite analysed in each igneous rock sampled in the Eden catchment. Factor 1 (F1) and Factor 2 (F2) explain 66.16% of the 8 original variables.

Table 4.4. Number of magnetite grains counted for each of the three main textures recognised in some representative rock samples and their mean grain size in μm. (1): Basalt, (2): Basaltic andesite, (3): Andesite.

Sample	Homogeneous	Trellis Ilmenite-Magnetite	Composite Ilmenite-Magnetite	Magnetite grain size (μm)
em8 (1)	93	0	0	75.46
em21 (1)	72	20	9	60.84
em43 (1)	250	0	0	6.71
em1 (2)	15	117	7	27.47
em15 (2)	54	0	39	22.54
em16 (2)	123	3	1	21.03
em3 (3)	66	6	25	29.03

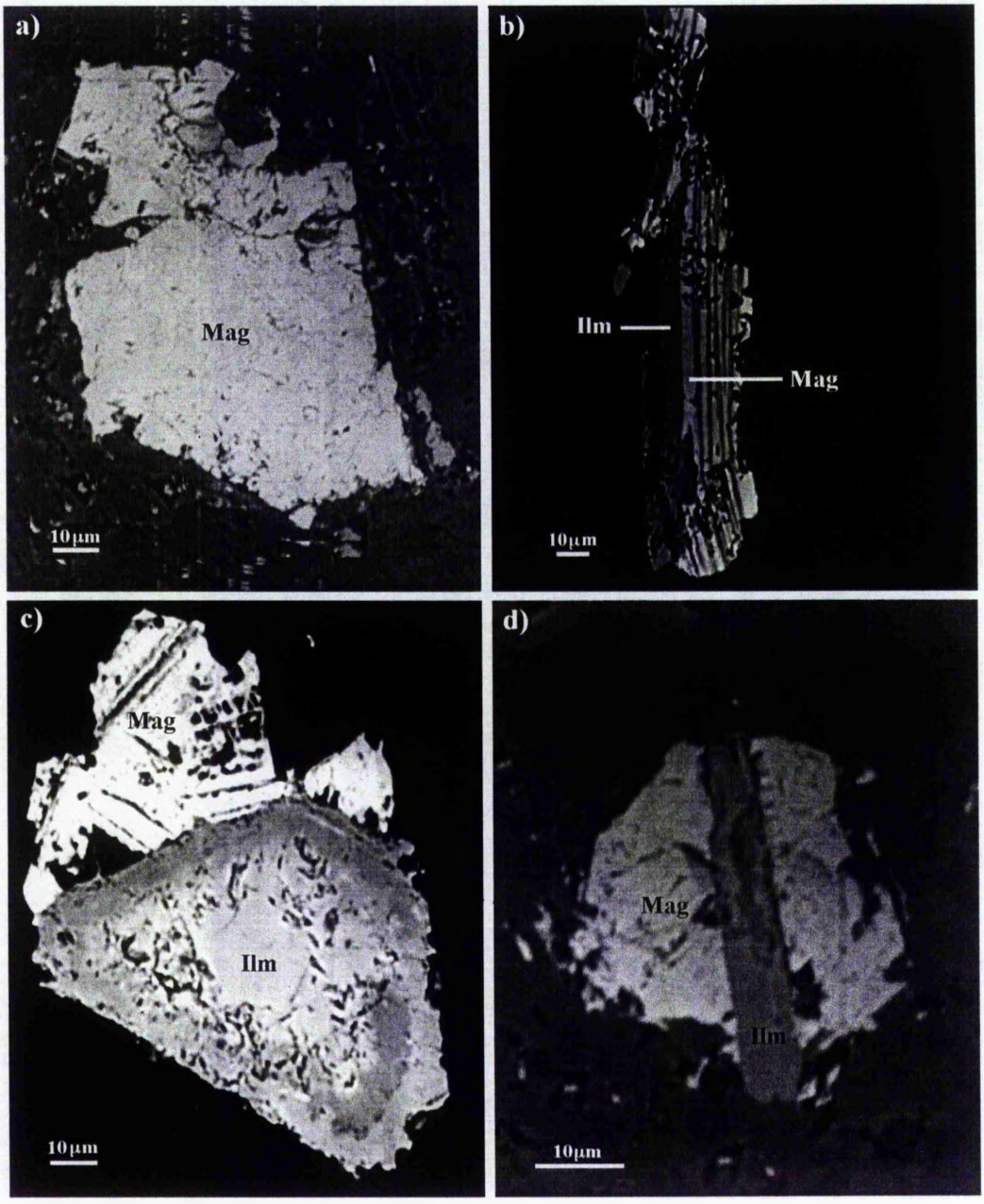

Plate 4.1. Main types of Fe-Ti oxide grains differentiated in the igneous rocks of the River Eden catchment on the basis of their textural relationship. a) Homogeneous magnetite grain, b) magnetite with trellis-type magnetite-ilmenite intergrowths, c) composite-type magnetite-ilmenite intergrowths, magnetite grain showing at the same time trellis-type magnetite-ilmenite intergrowths, d) composite-type magnetite-ilmenite intergrowths. Mag: magnetite, Ilm: ilmenite.

Analysis of weathered rock samples

In Chapter 2 the weathering of rocks in the catchment was described and some specific samples were taken for this study, representing the transition between source rock and sediment. Typical chemical weathering in basaltic rocks has spheroidal or onion-skin texture. Several attempts to prepare samples of the weathered rim (em25), known to be weathered under aerial conditions, for electron probe microanalysis were unsuccessful. The analysis of a similar section from the dolerite sample (em38) obtained from Holl Reservoir (NO 3225 7037) is known to be weathered under subaerial conditions (Chapter 3). An analysis of the magnetite grains found in a transverse section of Sample em38 shows various stages of chemical weathering. Magnetite is TiO_2- and FeO-poor in the external rim (i.e. more advanced chemical weathering stage) relative to the internal core area. The total sum of the nine oxides (SiO_2, TiO_2, Al_2O_3, FeO_{total}, MnO, MgO, CaO, Na_2O and K_2O) analysed in the magnetite grains also reveals an increase in values towards the central, relatively unweathered, core. This decrease in TiO_2, FeO and the total sum of weight percentage oxides in the magnetite grains is shown in Figure 4.6, where the data are compared with the mean chemical composition of the magnetite present in the fresh dolerite (Sample em38) as seen in Table 4.3.

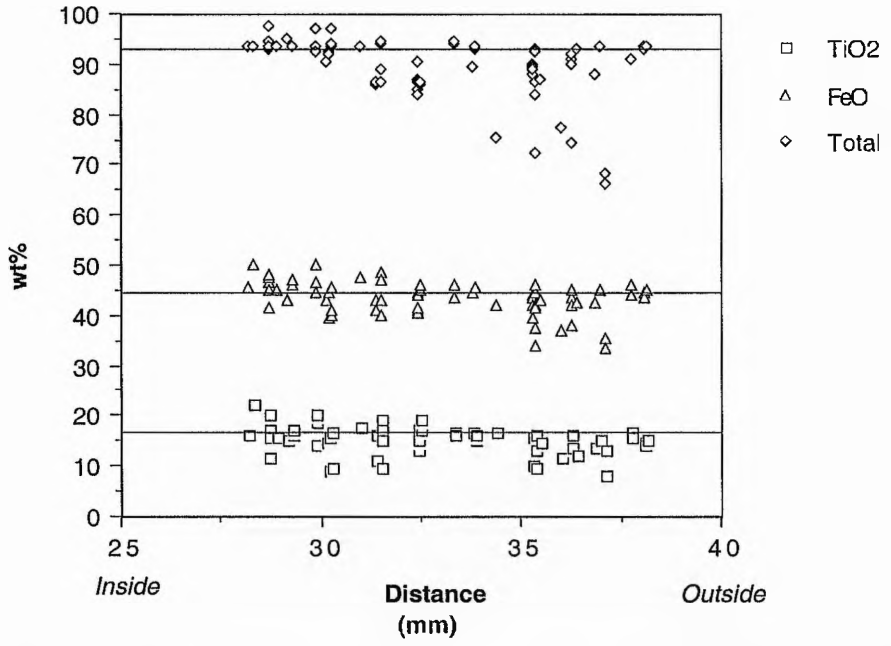

Figure 4.6. TiO_2, FeO and total sum of oxides, quoted as weight per cent, analysed in magnetite grains across a section of the em38 dolerite sample representing various stages of chemical weathering. The mean TiO_2, FeO and total sum of oxides values corresponding to all the magnetite grains analysed in the fresh dolerite sample (em38) are shown by a line.

Backscattered electron images revealed darker patches within the magnetite grains and especially on the edges and along internal grain fractures. These darker areas are enriched in SiO_2 (1.68-7.05%) and CaO (1.72-5%) with respect to the lighter areas (0.07-1.04% SiO_2 and 0.01-1.2% CaO). The same is observed when analysing the magnetite grains from the submerged dolerite sample (em39). In Figure 4.5 such enrichment in the SiO_2 and CaO content of magnetite in both dolerite samples (em38 and em39) is clearly seen.

4.1.3. Magnetic properties of the igneous and sedimentary rocks

As explained in Chapter 3, the magnetic properties of a material depend on three main factors: (1) mineralogy, (2) concentration and (3) grain size of the magnetic minerals (canted anti-ferromagnetic and ferrimagnetic minerals) present in the sample.

The χ_{lf}, χ_{ARM} and SIRM parameters (see Chapter 3) suggest important concentrations of magnetic minerals in all the Eden catchment igneous rocks (Figure 4.7), such concentrations generally decreasing from the basic to more acid rocks. However, in the sedimentary rocks such minerals are scarce, as in the case of sandstones which have low values for all these magnetic parameters, or they are even absent, as in the case of limestones which have weak negative susceptibility values (χ_{lf} = -0.2 m^3/kg) indicating that they are dominated by diamagnetic minerals (Dearing, 1994). These results agree with the X-ray diffraction data described in Chapter 3.

The normalised IRM acquisition curves (Figure 4.8a-d) show that basalt samples (except em36) are constituted mainly by magnetite, whilst dacite-rhyolite samples (except em30, which is not only chemically but also magnetically similar to the andesite samples) are made of hematite, with basaltic andesites and andesites containing different mixtures of magnetite and hematite. The tuffite sample (em36), classified as basalt (see section 4.1), is, however, mainly made of hematite, this difference in magnetic mineralogy (compared with the rest of basalt samples) being reflected in all magnetic properties. Sandstones show mixtures of magnetite and hematite (Figure 4.8e) with higher hematite contents than basaltic andesites and andesites. The $HIRM_{300}$ parameter (Figure 4.7) also suggests an increase in hematite concentration from basic to acid rocks.

The ratio of SIRM/χ_{lf} to $(Bo)_{CR}$ was found by Bradshaw and Thompson (1985) to 'give a good first guide to the mixing, petrology and granulometry of

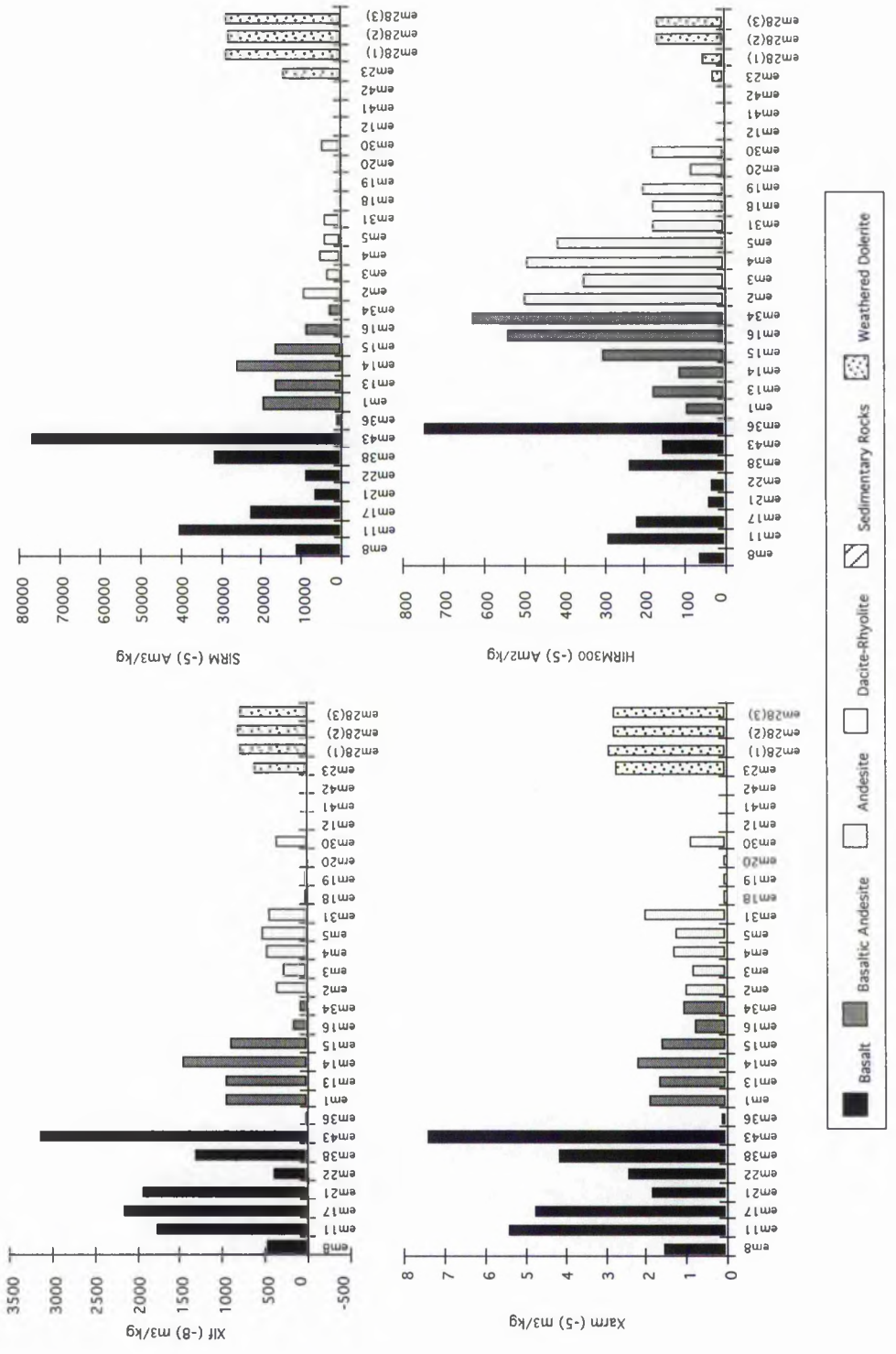

Figure 4.7. Main concentration-dependent magnetic parameters for all the Eden catchment rocks. χ_{lf}: Magnetic susceptibility, χ_{ARM}: Susceptibility of anhysteretic remanent magnetisation, SIRM: Saturation isothermal remanent magnetisation, $HIRM_{300}$: 'Hard' isothermal remanent magnetisation.

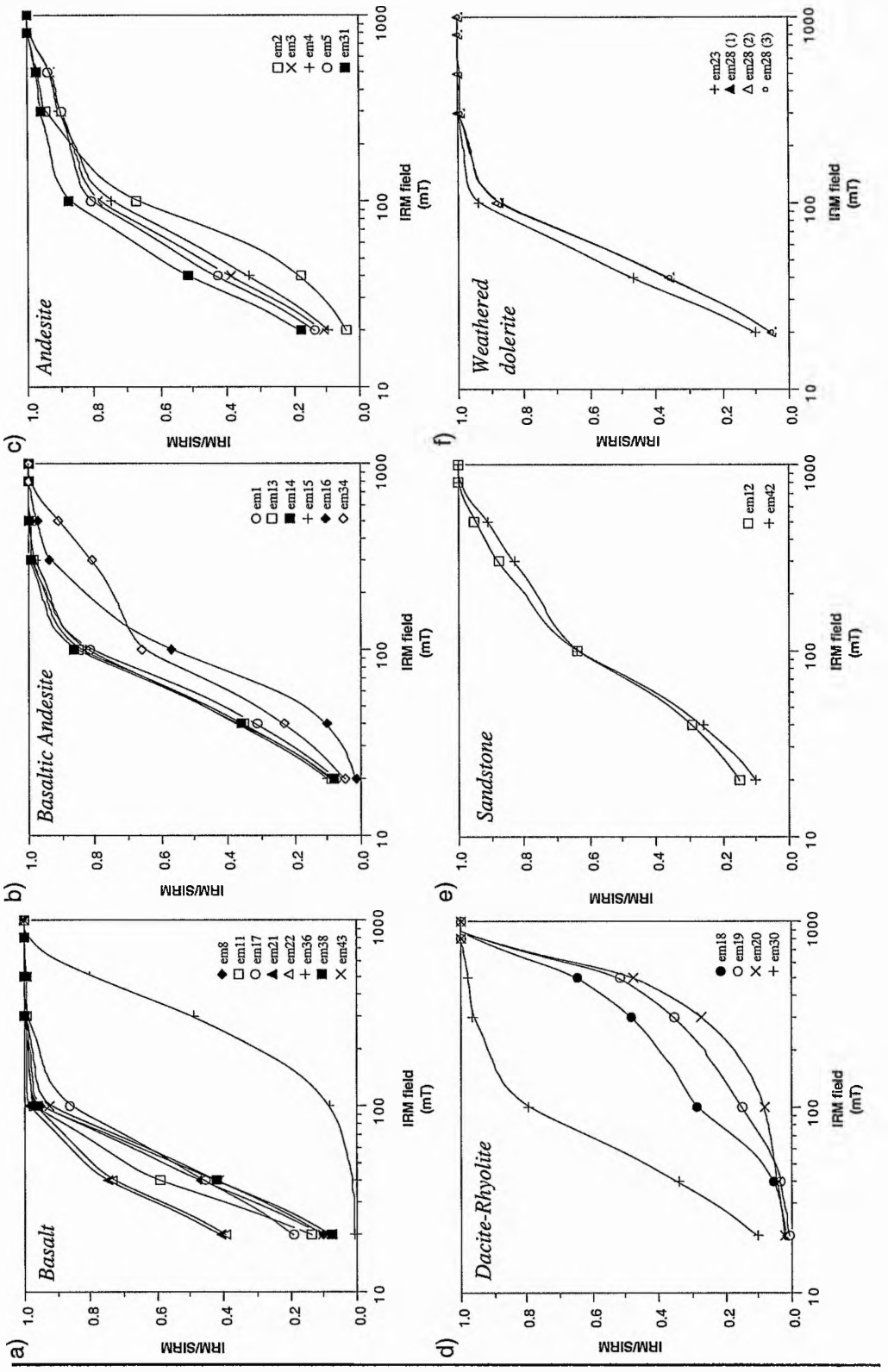

Figure 4.8. Normalised isothermal remanent magnetisation (IRM) acquisition curves for a) basalt, b) basaltic andesite, c) andesite, d) dacite-rhyolite, e) sandstone and f) weathered dolerite with onion-skin texture. Magnetite and hematite fields, after Thompson (1986), are shown in Figure 3.5.

natural magnetic minerals'. Figure 4.9 shows basalts tending to have a larger proportion of multidomain magnetite compared to basaltic andesites and andesites, which mainly have pseudo-single domain magnetite. The dacite-rhyolite samples are dominated by single domain hematite, and sedimentary rocks by single domain magnetite. No significant concentration of superparamagnetic (SP) magnetite grains is present in any of the rocks. These results are confirmed by frequency-dependent susceptibility ($\chi_{fd\%}$) values which are less than 10% for all the rock samples suggesting that they are dominated by multidomain and/or stable single domain grains (Dearing, 1994). Superparamagnetic magnetite is secondary being formed as a result of burning, pedogenesis or bacterial activities (Dearing, 1994), indicating that most magnetite grains present in the studied rocks are primary. However, it should be noted that the sedimentary rocks have higher $\chi_{fd\%}$ values (5-8%) compared with the igneous rocks (<2%), indicating a higher concentration of SP magnetite which could be the result of diagenetic processes, or even be inherited from a source material.

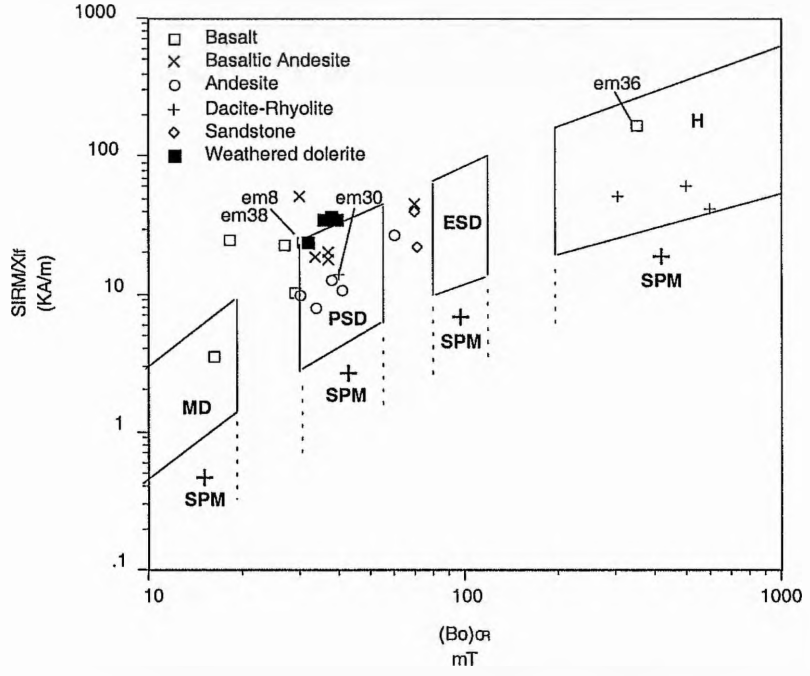

Figure 4.9. Ratio SIRM/χ_{lf} versus coercivity of remanence $(Bo)_{CR}$ diagram with grid schematically dividing magnetic mineralogies and magnetisation states. MD: Multidomain, PSD: Pseudo-single domain, and ESD: Elongated single domain magnetite, H: Single domain hematite, SPM: Superparamagnetic magnetite (after Thompson and Oldfield, 1986).

The ratio of SIRM to χ_{lf} (Figure 4.10a) has been used by several authors (e.g. Stober and Thompson, 1979; Thompson and Morton, 1979; Bradshaw and

Thompson, 1985) as an estimate of the concentration and grain size of magnetite in terms of the magnitude of these magnetic measurements and the ratio respectively. The results once again suggest an increase in concentration and grain size of magnetite from sedimentary rocks and more acid igneous rocks to basalts. Banerjee *et al.* (1981) proposed a variant on this latter method (Figure 4.1b) suggesting that χ_{ARM} can be used instead of SIRM measurements as χ_{ARM}/χ_{lf} may be more sensitive than SIRM/χ_{lf} in detecting certain grain size changes. Bradshaw and Thompson (1985) noted that, for non-interacting magnetite grains, χ_{ARM} corresponds approximately to the ratio SIRM/$(Bo)_{CR}$. However, no difference is evident between these plots for the rocks in this study.

A simultaneous R- and Q-mode factor analysis of the magnetic parameters (Figure 4.11) assists in their interpretation, the differences within and between rock groups being more readily apparent than in the raw data. The seven variables found to show most effectively the differences between the magnetic characteristics of the rock samples were used. The two factors plotted explain 67.73% of the variability in magnetic parameters of the rocks. Factor 1 is seen to be sensitive to those magnetic parameters-dependent on magnetic mineral assemblages and, simultaneously, on magnetic grain size. Magnetic susceptibility (χ_{lf}), anhysteretic remanent magnetisation (χ_{ARM}) and saturation isothermal remanent magnetisation (SIRM) are statistically correlated. However, these variables do not seem to be correlated with the high field isothermal remanent magnetisation ($HIRM_{300}$) which has negative factor loadings. This indicates that Factor 1 is able to discriminate mineral assemblages, with samples plotting close to the concentration-dependent magnetic parameters being mainly dominated by magnetite, whereas those samples which are close to the $HIRM_{300}$ parameters are dominated by hematite. Similarly, the coercivity of remanence $(Bo)_{CR}$ and the ratio χ_{ARM}/χ_{lf}, which are magnetic grain size-dependent parameters, are separated suggesting greater grain size in those samples closer to $(Bo)_{CR}$. Factor 2 separates concentration-dependent from magnetic grain size-dependent parameters.

The information from Figure 4.11 is basically the same as that of the bivariate plots (Figure 4.9 and 4.10). Differences in the magnetic parameters are seen within and between different rock groups, reflecting variations in the concentration, assemblage and grain size of the magnetic minerals. Although a clear discrimination of the rock samples on the basis of their magnetic parameters has not been found, a general trend is seen in which basalts are dominated by multidomain and/or stable single domain magnetite, whereas in the more acid rocks the relative proportion of hematite to magnetite increases and the magnetite grain size decreases slightly.

Sandstones are also dominated by magnetite but its concentration is very small in comparison with the igneous rocks, and its grain size tends to be smaller.

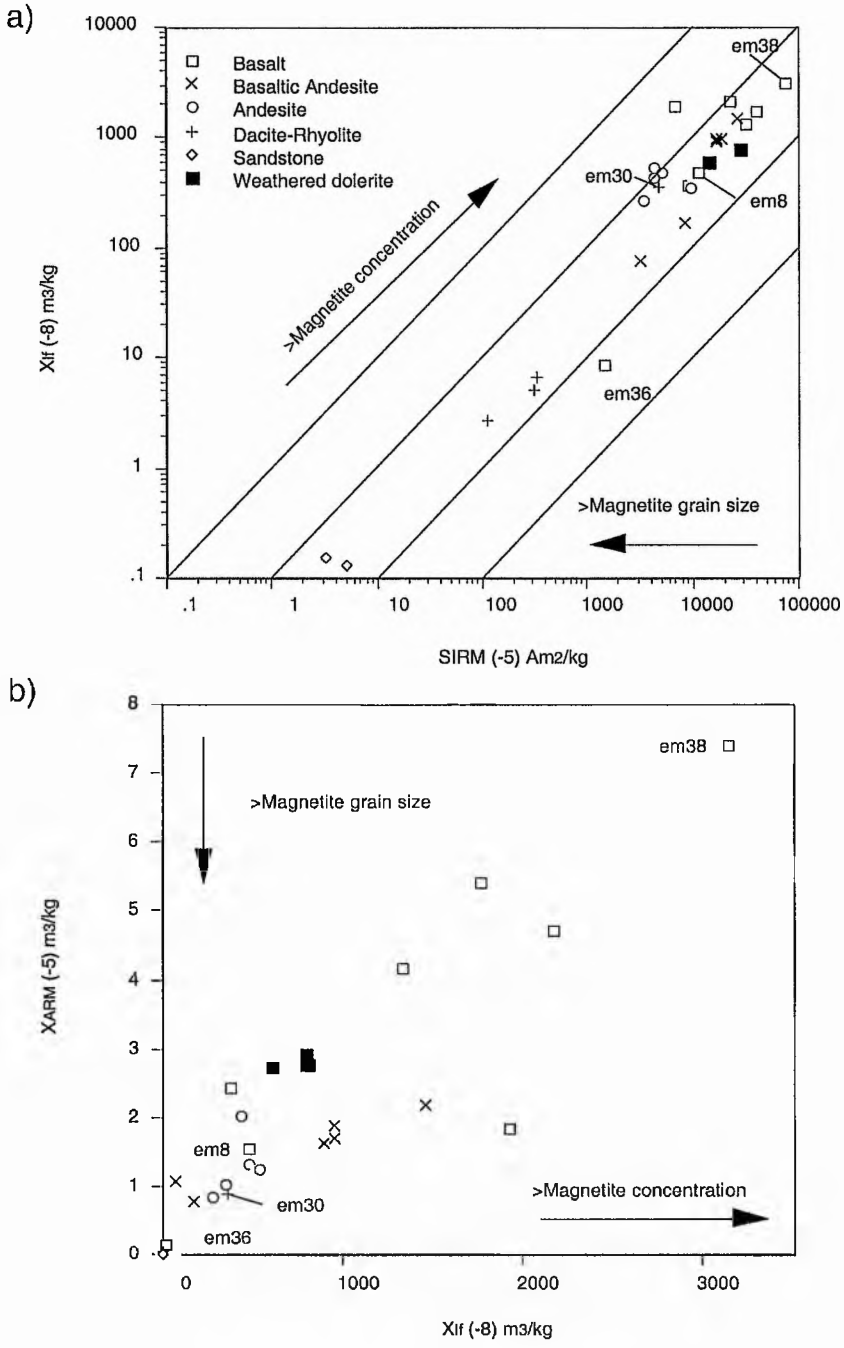

Figure 4.10. Scatter plots to estimate concentration and magnetite grain size in natural samples. a) Bilogarithmic magnetic susceptibility (χ_{lf}) versus saturation isothermal remanent magnetisation (SIRM), after Thompson and Oldfield (1986), b) susceptibility of anhysteretic remanent magnetisation (χ_{ARM}) versus magnetic susceptibility (χ_{lf}), after Banerjee *et al.* (1981).

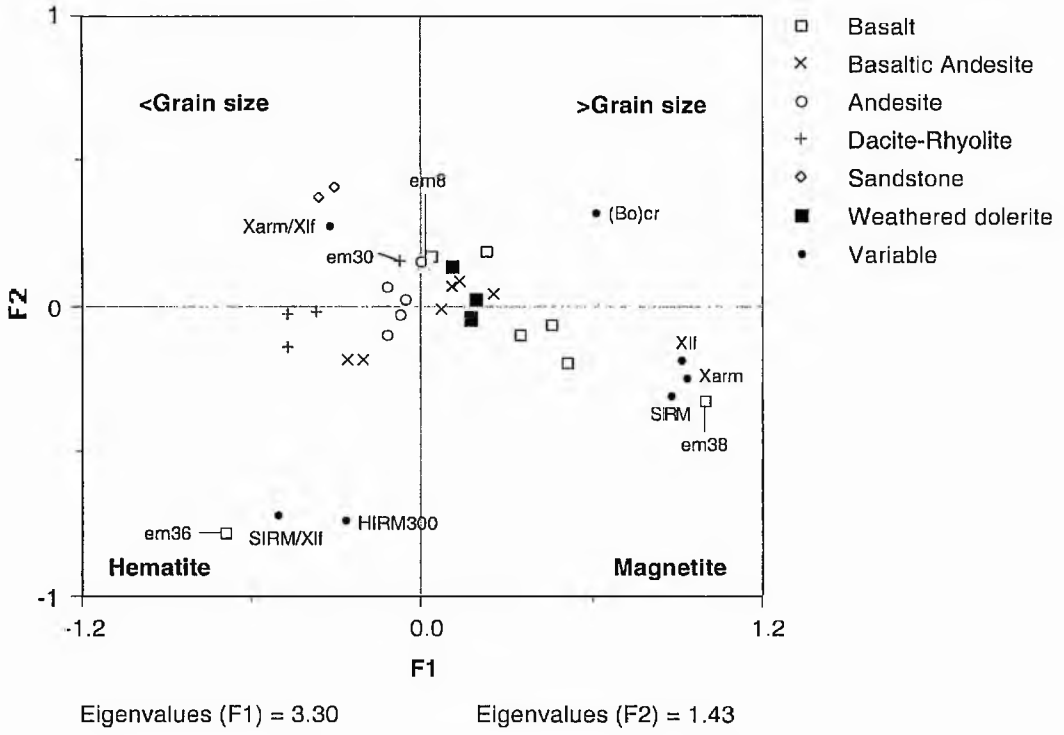

Figure 4.11. A simultaneous R- and Q-mode factor analysis of the main magnetic parameters measured in both igneous and sedimentary rocks sampled in the Eden catchment. Factor 1 (F1) and Factor 2 (F2) explain 67.73% of the 7 original variables.

Analysis of weathered rock samples

When comparing the magnetic parameters of a fresh dolerite sample (em8) with those of different mixing weathered layers (em23) and the soil resulting from the complete disintegration of the rock (em28(1), (2) and (3)), it is clearly seen from the χ_{lf}, χ_{ARM} and SIRM parameters (Figure 4.7) that all the weathered samples (em23 and em28) have higher concentration of magnetic minerals.

The normalised IRM acquisition curves (Figure 4.8f) suggest, however, that the weathered samples have a similar magnetic mineral assemblage compared with the fresh rock sample (em8). Thus, as confirmed by the $HIRM_{300}$ parameter (Figure 4.7), weathered samples are mainly made of magnetite, a slightly higher hematite concentration being observed in the soil sample (em28). On the other hand, both the $\chi_{fd\%}$ values (<2%) and the ratio of SIRM/χ_{lf} to $(Bo)_{CR}$ (Figure 4.9) indicate that, as in the fresh rock sample, weathered samples are dominated by single domain magnetite.

Figures 4.10 and 4.11 clearly show that whereas magnetic mineralogy and grain size remain basically unchangeable from fresh to weathered rock samples, magnetic concentration increases significantly. Such an increase in the concentration of magnetic minerals towards weathering may be explained by the loss of other non-magnetic minerals constituting the rock sample which, being more easily altered physically and chemically (such as plagioclase and pyroxene), could become part of the sediment more rapidly. Also, the slight decrease in magnetic grain size and in the relative concentration of magnetite with respect to hematite suggest the formation of secondary magnetic minerals (mainly SP magnetite and hematite) which concentration would undoubtely contribute to the increase in the values of χ_{lf} and SIRM.

The magnetic properties of Sample em38, which was weathered under subaqueous conditions do not seem to have been affected by the alteration of magnetite grains to sphene, the magnetic mineral assemblage (Figure 4.8a) and grain size (Figure 4.9) being within the range defined by all fresh basalt samples collected in the River Eden catchment.

4.1.4. Interrelationship between geochemistry and magnetism of rocks

The five groups of rocks (basalts, basaltic andesites, andesites, dacites-rhyolites, and sedimentary rocks), differentiated on the basis of their chemical composition in Subsection 4.1.1, show distinctive magnetic properties, indicating a close relationship between chemistry and magnetism, both being reflections of the mineralogy of the rocks. There are also variations in the chemical composition, concentration and grain size of the Fe-Ti oxides within each rock group. Magnetic mineral concentration, magnetite to hematite proportion, and magnetite grain size seem to decrease systematically towards the more acid igneous rocks, to a minimum (or even zero) in the sedimentary rocks. For the igneous rocks these results are in line with expectation, i.e. more acid magmas give lower magnetite/hematite ratios. Oxide abundance, distribution and composition depend on initial temperature, oxygen fugacity and TiO_2 and FeO abundance of the magma from which the rock crystallised. Basic magmas are enriched in FeO and TiO_2 compared with more acid magmas, and so they tend to contain larger concentrations of oxides. The initial temperatures of crystallisation, the cooling paths followed below the solidus, and the oxygen fugacity are the limiting factors chiefly responsible for compositional variations between titanomagnetites and ilmenites. Oxygen fugacity progressively increases from basic to acid suites, and so both Fe^{3+}:Fe^{2+} and Fe:Ti ratios also increase (Haggerty, 1976). This means that basic rocks will be characterised by ulvospinel-rich magnetite and pure ilmenite, whereas in more acid suites subsolidus

oxidation tends to lead to a decrease in TiO_2 content in the magnetite and an increase in the Fe_2O_3 content in the ilmenite (Buddington and Lindsley, 1964). The variability in the magnetite and ilmenite composition may be partially explained in terms of the oxidation state of the magma/rock.

The chemical homogeneity of the basalts was demonstrated in Subsection 4.1.1. However, Figure 4.7 shows that basalt samples have some differences in their magnetic properties. Samples em8, em21 and em22 tend to have even lower concentrations of magnetic oxides than the basaltic andesites. Also their magnetite grains (which are ulvospinel-rich) appear to have a larger grain size than the remaining basalt samples, which suggests variations in the conditions of oxide crystallisation.

At an early stage of this study a direct relationship was found between the ulvospinel-content in the magnetite and the magnetic susceptibility of the rocks, which was taken as an explanation of the variability of this magnetic parameter in chemically identical rocks (Appendix 7). However, additional data indicate that the magnetic susceptibility of the rocks is principally magnetite concentration-dependent (as shown also by Thompson and Oldfield, 1986; Dearing, 1994).

The dolerite weathering study revealed that the initial effects of subaerial weathering were very scant. However, they were detected by both chemical and magnetic analyses. Whilst microanalysis data show a slight decrease in FeO, TiO_2 and total weight percentages of magnetite towards more oxidised areas, magnetic data suggest a slightly higher relative hematite to magnetite concentration in the weathered samples with respect to the fresh rock. On the other hand, subaqueous weathering of dolerite involves an alteration of the titanomagnetite to sphene. This chemical alteration was not, however, found to significantly alter the magnetic properties of the rock.

Although rock samples are best grouped on the basis of their major element concentrations, there are also significant magnetic mineral differences between the rock groups. This is indicated by the simultaneous R- and Q-mode factor analysis of whole-rock chemistry, titanomagnetite chemistry and whole-rock magnetic parameters, which have proved to be efficient methods for interpreting the results and classifying the rock samples.

4.2. Mineral characterisation of glacial till

The glacial till deposits are a potential sediment source due to their extensive distribution over the River Eden catchment (Figure 2.2). An initial XRD analysis showed the presence of Fe-Ti oxides, and also of garnet (almandine variety) which indicates the provenance of at least some of the till from metamorphic rocks (Chapter 2). Mineral characterisation of till samples was carried out using a similar approach to that for rocks, including analysis of the Fe-Ti oxides present in the till, as well as measurement of the magnetic properties of bulk samples and of different particle size fractions.

4.2.1. Fe-Ti oxides in the glacial till

Some Fe-Ti oxides grains were separated from the Till BB1 sample in order to study their compositional range by electron probe microanalysis. Most grains were Ti-rich magnetite (titanomagnetite), however, unlike the titanomagnetite grains in the rock samples (Subsection 4.1.2), the till titanomagnetite has a wide span (Figure 4.12) ranging from ulvospinel (100% ulvospinel) to magnetite (99.99% magnetite) (Table 4.5). This compositional variability suggests different provenance for the titanomagnetite grains, as predicted in Chapter 2. Differences in the concentrations of some minor elements analysed in the titanomagnetite grains were also observed, with SiO_2 ranging from 0.11 to 13.96, Al_2O_3 from 0.01 to 4.71, MnO from 0 to 3.51, MgO from 0 to 0.95 and CaO from 0 to 1.35 (all in weight per cent). Nevertheless, a simultaneous R- and Q-mode factor analysis of the eight major and minor elements analysed for each titanomagnetite grain together with all grain compositions (Figure 4.13) suggests that this compositional variation in terms of trace elements concentration is not significant. Eigenvalues suggest that Factor 1 (F1) and Factor 2 (F2) explain 66.8% of the titanomagnetite composition variability in the glacial till. Factor 1 is mainly dominated by the Fe_2O_3, FeO and TiO_2 concentrations, showing the range in ulvospinel and magnetite relative proportions of the titanomagnetite grains. However, Factor 2 principally shows the range of concentration variability of minor elements measured in the titanomagnetite grains. This factor explains only 17.57% of the total composition variation. The mean chemical composition of the till titanomagnetite is presented in Table 4.6.

Ilmenite grains were found to be chemically similar in terms of both major and trace elements, with less than 19% in mol per cent of hematite (Fe_2O_3), as shown in Table 4.5.

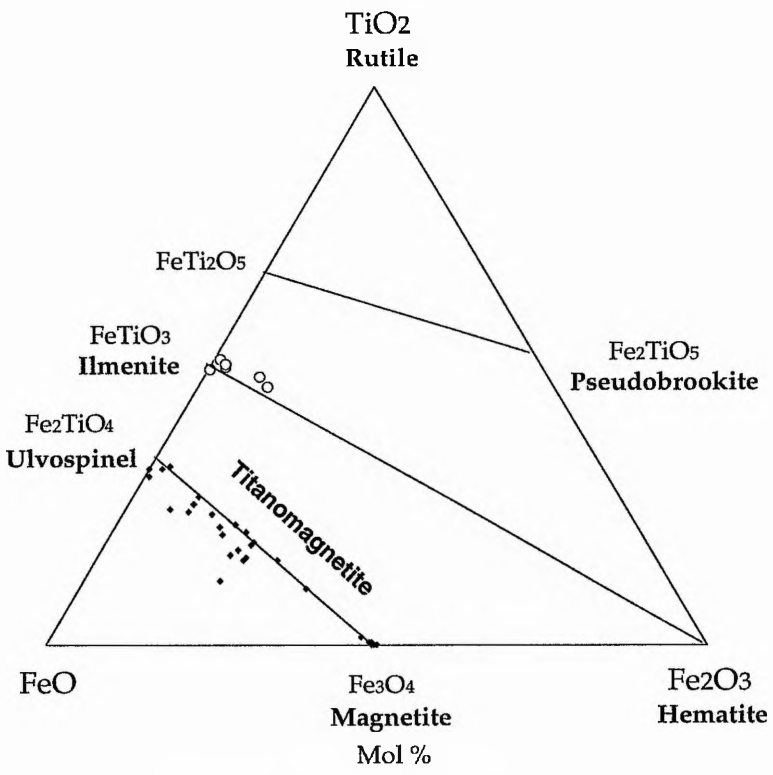

Figure 4.12. The system FeO-Fe_2O_3-TiO_2 showing the major high temperature solid solution series magnetite-ulvospinel, hematite-ilmenite, and pseudobrookite-$FeTi_2O_5$ plotted on a mol per cent basis, including the analysis of 28 magnetite and 6 ilmenite grains from the Till BB1 sample.

Table 4.5. Magnetite-ulvospinel and hematite-ilmenite relative proportions in mol per cent for magnetite and ilmenite grains analysed in Till BB1 sample, respectively.

Analysis number	2	4	5	6	7	8	10	11	12	13	14	15	16	17
Mol% Magnetite	50.44	47.05	27.96	1.75	55.59	5.59	0.00	98.88	28.36	55.17	58.99	29.63	65.08	42.99
Mol% Ulvospinel	49.56	52.95	72.04	98.25	44.41	94.41	100.00	1.12	71.64	44.83	41.01	70.37	34.92	57.01
Analysis number	18	19	22	23	25	26	27	28	29	30	31	32	33	34
Mol% Magnetite	99.99	99.49	64.75	96.79	37.27	77.76	45.86	99.58	56.21	59.53	8.72	99.88	21.73	55.28
Mol% Ulvospinel	0.01	0.51	35.25	3.21	62.73	22.24	54.14	0.42	43.79	40.47	91.28	0.12	78.27	44.72
Analysis number	1	3	9	20	21	24								
Mol% Hematite	14.79	4.17	18.05	1.70	4.00	0.00								
Mol% Ilmenite	85.21	95.83	81.95	98.30	96.00	100.00								

Backscattered electron images aid in the recognition of the morphology and texture of titanomagnetite grains. These grains tend to be angular, as found in the rock samples, with a mean grain size of 143 μm as estimated from 28 measured grains. They also show textural interrelationships with ilmenite; composite and trellis being the most common textures, with 20 homogeneous grains, 7 grains showing trellis texture and 1 composite grain counted.

Table 4.6. Mean values of eight principal elements (as weight per cent oxides) analysed in magnetite grains of glacial till sampled in the Eden catchment. And the relative proportion of magnetite and ulvospinel phases calculated from this mean titanomagnetite composition.

Sample	SiO_2	TiO_2	Al_2O_3	Fe_2O_3	FeO	MnO	MgO	CaO	mol % Magnetite	mol % Ulvospinel
Till BB1	1.10	13.60	1.00	33.30	42.69	0.60	0.14	0.29	55.09	44.91

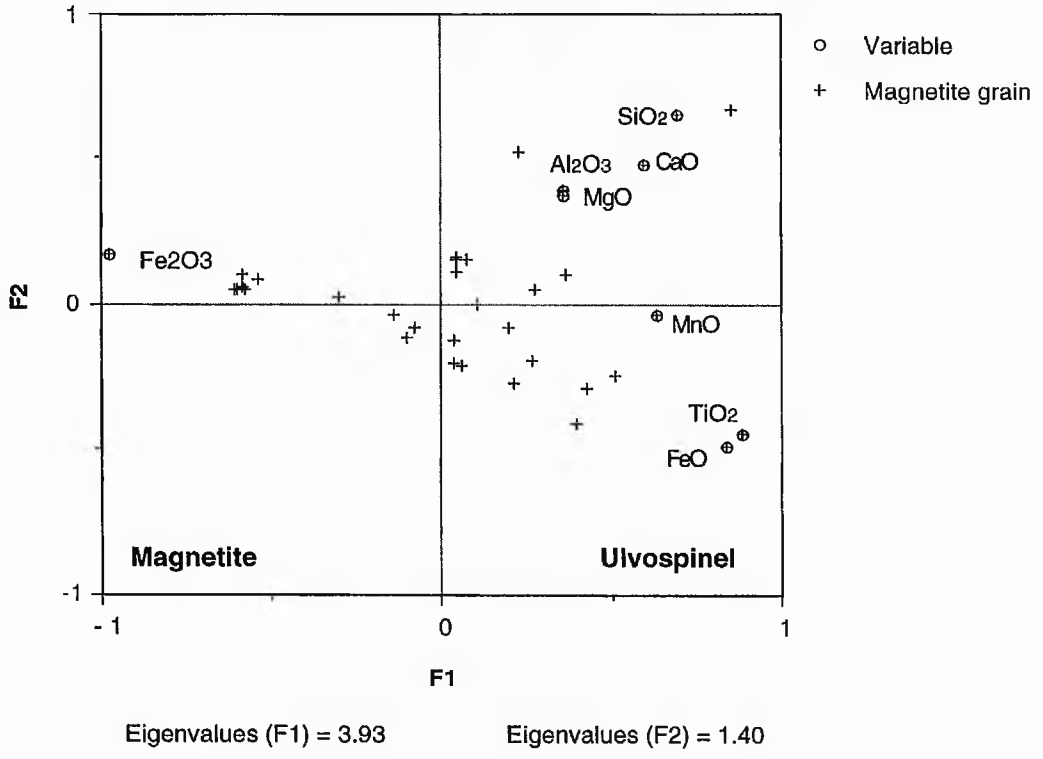

Figure 4.13. A simultaneous R- and Q-mode factor analysis of the eight major and minor element concentrations measured for titanomagnetite grains from Till BB1 sample. Factor 1 (F1) and Factor 2 (F2) explain 66.80% of the 8 original variables.

4.2.2. Magnetic properties of the glacial till

Two of the till samples (Till BB1 and Till BB4) were subdivided into 5 different particle size fractions in order to determine any variation in their particle size distribution, and also to determine if potential magnetic differences are a consequence of either their magnetic mineralogy or their particle size distribution, as observed by various authors (Thompson and Morton, 1979; Oldfield *et al.*, 1985; Oldfield and Yu, 1994). A third till sample (Till CB7) was analysed only as two bulk sub-samples.

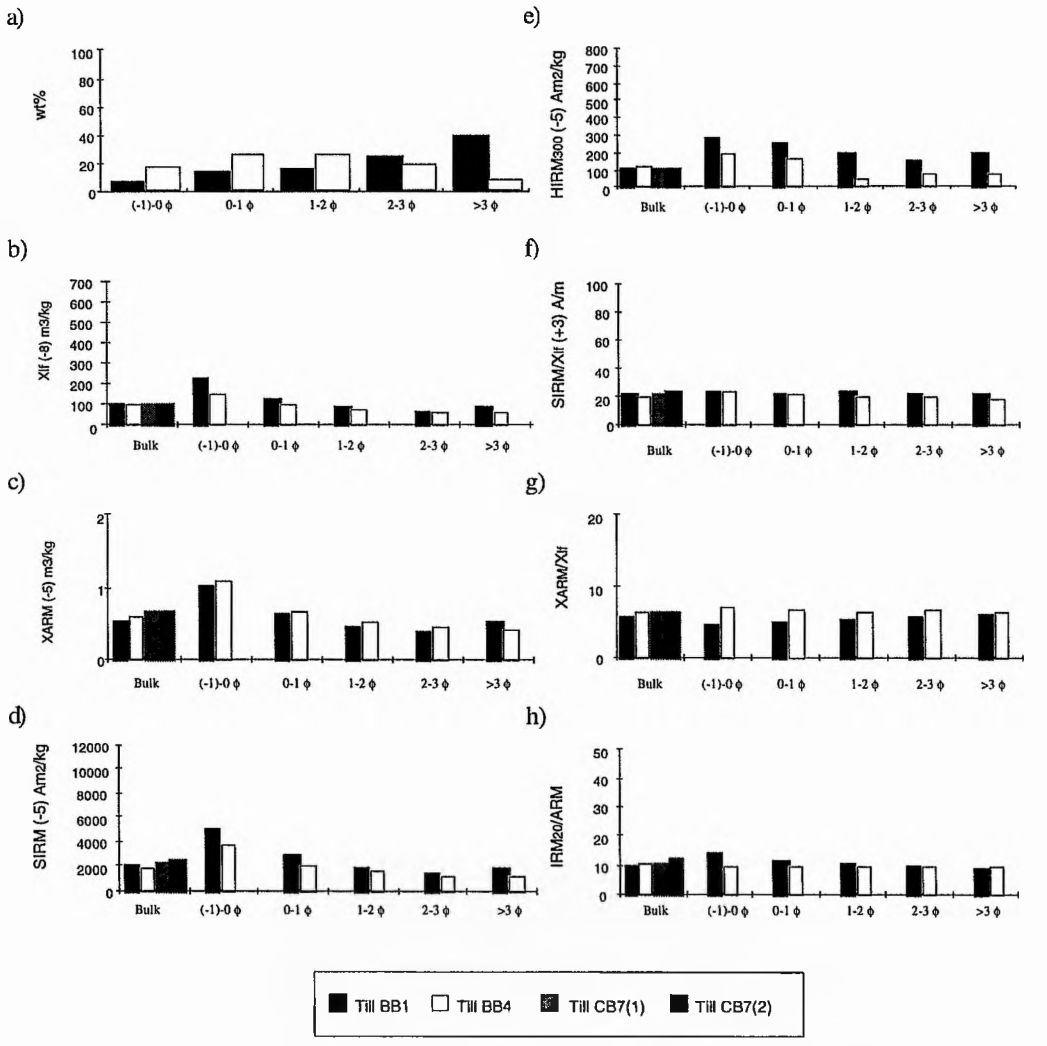

Figure 4.14. Particle size distribution in weight per cent and main magnetic parameters on a particle size basis for glacial till samples collected in the Barroway Burn (BB) and the Coalpit Burn (CB) courses. χ_{lf}: Magnetic susceptibility, χ_{ARM}: Susceptibility of anhysteretic remanent magnetisation (ARM), SIRM: Saturation isothermal remanent magnetisation, $HIRM_{300}$: High field isothermal remanent acquisition, IRM_{20}: Isothermal remanent magnetisation at 20 mT.

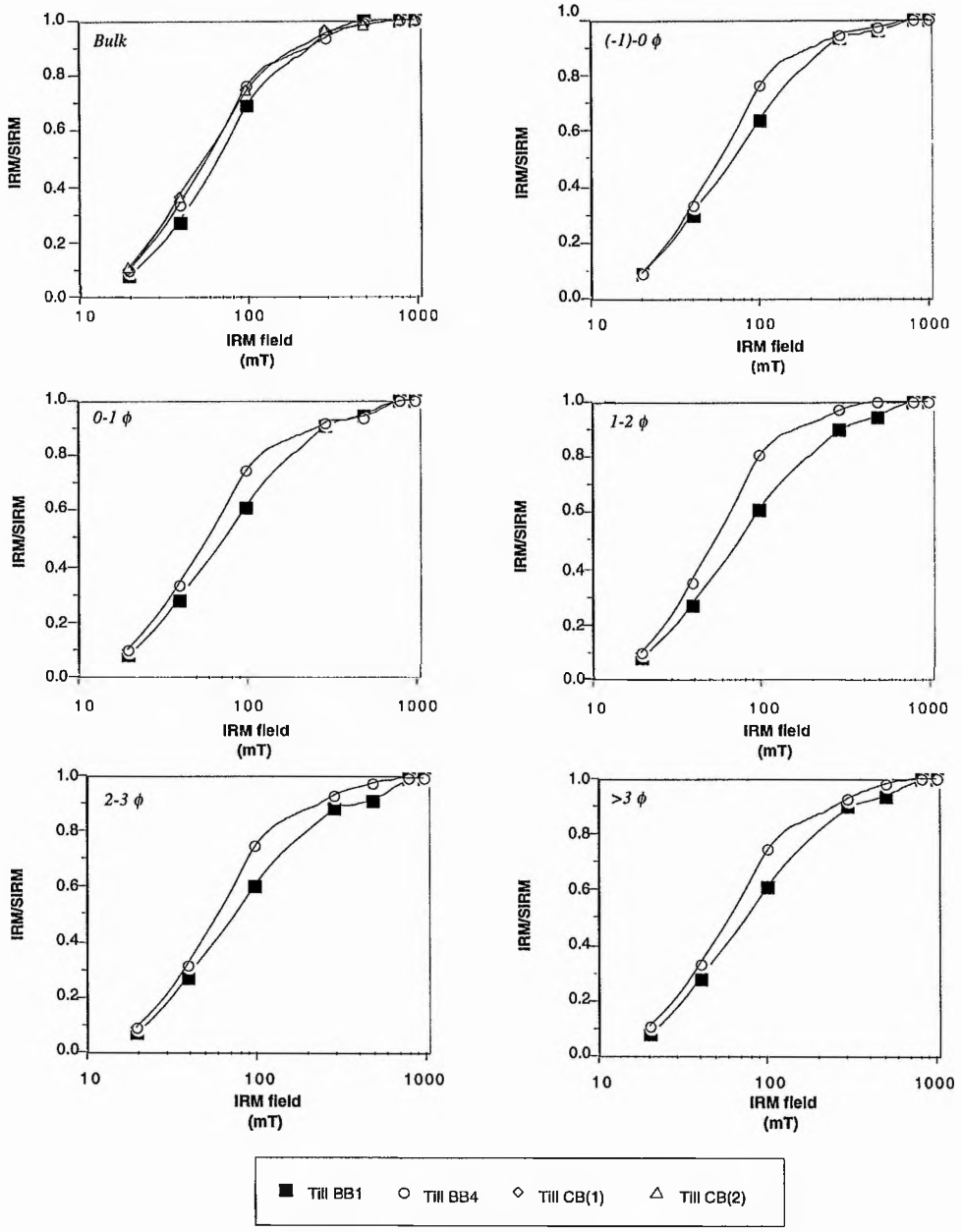

Figure 4.15. Normalised isothermal remanent magnetisation (IRM) acquisition curves on a particle size basis for till samples. Magnetite and hematite fields, after Thompson (1986), are shown in Figure 3.5.

Some difference in the particle size distribution of the samples is shown in Figure 4.14a. Whereas Till BB1 clearly comprises mostly of grains of >3 ϕ, Till BB4 is poorly sorted with similar proportions of -1 ϕ to 3 ϕ size fractions. Despite this, both till samples show similar magnetic distributions with ferrimagnetic minerals being mainly concentrated in the coarse fraction (-1 to 0 ϕ) as suggested by the magnetic susceptibility (χ_{lf}), the anhysteretic remanent magnetisation (χ_{ARM}) and

the saturation isothermal remanent magnetisation (SIRM) values (Figure 4.14b-d). The magnetic mineral assemblages are firstly shown using the normalised isothermal remanent magnetisation (IRM) curves (Figure 4.15). These curves indicate that all samples are composed of mixtures of magnetite and hematite which are present in approximately the same proportions in all size fractions. However, Till BB1 sample shows a greater hematite concentration than the Till BB4 sample, as was also found from the high field isothermal remanent magnetisation ($HIRM_{300}$) acquisition values (Figure 4.14e), which are an approximate indicator of hematite concentration (e.g. Yu and Oldfield, 1993).

Both the frequency-dependent susceptibility ($\chi_{fd\%}$) with values of less than 3%, and the ratio of the isothermal remanent magnetisation at 20 mT (IRM_{20}) to the anhysteretic remanent magnetisation (ARM) at less than 15, suggest a stable single domain magnetite dominance (Dearing, 1994 and Oldfield, 1991 respectively) in all samples. However, the SIRM/χ_{lf} and the χ_{ARM}/χ_{lf} ratios, considered potentially useful in magnetite granulometric studies and in determining mineral types in magnetite mixtures (Thompson *et al.*, 1980 and Banerjee *et al.*, 1981), show similar magnetic mineral assemblages in all samples but a slightly larger magnetic grain size in the Till BB1 than in the Till BB4. The same is observed in the coercivity of remanence $(Bo)_{CR}$ versus the SIRM/χ_{lf} ratio diagram (Figure 4.16).

The differences in magnetic assemblage and in magnetic grain size between these two till samples are clearly shown in Figure 4.17 where the demagnetisation parameter D versus the χ_{lf} diagram suggests a similar magnetic mineral concentration in the samples but a greater relative proportion of hematite to magnetite in the Till BB1 sample. The same is seen from the ratio of $(Bo)_{CR}$ to S-ratio which also indicates a slight difference in magnetic grain size as described above.

This magnetic variability observed between till samples is, however, insignificant compared with the variation in magnetic measurements found between rock samples within each rock group distinguished in Subsection 4.1.3. It is concluded that the glacial till deposit is homogeneous in terms of its magnetic mineralogy, being characterised by the presence of magnetite and hematite mixtures and by a pseudo-single domain magnetite dominance.

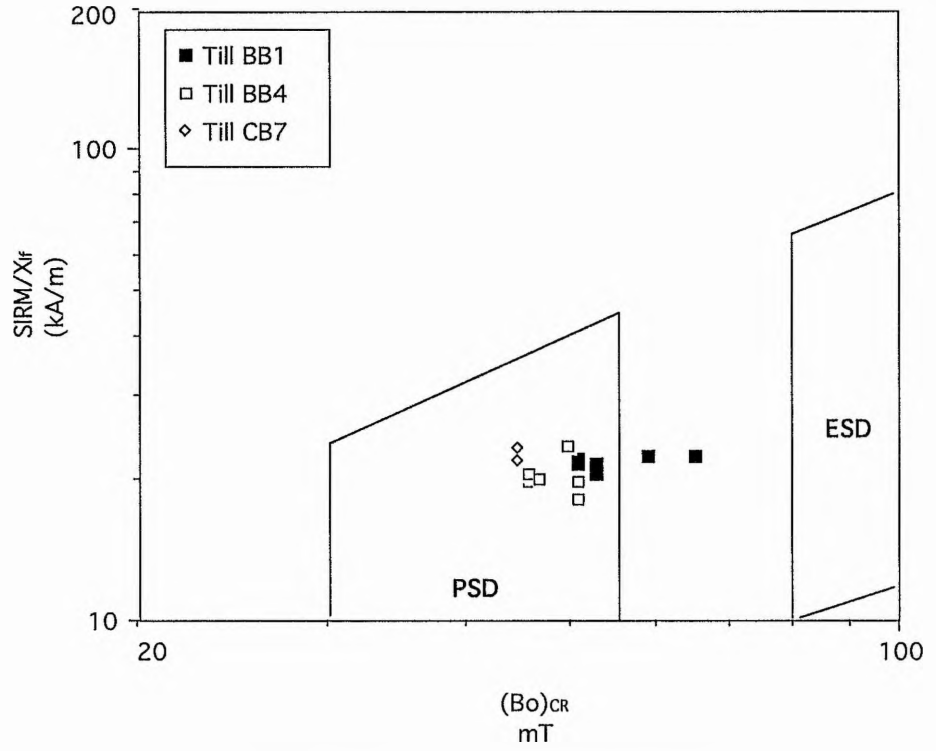

Figure 4.16. Ratio SIRM/χ_{lf} versus coercivity of remanence $(Bo)_{CR}$ diagram with grid schematically dividing magnetic mineralogies and magnetisation states for till samples. PSD: Pseudo-single domain, and ESD: Elongated single domain magnetite (after Thompson and Oldfield, 1986).

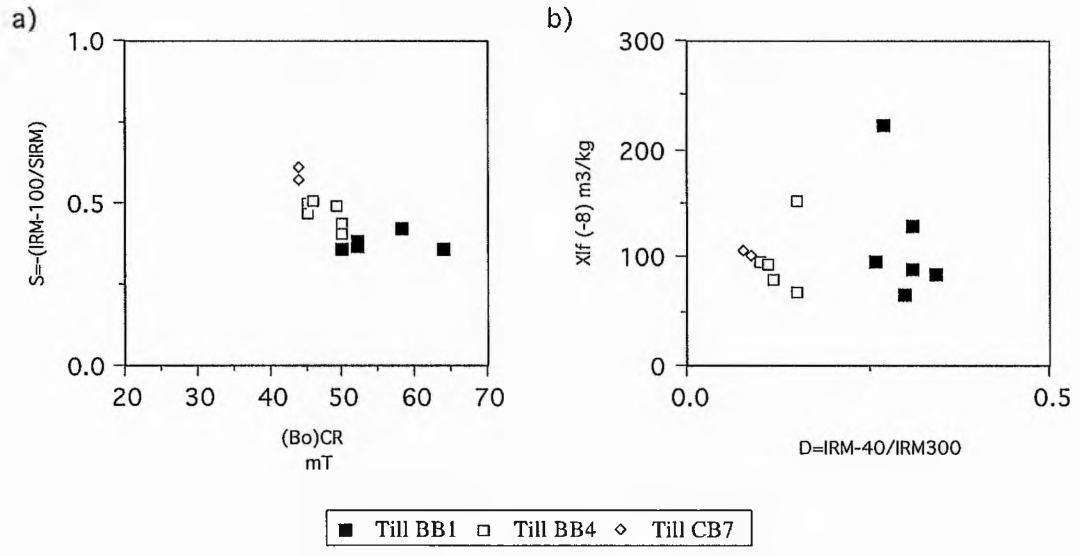

Figure 4.17. a) S-ratio (=-IRM_{-100}/SIRM) versus coercivity of remanence $(Bo)_{CR}$ diagram (after Stober and Thompson, 1979), and b) Magnetic susceptibility (χ_{lf}) versus demagnetisation parameter D (=IRM_{-40}/IRM_{300}) diagram for till samples (after Stott, 1986).

4.3. Mineral characterisation of stream sediments

An initial X-ray diffractometry analysis of all stream sediments sampled in the River Eden catchment showed the presence of Fe-Ti oxides accompanied in many cases by almandine garnet. In the section 4.2 garnet was identified as a characteristic of the glacial till. The presence of almandine, typical of metamorphic terrains such as the Scottish Highlands, in the stream sediments indicates that glacial till is also a source material for the stream sediments.

The composition of Fe-Ti oxides and the magnetic properties of the sediments from four tributaries of the River Eden were analysed. Two of the tributaries, the Barroway Burn and the Moonzie Burn, rise in the northern part of the Eden catchment, whilst the Kilgour Burn and the Coalpit Burn sourced in the southern part (Figure 1.1). Therefore, the Fe-Ti oxides present in these stream sediments will be derived mainly from the andesitic rocks in the cases of the Barroway Burn and the Moonzie Burn (Figure 3.2), and from the dolerites in the cases of the Kilgour Burn and the Coalpit Burn (Figure 3.3). The mineralogical characterisation of all these sediments can then be used to monitor any changes suffered by the Fe-Ti oxides in terms of their concentration, chemistry and grain size during the process of sediment formation and transport from these major source rocks.

4.3.1. Fe-Ti oxides in the stream sediments

Some representative samples of the bed sediments of each stream, including at least one from the apparent source and another one from the lower part of the course, were prepared for electron probe microanalysis of their magnetite and ilmenite grains. In the case of the River Eden, however, all sediment samples were analysed because significant mineralogical variations are to be expected due to the intermixing of sediments from several tributaries draining different source areas.

The compositional range of all the analysed Fe-Ti oxides was firstly tested by plotting the data in a FeO-Fe_2O_3-TiO_2 ternary diagram (Figure 4.4). All titanomagnetite grains show considerable scatter along the magnetite-ulvospinel solid solution line, as described for till samples (Figure 4.12) in section 4.2. A simultaneous R- and Q-mode factor analysis was then performed using the mean values of the eight principal elements (Table 4.7) measured in all magnetite grains in each sediment sample (Figure 4.18), in order to establish the compositional variations of the titanomagnetite grains in the stream sediment samples. The two

main factors explain 70.89% of the variability observed in the eight chemical elements analysed in the titanomagnetite grains. Factor 1 mainly reflects the content of three elements (Ti, Fe^{2+} and Fe^{3+}) in the titanomagnetite, showing the relative ulvospinel-magnetite proportions in the samples. Factor 2 is dominated by the variability in Mn and Al content of the titanomagnetite with large but opposite weightings. This statistical analysis clearly shows that, despite the wide compositional variation of the titanomagnetite grains within each stream, each fluvial system defines a particular field. This reflects a characteristic composition of the titanomagnetite grains within each stream which differs from one tributary to another. This was an unexpected result with each tributary preserving a clear fingerprint of its source material. Titanomagnetite grains from the Barroway Burn and the Moonzie Burn, both flowing over the andesitic rocks, appear enriched in the magnetite phase. Whereas the Kilgour Burn and the Coalpit Burn, which flow over the dolerites, transport dominantly ulvospinel-rich titanomagnetite grains.

Table 4.7. Mean values of eight principal elements (as weight per cent oxides) analysed in magnetite grains of the sediments sampled in the Eden catchment, and their relative proportion of magnetite and ulvospinel phases. BB: Barroway Burn, MB: Moonzie Burn, KB: Kilgour Burn, CB: Coalpit Burn, and RE: River Eden. Note that Na_2O and K_2O percentages have not been included as they are trace.

Sample	SiO_2	TiO_2	Al_2O_3	Fe_2O_3	FeO	MnO	MgO	CaO	mol % Magnetite	mol % Ulvospinel
BB3	1.12	12.30	0.91	38.12	35.31	0.48	0.50	0.65	60.82	39.18
BB6	1.44	16.40	1.37	27.01	42.49	0.47	0.12	0.52	45.21	54.79
BB7	0.76	13.53	1.05	35.34	40.95	0.45	0.21	0.22	56.68	43.32
MB1	0.76	13.37	1.16	36.25	39.05	0.37	0.25	0.19	57.59	42.41
MB4	1.03	13.66	0.95	33.36	40.60	0.42	0.33	0.20	55.02	44.98
KB1	1.65	18.21	1.18	21.94	46.65	0.82	0.14	0.52	37.64	62.36
KB6	0.94	15.41	1.52	29.65	41.60	0.64	0.24	0.20	49.08	50.92
CB1	2.82	18.72	1.04	17.11	47.20	0.39	0.07	1.53	31.41	68.59
CB5	1.76	15.27	1.44	24.94	45.09	0.38	0.19	0.67	45.00	55.00
CB6	6.68	18.71	1.32	15.74	46.31	0.35	0.24	0.84	29.65	70.35
RE1	0.87	13.16	1.49	34.97	42.64	0.41	0.25	0.14	57.10	42.90
RE2	0.57	10.60	1.48	44.10	40.48	0.33	0.23	0.05	67.58	32.42
RE3	1.99	15.21	1.43	24.70	43.94	0.29	0.13	0.83	44.86	55.14
RE4	1.47	17.19	1.24	22.47	44.97	0.35	0.34	0.45	39.57	60.43
RE5	1.38	15.41	1.20	29.14	41.95	0.40	0.33	0.37	48.65	51.35
RE6	1.41	17.64	0.98	22.55	46.11	0.43	0.07	0.40	39.04	60.96

The River Eden sediments, however, show a wider range of variability in the composition of their titanomagnetite grains. The field defined by the River Eden overlaps the fields of the four tributaries suggesting, as predicted above, that the

River Eden sediments result from mixtures of the sediments transported by all these streams.

The ilmenite grains analysed in all sediment samples show, as for rock and till samples, similar chemical compositions in terms of FeO, Fe_2O_3 and TiO_2 percentages, with less than 10% in mol per cent of hematite (Fe_2O_3).

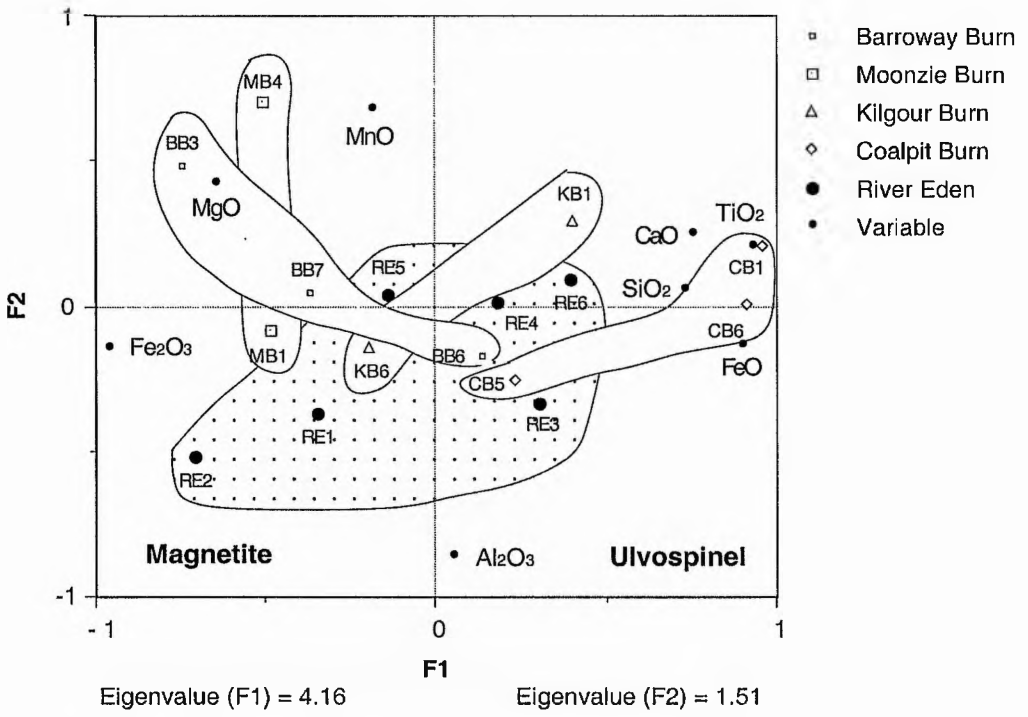

Figure 4.18. A simultaneous R- and Q-mode factor analysis of the mean composition of all grains of titanomagnetite analysed from the stream sediments sampled in the Eden catchment. Factor 1 (F1) and Factor 2 (F2) explain 70.89% of the 8 original variables.

Backscattered electron images enabled the recognition of magnetite grains altered to sphene, as described for some weathered dolerite samples (see subsection 4.1.2). A greater concentration of such grains is found in the southern part of the Eden catchment tributaries than in the streams from the northern part, as shown in Figure 4.18. The River Eden sediments also contain such altered magnetite grains (Plate 4.2), those samples with magnetite composition similar to the southern tributaries showing a major concentration. It is thus apparent that the chemical composition of the titanomagnetite grains transported by the River Eden and its tributaries is a good fingerprint for the determination of sediment provenance.

A textural analysis of the titanomagnetite grains was also performed. The number of grains showing the three main textures found (homogeneous, trellis and composite grains, as described by Grigsby, 1990 and Haggerty, 1991) in some selected sediment samples are presented in Table 4.8. An approximate estimate of the magnetite grain size is also included.

Even when mechanical abrasion of these grains may be anticipated as a consequence of fluvial transport, these grains appear to be angular or subangular suggesting either their resistance to both chemical weathering and mechanical abrasion, or simply their short distance of transport. However, some grains which are perfectly spheroidal (Plate 4.3) are also found rarely within the sediment samples. These grains show a patchy 'texture', and when light (in backscattered electron images) and dark zones are analysed (analyses 20 and 21 in RE2 sample, respectively, given in Appendix 4M) they differ slightly in their Si-, Ca-, Fe^{3+}- and Ti-content, the darker patches being Si-, Ca- and Fe^{3+}-enriched, and Ti-impoverished with respect to the light zones, suggesting an alteration to sphene as well as an oxidation of Fe^{2+} to Fe^{3+}. Such magnetite morphology has been found to result from industrial air pollution, mainly fly ash derived from coal combustion (e.g. Puffer *et al.*, 1980; Locke and Bertine, 1986), volcanism (e.g. Fredriksson and Martin, 1963), and extraterrestrial sources (e.g. Schmidt and Keil, 1966). In all these cases the magnetic spherules are composed of magnetite, which is mainly composed of Fe, although some low concentrations of other elements, such as Ti, Ca, Si, Al, K, Cu, Zn, V, Co, Ni and Mn, are also detected in those spherules resulting from industrial contamination (e.g. Doyle *et al.*, 1976; Puffer *et al.*, 1980; Locke and Bertine, 1986). However, Ni-rich spherules have been found to be of extraterrestrial origin, and those rich in Ti are typically of volcanic origin.

Fredriksson and Martin (1963) suggest that the high TiO_2 (5-10%) and MnO (0.5%) content in the magnetite spherules provides a criterion for distinguishing particles of volcanic origin. The magnetite spherules found in the sediment samples collected in the River Eden catchment show chemical similarity with the magnetite grains found in those samples, their TiO_2 and MnO contents corresponding to those described by Fredriksson and Martin (1963) as typically of volcanic origin. Therefore, it is concluded that magnetite spherules found in some of the stream sediment samples under study most probably correspond to reworked Devonian volcanic ashes.

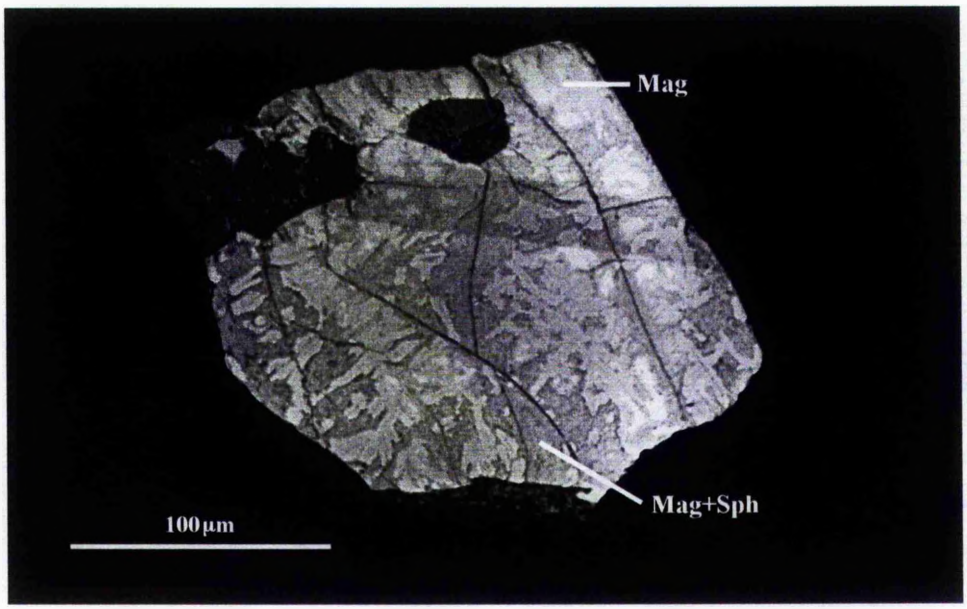

Plate 4.2. Detrital magnetite grain showing alteration to sphene. Mag: magnetite, Sph: sphene (see text for explanation).

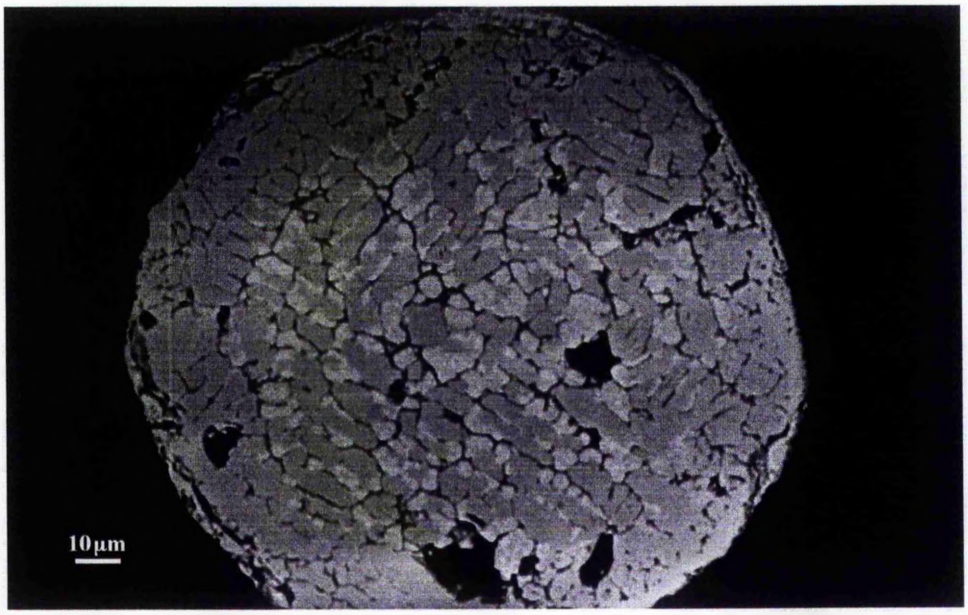

Plate 4.3. Magnetite spherule found in the River Eden sediment. Note darker rim and internal patches of the grain which are relatively Si-, Ca-, and Fe^{3+}-enriched, and Ti-impoverished (see text for explanation).

Table 4.8. Number of magnetite grains counted for each of the three main textures recognised in some representative sediment samples and their mean grain size in μm. BB: Barroway Burn, MB: Moonzie Burn, KB: Kilgour Burn, CB: Coalpit Burn, and RE: River Eden.

Sample	Homogeneous	Trellis Ilmenite-Magnetite	Composite Ilmenite-Magnetite	Magnetite grain size (μm)
BB3	16	1	0	119.7
BB6	26	6	0	155.6
BB7	30	4	2	155.3
MB1	25	1	1	195.1
MB4	24	4	1	143.6
KB1	30	0	0	136.4
KB6	21	8	1	146.8
RE1	14	14	4	139.2
RE2	22	4	3	215.5
RE3	23	4	1	183.9
RE4	21	9	2	194.9
RE5	15	15	1	135.4
RE6	16	6	5	196.9

4.3.2. Magnetic properties of the stream sediments

Each sediment sample was firstly subdivided on the basis of five particle sizes in order to ensure that differences in the magnetic properties of bulk samples are not due to differences in particle size distributions but rather their magnetic mineralogies (Thompson and Morton, 1979; Oldfield *et al.*, 1985; Oldfield and Yu, 1994).

When measuring the isothermal remanence magnetisation (IRM) a demagnetisation phenomenon was observed in most of the Coalpit Burn sediment samples involving a reduction in the magnitude of the IRM from 300 mT to 1 T applied magnetic fields. The difference in the values was, in all cases, less than 1%. However, due to the strong magnetism of the samples such a difference was significant in terms of the original values. The reasons for such behaviour in these samples could not be certainly determined. An additional error in measurements using the Molspin Fluxgate magnetometer results from the use of a calibration sample of $1424.16 * 10^{-8}$ A/m^2 for samples beyond this range. The magnetometer also showed some sensitivity to room temperature changes. Nevertheless, as all rock, till and the remainder of the stream sediment samples were measured under the same conditions without showing such a behaviour, other factors may be involved. Some authors (e.g. Lees, 1994) have observed demagnetisation cases due to magnetic grain interactions. Another possible factor could be the interaction between the

magnetometer and the sample due to the magnetic field created by the sample's remanent magnetisation. Several measurements of the sediment samples using decreasing sample volumes were made and finally similar or slightly greater IRM values for 500 mT and 1T than for 300 mT applied magnetic field intensities were obtained. This enabled the calculation of high field isothermal remanent acquisition parameters (HIRM) which are traditionally used as an estimate of the concentration of antiferromagnetic minerals. However, because of this analytical problem, the $HIRM_{100}$ of Bradshaw and Thompson (1985) was used for the stream sediment analysis instead of the $HIRM_{300}$ used for the rock and till samples. The S-ratio (=-IRM_{-100}/SIRM) and the demagnetisation parameter D (=IRM_{-40}/IRM_{300}) were found to be the best parameters to discriminate stream sediments in terms of their relative magnetite-hematite proportions, and therefore these were used in the statistical analyses.

Sediments in the River Eden tributaries

A similar particle size distribution is generally found in all the sediment samples collected in each individual stream but differences are observed between sediments of different streams. The Barroway Burn sediments are mainly composed of coarse sand (-1 to 1 ϕ in size), while in the Moonzie Burn, sediment samples show a wider range of particle size distributions from samples dominated by coarse sand (-1 to 0 ϕ in size) to samples dominated by finer sand (2 to 3 ϕ in size). The sediment samples collected along the Kilgour Burn are mainly 1 ϕ to 3 ϕ in size whilst the Coalpit Burn sediments appear to be less well sorted, varying from -1 ϕ to 3 ϕ in size (Figure 4.19).

The concentration-dependent magnetic parameters, magnetic susceptibility (χ_{lf}), susceptibility of anhysteretic remanent magnetisation (χ_{ARM}) and saturation isothermal remanent magnetisation (SIRM), suggest greater proportions of magnetic minerals in the coarse fractions (-1 to 1 ϕ) than in the finer fractions of the Barroway Burn sediments, the Moonzie Burn sediments and the Kilgour Burn sediments (Figure 4.19). However, in the Coalpit Burn sediments the magnetic minerals appear to be concentrated in the 1 ϕ to 2 ϕ size fraction. The normalised isothermal remanent magnetisation (IRM) acquisition curves (Figure 4.20) show that the assemblage of magnetic minerals within each stream sample is very similar in all size fractions, magnetite being dominant. In the Barroway Burn sediment samples there is a slight tendency of the relative hematite concentration to increase downstream. A similar trend towards coarser size fractions is found in the Coalpit Burn sediments whereas in the Moonzie Burn and the Kilgour Burn hematite tends to

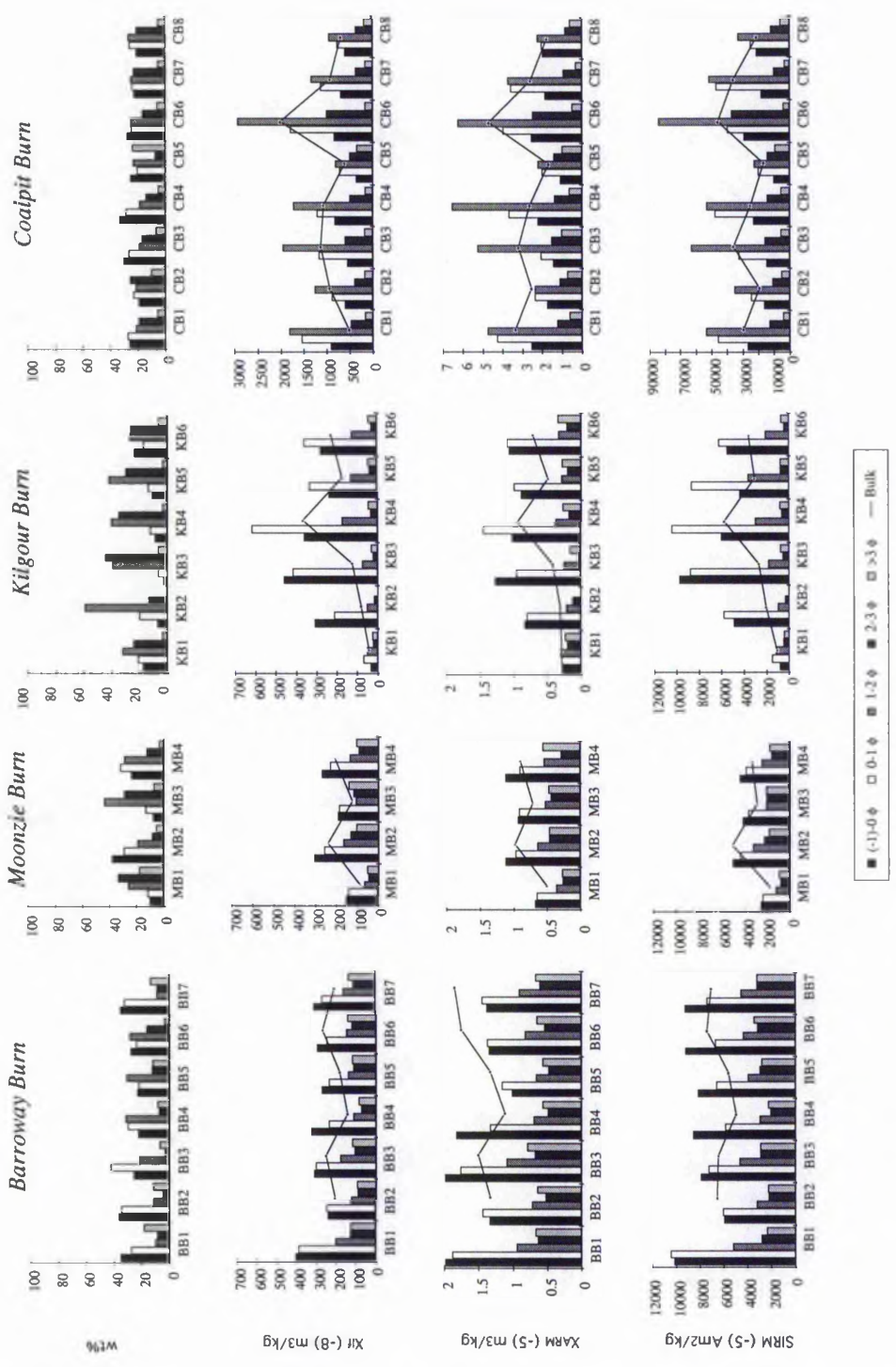

Figure 4.19. Particle size distribution in weight per cent and main concentration-dependent magnetic parameters on a particle size basis for all sediment samples collected in the Barroway Burn (BB), the Moonzie Burn (MB), the Kilgour Burn (KB) and the Coalpit Burn (CB). χ_{lf}: Magnetic susceptibility, χ_{ARM}: Susceptibility of anhysteretic remanent magnetisation, SIRM: Saturation isothermal remanent magnetisation.

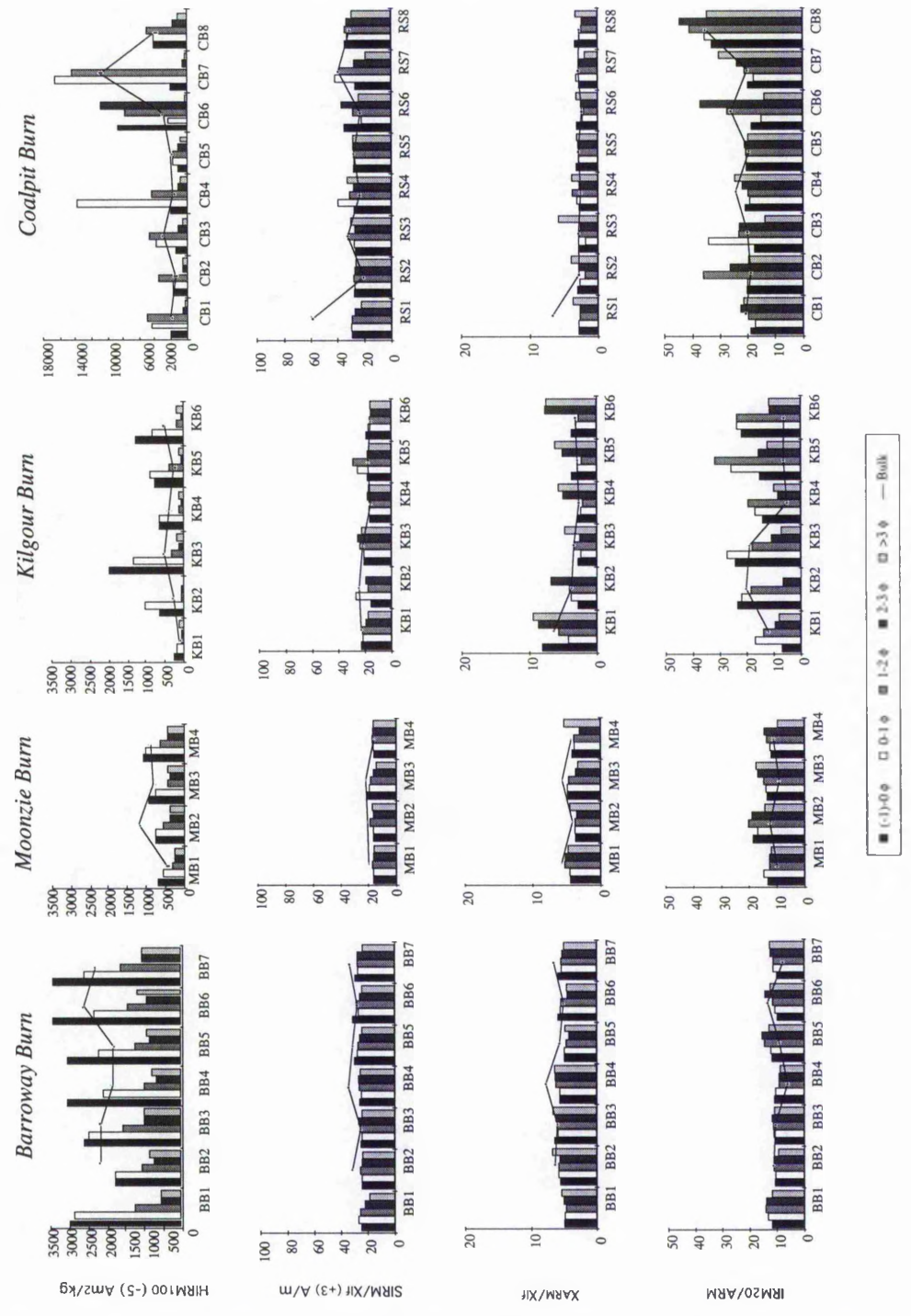

Figure 4.19. (continuation). Some main magnetic ratios indicating relative magnetite-hematite concentrations and variations in magnetic grain size on a particle size basis for all sediment samples collected in the Barroway Burn (BB), the Moonzie Burn (MB), the Kilgour Burn (KB) and the Coalpit Burn (CB). χ_{lf}: Magnetic susceptibility, χ_{ARM}: Susceptibility of anhysteretic remanent magnetisation (ARM), SIRM: Saturation isothermal remanent magnetisation, $HIRM_{100}$: High field isothermal remanent acquisition, IRM_{20}: Isothermal remanent magnetisation at 20 mT.

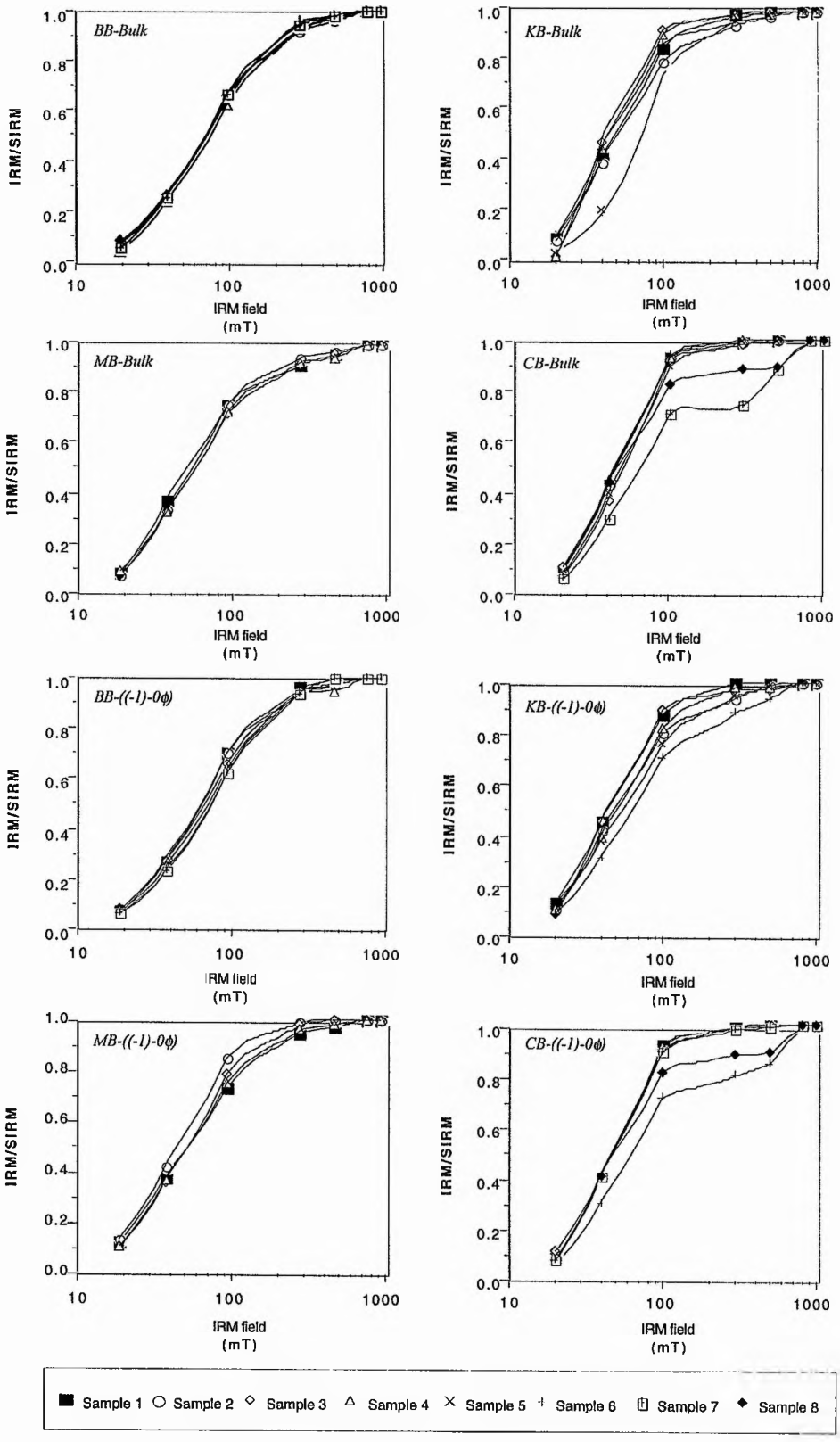
BB-Bulk
KB-Bulk
MB-Bulk
CB-Bulk
BB-((-1)-0ϕ)
KB-((-1)-0ϕ)
MB-((-1)-0ϕ)
CB-((-1)-0ϕ)
IRM/SIRM
IRM field (mT)
1.0
0.8
0.6
0.4
0.2
0.0
10
100
1000
Sample 1
Sample 2
Sample 3
Sample 4
Sample 5
Sample 6
Sample 7
Sample 8

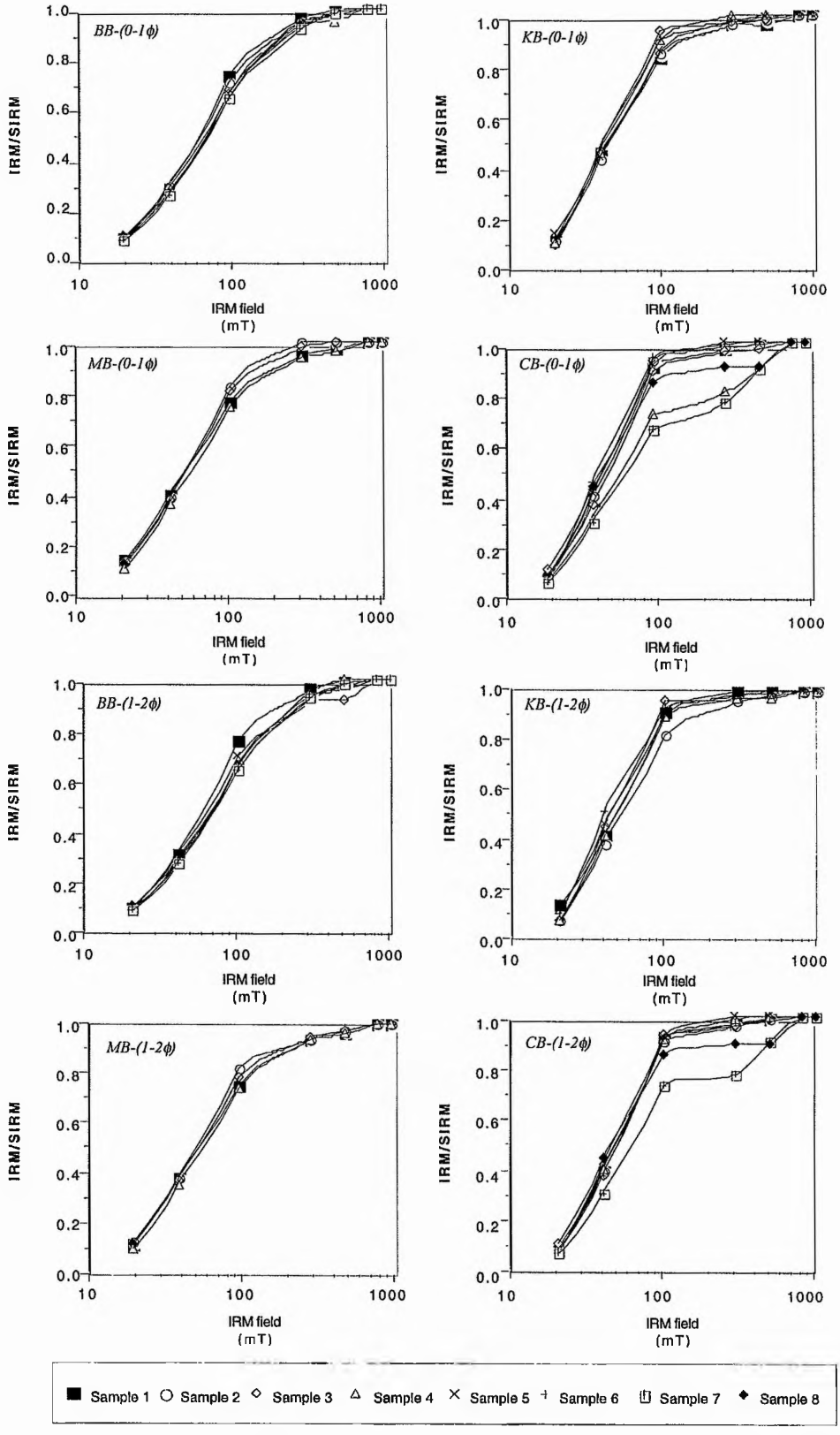
BB-(0-1ϕ)
KB-(0-1ϕ)
MB-(0-1ϕ)
CB-(0-1ϕ)
BB-(1-2ϕ)
KB-(1-2ϕ)
MB-(1-2ϕ)
CB-(1-2ϕ)
IRM/SIRM
IRM field (mT)
1.0
0.8
0.6
0.4
0.2
0.0
10
100
1000
Sample 1
Sample 2
Sample 3
Sample 4
Sample 5
Sample 6
Sample 7
Sample 8

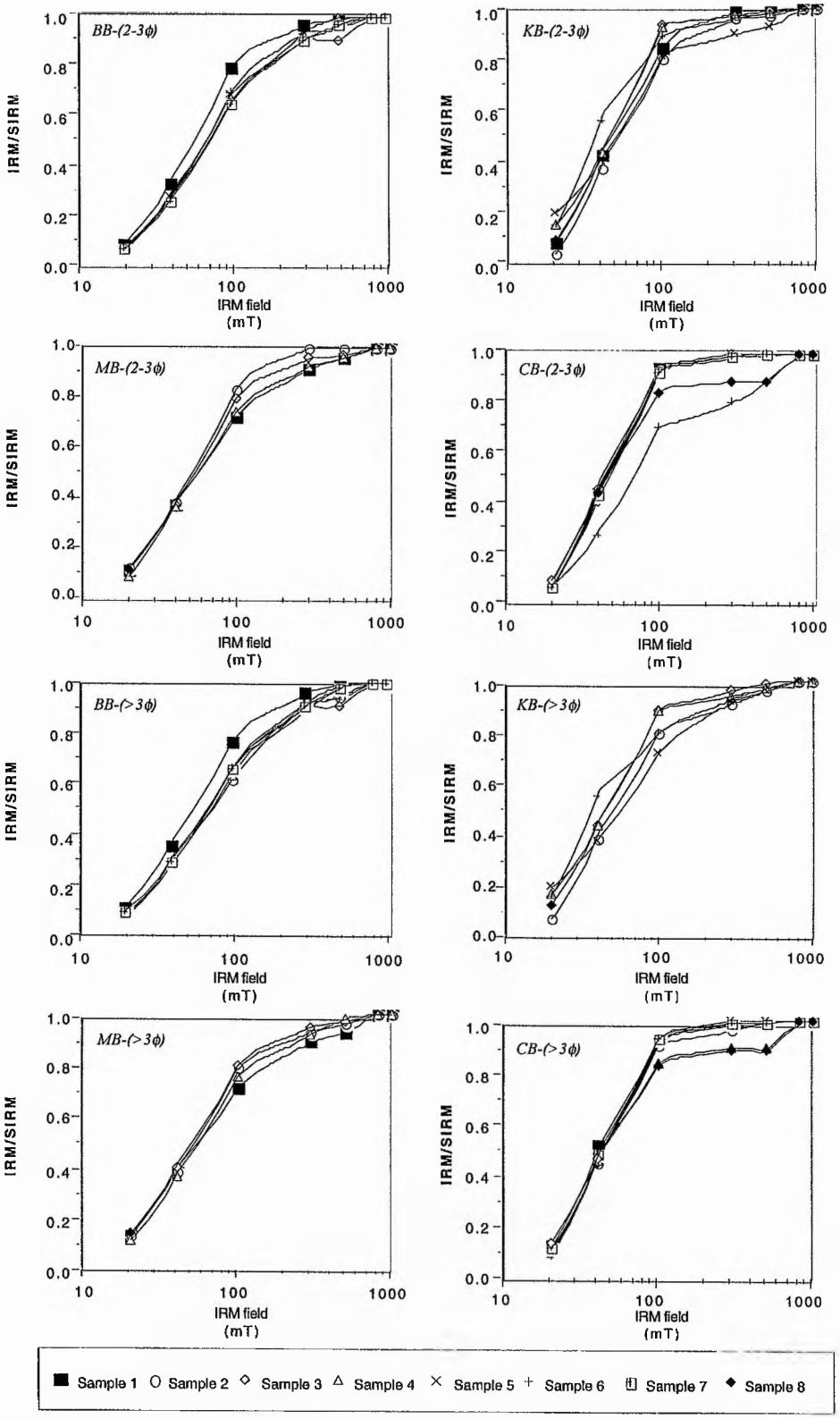

Figure 4.20. Normalised isothermal remanent magnetisation (IRM) acquisition curves on a particle size basis for the Barroway Burn (MB), the Moonzie Burn (MB), the Kilgour Burn (KB) and the Coalpit Burn (CB) sediments. Magnetite and hematite fields, after Thompson (1986), are shown in Figure 3.5.

concentrate in the fine size fractions (>2 ϕ). Similar conclusions are reached using the high field isothermal remanence acquisition ($HIRM_{100}$) (Figure 4.19).

The frequency-dependent susceptibility ($\chi_{fd\%}$) values are less than 4% for most of the sediment samples suggesting that, even when some superparamagnetic magnetite is present, the sediments are mainly dominated by multidomain and/or stable single domain magnetite (Dearing, 1994). The ratio of the isothermal remanent magnetisation at 20 mT (IRM_{20}) to the anhysteretic remanent magnetisation (ARM) suggests a similar magnetite grain size in all size fractions within and between the sediment samples, with values between 10 and 50 pointing to stable single domain magnetite dominance (Oldfield, 1991). The $SIRM/\chi_{lf}$ and χ_{ARM}/χ_{lf} ratios show similar values for all size fractions and sediment samples in each particular stream indicating similar magnetic mineral assemblages and grain sizes.

Magnetic data for bulk samples and for each size fraction of all samples from each stream were subjected to a simultaneous R- and Q-mode factor analysis (Figure 4.21) to differentiate the magnetic mineralogy within and between the sediment samples collected along the streams. The eigenvalues show that Factors 1 and 2 explain 98.44%, 84.07%, 96.05% and 82.09% of the variation in the five magnetic parameters found to be the best magnetic mineral characteriser (χ_{lf}, χ_{ARM}, SIRM, $(Bo)_{CR}$ and D), observed in the Barroway Burn, the Moonzie Burn, the Kilgour Burn and the Coalpit Burn sediments, respectively. Factor 1 seems to be strongly influenced by the concentration-dependent parameters, whereas Factor 2 is more strongly influenced by the assemblages in which greater proportions of hard magnetic minerals (e.g. hematite) are present, as well as by the magnetic grain size. All sediment samples in the Barroway Burn (Figure 4.21a) show similar magnetic properties indicating similar magnetic mineral assemblages and grain sizes. When comparing the samples on the basis of their particle size distribution it is clear that magnetite concentration increases towards the coarser size fractions in all the samples without any differences in hematite concentration and magnetite grain size. Similar results are obtained from the sediments sampled in the Moonzie Burn (Figure 4.21b) and in the Kilgour Burn (Figure 4.21c). In the Coalpit Burn sediments, magnetite still tends to concentrate in the coarser size fractions but the trend is not so clearly seen as in the other streams (Figure 4.21d). In this case an increase in hematite concentration towards coarser size fractions is more evident.

a) *Barroway Burn*

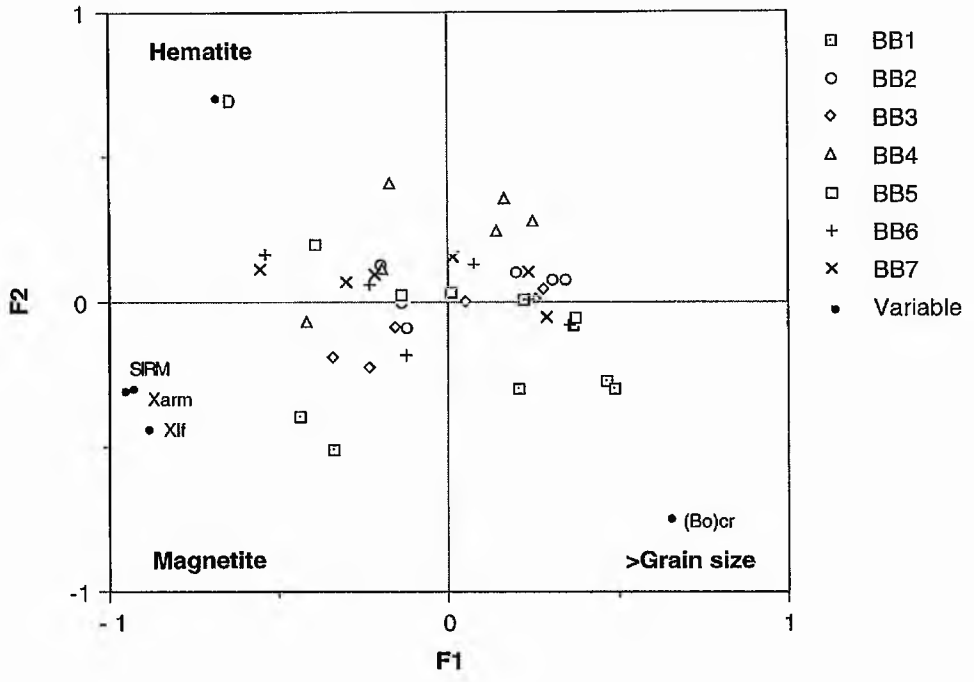

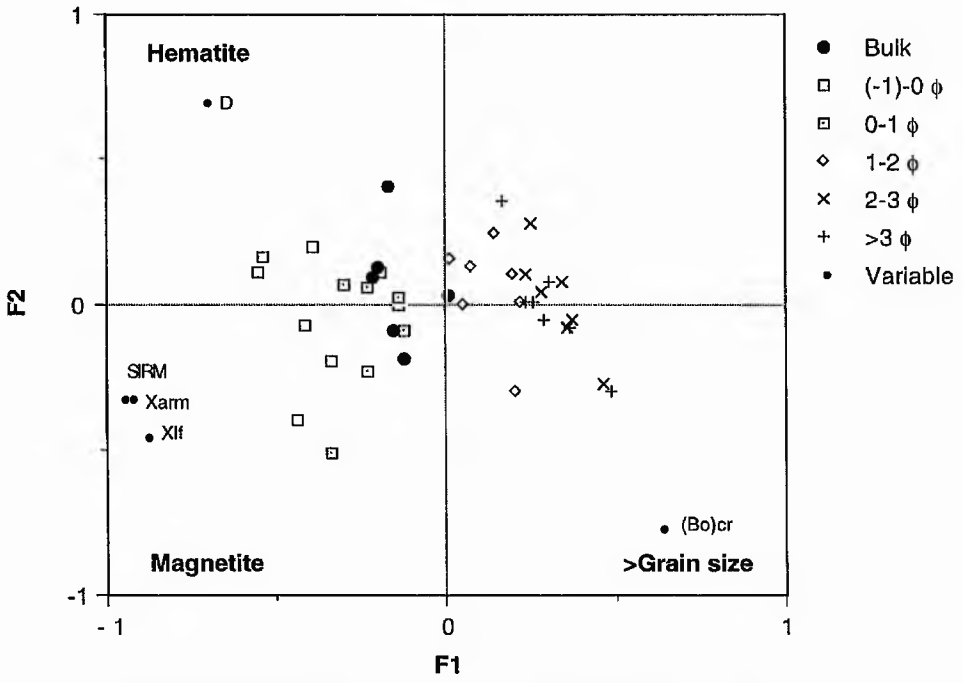

Eigenvalue (F1) = 3.45 Eigenvalue (F2) = 1.46

b) *Moonzie Burn*

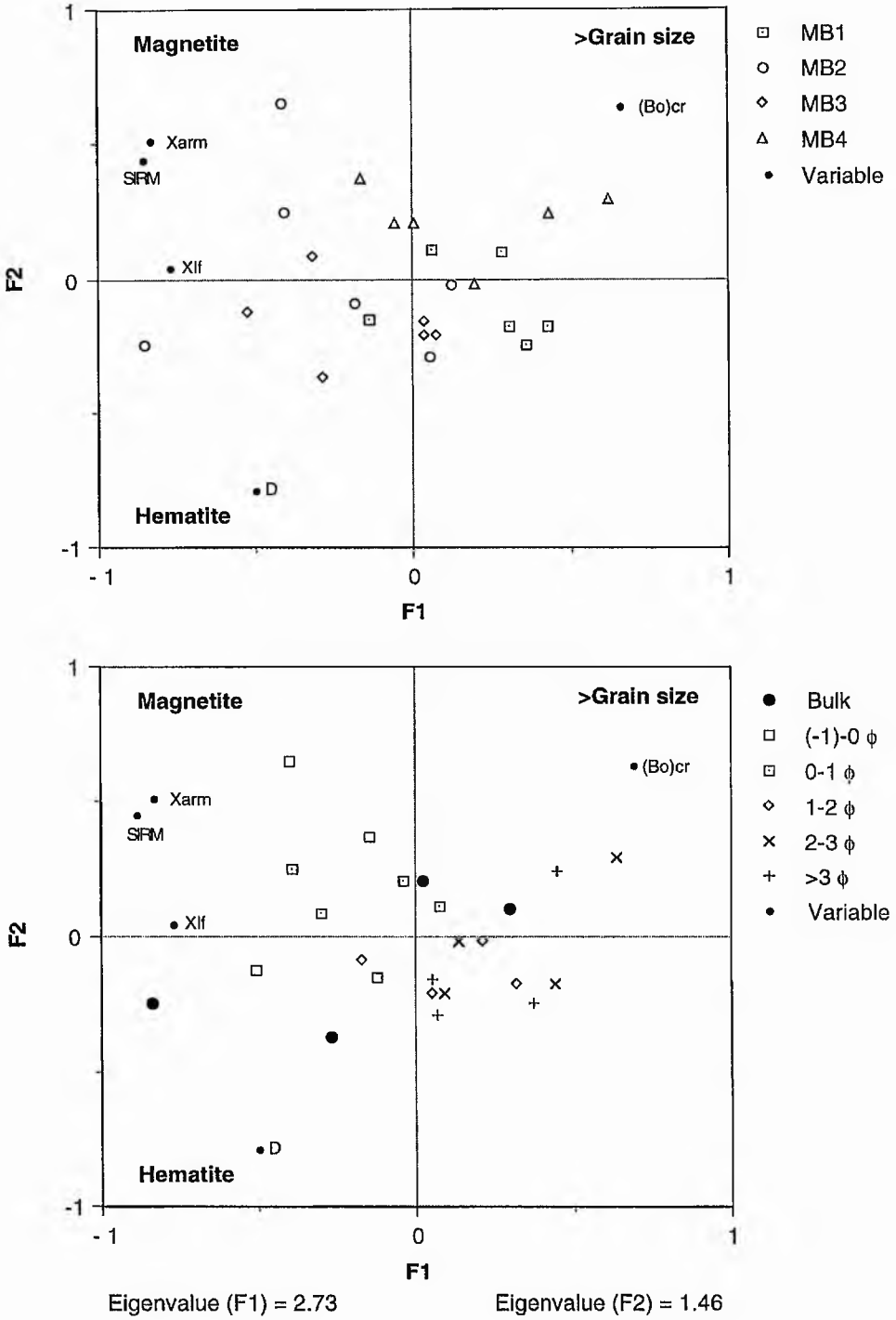

Eigenvalue (F1) = 2.73 Eigenvalue (F2) = 1.46

c) *Kilgour Burn*

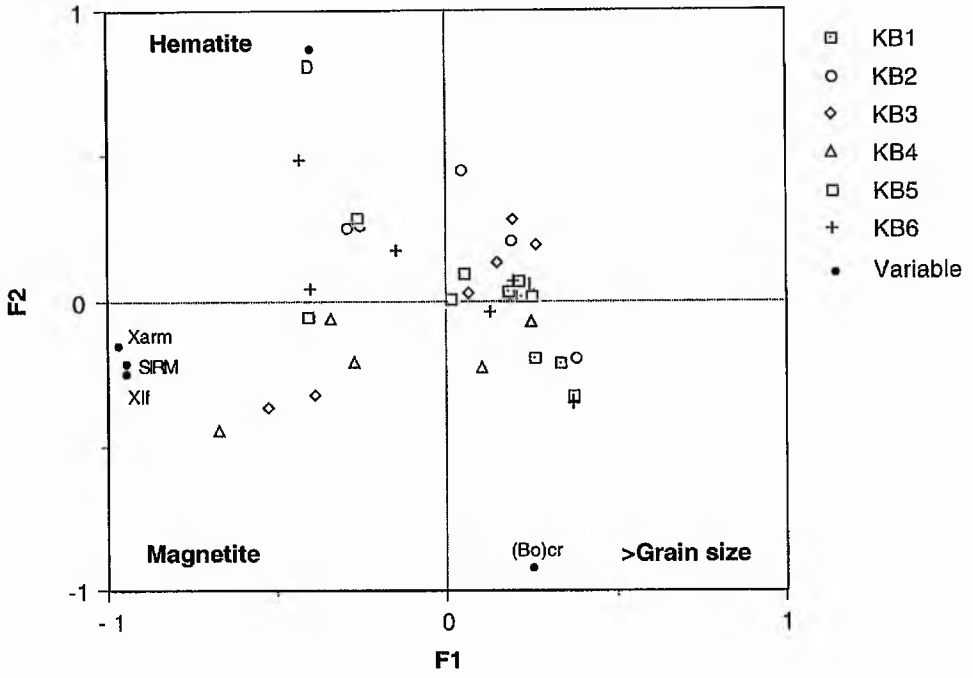

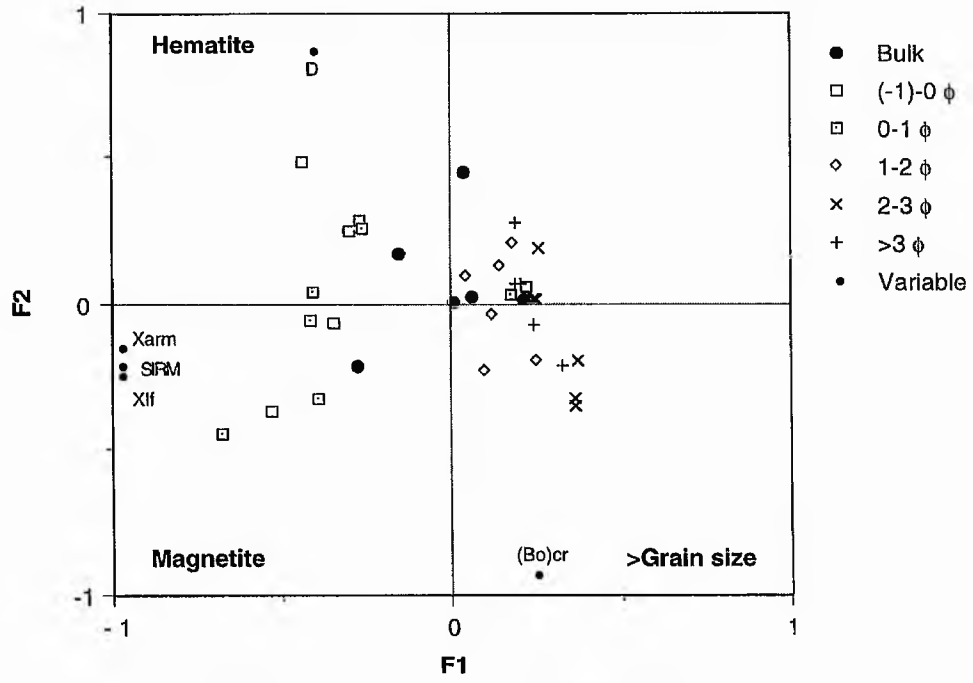

Eigenvalue (F1) = 3.02 Eigenvalue (F2) = 1.77

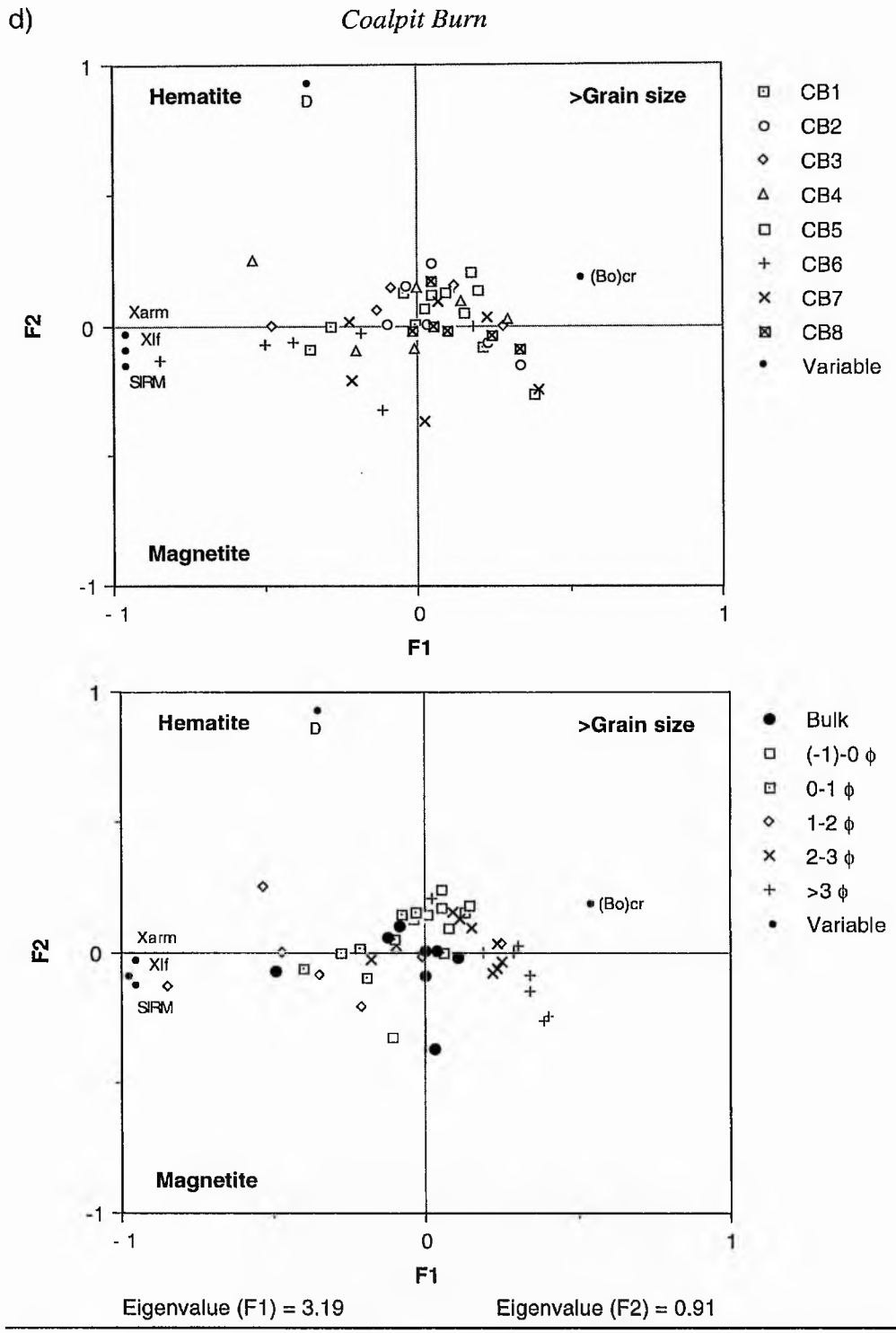

Figure 4.21. A simultaneous R- and Q-mode factor analysis of some of the main magnetic parameters measured in all sediment samples of a) the Barroway Burn, b) the Moonzie Burn, c) the Kilgour Burn, and d) the Coalpit Burn comparing the samples on the basis of their location and their particle size distributions. χ_{lf}: Magnetic susceptibility, χ_{ARM}: Susceptibility of anhysteretic remanent magnetisation, SIRM: Saturation isothermal remanent magnetisation, $(Bo)_{CR}$: Coercivity of remanence, D: Demagnetisation parameter ($=IRM_{-40}/IRM_{300}$).

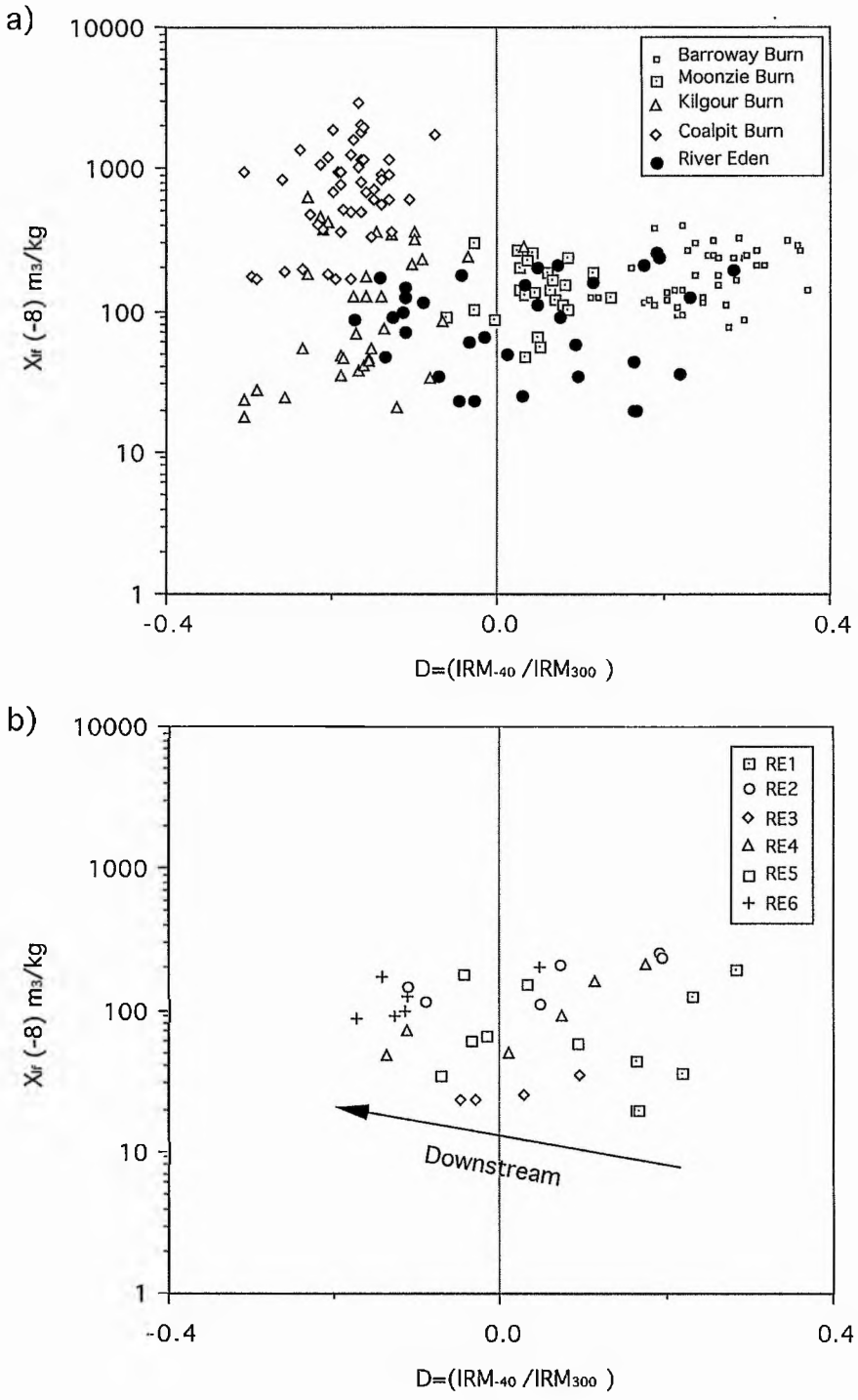

Figure 4.22. Magnetic susceptibility (χ_{lf}) versus demagnetisation parameter D (=IRM_{-40} /IRM_{300}) diagram for a) all stream sediments, and for b) the River Eden (RE) sediments (after Stott, 1986).

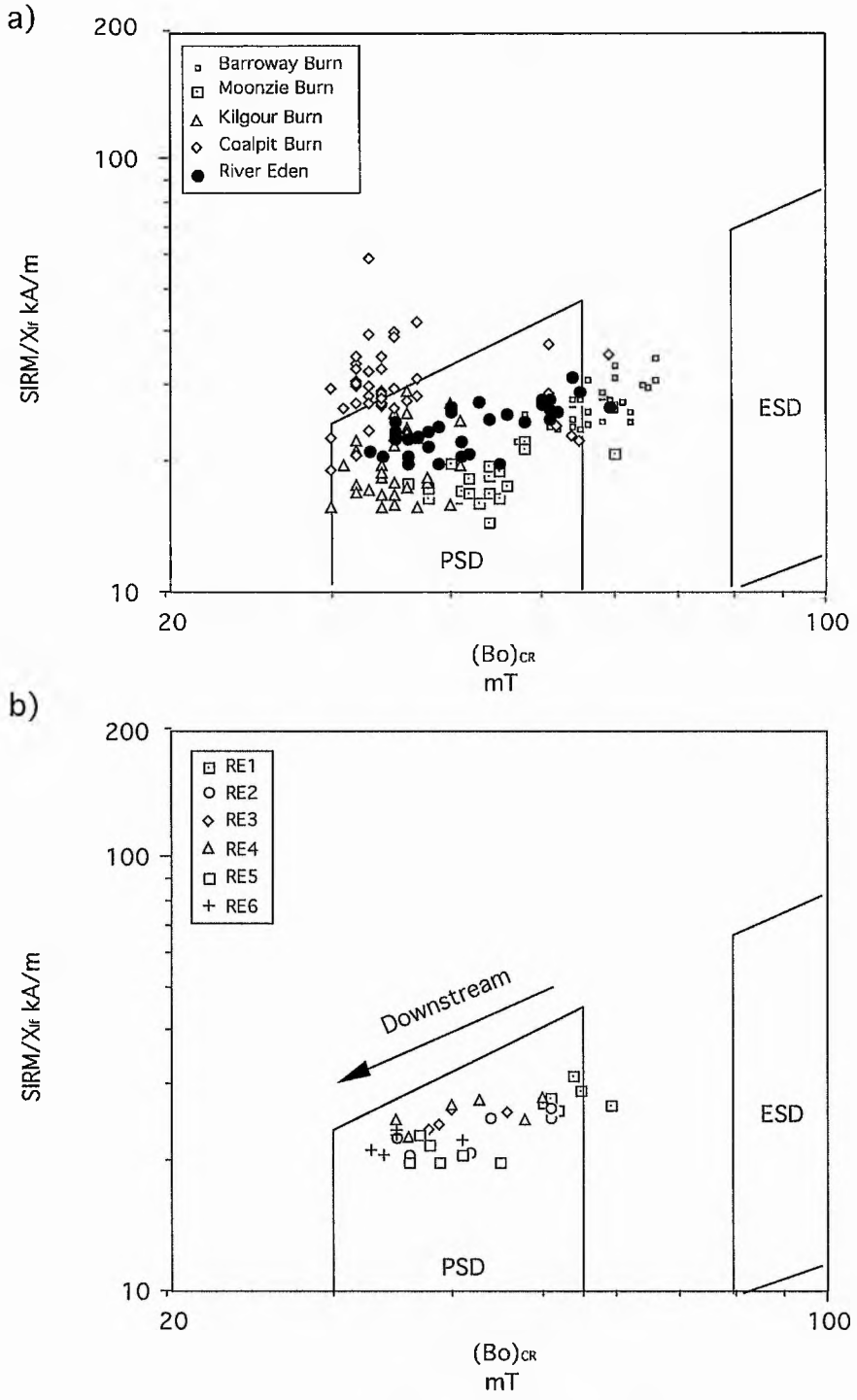

Figure 4.23. Ratio SIRM/χ_{lf} versus coercivity of remanence $(Bo)_{CR}$ diagram with grid schematically dividing magnetic mineralogies and magnetisation states for a) all stream sediments, and for b) the River Eden (RE) sediments. PSD: Pseudo-single domain, and ESD: Elongated single domain magnetite (after Thompson and Oldfield, 1986).

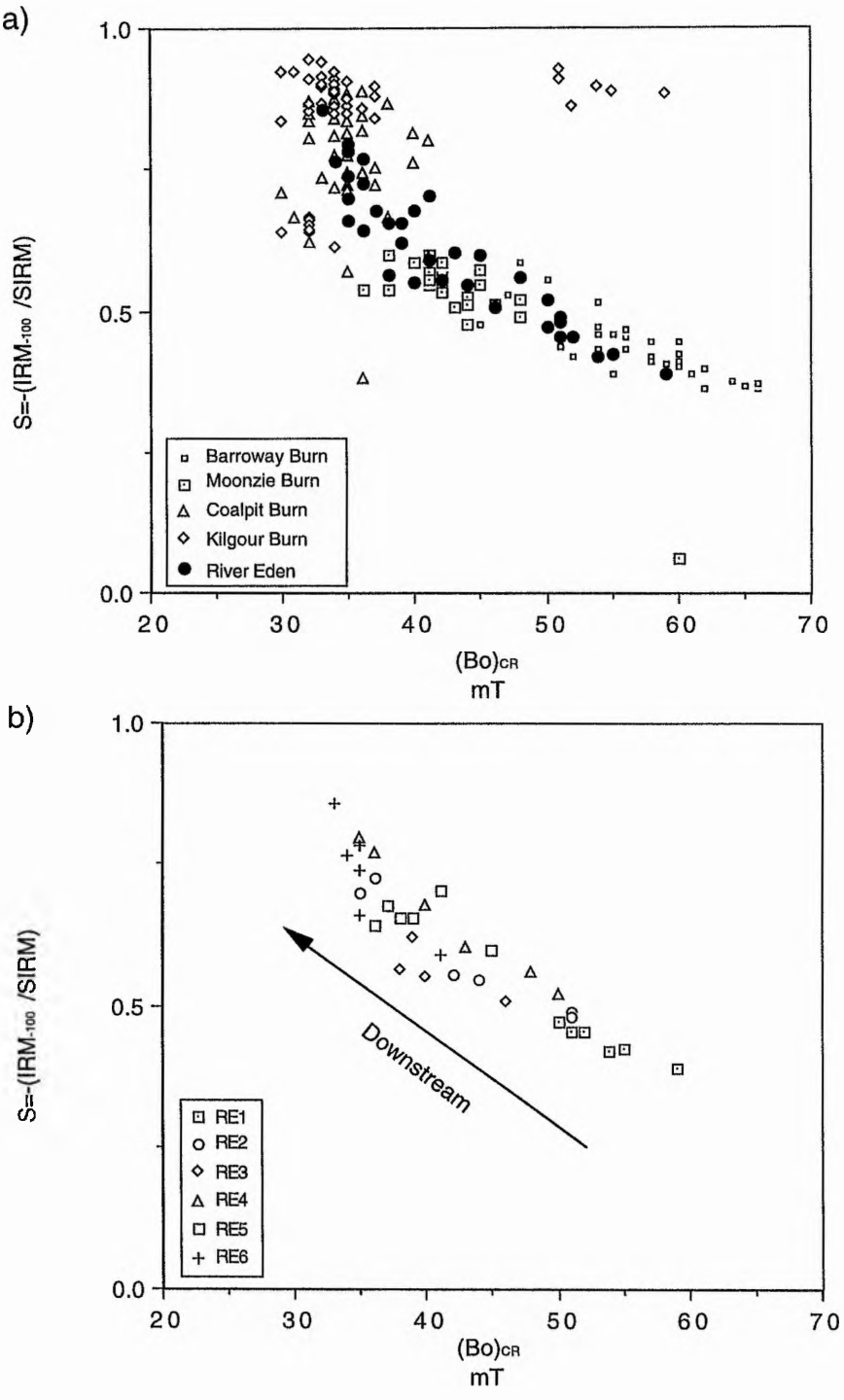

Figure 4.24. S-ratio (=-IRM_{-100}/SIRM) versus coercivity of remanence $(Bo)_{CR}$ diagram for a) all stream sediments, and for b) the River Eden (RE) sediments (after Stober and Thompson, 1979).

It is concluded from all these magnetic data that neither clear differences in the magnetic mineralogy nor in the grain size exist within and between the sediment samples along each stream, the magnetite concentration being the main cause of the variability in magnetic parameters. The magnetic properties of the bulk samples depend on the magnetic properties of each size fraction and on their particle size distribution. As sediment samples within each individual stream show similar particle size distributions then differences in magnetic properties of bulk samples are due principally to differences in magnetic mineral concentrations.

Although the sediments of each individual stream appear to be mineralogically similar, some differences were found when comparing the sediments of the four streams with one another. The χ_{lf}, χ_{ARM} and SIRM values (Figure 4.19) indicate that the Moonzie Burn, Barroway Burn, Kilgour Burn and Coalpit Burn sediments have increasing concentrations of magnetic minerals. A higher hematite concentration in the Coalpit Burn sediments compared with those of the Barroway Burn is indicated by the increase in the value of the demagnetisation parameter D (Figure 4.22a). On the other hand, the ratio of $(Bo)_{CR}$ to SIRM/χ_{lf}, which is a simple graphical method of recognising magnetic mixtures (Bradshaw and Thompson, 1985), shows in Figure 4.23a that although all sediment samples are dominated by pseudo-single domain magnetite, there is a trend of decreasing grain size towards the sediments of the Barroway Burn. The same results are seen in Figure 4.24a where the S-ratio of Stober and Thompson (1979) (useful in classifying samples with mixed magnetic mineralogy and detecting high hematite concentrations) versus the coercivity of remanence $(Bo)_{CR}$, shows that the four stream sediments clearly differ in their magnetite to hematite ratios and in magnetic grain size, both decreasing from the Coalpit Burn to the Barroway Burn sediments.

The comparison of the four stream sediments on the basis of their magnetic mineralogy was made by performing a simultaneous R- and Q-mode analysis (Figure 4.25) using the five most useful magnetic parameters (χ_{lf}, χ_{ARM}, SIRM, $(Bo)_{CR}$ and D). The eigenvalues show that Factors 1 and 2 explain 97.85% of the variation in the original five magnetic variables. Factor 1 is strongly influenced by the concentration-dependent parameters whilst Factor 2 is more strongly influenced by the assemblages in which greater proportions of hard magnetic minerals (e.g. hematite) are present, and by the magnetic grain size. The Barroway Burn, Moonzie Burn and Kilgour Burn sediments seem to have similar magnetite concentrations with increasing hematite concentration in the Barroway Burn sediments. The Coalpit Burn sediments, however, have higher magnetite concentrations and the lowest hematite concentrations. The magnetic grain size and the hematite concentration are inversely

related, sediments with lower hematite concentration showing larger magnetic grain size.

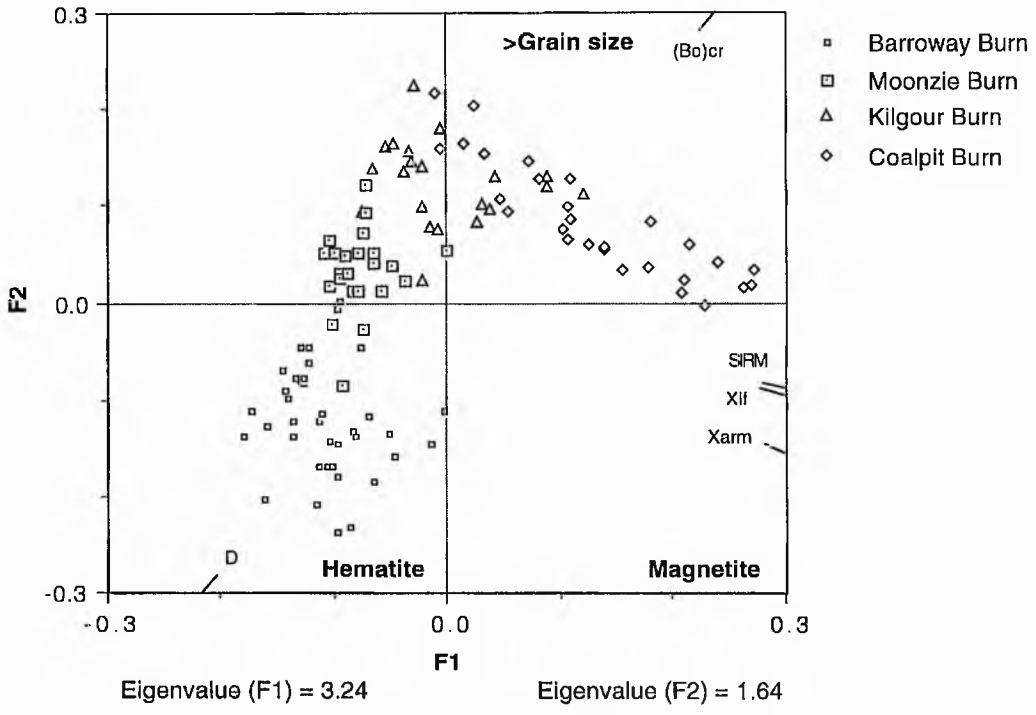

Figure 4.25. A simultaneous R- and Q-mode factor analysis of some of the main magnetic parameters measured in all stream sediments. χ_{lf}: Magnetic susceptibility, χ_{ARM}: Susceptibility of anhysteretic remanent magnetisation, SIRM: Saturation isothermal remanent magnetisation, $(Bo)_{CR}$: Coercivity of remanence, D: Demagnetisation parameter ($=IRM_{-40}/IRM_{300}$).

Sediments in the River Eden

The sediments sampled along the River Eden differ in their particle size distribution even though most samples appear to consist mainly of fine size fractions (>1 ϕ) (Figure 4.26). The magnetic properties, however, show a similar distribution for all sediment samples. The χ_{lf}, χ_{ARM} and SIRM parameters tend to be greater for the coarser size fractions (-1 to 1 ϕ) in all the River Eden sediments suggesting a concentration of magnetic minerals in such fractions (Figure 4.26b-d). The normalised isothermal remanence magnetisation (IRM) acquisition curves (Figure 4.27) for each sample show that, although the mineral assemblages are dominated by magnetite, some hematite may also be present. In all cases the hematite concentration appears to increase towards the coarser size fractions and, at the same time, the relative magnetite-hematite proportion increases downstream. Similar patterns are produced by the hard isothermal remanence magnetisation ($HIRM_{100}$)

which suggests a greater hematite concentration in the coarse fractions (-1 to 1 ϕ in size) in all sediment samples, and also a general decrease in the hematite concentration downstream (Figure 4.26e).

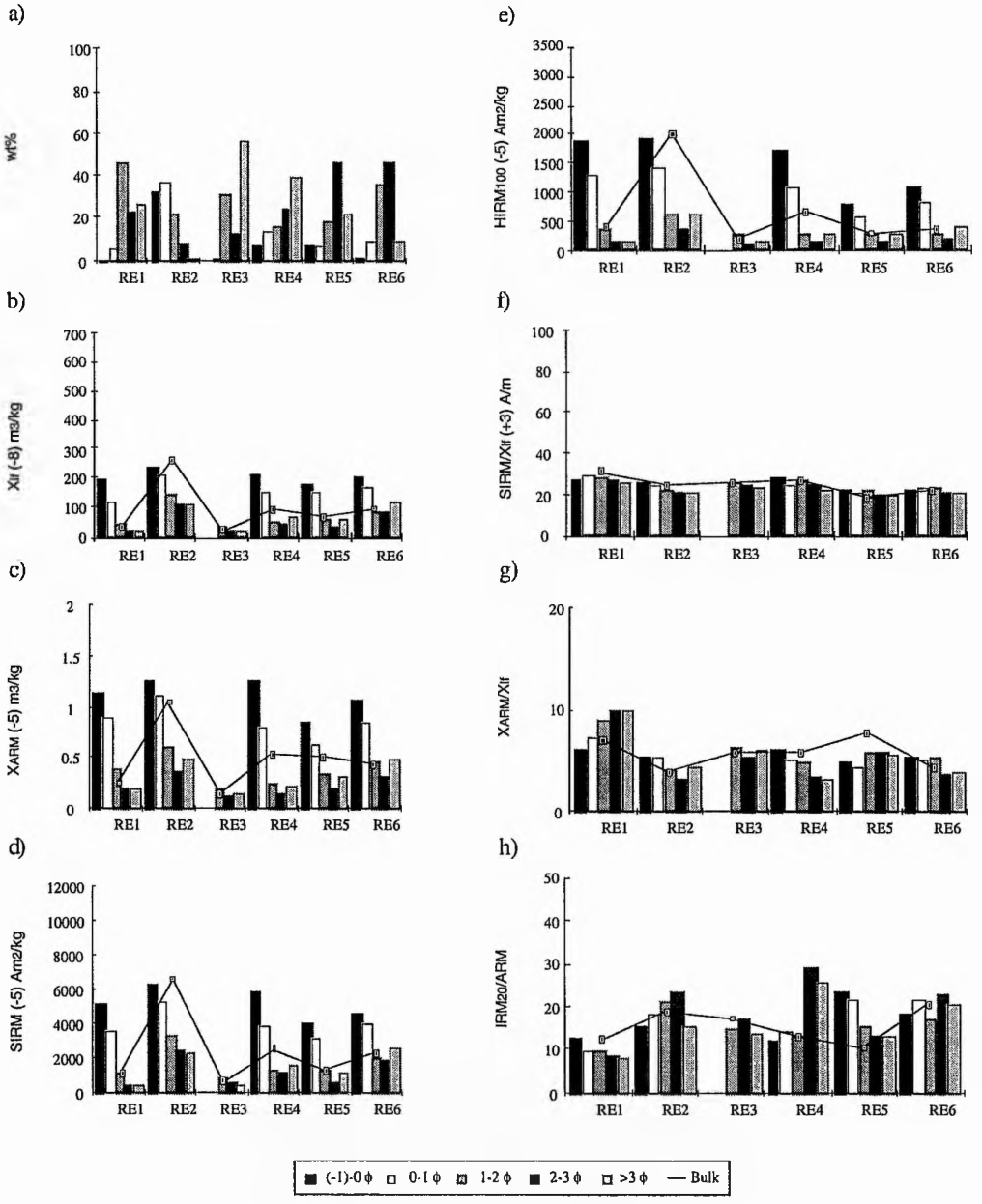

Figure 4.26. Particle size distribution in weight per cent and main concentration-dependent magnetic parameters on a particle size basis for all sediment samples collected in the River Eden (RE). χ_{lf}: Magnetic susceptibility, χ_{ARM}: Susceptibility of anhysteretic remanent magnetisation (ARM), SIRM: Saturation isothermal remanent magnetisation, $HIRM_{100}$: High field isothermal remanent acquisition at 100 mT, IRM_{20}: Isothermal remanent magnetisation at 20 mT.

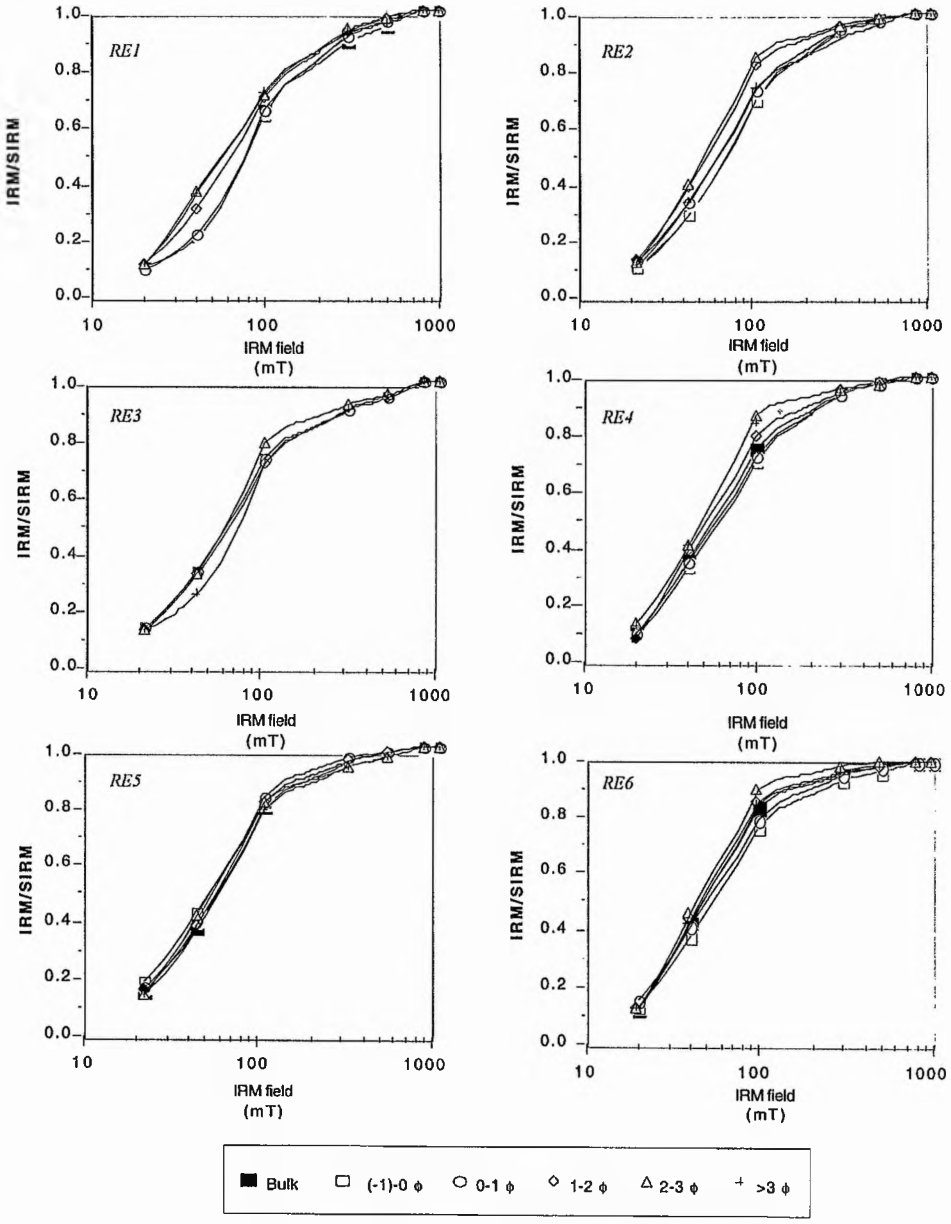

Figure 4.27. Normalised isothermal remanent magnetisation (IRM) acquisition curves on a particle size basis for the River Eden (RE) sediments. Magnetite and hematite fields, after Thompson (1986), are shown in Figure 3.5.

The frequency-dependent susceptibility ($\chi_{fd\%}$) values are, however, less than 3% suggesting that sediments are dominated by multidomain and/or stable single domain magnetite (Dearing, 1991). The ratio of IRM_{20} to ARM shows some slight variation within and between the River Eden sediments, however, all values range from 10 to 30, also suggesting a single domain magnetite dominance (Oldfield, 1991). The similar values of the ratios SIRM/χ_{lf} and χ_{ARM}/χ_{lf} (Figure 4.26f-g) for

all sediment samples confirm their homogeneity in terms of magnetic mineralogy and grain size.

The simultaneous R- and Q-mode factor analysis using the five best magnetic discriminants (χ_{lf}, χ_{ARM}, SIRM, $(Bo)_{CR}$ and D) for all the River Eden sediments is presented in Figure 4.28. Factors 1 and 2 combined explain 98.70% of the variation in the original variables. As in previous factor analyses, Factor 1 tends to reflect magnetic mineral concentration whereas Factor 2 reflects different magnetite-hematite assemblages and magnetic grain sizes. This analysis also highlights the magnetic mineral (mainly magnetite) concentration dependence of sediment magnetic properties. There is an increasing concentration in magnetic minerals towards the coarser size fractions whereas a downstream trend, consisting of an increasing relative magnetite to hematite concentration and magnetic grain size, is also observed.

The ratio of the magnetic susceptibility (χ_{lf}) to the demagnetisation parameter D (=IRM_{-40} /IRM_{300}) (Figure 4.22b) shows that, although the River Eden sediment samples cannot be discriminated on the basis of their magnetic mineral concentration, a trend in relative magnetite to hematite proportion may be seen which increases downstream. A similar trend is shown in the magnetic grain size when the ratio SIRM/χ_{lf} is plotted against the coercivity of remanence $(Bo)_{CR}$ (Figure 4.23b). All sediment samples are dominated by pseudo-single domain magnetite, as indicated by the IRM_{20}/SIRM data (Oldfield, 1991), but a range in magnetic grain size is observed in the samples, larger grains concentrating in progressively downstream sediments. This is supported by Figure 4.24b where the S-ratio (=-IRM_{-100}/SIRM) plotted versus the coercivity of remanence $(Bo)_{CR}$ shows a greater magnetite to hematite proportion, associated with larger magnetic grain size in downstream sediments. These unexpected results will be discussed in detail in Chapter 6.

It appears, therefore, that there is a difference in magnetic mineralogy in terms of mineral assemblages and magnetic grain size within the River Eden sediment samples, the magnetic mineral concentration also controlling the variability of magnetic parameters. The magnetism of the bulk samples is due therefore not only to their particle size distributions but also to differences in composition, concentration and grain size of magnetic minerals.

However, the River Eden sediments display a wider range of variability in magnetic properties compared with the four tributary stream sediments. In Figures 4.20, 4.21 and 4.22 the River Eden sediments plot in a scattered distribution

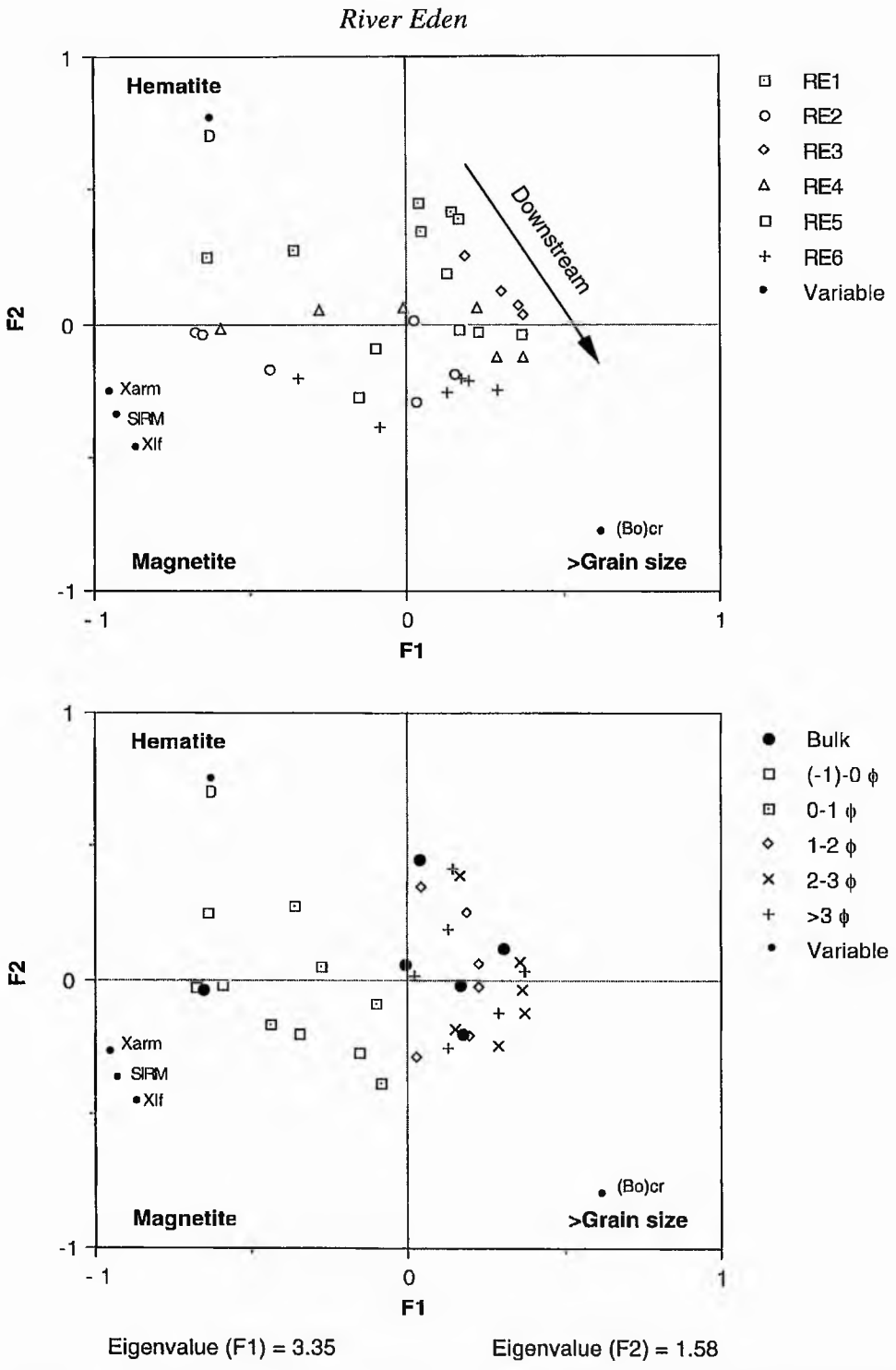

Figure 4.28. A simultaneous R- and Q-mode analysis of some of the main magnetic parameters measured in all sediment samples of the River Eden (RE) comparing the samples on the basis of their location and their particle size distribution. χ_{lf}: Magnetic susceptibility, χ_{ARM}: Susceptibility of anhysteretic remanent magnetisation, SIRM: Saturation isothermal remanent magnetisation, $(Bo)_{CR}$: Coercivity of remanence, D: Demagnetisation parameter (=IRM_{-40}/IRM_{300}).

overlapping the four groups defined by the tributary stream sediments. This indicates a mineral relationship between the River Eden and the tributary sediments, i.e. the sediments in the main channel are composed of different mixtures of the sediments supplied by the tributaries.

4.3.3. Interrelationship between chemical composition of magnetic mineralogy and magnetism of the stream sediments

Both chemical and magnetic analyses point to the homogeneity in terms of magnetic mineralogy within each of the tributary sediments of the River Eden. At the same time all streams can be distinguished as independent units. The River Eden sediments, however, show a greater magnetic mineral variability with chemical and magnetic characteristics overlapping those of the tributary streams suggesting a close mineral relationship between the River Eden and its tributaries.

The sediments transported by the Barroway Burn and the Moonzie Burn, which are known to be derived from the andesitic rocks (Figure 3.2) and the glacial till, are mainly composed of coarse sand (-1 to 1 ϕ in size). It is in such particle size fractions that most of ferrimagnetic minerals concentrate, magnetite-rich titanomagnetite being the dominant magnetic mineral. Some hematite is also found, but in relatively lower concentrations. Despite the similarity of these two stream sediments, some slight differences are observed, the Barroway Burn sediments showing greater hematite concentrations relative to magnetite, smaller magnetic grain size and titanomagnetites richer in the ulvospinel phase compared with the Moonzie Burn sediments.

The same characteristics are found in the Kilgour Burn and the Coalpit Burn sediments. The magnetic minerals present in these stream sediments are known to derive mainly from the dolerites (basalts) (Figure 3.3). The Kilgour Burn sediments are mainly 1 to 2 ϕ in size, the ferrimagnetic minerals being concentrated in the coarse fractions (-1 to 0 ϕ). On the other hand, the Coalpit Burn sediments are poorly sorted, i.e. they do not show a dominant particle size, but the ferrimagnetic minerals are mostly concentrated in the 1 to 2 ϕ size fractions. Magnetite, which is in most cases ulvospinel-rich titanomagnetite, is the principal magnetic mineral in all these sediments even when some hematite is also present. The Kilgour Burn sediments have relatively higher hematite concentrations than the Coalpit Burn sediments, but with similar magnetic grain size.

When comparing the ferrimagnetic minerals present in the sediments derived from the northern part of the Eden catchment (andesitic rocks and glacial till) with

those derived from the southern part of the Eden catchment (mainly dolerites), it is seen that they are more abundant as well as slightly larger grains in those from dolerites. Although the dominant ferrimagnetic mineral is magnetite in all sediments, hematite concentrations tend to be greater in the andesitic sediments. As mentioned above, a compositional difference is also found with magnetite being mostly ulvospinel-rich titanomagnetite in the Kilgour Burn and the Coalpit Burn sediments.

These results indicate that it is possible to discriminate sediments derived from different materials as well as those from a similar source on the basis of their ferrimagnetic mineral concentration, assemblages, chemical composition and grain size. This supports the suitability of such minerals as sedimentary provenance indicators.

5. Modelling

In Chapter 4 potential sediment sources present in the River Eden catchment were identified and mineralogically characterised on the basis of their magnetic characteristics and their Fe-Ti oxides chemical composition and morphology. These above results provide the basis on which to investigate the composition of the sediment transported by the River Eden and its tributaries in terms of the sources involved and the relative contribution of each source. In this chapter a statistical approach has been taken to modelling the sources and their contributions. Discriminant analysis provides a means of determining qualitatively the provenance of sediment by establishing the spatial relationships between the sediment sources and the sediment samples. In addition, linear programming has been used to estimate quantitatively the relative proportions of the source materials comprising the sediment samples. Thus, stream sediment samples collected in the River Eden catchment for this study are unmixed using both qualitative and quantitative approaches, the limitations of each method being discussed.

The system under consideration is very complex, with numerous variables and several sources. The application of the modelling methodologies led along various directions and produced various models for the provenance of sediment in the River Eden catchment. By changing the inputs and conditions of the models different outcomes may be possible. However, only those models which are consistent with local environmental conditions are presented in this chapter.

Although all models are quantitatively derived, the description of the model may be qualitative or quantitative, and this is used as the basis for the sections of this chapter.

5.1. Qualitative sedimentary provenance approach

Discriminant analysis was described in Chapter 3 as a method to estimate the separation between groups which, *a priori*, are known to differ from each other. This is a common statistical approach applied to geological problems. For example, some authors (e.g. Pearce and Cann, 1971; Pearce, 1974) have used discriminant functions based on major element oxides to distinguish different tectonically-defined basalt types. The discriminant functions resulting from the analysis also allow the

classification of unknown samples. Therefore, in sedimentary provenance studies, discriminant analysis may provide a means of, firstly, distinguishing sediment sources and, secondly, of determining the provenance of mixtures of sediments, as demonstrated by authors such as Darby (1984), Darby and Tsang (1986), Basu and Molinaroli (1989 and 1991), and Grigsby (1990 and 1992). All these authors used discriminant functions based on the chemical and textural characteristics of Fe-Ti oxides (magnetite and ilmenite) to group sediment samples derived from a unique and known origin, in order to recognise different sources and estimate the relative proportion of each source material (see Chapter 2).

5.1.1. Evaluation of the rocks and glacial till as sediment sources

In Chapter 4, six potential stream sediment sources were initially identified in the River Eden catchment: these comprise five rock groups differentiated on the basis of their chemical composition (basalts, basaltic andesites, andesites, dacite-rhyolites, and sedimentary rocks, including sandstones and limestones), and glacial till. Sedimentary rocks were found rarely to contain Fe-Ti oxides, whilst both igneous rocks and glacial till contain varying types and proportions of such minerals. Some differences were also seen in the grain size, texture, and mainly in the chemical composition of the Fe-Ti oxide (mainly magnetite) grains. The magnetic properties of all these materials considered as potential sources of sediments highlights the mineralogical differences among the groups and, for this reason, magnetic parameters, together with the results from the textural and chemical analysis of the magnetite grains, are used here as input parameters for discriminant analysis.

In order to establish which factors significantly and most successfully separate the six types of materials, Spearman's rank correlation coefficients and analyses of variance (Chapter 3) were first calculated, the results of these analyses being included in Appendix 5. The correlation coefficients show that most of the 28 magnetic parameters measured in the samples are significantly correlated, concentration-dependent magnetic parameters being the most highly positively correlated and, therefore, they will not effectively differentiate the groups when considered together. Major elements analysed in the magnetite grains are highly correlated, as expected. FeO and TiO_2 are positively correlated, their concentration being inversely proportional to the Fe_2O_3 concentration.

Analysis of variance tests whether the separation of the six potential sediment source materials considered is good by comparing the variation between groups with the within-group variation, for each magnetic parameter and each element

concentration in turn. However, as both analysis of variance and discriminant analysis assume normal distributions (Chapter 3), it is first necessary to know how closely the observed distributions approximate to the Gaussian distribution. This is tested by calculating the normal scores and then establishing the correlation between the original data and the normal scores of each variable for each group. When a significant correlation at a 0.05 level exists the distribution is considered to be normal. It is found that most of the magnetic variables are normally distributed, and even those which are not (basalts, basaltic andesites, andesites and glacial till) are close to normality (Table 5.1). A check was performed to test whether the results obtained from the analyses performed using raw data differ greatly from those obtained using normalised data (normalisation typically involving square roots or logs), and no significant differences were observed.

Table 5.1. Magnetic parameters and elements measured as oxides in magnetite grains found not to be normally distributed in each of the six potential stream sediment source materials distinguished in the River Eden catchment. Pearson's correlation coefficients between the original data and the calculated normal scores fall below the critical value for N number of samples the 95% confidence level, and therefore the hypothesis of normality is rejected. Note the low number of samples (N).

	Magnetic parameter	**Pearson's correlation coefficient**	**N**	**Critical value for a level of significance of $\alpha = 0.05$**
Basalts	$SIRM/\chi_{lf}$	$r_p = 0.7360$	5	$\alpha = 0.8804$
	MgO	$r_p = 0.8320$	7	$\alpha = 0.8955$
Basaltic Andesites	$(Bo)_{CR}$	$r_p = 0.8420$	7	$\alpha = 0.8955$
	χ_{ARM}/χ_{lf}	$r_p = 0.8090$		
	SiO_2	$r_p = 0.8500$		
	MgO	$r_p = 0.8160$		
Andesites	IRM_{-20}	$r_p = 0.8560$	5	$\alpha = 0.8804$
	IRM_{-40}	$r_p = 0.8600$		
	$HIRM_{40}$	$r_p = 0.8670$		
	$HIRM_{100}$	$r_p = 0.8500$		
	MnO	$r_p = 0.8060$	8	$\alpha = 0.9029$
Glacial Till	IRM_{-40}	$r_p = 0.6720$	8	$\alpha = 0.9030$
	$HIRM_{500}$	$r_p = 0.8880$		
	IRM_{20}/ARM	$r_p = 0.8950$		
	MgO	$r_p = 0.8690$	3	$\alpha = 0.8700$

The outcome of this analysis was that raw magnetic measurements were used in both the analysis of variance and the discriminant analysis, in preference to transformed variables, in order to represent the natural situation most closely. On the other hand, the concentration of the eight main elements analysed (as weight per cent oxides) in magnetite grains is found not to be normally distributed when all of the analyses are taken into account for the statistical analyses. Mean chemical composition of magnetite for each rock and glacial till sample, however, shows a normal distribution for most of the elements analysed. Those elements being non-normally distributed are given in Table 5.1, in which it is clear that, nevertheless, they are close to normality. As for the magnetic parameters, mean values of the magnetite chemical composition were used to perform both analyses of variance and discriminant analyses without any applied mathematical transformation.

All six main potential sediment sources

One-way analysis of variance (ANOVA) was carried out for each of the 28 magnetic parameters measured in 39 samples of the six potential sources of stream sediments identified in the River Eden catchment, and for each of the 8 elements analysed as oxides in magnetite grains from the samples. In the latter case two different analyses were undertaken, one using Mood's median test (Chapter 3) applied to all magnetite chemical analyses, and the second using one-way ANOVA applied to magnetite mean composition values.

Six groups are distinguished as potential sediment sources, including: basalts (em8, em11, em17, em21, em22, em38 and em43), basaltic andesites (em1, em13, em14, em15, em16, em31 and em34), andesites (em2, em3, em4, em5 and em30), dacite-rhyolites (em18, em19 and em20), sedimentary rocks (em12, em41 and em42), and glacial till (Till BB1 and Till BB4 (including bulk, (-1)-0 ϕ, 0-1 ϕ, 1-2 ϕ, 2-3 ϕ and >3 ϕ fractions), and Till CB7 (only bulk sample)). The tuffite sample (em36) was neither included in the analysis of variance nor in the discriminant analysis. This is due to its aberrant chemical-magnetic behaviour (Section 4.1), and its exclusion is justified on the grounds of being volumetrically insignificant as a potential sediment source, as shown in the geological map of the study area (Figure 2.1). Note also that the sedimentary rocks group is excluded from the analyses performed only using magnetite chemical composition data because magnetite was very scarce or absent in these rock types.

In most cases the mean values of each parameter for the different groups are well separated, the standard deviation values show a significant range of variability within the groups. The groups thus overlap making their separation difficult.

However, F-ratios (chi-square in Mood's median test) indicate whether or not the result of the analysis of variance for each variable is significant, i.e. if the test of the null hypothesis that the means (or medians in Mood's median test) of the groups are no different. In this context, with the exception of IRM_{-20}, all the magnetic parameters suggest that there is a significant difference among the means of the groups being considered. Using a chi-square test, with the exception of the Al_2O_3 concentration in magnetite grains, all the other analysed elements are likely to discriminate between the groups. Furthermore, considering magnetite mean compositions for each sample, only FeO seems to differ significantly between the groups. The greater the F-ratio or the chi-square value, and the smaller the p-value, the more effective the parameter will be in the discriminant analysis. In Table 5.2

Table 5.2. Variables found by one-way analysis of variance (ANOVA) to contribute most to the discrimination of the six potential stream sediment sources distinguished in the River Eden catchment. Critical value of F with 5 and 33 degrees of freedom is 3.64 at the 99% confidence level.

Variable	Source of variation	Sum of Squares	Degrees of freedom	Variance or mean square	F-ratio	p
χ_{lf}	Means	12521402	5	2504280	11.41	< 0.0001
	Within	7241830	33	219449		
	Total	19763232	38			
$\chi_{fd\%}$	Means	92.634	5	18.527	30.04	< 0.0001
	Within	20.354	33	0.617		
	Total	112.988	38			
χ_{ARM}	Means	65.900	5	13.180	14.66	< 0.0001
	Within	29.669	33	0.899		
	Total	95.569	38			
IRM_{20}	Means	71426128	5	14285226	23.67	< 0.0001
	Within	19917442	33	603559		
	Total	91343568	38			
IRM_{-40}	Means	430001792	5	86000360	10.58	< 0.0001
	Within	268217264	33	8127796		
	Total	698219072	38			
$(Bo)_{CR}$	Means	507852	5	101570	69.82	< 0.0001
	Within	48004	33	1455		
	Total	555856	38			
IRM_{20}/ARM	Means	3444.5	5	688.9	14.74	< 0.0001
	Within	1542.1	33	46.7		
	Total	4986.7	38			
D	Means	18.4241	5	3.6848	41.87	< 0.0001
	Within	2.9040	33	0.0880		
	Total	21.3281	38			

those parameters which contribute most to the discrimination of the six source materials are given.

Discriminant analysis was carried out using the SPSS statistical package. Basaltic andesites and andesites could not be separated successfully in any cases, and one-way analysis of variance indicates that the chemical composition of magnetite grains has poor discriminating power. When discriminant analysis was performed on magnetite chemical analyses, no successful discrimination was obtained. Thus, discriminant analysis used as a means of separating and differentiating the six types of potential sediment source materials resulted in a reduction of the groups to five, those being discriminated on the basis of their magnetic characteristics uniquely.

Discriminant functions, scaled eigenvectors, eigenvalues and the results of the tests of significance applied to each of the functions obtained from the discriminant analysis are given in Table 5.3. The SPSS program also displays the misclassified observations, indicating in this case that 92% of the grouped cases are correctly classified. Only three of the four discriminant functions obtained from the analyses are significant at a level of 0.01. Also, the eigenvalues indicate that Functions 1 and 2 contain a total of 83% of the information available for separating the 5 groups. The scaled eigenvector shows the largest scores for $\chi_{fd\%}$ (0.41) and D (0.75) parameters in Function 1. Therefore, Function 1 was the most effective at separating groups with low $\chi_{fd\%}$ and D values from those with high $\chi_{fd\%}$ and D values, i.e. those groups varying in magnetic grain size and in relative hematite to magnetite concentration (Appendix 2). On the other hand, the largest scores on the second function are for $\chi_{fd\%}$(-0.79) and SIRM/χ_{lf} (0.79). This Function 2 is the most effective at separating groups with high $\chi_{fd\%}$ and low SIRM/χ_{lf} from those with low $\chi_{fd\%}$ and high SIRM/χ_{lf}, i.e. groups varying in magnetic grain size and concentration of magnetic minerals (Appendix 2).

The discriminant functions used as axes in a scattergram show the location of the groups in the discriminant space. Figure 5.1 is a plot of Function 1 versus Function 2, the group boundaries being fitted by eye. The basalts, andesites and glacial till groups lie close together, whereas the dacite-rhyolites and the sedimentary rocks are clearly separated. In terms of the scaled eigenvectors, the basalts, andesites and sedimentary rocks occupy different fields because they differ in the concentration of magnetic minerals concentration and in grain size of such minerals, both increasing from sedimentary rocks to basalts. Whereas dacite-rhyolites, sedimentary rocks and glacial till show a greater relative hematite to magnetite

concentration than basalts and andesites. These results are wholly consistent with the findings of Chapter 4, adding confidence to the results of discriminant analysis.

Table 5.3. Results of discriminant analysis performed using magnetic parameters in order to separate spatially all the potential stream sediment sources distinguished in the River Eden catchment. The initial six sources are reduced to five by considering basaltic andesites and andesites altogether (see text for explanation).

	F1	F2	F3	F4
		Eigenvectors		
Constant	-1.1626437	-0.6437638	-1.5561036	-1.5764569
$\chi_{fd\%}$	0.5161189	-1.0013829	0.7508437	0.3137160
IRM_{20}	-0.0004082	0.0009459	-0.0011034	0.0001206
$HIRM_{100}$	-0.0001549	-0.0006320	-0.0006463	0.0010033
D	2.5708639	1.8604876	-0.2246964	0.6351680
$SIRM/\chi_{lf}$	0.0128825	0.0776118	0.0042304	-0.0178701
		Scaled eigenvectors		
$\chi_{fd\%}$	0.41061	-0.79667	0.59735	0.24958
IRM_{20}	-0.32227	0.74664	0.87096	0.09526
$HIRM_{100}$	-0.14497	-0.59123	-0.60456	0.93849
D	0.75800	0.54855	-0.06625	0.18727
$SIRM/\chi_{lf}$	0.13205	0.79556	-0.04336	-0.18318
		Discriminating efficiency		
Eigenvalues	8.9329	5.0395	2.5364	0.2213
% of variance	53.39	30.12	15.16	1.32
Cumulative %	53.39	83.52	98.68	100
		Test of significance		
Wilk's Lambda	0.0033859	0.038336	0.231529	0.818770
Chi-square	183.389	107.625	48.281	6.598
d.f.	20	12	6	2
p-value	<0.00001	<0.00001	<0.00001	0.0369
Chi-square at 0.01 significance level	37.6	26.2	16.8	9.22

Function 3 should not be ignored as it explains 15.16% of the total variation among the groups. The scaled eigenvectors show that IRM_{20} (0.87) and $HIRM_{100}$ (-0.60) have the greatest scores for this function. Thus, Function 3 is most effective in separating groups on the basis of their magnetite and hematite concentrations, as suggested by the IRM_{20} and $HIRM_{100}$ values (Appendix 2), respectively. However, the use of Function 3 in scatter plots does not improve the discrimination of groups and is not discussed further.

Discriminant function analysis provides not only a classification of groups known to differ from one another but also the possibility of classifying samples of unknown origin. Therefore, those functions which best separate the five potential stream sediment sources under consideration are used here to determine the location of the stream sediment samples in discriminant functions space and to understand their relationships with their potential source materials. The results are shown in Figure 5.1 indicating that most of the stream sediment samples approximately line up between the fields of basalt and sedimentary rocks. Only some Coalpit Burn sediment samples appear displaced on the left-hand corner of the diagram. Some anomalies were detected in the measurements of the isothermal remanent magnetisation acquired by the Coalpit Burn sediment samples at different magnetic field intensities (Chapter 4). Such anomalies are the most probable explanation for the results observed in Figure 5.1. Also sample MB4 plots away from the remaining Moonzie Burn samples along Function 2 axis. This is due to the greater $SIRM/\chi_{lf}$ value of the MB4 sample compared to the rest of the Moonzie Burn samples, as discussed in Chapter 4, as Function 2 was found to explain the separation of the groups in terms of their $\chi_{fd\%}$ and $SIRM/\chi_{lf}$ values.

No relationship seems to exist between the stream sediment samples and the dacite-rhyolite group. This suggests that even when such a group is a potential source of sediments in the River Eden catchment its actual contribution to the sediment budget may be small. This is consistent with the geology of the River Eden catchment in which neither dacites nor rhyolites constitute a volumetrically significant rock group (Figure 2.1). Indeed none of the chosen tributaries and any of the sampling points along the River Eden occur on these rock types (Figure 1.1). For this reason and for reasons of simplicity, the dacite-rhyolites group has been excluded as a source of stream sediments for the remainder of this study.

Both the Barroway Burn and the Moonzie Burn sediments plot within the glacial till group and along its boundary with the andesite group (Figure 5.1), whereas the Kilgour Burn and the Coalpit Burn sediments span the basalt and the andesite groups tracking towards the sedimentary rocks group. A boundary between

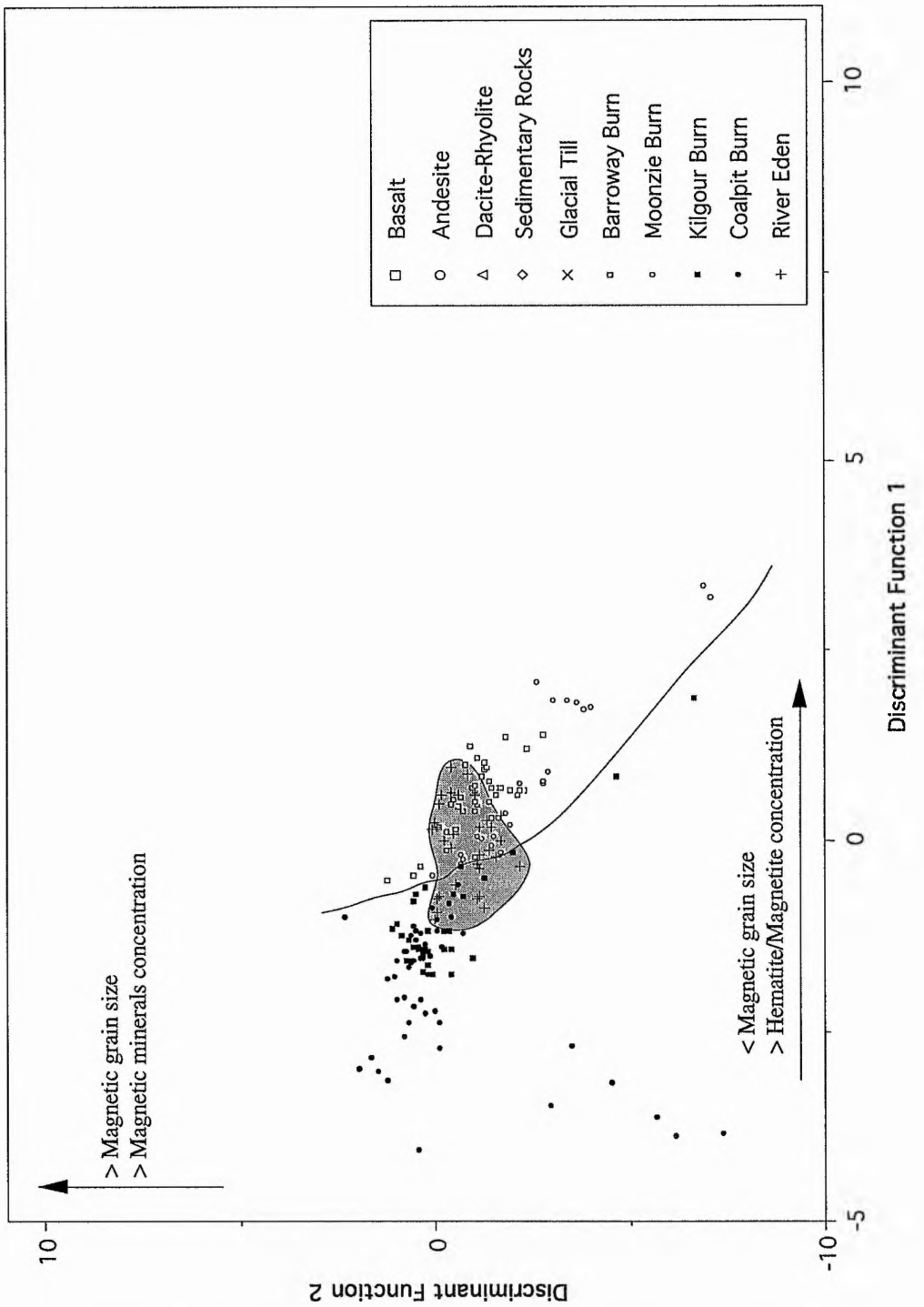

Figure 5.1. Plot of discriminant Function 1 versus discriminant Function 2 separating samples from five potential sources of stream sediments distinguished in the River Eden catchment. Stream sediment samples are also included in order to see their relationship with the sources (see text for explanation). Boundaries for rocks and glacial till groups, as well as for the River Eden sediments (shaded field), are fitted by eye. A line is also drawn which separates 'andesitic' from 'basaltic' stream sediment samples.

these sets of sediments is drawn in Figure 5.1. The sediments of the River Eden tributaries, Kilgour Burn and Coalpit Burn, are known to be derived principally from the basalts and the sedimentary rocks, whilst those transported by the Barroway Burn and the Moonzie Burn are known to be derived mainly from the andesites (Chapter 3).

Both the Barroway Burn and the Moonzie Burn sediments plot within the glacial till group and along its boundary with the andesite group (Figure 5.1), whereas the Kilgour Burn and the Coalpit Burn sediments span the basalt and the andesite groups tracking towards the sedimentary rocks group. A boundary between these sets of sediments is drawn in Figure 5.1. The sediments of the River Eden tributaries, Kilgour Burn and Coalpit Burn, are known to be derived principally from the basalts and the sedimentary rocks, whilst those transported by the Barroway Burn and the Moonzie Burn are known to be derived mainly from the andesites (Chapter 3).

The results observed in Figure 5.1 are interpreted as follows:

(1) The Coalpit Burn and the Kilgour Burn sediments comprise a mixture of basalts and sedimentary rocks in various proportions, the relative contribution of each source to the sediment sample being a function of its proximity to the field of the source groups. The reason that all the Kilgour Burn sediment samples and most of the Coalpit Burn sediments plot within the andesite group could be a reflection of the intermediate characteristics of the andesite group between those of the basalt and the sedimentary rocks.

(2) The Barroway Burn and the Moonzie Burn sediments are mixtures of andesites, glacial till and sedimentary rocks in various proportions.

(3) All the River Eden sediments plot within the andesite and the glacial till groups suggesting that they are mixtures of all four rock types and glacial till groups. However, due to the proximity of the basalt, andesite and glacial till groups in discriminant function space, the analysis fails to estimate the relative source proportions constituting the sediment samples. Furthermore, one of the andesite samples (indicated by a small arrow in Figure 5.1) introduces some doubt about the independence of the glacial till group as it could be a subgroup within the andesite group.

Basalts, andesites and glacial till

A further discriminant analysis, the results of which are given in Table 5.4, was performed with the aim of separating the basalt, andesite and glacial till groups. In this case 100% of the grouped cases were correctly classified. However, the second function obtained is not significant at a level of 0.01 and explains only 1.25%

Table 5.4. Results of discriminant analysis performed using magnetic parameters and magnetite mean composition in order to separate spatially the basalt, andesite and glacial till groups.

	F1	**F2**
	Eigenvectors	
Constant	146.9370851	1.5544114
IRM_{20}	-0.0028172	0.0008003
$HIRM_{100}$	0.0048761	-0.0002430
$(Bo)_{CR}$	1.3621568	0.1056286
FeO	-2.3959664	0.0368575
	Scaled eigenvectors	
IRM_{20}	-2.30914	0.65600
$HIRM_{100}$	5.84981	-0.29162
$(Bo)_{CR}$	7.85294	0.60896
FeO	-8.67097	0.13339
	Discriminating efficiency	
Eigenvalues	343.2917	4.3597
% of variance	98.75	1.25
Cumulative %	98.75	100
	Test of significance	
Wilk's Lambda	0.000542	0.186576
Chi-square	33.842	7.555
d.f.	8	3
p-value	<0.00001	0.0562
Chi-square at 0.01 significance level	20.1	11.3

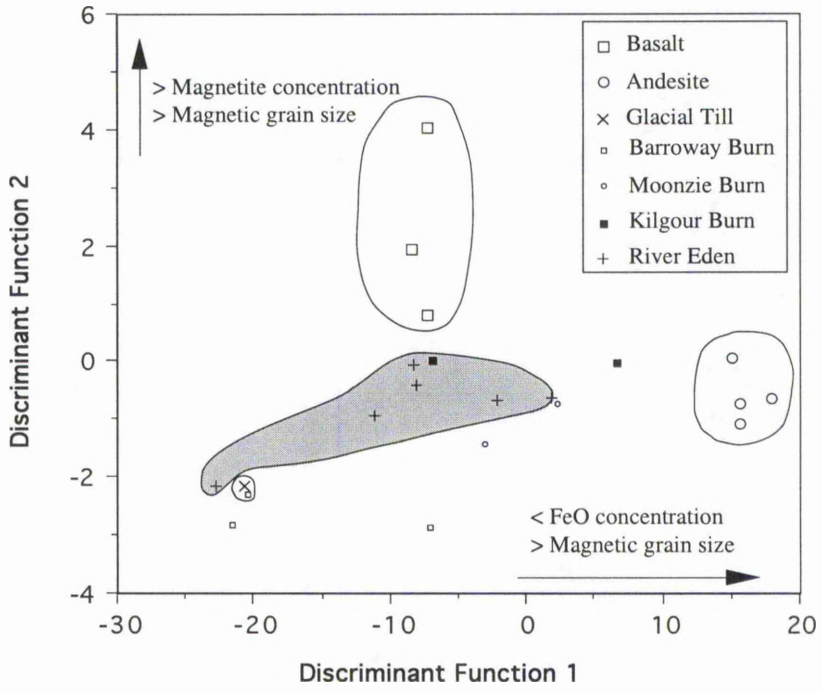

Figure 5.2. Plot of discriminant Function 1 versus discriminant Function 2 separating basalt, andesite and glacial till groups on the basis of magnetite mean composition and magnetic parameters of the samples. Stream sediment samples are also plotted in order to determine their relationship with these three potential sediment sources. Boundaries for rocks and glacial till groups, as well as for the River Eden sediments (shaded field), are fitted by eye.

of the total variation among the groups. The scaled eigenvectors indicate that discriminant Function 1 is the most effective at separating the groups on the basis of their magnetite FeO content and their magnetic grain size, which is consistent with their greater FeO (-8.67) and $(Bo)_{CR}$ (7.85) scores. Scaled eigenvectors for discriminant Function 2 show the largest scores for IRM_{20} and $(Bo)_{CR}$, suggesting an effective separation of the groups on the basis of their magnetite concentration and their magnetic grain size (Appendix 2). Using both discriminant functions in a scattergram (Figure 5.2) where samples of basalts, andesites and glacial till are plotted, the three groups appear well separated. As expected, Function 1 best separates the rocks and glacial till groups, nevertheless, the location of the groups along this function does not seem to agree with the results gives previously in Chapter 4. Function 1 best separates the groups on the basis of their magnetite FeO content and grain size, however, it was seen in Chapter 4 that both variables decrease from basalts to glacial till through the andesites.

Discriminant Function 2 is less effective at separating the groups compared with Function 1, but the variation in magnetite concentration and magnetic grain size observed in the groups along this function is consistent with the conclusions of Chapter 4, with both variables increasing towards the basalt group. As in the previous discriminant analysis, stream sediment samples are plotted in relation to the three source materials under consideration (Figure 5.2). The Kilgour Burn and the Moonzie Burn sediment samples plot close to the basalt and the andesite groups, whilst the Barroway Burn sediment samples are closer to the glacial till group. The latter is consistent with the proximity of the samples to an exposure of glacial till. The River Eden sediment samples span from the basalt and andesite groups towards the glacial till group, suggesting that such sediments result from a mixing process which involves all three source groups in varying proportions.

Basalts, andesites and sedimentary rocks

A third discriminant analysis was performed in order to obtain better separation of basalt, andesite and sedimentary rocks groups so as to estimate, qualitatively, the contribution of sedimentary rocks to the stream sediments. The analysis classified 95% of the grouped cases correctly. The results (Table 5.5) show that both discriminant functions are significant at a level of 0.01, with Function 1 explaining 91% of the distribution of the groups within the discriminant space and Function 2 containing approximately 9% of the total discriminating power. The scaled eigenvectors show the largest scores for χ_{ARM} and $\chi_{fd\%}$ in Function 1 and for IRM_{20} and χ_{ARM} in Function 2. Therefore, the three groups are separated on the basis of their magnetic grain size and of their magnetite concentration and grain size by the discriminant Functions 1 and 2, respectively. Rock samples are plotted within the discriminant space, along with the stream sediment samples (Figure 5.3). As with Figure 5.1, basalt and andesite samples fall in similar areas, in this case defining overlapping areas. With the exception of most of the Coalpit Burn sediments, the remaining tributary sediment samples plot within the andesite field, defining a trend towards the sedimentary rocks group. The River Eden sediment samples plot in a grouping from the andesite towards the sedimentary rocks groups.

In an attempt to better separate basalts from andesites, another discriminant analysis was performed using those two variables only which were found in the previous analysis to be the most effective at separating the three groups (basalts, andesites and glacial till) under consideration, on the basis of the significance of their Wilk's Lambda values. In Table 5.6, $\chi_{fd\%}$ and IRM_{20} show the lowest and the most significant Wilks' Lambda values at a 0.01 level with F-ratios of 71.45 and 21.77,

respectively, which are both significant at the 0.01 level, and are greater than the F-ratio values for $(Bo)_{CR}$ and χ_{ARM} (19.56 and 13.54, respectively). Thus, these two variables only are used in this new discriminant analysis, the results of which are included in Table 5.5 together with the results of the previous discriminant analysis.

Table 5.5. Results from the two discriminant analyses performed using magnetic parameters in order to spatially separate basalt, andesite and glacial till groups. In the first analysis the groups are discriminated on the basis of their $\chi_{fd\%}$, IRM_{20}, χ_{ARM} and $(Bo)_{CR}$ values, whereas in the second one the groups are discriminated on the basis of their $\chi_{fd\%}$ and IRM_{20} values.

	F1	**F2**	**F1**	**F2**
		Eigenvectors		
Constant	4.2090550	-1.8855999	-1.3766917	-2.1741461
$\chi_{fd\%}$	-1.4508579	0.3212243	1.2238407	0.4304854
IRM_{20}	-0.0009887	0.0015482	-0.0002993	0.0009012
χ_{ARM}	1.0511087	-0.6382809		
$(Bo)_{CR}$	0.0566865	-0.0017466		
		Scaled eigenvectors		
$\chi_{fd\%}$	-1.11850	0.24764	0.94349	0.33187
IRM_{20}	-1.04125	1.63054	-0.31524	0.94917
χ_{ARM}	1.31969	-0.80137		
$(Bo)_{CR}$	0.84571	-0.02606		
		Discriminating efficiency		
Eigenvalues	19.5917	1.8763	8.1792	1.5638
% of variance	91.26	8.74	83.95	16.05
Cumulative %	91.26	100	83.95	100
		Test of significance		
Wilk's Lambda	0.016884	0.347668	0.042493	0.390051
Chi-square	71.424	18.489	58.431	17.417
d.f.	8	3	4	1
p-value	<0.00001	0.0003	<0.00001	<0.00001
Chi-square at 0.01 significance level	20.1	11.3	13.3	6.64

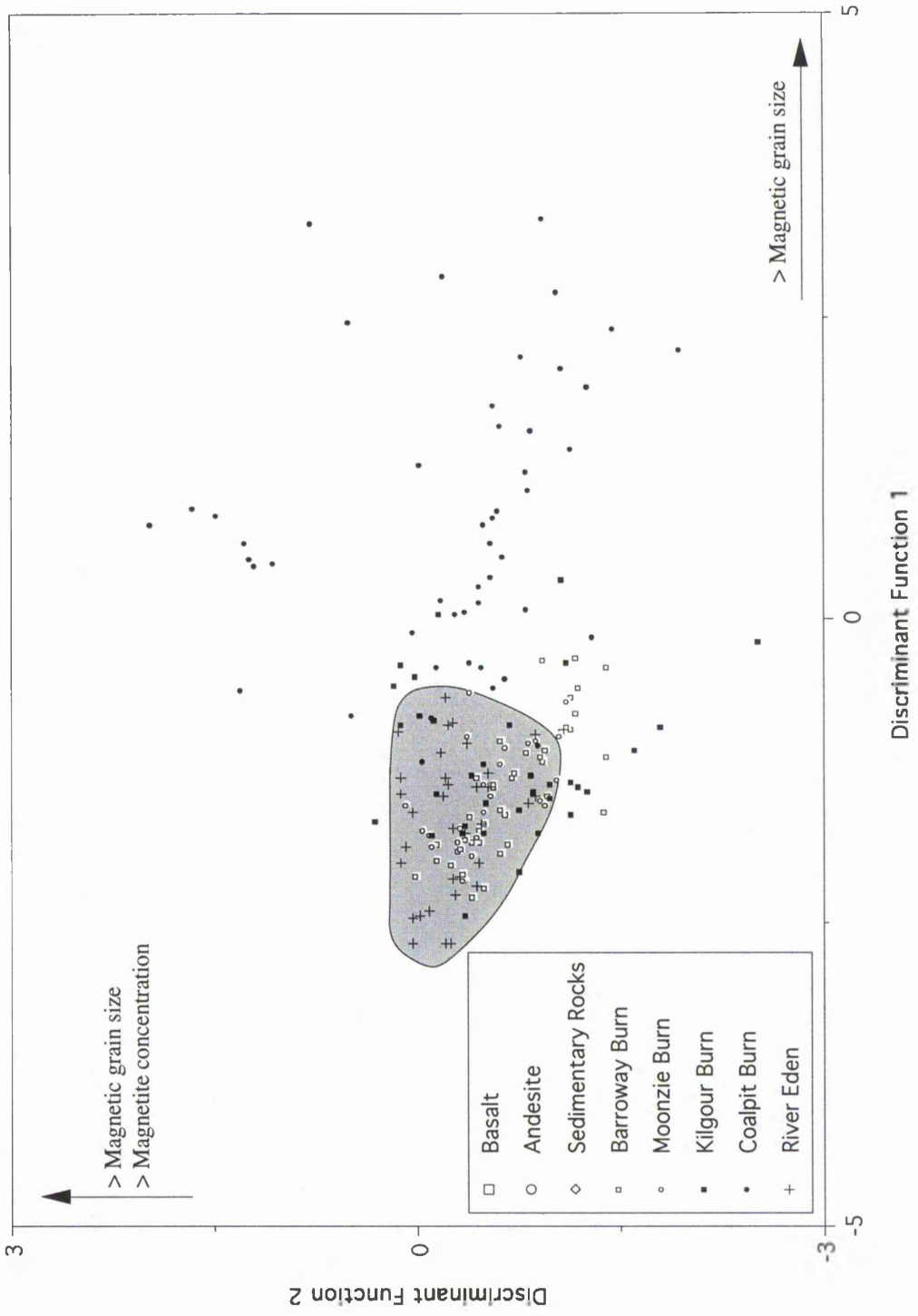

Figure 5.3. Plot of discriminant Function 1 versus discriminant Function 2 resulting from the first discriminant analysis performed for separating samples from basalt, andesite and sedimentary rocks groups. Stream sediment samples are also included in order to see their relationship with the sources (see text for explanation). Boundaries for rock groups, as well as for the River Eden sediments (shaded field), are fitted by eye.

Table 5.6. Wilk's Lambda and univariate F-ratio with 2 and 19 degrees of freedom for each of the four variables found to be the most effective at discriminating basalt, andesite and sedimentary rocks groups (see text for explanation). Critical F-ratio at a 0.01 significance level is equal to 5.93.

Variable	Wilk's Lambda	F-ratio	p
χ_{ARM}	0.41225	13.5442	0.0002
$(Bo)_{CR}$	0.32687	19.5631	<0.00001
$\chi_{fd\%}$	0.11734	71.4589	<0.00001
IRM_{20}	0.30375	21.7755	<0.00001

Once more, the percentage of correctly classified samples is 95%. Both discriminant functions are significant at a 0.01 level. Whereas Function 1 explains a total of 84% of the separation among the groups on the basis of their $\chi_{fd\%}$ values (i.e. their magnetic grain size variability), Function 2, which contains 16% of the total discriminating power, separates the groups principally on the basis of their IRM_{20} values (i.e. their magnetite concentration), as indicated by the scaled eigenvector scores.

In Figure 5.4 rock and stream sediment samples are plotted using both discriminant functions as axes. A similar overlap is found between the basalt and andesite groups as observed in Figure 5.3, and stream sediment samples show the same kind of trend as described from Figure 5.3. Thus, these latest two discriminant analyses suggest an important contribution from the sedimentary rocks to the sediments transported by the Barroway Burn, the Moonzie Burn and also the River Eden. However, the analyses fail to estimate the contribution of the sedimentary rocks in the mixing process which results in the formation of the sediments transported by the Coalpit Burn and principally by the Kilgour Burn. Most of the sediment samples collected from both these tributaries plot in the area defined by the andesite samples. However, due to the proximity of the basalt and andesite groups within the discriminant space, it is unclear whether the observed distribution of such sediment samples falls at the intersection of the basalt and andesite groups (suggesting a trivial influence of the sedimentary rocks), or whether they reflect some contribution from the sedimentary rocks which is diluting the characteristic magnetic signature of the basalts, thus leading to andesite magnetic characteristics which represent values intermediate between those characteristic of basalts and sedimentary rocks.

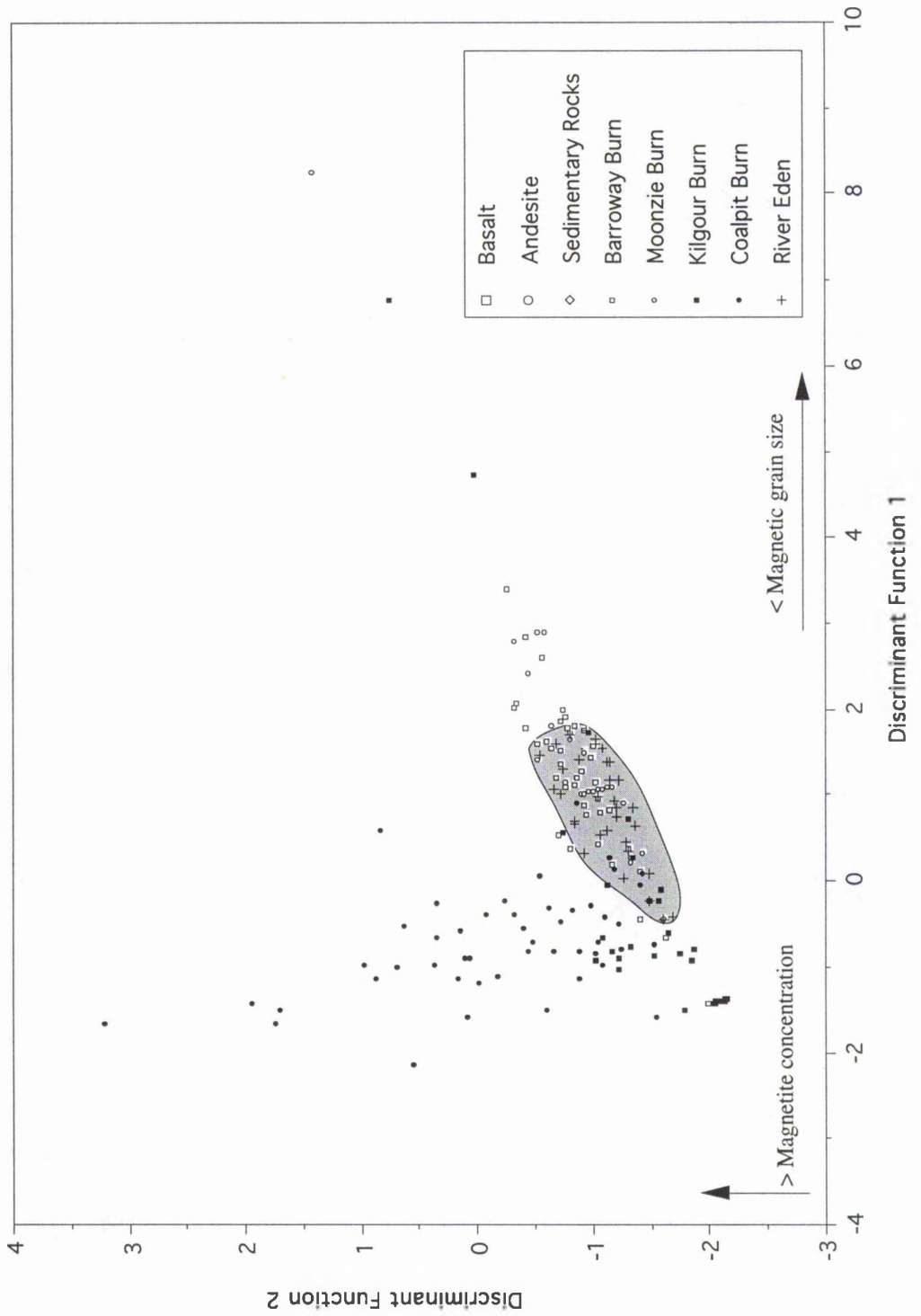

Figure 5.4. Plot of discriminant Function 1 versus discriminant Function 2 resulting from the second discriminant analysis performed for separating samples from basalts, andesites and sedimentary rocks groups. Stream sediment samples are also included in order to determine their relationship with the sources (see text for explanation). Boundaries for rocks groups, as well as for the River Eden sediments (shaded field), are fitted by eye.

5.1.2. Evaluation of tributary contribution to the the River Eden sediment

It is assumed that the sediments of the River Eden result from the mixing of the sediments transported by all of its tributaries. Therefore, in order to obtain a better estimation of the materials constituting those mixtures, a discriminant analysis was performed by considering the sediment samples of four tributaries as source materials rather than using the rock and glacial till samples as above. All parameters under consideration in this study were found to be non-normally distributed for each of the four streams. When using normalised data the percentage of grouped cases correctly classified increased from 87%, corresponding to the analysis using original data, to 89%. The three resulting discriminant functions using transformed data are significant at a 0.01 level, Functions 1 and 2 containing a total of 94% of the information available to discriminate the four River Eden tributaries under study (Table 5.7). The largest scaled eigenvector values are shown by IRM_{20}, IRM_{100} and $HIRM_{-100}$ in both functions, suggesting a discrimination of the River Eden tributary sediments on the basis of their magnetic mineralogy paragenesis and concentrations (Chapter 4). However, although good differentiation of the groups is achieved, the samples still occupy rather similar locations in discriminant space (Figure 5.5).

The River Eden sediment samples plotted within the discriminant space defined by discriminant Functions 1 and 2, they are seen (Figure 5.6) to fall mainly within the Barroway Burn and the Moonzie Burn regions. Both the results displayed on the basis of the sediment sample locations along the River Eden (Figure 5.6a), and on the basis of the magnetic characteristics of the different particle size fractions differentiated in the sediment samples (Figure 5.6b), show a slight pattern. An increasing influence from tributaries flowing mainly over basalts and sedimentary rocks (the Kilgour Burn and the Coalpit Burn) is observed towards the downstream River Eden sediment samples (from RE1 to RE6 samples in Figure 5.6a). Also, a slight tendency for the coarser particle size fraction ((-1) to 1 ϕ in size) to fall within the areas defined by the Barroway and the Moonzie Burns is observed (Figure 5.6b), whereas the finer fractions (>1 ϕ in size) plot 'closer' to the Kilgour Burn region. This might indicate a more basaltic origin for the finer particle sizes of the sediments and a more andesitic origin for the coarser fractions.

Nevertheless, it seems that the strong magnetic signature of the rock samples becomes diluted in the mixing process leading to a homogenisation of the magnetic parameter values of the sediments. Thus, discriminant analysis is found to fail in

Table 5.7. Results from the discriminant analyses performed using normalised magnetic parameters in order to spatially separate the Barroway Burn (BB), the Moonzie Burn (MB), the Kilgour Burn (KB) and the Coalpit Burn (CB) sediment samples.

	F1	F2	F3
	Eigenvectors		
Constant	2.0957949	-2.7698781	-8.1497970
χ_{lf}	0.4024862	1.3137957	-4.2152326
IRM_{20}	-0.6084944	-1.1652803	4.5349233
IRM_{100}	35.5467011	-26.1972475	29.7185334
IRM_{300}	-37.9669345	35.6921636	-37.9600513
$HIRM_{20}$	8.1243908	16.8535896	0.7109343
$HIRM_{-100}$	28.0487606	15.2182780	-39.2411628
$HIRM_{-300}$	-32.5271411	-39.1033307	47.6508023
	Scaled eigenvectors		
χ_{lf}	0.14395	0.46988	-1.50758
IRM_{20}	-0.19169	-0.36708	1.42858
IRM_{100}	11.75830	-8.66564	9.83043
IRM_{300}	-12.57753	11.82395	-12.57525
$HIRM_{20}$	2.72100	5.64457	0.23810
$HIRM_{-100}$	9.44999	5.12723	-13.22085
$HIRM_{-300}$	-11.02102	-13.24920	16.14530
	Discriminating efficiency		
Eigenvalues	8.9341	1.6522	0.6166
% of variance	79.75	14.75	5.50
Cumulative %	79.75	94.50	100.00
	Test of significance		
Wilk's Lambda	0.023478	0.233233	0.618577
Chi-square	530.864	205.984	67.967
d.f.	21	12	5
p-value	<0.00001	<0.00001	<0.00001
Chi-square at 0.01 significance level	39.0	26.2	15.1

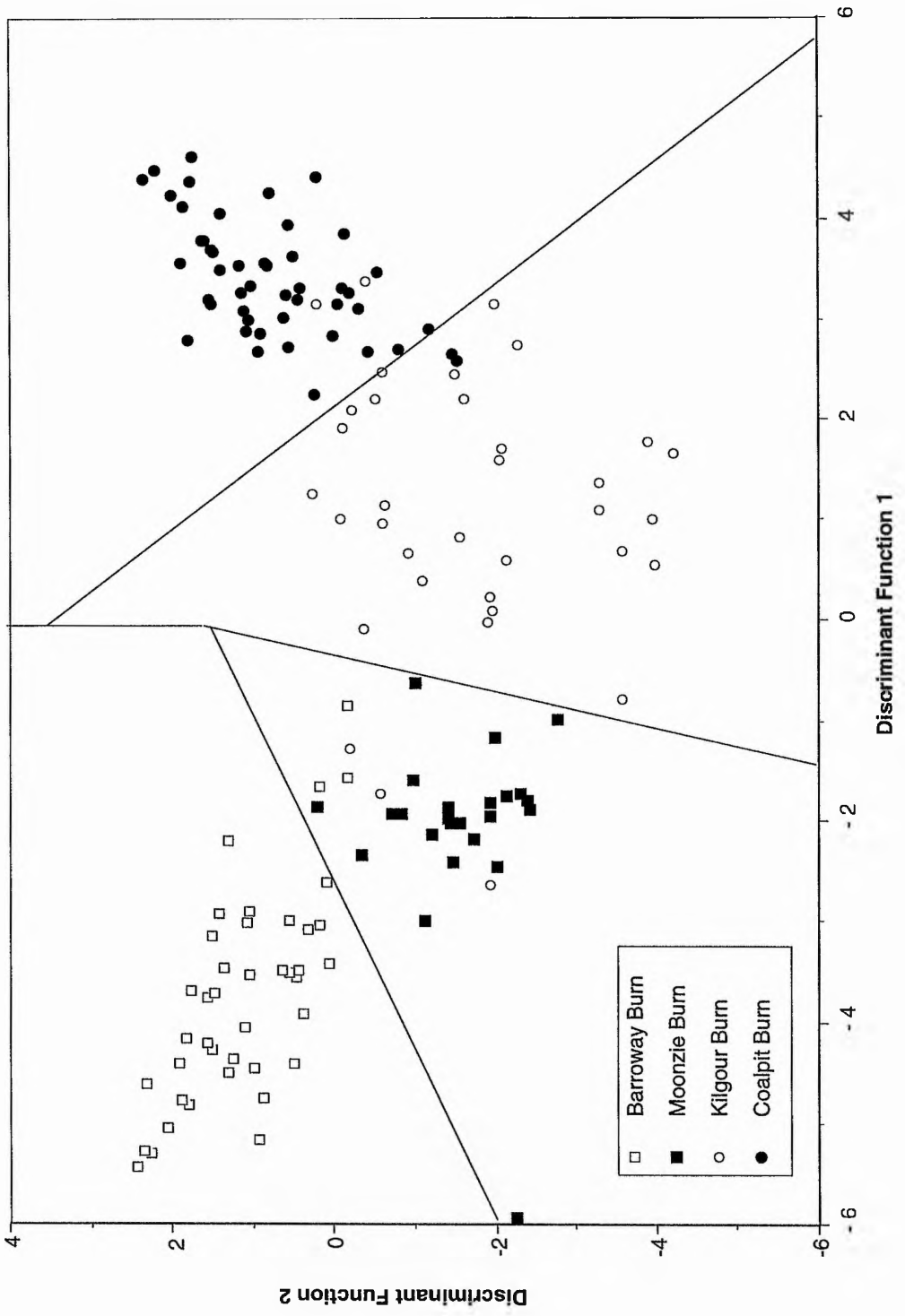

Figure 5.5. Plot of discriminant Function 1 versus discriminant Function 2 resulting from the discriminant analysis performed to differentiate sediment samples from the Barroway Burn (BB), the Moonzie Burn (MB), the Kilgour Burn (KB) and the Coalpit Burn (CB). The territorial map is fitted by eye.

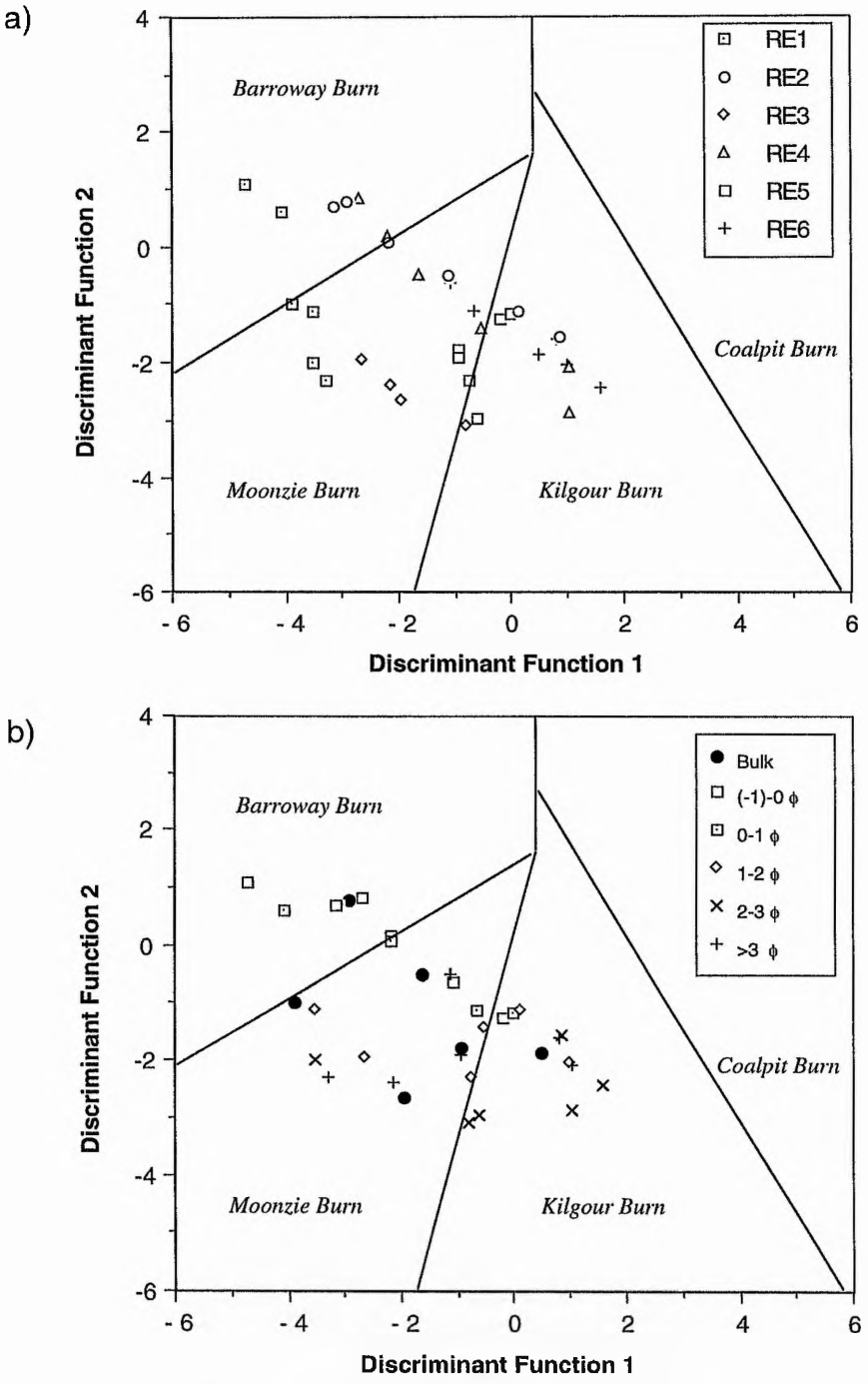

Figure 5.6. Plot of discriminant Function 1 versus discriminant Function 2 resulting from the discriminant analysis performed to differentiate sediment samples from the Barroway Burn (BB), the Moonzie Burn (MB), the Kilgour Burn (KB) and the Coalpit Burn (CB). The territorial map is fitted by eye as in Figure 5.5. The River Eden sediment samples are plotted in order to be classified on the basis of a) their sampling location and b) their particle size characteristics (see text for explanation).

satisfactorily modelling the provenance of those sediment samples resulting from mixtures of more than one, or perhaps two, sources due principally to the close location of the materials within the discriminant space, as a result of the similarity in the values of the variables under consideration.

5.1.3. Summary of the discriminant function analysis results

In summary, all four discriminant analyses discussed above provide qualitative estimations of the materials constituting the sediments sampled along four selected tributaries of the River Eden, as well as the sediments transported by the main channel of the River Eden. Firstly, they show that the characteristic magnetic signature of the source materials is the most powerful discriminator and that magnetite chemical composition, neither itself nor combined with the magnetic parameters, has a significant discriminating power. Even when all the magnetic and chemical composition of magnetic minerals results (Chapter 4) are used to analyse six main potential sediment source groups, discriminant analysis shows that, in practice, only four of these contribute significantly to the sediment samples. Thus, the Barroway Burn and the Moonzie Burn sediments, which are known to be principally of andesitic origin (Chapter 3) as well as glacial till, has a relatively minor contribution from the sedimentary rocks.

The Kilgour Burn and the Coalpit Burn sediments of basaltic origin are not successfully modelled by discriminant analysis. This is mainly due to the close proximity of the basalt and andesite groups within the discriminant space, as a simple consequence of their similar magnetic and mineralogical characteristics. Two possible explanations for the spatial distribution observed for these groups of sediments are offered: the sediments fall within the andesite field because of the overlap between the basalt and the andesite groups, in which case no sedimentary rocks contribution would be observed. Alternatively, some of the sediment is derived from the sedimentary rocks resulting in the attenuation or decrease in the basalt magnetic signature, driving it into the andesite field. The River Eden sediments appear grouped within an area located centrally within the discriminating space, mainly overlapping the andesite and the glacial till groups, with a trend towards the sedimentary rocks. All these sediment samples are mixtures of basalts, andesites, sedimentary rocks and glacial till, but a semiquantitative estimate of their relative proportions is difficult as the basalt and andesite groups are not easily resolved, and the dilution of the sources' magnetic signatures through the mixing process tends to homogenise the magnetic parameter values of the River Eden sediments.

5.2. Quantitative sedimentary provenance approach

As described in Chapter 3, programs based on linear algebraic calculations, such as SIMPLEX, may be used to estimate quantitatively the relative proportions of the materials in mixtures, i.e. to unmix mineral mixtures by mathematical methods. Such programs principally assume that the variables considered in the calculations are linearly additive, i.e. they are conservative and so the values of the variables measured in the mixture will be the result of the characteristic values of such variables in the sediment sources, as far as each source contributes to the mixture. Thus, as explained in Chapter 3, values of the variables corresponding to the mixture may be mathematically predicted using Equation 3.1.

Magnetic parameters are traditionally assumed to be linearly additive, and authors such as Yu and Oldfield (1989, 1993) have used them in linear programming to model sedimentary provenance, and environmentally sensible results have been obtained. However, Lees (1994) performed artificial mixing experiments and tested both the linear additivity of each of the three main magnetic characteristics measured in environmental studies (magnetic susceptibility, anhysteretic remanent magnetisation and isothermal remanent magnetisation), and the sensitivity of the linear programming model to the deviation of these parameters from the linear additivity. She found that in most cases predicted values obtained mathematically were lower than the measured values. The difference between theoretical and measured values for each magnetic variable was estimated. A minimum deviation of 5-7% from linear additivity was exhibited by magnetic susceptibility (χ_{lf}) which suggests that the Bartington Meter is linear (Lees, 1994). However, SIRM and HIRM parameters showed the largest errors (>10%) due to an increasing deviation from linearity with increasing parameter values and to an effective addition of the errors, respectively. Four possible explanations for the observed deviation of the magnetic measurements from linear additivity were offered by Lees (1997): the variability existing within each source material (source inhomogeneity), experimental error in the linearity measuring equipment, the presence of viscous grains, and a potential for magnetic grain interaction. However, linear programming was found to be sensitive to differences between predicted and measured values greater than 2.5%.

Lees (1994) also defined the limits to the use of magnetic properties in linear modelling. No more than four sources were modelled successfully and these have to be from the six (or fewer) main magnetic properties. Sources which were magnetically weak and/or constant multiples of other sources were always difficult to model. Also, sources which contributed less than 10% to the mixture were

difficult to recognise by linear programming unless they were magnetically strong, this figure being as high as 25% for magnetically weaker materials.

All these results were tested in environmental conditions using bedload sediment samples and also soil samples. The importance of intra-sample variability was confirmed, and the linearity of both the fractionating samples and the mathematical mixing was tested and found to be poor in both cases. Therefore, as a result of these limitations and errors derived from the use of magnetic parameters in linear modelling, Lees (1994) strongly cautioned against the use of such data as reliable quantitative estimates.

In the present study, two different datasets, morphological and especially chemical characterisation of Fe-Ti oxides and magnetic measurements, were used in order to establish the contribution of the different geological materials found in the River Eden catchment to the sediment mixtures transported by the River Eden and its tributaries. Results from discriminant analysis (Section 5.1) indicate that sediment sources are best differentiated on the basis of their magnetic properties. Nevertheless, the basalt, andesite and glacial till groups were found to plot very close together in discriminant space, some overlap being possible due to within-group variability. Evidence that all the sediment sources have been identified is contained in Figure 5.1; all sediment samples plotted within or between the areas defined by each of the sources. This suggests the suitability of linear programming to modelling sediment provenance using magnetic parameters. However, on the basis of Lees' (1994) work it seems that linear modelling would be negatively influenced by: (1) marked within-group variability; (2) great magnetic similarity of three of the four sediment sources; (3) andesites and glacial till having magnetic characteristics which are intermediate between basalts and sedimentary rocks (and therefore certain basalt and sedimentary rock mixtures show similar characteristics to andesite); and (4) sedimentary rocks having very weak magnetic signatures in contrast to basalts, andesites and glacial till such that this source contribution will probably only be detected above about 25%. Also important errors were detected in some of the magnetic measurements of stream sediment samples as a result of instrumental effects and possible magnetic grain interactions. These errors will also limit the reliability of the linear programming model.

Once all possible factors influencing the linear modelling of the stream sediments of the River Eden catchment have been defined, linear programming may then be applied with these factors in mind. Firstly, the linear additivity of each of the magnetic and chemical variables used in this study should be tested. In environmental studies, however, this is impossible as the proportion of the diverse

source materials, required to calculate the predicted value of each variable for each sediment sample (Equation 3.1) is the aim of the linear model. Nevertheless, magnetic measurements of bulk stream sediment samples may be used instead, applying Equation 3.1 to each of the particle size fraction subsamples, as an estimation. The data (Appendix 6) indicate that, as described by Lees (1994), there is a general tendency for the predicted values to be lower than the measured values for bulk samples. The difference between predicted and measured values is found to be the lowest for the χ_{lf} (-37.02%), IRM_{40} (-14.21%) and $HIRM_{-20}$ (-40.15%) magnetic parameters. A similar approach could not be performed for the data of chemical composition of magnetite grains as grains found only in the 2 to 3 ϕ in size fraction were analysed. The reason for this is that heavy liquid procedure, which was used to separate heavy minerals, requires a specific particle size for efficiency.

A unique value per variable is assigned to each source group in order to perform linear programming, despite the known within-group variability. Thus, mean values, mean plus the standard deviation (mean+sd) values and mean less the standard deviation (mean-sd) values are used in turn, as recommended by Lees (1994), in order to get a range of possible proportions which each source may contribute to the mixtures in terms of the natural variability of the source properties in the catchment.

The observed differences in the modelling results depending on the value assigned to each sediment source for each variable are considerable. These differences can be explained in terms of the variability existing within each sediment source, and also of the non-normal distribution of the dataset which, unfortunately, cannot be overcome as no transformation should be applied to the data when using the linear programming. This is highlighted by the similarity of the results obtained whether mean+sd or mean values are used, which both differ greatly from the mean-sd results. The mean, mean+sd, and mean-sd results are discussed in detail in Subsection 5.2.1, and tested in Subsection 5.2.3.

5.2.1. Modelling bulk sediment samples by using magnetic measurements

Bulk sediment samples were modelled using three different combinations of magnetic measurements: firstly, all magnetic parameters measured for this study (χ_{lf}, χ_{fd}, χ_{ARM}, IRM_{20}, IRM_{40}, IRM_{100}, IRM_{300}, IRM_{500}, SIRM, IRM_{-20}, IRM_{-40}, IRM_{-100}, IRM_{-300}, IRM_{-1000}, $HIRM_{20}$, $HIRM_{40}$, $HIRM_{100}$, $HIRM_{300}$, $HIRM_{500}$, $HIRM_{-20}$, $HIRM_{-40}$, $HIRM_{-100}$, $HIRM_{-300}$, $(Bo)_{CR}$ (Figure 5.7a), secondly, six main concentration-dependent magnetic parameters (χ_{lf}, IRM_{20}, IRM_{40}, IRM_{100}, IRM_{300}, SIRM) (Figure 5.7b), and finally, the three most linearly additive magnetic

parameters (χ_{lf}, IRM_{40}, $HIRM_{-20}$) (Figure 5.7c) were used. In all cases the four main sediment sources identified in this study were considered.

All results are shown in Figure 5.7. The most obvious outcome is that marked differences in the model outputs for each bulk sediment sample depend on the variables used, and also on the use of mean, mean+sd or mean-sd values. However, *a priori* knowledge of the sources of each stream sediment assists in testing the model results. Thus, as seen in earlier chapters, the Barroway Burn and the Moonzie Burn sediments are mainly composed of andesite and glacial till (see Figure 3.2) whereas the Kilgour Burn and the Coalpit Burn sediments are mainly composed of basalt, sedimentary rocks (mainly sandstones and limestones) and glacial till (see Figure 3.3).

The Barroway Burn bulk sediment samples (Figure 5.7A) modelled using mean-sd values show, in all three cases, a large proportion of basalt. As this is an environmentally meaningless model it can be rejected. On the other hand, the mean and mean+sd modelling results show for a) a major andesite contribution, glacial till is not detected at all; for b) glacial till appears to dominate the sediment samples, and in this case sedimentary rocks do not seem to contribute to the sediment formation (mainly observed from mean values); and for c) sedimentary rocks dominate the sediment samples, and as in case a) glacial till seems not to contribute to the sediments. On the basis of the environmental setting, model b) seems to be the most appropriate, suggesting that the Barroway Burn sediment is mainly composed of glacial till and andesite with a minor contribution from basalt, which, as indicated by Figure 3.2, is a volumetrically minor sediment source.

The sediment transported by the Moonzie Burn is expected to comprise mainly of sedimentary rocks. Models a) and b) (Figure 5.7B) using mean values show glacial till to be the dominant sediment source, whilst model c) suggests that the sediment is composed mainly of sedimentary rock fragments with a minor contribution from both andesite and basalt. On the other hand, similar results are seen in both models c) and b) for mean+sd values. In the latter model glacial till is also recognised as a contributor to the Moonzie Burn sediment. As in the Barroway Burn sediment sample modelling, mean-sd results may be rejected as they suggest andesite (models a) and b)) or glacial till (model c)) as the main sediment sources.

The limitation of linear programming in modelling the sediments in the River Eden catchment is clearly seen in Figures 5.7C and 5.7D, where the Kilgour Burn and the Coalpit Burn sediments, respectively, are found in several cases to be partly composed of andesite (using mean, mean+sd and mean-sd values in all three models

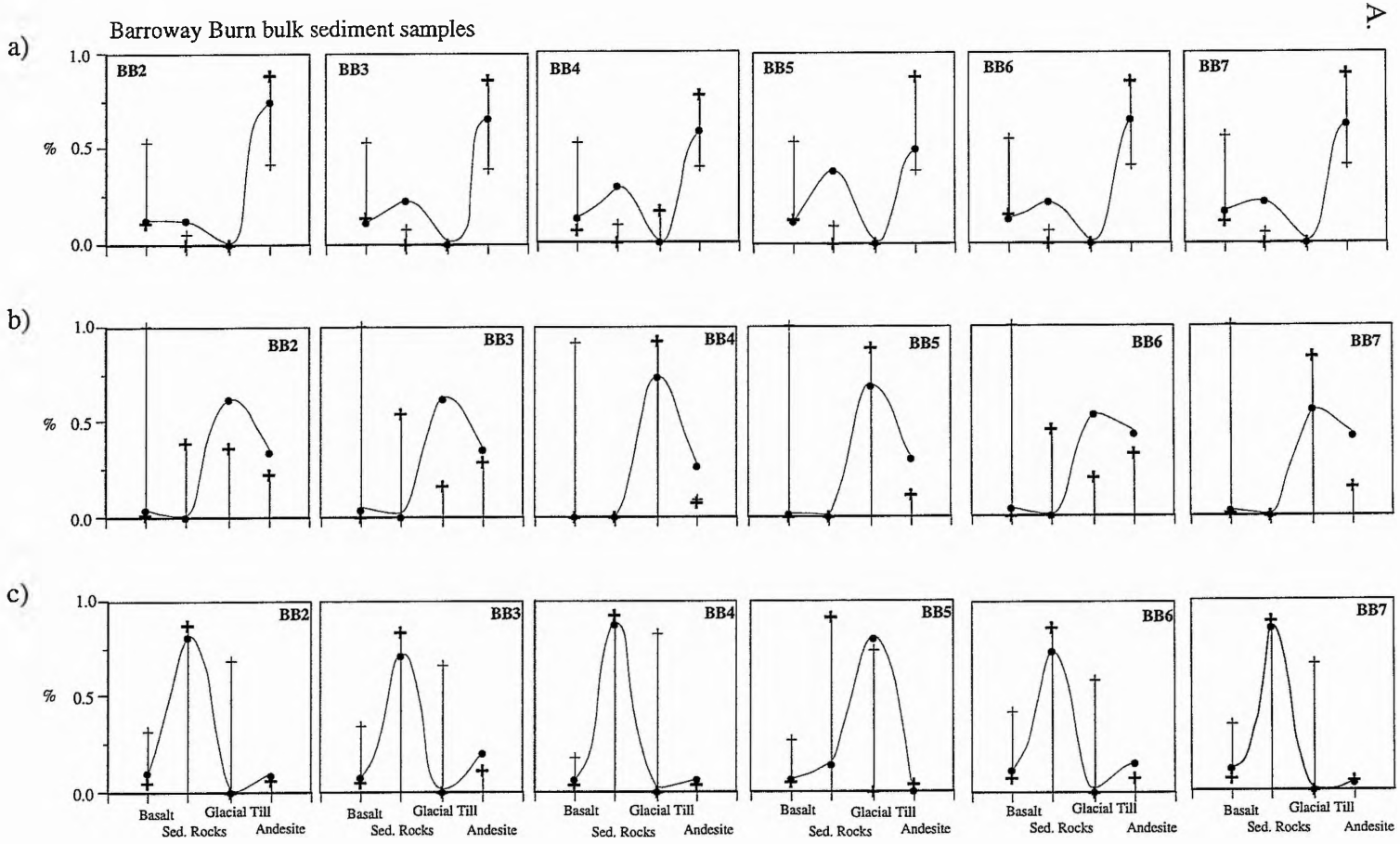
Barroway Burn bulk sediment samples
a)
b)
c)
BB2
BB3
BB4
BB5
BB6
BB7
%
1.0
0.5
0.0
Basalt
Sed. Rocks
Glacial Till
Andesite

B.

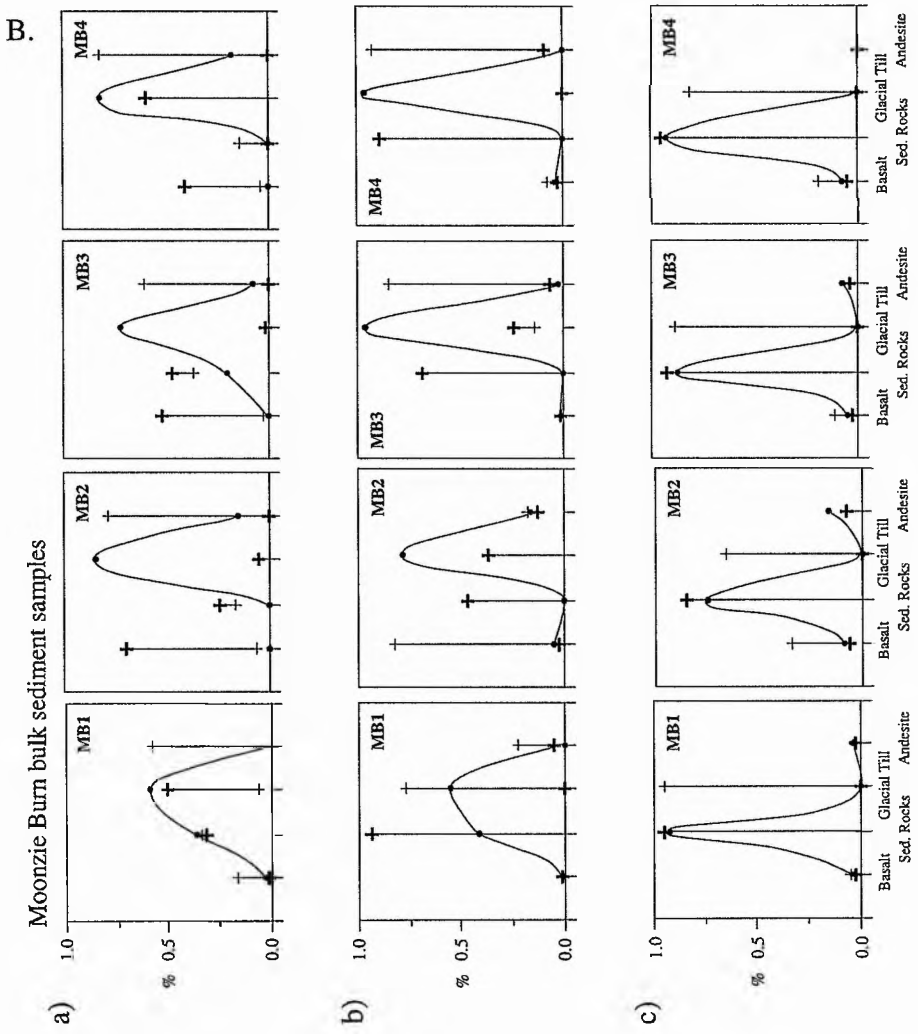
Moonzie Burn bulk sediment samples
a)
b)
c)
MB1
MB2
MB3
MB4
% 0.5
1.0
0.0
Basalt
Sed. Rocks
Glacial Till
Andesite

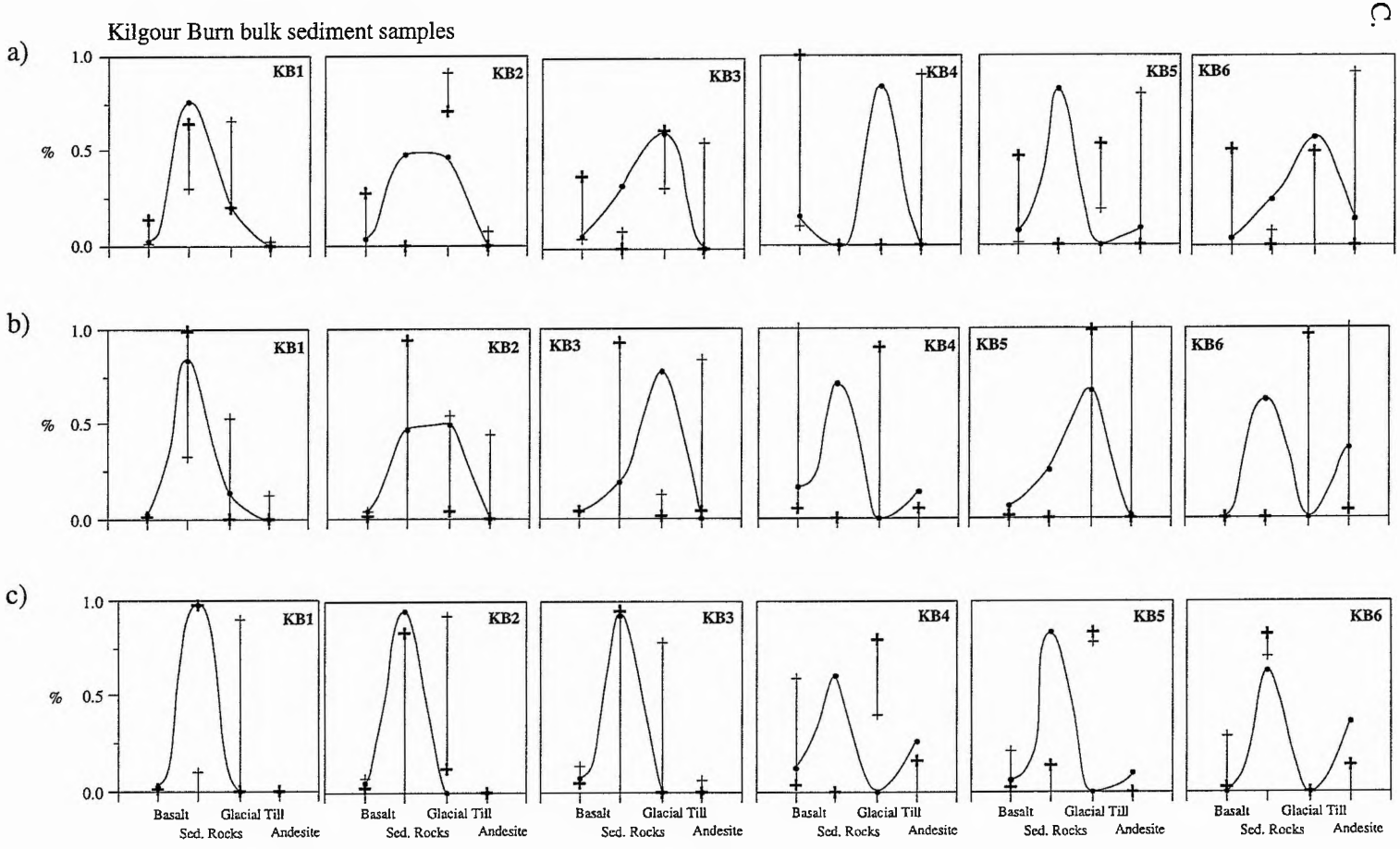
Kilgour Burn bulk sediment samples
a)
b)
c)
KB1
KB2
KB3
KB4
KB5
KB6
%
1.0
0.5
0.0
Basalt
Glacial Till
Sed. Rocks
Andesite

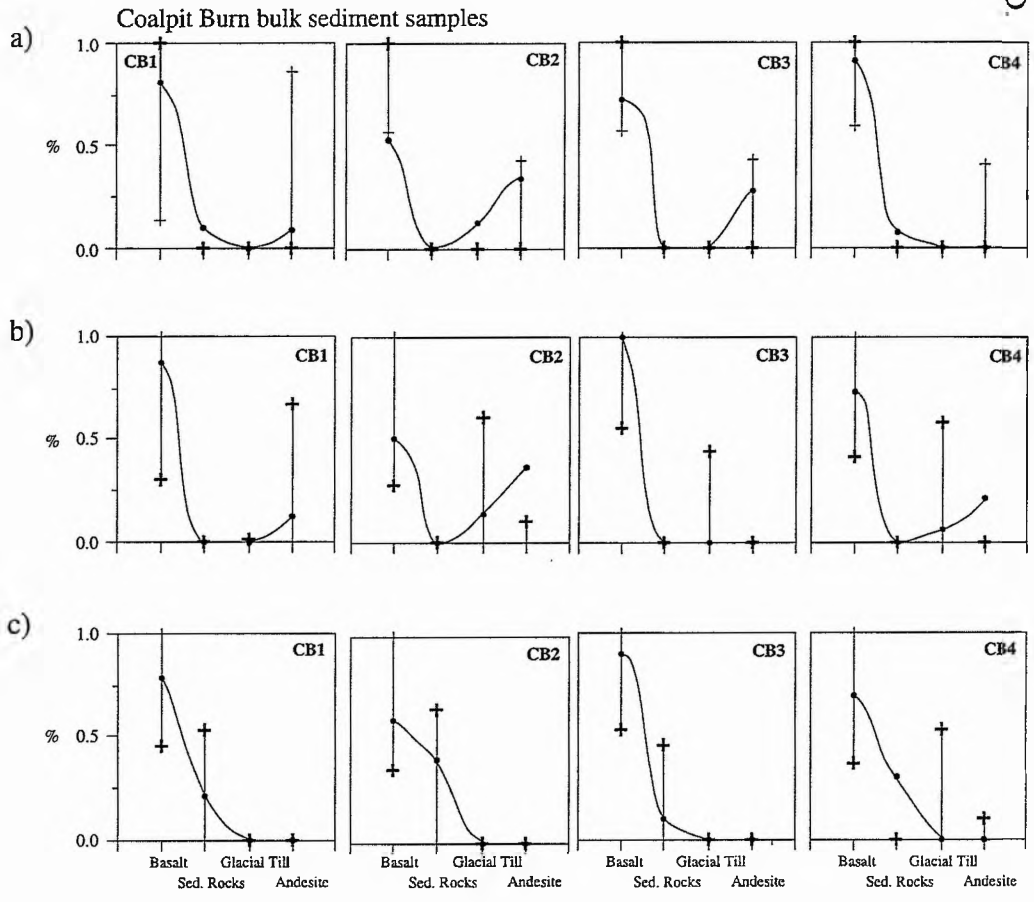
Coalpit Burn bulk sediment samples
a)
b)
c)
CB1
CB2
CB3
CB4
1.0
0.5
0.0
%
Basalt
Sed. Rocks
Glacial Till
Andesite

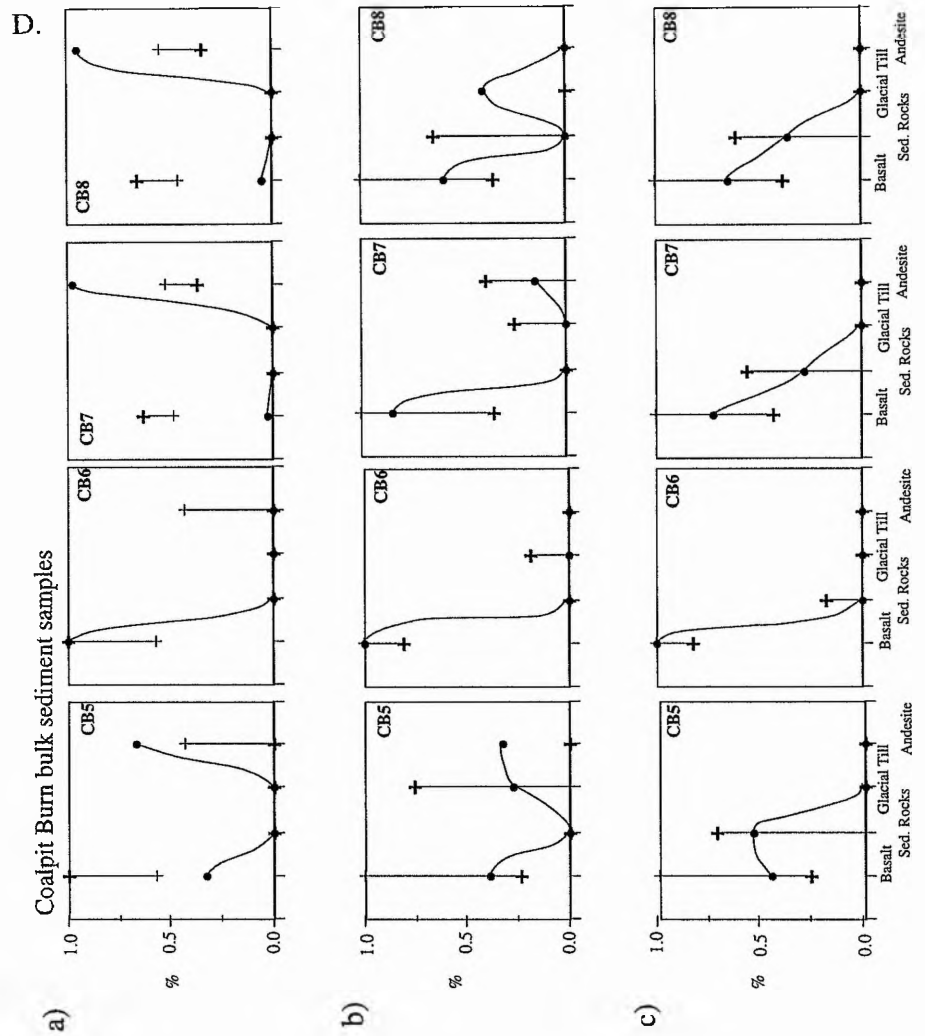

Figure 5.7. Linear programming results for bulk sediment samples from (A) the Barroway Burn (BB), (B) the Moonzie Burn (MB), (C) the Kilgour Burn (KB) and (D) the Coalpit Burn (CB). The mathematical unmixing approach is performed using (a) all magnetic parameters measured in this study, (b) χ_{lf}, IRM_{20}, IRM_{40}, IRM_{100}, IRM_{300} and SIRM, magnetic parameters, and (c) χ_{lf}, IRM_{40} and $HIRM_{-20}$, magnetic parameters. Also, modelling results for mean+sd (+), mean (•) and mean-sd (+) values of each variable assigned to each sediment source are shown (see text for explanation).

with magnetic measurements). These River Eden tributaries flow entirely over basalts and sedimentary rocks (Figure 3.3). The modelling results may then be explained in terms of the variability within the source groups as well as by their close proximity. The andesite contribution to the sediments tends to increase downstream (e.g. KB5, KB6, CB7 and CB8 samples). The reason for this effect could be a possible 'dilution' of the basalt magnetic signature during the transport of the magnetic mineral grains and the increasing contribution of sedimentary rocks (see Figure 3.3). Therefore, the resulting magnetic signature in the mixed sediments could be close to that of andesite or to glacial till.

The Kilgour Burn and the Coalpit Burn sediments are 'best' modelled using mean values of the three most linearly additive magnetic parameters (model c) in Figures 5.7C and 5.7D, respectively). This model suggests that the Kilgour Burn sediment is mainly composed of sedimentary rock fragments with a minor basalt contribution, whereas the Coalpit Burn sediment is mainly composed of basalt with a minor proportion of sedimentary rock fragments.

According to the results shown in Figure 5.7, the mean values of each magnetic parameter assigned to each sediment source group is suitable for linear modelling, even when the data show skewed distributions. Most of the bulk sediment samples collected in the River Eden catchment (expect the Barroway Burn samples) are more successfully modelled using the χ_{lf}, IRM_{40} and $HIRM_{-20}$ magnetic parameters in which cases the modelling results approximate to the environmentally expected results. However, it is also clear from these results that the deviation of the magnetic parameters from linear additivity, the magnetic variability within the sediment sources and the magnetic similarity of some of the sources, reduce the efficiency of the linear programming. Modelling results should therefore be considered as an approximate, semi-quantitative unmixing approach in such environmental studies.

The River Eden bulk sediment samples were modelled following the same procedure as described above, the results being shown in Figure 5.8. In this case the samples are expected to be mixes of varying proportions from the four main sources identified in the River Eden catchment. As before, modelling results using mean values of the magnetic parameters for each source group seem to be the most suitable. The all magnetic parameters model (Figure 5.8a) highlights the andesite and glacial till contributions to the sediment samples, which tend to be minor when using both the six magnetic parameters model (Figure 5.8b) or the three most linearly additive magnetic parameters model (Figure 5.8c). On the basis of all previous results obtained from modelling bulk sediment samples collected in four River Eden

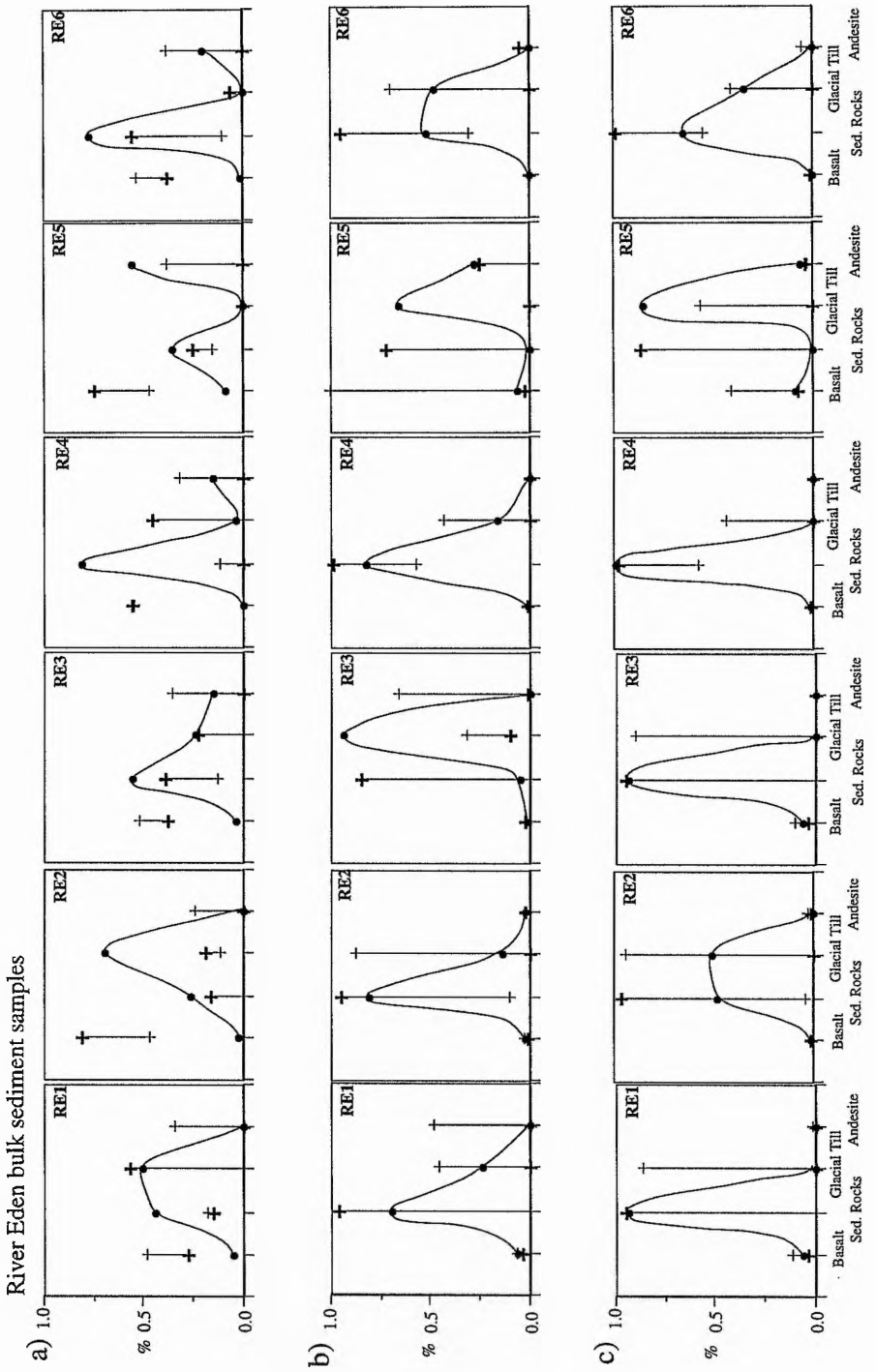

Figure 5.8. Linear programming results for the River Eden bulk sediment samples. The mathematical unmixing approach is performed using (a) all magnetic parameters measured in this study, (b) χ_{lf}, IRM_{20}, IRM_{40}, IRM_{100}, IRM_{300} and SIRM, magnetic parameters, and (c) χ_{lf}, IRM_{40} and $HIRM_{-20}$, magnetic parameters. Also, modelling results for mean+sd (+), mean (•) and mean-sd (+) values of each variable assigned to each sediment source are shown (see text for explanation).

tributaries, models using χ_{lf}, IRM_{40} and $HIRM_{-20}$ are considered the most consistent environmentally. Thus, the sediment in the main channel is primarily composed of sedimentary rock fragments with minor basalt and andesite contributions, supplemented to a small degree by glacial till in some localities. Samples RE1, RE2 and RE5 suggest an important proportion of glacial till in the sediment whereas samples RE3, RE4 and RE6 indicate no glacial till contribution.

5.2.2. Evaluation of using magnetic parameters and/or magnetite composition in modelling sediment fractions of 2 to 3 ϕ in size

In order to determine which of (1) magnetite composition data alone, (2) a combination of magnetite composition with magnetic data or (3) magnetic parameters alone gives the best results in linear modelling, sediment fractions of 2 to 3 ϕ in size were modelled. Magnetite grains of some selected sediment samples were concentrated and analysed. It was concluded that bulk sediment samples were 'best' modelled using the χ_{lf}, IRM_{40} and $HIRM_{-20}$ magnetic parameters (Figure 5.7) and, therefore, such parameters were also used in modelling the 2 to 3 ϕ size fraction of the selected sediment samples. The results obtained using these three magnetic parameters are given in section a) of Figure 5.9, whereas the results obtained using the chemical composition of magnetite grains are shown in section b) of the same figure. In section c) the model resulting from the use of both magnetite chemical composition and magnetic data is shown.

Figure 5.9A shows the results of the three models applied to some selected sediment samples from the Barroway Burn and the Moonzie Burn. The magnetic parameters point to sediment mainly derived from sedimentary rocks and glacial till. The sedimentary rock contribution observed in the Barroway Burn sediment samples is contrary to expectation (see above) and could be due to a lack of magnetite grains in this size fraction of the sediment, being composed mainly of non-magnetic minerals derived from andesite, basalt and glacial till (e.g. plagioclase, quartz, pyroxene, garnet). Results obtained from the eight main elements (Si, Ti, Al, Fe^{3+}, Fe^{2+}, Mn, Mg, Ca) analysed as oxides in magnetite grains indicate that, as expected, magnetite grains found in these two River Eden tributaries selected from the northern part of the catchment (Figure 1.1) were derived from andesite and glacial till. Alternatively, the combination of magnetism and magnetite composition suggests a model similar to the model from the magnetite chemistry alone, i.e. glacial till dominating the sediment samples.

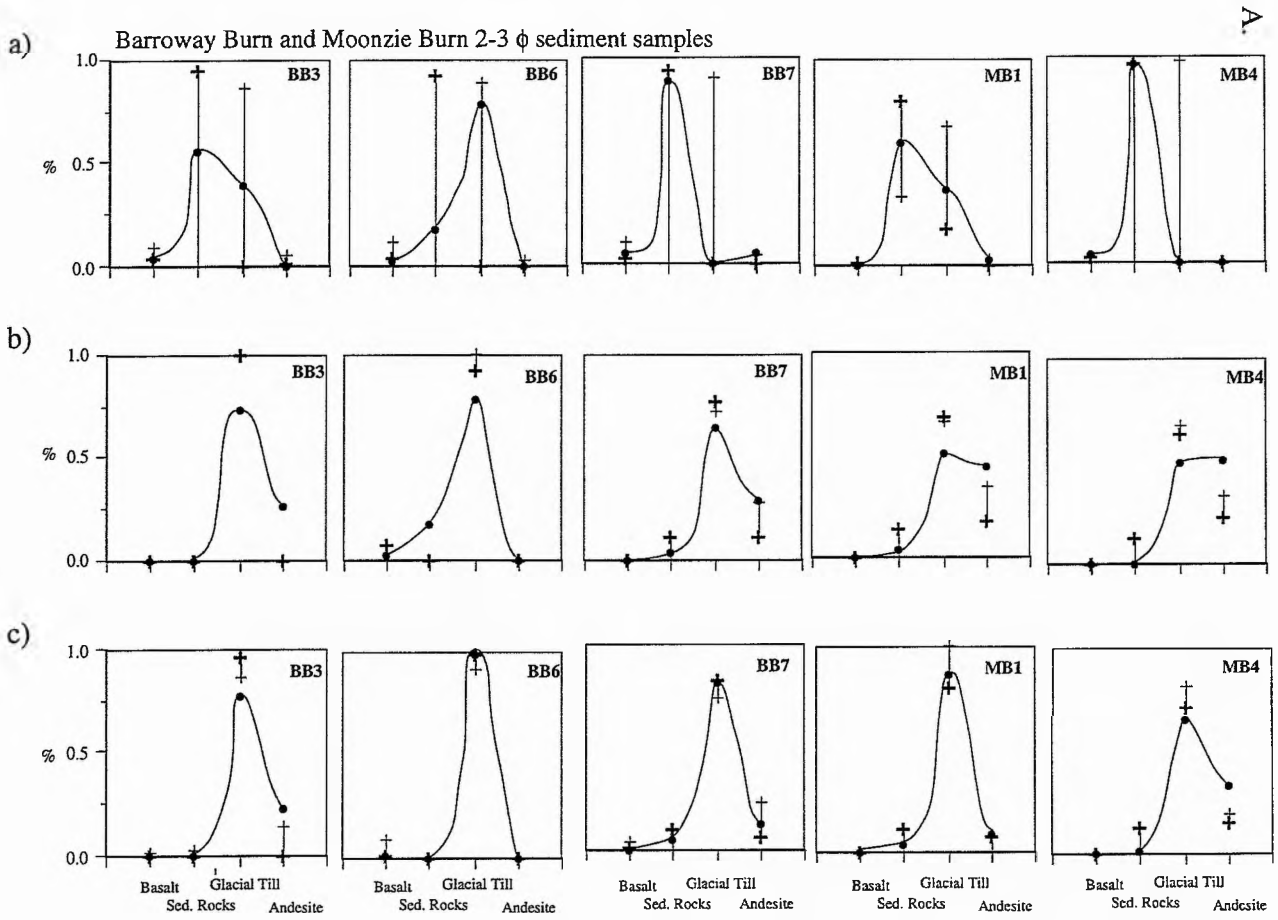
a)
Barroway Burn and Moonzie Burn 2-3 ϕ sediment samples
b)
c)
1.0
0.5
0.0
%
BB3
BB6
BB7
MB1
MB4
Basalt
Sed. Rocks
Glacial Till
Andesite

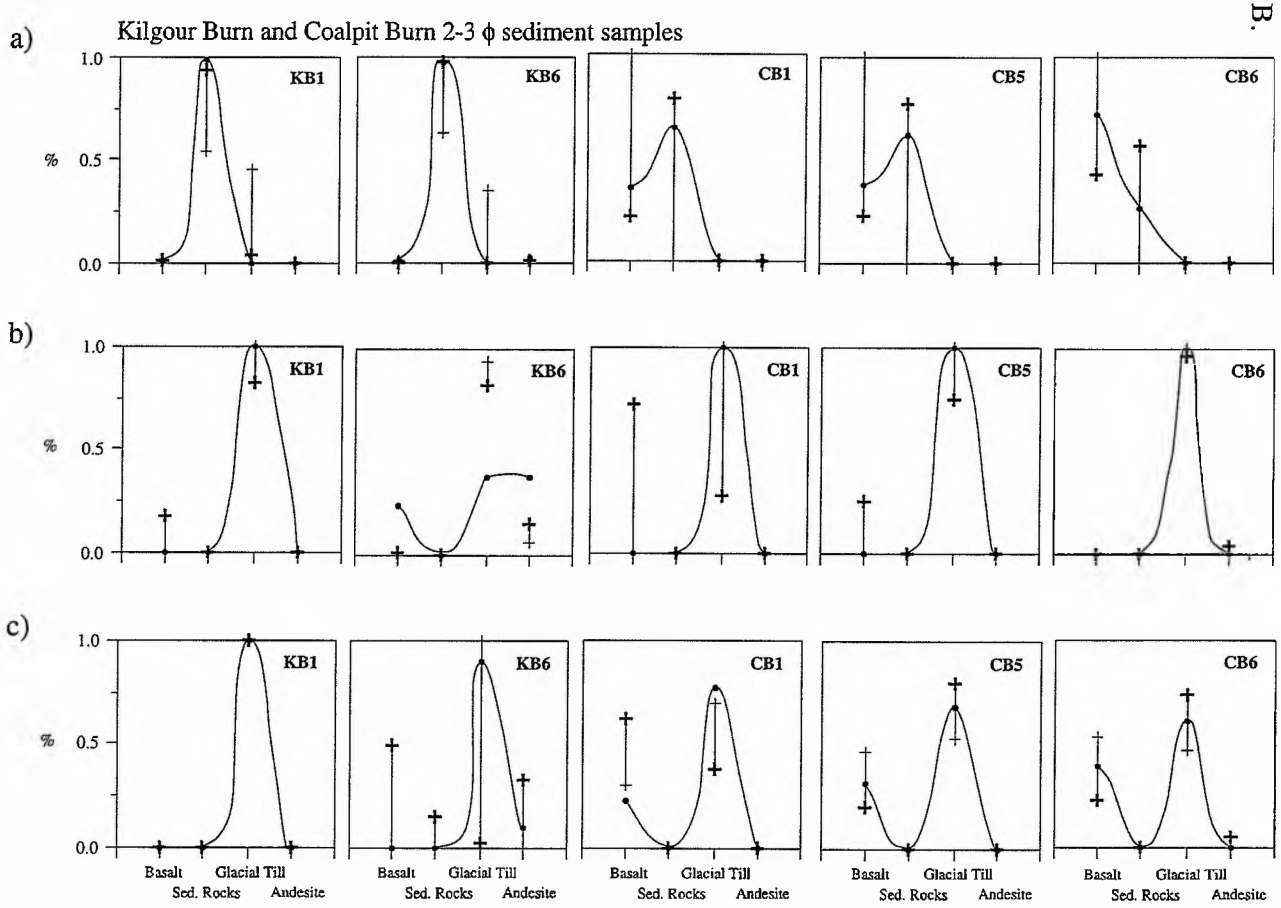
a)
Kilgour Burn and Coalpit Burn 2-3 ϕ sediment samples
KB1
KB6
CB1
CB5
CB6
%
1.0
0.5
0.0
b)
c)
Basalt
Sed. Rocks
Glacial Till
Andesite

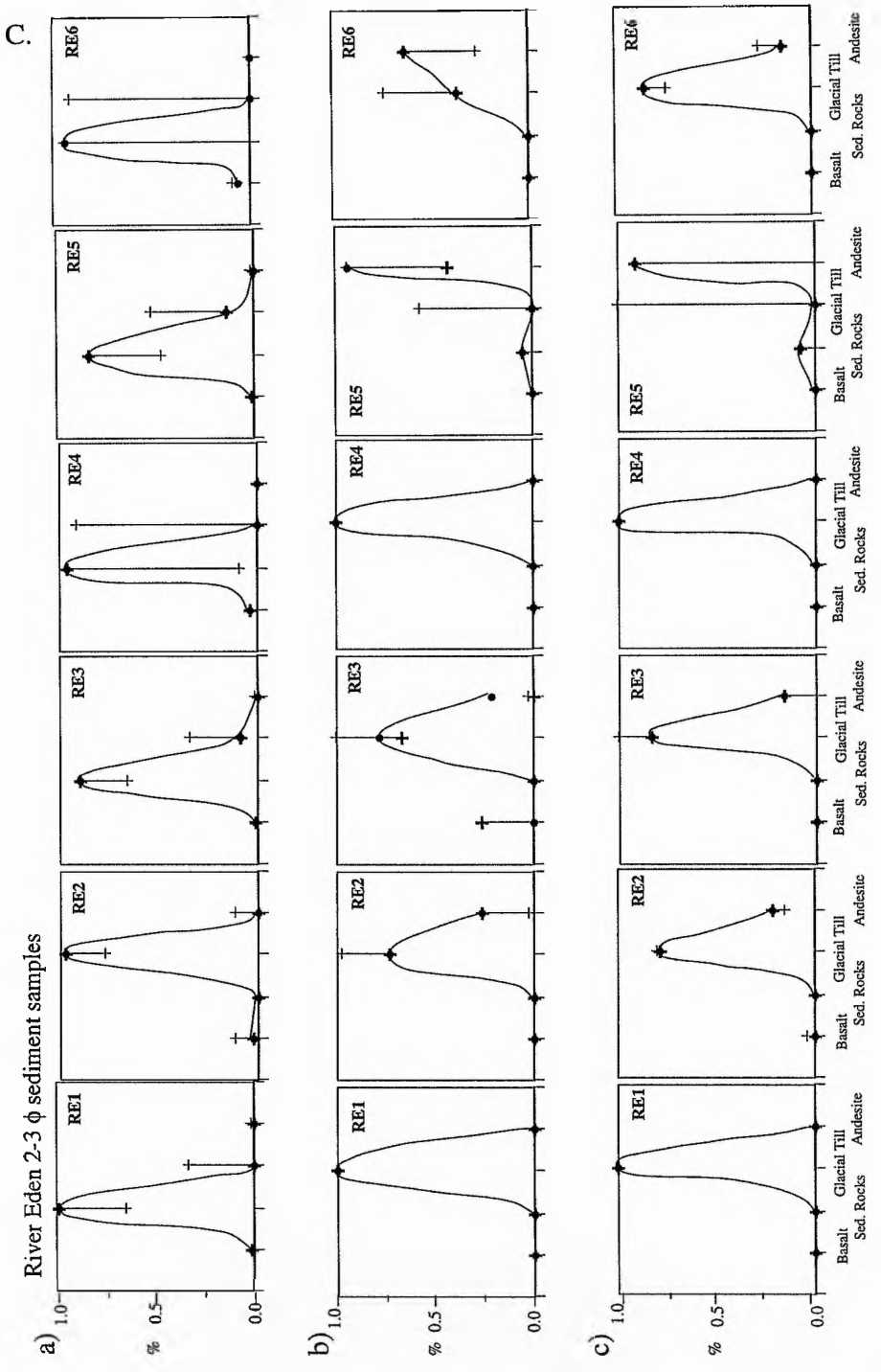

Figure 5.9. Linear programming results for selected (A) Barroway Burn (BB) and Moonzie Burn (MB) sediment samples, (B) Kilgour Burn (KB) and Coalpit Burn (CB) sediment samples, and (C) River Eden (RE) sediment samples. The mathematical unmixing approach is performed using (a) χ_{lf}, IRM_{40} and $HIRM_{-20}$, magnetic parameters, (b) eight main element measured as oxides in magnetite grains from the sediment samples, and (c) the combination of both (a) and (b) variables. Also, modelling results for mean+sd (+), mean (•) and mean-sd (+) values of each variable assigned to each sediment source are shown (see text for explanation).

The three model results corresponding to selected sediment samples from both the Kilgour Burn and the Coalpit Burn are shown in Figure 5.9B. The magnetic parameters model suggests that the Kilgour Burn samples are mainly made of sedimentary rocks, whereas the Coalpit Burn samples also show a major contribution from the basalts. Results based on magnetite composition show no difference between the sediments from these tributaries, suggesting that magnetite grains found in the analysed samples are derived from the glacial till. However, sample KB6 indicates that these results should be considered very carefully as magnetite derived from andesite is suggested by the model even when andesite is known not to contribute to the sediment transported by both of these tributaries in the southern part of the River Eden catchment (Figure 3.3). Results of the model c) are similar to results of the model b), although an influence from the magnetic parameters is evident for the Coalpit Burn sediment samples as model c) suggests that these sediments are mainly composed of glacial till and basalt.

Model conditions using magnetic parameters and/or magnetite chemical composition were applied to unmix the River Eden sediment samples (Figure 5.9C). The results show similar compositions for all the sediment samples. The model a), which is based uniquely on magnetic parameters, suggests that the River Eden sediment samples are mostly made of sedimentary rocks whereas models b) and c) point to glacial till as the main sediment source, with andesite being present in varying proportions.

The combined results (presented in Figure 5.9) suggest that magnetic parameters which were found to be the closest to the linear additivity are the most suitable parameters with which to model the sediment samples collected in the four River Eden tributaries. Magnetite composition fails to recognise the basalt contribution, suggesting that magnetite grains are mostly from the glacial till in all sediment samples. Some minor contribution from the sedimentary rocks, found in some of the Barroway Burn and Moonzie Burn sediment samples, suggests some doubt about the confidence of the results. However, the modelling results using combined magnetite composition and magnetic parameters data seem to be influenced principally by the magnetite composition as similar results are obtained when considering the magnetite composition only to model the sediment samples.

5.2.3. Testing the linear programming model: Modelling the provenance of stream sediment taken the Eden tributaries as sediment sources

Sediment samples collected in each of the four tributaries of the River Eden were considered as sources of the sediment transported along the River Eden. This provides an opportunity to test the output given by linear programming. Tables 5.8 and 5.9 show the results obtained when applying linear programming to unmix some stream sediment samples, taking the Barroway Burn, the Moonzie Burn, the Kilgour Burn and the Coalpit Burn as the sediment sources. The selected sediment samples from the Barroway Burn should be recognised by linear programming as having been derived only from the Barroway Burn whereas the selected sediment samples from the Moonzie Burn should be found to derive only from the Moonzie Burn, and so on. Sediment samples were modelled, firstly, using the most linearly additive magnetic parameters (χ_{lf}, IRM_{40} and $HIRM_{-20}$), secondly, considering only the seven main elements measured as oxides in magnetite grains, and finally, considering both the magnetite composition and the magnetic data, as in the previously discussed cases.

In both Table 5.8 and Table 5.9 results from the three modelling cases are given for the selected sediment samples collected in the Barroway Burn and the Moonzie Burn, and in the Kilgour Burn and the Coalpit Burn, respectively. In many cases the modelled sedimentary provenance does not accord with expectation. The total error of the model output corresponding to each of the three modelling cases considered (mean+sd, mean, and mean-sd values assigned to each source group) are given in Table 5.10. The smallest error is found when (1) assigning mean values of the three most linearly additive magnetic variables to each source group (33.8%); (2) mean-sd values of each of the eight main elements analysed in magnetite grains are used to unmix the sediment samples (26.6%); and (3) when mean-sd values of the magnetic and chemical variables measured in each source group are combined in the modelling approach (20.0%).

The same procedure applied to unmixing selected River Eden sediment samples shows a wide range of results depending, on the variables used and on the value assigned to each sediment source (Table 5.11). On this basis, however, three cases only are considered: (1) mean values of the magnetic parameters, which point to the Kilgour Burn sediment as the major source of the River Eden sediment in most cases, (2) mean-sd values of the magnetite composition, which suggest an andesitic origin for most of the magnetite grains transported by the River Eden and (3) the combination of magnetic and magnetite compositional variables, which show a greater variability in the contribution of each source group to the River Eden

Table 5.8. Linear programming model output for selected Barroway Burn (BB) and Moonzie Burn (MB) sediment samples when using (a) χ_{lf}, IRM_{40} and $HIRM_{-20}$, (b) eight main elements measured as oxides in magnetite grains, and (c) the combination of both (a) and (b) variables characterising the four River Eden tributaries under study (see text for explanation). Major sediment source contribution is shaded.

Sample		(a)				(b)				(c)			
		BB	**MB**	**KB**	**CB**	**BB**	**MB**	**KB**	**CB**	**BB**	**MB**	**KB**	**CB**
BB3 (2-3 ϕ)	Mean+sd	-	1.00	-	-	**0.84**	0.15	-	-	**0.69**	0.30	-	-
	Mean	**0.01**	0.52	0.46	-	**1.00**	-	-	-	**0.99**	-	-	-
	Mean-sd	**0.25**	0.66	0.08	-	**1.00**	-	-	-	**0.99**	-	-	0.01
BB3 (Bulk)	Mean+sd	**0.52**	0.47	-	-								
	Mean	**0.93**	-	-	0.07								
	Mean-sd	**0.61**	-	-	0.39								
BB6 (2-3 ϕ)	Mean+sd	-	1.00	-	-	-	0.46	0.45	0.08	**0.32**	0.47	0.20	-
	Mean	**0.27**	-	0.72	-	**0.98**	-	0.74	0.01	**0.97**	-	0.01	0.01
	Mean-sd	**0.80**	0.17	-	0.02	**0.17**	-	0.63	0.18	**0.36**	-	0.47	0.15
BB6 (Bulk)	Mean+sd	**0.99**	-	-	-								
	Mean	**0.88**	-	-	0.12								
	Mean-sd	**0.50**	-	-	0.50								
BB7 (2-3 ϕ)	Mean+sd	-	1.00	-	-	-	0.96	0.03	-	-	1.00	-	-
	Mean	**0.18**	-	0.81	-	**0.99**	-	-	-	**0.99**	-	-	-
	Mean-sd	**0.91**	-	0.06	0.03	-	0.85	0.14	-	**1.00**	-	-	-
BB7 (Bulk)	Mean+sd	-	0.69	0.30	-								
	Mean	**0.80**	-	0.12	0.08								
	Mean-sd	**0.65**	-	-	0.35								
MB1 (2-3 ϕ)	Mean+sd	-	**1.00**	-	-	-	**1.00**	-	-	-	**1.00**	-	-
	Mean	-	-	1.00	-	1.00	-	-	-	1.00	-	-	-
	Mean-sd	0.11	-	0.88	-	-	**0.99**	-	-	1.00	-	-	-
MB1 (Bulk)	Mean+sd	-	**1.00**	-	-								
	Mean	-	**1.00**	-	-								
	Mean-sd	1.00	-	-	-								
MB4 (2-3 ϕ)	Mean+sd	-	**1.00**	-	-	-	**1.00**	-	-	-	**1.00**	-	-
	Mean	-	-	1.00	-	1.00	-	-	-	1.00	-	-	-
	Mean-sd	-	-	0.91	0.08	.	**0.98**	-	0.02	-	**0.65**	0.34	-
MB4 (Bulk)	Mean+sd	-	**1.00**	-	-								
	Mean	-	**0.97**	-	0.02								
	Mean-sd	-	-	0.75	0.24								

Table 5.9. Linear programming model output for selected Kilgour Burn (KB) and Coalpit Burn (CB) sediment samples when using (a) χ_{lf}, IRM_{40} and $HIRM_{-20}$, (b) eight main elements measured as oxides in magnetite grains, and (c) the combination of both (a) and (b) variables characterising the four River Eden tributaries under study (see text for explanation). Major sediment source contribution is shaded.

Sample		(a)				(b)				(c)			
		BB	**MB**	**KB**	**CB**	**BB**	**MB**	**KB**	**CB**	**BB**	**MB**	**KB**	**CB**
KB1 (2-3 ϕ)	Mean+sd	-	1.00	-	-	-	0.05	**0.94**	-	-	0.15	**0.84**	-
	Mean	-	-	**1.00**	-	0.98	-	-	0.01	0.98	-	-	0.01
	Mean-sd	-	-	**1.00**	-	-	-	**0.82**	0.17	-	-	**1.00**	-
KB1 (Bulk)	Mean+sd	-	1.00	-	-								
	Mean	-	-	**1.00**	-								
	Mean-sd	-	-	**0.94**	0.05								
KB6 (2-3 ϕ)	Mean+sd	-	1.00	-	-	-	0.77	**0.22**	-	-	1.00	-	-
	Mean	-	-	**1.00**	-	0.99	-	**0.01**	-	0.98	-	**0.10**	-
	Mean-sd	-	-	**1.00**	-	-	-	**0.99**	-	-	-	**1.00**	-
KB6 (Bulk)	Mean+sd	-	1.00	-	-								
	Mean	1.00	-	-	-								
	Mean-sd	0.79	-	-	0.20								
CB1 (2-3 ϕ)	Mean+sd	-	-	0.78	**0.21**	-	-	0.04	**0.95**	0.67	-	-	**0.32**
	Mean	-	-	0.35	**0.65**	0.97	-	-	**0.03**	0.82	-	-	**0.18**
	Mean-sd	-	-	-	**1.00**	-	-	-	**1.00**	-	-	-	**1.00**
CB1 (Bulk)	Mean+sd	-	0.35	-	**0.64**								
	Mean	-	-	-	**1.00**								
	Mean-sd	-	-	-	**1.00**								
CB5 (2-3 ϕ)	Mean+sd	-	0.03	0.72	**0.24**	-	0.57	0.14	**0.27**	-	0.57	0.15	**0.27**
	Mean	-	-	0.30	**0.70**	0.97	-	0.01	**0.02**	0.68	-	0.01	**0.30**
	Mean-sd	-	-	-	**1.00**	0.36	0.06	0.18	**0.39**	-	-	-	**1.00**
CB5 (Bulk)	Mean+sd	-	0.64	-	**0.35**								
	Mean	0.15	-	-	**0.85**								
	Mean-sd	-	-	-	**1.00**								
CB6 (2-3 ϕ)	Mean+sd	0.39	-	-	**0.61**	-	0.03	-	**0.95**	-	0.24	-	**0.75**
	Mean	-	-	-	**1.00**	0.87	0.01	-	**0.12**	0.57	-	-	**0.42**
	Mean-sd	-	-	-	**1.00**	-	-	-	**1.00**	-	-	-	**1.00**
CB6 (Bulk)	Mean+sd	-	-	-	**1.00**								
	Mean	-	-	-	**1.00**								
	Mean-sd	-	-	-	**1.00**								

Table 5.10. Percentage of error calculated for the linear programming model output data shown in Table 5.8 and Table 5.9 when using (a) χ_{lf}, IRM_{40} and $HIRM_{-20}$, (b) eight main elements measured as oxides in magnetite grains, and (c) the combination of both (a) and (b) variables characterising the four River Eden tributaries under study (see text for explanation).

	(a)	(b)	(c)
Mean+sd	57.20%	38.30%	48.10%
Mean	33.80%	68.50%	60.50%
Mean-sd	36.70%	26.60%	20.00%

sediment, suggesting that there is more mixing downstream. Comparing these results with those obtained from discriminant analysis (Section 5.1), the use of mean-sd values of magnetic parameters and magnetite composition leads to results similar to those shown in Figure 5.6.

5.2.4. Summary of the linear programming results

The suitability of linear programming to quantitatively unmix the stream sediments of the River Eden catchment is therefore found to be limited. Modelling results have highlighted the importance of linear additivity of the variables used in the mathematical approach. Thus, the most environmentally sensible results were obtained when using the most linearly additive magnetic parameters. However, such results were found to be crude estimates of sediment provenance as significant errors were detected. Neither the use of magnetite composition nor the combination of both magnetic measurements and magnetite chemistry improved the results. Nevertheless, in all cases, mean values were found to be adequate in characterising sediment source, despite the variability within each source.

Use of the linear programming model did not provide much more useful information than was obtained using discriminant function analysis (Section 5.1) in quantifying sedimentary provenance. However, this analysis of this kind of modelling has highlighted the suitability and importance of magnetic measurements as sedimentary provenance indicators.

Table 5.11. Linear programming model output for selected River Eden (RE) sediment samples when using (a) χ_{lf}, IRM_{40} and $HIRM_{-20}$, (b) eight main elements measured as oxides in magnetite grains, and (c) the combination of both (a) and (b) variables characterising the four River Eden tributaries under study (see text for explanation).

Sample		(a)				(b)				(c)			
		BB	**MB**	**KB**	**CB**	**BB**	**MB**	**KB**	**CB**	**BB**	**MB**	**KB**	**CB**
RE1	Mean+sd	-	1.00	-	-	0.41	0.45	0.13	-	0.11	0.59	0.29	-
(2-3 ϕ)	Mean	-	-	1.00	-	0.98	-	-	0.01	0.98	-	-	0.01
	Mean-sd	-	-	1.00	-	-	0.30	0.55	0.16	0.39	0.46	0.07	0.08
RE1	Mean+sd	-	1.00	-	-								
(Bulk)	Mean	-	-	1.00	-								
	Mean-sd	0.02	-	0.96	-								
RE2	Mean+sd	-	1.00	-	-	0.18	0.77	0.01	0.03	0.27	0.72	-	-
(2-3 ϕ)	Mean	0.04	0.94	-	0.01	0.99	-	-	0.01	0.98	-	-	-
	Mean-sd	-	0.98	-	0.02	0.20	0.65	-	0.15	0.39	0.46	0.07	0.08
RE2	Mean+sd	0.42	0.56	-	0.02								
(Bulk)	Mean	0.88	-	-	0.12								
	Mean-sd	0.50	-	-	0.50								
RE3	Mean+sd	-	1.00	-	-	0.25	0.69	-	0.06	0.42	0.52	0.05	-
(2-3 ϕ)	Mean	-	-	1.00	-	0.98	-	-	0.01	0.98	-	-	0.01
	Mean-sd	-	-	1.00	-	0.23	0.55	-	0.21	-	-	1.00	-
RE3	Mean+sd	-	1.00	-	-								
(Bulk)	Mean	-	-	1.00	-								
	Mean-sd	-	-	1.00	-								
RE4	Mean+sd	-	1.00	-	-	-	1.00	-	-	1.00	-	-	-
(2-3 ϕ)	Mean	-	-	1.00	-	0.97	-	0.01	0.02	0.97	0.01	-	0.01
	Mean-sd	-	-	0.94	0.05	-	0.27	-	0.71	-	-	0.88	0.12
RE4	Mean+sd	-	1.00	-	-								
(Bulk)	Mean	-	-	0.99	0.01								
	Mean-sd	0.23	-	0.63	0.14								
RE5	Mean+sd	-	1.00	-	-	-	1.00	-	-	-	1.00	-	-
(2-3 ϕ)	Mean	-	-	1.00	-	0.98	-	0.01	-	0.98	-	0.01	-
	Mean-sd	-	0.01	0.98	-	-	1.00	-	-	-	0.07	0.93	-
RE5	Mean+sd	-	1.00	-	-								
(Bulk)	Mean	-	-	1.00	-								
	Mean-sd	0.32	0.08	0.59	-								
RE6	Mean+sd	-	1.00	-	-	-	1.00	-	-	-	1.00	-	-
(2-3 ϕ)	Mean	-	0.13	0.86	-	0.98	-	0.01	-	0.98	-	0.01	-
	Mean-sd	0.19	-	0.66	0.13	-	1.00	-	-	-	0.80	0.18	-
RE6	Mean+sd	-	1.00	-	-								
(Bulk)	Mean	-	0.80	0.20	-								
	Mean-sd	0.22	0.01	0.59	0.16								

5.3. Summary and conclusions

Discriminant function analysis provides a good qualitative sedimentary provenance model. Results agree with those given in Chapter 4, suggesting that the northern Eden tributaries' (Barroway Burn and Moonzie Burn) sediment is mainly composed of andesite and glacial till, whilst sediment sampled in the southern Eden tributaries (Kilgour Burn and Coalpit Burn) is mainly derived from basalt and sedimentary rocks. Differences in the sediment transported by streams flowing over similar materials (rocks and till) are due to variations in the relative contribution of the sources. Thus, the Barroway Burn sediment shows a greater contribution from the glacial till than the Moonzie Burn sediment. Similarly, the Kilgour Burn sediment shows a greater contribution from sedimentary rocks than the Coalpit Burn sediment. On the other hand, all sediment samples from the main course of the River Eden show similar characteristics, suggesting a tendency of the mixing fluvial process to homogenise the mineral assemblage. Nevertheless, downstream variation in the tributary supply is detected.

Discriminant function analysis results also set up the basis for linear programming modelling as it highlights the greater discriminant power of the magnetic measurements over the magnetite chemical composition, and also that all sediment sources have been identified, being classified as basalts, andesites, sedimentary rocks and glacial till. All these sources are clearly differentiated on the basis of their magnetic properties, however, their proximity within the discriminant space makes the model interpretation difficult, the detailed information resulting from the interpretation of the analytical data (Chapter 4) being necessary.

Linear programming modelling underlines the power of magnetic measurements in modelling approach over magnetite composition. However, a quantitative estimate of sediment provenance fails, due principally to the non-linear additivity of the variables, and the interrelationship of the source magnetic characteristics.

The importance of a very detailed characterisation of sources and sediment is highlighted in order to make an adequate environmental interpretation of both qualitative and quantitative models.

6. Discussion

The analytical and statistical results presented in Chapters 4 and 5 were obtained in this study in order to address three main issues: (1) the chemical and physical changes of Fe-Ti oxides from rocks to sediments, (2) the provenance of sediments in the River Eden and its tributaries, and (3) the evaluation of geochemical and magnetic measurements in sedimentary environmental studies. These issues are discussed using data and conclusions derived in previous chapters. The form that further research might take in order to understand such systems better is also discussed.

6.1. Chemical and physical changes suffered by the Fe-Ti oxides from rocks and till to stream sediment

The process of rocks being weathered to create sediment involves chemical alteration, physical abrasion and separation of minerals. As mentioned in Chapter 2, however, heavy minerals are often characterised by their high chemical stability. In Chapter 4 it was shown that during the initial subaerial chemical degradation of igneous rocks present in the Eden catchment the Fe-Ti oxides did not suffer significant compositional change. The principal change was a slight decrease in the weight percentage of FeO, TiO_2 and the total sum of elements measured in magnetite grains towards the more advanced chemical weathering stages of the rock, suggesting initial magnetite oxidation, perhaps to a metastable oxyhydroxide phase (e.g. goethite, lepidocrocite or limonite) which, in time, will convert to hematite. However, surprisingly, FeO depletion in the magnetite grains is not accompanied by an increase in Fe_2O_3. This might be due to a removal of Fe^{2+} in solution.

Magnetic measurements, however, also successfully detected such an oxidation of the magnetite grains towards increasing weathering stages of the rock. They also indicated a relatively increased concentration of magnetic minerals with weathering. This may be due to the differential removal of mineral phases which are more susceptible to chemical and physical alteration. Again this was not the objective of study and remains unconstrained.

The total chemical and physical degradation of the rock transforms it into sediment which becomes part of the fluvial system defining the River Eden catchment. The Fe-Ti oxides initially become part of the stream sediments being fresh chemically and morphologically reflecting their parental characteristics. Subsequently they suffer chemical and physical abrasion during transport in river water.

Magnetite grains from a rock sample known to be weathered under subaqueous conditions (em39) were analysed, being found to be partially replaced by sphene ($CaTiSiO_5$). Van der Voo *et al.* (1993) described a similar alteration feature with primary titanomagnetite giving pure magnetite (Fe_3O_4) and sphene ($CaTiSiO_5$). They ascribed it to late hydrothermal circulation, which is common at relatively low temperatures in igneous rocks and often results in the alteration of primary Mg-silicates to chlorite. In the River Eden catchment study none of the magnetite grains analysed in fresh rock samples was found to be altered to sphene and, on the other hand, SiO_2- and CaO-content increased towards the rim of the magnetite grain and along internal fractures. The same phenomenon was observed in numerous magnetite grains analysed from stream sediment samples. These magnetite grains showed abundant internal fractures infilled with a SiO_2-rich phase (a precise chemical analysis could not be performed due to the very small width of such fractures). Electron probe microanalysis of the altered areas in the stream magnetite grains revealed stoichiometric occasional sphene (see for example analyses 37 in BB6 sample and 39 in RE4 sample given in Appendix 4) apparently as a result of hydrological alteration of the magnetite. A general trend was found in which magnetite alteration was more frequent in those magnetite grains derived from basaltic rocks (Figure 4.18), perhaps being due to higher TiO_2-content in the magnetite within more basic rocks (Chapter 4).

Such secondary origin of sphene may also be found replacing ilmenite, but in this study stream ilmenite grains appear chemically unaltered suggesting a higher chemical resistance of the ilmenite grains compared with magnetite grains.

The magnetic properties of rocks did not seem to be affected by the alteration of magnetite to sphene (Section 4.1). When comparing magnetic properties of sediment sources (rocks and glacial till) with stream sediments a similar magnetic mineral paragenesis is suggested in both source material and sediment. This accords with the electron probe microanalysis data of magnetite and ilmenite grains which suggest that no significant compositional changes are produced during the transport of Fe-Ti grains, at least in terms of their FeO-, Fe_2O_3- and TiO_2-contents. Thus, the hematite concentration shown by magnetic measurements of stream sediment

samples seems to be derived from rocks and till and not as a result of an oxidation of magnetite and/or ilmenite grains.

Backscattered electron images were used to estimate the mean grain size of magnetite in various rock and glacial till samples, in order to examine the relationship of magnetite grain size with fluvial sediment transport. The results were rather unexpected as till and sediment samples showed much greater mean grain size than any of the rock samples (Subsections 4.1.2, 4.2.1 and 4.3.1). Two main reasons are offered in explanation: (1) streams lead to selective mineral concentration in terms of grain size, and (2) sampling preparation for electron probe microanalysis, including sieving, heavy liquid and hand-magnet separation of the magnetite grains, leads to preferential selection of magnetite grains on the basis of their grain size. However, with the generated data for this study, the relative importance of each of these reasons could not be assessed.

Magnetic measurements appeared to provide the best method of estimating magnetite grain size. There are small differences in the grain size of the magnetite constituting the rocks with a tendency to increase towards the more basic rocks (Chapter 4). Glacial till was found to be composed of magnetite of similar grain size to andesitic rocks (Figures 4.9 and 4.16). Stream sediments showed some variability in magnetite grain size, however, such variability was found to be within the magnetite grain size range defined by all rock and till samples. Therefore, no changes in magnetite grain size were found in the sediment as a result of fluvial transport, and this morphological characteristic was found to be an excellent source fingerprint (Section 4.3). However, sediments sampled along the River Eden showed, surprisingly, a downstream increase in magnetite grain size. A similar downstream trend was also observed for ulvospinel-rich magnetite and for relative magnetite to hematite concentration (Figure 4.28). A clue to understanding such a counter-intuitive distribution of magnetic mineralogy along the River Eden is in the topography and distribution of the tributaries within the River Eden catchment (Figure 4.1). The higher relief in the southern part (maximum height of 424 m) compared to the northern part (maximum height of 285 m) of the Eden catchment, and most northerly tributaries join the River Eden at points closer to its source than the southern tributaries which tend to discharge their water and sediment mainly towards the River Eden mouth. All this suggests a decreasing concentration of magnetite derived from andesitic rocks and glacial till at the same time as an increasing concentration of magnetite derived mainly from basaltic rocks downstream.

Variations in texture or shape of magnetite grains during fluvial transport were not observed. Chemical and physical resistance of magnetite grains during the initial degradation of rocks to become sediment and during its transport by the River Eden and its tributaries gives confidence to their use as sedimentary provenance indicators in the catchment.

6.2. Provenance of the sediment in the River Eden catchment: Evaluation of qualitative and quantitative approaches

A first step in any sedimentary provenance study is to identify and differentiate all potential sediment sources in the study area. From this study six main potential sediment sources were recognised in the River Eden catchment on the basis of their chemical and magnetic characteristics (Chapter 4), namely: basalts, basaltic andesites, andesites, dacite-rhyolites, glacial till and sedimentary rocks (principally sandstones and limestones).

A second essential requirement in provenance studies is to identify a provenance indicator, i.e. a characteristic of the source material (e.g. whole-source chemistry, magnetism or mineralogy) which makes it unique and perfectly distinguishable from any other potential source and, at the same time, which remains unmodified during the geological cycle involving rock transformation to sediment (and potentially back to sedimentary rock). The chemical and magnetic differences seen among the six main sediment sources from the River Eden catchment derive from their mineralogical differences. Therefore, heavy minerals which are generally regarded as highly resistant (Chapter 2) may be used in this study as provenance indicators. An initial general mineral characterisation of the source materials revealed (Chapters 3 and 4) that the most common heavy minerals found in the majority of sources (with the exception of the sedimentary rocks) are Fe-Ti oxides (mainly ilmenite and magnetite). As discussed above, ilmenite was found to be chemically more resistant to change than magnetite. However, its similar chemical and morphological characteristics in all source materials, where present, reject its use as provenance indicator. On the other hand, compositional and morphological (i.e. texture, grain size, shape) features of magnetite and magnetic characteristics reveal significant differences between the primary sources. The interpretation of the statistical data shows that in the igneous rocks there is a trend defined by a decrease in relative ulvospinel-rich to magnetite-rich titanomagnetite concentration, in relative magnetite to hematite concentration, in magnetite grain size, and generally in the concentration of magnetic minerals towards the more acid rocks. Magnetite in glacial

till shows a wide compositional variability in terms of its three major elements (FeO, Fe_2O_3 and TiO_2), as expected in this kind of sedimentary deposit. Magnetic characteristics of the till suggest, however, similar relative magnetite to hematite concentrations, magnetite grain size and concentration of magnetic minerals as the andesite. Sandstones are found to contain a minor component of hematite according to magnetic parameters.

A similar approach was used to test the suitability of the magnetite characteristics as provenance indicators by comparing the results from sediments with those obtained from the analysis of source materials. The four tributaries were selected in such a way that their sediment sources are known *a priori*, the number of sources being a maximum of two for each stream. Thus, the Barroway Burn and the Moonzie Burn (from the northern part of the River Eden catchment) derive sediment mainly from andesitic rocks and glacial till, whilst the Kilgour Burn and the Coalpit Burn (from the southern part of the River Eden catchment) derive sediment mainly from basalt and sedimentary rocks. The results were very satisfactory as magnetite found in the northern tributaries presented a composition and grain size within the range defined by both andesitic rocks and glacial till whereas magnetite from the southern tributaries shows a relative TiO_2 enrichment and a greater grain size typical of basalts. Each tributary sediment was found to define an independent group, i.e. the magnetic mineral characteristics of the sediments derived from the same sources appear, however, 'unmixed', to define unique and independent groups (e.g. Figure 4.25). This is partly due to the heterogeneity existing within each source group which though minimal in comparison with the heterogeneity between source groups, must always be kept in mind in environmental studies. Also, the selective transport and deposition of sediment particles by the fluvial system must be taken into account on the basis of, mainly, their size, shape and density but also the energy of the system (directly dependent on the stream flow and the topography of the area) and possible barriers (e.g. large rocks or trees) along the stream course. A third factor possibly affecting the results is the relative proportion of each of the sources mixed to form the sediment. This last factor is particularly important when measuring magnetic parameters as most of them are, theoretically, linearly additive due to their magnetic concentration dependence (Chapter 3). Understanding this system better is very important as, at first sight, the method seems to provide a means of identifying individual tributaries, and thus providing an important new environmental tool.

The River Eden sediment samples show, as expected, a greater variability, in terms of magnetic mineral characteristics, than any of the tributaries as a result of a more complex mixing process involving a greater number of sources. Despite the

heterogeneity the results are within the range defined by all six considered sediment sources, closely grouped over the four tributary areas (Figures 4.22, 4.23 and 4.24). This data, together with the downstream mineralogical trend described and discussed above (Section 6.1), underlines the conservative magnetite source fingerprint in the sediment transported by the River Eden.

Discriminant function analysis (Chapter 3) provides a qualitative and/or a semi-quantitative estimation of the sediment origin. In this study, sources are most successfully discriminated by magnetic measurements, as magnetite chemical composition differs significantly between sources, although the signature is not unique (Figures 4.5 and 4.13). When sources and sediment samples are plotted in discriminant space using their magnetic characteristics, there is overlap between sediment and source materials (Figure 5.1). This suggests that all main potential sources of the sediment transported by the River Eden fluvial system have probably been identified. Also it is observed that whilst dacite-rhyolite was considered as a potential sediment source in the study area this group does not contribute significantly to the formation of the sediment samples. On the other hand, the similarity between basaltic andesites and andesites, which occupy the same discriminant space, has been highlighted. Thus, discriminant analysis effectively reduced the number of sediment sources from six to four: basalts, andesites, glacial till and sedimentary rocks. The andesite and glacial till groups are difficult to be distinguished, being located between basalt and sedimentary rocks groups in discriminant function space (Figure 5.1).

Most sediment samples surprisingly overlap the andesite and glacial till groups (Figures 5.1, 5.3 and 5.4) even when, as discussed earlier, the sediments of the Kilgour Burn and the Coalpit Burn are derived from basalts and sedimentary rocks without any andesite contribution. This may be explained by the fact that andesite and glacial till groups are very close to the basalt group and occupy an intermediate place between such a group and the sedimentary rocks group. Thus, sediment resulting from a mixture of basalt and sedimentary rocks shows magnetic characteristics similar to sediment composed mainly of andesite. Therefore, it is seen that in such circumstances, markedly different sedimentary provenance may, however, give sediment with similar magnetic characteristics. With this in mind, it is seen that the sediment of the Kilgour Burn shows a greater contribution from sedimentary rocks than that of the Coalpit Burn, whilst the sediment of the Barroway Burn is dominated by glacial till in contrast with that of the Moonzie Burn which shows both andesite and glacial till contributions. This agrees with the results presented in Chapter 4 and also with the environmental observations: the Kilgour

Burn sediment samples were collected mainly along a sedimentary bank presenting a greater topographic slope compared with the Coalpit Burn (Figure 3.3) which would be expected to lead to a greater relative contribution from the sedimentary rocks. As sedimentary rocks were found to be essentially composed of non-magnetic minerals their contribution to the sediment will result in a dilution or decrease in the strong intensity of the magnetic signature characteristic of the basalts. Similarly, field observations showed a more widespread occurrence of glacial till along the Barroway Burn course compared with that of the Moonzie Burn (Figures 1.1 and 2.2).

The River Eden sediment samples overlap both the andesite and glacial till groups, a slight trend towards glacial till magnetic characteristics being observed (Figure 5.1). The results presented in Chapter 4 suggest that magnetic minerals transported by the River Eden are derived dominantly from basalts, andesites and glacial till along its northern and southern tributaries. However, an important contribution from the sedimentary rocks to the River Eden sediment might be expected as its main course flows mainly along the Upper Devonian sandstones (Figures 1.1, 2.1 and 2.2). Such sandstones are easily eroded as a consequence of their weak cementation (Chapter 2) and thus, the bed of the River Eden is observed to be covered with sand deposits. The sandstone contribution to the sediment of the River Eden is shown when the basalt, andesite and sedimentary rocks groups are considered (Figures 5.3 and 5.4). As explained above, this non-magnetic contribution to the River Eden sediment leads to a weakness of the magnetic signature derived from the igneous rocks and the glacial till. However, it was found that due to the specific magnetic properties of the basalt, andesite and glacial till groups, sediment samples resulting from different mixtures of different source materials may show very similar resulting magnetic characteristics, a fact which makes the estimation of the relative contributions of each source material to the resulting mixed sediment difficult.

Sampling location plays a major role in the sediment composition as a function of proximity of the tributaries to the main river channel. However, the similarity of the sample characteristics suggests that the complex mixing process involving the various sources which occur during sediment transport by the River Eden have a tendency to homogenise the magnetic properties of the sediment along the river course.

Discriminant function analysis provides a good qualitative means of modelling of the sediment provenance of the tributaries of the River Eden . However, as in any mathematical approach a through interpretation of the results requires a

deep knowledge of the characteristics of the sediment sources which in this particular study involves mainly composition, grain size and concentration of magnetite, as well as the geological and geographical (topography, tributaries distribution) settings. Although complex mixing involving numerous sources (at least four main sources) makes recognition of the relative contribution of each source difficult, the results show a clear source fingerprint for the sediment.

The SIMPLEX model has a number of constraints when applied to environmental studies (Chapter 5). Here, none of the models was found to be environmentally consistent when considering either rocks and glacial till or the four Eden tributaries as sedimentary sources. The main factors responsible for the failure of the quantitative approach in this sedimentary provenance study are suggested to be: (1) the similarity of the magnetic mineral characteristics of the different sediment sources, (2) the intermediate magnetic characteristics of the andesite and glacial till groups between the basalt and sedimentary rocks groups, and (3) the fact that linearly additive magnetic parameters are all interdependent, being magnetic mineral concentration-dependent. Ideally, other independent variables could be included to make discrimination more efficient.

Qualitative model of sediment provenance in the River Eden catchment

In Figure 6.1 is presented a qualitative summary of the provenance model obtained in this study for the stream sediments of the River Eden catchment. The results shown are derived from the knowledge of the geology and topography of the study area, and of the magnetic mineral composition of the potential sediment sources. Statistical approaches have also assisted in the interpretation of data interrelationships.

Figure 6.1 highlights the importance of geological and hydrographical settings (both intimately related to the topography) to the composition of the stream sediment samples, and also the environmental consistency of both geochemical and magnetic results. This is clearly appreciated when modelling the four Eden tributaries whose sediment sources are known *a priori* from the geological map (Figures 2.1 and 2.2). Thus, the northern tributaries (Barroway Burn and Moonzie Burn) transport sediment principally derived from andesitic rocks and till. However, the dominance of glacial till with respect to the contribution from andesitic rocks is clearly seen in the Barroway Burn sediment compared with the Moonzie Burn sediment. Such sediment composition variability between these two tributaries, as well as the variability observed in the composition of each sediment sample

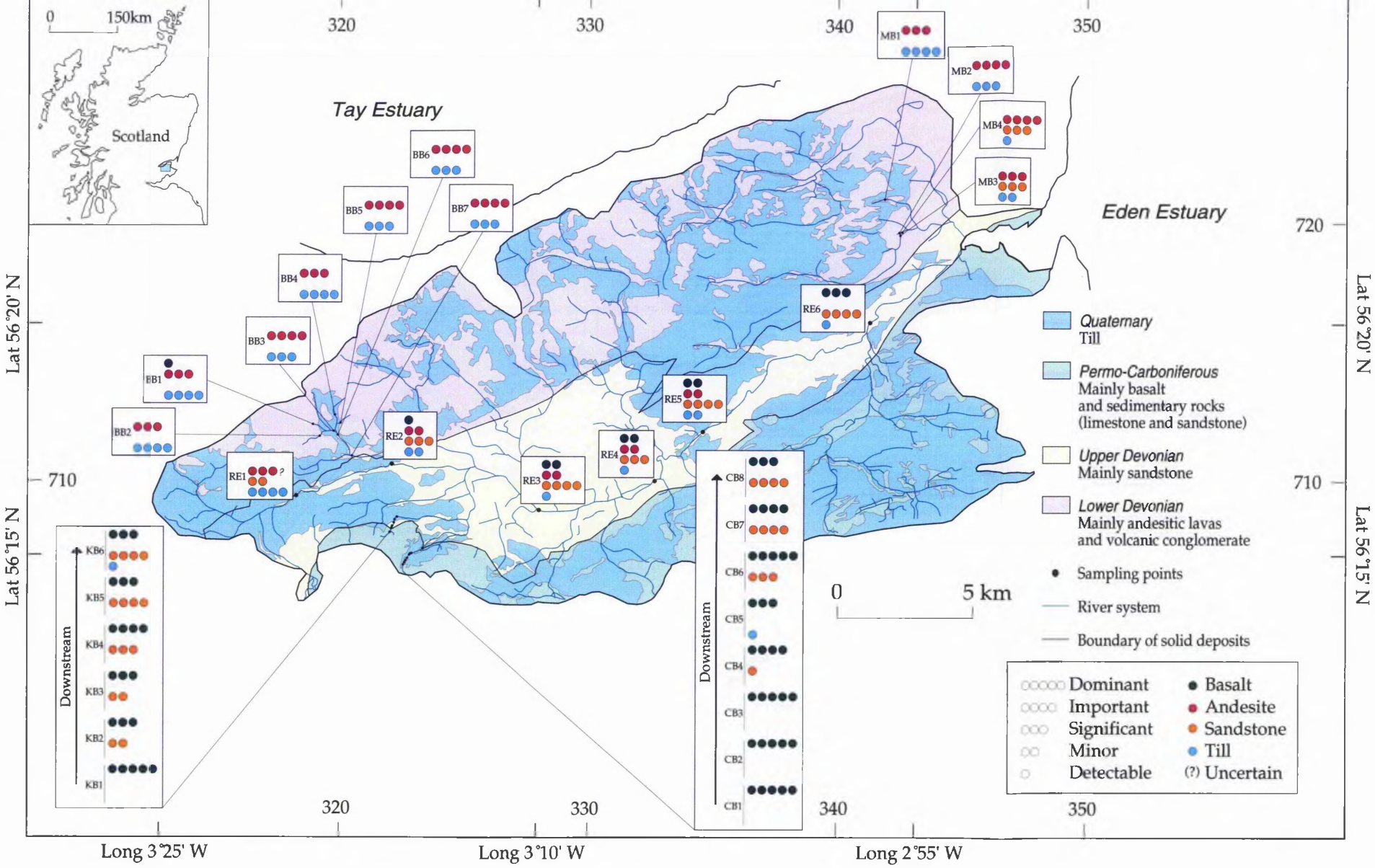

Figure 6.1. Provenance model for each stream sediment sample collected in the River Eden catchment, where four main sediment sources are distinguished (see text for explanation). BB: Barroway Burn, MB: Moonzie Burn, KB: Kilgour Burn, CB: Coalpit Burn, RE: River Eden.

collected along each tributary, is found to be due to differences in the sources present at the sampling points.

On the other hand, the sediments of the southern Eden tributaries (Kilgour Burn and Coalpit Burn) are found (as expected) to be mainly composed of basalt and sedimentary rocks (principally sandstone). These tributaries provide a means of observing the influence of both geology and topography on sediment composition. Downstream sampling along both tributaries shows an increasing contribution of sandstone relative to basalt. However, such an increase in the proportion of sandstone in the sediment is found to be more rapid in the Kilgour Burn sediment than in the Coalpit Burn sediment. These results may be explained in terms of topographic differences (Figure 3.3) as a steeper slope would favour the erosion of the sources, and so the formation of sediment transported by the river flow. The slope of the Kilgour Burn course flowing over sandstone is markedly more pronounced than that of the Coalpit Burn course and, therefore, the easily erodible sandstone is believed to contribute more greatly to the sediment of this tributary as compared with the Coalpit Burn. All these environmentally consistent results obtained from the study of the Eden tributaries provide a strong basis for the modelling of the provenance of sediment in the River Eden. The contribution of all four main sediment sources (basalt, andesite, sandstone and till) identified in the Eden catchment are successfully detected in most of the sediment samples collected along the main channel of the River Eden. The exceptions are Samples RE1 and RE6 where basalt and andesite are respectively not detected. As mentioned in Chapter 5, basalt contribution could be hidden by the andesite contribution because of the intermediate characteristics of andesite between those of basalt and sandstone. For this reason the andesite contribution to Sample RE1 is indicated as uncertain. The marked basalt signature in Sample RE6 could, however, be masking the andesite signature.

The significant contribution of the sandstone to the sediment along the River Eden course is observed. However, the basalt contribution tends to be more significant downstream, whilst the andesite and, principally, the till contributions tend to decrease. The reason for this downstream variation in the sediment composition of the River Eden is found in the geographical distribution of the river system. Whereas the River Eden is predominantly supplied in its upper reaches by the northern tributaries, i.e. those which flow over the Lower Devonian andesitic rocks, the importance of the southern tributaries, flowing over the Carboniferous basaltic rocks, increases through the lower reaches towards the River Eden mouth. Thus, the proximity of Sample RE6 to the confluence of an important southern

tributary system (in terms of its length and the volume of basaltic rocks over which flows) to the Eden course is significant and could explain the marked basalt contribution to the composition of this sample.

From Figure 6.1 it may be appreciated that, although a quantification of the sediment composition in the River Eden catchment has not been possible, an environmentally sensible qualitative provenance model is derived from this study. This affirms the suitability of both geochemical and magnetic approaches in sedimentary provenance studies which clearly enable sediment samples to be distinguished within and between stream systems in terms of their origin.

6.3. Evaluation of geochemical and magnetic measurements in mineral characterisation and sedimentary provenance studies

Numerous authors have used chemical and textural characteristics of Fe-Ti oxides (mainly magnetite and/or ilmenite), and magnetic measurements separately as sedimentary provenance indicators (Chapter 2). In this study, however, both approaches have been combined in a more complete magnetic mineral characterisation of the sediment and its sources in the River Eden catchment.

Authors such as Darby and Tsang (1987) Basu and Molinaroli (1989, 1991), and Schneiderman (1995) found marked chemical differences (principally in Ti-, Al- and Mg-contents) in detrital ilmenite derived from igneous and metamorphic rocks. Similarly, Grigsby (1992) discriminated successfully detrital ilmenite grains derived from plutonic and volcanic rocks. In the River Eden catchment, where ilmenite grains from basaltic and andesitic rocks have been studied chemically and texturally, no differences have been found which led to reject this Fe-Ti oxide as provenance indicator (Chapter 4).

Grigsby (1990), by studying chemical and textural characteristics of detrital magnetite grains derived from plutonic, volcanic and metamorphic rocks, discriminated intermediate from felsic volcanic rock origins. However, magnetite grains derived from mafic volcanic rocks were found to widely vary, principally, in Ti-content. Thus, mafic and felsic volcanic rock sources could only be differentiated on the basis of the relative proportions of trellis-type and composite-type ilmenite-magnetite intergrowths (Plate 4.1). In the River Eden catchment, magnetite has been found to be both chemically and texturally variable within each rock sample and between different rock samples. However, whereas the textural variability is not

found to be rock-type discriminating, the magnetite chemistry varies related to the whole-rock chemistry. Thus, each rock type (basalt, basaltic andesite, andesite, dacite-rhyolite) has a characteristic Ti-content magnetite (Subsection 4.1.2). Nevertheless, as concluded by all above authors, magnetite compositional variability between source groups (rocks and till) was not found to be discriminating enough by itself as to provide a successful quantitative provenance model.

Magnetic parameters have been successfully applied in detecting changes in source contributions to the sediment found in reservoirs, lakes and river catchments (e.g. Stober and Thompson, 1979; Oldfield *et al.*, 1979; Walling *et al.*, 1979; Bradshaw and Thompson, 1985; Oldfield *et al.*, 1985; Stott, 1986; Andrews and Jennings, 1987; Walden *et al.*, 1995). However, although some quantitative sediment provenance models have also been derived only from the use of magnetic parameters (e.g. Yu and Oldfield, 1989, 1993; Lees, 1994; Walden *et al.*, 1997), major limitations were detected (Chapter 5).

In this study, magnetic measurements provided information about the mineralogy of both sources and sediment in the form of relative concentrations of different magnetic minerals found in each source group and of the total magnetic mineralogy between the groups. This concentration variability, together with differences in magnetic grain size suggested by the magnetic measurements, is found to be distinctive in a similar manner as the magnetite chemical variability, i.e. the variability is associated with whole-chemical composition differentiating the rocks and glacial till groups (Chapter 4). This magnetic mineral concentration dependence of the magnetic parameters leads to the recognition of the influence in sediment formation of non-magnetite-bearing materials, in the form of the local sedimentary rocks. The greater the contribution of non-magnetic minerals to the sediment, the lower the magnetic signature of the sediment as a consequence of the dilution of magnetite grains with other mineral grains (e.g. quartz).

Important advantages have been found in combining magnetite compositional and textural analyses, and magnetic measurements to both mineral characterisation and sedimentary provenance modelling.

Both chemical and magnetic approaches give coherent results while at the same time complementing to each other. Chemical analysis of minerals defines variations under both subaerial and subaqueous conditions, but while magnetic parameters recognise the subaerial weathering of the Fe-Ti oxides they do not detect the subaqueous alteration of titanomagnetite to sphene (Section 6.1). The chemical approach was found to be the most successful means of monitoring the magnetite

transfer from rocks to sediment, thus supporting its suitability as a provenance indicator. Also, magnetite compositional knowledge leads to a better understanding of the magnetic characteristics of the materials. Thus, the use of magnetic parameters indicates an increasing hematite contribution towards more acid rocks (greater SiO_2 concentration). However, as seen from magnetite chemical analysis, this is not an indication of rock weathering, but it is due to oxidation of the magnetite thereby an increasing Fe_2O_3-content associated with a depletion in FeO- and TiO_2-content in the magnetite during rock formation (Section 4.1). Furthermore, magnetic measurements were found to supply more information about mineralogy of sources and sediment in terms of their magnetic mineral concentration and grain size, and thus also the best means of estimating the contribution of non-magnetite-bearing materials to the sediment (although the method does not resolve what these materials might be).

Chemical and magnetic parameters, both separately and combined give good qualitative estimates of the sediment provenance in the River Eden catchment. However, a quantitative estimation by statistical methods has not been very successful. Magnetite chemistry, which independently would be reflecting the origin of magnetite grains origin, shows a minor variability between the sources which, together with their great intra-group variability, makes this dataset not sufficiently discriminating to provide a quantitative model. Similarly, magnetic parameters show an important intra-group variability, however, their intergroup differences are insufficient to discriminate sources (Chapter 5). In this study, the interrelationship observed in the magnetic properties of the groups (i.e. their mutual dependency) is found to be principally responsible for the failure of magnetic parameters in successful quantitative modelling.

6.4. Future work: Improving the quantitative sedimentary provenance modelling in river catchments

A major limitation to the accurate estimation (quantification) of the sources contributing to the stream sediment in the River Eden catchment has been found to be the impossibility of perfectly discriminating three of the main sediment sources of the catchment, namely: basalts, andesites and glacial till. Hence, it is found that more discriminating and independent variables would be required.

Diverse methodologies have been traditionally developed in sedimentary provenance studies. Among them, there are found several which could potentially

improve the provenance modelling results in river catchments where, as in the River Eden catchment, markedly magnetically distinctive materials are present.

Electron probe microanalysis does not discriminate the different Fe oxidation stages. Thus, Mössbauer spectrometry is suggested as an alternative technique which may be applied to the study of these three materials in an attempt to obtain a more accurate mineralogical characterisation. This technique has been found to be very successful in the identification of minerals differentiated by their relative Fe^{2+}/Fe^{3+} (e.g. magnetite, maghemite, hematite, goethite) contents.

An alternative analytical technique which could provide more detailed information on the different Fe-Ti oxides and their relative proportions can be obtained using VSM (Vibrating Sample Magnetometer). The hysteresis loop can be used to derive several valuable parameters (for details see e.g. Jiles, 1991; Lees, 1994). The saturation remanence to saturation magnetisation ratio versus the coercivity of remanence to coercive force ratio give information about magnetic grain size (e.g. Radhakrihnamurty and Deutsch, 1974; Day *et al.*, 1977; King *et al.*, 1982; Hodych, 1996). Also the saturation magnetisation is proportional to the concentration of magnetic minerals (canted anti-ferromagnetic and ferrimagnetic minerals) being grain size- and interaction-independent. However, Lees (1994) found using VSM parameters in sedimentary provenance studies, that the linear additivity of VSM measurements as well as experimental problems are still in need of resolution.

A general assessment of the magnetic instruments' accuracy and behaviour is required, principally when measuring strongly magnetic natural materials, in order to understand the reasons for the 'apparent' demagnetisation phenomena observed when measuring some stream sediment samples (Chapter 4).

Perhaps the best way forward is to identify parameters which are independent of magnetic data. Analysis of the sediment constituents of the River Eden directed at assessing the contribution of the glacial till to the sediment on the basis of minerals found uniquely in it (especially garnet) is a promising method for constraining this particular input to the sediment.

Numerous authors have already successfully applied radiogenic isotopic measurements of Sr, Nd, and Pb (e.g. Linn *et al.*, 1991; McCaffrey, 1994; Vroon *et al.*, 1995; Boghossian *et al.*, 1996; Evans, 1996; Glover *et al.*, 1996; Goldstein *et al.*, 1997; Graham *et al.*, 1997; McDaniel *et al.*, 1997), in sedimentary provenance studies. Another way to distinguish the contribution of basalts and andesites could be

isotopic measurements of whole-rock and whole-sediment samples as these two rock types show differences in, for example, Sr-content associated to their petrogenesis. Similarly, REE distributions in rock and bulk sediment samples might be used as tracers of sedimentary provenance (e.g. Condie *et al.*, 1995).

Finding those variables which best discriminate the potential sedimentary sources in a study area will certainly improve the results derived from linear programming. However, a better understanding of mathematical methods would be required in order to develop a better mathematical approximation to the complex environmental processes.

An accurate estimation of sediment provenance will lead to a better understanding of fluvial dynamics. Such information is important in constraining the transport of clastic material in rivers and relating them to sources, flow rates, topography, geological setting, etc.

Anthropogenic effects have not been detected in this study. However, numerous authors have found that pollution can be detected by compositional and textural analyses of magnetite spherules (e.g. Puffer *et al.*, 1980; Goldberg *et al.*, 1981; Hansen *et al.*, 1981), as well as by magnetic measurements (e.g. Hunt *et al.*, 1984; Oldfield *et al.*, 1985; Hunt, 1986; Locke and Bertine, 1986). The suitability of both approaches in sedimentary provenance studies has been addressed here and it is suggested that both approaches might be successfully combined. Hutchinson (1995) has estimated the erosion status and the rate of sedimentation in river catchment by using a combination of magnetic and geochemical (radiometric ^{137}C and ^{210}Pb) techniques. Both geochemical and magnetic parameters might then be appropriate in modelling the anthropogenic impact of deforestation or quarrying in the environment.

7. Conclusions

This study aimed to characterise the inputs into the Eden catchment using mineralogical provenance indicators. The aim was achieved, at least in part, and the principal conclusions are listed below.

7.1. Mineral composition as provenance indicator

1. Magnetite chemical composition along with magnetic measurements is a viable approach to determine provenance for sediment in the River Eden catchment.

2. Despite differences in its internal texture (homogeneous grains, and trellis and composite magnetite-ilmenite intergrowths) there is not a distinctive magnetite characteristic between the different sources found in the catchment. However, magnetite composition, although variable within each source group, is clearly a source discriminator.

3. Magnetite is compositionally altered by weathering processes involved principally in rock degradation and fluvial transport of the resulting sediment. Results suggest a subaerial oxidation of the magnetite, possibly to an oxyhydroxide phase (such as goethite, lepidocrocite or limonite), and an alteration to sphene under subaqueous conditions. However, as shown by both geochemical and magnetic measurements, these compositional variations of the magnetite due to weathering do not obliterate the original source fingerprint in detrital magnetite found in stream sediment samples.

7.2. Magnetic parameters as provenance indicators

1. Magnetic parameters are found to be better source discriminators than magnetite composition as they provide additional information in terms of composition, concentration, and grain size of the magnetic mineral paragenesis of the samples.

7.3. Use of statistical modelling techniques

1. Scattergrams, simultaneous R- and Q-mode factor analysis and discriminant function analysis applied to both geochemical and magnetic data lead to a good qualitative model of the provenance of stream sediments in the catchment. The four main sediment sources (basalts, andesites, glacial till and sedimentary rocks) in the River Eden catchment are identified and their relative contribution to the sediment approximately estimated.

2. Limited success is achieved in the quantitative modelling of sediment provenance when using linear programming, mainly as a consequence of the small compositional contrast between magnetite grains derived from different parent rocks, and the interdependence existing between the magnetic parameters.

7.4. Application to the River Eden catchment

1. Four selected tributaries of the River Eden show that, although the sediment found in each stream might be derived from the same known sources, each tributary sediment is found to be clearly distinct in terms of magnetic mineral composition, grain size, and concentration. This results from a combination of the source characteristic mineralogy and the relative proportions in which sediment derived from different sources is mixed during fluvial transport.

2. The impact of tributaries on the magnetite signature of sediments in the downstream course of the main River Eden channel is significant. A clear dominance of detrital magnetite characteristic of derivation from basaltic sources is found associated with an increasing contribution from southern tributaries joining the River Eden towards its mouth.

7.5. General conclusions

1. This study clearly demonstrates the discriminating power available from the use of magnetite composition, grain size and concentration to distinguish the adjacent drainage basins, even basins with similar source rocks but in different proportions being able to be distinguished. Thus, properties of magnetite derived from known source materials (rocks and till) serve as the basis for establishing

quantitative criteria for determining the provenance of stream sediments in the Eden catchment, along with alternative independent discriminating data.

2. Complementary data obtained from alternative methods, such as heavy mineral suites modal analysis and isotopic measurements of bulk sediment samples, etc., are required in order to reach a better discrimination of mineralogically similar sources on the basis of their independent and conservative characteristics.

3. A major application of the results obtained in this study could be the use of the potential of geochemical and magnetic approaches as sedimentary provenance indicators in estimating the human impact on the environment, principally in terms of pollution tracing.

This thesis has provided a detailed view of the chemical and physical effects of weathering and abrasion processes on Fe-Ti oxide minerals from rock to sediment. The suitability of both mineral chemical composition and magnetic parameters as sedimentary provenance indicators has been confirmed but, furthermore, the increasing potential of the combination of both geochemical and magnetic techniques has been shown. The importance of using geochemical parameters for a better understanding and a greater efficiency of magnetic characteristics of natural materials used in magnetic mineral characterisation and sedimentary provenance environmental studies has been highlighted.

References

Abdalla A.Y. and **Whyte F.**, 1979, The influence of bedrock on heavy mineral content of streams within a glaciated area of Perthshire. *Scott. J. Geol.*, **15**, 129-138.

Andrews T.J. and **Jennings A.E.**, 1987, Influence of sediment source and type on the magnetic susceptibility of fiord and shelf deposits, Baffin Island and Baffin Bay, N.W.T. *Can. J. Earth Sci.*, **24**, 1386-1401.

Armstrong M., Paterson, I.B. and **Browne M.A.E.**, 1985, Geology of the Perth and Dundee district. *Mem. Brit. Geol. Surv.*, Sheets 48W, 48E, 49, 108 pp.

Banerjee S.K., King J. and **Marvin J.**, 1981, A rapid method for magnetic granulometry with applications to environmental studies. *Geophys. Res. Lett.*, **8**, 333-336.

Basu A. and **Molinaroli E.**, 1989, Provenance characteristics of detrital opaque Fe-Ti oxide minerals. *J. Sed. Petrol.*, **59**, 922-934.

Basu A. and **Molinaroli E.**, 1991, Reliability and application of detrital opaque Fe-Ti oxide minerals in provenance determination. In: Morton A.C., Todd S.P. and Haughton P.D.W. (eds.), *Developments in Sedimentary Provenance Studies*. Spec. Publ. Geol. Soc. Lond., **57**, 56-65.

Björck S., Dearing J.A. and **Johnson A.**, 1982, Magnetic susceptibility of Late Wechselian deposits in south-eastern Sweden. *Boreas*, **11**, 99-111.

Boghossian N.D., Patchett P.J., Ross G.M. and **Gehrels G.E.**, 1996, Nd isotopes and the source of sediments in the Miogeocline of the Canadian Cordillera. *J. Geol.*, **104**, 259-277.

Boulton G.S., Peacock J.D. and **Sutherland D.G.**, 1991, Quaternary. In: Craig G.Y. (ed.), *Geology of Scotland.* Geol. Soc. Lond., 503-543.

Bradshaw R. and **Thompson R.**, 1985, The use of magnetic measurements to investigate the mineralogy of Iceland lake sediments and to study catchment processes. *Boreas*, **14**, 203-215.

Buddington A.F. and **Lindsley D.H.**, 1964, Iron-titanium oxide minerals and synthetic equivalents. *J. Petrol.*, **5**, 310-357.

Butler R.F. and **Banerjee S.K.**, 1975, Theoretical single-domain grain size range in magnetite and titanomagnetite. *J. Geophys. Res.*, **80**, 4049-4058.

Cawood P.A., 1983, Modal composition and detrital clinopyroxene geochemistry of lithic sandstones from the New England Fold Belt (east Australia): A Paleozoic forearc terrace. *Bull. Geol. Soc. Amer.*, **94**, 1199-1214.

Chisholm J.I., 1971, The stratigraphy of the post-glacial marine transgression in N.E. Fife. *Bull. Geol. Surv. Great Britain*, **37**, 91-107.

Chisholm J.I. and **Dean J.M.**, 1974, The Upper Old Red Sandstone of Fife and Kinross: a fluviatile sequence with evidence of marine incursion. *Scott. J. Geol.*, **10**, 1-30.

Clark D.A., 1983, Comments on Magnetic Petrophysics. *Bull. Austr. Soc. Explor. Geophys.*, **14**, 49-62.

Darby D.A. and **Tsang Y.W.**, 1987, Variation in ilmenite element composition within and among drainage basins: Implications for provenance. *J. Sed. Petrol.*, **57**, 831-838.

Davis J.C., 1986, *Statistics and data analysis in geology*. John Wiley & Sons, Inc., U.S.A., 646 pp.

Day R., **Fuller M.** and **Schmidt V.A.**, 1977, Hysteresis properties of titanomagnetites: grain-size and compositional dependence. *Phys. Earth Planet. Int.*, **13**, 260-267.

Dearing J.A., **Maher B.A.** and **Oldfield F.**, 1985, Geomorphological linkages between soils and sediments: the role of magnetic measurements. In: Richards K.S., Arnett R.R. and Ellis S. (eds.), *Geomorphology and soils*. George Allen & Unwin, London, 245-266.

Dearing J.A., 1994, *Environmental magnetic susceptibility: Using the Bartington MS2 system*. Kenilworth: Chi Publishing, 104 pp.

Doyle L.J., **Hopkins T.L.** and **Betzer P.R.**, 1976, Black magnetic spherule fallout in the eastern Gulf of Mexico. *Science*, **194**, 1157-1159.

Droop G.T.R., 1987, A general equation for estimating Fe^{3+} concentrations in ferromagnesian silicates and oxides from microprobe analyses, using stoichiometric criteria. *Mineral. Mag.*, **51**, 431-435.

Duck RW. and **McManus J.**, 1990, Relationships between catchment characteristics, land use and sediment yield in the Midland Valley of Scotland. In: Boardman J., Foster I.D.L. and Dearing J.A. (eds.), *Soil Erosion on Agricultural Land*. John Wiley, London, 285-299.

Evans J.A., 1996, Dating the transition of smectite to illite in Paleozoic mudrocks using the Rb-Sr whole-rock technique. *J. Geol. Soc. Lon.*, **153**, 101-108.

Forsyth I.H. and **Chisholm M.A.**, 1977, The Geology of East Fife. *Mem. Brit. Geol. Surv.*, Sheets 41 and 49, 284 pp.

Francis E.H. and **Walker B.H.**,1987, Emplacement of alkali-dolerite sills relative to extrusive volcanism and sedimentary basins in the Carboniferous of Fife, Scotland. *Trans. Roy. Soc. Edin.: Earth Sci.*, 77, 309-323.

Fredriksson K. and **Martin L.R.**, 1963, The origin of black spherules found in Pacific island, deep-sea sediments, and Antarctic ice. *Geochim. Cosmochim. Acta*, **27**, 245-248.

Gandy M.K., 1975, The petrology of the Lower Old Red Sandstone lavas of the eastern Sidlaw Hills, Perthshire, Scotland. *J. Petrol.*, **16**, 189-211.

Geikie A., 1900, The Geology of central and western Fife and Kinross. *Mem. Brit. Geol. Surv.*, Sheets 40, 32 and 48, 284 pp.

Glover B.W., Leng M.J. and **Chisholm J.I.**, 1996, A second major fluvial sourceland for the Silesian Pennine Basin of northern England. *J. Geol. Soc. Lon.*, **153**, 901-906.

Goldberg E.D., Hodge V.F., Griffin J.J. and **Koide M.**, 1981, Impact of fossil fuel combustion on the sediments of Lake Michigan. *Env. Sci. Tech.*, **15**, 466-471.

Goldstein S., Arndt N.T. and **Stallard R.F.**, 1997, The history of a continent from U-Pb ages of zircons from Orinoco River sand and Sm-Nd isotopes in Orinoco basin river sediments. *Chem. Geol.*, **139**, 271-286.

Condie K.C., Dengate J. and **Cullers R.L.**, 1995, Behaviour of rare-earth elements in a paleoweathering profile on granodiorite in the front range, Colorado, USA. *Geochim. Cosmochim. Acta*, **59**, 279-294.

Graham I.J., Glasby G.P. and **Churchman, G.J.**, 1997, Provenance of the detrital component of deep-sea sediments from the SW Pacific Ocean based on mineralogy, geochemistry and Sr isotopic composition. *Mar. Geol.*, **140**, 75-96.

Grigsby J.D., 1990, Detrital magnetite as a provenance indicator. *J. Sed. Petrol.*, **60**, 940-951.

Grigsby J.D., 1992, Chemical fingerprinting in detrital ilmenite: a viable alternative in provenance research?. *J. Sed. Petrol.*, **62**, 331-337.

Haggerty S.E., 1976, Opaque mineral oxides in terrestrial igneous rocks. In: Rumble D. (ed.), *Oxide minerals*. Short Course Notes, Mineral. Soc. Amer., **3**, 101-300.

Haggerty S.E., 1991, Oxide textures-a mini-atlas. In: Lindsley D.H. (ed.), *Oxide minerals: petrologic and magnetic significance*. Reviews in Mineralogy, Mineral. Soc. Amer., **25**, 129-219.

Hansen L.D., Silberman D. and **Fisher G.L.**, 1981, Crystalline components of stack-collected, size-fractionated coal fly ash. *Env. Sci. Tech.*, **15**, 1057-1062.

Haughton P.D. and **Farrow C.M.**, 1989, Compositional variations in Lower Old Red Sandstone garnets from the Midland Valley of Scotland and the Anglo-Welsh Basin. *Geol. Mag.*, **126**, 373-396.

Henry D.J. and **Dutrow B.L.**, 1992, Tourmaline in a low grade clastic metasedimentary rock: An example of the petrogenetic potential of tourmaline. *Contrib. Mineral. Petrol.*, **112**, 203-218.

Henry D.J., Lu G. and **McCabe C.**, 1994, Epigenetic tourmaline in sedimentary red-beds: An example from the Silurian Rose Hill Formation, Virginia. *Canad. Mineral.*, **32**, 599-605.

Hiscott R.N., 1978, Provenance of Ordovician deep-water sandstones, Tourelle Formation, Quebec, and implications for initiation of the Taconic orogeny. *Can. J. Earth Sci.*, **15**, 1579-1597.

Hodych, J.P., 1996. Inferring domain state from magnetic hysteresis in high coercivity dolerites bearing magnetite with ilmenite lamellae. *Earth Planet. Sci. Lett.*, **142**, 523-533.

Hunt A., 1986, The application of mineral magnetic methods to atmospheric aerosol discrimination. *Phys. Earth Planet. Int.*, **42**, 10-21.

Hunt A., Jones J. and **Oldfield F.**, 1984, Magnetic measurements and heavy metals in atmospheric particulates of anthropogenic origin. *Sci. Tot. Environ.*, **33**, 129-139.

Hutchinson S.M., 1995, Use of magnetic and radiometric measurements to investigate erosion and sedimentation in a British upland catchment. *Earth Surf. Proc. Land.*, **20**, 293-314.

Irvine T.N. and **Baragar W.R.A.**, 1971, A guide to the chemical classification of the common volcanic rocks. *Can. J. Earth Sci.*, **8**, 523-548.

Jiles D., 1991, *Introduction to Magnetism and Magnetic Materials*. Chapman & Hall, London, 440 pp.

King J., Banerjee S.K., Marvin J. and **Ozdemir O.**, 1982, A comparison of different magnetic methods of determining the relative grain size of magnetite in natural materials: Some results from lake sediments. *Earth Planet. Sci. Lett.*, **59**, 404-419.

Kuno H., 1968, Differentiation of basalt magmas. In: Hess H.H. and Poldervaart A. (eds.), *Basalts: The Poldervaart treatise on rocks of basaltic composition*, Vol. 2. Interscience, New York, pp. 623-688.

Laxton J.L. and **Ross D.L.**, 1981, The sand and gravel resources of the country around Newport-on-Tay, Fife Region. Description of 1:25000 sheet NO 42 and parts of NO 32 and 52. *Min. Assess. Report,* **89**, 96 pp.

Lees J.A., 1994, *Modelling the magnetic properties of natural and environmental materials*. Unpublished Ph.D. Thesis, University of Coventry, UK.

Lees J.A., 1997, Mineral magnetic properties of mixtures of environmental and synthetic materials: linear additivity and interactions effects. *Geophys. J. Int.*, **131**, 335-336.

Le Maitre R.W., 1982, *Numerical petrology*. Developments in petrology, **8**. Elsevier Scientific Publishing Company, Amsterdam, 281 pp.

Le Maitre R.W., Baterman P., Dudek A., Keller J., Lameyre Le Bas M.J., Sabine P.A., Schmid R., Sorensen H., Streckeisen A., Woolley A.R. and Zanettin, B., 1989, *A classification of igneous rocks and glossary of terms*. Blackwell Scientific, Oxford, 193 pp.

Linn A.M., Depaolo D.J. and **Ingersoll R.V.**, 1991, Nd-Sr isotopic provenance analysis of Upper Cretaceous Great Valley fore-arc sandstones. *Geology*, **19**, 803-806.

Locke G. and **Bertine K.K.**, 1986, Magnetite in sedimentas as an indicator of coal combustion. *Appl. Geochem.*, **1**, 345-356.

Macdonald R., Gottfried D., Farrington M.J., Brown F.W. and **Skinner N.G.**, 1981, Geochemistry of a continental tholeiite suite: Late Palaeozoic quartz dolerite dykes of Scotland. *Trans. Roy. Soc. Edin.: Earth Sci.*, **72**, 57-74.

Maher B.A., 1988, Magnetic properties of some synthetic sub-micron magnetites. *Geophys. J.*, **94** , 83-96.

McCaffrey W.D., 1994, Sm-Nd isotopic characteristics of sedimentary provenance - the Windermere supergroup of NW England. *J. Geol. Soc. Lon.*, **151**, 1017-1021.

McDaniel D.K., Sevigny J.H., Hanson G.N. and **McLennan S.M.**, 1997, Grenvillian provenance for the amphibolite-grade Trap Falls Formation: implications for early Paleozoic tectonic history of New England. *Can. J. Earth Sci.*, **34**, 1286-1294.

Morton A.C., 1987, Influences of provenance and diagenesis on detrital garnet suites in the Forties Sandstone, Paleocene, central North Sea. *J. Sed. Petrol.*, **57**, 1027-1032.

Morton A.C., 1991. Geochemical studies of detrital heavy minerals and their application to provenance research. In: Morton A.C., Todd S.P. and Haughton P.D.W. (eds.), *Developments in Sedimentary Provenance Studies*. Spec. Publ. Geol. Soc. Lond., **57**, 31-45.

Nedler J.A. and **Mead R.**, 1965, A simplex method for function minimization. *Comput. J.*, 7, 308-313.

Oldfield F., 1991, Environmental magnetism - a personal perspective. *Quater. Sci. Rev.*, **10**, 73-85.

Oldfield F., 1994, Toward the discrimination of fine-grained ferrimagnets by magnetic measurements in lake and near-shore marine sediments. *J. Geophys. Res.*, **99**, 9045-9050.

Oldfield F. and **Yu L.**, 1994, The influence of particle size variations on the magnetic properties of sediments from the north-eastern Irish Sea. *Sedimentology*, **41**, 1093-1108.

Oldfield F., Maher B.A., Donoghue J. and **Pierce J.**, 1985, Particle-size related, mineral magnetic source sediment linkages in the Rhode River catchment, Maryland, USA. *J. Geol. Soc. London*, **142**, 1035-1046.

Oldfield F., Rummery T.A., Thompson R. and **Walling D.E.**, 1979, Identification of suspended sediment sources by means of magnetic measurements: Some preliminary results. *Water Resources Res.*, **15**, 211-218.

Oldfield F., Hunt A., Jones M.D.H., Chester R., Dearing J.A., Olsson L. and **Prospero J.M.**, 1985, Magnetic differentiation of atmospheric dusts. *Nature*, **317**, 516-518.

O'Reilly W.O., 1984, *Rock and Mineral Magnetism*. Blackie, Glasgow, 220 pp.

Owen M.R., 1987, Hafnium content of detrital zircons, a new tool for provenance study. *J. Sed. Petrol.*, **57**, 824-830.

Pearce J.A. and **Cann J.R.**, 1971, Ophiolite origin investigated by discriminant analysis using Ti, Zr, and Y. *Earth. Planet. Sci. Lett.*, **12**, 339-349.

Pearce J.A., 1976, Statistical analysis of major element patterns in basalts. *J. Petrol.*, **17**, 15-43.

Peccerillo R. and **Taylor S.R.**, 1976, Geochemistry of Eocene calc-alkaline volcanic rocks from the Kastamonu area, northern Turkey. *Contrib. Mineral. Petrol.*, **58**, 63-81.

Puffer J.H., Russell E.W. and **Rampino M.R.**, 1980, Distribution and origin of magnetite spherules in air, waters, and sediments of the grester New York city area and the northern Atlantic Ocean. *J. Sed. Petrol.*, **50**, 247-256.

Putnis A., 1992, *Introduction to mineral sciences*. Cambridge University Press, 457 pp.

Radhakrishnamurty, C. and **Deutsch, E.R.**, 1974, Magnetic techniques for ascertaining the nature of iron oxides grains in basalts. *J. Geophys.*, **40**, 453-465.

Razjigaeva N.G. and **Naumova V.V.**, 1992, Trace element composition of detrital magnetite from coastal sediments of northwestern Japan Sea for provenance study. *J. Sed. Petrol.*, **62**, 802-809.

Rickwood P.C., 1989, Boundary lines within petrologic diagrams which use oxides of major and minor elements. *Lithos*, **22**, 247-263.

Rollinson H., 1993, *Using geochemical data: Evaluation, presentation, interpretation*. Longman Scientific & Technical, Essex, 352 pp.

Schmidt R.A. and **Keil K.**, 1966, Electron microprobe study of spherules from Atlantic Ocean sediments. *Geochim. Cosmochim. Acta*, **30**, 471-478.

Schneiderman J.S., 1995, Detrital opaque oxides as provenance indicators in River Nile sediments. *J. Sed Res.*, **65**, 668-674.

Snowball I.F., 1995, *Electromagnetic units and their use in mineral magnetic studies*. Lund: Chi Publishing, 12 pp.

Stober J.C. and **Thompson R.**, 1979, An investigation into the source of magnetic minerals in some Finnish lake sediments. *Earth Planet. Sci. Lett.*, **45**, 464-474.

Stott A.P., 1986, Sediment tracing in a reservoir-catchment system using a magnetic mixing model. *Phys. Earth Planet. Int.*, **42**, 105-112.

Temple J.T., 1978, The use of factor analysis in geology. *Math. Geol.*, **10**, 379-387.

Thirlwall M.F., 1981, Implications for Caledonian plate tectonic models of chemical data from volcanic rocks of the British Old Red Sandstone. *J. Geol. Soc. London*, **138**, 123-138.

Thirlwall M.F., 1983, Discussion on implications for Caledonian plate tectonic models of chemical data from volcanic rocks of the British Old Red Sandstone. *J. Geol. Soc. London*, **140**, 315-318.

Thompson R., 1986, Modelling magnetization data using SIMPLEX. *Physics Earth Planet. Int.*, **42**, 113-127.

Thompson R. and **Morton D.J.**, 1979, Magnetic susceptibility and particle-size distribution in recent sediments of the Loch Lomond drainage basin, Scotland. *J. Sed. Petrol.*, **49**, 801-812.

Thompson R. and **Oldfield F.**, 1986, *Environmental Magnetism*. Allen & Unwin, London, 227 pp.

Thompson R., Bloemendal J., Dearing J.A., Oldfield F., Rummery T.A., Stober J.C. and **Turner G.M.**, 1980, Environmental applications of magnetic measurements. *Science*, **207**, 481-486.

Van der Voo R., Fang W., Wang Z., Suk D., Peacor D.R. and **Liang Q.**, 1993, Paleomagnetism and electron microscopy of the Emeishan Basalts, Yunnan, China. *Tectonophys.*, **221**, 367-379.

Vroon P.Z., Vanbergen M.J., Klaver G.J. and **White W.M.**, 1995, Strontium, neodymium, and lead isotopic and trace-element signatures of the East Indonesian sediments - provenance and implications for Banda arc magma genesis. *Geochim Cosmochim. Acta*, **59**, 2573-2598.

Walden J. and **Smith J.P.**, 1995, Factor analysis: A practical application. In: Maddy D. and Brew J.S. (eds.), *Statistical modelling of Quaternary Science data.* Technical Guide Series, **5**, 39-64. Quaternary Research Association, Cambridge.

Walden J., Slattery M.C. and **Burt T.P.**, 1997, Use of mineral magnetic measurements to fingerprint suspended sediment sources: Approaches and techniques for data analysis. *J. Hydrol.*, **202**, 353-372.

Walden J., Smith J.P. and **Dackombe R.V.**, 1992a, Mineral magnetic analyses as a means of lithostratigraphic correlation and provenance indication of glacial diamicts: intra- and inter-unit variation. *J. Quater. Sci.*, 7, 257-270.

Walden J., Smith J.P. and **Dackombe R.V.**, 1992b, The use of simultaneous R- and Q-mode factor analysis as a tool for assisting interpretation of mineral magnetic data. *Math. Geol.*, **24**, 227-247.

Walden J., Smith J.P. and **Dackombe R.V.**, 1996, A comparison of mineral magnetic, geochemical and mineralogical techniques for compositional studies of glacial diamictons. *Boreas*, **25**, 115-130.

Walden J., Smith J.P., Dackombe R.V. and **Rose J.**, 1995, Mineral magnetic analyses of glacial diamicts from the Midland Valley of Scotland. *Scott. J. Geol.*, **31**, 79-89.

Walker B.H. and **Francis E.H.**, 1987, High-level emplacement of an olivine-dolerite sill into Namurian sediments near Cardenden, Fife. *Trans. Roy. Soc. Edin.: Earth Sci.*, **77**, 295-307.

Walling D.E., Peart M.R., Oldfield F. and **Thompson R.**, 1979, Suspended sediment sources identified by magnetic measurements. *Nature*, **281**, 110-113.

Yu L. and **Oldfield F.**, 1989, A multivariate mixing model for identifying sediment source from magnetic measurements. *Quater. Res.*, **32**, 168-181.

Yu L. and **Oldfield F.**, 1993, Quantitative sediment source ascription using magnetic measurements in a reservoir-catchment system near Níjar, S.E. Spain. *Earth Surf. Proc. Land.*, **18**, 441-454.

Appendices

Appendix 1

In this appendix, both sample preparation and instrumentation used for analysis are described, distinguishing between chemical and magnetic analytical procedures.

Geochemical instrumentation

Whole rock chemical composition of rock samples was determined by X-ray fluorescence spectrometry. The identification of heavy minerals present in rocks, glacial till and river sediments, and their chemical and textural analyses were made by X-ray diffractometry and electron microprobe, respectively.

Rock samples were prepared for analysis by first removing all surface weathering using a wet surface grinding Al_2O_3 wheel. The samples were then reduced in size with a Lake and Elliot hydraulic splitter with stainless steel jaws, and a Sturtevant jaw crusher with steel jaws. After this, samples were crushed using a tungsten carbide Tema swing mill for 3.3 minutes for XRF analysis, and sieved, in order to obtain different particle size fractions ((-1)-0 ϕ, 0-1 ϕ, 1-2 ϕ, 2-3 ϕ, and > 3 ϕ), for XRD and electron microprobe analysis. Till and sediment samples were oven-dried at 40 °C and then sieved, obtaining the same particle size fractions as for rock samples.

X-ray fluorescence spectrometry

A Philips 1450/20 sequential spectrometer was used for rock chemistry analyses. The operating conditions were at 50 kV and 30 mA when analysing major elements (Si, Ti, Al, Fe, Mn, Mg, Ca, Na, K and P), and at 60 kV and 30 mA when analysing trace elements (Nb, Zr, Y, Sr, U, Rb, Th, Pb, Ga, Zn, Cu, Ni, Cr, Ce, Sc, V, Ba and La). A Rh anode X-ray tube was used for primary excitation and a range of International Rock Standards were used for calibration the analysis.

Major elements were determined using fused glass beads prepared from 2.666 g of Spectroflux 105 (Johnson Matthey) placed in a platinum crucible and melted in the oven at 950 °C for 10 minutes. 0.5 g of rock powder and 0.06 g of NH_4NO_3 were then added and the mixture placed back into the oven for 20 minutes at the same temperature. After removal from the oven, samples were cooled down at room temperature. As soon as they were cold, they were weighted and then melted with a Meker Burner, each sample being quickly poured into a aluminium disc (32 mm in diameter), which is surrounded by a brass ring and placed on a hot plate at a

temperature of 230 °C. An aluminium plunger was immediately brought down gently on top of the melt to mould and quench it. The sample was kept on the aluminium disc, placed on the hot plate, and the temperature allowed to fall slowly.

Trace elements were determined using powder briquettes prepared from 9 g of sample, mixed with 15 drops of Moviol binder and kept under 14 tons/in^2 of pressure for 5 minutes in a 30 ton C-30 press. The briquettes were then dried in the oven overnight.

Two glass beads and powder briquettes were made per rock sample and duplicate analyses compared. The quoted result is the mean value of duplicate analyses.

X-ray diffractometry

A Philips 1050 goniometer and a Hiltonbrooks DG2 generator were used to identify heavy mineral species present in rock, glacial till and sediment samples. The operating conditions were at 40 kV and 30 mA, using an X-ray tube with Cu or Co anode, a 1° divergence slit, a 0.2 mm receiving slit, and a graphite monochromator.

For X-ray diffraction analysis, the 2-3 ϕ particle size fraction of each sample was poured into a glass separating funnel containing tetrabromoethane (specific gravity 2.96 at 20°C), and left for 2 hours, in the case of rock samples, and for 45 minutes, in the case of glacial till and sediment samples. The heavy mineral fraction deposited at the bottom of the funnel was then removed, cleaned and dried. Approximately 1 g of this fraction was very finely crushed using an agate mortar, and then acetone was added to produce a thin slurry which was spread on a piece of glass bonded to an aluminium specimen holder which was placed directly in the diffractometer after the acetone evaporated.

Electron probe microanalysis

A JEOL JCXA-733 Superprobe was used for the point analysis and textural characterisation (by backscattered electron images) of minerals. The operating conditions were typically an accelerating voltage of 15 kV and a probe current of 20 nA. The standards used were: wollastonite for Si and Ca, rutile for Ti, corundum for Al, pure Fe and Mn metal, periclase for Mg, albite for Na, and orthoclase for K.

Polished thin sections of rocks were used for probe analysis. In sediments, grains of Fe-Ti oxides were picked out from the heavy mineral fraction by using a hand magnet (yielding mainly magnetite), and by hand-picking under the

microscope. These grains were then placed onto a holder and covered with resin which, when cured, was polished and coated with a conducting layer of carbon before being placed into the microprobe.

Magnetism instrumentation

The magnetic properties of rock, glacial till, and river sediment samples were measured by magnetising them, firstly, with a Bartington MS2B sensor, secondly, a Molspin AC field magnetiser, and finally a Molspin pulse magnetiser, in order of increasing magnetic field intensity. This sequence was used because at strong magnetic fields magnetisation becomes irreversible. The remanence acquired at each stage was measured using a Molspin Fluxgate magnetometer, ensuring that less than 1 or 2 minutes elapsed after the magnetisation of the sample.

Rock samples were prepared, for measurement in these instruments, by cutting cylindrical cores of approximately 10 cm^3, whilst glacial till and river sediment samples were dried in the oven at a temperature of 40 °C, and packed in standard 10 cm^3 plastic pots.

Susceptibility meter

A MS2B single sample dual frequency susceptibility sensor (Bartington Instruments Ltd.) was used to measure the magnetic susceptibility of the samples at both low (0.47 kHz) and high (4.6 kHz) frequencies. A detailed description of the sensor itself, measurement procedures, calibration, accuracy and precision, and data interpretation has been given by Dearing (1994).

As packed sediment samples have unknown volumes and densities, the calculation of mass specific susceptibility must be done as described by Snowball (1995). In practice, this is simplified by dividing the susceptibility value by the mass of sample less loss-on-ignition. The result is divided by 10 to give units of 10^{-6} m^3/kg.

Anhysteretic magnetiser

A Molspin AC field magnetiser was used to apply a weak, steady magnetic field (0.04 mT) superimposed on a stronger alternating field (98 mT), in order to measure the anhysteretic remanent magnetisation acquired by the sample.

Pulse magnetiser

A Molspin pulse magnetiser was used to apply increasingly stronger magnetic fields. Firstly, six forward magnetic fields of 20 mT, 40 mT, 100 mT, 300 mT, 500 mT, and 1000 mT were applied, and then five backwards fields of -20 mT, -40 mT, -100 mT, -300 mT, and -1000 mT.

Fluxgate magnetometer

A Molspin Fluxgate magnetometer, controlled by software running on a PC, was used to measure the remanence induced in the samples by both the AC field and the pulse magnetisers. The measure of each sample was made in about 6 seconds (short spin time).

The remanence values displayed on the computer are in units of 10^{-8} Am^2. They were then divided by the mass of the sample less loss-on-ignition, giving units of 10^{-5} Am^2/kg.

Appendix 2

In this appendix the magnetic parameters most commonly used in environmental studies are described, including their interpretation in natural samples. The below definitions have been adapted from Dearing *et al.* (1985), Oldfield *et al.* (1985), Yu and Oldfield (1989), Oldfield (1991).

Magnetic susceptibility (χ): This is measured within a small magnetic field (< 1 mT) and is reversible (no remanence induced). It can be measured on a volume (K) or mass specific (χ) basis. Volume susceptibility (K) is the ratio of the volume magnetisation induced to the intensity of the magnetising field, and so a dimensionless quantity, expressed in 10^{-5} SI units. Specific susceptibility (χ) is the ratio of the volume susceptibility to the density of the sample, measured in m^3/kg. This measurement is roughly proportional to the concentration of ferrimagnetic minerals within a sample, although it is also sensitive to changes in grain size.

Instrumentation : MS2B single sample dual frequency susceptibility sensor (Bartington Instruments Ltd.)

Frequency-dependent susceptibility (χ_{fd}): This is the variation of susceptibility when measured at two different frequencies: a low frequency of 0.47 kHz (χ_{lf}) and a higher frequency of 4.7 kHz (χ_{hf}). This parameter indicates the presence of ferrimagnetic grains lying at the SSD/SP boundary (~0.03 μm). At higher frequencies, a proportion of these grains will become blocked in and will no longer contribute to χ as SP but as SD grains. It can be expressed as mass specific (χ_{fd}) dual frequency-dependent susceptibility, or as a percentage ($\chi_{fd\%}$) frequency-dependent susceptibility.

$$\chi_{fd} = \chi_{lf} - \chi_{hf}\ (m^3/kg) \quad \text{or} \quad \chi_{fd\%} = ((\chi_{lf} - \chi_{hf})/\chi_{lf}) * 100$$

Instrumentation : MS2B single sample dual frequency susceptibility sensor (Bartington Instruments Ltd.)

Anhysteretic remanent magnetisation (ARM): This is acquired by a sample when subjected to a decreasing alternating field (from 100 to 0 mT) with a weak steady field (0.4 mT) superimposed. This parameter is sensitive to the concentration of fine grain size SSD (0.02-0.04 μm) of ferrimagnetic minerals in a sample. ARM is measured in Am^2/kg.

Instrumentation : Anhysteretic magnetiser and Fluxgate magnetometer (Molspin Ltd.)

Susceptibility of ARM (χ_{ARM}): This is the ratio of ARM to the steady field used (0.04 mT = 31.84 A/m). χ_{ARM} (in m^3/kg) is sensitive to fine grain sizes, values increasing with decreasing grain size (King *et al.*, 1982).

Isothermal remanent magnetisation (IRM): This is the remanent magnetisation in a sample after a magnetic field has been applied. The IRM acquired after a magnetic field of 20 mT applied (IRM_{20}) is also called 'soft' isothermal remanent magnetisation and it can be used as an approximate measure of the total concentration of remanence-carrying ferrimagnets. The original IRM data are divided by sample mass and measured in Am^2/kg.

Instrumentation : Pulse magnetiser (max. field 1 T) and Fluxgate magnetometer (Molspin Ltd.)

Saturation isothermal remanent magnetisation (SIRM): This is the highest level of magnetic remanence that can be induced in a sample by application of a high field (here 1 Tesla). SIRM (in Am^2/kg) is an indicator of the volume concentration of magnetic minerals in a sample, but also responds to grain size variations.

Instrumentation : Pulse magnetiser (max. field 1 T) and Fluxgate magnetometer (Molspin Ltd.)

Coercivity of remanence ($(Bo)_{CR}$): This is the reverse field required to reduce SIRM to zero. $(Bo)_{CR}$ can be used to determine magnetic mineralogy and grain size. Magnetite shows values < -100 mT and for hematite $(Bo)_{CR}$ > -100 mT (Oldfield et al., 1985). On the other hand, the smaller the magnetite grain size, the bigger the $(Bo)_{CR}$ value (Thompson and Morton, 1979).

Instrumentation : Pulse magnetiser (maximum field 1 T) and Fluxgate magnetometer (Molspin Ltd.)

Reverse saturation: This is the highest level of remanent magnetisation (in Am^2/kg) reached by a sample when a reverse magnetic field, following a strong forward field (1 T), is applied. Magnetite appears fully reverse saturated in back fields of < -300 mT, and hematite in fields of > -300 mT (Oldfield *et al.*, 1985).

Instrumentation : Pulse magnetiser (max. field 1 T) and Fluxgate magnetometer (Molspin Ltd.)

High field isothermal remanent magnetisation (HIRM): This is the difference between SIRM and IRM (in Am^2/kg). $HIRM_{100}$ and $HIRM_{300}$ can be used as an approximate measure of the concentration of remanence-carrying hematite and goethite in a sample.

Instrumentation : Pulse magnetiser (max. field 1 T) and Fluxgate magnetometer (Molspin Ltd.)

ARM/χ_{lf}: High values indicate finer grain sizes, around SSD, of ferrimagnetic minerals in a sample (Banerjee *et al.*, 1981; King *et al.*, 1982; Oldfield, 1994). It is quoted in A/m units.

χ_{ARM}/SIRM: This ratio is sensitive to magnetite and maghemite grain sizes. Increases in magnetite grain size are indicated by an increase in the value of the ratio, a value of 0.1 indicating coarse grained primary crystals, and a value of 1 indicating very fine (probably pedogenic secondary) crystals. It is quoted in A/m units.

SIRM/χ_{lf}: This ratio is sensitive to mineral type, concentration of strong magnetic minerals and grain size, and is reduced by increased ferrimagnetic versus canted antiferromagnetic mineral contribution, increased grain size from SD upwards, and an increase in SP contribution to χ_{lf}. It is quoted in A/m units.

SIRM/ARM: This indicates SSD grains in a sample. High values (> 100) generally indicate MD grains, low values (< 30) indicate SSD dominance (Yu and Oldfield, 1993). It is a dimensionless parameter.

'S' ratio (=-IRM_{-100}/SIRM): This ratio discriminates between ferri- and canted antiferromagnetic minerals. The closer the value to 1, the greater the magnetite concentration in the sample, with respect to the hematite concentration (Stober and Thompson, 1979). It is a dimensionless parameter.

Demagnetisation parameter D (=-IRM_{-40}/IRM_{300}): This ratio also discriminates between ferri- and canted antiferromagnetic minerals. The smaller the value, the greater the magnetite concentration in the sample with respect to the hematite concentration (Stott, 1986). It is a dimensionless parameter.

Appendix 3

Two short MINITAB macros, RQ.MTB and STANDARD.MTB, created using a text editor, in order to achieve most efficiently the algebraic calculations required to perform a simultaneous R- and Q-mode factor analysis (see Subsection 3.5.3). Note that these macros are suitable only for a maximum of 20 variables. For data sets with larger numbers of variables, some alterations will be necessary.

1. RQ.MTB macro

Variables set up

```
PRINT K1 K2 K3 K4 K5 K6 K7
LET K21=K2+K3-1
LET K22=K4+K3-1
LET K23=K5+K3-1
LET K24=K2+1
LET K25=K4+1
LET K26=K5+1
LET K31=K1
LET K32=K2

EXEC 'STANDARD' K3

COPY CK2-CK21 M2
ERASE CK2-CK21
TRANSPOSE M2 M3
MULTIPLY M3 M2 M4

PRINT M4

EIGEN M4 CK2 M6
SQRT CK2 CK24
DIAGONAL CK24 M7
MULT M6 M7 M8
MULT M2 M6 M9
COPY M8 CK4-CK22
COPY M9 CK5-CK23
```

Output

Proportion of the original variation explained by each new factor

PRINT CK6,CK2

R-mode (variable) factor loadings

PRINT CK6,CK4-CK22

Q-mode (sample) factor loadings

PRINT CK7,CK5-CK23

Plot variable loadings on factor 1 and 2

LPLOT CK25,CK4,CK6

Plot sample loadings on factor 1 and 2

LPLOT CK26,CK5,CK7

Analysis complete

2. STANDARD.MTB macro

```
let ck32=(ck31-mean(ck31)
let k33=sqrt(ssq(ck32/n(ck32))
let ck32=ck32/(k33*(sqrt(n(ck32))))
let k40=mean(ck31)
```

Print mean and std dev

PRINT K40,K33

```
let k31=k31+1
let k32=k32+1
```

Prior to executing the macros, seven MINITAB constants need to be set up using the command *let* (e.g. let K1=2). These constants will tell the macros diverse information.

Constant	*Tells the macros*
K1	The column which contains the first variable of the raw data
K2	The first empty column into which the standardised version of the data raw can be placed
K3	The number of variables used in the analysis
K4	The first empty column to use when storing the R-mode (variable) loadings
K5	The first empty column to use when storing the Q-mode (sample) loadings
K6	The column number containing the number of variables
K7	The column number containing the number of samples

The command *exec 'rq'* will then run the macros which will firstly standardise the original raw data matrix (*n* rows by *m* columns) (M1) placing the standardised data into a MINITAB matrix format (M2). Each element of the original raw data matrix has its column (variable) mean subtracted from it, and it is then divided by the product of the column (variable) standard deviation and the square root of *n* (number of samples), in order to standardise the data. Subsequently, the standardised data matrix (*n* rows by *m* columns) is transposed, i.e. columns turned to rows and rows turned to columns, to give a matrix which has *m* rows by *n* columns (M3). The product of the standardised data matrix (M2) multiplied by its transposed matrix (M3) will result in the correlation matrix (M4) between the variables from which eigenvectors and eigenvalues are extracted.

The eigenvectors are used to form a matrix (M6) and the square roots of the eigenvalues are used to form a diagonal matrix (M7). The R-mode (variable) factor loading matrix (M8) is obtained by multiplying M6 and M7 matrices, each column representing the loadings of the original variables on an individual factor. On the other hand, the Q-mode (sample) factor loading matrix (M9) results from multiplying the M2 and M6 matrices, each column representing the loadings of the original samples on an individual factor.

The factor loadings for either the variables or samples for any two of the factors are then plotted (*LPLOT* command), producing a scatter diagram which will show the position of both the original variables and the samples in the new factor space. The same axes are used in both plots to allow the relationship between the samples and the variables to be judged more clearly.

Appendix 4

In this appendix all data obtained from the analyses of rock and stream sediment samples collected in the River Eden catchment using both geochemical and magnetic methods as described in Chapter 3 are presented. These data include: X-ray fluorescence analysis of whole-rock samples of the igneous rocks (A); electron probe microanalysis of magnetite and ilmenite grains contained in the igneous rocks (B and D, respectively), glacial till (F and G) and in the sediments sampled from the Barroway Burn (I and N), the Moonzie Burn (J and O), the Kilgour Burn (K and P), the Coalpit Burn (L and Q) and the River Eden (M and R); electron probe microanalysis of magnetite grains along a transverse section (distance Y) of a weathered dolerite sample (em25) (C); and principal magnetic parameters measured in whole-rock samples of both igneous and sedimentary rocks (E), glacial till (H), and sediments from the River Eden tributaries located in the northern part of the catchment (S), those tributaries flowing through the southern part (T), and also from the River Eden (U).

The numbers assigned to each electron probe microanalysis consist of two parts: the first indicates the number of the analysis performed, and the second represents the number of the sample from which the Fe-Ti oxide grain is analysed. Analysed elements are presented as oxides weight per cent. The total Fe was analysed as FeO and recalculated to weight percent Fe_2O_3 and FeO following the procedure of Droop (1987).

List of contents

A. Whole-rock chemistry of representative igneous rock samples from the River Eden catchment. Andesite: em1 to em34, Volcanic conglomerate: em33, Felsite: em20, Tuffite: em36, Dolerite: em8 to em39. The total Fe is given as Fe_2O_3. Major elements quoted as weight percentage oxides and trace elements quoted in ppm.

Sample	em1	em2	em3	em4	em5	em13	em14	em15	em16	em18	em19	em29	em30	em34	em33	em20	em36	em8	em11	em17	em21	em22	em38	em39
SiO_2	56.00	59.54	59.31	59.88	60.19	56.72	56.81	56.03	56.56	65.36	65.68	57.28	66.47	56.57	58.11	72.80	50.19	49.09	50.37	48.18	48.50	47.95	48.91	48.69
TiO_2	1.19	0.71	0.75	0.73	0.73	1.08	1.09	1.07	1.05	0.52	0.52	1.09	0.51	1.16	0.87	0.11	1.07	2.31	2.01	2.35	1.79	1.81	2.90	2.96
Al_2O_3	15.71	17.06	17.85	17.64	17.83	17.96	18.11	17.85	18.08	16.12	16.08	18.31	15.77	16.41	17.95	13.64	14.69	13.39	14.11	13.97	14.27	14.01	12.97	12.96
Fe_2O_3	6.30	5.26	5.46	5.55	5.32	7.06	7.15	7.24	6.88	3.73	4.04	7.02	3.58	6.98	6.11	1.15	6.77	13.24	12.29	12.86	11.78	11.68	16.00	16.31
MnO	0.09	0.09	0.07	0.08	0.08	0.13	0.12	0.12	0.12	0.04	0.04	0.15	0.06	0.14	0.08	0.10	0.23	0.16	0.17	0.17	0.17	0.17	0.20	0.21
MgO	3.77	3.42	3.02	2.15	2.21	2.24	2.20	2.15	1.79	0.73	0.75	2.23	1.22	2.63	1.99	0.24	3.66	6.54	6.47	7.32	7.88	7.89	5.66	5.82
CaO	6.07	0.94	1.70	3.08	3.08	5.17	5.24	5.31	5.89	0.49	0.48	5.29	2.29	3.65	0.70	1.46	6.69	8.27	9.11	8.24	8.66	8.78	8.35	8.24
Na_2O	3.98	3.73	4.60	4.87	4.91	4.88	4.78	4.67	4.85	2.24	1.76	4.77	5.27	3.93	5.91	2.49	0.24	2.74	3.15	3.76	3.40	3.47	2.28	2.21
K_2O	2.21	5.87	5.40	3.43	3.83	1.90	1.90	1.87	1.91	5.86	6.03	1.91	2.50	3.61	3.06	4.74	2.15	0.97	1.32	0.64	0.99	0.99	1.19	1.18
P_2O_5	0.45	0.40	0.42	0.42	0.42	0.62	0.62	0.62	0.61	0.22	0.21	0.62	0.23	0.28	0.27	0.07	0.23	0.31	0.25	0.21	0.37	0.37	0.28	0.27
Loss	4.60	3.40	2.00	1.40	2.20	1.50	1.40	2.90	2.60	4.20	4.40	1.70	2.30	5.20	5.20	3.20	14.30	3.80	1.00	3.00	2.40	1.80	1.80	1.90
Total	100.37	100.42	100.58	99.23	100.80	99.24	99.40	99.80	100.34	99.49	99.96	100.35	100.20	100.56	100.25	99.96	100.22	100.82	100.25	100.70	100.21	98.92	100.51	100.73
Ba	735	760	706	577	578	488	481	457	508	607	647	460	647	799	608	955	271	316	346	186	328	312	297	317
Rb	47	87	66	57	57	40	42	40	28	147	149	42	58	50	65	107	35	25	27	16	20	18	30	29
Sr	729	186	272	437	424	606	607	595	625	52	54	606	486	417	308	161	483	336	398	471	402	411	347	347
Cr	157	4	5	4	11	3	6	7	5	8	8	4	21	70	27	1	69	771	103	149	264	246	25	25
Cu	24	7	13	8	5	6	7	6	9	84	105	7	7	14	22	2	10	54	68	150	53	52	84	83
Ni	94	2	3	1	6	4	5	4	1	13	13	5	14	37	21	1	29	55	64	109	173	149	41	38
Pb	11	9	13	24	23	9	9	13	15	14	13	10	24	32	13	14	6	2	1	3	0	0	1	1
Sc	15	4	6	6	6	11	12	11	12	2	1	11	4	14	8	3	20	26	26	30	24	21	34	35
V	110	39	49	45	47	59	62	68	62	39	43	66	47	131	97	0	137	377	303	353	200	198	529	542
Zn	69	59	62	59	60	83	80	89	75	22	22	82	74	94	349	14	58	99	101	96	95	92	120	126
La	42	31	32	34	35	41	34	31	35	31	33	32	33	30	27	20	20	20	18	11	21	21	20	21
Ce	88	73	73	81	80	6	74	75	82	61	64	770	67	67	51	27	51	54	46	32	44	43	54	51
Ga	17	18	22	18	20	21	22	22	21	20	20	20	17	18	15	18	16	22	21	20	21	20	24	25
Nb	17	13	14	14	14	11	13	13	13	13	13	13	13	11	14	20	8	14	14	13	30	29	13	11
U	2	1	3	1	1	1	0	1	0	2	1	1	2	0	2	0	0	0	1	1	0	0	0	0
Th	6	4	7	7	8	5	6	7	5	13	14	6	13	6	10	13	4	6	1	2	2	2	3	2
Y	20	26	28	28	28	35	35	34	33	18	19	35	19	24	19	25	21	29	29	24	24	24	36	34
Zr	270	285	305	303	304	290	287	285	286	291	296	292	237	212	242	108	166	164	167	128	142	141	190	186

B. Electron probe microanalysis of magnetite from the River Eden catchment igneous rocks.

Point	1-1	4-1	5-1	7-1	9-1	11-1	13-1	14-1	16-1	19-1	20-1	21-1	22-1	23-1	24-1
SiO2	0.39	0.39	0.33	0.45	0.85	0.37	0.41	0.19	0.40	0.33	0.21	0.48	0.38	0.36	0.40
TiO2	10.51	12.50	14.53	12.11	1.12	7.00	11.34	17.33	14.01	13.09	15.25	7.34	4.32	2.79	3.50
Al2O3	0.55	1.24	1.18	0.19	0.88	0.92	0.32	0.93	1.06	0.84	1.11	0.54	0.59	1.44	0.38
FeO	79.78	79.07	72.77	76.33	86.12	83.96	77.17	72.45	79.14	79.47	74.23	82.99	86.86	86.87	88.82
MnO	0.43	0.45	0.45	0.33	0.41	0.28	1.65	2.13	0.38	0.34	2.34	0.38	0.68	0.40	0.46
MgO	0.48	0.93	0.69	0.46	0.31	0.33	0.00	0.00	0.66	0.50	0.00	0.35	0.97	0.58	0.31
CaO	0.01	0.00	0.04	0.02	0.07	0.04	0.08	0.02	0.03	0.05	0.04	0.05	0.03	0.11	0.03
Na2O	0.00	0.00	0.00	0.00	0.00	0.00	0.00	0.00	0.00	0.00	0.00	0.00	0.00	0.00	0.00
K2O	0.00	0.00	0.06	0.04	0.05	0.06	0.04	0.00	0.01	0.00	0.02	0.05	0.04	0.00	0.00
Total	92.15	94.58	90.03	89.91	89.81	92.94	91.00	93.05	95.70	94.63	93.20	92.17	93.85	92.54	93.89
Fe2O3	45.06	42.16	34.80	40.51	61.25	52.57	42.58	31.38	39.93	41.39	35.57	51.51	59.53	60.42	61.02
FeO	39.23	41.13	41.46	39.87	31.00	36.65	38.85	44.22	43.21	42.23	42.22	36.64	33.29	32.50	33.91
Total	96.66	98.80	93.52	93.97	95.94	98.21	95.26	96.19	99.70	98.77	96.76	97.33	99.82	98.59	100.01

Point	25-1	26-1	27-1	28-1	29-1	30-1	31-1	33-1	34-1	35-1	36-1	16-2	18-2	19-2	24-2
SiO2	0.23	0.36	0.33	0.31	0.33	0.32	0.34	0.27	0.27	0.29	0.19	0.20	0.41	0.32	2.07
TiO2	2.02	3.64	13.12	7.70	9.25	12.30	15.98	8.91	17.24	4.23	15.08	13.76	11.85	13.10	2.67
Al2O3	0.63	0.44	0.59	1.13	0.77	0.11	0.75	0.39	0.65	0.91	0.83	1.02	0.93	0.99	0.72
FeO	85.90	88.00	76.40	82.98	82.40	79.76	75.56	81.32	70.60	88.43	77.26	79.41	77.66	77.42	87.01
MnO	0.17	0.58	1.84	0.21	0.17	0.90	0.50	0.18	2.52	0.04	0.32	0.51	0.58	0.31	0.42
MgO	0.28	0.82	0.00	0.35	0.47	0.00	1.06	0.45	0.00	0.27	0.63	0.25	0.62	0.70	0.00
CaO	0.10	0.03	0.14	0.02	0.10	0.09	0.04	0.07	0.19	0.07	0.04	0.02	0.04	0.10	0.27
Na2O	0.00	0.16	0.14	0.00	0.00	0.00	0.00	0.00	0.10	0.00	0.00	0.00	0.00	0.00	0.00
K2O	0.05	0.04	0.02	0.00	0.00	0.05	0.00	0.00	0.01	0.12	0.01	0.02	0.11	0.04	0.10
Total	89.38	94.06	92.57	92.69	93.49	93.53	94.23	91.59	91.57	94.36	94.37	95.18	92.19	92.98	93.27
Fe2O3	60.96	61.83	40.39	50.72	48.56	42.98	35.51	48.50	31.03	59.68	37.50	40.34	41.84	40.18	57.71
FeO	31.05	32.35	40.05	37.34	38.70	41.08	43.61	37.68	42.68	34.72	43.51	43.11	40.00	41.26	35.08
Total	95.49	100.26	96.61	97.76	98.35	97.83	97.79	96.45	94.68	100.33	98.12	99.22	96.38	97.00	99.05

Point	25-2	26-2	27-2	29-2	30-2	31-2	32-2	35-3	36-3	38-3	39-3	40-3	41-3	42-3	43-3
SiO2	2.43	1.28	6.64	0.45	0.38	0.72	0.41	0.21	0.80	1.01	0.86	0.55	1.24	3.32	1.62
TiO2	5.84	3.54	4.77	3.55	15.37	3.50	12.88	5.28	4.34	3.84	5.37	8.65	2.14	2.13	2.32
Al2O3	0.29	1.76	2.37	1.29	0.86	3.40	0.59	0.67	0.52	0.38	0.60	1.10	0.44	1.78	0.55
FeO	79.99	84.15	75.66	89.08	77.30	86.83	74.95	87.40	88.91	87.72	86.20	80.70	89.36	83.78	87.47
MnO	0.17	0.75	0.03	0.19	0.35	0.42	0.42	1.49	0.45	0.60	0.71	0.61	0.28	0.35	0.40
MgO	0.00	0.24	4.99	0.10	0.02	0.26	0.27	0.00	0.00	0.00	0.00	0.00	0.00	0.89	0.00
CaO	0.30	0.05	0.06	0.07	0.06	0.04	0.06	0.01	0.10	0.14	0.14	0.20	0.10	0.26	0.16
Na2O	0.00	0.09	0.20	0.00	0.00	0.00	0.00	0.00	0.00	0.11	0.19	0.00	0.00	0.13	0.22
K2O	0.10	0.06	0.80	0.01	0.05	0.05	0.12	0.03	0.00	0.01	0.04	0.11	0.06	0.14	0.14
Total	89.12	91.92	95.51	94.74	94.38	95.23	89.68	95.08	95.11	93.80	94.11	91.91	93.61	92.78	92.88
Fe2O3	47.72	55.92	46.49	60.17	36.13	57.45	38.38	58.19	58.82	58.94	56.47	47.66	61.41	55.06	60.34
FeO	37.05	33.83	33.82	34.94	44.79	35.14	40.41	35.03	35.98	34.68	35.38	37.81	34.10	34.23	33.18
Total	93.89	97.52	100.17	100.77	98.00	100.98	93.52	100.91	101.00	99.71	99.77	96.68	99.76	98.29	98.92

B. (continuation)

Point	44-3	45-3	46-3	47-3	48-3	49-3	50-3	51-3	53-3	54-3	56-3	57-3	3-4	4-4	1-5	2-5
SiO2	1.95	1.39	3.21	2.22	1.86	0.75	1.86	1.95	0.59	1.72	1.29	1.81	2.13	0.28	0.94	0.41
TiO2	2.76	1.63	2.20	3.41	4.13	4.08	1.22	1.31	7.34	3.75	1.96	2.02	2.75	1.99	3.42	3.75
Al2O3	0.49	0.53	1.26	0.49	0.68	0.91	0.57	0.53	0.81	0.53	0.70	0.79	0.84	2.73	2.62	2.96
FeO	86.37	75.63	82.48	84.37	84.87	85.92	87.59	87.60	81.19	83.41	85.05	80.77	85.28	83.13	82.07	81.59
MnO	0.49	0.12	0.09	0.41	0.42	0.91	0.19	0.30	0.24	0.31	0.44	0.23	0.13	0.72	0.55	0.49
MgO	0.00	0.00	0.27	0.00	0.00	0.19	0.00	0.00	0.11	0.00	0.00	0.00	0.35	0.51	0.33	0.58
CaO	0.19	0.23	0.13	0.19	0.16	0.10	0.21	0.17	0.06	0.16	0.10	0.39	0.13	0.07	0.02	0.07
Na2O	0.09	0.00	0.00	0.06	0.30	0.00	0.04	0.02	0.00	0.00	0.00	0.00	0.00	0.00	0.00	0.00
K2O	0.14	0.06	0.08	0.14	0.06	0.17	0.08	0.11	0.08	0.10	0.02	0.08	0.03	0.00	0.03	0.00
Total	92.48	79.58	89.71	91.28	92.47	93.02	91.76	91.99	90.40	89.97	89.56	86.08	91.64	89.43	89.97	89.86
Fe2O3	57.94	51.59	52.61	54.91	55.62	57.92	60.40	60.19	49.49	54.13	58.23	54.30	56.08	58.32	54.16	54.39
FeO	34.23	29.21	35.13	34.96	34.82	33.80	33.24	33.44	36.66	34.70	32.66	31.90	34.82	30.65	33.34	32.65
Total	98.29	84.75	94.97	96.78	98.04	98.82	97.81	98.02	95.36	95.39	95.39	91.52	97.25	95.27	95.39	95.30

Point	3-5	4-5	5-5	6-5	7-5	8-5	9-5	10-5	11-5	12-5	13-5	14-5	15-5	16-5	18-5	19-5
SiO2	2.80	2.91	0.51	2.48	0.23	0.17	0.23	0.72	10.76	5.49	4.26	1.46	2.09	1.31	3.08	0.38
TiO2	0.39	0.31	3.63	0.44	4.21	22.18	8.92	1.44	2.06	2.74	2.61	1.02	7.81	2.84	4.90	2.66
Al2O3	0.77	0.68	1.97	0.28	1.69	0.03	0.12	2.14	2.85	1.50	1.39	0.41	0.54	0.22	0.62	1.46
FeO	83.52	84.78	81.60	85.71	85.96	68.73	81.07	82.67	72.34	76.50	78.82	84.48	80.70	86.52	83.27	82.46
MnO	0.05	0.12	0.81	0.15	0.34	0.39	0.51	0.52	0.29	0.11	0.16	0.21	0.45	0.58	0.22	0.80
MgO	0.00	0.00	0.17	0.03	0.83	1.47	1.97	0.57	1.01	0.77	0.07	0.00	0.00	0.00	0.00	0.09
CaO	0.31	0.29	0.09	0.12	0.02	0.04	0.10	0.10	0.27	0.31	0.34	0.16	0.35	0.22	0.28	0.94
Na2O	0.02	0.00	0.00	0.00	0.00	0.00	0.00	0.00	0.53	0.00	0.00	0.00	0.00	0.01	0.00	0.00
K2O	0.09	0.06	0.04	0.12	0.00	0.01	0.06	0.15	0.50	0.44	0.07	0.04	0.04	0.05	0.17	0.08
Total	87.95	89.15	88.82	89.32	93.28	93.02	92.98	88.30	90.60	87.85	87.72	87.77	91.98	91.75	92.54	88.88
Fe2O3	56.68	57.42	54.74	58.99	58.15	23.35	50.94	58.59	35.79	45.17	47.36	58.85	46.19	58.70	50.28	57.95
FeO	32.52	33.12	32.35	32.63	33.63	47.72	35.23	29.95	40.14	35.86	36.19	31.52	39.14	33.70	38.03	30.31
Total	93.63	94.90	94.30	95.23	99.10	95.35	98.08	94.17	94.18	92.37	92.46	93.66	96.60	97.63	97.58	94.68

Point	20-5	21-5	22-5	23-5	24-5	25-5	27-5	28-5	29-5	30-5	31-5	32-5	34-5	35-5	36-5	37-5
SiO2	3.06	0.47	0.69	0.96	0.35	0.20	3.60	3.21	3.42	0.97	0.89	0.19	0.29	0.29	0.46	0.39
TiO2	2.13	1.61	4.95	1.95	1.29	3.19	1.70	1.50	1.58	2.19	2.55	1.68	31.34	2.38	1.94	1.62
Al2O3	1.26	1.51	1.59	0.52	0.86	1.29	1.38	0.96	1.23	0.47	0.34	3.88	0.47	2.36	2.11	2.18
FeO	80.17	83.09	80.33	84.55	87.19	82.65	73.14	77.80	79.31	86.11	84.79	83.22	61.62	84.46	83.08	84.84
MnO	0.10	0.25	0.84	0.21	0.20	0.74	0.16	0.21	0.24	0.20	0.12	0.26	1.09	0.51	0.51	0.31
MgO	0.15	0.82	0.00	0.00	0.07	0.20	0.26	0.32	0.35	0.00	0.00	0.60	0.76	0.43	0.25	0.44
CaO	0.60	0.10	0.04	0.13	0.10	0.04	0.34	0.30	0.31	0.08	0.11	0.04	0.03	0.10	0.03	0.06
Na2O	0.00	0.00	0.00	0.00	0.00	0.00	0.00	0.00	0.00	0.00	0.00	0.00	0.00	0.00	0.00	0.13
K2O	0.07	0.13	0.00	0.02	0.04	0.09	0.01	0.04	0.03	0.00	0.01	0.01	0.05	0.00	0.06	0.06
Total	87.54	87.99	88.43	88.34	90.11	88.39	80.59	84.35	86.47	90.02	88.81	89.87	95.65	90.54	88.45	90.03
Fe2O3	51.53	59.50	51.55	58.41	62.26	57.05	45.65	50.43	50.97	59.14	57.89	58.12	5.11	58.70	57.96	60.47
FeO	33.81	29.55	33.94	32.00	31.16	31.32	32.06	32.42	33.44	32.89	32.70	30.91	57.02	31.65	30.93	30.43
Total	92.70	93.95	93.59	94.19	96.35	94.11	85.16	89.40	91.58	95.95	94.61	95.69	96.16	96.42	94.25	96.08

B. (continuation)

Point	42-5	43-5	2-8	4-8	6-8	7-8	8-8	9-8	11-8	13-8	15-8	16-8	17-8	19-8	24-8	29-8
SiO2	2.13	0.28	0.29	0.19	0.17	0.28	3.41	1.19	0.29	0.24	0.26	0.24	0.34	0.38	0.16	0.34
TiO2	2.75	1.99	17.55	17.62	18.63	15.45	21.92	16.20	18.70	18.65	18.68	18.76	10.67	16.76	18.96	19.52
Al2O3	0.84	2.73	1.45	1.60	1.29	1.47	0.90	1.23	1.65	1.64	1.82	1.65	0.70	1.67	1.46	1.71
FeO	85.28	83.13	72.91	72.39	71.58	75.40	64.51	72.22	70.35	72.15	71.02	72.34	71.82	73.18	72.35	72.60
MnO	0.13	0.72	0.46	0.39	0.65	0.41	0.00	0.34	0.52	0.58	0.45	0.57	0.28	0.59	0.49	0.56
MgO	0.35	0.51	0.00	0.00	0.00	0.00	0.51	0.10	0.00	0.00	0.00	0.00	0.00	0.00	0.00	0.00
CaO	0.13	0.07	0.07	0.04	0.05	0.02	0.16	0.11	0.05	0.03	0.15	0.08	0.29	0.10	0.05	0.11
Na2O	0.00	0.00	0.00	0.00	0.00	0.00	0.00	0.00	0.00	0.00	0.03	0.12	0.00	0.00	0.00	0.00
K2O	0.03	0.00	0.04	0.00	0.05	0.00	0.01	0.00	0.03	0.03	0.02	0.06	0.04	0.04	0.00	0.00
Total	91.64	89.43	92.77	92.21	92.44	93.03	91.43	91.39	91.59	93.32	92.42	93.82	84.15	92.72	93.47	94.84
Fe2O3	56.08	58.32	29.88	29.31	27.90	34.34	12.93	29.65	26.34	27.88	26.96	28.49	38.63	30.99	27.70	26.81
FeO	34.82	30.65	46.02	46.02	46.48	44.50	52.88	45.53	46.65	47.06	46.76	46.70	37.06	45.29	47.42	48.48
Total	97.25	95.27	95.76	95.15	95.23	96.47	92.72	94.36	94.22	96.11	95.12	96.67	88.01	95.83	96.24	97.52

Point	30-8	32-8	34-8	35-8	36-8	37-8	38-8	39-8	1-13	8-13	9-13	13-13	18-13	23-13	27-13	28-13
SiO2	0.57	0.31	0.29	0.19	0.38	0.44	0.78	3.49	2.26	2.51	2.03	0.23	2.02	0.38	0.29	0.33
TiO2	15.22	16.51	18.00	18.27	20.12	18.53	14.25	20.49	27.56	25.97	28.62	27.30	24.71	26.69	28.87	26.08
Al2O3	1.13	1.53	1.34	1.45	1.66	1.19	1.34	1.02	0.82	0.47	0.56	0.67	0.29	0.80	0.64	0.79
FeO	75.66	75.43	75.07	74.15	72.07	72.49	75.54	67.09	62.73	67.62	60.46	64.80	63.65	67.03	64.84	67.96
MnO	0.72	0.44	0.61	0.35	0.53	0.55	0.73	0.18	1.68	0.89	1.80	1.12	2.36	1.80	0.56	1.06
MgO	0.00	0.00	0.00	0.00	0.00	0.00	0.00	0.32	0.91	0.17	0.53	0.31	0.50	0.15	0.87	0.03
CaO	0.02	0.05	0.06	0.09	0.14	0.13	0.11	0.33	0.93	0.05	0.14	0.07	0.30	0.05	0.09	0.07
Na2O	0.00	0.00	0.00	0.00	0.00	0.04	0.00	0.00	0.00	0.03	0.00	0.00	0.00	0.00	0.00	0.13
K2O	0.00	0.00	0.00	0.00	0.04	0.00	0.01	0.00	0.03	0.13	0.05	0.01	0.12	0.03	0.00	0.04
Total	93.31	94.26	95.37	94.49	94.94	93.36	92.74	92.93	96.90	97.84	94.29	94.50	93.95	96.94	96.14	96.47
Fe2O3	34.73	32.91	30.93	29.83	25.66	28.32	35.58	16.56	8.71	12.22	5.21	12.21	13.53	14.69	10.36	16.15
FeO	44.41	45.82	47.24	47.30	48.98	47.01	43.52	52.19	54.89	56.62	55.76	53.82	51.47	53.81	55.52	53.43
Total	96.79	97.56	98.46	97.48	97.51	96.20	96.31	94.59	97.78	99.06	94.81	95.72	95.30	98.42	97.18	98.09

Point	31-13	33-13	34-13	35-13	36-13	73-14	76-14	78-14	79-14	82-14	85-14	86-14	87-14	88-14	89-14	90-14
SiO2	0.13	0.42	0.32	0.34	0.65	0.37	0.29	0.35	0.29	0.31	0.25	0.35	0.24	0.24	0.20	0.24
TiO2	22.08	17.33	23.85	23.13	26.47	15.82	14.67	11.02	13.41	16.49	8.75	10.66	16.55	18.61	1.61	10.76
Al2O3	0.31	0.06	0.14	0.34	0.82	1.03	0.88	1.21	0.85	0.79	0.53	1.14	1.02	1.10	0.88	0.57
FeO	72.64	74.22	69.82	69.42	66.68	75.02	76.18	78.65	78.11	71.18	78.31	76.12	75.16	70.78	87.68	76.37
MnO	0.69	1.43	2.20	0.97	1.37	0.40	0.64	0.46	0.71	2.92	0.60	0.54	0.77	0.66	0.84	0.13
MgO	0.00	0.03	0.00	0.16	0.25	0.20	0.19	0.15	0.09	0.00	0.50	0.62	0.70	1.15	0.71	0.18
CaO	0.00	0.11	0.02	0.03	0.13	0.04	0.02	0.10	0.04	0.03	0.07	0.06	0.04	0.00	0.07	0.11
Na2O	0.00	0.00	0.00	0.10	0.00	0.00	0.00	0.00	0.00	0.00	0.00	0.00	0.00	0.00	0.00	0.00
K2O	0.02	0.09	0.05	0.04	0.00	0.00	0.06	0.05	0.00	0.02	0.01	0.01	0.00	0.03	0.01	0.01
Total	95.87	93.69	96.40	94.52	96.35	92.87	92.93	91.98	93.50	91.74	89.03	89.50	94.48	92.57	91.98	88.37
Fe2O3	24.57	32.59	21.10	21.35	14.03	33.92	36.83	43.10	39.74	32.07	46.84	42.27	34.20	28.73	63.67	41.99
FeO	50.53	44.89	50.83	50.21	54.05	44.50	43.04	39.86	42.35	42.32	36.16	38.08	44.38	44.92	30.39	38.59
Total	98.33	96.95	98.51	96.66	97.75	96.27	96.61	96.29	97.48	94.96	93.72	93.73	97.91	95.45	98.36	92.58

B. (continuation)

Point	92-14	93-14	96-14	97-14	99-14	100-14	103-14	105-14	1-15	3-15	5-15	6-15	7-15	9-15	10-15	11-15
SiO2	0.32	0.40	0.30	0.64	0.28	0.34	0.29	0.30	0.61	0.37	0.39	0.25	0.41	0.28	0.38	0.35
TiO2	5.98	8.16	1.48	8.25	20.35	11.92	18.24	14.85	11.66	11.25	11.12	11.83	12.00	11.94	11.95	11.95
Al2O3	3.52	1.55	1.13	0.59	0.59	0.19	0.17	0.81	1.00	0.85	1.06	1.05	1.07	1.09	0.74	0.84
FeO	80.66	81.50	88.88	81.05	67.57	74.49	70.50	75.71	77.69	76.47	77.10	77.88	76.22	75.79	70.34	76.16
MnO	0.21	0.48	0.68	0.39	0.49	0.53	0.77	2.20	1.48	1.33	0.18	0.90	0.48	0.78	0.62	0.67
MgO	0.25	0.20	0.74	0.44	0.76	0.36	0.43	0.00	0.14	0.00	0.28	0.00	0.01	0.00	0.37	0.23
CaO	0.10	0.12	0.01	0.06	0.05	0.14	0.09	0.00	0.58	0.10	0.14	0.09	0.07	0.06	0.21	0.11
Na2O	0.00	0.00	0.00	0.00	0.00	0.00	0.01	0.00	0.00	0.00	0.04	0.00	0.00	0.00	0.00	0.00
K2O	0.04	0.03	0.00	0.04	0.02	0.05	0.03	0.01	0.05	0.05	0.03	0.00	0.04	0.06	0.05	0.05
Total	91.08	92.42	93.22	91.46	90.10	88.00	90.53	93.88	93.21	90.42	90.35	92.00	90.29	90.00	84.66	90.35
Fe2O3	50.08	48.79	64.24	48.68	23.61	39.74	28.68	37.01	42.43	41.78	41.96	41.71	39.74	39.98	36.42	40.50
FeO	35.60	37.59	31.07	37.25	46.32	38.73	44.69	42.41	39.51	38.87	39.34	40.34	40.46	39.81	37.57	39.71
Total	96.10	97.31	99.65	96.34	92.46	91.98	93.40	97.59	97.46	94.60	94.55	96.17	94.27	94.00	88.31	94.41

Point	13-15	15-15	17-15	18-15	19-15	20-15	21-15	22-15	24-15	26-15	29-15	30-15	32-15	33-15	35-15	36-15
SiO2	0.26	0.38	0.68	0.21	0.34	0.25	0.12	0.46	0.30	0.22	0.21	0.21	0.22	0.26	0.29	0.32
TiO2	11.27	11.70	9.61	10.41	11.31	12.58	10.98	10.82	9.19	15.00	11.97	16.07	14.87	12.77	12.89	10.21
Al2O3	1.03	0.97	1.67	0.70	1.25	0.78	1.11	1.23	1.44	1.16	0.95	1.21	1.39	0.71	1.20	1.01
FeO	76.65	77.89	73.76	79.14	77.45	76.58	77.25	73.68	78.97	74.02	77.45	72.07	73.63	76.23	74.43	76.44
MnO	0.80	0.81	0.19	0.40	0.62	0.80	0.95	0.81	0.53	1.22	0.54	1.63	1.07	0.33	1.64	0.81
MgO	0.00	0.00	1.53	0.20	0.00	0.46	0.00	0.00	0.56	0.00	0.28	0.06	0.01	0.00	0.00	0.02
CaO	0.09	0.02	0.16	0.07	0.09	0.06	0.10	0.20	0.13	0.08	0.13	0.10	0.11	0.09	0.11	0.05
Na2O	0.00	0.00	0.10	0.00	0.00	0.00	0.00	0.00	0.00	0.00	0.02	0.00	0.00	0.00	0.00	0.00
K2O	0.05	0.02	0.13	0.05	0.06	0.02	0.02	0.10	0.02	0.01	0.01	0.00	0.04	0.02	0.03	0.03
Total	90.14	91.78	87.84	91.18	91.13	91.52	90.53	87.30	91.14	91.71	91.56	91.35	91.33	90.41	90.58	88.89
Fe2O3	41.58	41.62	42.88	44.79	41.78	40.44	42.67	39.78	46.31	34.87	41.60	32.37	34.64	39.00	38.24	42.68
FeO	39.23	40.44	35.18	38.83	39.86	40.18	38.85	37.88	37.30	42.64	40.02	42.94	42.45	41.14	40.03	38.04
Total	94.30	95.94	92.13	95.66	95.31	95.57	94.80	91.28	95.77	95.20	95.73	94.59	94.80	94.32	94.41	93.16

Point	37-15	38-15	40-16	41-16	42-16	43-16	44-16	45-16	48-16	50-16	52-16	53-16	54-16	55-16	56-16	58-16
SiO2	0.21	0.31	0.98	0.70	0.27	0.06	0.29	0.35	0.32	0.31	2.77	0.57	0.29	0.41	0.21	0.17
TiO2	11.26	9.99	17.71	10.26	24.01	17.20	19.55	20.82	19.64	17.86	1.70	27.01	18.78	20.28	19.53	22.02
Al2O3	0.96	0.83	0.98	0.52	0.65	0.59	1.09	0.89	0.35	0.59	0.21	0.63	1.01	0.95	0.89	0.06
FeO	77.89	77.08	69.25	78.13	63.51	71.84	68.49	68.07	66.90	71.76	81.31	62.21	70.94	67.45	70.59	67.22
MnO	0.97	0.62	2.94	1.35	0.44	0.40	0.31	0.26	0.43	0.30	0.14	0.24	0.97	0.68	0.59	0.50
MgO	0.00	0.55	0.53	0.68	2.23	1.18	0.62	0.67	0.89	0.48	0.00	0.57	1.97	1.43	1.00	0.45
CaO	0.11	0.06	0.00	0.03	0.12	0.11	0.08	0.10	0.13	0.19	0.27	0.26	0.03	0.08	0.05	0.08
Na2O	0.00	0.00	0.00	0.00	0.00	0.00	0.00	0.03	0.02	0.00	0.00	0.00	0.00	0.09	0.00	0.00
K2O	0.01	0.00	0.02	0.00	0.01	0.02	0.04	0.03	0.03	0.00	0.12	0.04	0.03	0.00	0.05	0.01
Total	91.43	89.44	92.43	91.66	91.23	91.40	90.45	91.22	88.70	91.49	86.53	91.52	94.03	91.37	92.91	90.52
Fe2O3	42.69	44.06	28.41	44.63	17.66	31.94	24.83	22.98	24.41	29.55	53.65	10.03	29.93	24.58	27.36	21.20
FeO	39.48	37.43	43.69	37.96	47.62	43.10	46.14	47.39	44.93	45.17	33.03	53.18	44.01	45.33	45.97	48.13
Total	95.70	93.85	95.27	96.13	93.00	94.60	92.94	93.52	91.15	94.45	91.90	92.52	97.02	93.83	95.65	92.63

B. (continuation)

Point	59-16	63-16	65-16	66-16	68-16	70-16	71-16	2-17	3-17	4-17	10-17	11-17	13-17	14-17	15-17	17-17
SiO2	0.46	0.33	0.28	0.17	0.21	0.31	0.27	3.96	0.28	3.78	1.60	0.54	0.57	1.82	2.10	1.14
TiO2	21.28	17.44	18.08	20.33	19.84	20.70	22.71	0.12	4.90	0.14	0.12	5.48	5.00	1.09	0.04	13.61
Al2O3	0.13	0.05	0.88	0.97	0.78	0.56	0.41	0.45	1.16	0.35	0.13	2.27	0.84	0.45	0.00	0.74
FeO	66.66	70.75	70.32	69.03	68.64	69.09	66.18	84.57	85.85	84.54	88.74	81.86	83.99	83.65	87.98	74.81
MnO	0.40	0.41	0.44	0.58	0.49	1.08	0.40	0.06	0.23	0.12	0.07	0.28	0.25	0.24	0.06	0.46
MgO	0.25	0.16	0.65	1.17	1.27	0.87	0.71	1.29	0.06	0.98	0.48	0.53	0.00	0.34	0.14	0.12
CaO	0.09	0.12	0.04	0.07	0.10	0.04	0.02	0.19	0.20	0.23	0.12	0.27	0.40	0.13	0.06	0.58
Na2O	0.00	0.00	0.00	0.00	0.00	0.00	0.03	0.00	0.00	0.04	0.02	0.00	0.00	0.05	0.00	0.00
K2O	0.03	0.05	0.06	0.02	0.01	0.03	0.01	0.06	0.00	0.06	0.02	0.00	0.06	0.03	0.02	0.10
Total	89.30	89.31	90.74	92.33	91.33	92.67	90.75	90.69	92.66	90.23	91.29	91.23	91.09	87.80	90.39	91.54
Fe2O3	20.93	29.34	28.42	25.35	25.78	24.84	19.50	57.34	56.42	57.50	63.63	52.36	54.85	58.12	61.77	36.21
FeO	47.83	44.35	44.75	46.22	45.44	46.74	48.63	32.98	35.08	32.80	31.48	34.74	34.63	31.35	32.40	42.23
Total	91.40	92.24	93.59	94.86	93.91	95.16	92.70	96.44	98.31	95.99	97.67	96.47	96.59	93.62	96.58	95.17

Point	18-17	2-18	3-18	4-18	7-18	8-18	16-18	17-18	21-18	22-18	23-18	27-18	34-18	35-18	36-18	37-18
SiO2	0.91	0.41	0.48	0.30	0.92	0.00	0.00	0.00	0.00	0.10	0.10	0.36	0.59	0.76	0.65	0.66
TiO2	4.67	6.44	23.51	3.53	6.58	3.71	11.59	8.20	7.50	8.62	4.53	8.95	11.16	18.91	5.51	6.72
Al2O3	0.67	0.27	0.00	0.39	0.51	0.31	0.22	0.15	0.25	0.00	0.55	1.17	1.00	0.91	0.77	0.85
FeO	82.06	78.21	49.12	78.50	74.66	83.21	75.20	77.72	80.00	78.74	82.29	75.25	73.12	65.35	79.54	77.77
MnO	0.31	0.27	1.80	0.26	0.11	0.21	0.65	0.74	0.22	0.28	0.62	0.66	0.39	0.54	0.58	0.22
MgO	0.42	0.00	0.00	0.00	0.00	0.00	0.30	0.00	0.00	0.00	0.00	0.09	0.32	0.46	0.00	0.07
CaO	0.34	0.11	0.18	0.06	0.08	0.08	0.06	0.16	0.02	0.06	0.06	0.11	0.02	0.06	0.08	0.29
Na2O	0.00	0.11	0.00	0.00	0.00	0.00	0.00	0.02	0.01	0.33	0.00	0.08	0.08	0.00	0.00	0.00
K2O	0.06	0.09	0.13	0.08	0.31	0.02	0.07	0.07	0.03	0.07	0.03	0.04	0.05	0.05	0.08	0.11
Total	89.45	85.89	75.21	83.10	83.17	87.53	88.08	87.05	88.03	88.19	88.19	86.71	86.71	87.04	87.21	86.68
Fe2O3	53.89	49.49	6.08	53.20	45.68	56.85	41.28	47.54	49.44	48.52	55.08	43.75	38.93	22.60	50.77	47.88
FeO	33.57	33.67	43.64	30.63	33.56	32.06	38.05	34.94	35.51	35.07	32.72	35.88	38.09	45.01	33.86	34.68
Total	94.84	90.85	75.82	88.43	87.75	93.22	92.22	91.81	92.98	93.05	93.70	91.09	90.61	89.30	92.30	91.48

Point	39-18	41-18	47-18	48-18	51-18	53-18	54-18	56-18	57-18	59-18	63-18	2-19	3-19	4-19	10-19	11-19
SiO2	0.52	0.37	0.31	0.34	1.78	0.62	0.45	0.42	0.49	0.47	0.68	0.40	0.69	0.35	2.29	0.24
TiO2	7.53	10.18	7.92	9.67	8.48	7.12	4.07	6.57	23.19	29.77	12.14	5.13	5.77	11.17	5.84	22.64
Al2O3	0.85	0.76	1.10	0.64	1.52	0.69	0.93	0.78	0.81	0.41	1.02	0.98	0.85	0.56	0.68	0.31
FeO	77.68	75.89	77.67	76.24	72.32	75.83	81.69	78.30	60.57	56.02	70.93	78.79	80.02	75.64	78.89	63.60
MnO	0.26	0.33	0.61	0.12	0.39	0.16	0.31	0.21	1.88	2.38	1.57	0.27	0.21	0.44	0.13	1.61
MgO	0.07	0.22	0.17	0.00	0.13	0.13	0.09	0.00	0.51	0.43	0.00	0.21	0.08	0.23	0.02	0.94
CaO	0.26	0.09	0.06	0.19	0.17	0.42	0.05	0.06	0.00	0.03	0.05	0.07	0.18	0.09	0.11	0.03
Na2O	0.06	0.00	0.05	0.00	0.00	0.00	0.00	0.00	0.00	0.12	0.00	0.00	0.00	0.00	0.00	0.00
K2O	0.08	0.06	0.03	0.02	0.19	0.09	0.13	0.04	0.05	0.12	0.04	0.04	0.02	0.03	0.08	0.03
Total	87.30	87.89	87.90	87.23	84.97	85.06	87.72	86.38	87.51	89.75	86.43	85.89	87.82	88.51	88.04	89.39
Fe2O3	47.17	42.40	46.88	42.97	39.48	46.17	54.57	48.43	14.91	4.01	35.99	50.97	50.42	41.03	46.69	18.92
FeO	35.23	37.74	35.48	37.58	36.79	34.29	32.58	34.72	47.16	52.41	38.54	32.92	34.64	38.72	36.88	46.57
Total	92.03	92.14	92.60	91.53	88.92	89.69	93.19	91.23	89.00	90.15	90.03	90.99	92.87	92.62	92.72	91.29

B. (continuation)

Point	13-19	16-19	17-19	19-19	20-19	21-19	22-19	24-19	28-19	29-19	32-19	33-19	34-19	37-19	39-19	40-19
SiO2	0.31	1.63	0.50	0.75	0.60	0.85	0.75	0.75	0.37	0.83	0.47	0.77	0.65	1.10	1.05	1.26
TiO2	22.24	4.52	16.66	5.10	4.50	9.03	7.17	4.81	4.88	0.46	10.21	4.24	6.67	7.69	3.79	7.10
Al2O3	0.46	0.83	0.53	0.89	1.09	0.66	0.74	0.70	1.30	0.11	0.87	0.64	0.72	0.93	0.23	0.61
FeO	63.70	78.89	72.12	79.43	80.38	75.41	77.11	81.65	81.45	85.38	74.91	80.99	79.09	78.03	82.32	78.78
MnO	1.55	0.15	0.66	0.20	0.23	0.20	0.17	0.27	0.26	0.00	0.38	0.18	0.28	0.17	0.02	0.09
MgO	0.84	0.10	0.57	0.11	0.19	0.13	0.06	0.13	0.09	0.00	0.29	0.00	0.07	0.06	0.00	0.00
CaO	0.04	0.04	0.09	0.03	0.27	0.80	0.14	0.02	0.02	0.10	0.05	0.13	0.11	0.15	0.08	0.11
Na2O	0.00	0.00	0.00	0.00	0.00	0.06	0.00	0.00	0.00	0.00	0.00	0.00	0.03	0.00	0.00	0.00
K2O	0.01	0.16	0.04	0.09	0.06	0.04	0.05	0.06	0.00	0.03	0.05	0.06	0.06	0.01	0.02	0.06
Total	89.14	86.33	91.18	86.61	87.32	87.16	86.18	88.39	88.36	86.90	87.23	87.01	87.68	88.14	87.50	88.00
Fe2O3	19.09	49.85	31.51	50.84	52.77	43.42	46.34	52.95	52.85	61.29	41.45	53.08	48.88	45.49	54.09	46.71
FeO	46.51	34.04	43.77	33.69	32.89	36.34	35.40	34.01	33.89	30.23	37.61	33.22	35.11	37.10	33.64	36.75
Total	91.05	91.32	94.33	91.70	92.60	91.51	90.82	93.70	93.65	93.04	91.38	92.33	92.58	92.69	92.92	92.67

Point	1-20	2-20	4-20	5-20	7-20	8-20	10-20	11-20	14-20	15-20	17-20	18-20	19-20	20-20	21-20	22-20
SiO2	0.24	0.23	0.39	0.33	0.25	0.22	0.25	0.36	0.37	0.40	0.21	0.24	0.16	0.40	0.42	3.73
TiO2	3.16	2.88	3.57	3.41	3.50	3.99	3.29	2.87	3.65	3.46	3.79	3.85	3.78	4.00	4.05	3.33
Al2O3	1.70	1.61	1.70	1.65	1.37	1.59	1.54	1.64	1.32	1.84	1.61	1.68	1.74	1.59	0.77	3.40
FeO	74.29	76.14	74.53	73.56	72.73	73.75	72.96	74.95	72.34	68.92	72.02	72.94	73.41	72.78	78.08	69.86
MnO	6.68	5.90	6.49	5.91	6.61	6.76	7.47	6.31	7.19	6.69	8.22	7.06	6.73	6.78	2.76	6.08
MgO	1.22	1.09	1.31	1.51	1.39	1.62	1.36	1.18	1.42	1.10	1.21	1.19	1.67	1.60	0.55	1.45
CaO	0.01	0.01	0.03	0.00	0.00	0.01	0.02	0.00	0.06	0.05	0.00	0.01	0.02	0.03	0.03	0.06
Na2O	0.00	0.00	0.00	0.00	0.00	0.00	0.00	0.00	0.00	0.00	0.00	0.16	0.00	0.00	0.00	0.00
K2O	0.00	0.04	0.06	0.05	0.01	0.00	0.03	0.06	0.05	0.03	0.06	0.02	0.02	0.02	0.01	0.18
Total	87.29	87.89	88.07	86.42	85.86	87.94	86.92	87.38	86.39	82.48	87.11	87.15	87.51	87.20	86.67	88.09
Fe2O3	56.14	57.29	55.68	55.07	54.89	55.32	55.93	56.68	54.85	51.37	55.01	55.23	55.46	54.34	54.17	45.97
FeO	23.77	24.58	24.42	24.00	23.33	23.97	22.64	23.95	22.98	22.69	22.51	23.24	23.50	23.89	29.34	28.50
Total	92.91	93.63	93.65	91.93	91.36	93.48	92.52	93.05	91.88	87.62	92.62	92.68	93.07	92.64	92.09	92.69

Point	23-20	24-20	25-20	27-20	28-20	4-21	9-21	11-21	12-21	13-21	17-21	18-21	20-21	22-21	23-21	24-21
SiO2	0.59	0.30	0.31	0.43	0.28	0.41	1.24	0.35	0.37	0.52	0.24	0.23	0.31	0.62	0.38	0.93
TiO2	3.52	2.63	3.68	3.98	3.39	27.88	22.43	26.18	24.71	25.83	26.55	25.37	25.84	26.61	23.23	24.69
Al2O3	0.72	1.59	1.55	1.35	1.09	0.53	0.11	0.40	0.09	0.15	0.46	0.07	0.53	0.70	0.18	0.28
FeO	77.93	73.24	74.55	71.98	73.62	64.78	64.54	62.97	65.17	66.58	67.23	68.65	67.69	62.73	67.04	65.56
MnO	2.59	6.54	6.75	6.41	6.70	1.11	1.62	1.55	1.53	2.01	1.68	1.70	1.91	2.25	1.93	0.66
MgO	0.28	0.59	1.36	1.15	1.00	0.45	0.00	0.00	0.00	0.04	0.05	0.00	0.11	0.00	0.00	0.18
CaO	0.02	0.01	0.01	0.03	0.00	0.02	0.18	0.07	0.22	0.12	0.12	0.09	0.10	0.18	0.07	0.60
Na2O	0.00	0.00	0.05	0.00	0.00	0.10	0.00	0.00	0.00	0.00	0.07	0.00	0.00	0.00	0.13	0.05
K2O	0.04	0.08	0.03	0.03	0.08	0.00	0.12	0.02	0.00	0.04	0.04	0.00	0.01	0.01	0.01	0.04
Total	85.69	84.98	88.29	85.36	86.17	95.28	90.23	91.55	92.09	95.29	96.43	96.12	96.49	93.10	92.97	92.97
Fe2O3	54.06	55.32	56.14	52.99	55.52	11.69	17.41	12.20	16.00	15.70	15.61	17.98	16.58	11.45	20.00	15.47
FeO	29.28	23.46	24.03	24.30	23.66	54.26	48.87	51.99	50.77	52.45	53.19	52.48	52.77	52.42	49.04	51.63
Total	91.11	90.52	93.92	90.67	91.73	96.45	91.97	92.77	93.70	96.86	97.99	97.92	98.15	94.25	94.97	94.52

B. (continuation)

Point	28-21	33-21	34-21	1-22	3-22	4-22	9-22	11-22	25-22	27-22	28-22	29-22	31-22	32-22	33-22	1-29
SiO2	0.17	0.75	0.35	0.55	0.24	0.44	0.55	0.47	0.31	0.27	0.19	0.19	0.28	0.29	0.64	1.28
TiO2	25.19	25.39	27.65	27.46	26.13	25.32	23.19	20.12	22.11	15.83	31.24	34.26	13.90	13.75	14.63	19.84
Al2O3	0.29	0.65	0.29	0.32	0.46	0.59	0.93	0.38	0.74	0.73	0.00	0.00	1.71	1.97	0.25	1.12
FeO	66.25	64.62	68.24	70.23	71.39	72.43	70.92	73.60	67.35	71.48	46.70	46.97	67.63	64.81	65.51	64.23
MnO	1.63	2.01	0.73	1.35	1.36	1.28	1.23	2.16	3.00	0.55	0.61	0.49	0.50	2.57	1.69	2.71
MgO	0.00	0.00	0.33	0.08	0.02	0.02	0.22	0.00	0.00	0.22	0.51	0.21	0.48	0.04	0.34	0.31
CaO	0.07	0.05	0.04	0.08	0.03	0.01	0.19	0.43	0.18	0.01	0.03	0.03	0.03	0.02	0.03	0.15
Na2O	0.00	0.00	0.00	0.00	0.01	0.00	0.00	0.00	0.00	0.00	0.00	0.00	0.00	0.00	0.00	0.00
K2O	0.03	0.00	0.01	0.02	0.00	0.00	0.02	0.03	0.05	0.02	0.04	0.01	0.00	0.00	0.00	0.01
Total	93.62	93.46	97.64	100.09	99.64	100.08	97.25	97.20	93.74	89.10	79.32	82.16	84.53	83.44	83.08	89.66
Fe2O3	16.42	13.92	13.98	15.54	18.51	19.84	21.60	28.80	22.07	31.78	0.00	0.00	31.22	30.13	29.52	20.91
FeO	51.47	52.09	55.66	56.24	54.74	54.58	51.48	47.69	47.49	42.88	46.70	46.97	39.53	37.69	38.95	45.42
Total	95.27	94.85	99.04	101.64	101.50	102.07	99.41	100.08	95.95	92.28	79.32	82.16	87.65	86.45	86.03	91.75

Point	2-29	3-29	4-29	5-29	6-29	7-29	8-29	10-29	11-29	12-29	13-29	14-29	15-29	17-29	19-29	21-29
SiO2	0.88	0.61	0.70	0.24	0.26	0.53	0.55	0.46	0.15	0.35	0.39	5.23	0.29	0.27	0.37	0.19
TiO2	21.41	18.51	17.03	17.16	18.89	18.13	16.23	19.25	18.25	16.59	15.86	21.13	16.61	16.94	16.36	16.10
Al2O3	1.25	1.17	0.96	0.91	0.89	1.04	0.97	0.83	1.04	0.93	0.65	0.58	1.02	0.91	1.14	0.82
FeO	65.22	66.08	69.59	69.30	69.82	68.92	70.72	67.77	69.23	71.45	70.32	61.85	71.53	70.54	69.69	70.60
MnO	2.08	2.52	2.27	2.52	2.42	2.48	2.09	2.47	2.61	2.40	2.12	1.72	2.24	2.26	2.19	2.40
MgO	0.38	0.15	0.01	0.00	0.00	0.00	0.04	0.00	0.00	0.00	0.00	0.51	0.02	0.00	0.00	0.00
CaO	0.03	0.08	0.03	0.16	0.04	0.05	0.10	0.08	0.01	0.06	0.15	1.17	0.04	0.01	0.82	0.10
Na2O	0.05	0.00	0.00	0.00	0.00	0.00	0.00	0.00	0.00	0.00	0.13	0.00	0.00	0.00	0.00	0.00
K2O	0.00	0.00	0.00	0.00	0.00	0.01	0.02	0.00	0.02	0.06	0.01	0.02	0.00	0.03	0.00	0.03
Total	91.30	89.11	90.58	90.29	92.32	91.15	90.72	90.85	91.31	91.82	89.62	92.21	91.75	90.96	90.56	90.22
Fe2O3	19.87	24.76	28.86	29.61	27.49	27.34	31.06	25.24	28.17	31.75	32.27	11.23	31.57	30.51	31.00	32.05
FeO	47.34	43.80	43.62	42.66	45.08	44.32	42.77	45.06	43.88	42.88	41.28	51.75	43.12	43.09	41.79	41.76
Total	93.29	91.59	93.47	93.26	95.07	93.89	93.83	93.38	94.13	95.00	92.86	93.33	94.91	94.02	93.67	93.43

Point	23-29	24-29	26-29	27-29	29-29	30-29	31-29	34-29	1-30	3-30	6-30	8-30	10-30	12-30	13-30	15-30
SiO2	0.23	0.17	0.23	0.36	0.31	0.26	0.27	0.24	1.81	0.42	0.21	0.36	0.32	1.04	1.03	1.13
TiO2	14.41	16.51	18.05	17.94	15.79	13.70	14.44	13.21	6.67	11.39	11.34	9.60	10.55	6.49	2.00	2.62
Al2O3	1.25	0.70	0.62	0.67	1.36	0.98	0.85	0.80	0.47	0.54	0.91	1.35	1.20	1.01	0.30	0.60
FeO	73.47	70.61	71.22	70.53	72.16	75.07	75.77	76.01	74.28	75.68	76.38	78.87	75.06	75.11	81.94	79.91
MnO	1.94	2.22	2.32	2.44	2.23	1.97	2.08	2.08	0.64	0.62	0.48	0.29	3.57	0.37	0.44	0.46
MgO	0.00	0.00	0.00	0.00	0.00	0.00	0.00	0.00	0.25	0.01	0.29	0.43	0.00	0.32	0.00	0.00
CaO	0.11	0.09	0.07	0.11	0.06	0.15	0.08	0.10	0.25	0.10	0.08	0.05	0.04	0.45	0.15	0.47
Na2O	0.00	0.02	0.00	0.00	0.00	0.00	0.00	0.00	0.17	0.00	0.00	0.01	0.01	0.00	0.00	0.00
K2O	0.02	0.02	0.01	0.03	0.00	0.05	0.04	0.00	0.01	0.02	0.00	0.03	0.02	0.09	0.02	0.02
Total	91.44	90.33	92.52	92.09	91.90	92.16	93.52	92.44	84.55	88.78	89.69	90.99	90.77	84.87	85.88	85.21
Fe2O3	35.79	31.51	29.80	29.40	32.89	38.15	37.71	39.53	44.49	40.50	41.46	45.25	43.17	46.00	56.57	54.25
FeO	41.26	42.26	44.40	44.08	42.56	40.74	41.84	40.44	34.24	39.23	39.08	38.15	36.21	33.72	31.03	31.09
Total	95.03	93.48	95.51	95.04	95.19	95.98	97.30	96.40	89.01	92.83	93.84	95.52	95.09	89.47	91.55	90.64

B. (continuation)

Point	17-30	18-30	20-30	21-30	23-30	24-30	25-30	26-30	27-30	29-30	32-30	33-30	34-30	36-32	38-32	40-32
SiO2	1.55	1.79	1.40	1.07	1.05	0.25	2.49	0.63	0.90	1.67	0.26	1.33	1.62	0.20	0.31	0.47
TiO2	6.70	6.00	4.25	15.28	8.70	11.75	0.53	5.16	2.15	5.36	8.25	5.02	2.54	17.53	17.71	18.05
Al2O3	0.61	0.54	0.52	0.51	0.68	1.07	1.13	0.72	0.30	0.39	0.38	0.26	0.38	1.67	1.89	1.94
FeO	74.53	74.78	77.20	67.84	75.86	71.74	80.21	78.49	81.00	72.22	78.33	78.48	81.12	66.71	67.03	64.68
MnO	0.45	0.58	0.72	0.29	0.35	1.01	0.09	0.68	0.30	0.69	0.82	0.69	0.48	3.53	4.44	3.97
MgO	0.00	0.00	0.00	0.24	0.15	0.46	0.00	0.00	0.00	0.24	0.01	0.00	0.00	0.00	0.45	0.17
CaO	0.21	0.27	0.25	0.24	0.12	0.11	0.15	0.19	0.23	0.30	0.06	0.14	0.27	0.00	0.00	0.04
Na2O	0.10	0.00	0.21	0.00	0.00	0.07	0.00	0.00	0.00	0.07	0.00	0.00	0.00	0.00	0.00	0.00
K2O	0.03	0.04	0.00	0.05	0.10	0.00	0.07	0.03	0.04	0.03	0.01	0.01	0.00	0.01	0.05	0.05
Total	84.17	84.01	84.54	85.51	87.00	86.46	84.67	85.90	84.93	80.96	88.11	85.92	86.42	89.66	91.88	89.36
Fe2O3	44.28	44.77	50.46	28.62	43.22	38.26	54.13	50.55	55.95	44.71	47.09	49.65	54.27	27.52	28.59	25.40
FeO	34.69	34.50	31.79	42.08	36.97	37.31	31.49	33.00	30.66	31.99	35.96	33.80	32.28	41.95	41.30	41.82
Total	88.60	88.50	89.60	88.37	91.33	90.29	90.09	90.96	90.53	85.44	92.82	90.90	91.86	92.42	94.75	91.91

Point	42-32	43-32	44-32	46-32	47-32	49-32	36-33	37-33	39-33	40-33	42-33	43-33	44-33	45-33	46-33	47-33
SiO2	1.25	2.40	1.73	0.12	0.28	0.23	0.83	0.73	0.32	0.54	3.33	0.49	0.99	0.20	4.00	0.21
TiO2	6.61	14.07	2.04	5.20	5.95	3.88	8.89	11.20	11.21	15.80	13.47	15.75	15.33	13.46	14.80	16.14
Al2O3	4.16	1.88	0.54	1.94	2.22	2.58	1.14	0.98	0.83	1.11	3.23	1.16	1.27	2.85	2.52	1.12
FeO	76.15	49.41	81.42	78.45	78.02	79.66	74.39	71.87	71.69	64.61	63.09	65.73	66.07	70.51	61.49	67.53
MnO	0.76	0.19	0.48	0.20	0.30	0.38	1.64	2.46	3.01	1.37	1.67	1.70	1.47	0.65	1.34	1.29
MgO	1.38	1.02	0.00	2.03	2.21	1.63	0.14	0.00	0.19	0.00	0.38	0.00	0.00	2.19	0.23	0.00
CaO	0.02	1.73	0.26	0.03	0.03	0.06	0.05	0.10	0.32	0.03	0.03	0.01	0.04	0.00	0.14	0.04
Na2O	0.00	0.00	0.00	0.00	0.00	0.00	0.00	0.00	0.00	0.00	0.05	0.15	0.06	0.15	0.54	0.01
K2O	0.14	0.11	0.09	0.00	0.00	0.02	0.00	0.00	0.01	0.02	0.03	0.03	0.05	0.00	0.17	0.05
Total	90.48	70.80	86.58	87.96	89.00	88.44	87.08	87.34	87.58	83.47	85.26	85.01	85.28	90.02	85.24	86.39
Fe2O3	46.02	16.04	55.12	52.84	51.38	54.63	42.68	38.45	40.01	26.40	23.28	28.24	27.62	36.47	21.67	28.73
FeO	34.74	34.97	31.82	30.91	31.78	30.50	35.98	37.27	35.69	40.85	42.14	40.32	41.22	37.69	41.99	41.68
Total	95.08	72.41	92.10	93.26	94.14	93.92	91.35	91.19	91.58	86.11	87.60	87.84	88.04	93.67	87.41	89.27

Point	48-33	49-33	51-33	53-33	54-33	1-34	3-34	4-34	5-34	8-34	9-34	10-34	12-34	14-34	15-34	16-34
SiO2	0.31	0.21	0.32	0.30	2.05	0.30	0.29	0.31	0.86	2.35	0.25	0.17	0.36	0.29	1.40	0.16
TiO2	16.13	7.19	5.96	9.26	4.33	12.53	14.42	15.25	7.42	1.40	8.66	8.13	11.25	10.37	9.16	7.11
Al2O3	2.14	0.65	0.69	1.66	0.72	2.28	2.54	2.13	1.13	0.47	0.82	1.01	2.15	2.93	3.86	1.37
FeO	67.79	77.66	78.73	77.36	80.70	72.47	70.55	70.39	76.28	80.50	74.66	74.27	71.67	71.05	68.00	75.24
MnO	3.25	0.74	0.68	1.37	0.08	0.11	0.13	0.19	0.31	1.13	0.37	0.35	0.21	0.09	0.11	0.21
MgO	0.32	2.60	2.14	0.85	0.08	1.27	1.63	1.12	3.21	0.00	2.03	2.95	2.41	2.99	3.46	3.81
CaO	0.01	0.02	0.05	0.03	0.04	0.02	0.04	0.00	0.06	0.27	0.02	0.06	0.06	0.07	0.07	0.03
Na2O	0.00	0.00	0.00	0.07	0.00	0.00	0.00	0.00	0.00	0.00	0.00	0.00	0.00	0.00	0.00	0.00
K2O	0.00	0.02	0.01	0.01	0.08	0.03	0.02	0.02	0.08	0.03	0.01	0.00	0.01	0.05	0.04	0.03
Total	89.95	89.09	88.58	90.90	88.07	89.00	89.60	89.40	89.36	86.14	86.83	86.94	88.13	87.85	86.08	87.94
Fe2O3	29.92	51.32	52.85	46.07	50.45	37.13	33.54	31.85	49.27	54.55	45.93	47.59	39.77	41.02	38.49	50.58
FeO	40.87	31.48	31.18	35.90	35.31	39.06	40.38	41.72	31.95	31.41	33.33	31.45	35.88	34.14	33.36	29.73
Total	92.94	94.23	93.87	95.51	93.12	92.72	92.96	92.59	94.29	91.61	91.43	91.70	92.11	91.95	89.94	93.01

B. (continuation)

Point	17-34	18-34	19-34	21-34	23-34	25-34	26-34	28-34	29-34	30-34	32-34	32-34	33-34	35-34	11-35	12-35
SiO2	5.22	0.32	0.67	0.23	0.30	0.27	0.15	0.13	0.26	0.22	0.35	0.35	0.25	0.27	0.52	1.69
TiO2	5.69	6.86	6.83	6.79	11.48	9.22	11.20	7.63	6.60	8.06	5.45	5.45	6.13	17.38	6.40	15.73
Al2O3	2.37	1.57	2.05	3.08	2.69	2.16	1.95	3.13	0.79	3.02	0.45	0.45	0.92	0.74	1.24	2.91
FeO	69.64	74.47	74.79	75.53	71.16	67.85	73.24	74.14	77.89	72.72	75.54	75.54	73.86	65.81	78.67	66.99
MnO	0.20	0.24	0.37	0.13	0.01	0.11	0.30	0.11	0.34	0.14	0.65	0.65	0.76	0.44	0.19	0.62
MgO	2.40	3.47	3.84	2.76	2.79	3.83	2.25	3.51	3.02	2.86	2.48	2.48	3.09	2.23	0.00	0.63
CaO	0.05	0.04	0.04	0.01	0.01	0.00	0.03	0.01	0.06	0.00	0.03	0.03	0.04	0.05	0.03	0.04
Na2O	0.11	0.00	0.10	0.00	0.00	0.00	0.00	0.00	0.00	0.00	0.00	0.00	0.00	0.00	0.00	0.00
K2O	0.32	0.04	0.05	0.00	0.00	0.01	0.00	0.01	0.03	0.00	0.01	0.01	0.01	0.00	0.07	0.09
Total	86.00	87.00	88.75	88.53	88.44	83.45	89.11	88.66	88.98	87.01	84.97	84.97	85.05	86.93	87.13	88.69
Fe2O3	38.26	49.54	50.00	48.63	39.18	41.52	41.27	47.65	52.41	45.05	51.66	51.66	50.34	28.04	48.55	25.73
FeO	35.21	29.89	29.80	31.77	35.90	30.48	36.11	31.27	30.73	32.18	29.05	29.05	28.56	40.58	34.99	43.84
Total	89.83	91.97	93.76	93.40	92.37	87.61	93.25	93.43	94.23	91.52	90.14	90.14	90.09	89.74	91.99	91.26

Point	13-35	14-35	15-35	16-35	17-35	18-35	19-35	20-35	21-35	22-35	23-35	24-35	26-35	27-35	28-35	29-35
SiO2	6.64	2.28	1.21	0.93	1.36	1.55	0.36	0.23	0.97	5.81	0.45	5.10	0.23	0.37	1.18	0.59
TiO2	18.12	11.07	8.09	14.46	12.27	17.43	7.13	16.33	15.70	2.14	6.90	1.40	19.12	18.04	15.84	19.76
Al2O3	3.34	2.83	1.43	0.75	1.06	1.08	4.50	2.45	2.77	1.69	0.43	0.97	1.34	2.36	0.50	0.38
FeO	55.73	67.78	75.40	70.89	71.08	64.49	68.26	69.97	68.73	75.12	79.16	80.58	68.41	65.76	69.45	68.43
MnO	0.86	0.99	0.99	0.22	1.27	1.95	3.34	0.25	0.21	0.05	0.27	0.06	0.25	0.27	0.34	0.05
MgO	3.65	0.90	0.07	0.57	0.73	0.64	1.03	2.54	2.40	0.54	0.00	0.00	2.47	3.67	0.83	0.78
CaO	0.17	0.08	0.06	0.03	0.02	0.07	0.03	0.04	0.06	0.17	0.08	0.07	0.00	0.02	0.04	0.01
Na2O	0.00	0.00	0.00	0.00	0.00	0.00	0.00	0.13	0.00	0.00	0.00	0.00	0.00	0.00	0.00	0.00
K2O	0.36	0.10	0.09	0.07	0.03	0.03	0.06	0.08	0.05	0.62	0.10	0.11	0.05	0.00	0.13	0.06
Total	88.95	86.05	87.34	87.91	87.82	87.25	84.71	92.03	90.90	86.14	87.38	88.33	92.01	90.57	88.39	90.08
Fe2O3	10.27	32.23	43.34	32.33	35.36	23.71	42.16	32.76	30.38	44.29	48.98	48.71	27.69	27.87	29.75	24.38
FeO	46.50	38.78	36.40	41.79	39.26	43.16	30.33	40.49	41.40	35.27	35.08	36.74	43.50	40.68	42.68	46.49
Total	89.90	89.26	91.67	91.15	91.36	89.62	88.93	95.31	93.94	90.57	92.29	93.17	94.65	93.27	91.29	92.52

Point	30-35	31-35	32-35	33-35	34-35	35-35	36-35	38-36	39-36	40-36	41-36	42-36	43-36	44-36	45-36	46-36
SiO2	2.45	1.44	1.16	1.22	3.20	7.27	6.78	0.22	0.29	0.21	0.15	0.33	0.31	0.29	0.38	0.14
TiO2	1.87	13.73	12.58	4.50	29.71	3.13	1.25	7.81	7.80	7.82	3.08	1.52	7.35	7.65	7.18	6.79
Al2O3	1.30	1.84	0.88	1.20	2.81	1.89	2.85	0.31	0.32	0.40	0.02	0.06	0.33	0.35	0.28	0.29
FeO	80.64	66.56	67.62	77.48	48.72	72.63	74.11	76.05	75.59	77.99	81.52	82.96	78.98	78.90	77.70	79.76
MnO	0.01	1.16	2.55	1.24	0.75	0.07	0.14	0.24	0.19	0.08	0.00	0.01	0.08	0.16	0.16	0.13
MgO	0.09	0.51	0.46	0.00	2.48	1.64	2.37	1.24	1.53	0.76	0.00	0.00	0.84	0.77	0.59	0.70
CaO	0.30	0.09	0.06	0.04	0.09	0.23	0.20	0.29	0.94	0.25	0.08	0.13	0.26	0.25	0.22	0.34
Na2O	0.00	0.00	0.00	0.00	0.00	0.00	0.10	0.00	0.00	0.00	0.00	0.00	0.00	0.03	0.00	0.00
K2O	0.11	0.09	0.06	0.06	0.01	0.73	0.13	0.00	0.00	0.00	0.05	0.08	0.06	0.00	0.00	0.00
Total	86.79	85.45	85.35	85.73	87.83	87.69	88.11	86.16	86.65	87.51	84.89	85.08	88.20	88.40	86.50	88.14
Fe2O3	52.94	29.41	33.55	49.73	0.00	40.26	43.95	47.48	47.99	48.06	56.25	59.18	49.56	49.05	48.30	50.99
FeO	32.99	40.10	37.43	32.73	48.72	36.40	34.56	33.33	32.40	34.74	30.90	29.70	34.39	34.76	34.24	33.87
Total	92.05	88.35	88.71	90.71	87.76	91.64	92.33	90.92	91.45	92.33	90.53	91.01	93.17	93.31	91.34	93.25

B. (continuation)

Point	47-36	48-36	49-36	50-36	51-36	52-36	53-36	54-36	55-36	56-36	38-38	39-38	40-38	41-38	43-38	44-38
SiO2	0.24	0.51	0.20	0.22	0.12	0.17	0.50	0.28	0.44	0.43	3.52	0.54	0.68	4.30	1.04	3.95
TiO2	6.59	1.87	1.48	3.74	5.19	1.55	1.30	2.03	1.87	3.53	15.59	15.71	16.87	15.46	17.06	16.50
Al2O3	0.27	0.29	0.02	0.58	0.50	0.00	0.54	0.00	0.12	0.36	0.66	1.00	0.61	0.59	0.52	0.62
FeO	79.56	83.37	83.76	81.41	81.71	84.16	80.29	83.31	82.52	80.12	69.02	72.62	71.60	67.82	70.82	68.51
MnO	0.14	0.11	0.08	0.13	0.10	0.06	0.00	0.05	0.02	0.01	0.33	1.52	0.68	0.46	1.17	0.34
MgO	0.69	0.06	0.00	0.43	0.72	0.00	0.13	0.00	0.05	0.18	0.00	0.06	0.00	0.00	0.00	0.02
CaO	0.82	0.74	0.56	0.54	0.55	0.24	0.47	0.01	0.12	0.17	2.62	0.24	0.25	3.28	0.22	3.18
Na2O	0.00	0.00	0.00	0.00	0.00	0.00	0.14	0.00	0.00	0.00	0.00	0.00	0.00	0.00	0.06	0.00
K2O	0.00	0.03	0.00	0.04	0.02	0.00	0.08	0.09	0.04	0.06	0.02	0.00	0.01	0.02	0.00	0.02
Total	88.31	86.97	86.10	87.09	88.90	86.19	83.44	85.76	85.18	84.86	91.76	91.68	90.69	91.92	90.90	93.13
Fe2O3	51.39	59.19	60.31	55.91	54.74	60.27	58.03	58.80	58.13	54.28	26.57	32.82	29.80	25.20	28.96	24.80
FeO	33.32	30.11	29.49	31.10	32.45	29.93	28.08	30.39	30.21	31.28	45.11	43.09	44.78	45.14	44.77	46.19
Total	93.45	92.90	92.14	92.69	94.39	92.22	89.25	91.65	91.00	90.29	94.42	94.97	93.67	94.45	93.80	95.61

Point	46-38	47-38	49-38	50-38	51-38	54-38	55-38	57-38	58-38	61-38	62-38	64-38	65-38	66-38	67-38	68-38
SiO2	0.20	3.86	4.11	0.07	0.50	2.94	0.23	3.24	0.29	0.37	0.65	1.96	0.63	0.32	3.69	0.49
TiO2	15.64	16.41	14.95	14.05	16.18	15.73	14.60	16.55	16.44	15.99	17.35	15.22	14.53	16.04	16.56	14.16
Al2O3	1.07	0.74	0.50	1.02	0.92	0.68	1.20	0.57	0.95	0.98	0.69	0.52	0.81	0.95	0.55	0.76
FeO	73.51	67.40	69.01	75.23	72.75	68.97	73.25	67.79	71.58	69.04	71.20	70.61	71.87	73.21	68.25	75.70
MnO	1.08	0.34	0.23	0.61	1.92	0.30	0.78	0.32	0.82	1.95	0.43	0.51	1.80	0.91	0.29	1.36
MgO	0.00	0.01	0.00	0.03	0.00	0.00	0.00	0.00	0.15	0.02	0.00	0.00	0.05	0.00	0.02	0.00
CaO	0.03	2.77	2.99	0.17	0.27	2.23	0.08	2.55	0.18	0.21	0.24	1.72	0.14	0.01	2.98	0.09
Na2O	0.00	0.14	0.00	0.00	0.00	0.00	0.00	0.09	0.00	0.00	0.00	0.00	0.00	0.00	0.00	0.00
K2O	0.01	0.02	0.04	0.00	0.00	0.05	0.01	0.00	0.00	0.02	0.04	0.00	0.00	0.00	0.00	0.00
Total	91.55	91.67	91.84	91.18	92.54	90.90	90.14	91.09	90.40	88.58	90.60	90.54	89.83	91.43	92.35	92.57
Fe2O3	33.59	24.37	26.80	37.01	32.66	27.06	34.45	25.18	31.08	30.41	28.78	30.31	33.89	32.51	24.73	37.06
FeO	43.28	45.46	44.90	41.93	43.36	44.62	42.25	45.13	43.61	41.68	45.30	43.34	41.37	43.96	46.00	42.36
Total	94.91	94.11	94.52	94.88	95.81	93.61	93.59	93.61	93.51	91.62	93.48	93.58	93.22	94.68	94.82	96.28

Point	69-38	1-39	2-39	4-39	5-39	6-39	8-39	9-39	11-39	13-39	14-39	15-39	16-39	18-39	19-39	21-39
SiO2	3.31	4.04	0.15	0.23	4.86	0.35	0.25	4.53	0.23	0.38	3.24	4.33	0.44	0.42	0.36	0.55
TiO2	18.00	14.20	14.68	14.11	14.81	10.98	14.41	13.94	11.05	12.24	14.82	14.41	12.57	12.42	15.87	12.83
Al2O3	0.49	0.58	1.00	0.96	0.63	1.36	1.05	0.56	1.25	0.97	0.68	0.68	0.68	0.93	1.03	0.93
FeO	66.79	68.46	73.10	71.92	64.68	76.08	73.15	66.80	79.28	75.43	68.31	67.66	75.28	74.53	70.27	71.99
MnO	0.36	0.38	0.80	0.67	0.35	0.83	1.73	0.40	1.01	1.53	0.44	0.28	1.07	1.65	1.56	1.69
MgO	0.00	0.00	0.31	0.00	0.00	0.05	0.06	0.00	0.00	0.01	0.00	0.00	0.00	0.07	0.00	0.00
CaO	2.29	3.08	0.08	0.07	3.40	0.15	0.04	3.27	0.16	0.12	2.37	3.03	0.11	0.21	0.38	0.83
Na2O	0.00	0.07	0.06	0.06	0.00	0.00	0.10	0.00	0.00	0.00	0.00	0.00	0.00	0.00	0.00	0.00
K2O	0.01	0.01	0.01	0.02	0.00	0.00	0.03	0.02	0.03	0.02	0.02	0.03	0.00	0.01	0.07	0.01
Total	91.25	90.82	90.18	88.05	88.72	89.80	90.81	89.53	93.00	90.70	89.88	90.41	90.15	90.24	89.52	88.83
Fe2O3	21.86	27.87	35.16	34.45	22.74	41.21	35.91	26.06	43.93	39.73	27.39	26.08	38.80	39.01	31.45	36.85
FeO	47.12	43.38	41.46	40.92	44.22	38.99	40.83	43.35	39.75	39.68	43.67	44.19	40.37	39.43	41.96	38.83
Total	93.44	93.61	93.70	91.50	91.00	93.93	94.41	92.13	97.40	94.68	92.62	93.02	94.04	94.15	92.67	92.52

B. (continuation)

Point	22-39	23-39	24-39	25-39	26-39	27-39	30-39	31-39	33-39	35-39	36-39	1-43	2-43	3-43	4-43	5-43
SiO2	3.96	0.34	5.00	0.22	4.30	4.17	0.24	7.05	2.23	3.38	0.26	0.35	0.38	0.40	0.61	0.40
TiO2	13.70	16.06	15.32	12.64	15.09	14.94	13.62	9.92	7.69	14.82	14.94	18.26	20.32	20.54	20.47	22.24
Al2O3	0.56	1.09	0.88	0.87	0.36	0.49	0.90	0.59	0.98	0.44	1.01	7.72	0.96	1.23	1.01	0.83
FeO	67.19	71.78	66.26	76.79	65.06	66.79	72.34	67.53	77.59	69.63	72.58	61.54	70.66	69.39	67.04	66.71
MnO	0.46	1.64	0.32	0.71	0.42	0.29	1.91	0.28	0.48	0.20	2.02	0.73	1.52	1.63	1.23	2.35
MgO	0.00	0.16	0.00	0.09	0.00	0.00	0.02	0.00	0.00	0.00	0.00	3.92	0.29	0.37	0.19	0.00
CaO	3.14	0.12	3.46	0.05	2.82	2.87	0.05	5.00	1.87	2.02	0.12	0.01	0.08	0.59	0.59	0.33
Na2O	0.00	0.00	0.00	0.00	0.00	0.09	0.00	0.00	0.00	0.00	0.00	0.00	0.00	0.02	0.36	0.00
K2O	0.00	0.01	0.00	0.00	0.05	0.00	0.00	0.01	0.00	0.00	0.03	0.00	0.03	0.03	0.05	0.05
Total	89.00	91.19	91.25	91.37	88.11	89.64	89.07	90.39	90.84	90.48	90.96	92.53	94.23	94.21	91.55	92.90
Fe2O3	27.54	32.18	22.88	39.90	23.42	25.28	36.06	29.02	44.90	27.69	34.58	22.33	25.77	25.10	24.21	20.85
FeO	42.41	42.82	45.67	40.88	43.99	44.05	39.90	41.42	37.18	44.71	41.47	41.44	47.47	46.80	45.26	47.94
Total	91.76	94.41	93.54	95.36	90.45	92.17	92.69	93.30	95.34	93.26	94.42	94.77	96.81	96.72	93.97	94.98

Point	6-43	7-43	8-43	9-43	10-43	11-43	12-43	13-43	14-43	15-43	16-43	17-43	18-43	19-43	20-43	21-43
SiO2	1.68	0.49	0.41	0.41	0.28	0.36	0.46	0.62	0.36	0.34	0.29	0.38	0.31	0.87	0.34	0.31
TiO2	23.46	22.12	21.03	20.51	22.38	22.75	20.66	20.20	21.65	19.53	22.02	22.30	23.17	22.78	22.92	24.33
Al2O3	0.63	2.13	2.58	2.49	3.31	2.89	3.74	3.75	3.69	5.46	3.14	3.71	1.34	1.06	2.72	0.61
FeO	60.33	68.54	69.16	67.41	65.64	67.31	66.04	65.00	66.11	63.52	65.24	65.85	68.79	65.01	65.86	67.63
MnO	0.65	0.75	0.95	0.97	0.89	0.87	0.85	0.74	0.76	0.72	0.77	0.76	1.01	1.88	1.21	1.72
MgO	0.00	0.07	0.42	1.18	2.14	2.16	2.64	2.57	2.16	2.93	2.51	2.83	0.20	0.00	0.94	0.00
CaO	2.82	0.32	0.30	0.20	0.17	0.05	0.11	0.39	0.12	0.10	0.12	0.12	0.23	1.20	0.25	0.21
Na2O	0.00	0.00	0.00	0.00	0.00	0.00	0.00	0.31	0.00	0.00	0.00	0.00	0.00	0.00	0.01	0.00
K2O	0.06	0.05	0.03	0.04	0.02	0.04	0.01	0.04	0.02	0.01	0.01	0.00	0.02	0.04	0.00	0.00
Total	89.63	94.46	94.87	93.19	94.82	96.43	94.51	93.63	94.87	92.61	94.11	95.94	95.06	92.83	94.24	94.81
Fe2O3	13.45	20.41	22.77	23.17	20.28	21.05	22.90	23.97	21.15	22.09	20.87	20.87	20.13	18.37	18.66	18.30
FeO	48.22	50.17	48.67	46.55	47.40	48.36	45.43	43.43	47.08	43.63	46.46	47.07	50.68	48.48	49.06	51.16
Total	90.97	96.51	97.15	95.51	96.85	98.53	96.80	96.03	96.99	94.82	96.20	98.03	97.07	94.67	96.11	96.65

Point	22-43	23-43	24-43	25-43
SiO2	0.35	0.33	0.37	0.32
TiO2	22.66	21.26	22.48	23.06
Al2O3	0.76	1.00	1.88	1.78
FeO	67.99	68.69	67.03	66.38
MnO	1.40	0.98	0.98	1.30
MgO	0.28	0.16	0.66	1.05
CaO	0.37	0.31	0.13	0.19
Na2O	0.00	0.00	0.00	0.00
K2O	0.06	0.10	0.03	0.01
Total	93.86	92.82	93.55	94.09
Fe2O3	21.07	22.95	19.85	19.51
FeO	49.03	48.04	49.17	48.82
Total	95.97	95.12	95.53	96.04

C. Electron probe microanalysis of magnetite from weathered dolerite sample.
Distances X and Y (along and across the sample respectively) are measured in mm (*).

Point	Distance X	Distance Y	SiO2	TiO2	Al2O3	Fe2O3	FeO	MnO	MgO	CaO	Na2O	K2O	Total
13	18.90	28.20	3.99	16.00	0.58	24.27	45.33	0.35	0.03	2.98	0.00	0.03	93.57
12	19.40	28.30	1.08	22.11	0.43	18.66	50.15	0.32	0.00	0.44	0.00	0.00	93.19
14	19.70	28.70	4.58	16.93	0.56	21.83	46.71	0.36	0.00	3.53	0.00	0.00	94.50
15	18.60	28.70	9.32	17.05	0.71	10.05	47.51	0.26	0.01	7.79	0.00	0.05	92.75
16	18.60	28.70	1.11	20.15	0.65	25.22	48.02	1.20	0.18	0.67	0.04	0.02	97.27
17	17.70	28.70	4.63	15.57	0.69	23.52	44.87	0.40	0.00	3.70	0.00	0.04	93.41
18	17.70	28.70	5.69	11.41	0.75	29.06	41.48	0.30	0.00	4.62	0.00	0.01	93.34
20	22.40	28.90	4.61	15.45	0.68	23.85	45.03	0.43	0.00	3.55	0.00	0.00	93.60
19	23.50	29.30	5.13	17.36	0.61	19.13	46.86	0.33	0.00	4.03	0.00	0.04	93.49
21	22.40	29.30	4.08	16.05	0.77	23.57	46.00	0.32	0.00	2.50	0.00	0.07	93.35
22	22.40	29.20	0.36	15.40	0.84	33.93	42.75	1.44	0.03	0.13	0.00	0.00	94.87
1	15.75	29.90	0.19	18.50	0.86	29.93	46.62	0.92	0.10	0.06	0.00	0.00	97.16
2	15.75	29.90	6.49	14.37	0.79	21.52	44.59	0.17	0.00	5.34	0.00	0.00	93.27
3	15.75	29.90	9.46	20.06	0.95	3.54	49.87	0.17	0.00	8.52	0.00	0.00	92.58
25	19.90	30.15	3.66	14.50	0.43	26.04	42.87	0.31	0.00	2.83	0.00	0.01	90.64
23	23.30	30.20	5.75	9.27	1.28	32.35	39.38	0.19	0.17	3.90	0.15	0.03	92.48
24	23.30	30.20	6.20	15.02	0.74	20.25	44.36	0.30	0.00	5.34	0.00	0.00	92.22
26	17.50	30.25	3.62	15.62	0.61	24.77	44.55	0.34	0.03	2.58	0.00	0.02	92.14
27	16.30	30.30	4.06	16.83	0.56	22.69	45.67	0.24	0.00	3.24	0.06	0.05	93.39
28	14.20	30.30	4.08	9.75	0.77	36.28	39.85	0.24	0.04	3.05	0.00	0.02	94.06
4	30.30	30.30	6.80	9.51	0.75	32.71	41.01	0.26	0.00	5.68	0.00	0.01	96.74
30	24.20	31.00	6.29	17.90	0.80	15.33	47.70	0.27	0.00	5.00	0.05	0.02	93.36
32	18.90	31.40	3.78	16.04	0.53	19.25	43.09	0.37	0.00	2.71	0.00	0.00	85.76
33	18.90	31.40	8.56	11.21	0.65	18.48	40.88	0.30	0.00	6.39	0.00	0.01	86.47
34	16.60	31.50	8.48	9.47	0.61	23.91	39.79	0.27	0.00	6.45	0.00	0.05	89.02
35	12.20	31.50	4.43	19.05	0.42	17.68	48.60	0.32	0.00	3.24	0.00	0.01	93.74
36	6.40	31.50	4.30	17.31	0.40	22.08	46.98	0.33	0.00	3.24	0.00	0.04	94.68
31	20.90	31.50	4.77	15.10	0.70	19.16	43.04	0.28	0.00	3.41	0.00	0.00	86.47
37	21.50	32.45	3.72	17.25	0.60	17.84	44.66	0.32	0.00	2.61	0.00	0.01	87.01
38	20.90	32.45	0.71	14.83	0.69	28.49	40.77	0.71	0.00	0.14	0.00	0.00	86.34
39	17.10	32.45	5.40	16.34	0.75	14.13	43.88	0.24	0.00	3.94	0.00	0.01	84.69
40	15.70	32.45	3.75	13.31	0.91	22.66	40.60	0.82	0.13	1.47	0.00	0.05	83.70
41	15.70	32.45	0.33	15.36	0.93	31.00	41.32	1.34	0.08	0.13	0.00	0.01	90.50
42	11.20	32.50	6.52	17.16	0.63	11.30	44.80	0.17	0.00	5.25	0.04	0.01	85.89
43	11.20	32.50	5.91	19.44	0.62	8.58	45.94	1.21	0.16	4.36	0.00	0.10	86.31
6	14.20	33.35	4.17	16.44	0.60	23.07	46.09	0.31	0.00	3.01	0.00	0.02	93.71
7	14.20	33.35	0.20	16.39	0.97	32.36	43.29	0.55	0.22	0.15	0.12	0.02	94.27
46	14.10	33.80	3.77	16.45	0.45	21.09	44.60	0.32	0.00	2.71	0.00	0.01	89.41
45	23.10	33.90	5.72	15.33	0.70	21.27	45.53	0.22	0.00	4.23	0.00	0.04	93.05
44	23.80	33.90	3.93	16.14	0.57	24.05	45.50	0.28	0.00	2.85	0.00	0.06	93.39
8	13.85	34.40	6.31	16.67	0.65	5.07	41.85	0.21	0.00	4.47	0.00	0.00	75.23
47	24.00	35.30	3.42	15.07	0.57	24.82	43.77	0.27	0.00	2.15	0.00	0.02	90.09
48	19.60	35.30	4.45	15.33	0.63	20.42	43.31	0.31	0.00	3.29	0.00	0.00	87.74
49	19.60	35.30	6.30	10.22	0.59	27.49	39.15	0.61	0.02	5.00	0.00	0.01	89.39
50	19.60	35.30	3.59	15.65	0.59	22.66	41.84	1.78	0.00	2.82	0.00	0.03	88.96
51	19.10	35.40	4.67	15.23	0.81	17.30	42.17	0.30	0.00	3.32	0.00	0.05	83.84

C. (continuation)

Point	Distance X	Distance Y	SiO2	TiO2	Al2O3	Fe2O3	FeO	MnO	MgO	CaO	Na2O	K2O	Total
52	19.10	35.40	0.37	13.17	1.06	31.99	37.34	2.09	0.00	0.15	0.00	0.02	86.19
54	14.70	35.40	4.87	9.71	0.71	19.70	33.84	0.17	0.00	3.42	0.00	0.02	72.44
55	7.30	35.40	4.04	15.21	0.63	24.96	44.44	0.33	0.00	2.95	0.00	0.04	92.58
56	7.30	35.40	4.07	13.36	0.59	28.88	41.27	1.13	0.01	3.71	0.00	0.00	93.02
57	6.50	35.40	5.88	16.22	0.41	19.28	45.93	0.20	0.00	4.71	0.00	0.01	92.64
53	18.60	35.50	6.16	14.79	0.62	17.29	43.06	0.34	0.00	4.80	0.00	0.00	87.05
9	14.20	36.00	4.62	11.72	0.71	19.65	37.01	0.25	0.00	3.25	0.00	0.01	77.21
58	21.40	36.30	6.13	13.91	0.35	22.23	43.60	0.26	0.00	4.36	0.07	0.02	90.92
59	21.40	36.30	0.35	14.79	0.64	33.47	42.07	0.45	0.06	0.23	0.00	0.00	92.06
60	18.60	36.30	4.86	16.21	0.56	19.52	45.20	0.33	0.00	3.42	0.00	0.01	90.11
61	14.40	36.30	4.80	13.49	0.59	13.80	37.84	0.25	0.00	3.34	0.00	0.00	74.10
62	7.90	36.40	5.60	12.28	0.53	27.51	42.27	0.29	0.00	4.36	0.00	0.02	92.85
63	18.10	36.90	5.67	13.80	0.55	20.74	42.54	0.18	0.00	4.18	0.00	0.01	87.67
66	5.70	37.00	4.56	15.12	0.61	24.68	44.89	0.31	0.08	3.33	0.00	0.01	93.59
64	14.00	37.10	4.49	12.89	0.50	10.20	35.13	0.25	0.00	2.72	0.00	0.00	66.18
65	14.00	37.10	8.84	8.10	0.52	11.40	33.13	0.18	0.00	6.10	0.00	0.02	68.29
10	14.20	37.80	1.73	16.53	0.94	25.88	43.83	1.73	0.17	0.17	0.00	0.02	91.00
11	14.20	37.80	6.90	15.73	0.69	16.53	45.80	0.06	0.00	5.36	0.00	0.00	91.07
68	7.60	38.10	4.60	14.86	0.48	25.24	44.53	0.44	0.04	3.43	0.00	0.00	93.62
69	9.60	38.10	2.81	14.30	0.48	29.64	43.21	0.38	0.00	1.93	0.00	0.01	92.77
67	6.30	38.20	4.51	15.07	0.53	24.91	44.77	0.26	0.00	3.45	0.00	0.01	93.50

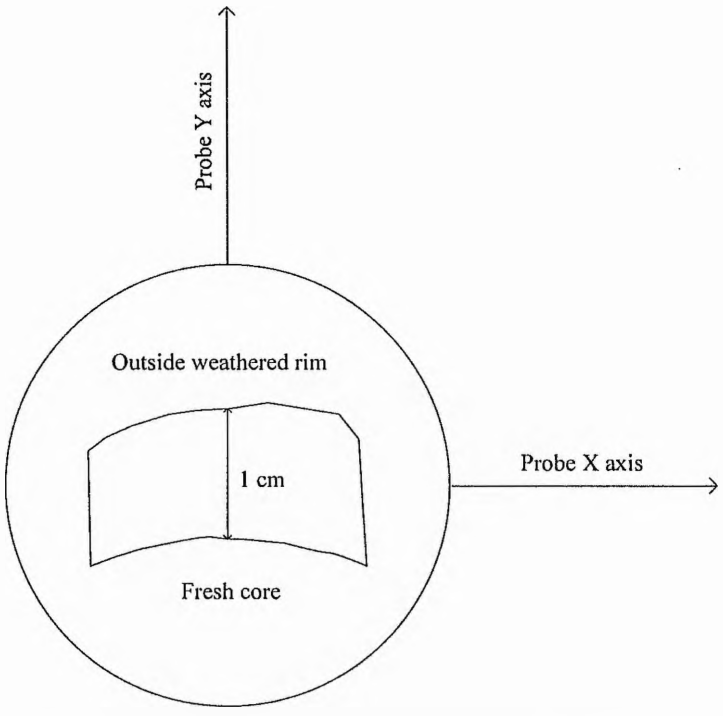

(*) Sketch of a dolerite sample exhibiting spheroidal or onion-skin weathering texture showing its position relative to the reference positional axes of the electron probe.
Increasing weathering of the titanomagnetite mineral grains is detected along Y axis.

D. Electron probe microanalysis of ilmenite from the River Eden catchment igneous rocks.

Point	2-1	6-1	8-1	10-1	12-1	15-1	17-1	18-1	32-1	17-2	20-2	21-2	22-2	23-2	28-2
SiO2	0.37	0.32	0.26	0.35	0.24	0.22	0.25	0.31	0.27	0.04	0.65	0.11	0.06	0.11	0.30
TiO2	48.33	48.70	54.41	49.41	49.14	51.37	49.76	50.62	54.05	47.72	44.77	44.80	46.20	44.34	43.72
Al2O3	0.21	0.10	0.26	0.10	0.00	0.07	0.02	0.05	0.05	0.00	0.16	0.14	0.25	0.21	0.08
FeO	45.40	44.61	37.14	46.99	47.58	46.63	45.04	44.15	51.34	46.87	47.65	48.61	38.85	48.29	46.95
MnO	0.21	0.35	1.07	1.39	2.67	1.31	1.22	1.36	1.07	0.83	0.76	0.68	3.23	0.52	0.71
MgO	0.09	0.66	1.58	2.23	0.00	1.71	1.41	1.79	2.69	1.13	0.09	5.05	5.20	5.06	1.18
CaO	0.09	0.04	0.11	0.04	0.06	0.01	0.10	0.04	0.08	0.03	0.11	0.00	0.01	0.01	0.01
Na2O	0.00	0.00	0.00	0.00	0.00	0.00	0.00	0.00	0.00	0.00	0.00	0.00	0.05	0.00	0.00
K2O	0.01	0.05	0.06	0.03	0.02	0.02	0.01	0.02	0.00	0.03	0.13	0.03	0.03	0.00	0.00
Total	94.70	94.84	94.89	100.53	99.70	101.33	97.81	98.35	109.54	96.65	94.31	99.42	93.87	98.54	92.94
Fe2O3	2.21	2.39	0.00	8.51	6.59	5.13	4.33	3.26	9.33	7.65	8.95	19.96	11.20	19.81	11.21
FeO	43.42	42.46	37.14	39.33	41.65	42.01	41.14	41.22	42.94	39.99	39.60	30.65	28.77	30.47	36.86
Total	94.93	95.08	94.89	101.39	100.36	101.84	98.25	98.68	110.48	97.41	95.20	101.42	94.99	100.52	94.06

Point	17-5	26-5	1-8	3-8	10-8	12-8	14-8	20-8	22-8	23-8	25-8	26-8	27-8	31-8	33-8
SiO2	0.47	0.26	0.05	0.20	0.28	0.30	0.14	0.14	0.28	0.14	0.25	0.21	0.15	0.24	0.10
TiO2	51.48	50.74	49.50	52.10	49.68	49.57	51.61	49.12	47.86	50.14	49.68	50.16	51.24	53.02	50.86
Al2O3	0.05	0.10	0.08	0.00	0.02	0.10	0.03	0.00	0.00	0.04	0.04	0.00	0.08	0.00	0.04
FeO	35.22	37.82	48.77	46.59	47.96	48.87	45.62	47.75	48.24	48.63	49.14	47.69	48.46	46.68	50.27
MnO	5.29	3.63	0.15	0.20	0.17	0.25	0.43	0.18	0.24	0.19	0.26	0.23	0.23	0.21	0.19
MgO	1.89	0.55	0.15	0.02	0.19	0.23	0.30	0.14	0.07	0.15	0.18	0.34	0.10	0.16	0.10
CaO	0.08	0.10	0.03	0.20	0.03	0.04	0.03	0.02	0.07	0.00	0.06	0.10	0.02	0.07	0.00
Na2O	0.00	0.00	0.00	0.00	0.01	0.00	0.00	0.00	0.00	0.00	0.00	0.00	0.02	0.00	0.00
K2O	0.02	0.03	0.00	0.00	0.02	0.01	0.01	0.03	0.04	0.00	0.03	0.03	0.00	0.04	0.02
Total	94.50	93.22	98.71	99.32	98.35	99.36	98.16	97.37	96.79	99.29	99.64	98.76	100.29	100.41	101.57
Fe2O3	0.00	0.00	5.14	0.00	3.99	5.16	0.06	5.12	6.01	4.25	5.45	3.75	3.00	0.00	5.37
FeO	35.22	37.82	44.14	46.59	44.38	44.22	45.57	46.63	42.83	44.81	44.23	44.31	45.76	46.68	45.44
Total	94.50	93.22	99.23	99.32	98.75	99.88	98.17	105.23	97.39	99.71	100.18	99.13	100.59	100.41	102.11

Point	40-8	1-11	2-11	5-11	6-11	7-11	9-11	11-11	12-11	14-11	15-11	2-13	5-13	7-13	12-13
SiO2	0.16	0.45	0.36	0.22	0.19	0.26	6.22	0.11	0.26	0.19	0.52	0.33	0.09	0.36	0.13
TiO2	52.75	49.60	44.50	48.04	51.22	49.01	47.79	50.21	59.29	50.99	51.25	52.09	52.02	51.51	50.82
Al2O3	0.01	0.08	0.03	0.00	0.06	0.00	2.53	0.01	0.11	0.01	0.03	0.00	0.00	0.00	0.00
FeO	51.23	47.61	48.20	50.48	49.30	48.16	34.39	47.39	29.25	48.59	47.65	46.09	46.38	46.53	47.72
MnO	0.26	0.44	0.46	0.31	0.50	0.32	0.00	0.66	0.13	0.39	0.48	0.64	0.82	0.62	0.85
MgO	0.19	0.00	0.04	0.20	0.00	0.01	0.18	0.00	0.06	0.00	0.00	0.54	0.30	0.60	0.08
CaO	0.04	0.02	0.00	0.11	0.05	0.12	0.03	0.12	0.09	0.07	0.05	0.03	0.03	0.13	0.05
Na2O	0.06	0.00	0.00	0.00	0.06	0.00	0.00	0.00	0.00	0.00	0.03	0.00	0.00	0.00	0.04
K2O	0.02	0.26	0.14	0.04	0.05	0.01	1.23	0.05	0.11	0.04	0.10	0.03	0.05	0.03	0.03
Total	104.72	98.45	93.73	99.38	101.41	98.01	92.38	98.54	89.29	100.29	100.10	99.75	99.68	99.77	99.72
Fe2O3	5.12	4.13	9.69	8.82	4.44	4.79	0.00	3.39	0.00	3.43	2.12	0.65	1.17	1.90	3.54
FeO	46.63	43.90	39.48	42.54	45.30	43.85	34.39	44.33	29.25	45.51	45.75	45.51	45.32	44.82	44.53
Total	105.23	98.86	94.71	100.27	101.86	98.37	92.38	98.88	89.29	100.63	100.31	99.81	99.80	99.96	100.07

D. (continuation)

Point	15-13	20-13	21-13	22-13	24-13	26-13	29-13	30-13	32-13	37-13	38-13	74-14	75-14	77-14	80-14
SiO2	0.20	0.16	0.15	0.05	0.45	0.20	0.28	0.15	0.20	0.03	0.11	0.18	0.23	0.31	0.07
TiO2	51.76	52.79	52.71	53.32	52.46	52.37	53.74	53.40	53.31	52.71	52.73	48.30	49.11	50.21	47.04
Al2O3	0.01	0.04	0.00	0.00	0.08	0.01	0.01	0.01	0.06	0.04	0.00	0.11	0.01	0.04	0.09
FeO	46.36	46.36	44.96	45.87	45.82	46.29	47.43	45.96	46.17	46.57	46.23	48.01	45.71	45.38	46.29
MnO	0.72	0.55	0.66	0.93	0.82	0.54	0.79	0.85	0.80	0.68	0.61	1.46	3.30	1.71	1.49
MgO	0.32	1.04	1.13	0.57	0.70	1.01	0.29	0.65	0.47	0.38	0.23	0.81	0.25	0.68	0.82
CaO	0.06	0.03	0.16	0.07	0.13	0.04	0.05	0.05	0.06	0.01	0.04	0.05	0.05	0.10	0.05
Na2O	0.00	0.00	0.01	0.54	0.00	0.14	0.00	0.00	0.00	0.00	0.00	0.00	0.00	0.00	0.00
K2O	0.02	0.01	0.02	0.35	0.04	0.00	0.01	0.02	0.09	0.03	0.00	0.01	0.02	0.03	0.03
Total	99.43	100.99	99.79	101.70	100.50	100.61	102.59	101.10	101.15	100.45	99.94	98.93	98.69	98.45	95.89
Fe2O3	1.09	1.31	0.40	3.87	0.53	2.23	0.20	0.00	0.00	0.66	0.00	8.18	5.76	3.33	7.82
FeO	45.38	45.18	44.60	42.39	45.34	44.28	47.25	45.96	46.17	45.98	46.23	40.65	40.52	42.39	39.26
Total	99.54	101.12	99.83	102.09	100.56	100.83	102.61	101.10	101.15	100.51	99.94	99.75	99.27	98.78	96.67

Point	81-14	83-14	84-14	91-14	94-14	101-14	106-14	107-14	2-15	4-15	8-15	12-15	14-15	16-15	23-15
SiO2	0.34	0.19	2.24	0.48	0.39	0.18	0.29	0.39	0.11	0.29	0.69	0.15	0.05	0.29	0.20
TiO2	33.42	49.29	54.96	43.71	49.20	51.49	50.41	56.42	48.87	49.50	47.88	48.92	49.11	49.99	48.37
Al2O3	0.58	0.06	0.24	0.51	0.17	0.02	0.14	0.11	0.04	0.08	0.13	0.06	0.02	0.03	0.05
FeO	58.32	45.75	37.07	47.54	43.79	40.87	47.27	37.89	45.15	44.96	45.36	45.75	46.57	45.61	46.09
MnO	0.87	1.25	0.19	1.28	0.57	0.42	1.32	1.36	1.15	1.26	1.13	1.08	1.01	1.05	1.08
MgO	0.43	1.28	0.27	0.57	0.61	0.16	0.61	1.18	1.60	2.12	1.70	1.67	1.73	1.81	1.97
CaO	0.05	0.08	0.11	0.02	0.00	0.08	0.03	0.08	0.08	0.17	0.04	0.07	0.03	0.10	0.06
Na2O	0.00	0.00	0.00	0.00	0.00	0.00	0.00	0.00	0.00	0.00	0.00	0.00	0.02	0.00	0.00
K2O	0.02	0.04	0.01	0.01	0.04	0.08	0.00	0.03	0.00	0.03	0.10	0.03	0.06	0.03	0.06
Total	94.03	97.92	95.09	94.12	94.77	93.29	100.07	97.46	96.99	98.39	97.02	97.73	98.59	98.91	97.87
Fe2O3	32.91	5.49	0.00	11.13	0.95	0.00	4.49	0.00	5.74	6.06	6.63	6.47	7.47	5.35	8.00
FeO	28.70	40.81	37.07	37.53	42.94	40.87	43.23	37.89	39.98	39.51	39.39	39.93	39.85	40.79	38.89
Total	97.33	98.47	95.09	95.23	94.86	93.29	100.51	97.46	97.57	99.00	97.68	98.38	99.34	99.45	98.67

Point	28-15	31-15	34-15	57-16	61-16	62-16	64-16	9-18	12-18	14-18	16-18	17-18	18-18	19-18	20-18
SiO2	0.15	0.25	0.22	0.34	2.37	0.76	0.40	0.94	0.68	0.16	0.25	0.29	0.20	0.48	0.20
TiO2	49.04	50.38	47.67	31.27	53.41	50.11	53.55	32.32	35.29	43.99	44.79	49.28	53.11	40.79	51.22
Al2O3	0.00	0.03	0.03	0.63	0.00	0.06	0.13	0.54	0.38	0.11	0.12	0.22	0.11	0.36	0.08
FeO	46.81	43.41	47.97	59.34	36.49	40.46	36.73	53.63	50.88	45.59	44.07	37.24	31.18	39.51	36.21
MnO	1.03	1.06	0.93	0.21	0.58	0.49	1.60	1.07	0.79	4.29	4.07	0.47	5.23	2.43	1.32
MgO	0.82	3.14	1.23	0.52	0.79	0.74	3.07	0.00	0.00	0.87	0.94	0.61	0.55	0.59	0.99
CaO	0.12	0.09	0.01	0.06	0.27	0.15	0.08	0.10	0.52	0.00	0.02	0.05	0.01	0.08	0.04
Na2O	0.02	0.00	0.00	0.00	0.05	0.00	0.00	0.05	0.00	0.04	0.00	0.00	0.01	0.00	0.00
K2O	0.02	0.04	0.00	0.02	0.02	0.05	0.05	0.28	0.05	0.01	0.02	0.04	0.09	0.12	0.02
Total	98.01	98.39	98.06	92.38	93.97	92.81	95.61	88.93	88.59	95.07	94.27	88.20	90.48	84.35	90.09
Fe2O3	5.94	5.23	8.87	35.64	0.00	0.00	0.00	28.59	22.17	13.27	10.42	0.00	0.00	6.91	0.00
FeO	41.47	38.71	39.99	27.27	36.49	40.46	36.73	27.90	30.93	33.64	34.69	37.24	31.18	33.29	36.21
Total	98.61	98.91	98.94	95.94	93.97	92.81	95.61	91.80	90.81	96.40	95.32	88.20	90.48	85.04	90.09

D. (continuation)

Point	52-18	55-18	58-18	61-18	5-19	8-19	26-19	30-19	36-19	38-19	1-21	2-21	5-21	6-21	7-21
SiO2	0.16	0.49	0.38	0.18	0.15	0.38	0.47	0.17	0.31	0.23	0.13	0.24	0.29	0.16	0.17
TiO2	49.89	44.27	36.67	52.85	47.55	50.39	53.14	50.67	49.05	44.13	51.12	49.87	51.10	50.77	50.58
Al2O3	0.28	0.34	0.38	0.40	0.06	0.14	0.28	0.10	0.04	0.15	0.13	0.02	0.02	0.02	0.01
FeO	37.81	34.42	49.18	32.65	38.70	38.33	33.77	36.05	41.19	43.92	46.68	47.36	46.43	46.89	46.48
MnO	0.95	4.13	3.11	0.65	3.47	0.07	0.80	3.66	1.32	1.42	0.93	0.64	0.86	0.68	0.65
MgO	1.94	0.46	0.66	2.34	0.83	0.70	1.56	0.62	0.51	0.37	0.45	0.29	0.32	0.23	0.34
CaO	0.03	0.12	0.01	0.05	0.09	0.08	0.11	0.07	0.09	0.01	0.00	0.04	0.08	0.04	0.10
Na2O	0.00	0.10	0.00	0.06	0.00	0.00	0.00	0.00	0.00	0.00	0.00	0.00	0.00	0.00	0.00
K2O	0.03	0.09	0.05	0.04	0.02	0.03	0.06	0.01	0.01	0.00	0.00	0.00	0.01	0.00	0.03
Total	91.08	84.42	90.44	89.23	90.86	90.13	90.19	91.35	92.51	90.23	99.44	98.46	99.09	98.79	98.36
Fe2O3	0.00	0.00	22.48	0.00	1.01	0.00	0.00	0.00	0.00	6.73	2.56	3.81	1.86	2.43	2.52
FeO	37.81	34.42	28.96	32.65	37.79	38.33	33.77	36.05	41.19	37.87	44.38	43.94	44.75	44.70	44.21
Total	91.08	84.42	92.69	89.23	90.96	90.13	90.19	91.35	92.51	90.90	99.69	98.84	99.28	99.03	98.61

Point	8-21	21-21	25-21	26-21	27-21	31-21	32-21	35-21	36-21	38-21	2-22	6-22	8-22	13-22	15-22
SiO2	0.20	0.27	0.11	0.11	0.19	0.03	0.24	0.17	0.16	0.19	0.18	0.17	0.10	0.23	0.29
TiO2	50.76	50.99	52.29	52.04	53.19	51.85	51.15	52.48	50.67	48.12	47.34	46.82	50.99	51.79	47.25
Al2O3	0.02	0.00	0.02	0.00	0.05	0.00	0.06	0.05	0.07	0.04	0.00	0.02	0.00	0.02	0.04
FeO	46.60	45.97	46.37	46.02	46.00	46.76	46.07	46.36	46.20	48.42	47.67	45.55	46.30	47.69	47.55
MnO	0.65	0.72	0.68	0.84	0.83	0.68	0.67	0.74	0.62	1.20	0.71	0.61	0.76	0.58	0.58
MgO	0.70	0.51	0.77	0.72	1.06	0.55	0.56	0.79	0.97	0.22	0.52	0.99	0.74	0.23	0.71
CaO	0.07	0.03	0.11	0.05	0.02	0.03	0.15	0.03	0.15	0.11	0.02	0.05	0.07	0.00	0.03
Na2O	0.00	0.00	0.00	0.00	0.00	0.15	0.00	0.00	0.00	0.00	0.08	0.00	0.08	0.00	0.00
K2O	0.02	0.05	0.02	0.04	0.00	0.00	0.01	0.01	0.02	0.02	0.03	0.00	0.00	0.01	0.04
Total	99.02	98.54	100.36	99.82	101.52	100.05	98.91	100.62	98.85	98.32	96.55	94.21	99.04	100.56	96.49
Fe2O3	3.06	1.80	1.62	1.54	0.76	2.77	1.85	1.31	3.37	7.47	7.79	6.31	3.18	2.08	7.46
FeO	43.84	44.35	44.91	44.63	45.32	44.27	44.41	45.17	43.16	41.69	40.66	39.87	43.44	45.83	40.84
Total	99.33	98.72	100.52	99.97	101.41	100.33	99.10	100.75	99.18	99.07	97.33	94.85	99.35	100.77	97.24

Point	16-22	20-22	24-22	13-22	9-29	16-29	18-29	20-29	22-29	25-29	28-29	32-29	33-29	7-30	9-30
SiO2	0.17	0.24	0.09	0.23	0.71	1.80	0.11	0.33	0.12	0.17	0.24	0.21	0.17	0.21	0.06
TiO2	49.18	52.57	42.21	51.79	40.20	28.87	49.99	49.31	49.50	48.33	48.30	48.47	47.67	49.99	52.32
Al2O3	0.03	0.01	0.07	0.02	0.38	0.68	0.08	0.07	0.02	0.00	0.03	0.05	0.07	0.01	0.11
FeO	45.96	46.66	47.20	47.69	52.84	58.81	44.25	44.79	44.94	44.96	46.19	45.99	46.47	44.24	36.74
MnO	0.70	0.56	0.59	0.58	1.17	1.55	0.87	0.85	0.84	0.81	0.69	0.96	0.76	0.83	1.06
MgO	1.13	0.02	0.66	0.23	0.79	0.92	1.70	0.80	2.09	1.41	0.94	0.84	1.23	1.30	1.37
CaO	0.04	0.07	0.03	0.00	0.10	0.12	0.21	0.18	0.10	0.09	0.08	0.11	0.18	0.06	0.07
Na2O	0.00	0.00	0.00	0.00	0.00	0.00	0.00	0.14	0.00	0.11	0.00	0.00	0.06	0.00	0.06
K2O	0.00	0.00	0.01	0.01	0.00	0.01	0.01	0.00	0.01	0.03	0.01	0.05	0.02	0.06	0.03
Total	97.19	100.12	90.86	100.56	96.17	92.76	97.22	96.47	97.61	95.92	96.47	96.68	96.62	96.69	91.81
Fe2O3	4.77	0.00	12.17	2.08	20.60	37.88	3.73	3.59	5.55	5.94	5.49	5.45	7.67	2.68	0.00
FeO	41.66	46.66	36.25	45.83	34.30	24.72	40.90	41.56	39.94	39.61	41.25	41.08	39.56	41.83	36.74
Total	97.67	100.12	92.08	100.77	98.24	96.55	97.59	96.83	98.16	96.51	97.02	97.22	97.39	96.96	91.81

D. (continuation)

Point	11-30	19-30	22-30	30-30	31-30	37-32	39-32	45-32	48-32	50-32	50-33	2-34	6-34	7-34	11-34	13-34
SiO2	0.69	0.16	0.16	0.33	0.18	2.85	2.72	0.20	0.18	0.13	0.23	0.71	1.27	0.33	0.27	1.74
TiO2	49.58	49.72	47.99	54.34	51.98	58.59	38.83	39.61	43.01	37.94	35.56	31.64	34.28	53.20	39.81	38.12
Al2O3	0.18	0.14	0.00	0.12	0.05	1.13	1.70	3.23	2.52	4.02	1.03	3.88	2.30	0.17	1.59	3.95
FeO	37.80	37.80	39.45	31.45	36.79	28.62	44.84	45.92	43.32	47.48	51.44	54.65	49.33	35.10	45.10	44.41
MnO	1.11	0.76	1.51	1.09	0.48	1.35	2.18	0.10	0.26	0.15	0.42	0.07	0.24	2.15	0.21	0.15
MgO	0.04	1.95	1.12	0.62	1.33	0.00	0.10	2.75	3.95	2.29	2.85	1.29	3.66	2.47	3.68	2.92
CaO	0.11	0.05	0.63	0.33	0.04	0.26	0.22	0.04	0.02	0.05	0.04	0.07	0.02	0.05	0.02	0.08
Na2O	0.00	0.00	0.00	0.00	0.00	0.00	0.00	0.01	0.00	0.00	0.00	0.00	0.00	0.00	0.00	0.00
K2O	0.05	0.03	0.01	0.04	0.01	0.17	0.28	0.02	0.04	0.04	0.03	0.02	0.24	0.02	0.07	0.13
Total	89.54	90.62	90.87	88.32	90.86	92.96	90.86	91.88	93.28	92.08	91.61	92.34	91.34	93.49	90.75	91.50
Fe2O3	0.00	0.00	0.50	0.00	0.00	0.00	11.29	16.89	13.17	19.55	27.60	30.99	27.25	0.00	17.76	15.42
FeO	37.80	37.80	38.99	31.45	36.79	28.62	34.68	30.72	31.47	29.88	26.61	26.76	24.81	35.10	29.11	30.53
Total	89.54	90.62	90.92	88.32	90.86	92.96	91.99	93.57	94.60	94.04	94.37	95.44	94.07	93.49	92.53	93.05

Point	20-34	22-34	24-34	27-34	31-34	34-34	37-38	42-38	45-38	53-38	56-38	59-38	60-38	63-38	3-39	7-39
SiO2	3.16	0.16	0.20	0.26	0.31	0.31	0.30	0.21	0.18	0.19	0.33	0.10	0.13	0.24	0.04	0.08
TiO2	38.28	37.36	38.86	42.83	37.73	36.48	49.71	49.52	49.76	49.34	49.87	48.68	49.82	49.35	45.54	44.19
Al2O3	2.25	4.33	3.59	2.72	3.60	1.66	0.09	0.00	0.04	0.04	0.07	0.08	0.10	0.00	0.00	0.05
FeO	43.72	46.18	45.44	41.15	43.70	48.93	47.22	47.75	48.16	47.99	49.00	48.43	47.59	47.55	48.48	47.99
MnO	0.21	0.00	0.05	0.20	0.11	0.19	0.55	0.44	0.48	0.51	0.41	0.45	0.58	0.48	0.53	0.47
MgO	3.66	2.65	2.66	4.39	3.57	2.33	0.64	0.17	0.44	0.50	0.41	0.23	0.60	0.34	0.45	0.22
CaO	0.02	0.03	0.03	0.01	0.07	0.05	0.08	0.01	0.00	0.00	0.03	0.05	0.08	0.10	0.02	0.07
Na2O	0.32	0.00	0.00	0.07	0.00	0.00	0.00	0.00	0.00	0.00	0.00	0.00	0.00	0.00	0.00	0.00
K2O	0.22	0.00	0.00	0.00	0.03	0.04	0.01	0.00	0.00	0.00	0.00	0.00	0.00	0.00	0.00	0.03
Total	91.83	90.70	90.82	91.63	89.13	89.97	98.59	98.10	99.06	98.57	100.11	98.02	98.89	98.06	95.06	93.09
Fe2O3	16.04	19.05	16.75	11.88	17.84	22.50	4.42	4.13	4.95	5.34	5.47	6.08	4.87	4.55	9.80	10.21
FeO	29.29	29.04	30.36	30.46	27.64	28.68	43.24	44.04	43.71	43.18	44.08	42.96	43.21	43.46	39.66	38.80
Total	93.43	92.61	92.50	92.81	90.92	92.22	99.03	98.51	99.56	99.11	100.66	98.63	99.38	98.51	96.04	94.12

Point	12-39	17-39	28-39	29-39	32-39	34-39
SiO2	0.14	0.06	0.09	0.15	0.11	0.19
TiO2	44.03	44.46	44.43	43.92	44.81	42.24
Al2O3	0.02	0.11	0.01	0.05	0.01	0.00
FeO	47.84	48.15	47.64	48.92	48.07	46.39
MnO	0.50	0.50	0.66	0.31	0.63	0.57
MgO	0.50	0.37	0.08	0.20	0.43	0.44
CaO	0.01	0.04	0.01	0.00	0.05	0.04
Na2O	0.00	0.00	0.00	0.00	0.00	0.00
K2O	0.00	0.00	0.06	0.00	0.01	0.03
Total	93.05	93.68	92.98	93.55	94.13	89.89
Fe2O3	10.52	10.34	9.53	11.00	10.15	10.74
FeO	38.37	38.84	39.07	39.02	38.94	36.72
Total	94.10	94.71	93.93	94.65	95.14	90.96

E. Magnetic properties of rocks from the River Eden catchment.

Sample	wt (g)	X_{lf}(-8) (m^3/kg)	X_{hf}(-8) (m^3/kg)	X_{fd} %	Xarm(-5) (m^3/kg)	IRM_{20}(-5) (Am^2/Kg)	IRM_{40}(-5) (Am^2/Kg)	IRM_{100}(-5) (Am^2/Kg)	IRM_{300}(-5) (Am^2/Kg)	IRM_{500}(-5) (Am^2/Kg)	SIRM(-5) (Am^2/Kg)	IRM_{-20}(-5) (Am^2/Kg)	IRM_{-40}(-5) (Am^2/Kg)	IRM_{-100}(-5) (Am^2/Kg)	IRM_{-300}(-5) (Am^2/Kg)	IRM_{-1000}(-5) (Am^2/Kg)
em1	32.34	952.94	946.45	0.68	1.89	1464.29	6134.53	15923.44	19440.88	19475.48	19539.24	9570.06	-1571.43	-15550.76	-19162.42	-19692.09
em2	31.27	350.85	349.57	0.36	1.01	402.71	1679.74	6299.99	8894.33	9108.81	9395.93	6549.62	2868.12	-4667.19	-8507.57	-9374.05
em3	31.36	277.60	275.87	0.62	0.85	372.56	1350.71	2729.73	3120.09	3231.06	3472.42	1650.27	-253.45	-2224.42	-2817.90	-3426.38
em4	32.42	475.58	473.18	0.51	1.34	489.98	1721.45	3878.16	4672.63	4830.03	5163.66	2783.30	282.65	-3037.01	-4218.96	-5120.06
em5	32.11	533.49	531.16	0.44	1.27	588.32	1824.98	3432.33	3813.17	3958.93	4231.41	1715.25	-551.23	-2821.75	-3361.54	-4180.39
em8	33.97	481.57	480.40	0.24	1.54	1195.23	5340.33	10887.71	11392.51	11453.81	11459.08	5052.63	-2787.93	-10694.57	-11350.14	-11463.99
em11	34.87	1769.82	1756.05	0.78	5.42	5606.84	23907.95	39256.40	40118.65	40361.31	40411.29	11782.84	-18384.03	-39350.72	-39926.32	-40335.49
em12	22.24	0.15	0.14	6.06	0.01	0.48	0.93	2.05	2.81	3.04	3.19	2.27	1.11	-0.76	-2.16	-2.86
em13	32.82	959.14	954.36	0.50	1.69	1490.91	5891.35	14239.94	16613.86	16709.81	16790.32	7748.14	-1751.85	-12975.14	-15942.31	-16128.71
em14	32.61	1467.26	1460.36	0.47	2.18	2200.10	9488.04	22681.80	26117.99	26145.11	26233.52	11237.34	-2855.71	-21186.75	-25391.17	-25430.30
em15	32.53	903.31	898.08	0.58	1.61	1669.08	6156.50	13829.16	16342.63	16580.69	16649.01	7305.50	-2466.09	-13181.65	-15966.95	-16757.34
em16	32.12	169.13	166.60	1.49	0.76	145.30	879.28	5019.08	8231.34	8552.64	8770.06	7085.51	-4205.51	-3164.19	-8120.85	-8768.19
em17	34.29	2170.90	2164.19	0.31	4.73	4301.62	10328.45	19427.72	22320.32	22386.01	22542.19	5406.29	-5482.06	-17260.47	-21587.63	-21613.80
em18	27.93	6.75	6.56	2.76	0.02	5.19	17.78	97.67	164.21	220.74	340.90	312.47	256.07	137.91	9.93	-308.48
em19	27.74	5.20	5.07	2.56	0.02	2.72	10.42	47.94	111.80	163.12	315.60	295.30	262.35	189.70	101.70	-262.93
em20	30.45	2.75	2.64	3.94	0.01	2.03	4.88	9.51	30.56	54.17	113.66	109.22	103.78	91.57	56.99	-87.44
em21	32.56	1930.71	1925.79	0.25	1.84	2814.30	5146.03	6772.78	6802.72	6817.96	6846.78	-1595.13	-4910.96	-6765.38	-6803.33	-6832.23
em22	35.04	375.09	373.84	0.33	2.45	3623.81	6755.96	8903.37	9192.53	9223.70	9226.79	-845.04	-5567.46	-8317.50	-8852.27	-8918.76
em30	30.62	354.34	352.42	0.54	0.89	508.31	1685.48	3925.39	4735.94	4802.85	4915.72	2303.42	-54.38	-3277.89	-4463.00	-4705.79
em31	29.69	436.57	426.73	2.25	2.03	765.30	2231.13	3785.22	4146.76	4206.63	4322.86	1384.89	-1230.24	-3253.12	-3859.26	-4123.89
em34	28.77	74.40	72.98	1.92	1.08	180.40	745.01	2179.39	2663.98	2987.00	3294.64	2590.25	1402.49	-1042.32	-2100.27	-3349.83
em36	31.39	8.62	8.47	1.74	0.13	6.17	20.06	123.18	726.58	1184.55	1474.53	1440.89	1389.82	1191.17	165.52	-1464.95
em38	35.20	3144.50	3120.35	0.77	7.42	5907.28	32527.96	74041.34	76913.60	76928.29	77071.11	34888.18	-16931.19	-73771.15	-77351.47	-77420.36
em41	32.60	-0.20	-0.21	5.01	0.00	0.13	0.13	0.24	0.32	0.33	0.33	0.30	0.23	0.05	-0.11	-0.14
em42	27.53	0.12	0.11	8.33	0.01	0.52	1.33	3.28	4.28	4.70	5.14	3.38	1.80	-1.46	-3.57	-4.89
em43	36.29	1331.13	1313.49	1.33	4.16	3206.80	13193.69	29262.39	31370.37	31380.13	31607.69	14135.44	-5458.39	-28145.98	-31345.02	-31561.58
Weathered dolerite sample																
em23	9.76	606.27	599.92	1.05	2.74	1494.69	6754.50	13535.49	14366.28	14373.68	14395.42	6709.40	-3087.58	-12510.90	-13842.74	-13875.11
em28(1)	7.00	789.92	780.09	1.24	2.91	1471.66	10143.87	24935.46	28304.91	28329.14	28356.99	16332.16	-879.39	-22504.97	-27485.48	-27523.45
em28(2)	8.33	803.46	794.72	1.09	2.77	1468.60	10103.99	24966.18	27983.00	28079.95	28149.70	16008.54	-538.73	-22529.78	-27101.85	-27135.76
em28(3)	7.10	795.13	786.08	1.14	2.77	1489.32	10280.72	24928.28	28105.91	28150.24	28274.25	15833.38	-1911.66	-22867.06	-27177.77	-27338.85

E. (continuation)

Sample	$HIRM_{20}(-5)$ (Am^2/Kg)	$HIRM_{40}(-5)$ (Am^2/Kg)	$HIRM_{100}(-5)$ (Am^2/Kg)	$HIRM_{300}(-5)$ (Am^2/Kg)	$HIRM_{500}(-5)$ (Am^2/Kg)	$HIRM_{-20}(-5)$ (Am^2/Kg)	$HIRM_{-40}(-5)$ (Am^2/Kg)	$HIRM_{-100}(-5)$ (Am^2/Kg)	$HIRM_{-300}(-5)$ (Am^2/Kg)	$(Bo)_{cr}$ (mT)	Rev.Sat. (mT)
em1	18074.95	13404.71	3615.80	98.36	63.76	9969.18	21110.67	35089.99	38701.65	-37	-380
em2	8993.22	7716.19	3095.94	501.60	287.12	2846.31	6527.81	14063.12	17903.50	-60	-1000
em3	3099.86	2121.71	742.69	352.33	241.36	1822.15	3725.87	5696.84	6290.32	-38	-1000
em4	4673.68	3442.21	1285.51	491.03	333.64	2380.36	4881.01	8200.67	9382.62	-41	-1000
em5	3643.08	2406.43	799.07	418.24	272.48	2516.15	4782.63	7053.16	7592.94	-34	-1000
em8	10263.85	6118.75	571.36	66.57	5.26	6406.44	14247.01	22153.64	22809.21	-31	-1000
em11	34804.46	16503.34	1154.90	292.65	49.99	28628.46	58795.32	79762.02	80337.62	-27	-100
em12	2.72	2.27	1.14	0.38	0.15	0.93	2.09	3.95	5.35	-71	-1000
em13	15299.41	10898.96	2550.37	176.45	80.50	9042.18	18542.17	29765.46	32732.62	-37	-1000
em14	24033.42	16745.48	3551.72	115.52	88.41	14996.18	29089.23	47420.27	51624.69	-37	-1000
em15	14979.93	10492.52	2819.86	306.38	68.32	9343.51	19115.10	29830.66	32615.96	-34	-560
em16	8624.76	7890.79	3750.99	538.72	217.42	1684.56	12975.57	11934.26	16890.91	-30	-1000
em17	18240.57	12213.74	3114.47	221.87	156.18	17135.89	28024.25	39802.66	44129.81	-29	-1000
em18	335.71	323.12	243.23	176.69	120.15	28.43	84.83	202.98	330.97	-310	-1000
em19	312.89	305.18	267.67	203.80	152.48	20.30	53.25	125.90	213.91	-500	-1000
em20	111.62	108.78	104.14	83.10	59.48	4.43	9.87	22.09	56.67	-600	-1000
em21	4032.49	1700.75	74.00	44.06	28.83	8441.91	11757.75	13612.16	13650.11	-16	-1000
em22	5602.98	2470.83	323.42	34.26	3.09	10071.83	14794.25	17544.29	18079.06	-18	-1000
em30	4407.42	3230.24	990.33	179.78	112.87	2612.31	4970.10	8193.61	9378.72	-40	-1000
em31	3557.56	2091.73	537.64	176.09	116.22	2937.97	5553.10	7575.97	8182.11	-30	-1000
em34	3114.24	2549.64	1115.26	630.66	307.64	704.39	1892.15	4336.97	5394.92	-70	-900
em36	1468.36	1454.46	1351.35	747.95	289.97	33.64	84.70	283.36	1309.00	-350	-1000
em38	71163.83	44543.16	3029.77	157.51	142.82	42182.94	94002.30	150842.26	154422.58	-32	-300
em41	0.20	0.19	0.09	0.01	0.00	0.02	0.10	0.28	0.44	-130	-1000
em42	4.62	3.81	1.86	0.86	0.44	1.76	3.34	6.60	8.71	-70	-1000
em43	28400.89	18413.99	2345.29	237.32	227.56	17472.24	37066.08	59753.67	62952.71	-32	-800
Weathered dolerite sample.											
em23	12900.73	7640.92	859.93	29.14	21.75	7686.02	17483.00	26906.32	28238.16	-32	-1000
em28(1)	26885.33	18213.12	3421.53	52.08	27.85	12024.83	29236.38	50861.96	55842.47	-38	-1000
em28(2)	26681.10	18045.71	3183.52	166.70	69.75	12141.16	28688.43	50679.48	55251.55	-39	-1000
em28(3)	26784.94	17993.54	3345.97	168.34	124.01	12440.88	30185.91	51141.31	55452.03	-36	-1000

F. Electron probe microanalysis of magnetite from the Till BB1 sample.

Point	2-1	4-1	5-1	6-1	7-1	8-1	10-1	11-1	12-1	13-1	14-1	15-1	16-1	17-1	18-1	19-1
SiO2	0.59	3.53	1.00	3.47	0.40	3.45	13.96	0.20	2.16	2.89	3.02	3.57	0.33	1.73	0.12	0.40
TiO2	15.62	15.56	22.72	28.03	14.60	28.56	21.49	0.38	21.81	12.62	11.88	18.98	11.47	17.11	0.01	0.17
Al2O3	2.55	1.15	0.99	0.77	1.14	0.47	1.29	0.16	1.03	1.63	1.17	1.20	1.27	0.98	0.33	0.18
FeO	70.47	70.69	65.45	58.62	76.22	57.65	42.67	92.25	66.13	70.38	72.78	62.05	78.24	69.17	90.52	91.54
MnO	3.51	0.60	1.37	0.47	0.43	1.56	2.03	0.20	1.42	0.35	0.73	0.83	0.96	0.49	0.00	0.05
MgO	0.04	0.11	0.09	0.30	0.17	0.00	0.40	0.00	0.35	0.90	0.92	0.95	0.21	0.27	0.12	0.00
CaO	0.04	2.34	0.57	0.78	0.24	4.12	11.36	0.00	0.14	0.22	0.21	0.36	0.26	0.17	0.10	0.04
Na2O	0.00	0.00	0.00	0.00	0.00	0.00	0.00	0.00	0.00	0.00	0.00	0.00	0.00	0.00	0.00	0.00
K2O	0.00	0.00	0.00	0.00	0.00	0.00	0.00	0.00	0.00	0.00	0.00	0.00	0.00	0.00	0.00	0.00
Total	92.81	93.98	92.19	92.44	93.20	95.82	93.20	93.19	93.04	88.99	90.71	87.96	92.73	89.92	91.20	92.38
Fe2O3	31.74	27.60	17.61	1.00	36.48	3.38	0.00	67.55	17.23	31.01	34.09	15.96	42.67	25.75	66.94	66.86
FeO	41.91	45.86	49.60	57.72	43.39	54.62	42.67	31.46	50.63	42.48	42.10	47.70	39.84	46.00	30.28	31.38
Total	95.99	96.74	93.95	92.54	96.85	96.16	93.20	99.96	94.77	92.09	94.12	89.56	97.01	92.50	97.90	99.08

Point	22-1	23-1	25-1	26-1	27-1	28-1	29-1	30-1	31-1	32-1	33-1	34-1
SiO2	5.84	0.34	0.87	0.36	0.50	0.26	3.25	4.51	0.59	0.22	6.71	0.32
TiO2	7.40	1.06	19.32	7.31	17.67	0.15	11.91	11.14	29.87	0.04	19.54	14.27
Al2O3	4.71	0.60	1.53	1.39	0.84	0.07	2.79	1.16	0.38	0.01	1.28	2.41
FeO	64.08	89.50	68.09	83.14	72.23	92.64	71.15	70.53	60.37	92.99	59.70	75.04
MnO	1.24	0.05	0.50	0.42	1.28	0.01	0.58	1.04	1.47	0.00	0.22	0.43
MgO	0.87	0.08	0.00	0.14	0.16	0.00	0.26	0.17	0.35	0.00	0.00	0.00
CaO	0.26	0.00	0.19	0.01	0.08	0.00	0.13	3.02	0.49	0.07	5.31	0.16
Na2O	0.00	0.00	0.00	0.00	0.00	0.00	0.00	0.00	0.00	0.00	0.00	0.00
K2O	0.00	0.00	0.00	0.00	0.00	0.00	0.00	0.00	0.00	0.00	0.00	0.00
Total	84.39	91.63	90.49	92.75	92.75	93.12	90.06	91.56	93.53	93.34	92.77	92.62
Fe2O3	27.12	64.11	22.92	51.00	29.88	67.95	30.52	32.70	5.70	68.51	10.83	35.22
FeO	39.67	31.80	47.46	37.25	45.34	31.50	43.69	41.11	55.24	31.34	49.95	43.34
Total	87.11	98.05	92.79	97.86	95.75	99.93	93.12	94.84	94.10	100.20	93.85	96.15

G. Electron probe microanalysis of ilmenite from the Till BB1 sample.

Point	1-1	3-1	9-1	20-1	21-1	24-1
SiO2	0.49	0.19	1.23	1.53	0.25	5.90
TiO2	43.27	50.76	41.43	49.20	48.47	43.97
Al2O3	0.25	0.06	0.38	0.21	0.04	2.74
FeO	48.57	47.26	50.98	42.95	44.81	40.09
MnO	2.35	0.80	1.11	2.52	0.38	1.28
MgO	0.91	0.97	1.07	0.41	1.21	1.12
CaO	0.33	0.04	0.87	1.07	0.13	0.67
Na2O	0.00	0.00	0.00	0.00	0.00	0.00
K2O	0.00	0.00	0.00	0.00	0.00	0.00
Total	96.17	100.08	97.06	97.90	95.29	95.76
Fe2O3	15.00	4.41	18.21	1.70	4.03	0.00
FeO	35.08	43.30	34.59	41.43	41.18	40.09
Total	97.67	100.52	98.88	98.06	95.69	95.76

H. Magnetic propeties of till samples from the River Eden catchment.

Sample	wt (g)	X_{lf}(-8) (m^3/kg)	X_{hf}(-8) (m^3/kg)	X_{fd} %	Xarm(-5) (m^3/kg)	IRM_{20}(-5) (Am^2/Kg)	IRM_{40}(-5) (Am^2/Kg)	IRM_{100}(-5) (Am^2/Kg)	IRM_{300}(-5) (Am^2/Kg)	IRM_{500}(-5) (Am^2/Kg)	SIRM(-5) (Am^2/Kg)	IRM_{-20}(-5) (Am^2/Kg)	IRM_{-40}(-5) (Am^2/Kg)
Till BB1(Bulk)	12.28	95.30	92.86	2.56	0.53	171.16	574.98	1471.38	2033.36	2136.04	2143.46	1275.94	537.25
(-1)-0 Φ	9.16	221.52	216.06	2.46	1.01	456.86	1511.89	3250.22	4761.68	4850.17	5044.63	3180.05	1287.87
0-1 Φ	9.86	129.87	126.83	2.34	0.64	233.86	796.72	1758.62	2625.10	2744.83	2879.67	1844.36	810.63
1-2 Φ	10.03	83.79	82.79	1.19	0.44	150.12	519.91	1157.41	1712.62	1816.76	1912.12	1195.31	589.16
2-3 Φ	10.88	66.19	66.19	0.00	0.38	116.65	410.74	885.26	1303.27	1343.81	1458.82	901.45	394.62
>3 Φ	8.28	89.40	88.20	1.35	0.54	149.55	524.26	1138.81	1682.37	1758.37	1876.65	1171.70	518.67
Till BB4(Bulk)	8.25	94.55	92.12	2.56	0.60	196.17	635.27	1478.35	1799.66	1893.13	1917.04	989.04	197.82
(-1)-0 Φ	6.99	151.75	147.46	2.83	1.09	323.56	1193.73	2803.34	3463.82	3535.45	3656.84	1969.13	517.72
0-1 Φ	6.95	96.35	93.47	2.99	0.68	201.19	664.67	1526.80	1867.52	1903.09	2027.41	916.09	183.59
1-2 Φ	8.02	79.83	78.58	1.56	0.53	161.82	561.88	1313.96	1572.55	1618.42	1625.32	853.49	180.95
2-3 Φ	7.44	65.86	64.52	2.04	0.45	133.71	429.95	1012.37	1257.96	1305.59	1335.08	681.05	183.00
>3 Φ	8.07	66.91	65.67	1.85	0.43	133.47	402.71	929.61	1152.55	1210.73	1235.35	624.32	175.65
Till RS7 (1)	12.11	101.84	100.50	1.31	0.65	230.16	808.26	1707.81	2168.05	2232.10	2270.18	1209.05	188.25
Till RS7 (2)	11.06	105.78	104.72	1.00	0.68	265.81	901.88	1894.80	2402.56	2466.63	2511.13	1414.29	198.27

Sample	IRM_{-100}(-5) (Am^2/Kg)	IRM_{-300}(-5) (Am^2/Kg)	IRM_{-1000}(-5) (Am^2/Kg)	$HIRM_{20}$(-5) (Am^2/Kg)	$HIRM_{40}$(-5) (Am^2/Kg)	$HIRM_{100}$(-5) (Am^2/Kg)	$HIRM_{300}$(-5) (Am^2/Kg)	$HIRM_{500}$(-5) (Am^2/Kg)	$HIRM_{-20}$(-5) (Am^2/Kg)	$HIRM_{-40}$(-5) (Am^2/Kg)	$HIRM_{-100}$(-5) (Am^2/Kg)	$HIRM_{-300}$(-5) (Am^2/Kg)	$(Bo)_{cr}$ (mT)	Rev.Sa (mT)
Till BB1(Bulk)	-765.09	-1691.97	-1963.45	1972.31	1568.49	672.09	110.11	7.42	867.52	1606.21	2908.55	3835.43	-50	-1000
(-1)-0 Φ	-2117.39	-5295.03	-5921.17	4587.77	3532.74	1794.41	282.96	194.46	1864.58	3756.77	7162.03	10339.67	-58	-280
0-1 Φ	-1075.78	-2869.24	-3049.10	2645.81	2082.94	1121.04	254.57	134.84	1035.31	2069.03	3955.45	5748.90	-52	-300
1-2 Φ	-687.77	-1874.43	-2034.79	1762.00	1392.21	754.71	199.50	95.36	716.81	1322.96	2599.89	3786.55	-64	-310
2-3 Φ	-557.90	-1402.91	-1515.90	1342.17	1048.08	573.55	155.54	115.00	557.36	1064.19	2016.71	2861.73	-50	-320
>3 Φ	-705.32	-1770.19	-1977.53	1727.10	1352.39	737.84	194.27	118.28	704.94	1357.98	2581.96	3646.84	-52	-340
Till BB4(Bulk)	-952.40	-1463.07	-1727.31	1720.87	1281.77	438.69	117.38	23.92	928.00	1719.22	2869.44	3380.11	-45	-1000
(-1)-0 Φ	-1801.30	-2844.54	-3240.89	3333.27	2463.11	853.50	193.01	121.39	1687.70	3139.11	5458.14	6501.37	-49	-1000
0-1 Φ	-950.14	-1509.74	-1731.39	1826.22	1362.74	500.60	159.89	124.32	1111.32	1843.82	2977.55	3537.14	-45	-1000
1-2 Φ	-826.87	-1242.86	-1490.83	1463.50	1063.44	311.36	52.78	6.90	771.83	1444.37	2452.19	2868.18	-46	-1000
2-3 Φ	-593.19	-943.35	-1197.24	1201.37	905.13	322.72	77.12	29.49	654.03	1152.08	1928.27	2278.43	-50	-1000
>3 Φ	-506.99	-857.16	-1132.47	1101.88	832.64	305.74	82.80	24.62	611.03	1059.70	1742.34	2092.50	-50	-1000
Till RS7 (1)	-1302.32	-2008.08	-2218.37	2040.02	1461.92	562.36	102.12	38.08	1061.12	2081.92	3572.50	4278.26	-44	-1000
Till RS7 (2)	-1532.89	-2388.88	-2590.48	2245.32	1609.25	616.32	108.57	44.50	1096.84	2312.85	4044.02	4900.01	-44	-390

I. Electron probe microanalysis of magnetite from the Barroway Burn (BB) sediments.

Point	5-3	6-3	9-3	10-3	13-3	14-3	15-3	16-3	17-3	26-3	32-3	34-3	37-3	40-3	44-3	1-6
SiO2	7.40	1.84	0.42	1.99	0.74	0.20	0.28	0.40	0.27	0.27	9.73	6.91	0.78	0.32	8.65	0.59
TiO2	13.14	29.31	0.21	9.42	18.40	0.04	0.07	0.01	0.00	4.26	22.38	23.05	0.08	20.38	40.64	17.66
Al2O3	1.37	0.53	0.06	1.15	1.26	0.10	0.36	0.00	0.34	0.46	2.03	0.83	0.52	2.35	2.07	1.30
FeO	63.69	59.31	90.82	80.36	74.09	81.72	86.82	79.95	78.02	85.11	50.87	55.38	84.29	69.01	22.68	69.21
MnO	0.38	0.13	0.23	0.19	1.04	0.13	0.99	1.60	1.76	0.28	0.31	0.14	0.34	1.46	1.54	0.66
MgO	0.48	0.20	0.43	0.06	0.13	0.00	3.09	11.52	13.05	0.17	0.82	0.01	1.48	0.17	0.60	0.04
CaO	5.16	0.87	0.44	1.58	0.04	0.13	0.41	0.16	0.10	0.28	6.69	5.26	0.42	0.35	5.33	0.10
Na2O	0.00	0.00	0.00	0.00	0.00	0.00	0.00	0.00	0.00	0.07	0.05	0.03	0.00	0.00	0.17	0.00
K2O	0.00	0.03	0.02	0.00	0.00	0.03	0.00	0.00	0.00	0.03	0.01	0.03	0.00	0.00	0.02	0.01
Total	91.62	92.21	92.63	94.76	95.69	82.33	92.01	93.64	93.54	90.92	92.90	91.64	87.90	94.03	81.69	89.58
Fe2O3	21.67	2.61	67.45	44.57	29.38	60.38	68.77	75.08	75.80	57.71	0.00	2.95	63.30	23.82	0.00	26.69
FeO	44.19	56.96	30.13	40.25	47.64	27.39	24.94	12.39	9.81	33.18	50.87	52.72	27.33	47.57	22.68	45.19
Total	93.79	92.47	99.39	99.22	98.63	88.38	98.90	101.16	101.13	96.70	92.90	91.93	94.24	96.42	81.69	92.25

Point	3-6	4-6	6-6	7-6	8-6	10-6	11-6	12-6	13-6	16-6	17-6	19-6	20-6	23-6	24-6	27-6
SiO2	2.74	0.38	3.80	3.87	6.41	4.85	0.35	6.50	3.02	0.30	0.29	2.59	0.79	4.67	0.33	0.49
TiO2	18.58	11.40	13.70	19.64	32.24	13.35	22.33	21.58	15.94	22.12	6.39	17.42	14.88	14.80	13.70	0.02
Al2O3	1.67	0.74	1.63	0.91	1.09	1.14	1.05	1.71	0.74	1.38	3.21	1.28	1.86	1.28	1.61	0.04
FeO	66.00	76.24	68.29	65.34	43.05	67.52	68.02	54.46	67.79	71.37	80.98	65.97	72.47	67.69	75.50	83.31
MnO	1.21	0.74	0.46	0.50	3.03	0.39	0.48	0.52	0.44	0.58	0.35	1.67	0.32	0.55	0.58	0.03
MgO	0.00	0.00	0.00	0.13	0.28	0.00	0.46	0.23	0.05	0.35	0.74	0.40	0.17	0.00	0.00	0.02
CaO	2.04	0.21	2.86	3.17	5.41	3.98	0.25	5.34	1.90	0.02	0.00	0.88	0.31	4.01	0.14	0.19
Na2O	0.00	0.00	0.00	0.00	0.00	0.00	0.02	0.00	0.00	0.00	0.00	0.00	0.00	0.00	0.00	0.00
K2O	0.00	0.02	0.00	0.02	0.00	0.00	0.00	0.00	0.02	0.02	0.00	0.02	0.00	0.02	0.00	0.00
Total	92.24	89.73	90.75	93.58	91.52	91.23	92.98	90.34	89.90	96.12	91.96	90.23	90.79	93.01	91.85	84.10
Fe2O3	21.25	41.05	27.80	18.51	0.00	27.09	20.77	4.92	25.52	23.12	50.53	23.07	32.26	25.76	36.82	61.05
FeO	46.87	39.30	43.27	48.69	43.05	43.14	49.33	50.03	44.83	50.56	35.51	45.21	43.44	44.51	42.36	28.38
Total	94.37	93.85	93.53	95.43	91.52	93.94	95.05	90.83	92.46	98.44	97.02	92.54	94.02	95.59	95.54	90.21

Point	28-6	29-6	30-6	31-6	33-6	34-6	36-6	37-6	38-6	40-6	41-6	42-6	44-6	45-6	46-6	47-6
SiO2	7.56	0.76	6.52	0.31	0.38	0.29	4.58	30.46	0.70	6.35	0.58	2.48	3.89	1.79	0.38	1.25
TiO2	21.25	9.44	16.33	6.96	8.02	17.00	16.18	26.90	16.88	19.47	11.44	33.69	19.12	16.63	17.78	10.40
Al2O3	1.08	1.03	1.00	1.19	0.78	1.85	0.86	3.81	1.08	0.84	1.81	1.03	0.98	1.10	1.32	0.82
FeO	56.46	79.01	64.22	82.38	81.27	72.13	66.64	9.67	71.80	61.19	78.08	43.30	62.33	70.36	72.89	75.46
MnO	0.38	0.74	0.56	0.64	0.28	1.87	0.29	0.04	0.43	0.06	0.94	0.45	0.19	0.54	0.55	0.63
MgO	0.05	0.03	0.05	0.01	0.00	0.02	0.00	2.19	0.00	0.00	0.21	0.35	0.12	0.00	0.01	0.29
CaO	6.30	0.61	5.29	0.01	0.07	0.12	2.95	23.45	0.33	5.32	0.19	1.25	3.46	1.51	0.15	0.26
Na2O	0.00	0.00	0.00	0.00	0.00	0.00	0.00	0.00	0.00	0.00	0.00	0.20	0.12	0.00	0.00	0.00
K2O	0.00	0.02	0.00	0.01	0.01	0.00	0.02	0.00	0.00	0.00	0.02	0.03	0.01	0.01	0.02	0.00
Total	93.09	91.63	93.98	91.52	90.81	93.28	91.52	96.52	91.22	93.23	93.27	82.78	90.23	91.93	93.10	89.12
Fe2O3	5.87	45.30	19.24	51.14	48.75	30.86	22.30	0.00	29.52	12.78	41.84	0.00	17.42	28.07	29.59	40.49
FeO	51.18	38.25	46.90	36.36	37.40	44.36	46.57	9.67	45.24	49.68	40.43	43.30	46.66	45.10	46.26	39.02
Total	93.67	96.17	95.91	96.65	95.70	96.37	93.75	96.52	94.17	94.51	97.46	82.78	91.98	94.74	96.07	93.17

I. (continuation)

Point	1-6L	6-6L	9-6L	11-6L	18-6L	19-6L	20-6L	1-7	2-7	3-7	5-7	8-7	9-7	10-7	11-7	12-7
SiO2	0.92	13.26	0.38	8.39	0.86	0.25	0.32	0.24	0.29	0.19	6.69	1.09	0.39	0.22	6.85	0.44
TiO2	13.07	4.20	22.15	31.96	10.76	15.85	14.68	0.00	17.00	10.89	23.46	11.45	20.07	16.63	14.18	17.54
Al2O3	0.51	4.31	0.26	2.15	1.34	1.59	1.68	0.06	0.67	1.24	1.82	0.87	1.48	0.89	1.70	1.36
FeO	75.37	53.52	68.47	37.57	76.74	74.87	74.93	93.70	76.19	80.31	56.52	77.69	70.12	73.72	62.04	73.48
MnO	0.29	0.35	0.48	1.00	0.30	1.16	1.57	0.00	0.50	0.68	1.27	1.50	0.07	0.14	0.56	1.20
MgO	0.00	5.02	0.25	1.97	0.09	1.09	0.77	0.00	0.00	0.00	0.11	0.08	0.14	0.58	0.15	0.06
CaO	0.18	1.49	0.02	0.53	0.21	0.00	0.04	0.01	0.19	0.03	5.50	0.12	0.10	0.01	5.99	0.08
Na2O	0.04	0.62	0.00	0.67	0.00	0.00	0.00	0.00	0.00	0.00	0.00	0.00	0.00	0.00	0.16	0.00
K2O	0.02	0.16	0.00	0.73	0.02	0.00	0.00	0.01	0.01	0.00	0.00	0.00	0.03	0.00	0.03	0.00
Total	90.40	82.93	92.01	84.97	90.32	94.82	94.00	94.01	94.84	93.33	95.36	92.80	92.41	92.20	91.67	94.16
Fe2O3	37.10	19.75	21.11	0.00	40.89	35.37	36.75	69.01	33.51	44.53	4.12	41.27	24.13	32.48	21.12	30.64
FeO	41.98	35.75	49.47	37.57	39.94	43.04	41.86	31.60	46.03	40.24	52.81	40.56	48.41	44.49	43.03	45.91
Total	94.12	84.91	94.12	84.97	94.41	98.36	97.68	100.92	98.19	97.79	95.77	96.94	94.83	95.45	93.78	97.23

Point	13-7	14-7	15-7	16-7	17-7	18-7	20-7	21-7	22-7	23-7	24-7	25-7	27-7	28-7	30-7	31-7
SiO2	0.36	0.37	0.16	0.35	1.16	0.27	2.07	5.34	6.69	5.05	0.81	0.27	0.89	0.40	0.48	0.53
TiO2	15.93	11.96	0.04	11.63	3.91	33.18	15.35	1.50	7.03	2.65	13.41	19.98	17.85	15.91	20.14	0.07
Al2O3	2.04	0.93	0.00	3.11	0.45	0.31	0.70	0.88	1.04	0.80	1.03	1.46	0.81	0.75	0.93	0.02
FeO	72.18	77.77	92.20	73.85	83.93	62.39	73.33	79.31	72.63	78.74	76.11	70.67	73.51	74.24	70.71	83.38
MnO	0.47	1.66	0.00	0.62	0.24	1.00	0.32	0.24	0.34	0.20	0.42	0.77	1.20	0.58	1.17	0.10
MgO	0.00	0.07	0.00	2.48	0.00	0.41	0.00	1.75	0.00	1.18	0.00	0.43	0.33	0.04	0.16	0.00
CaO	0.06	0.09	0.03	0.07	0.84	0.05	1.32	0.55	5.21	1.34	0.59	0.04	0.03	0.44	0.34	0.20
Na2O	0.00	0.00	0.00	0.00	0.04	0.00	0.00	0.00	0.00	0.14	0.00	0.00	0.00	0.00	0.00	0.00
K2O	0.01	0.00	0.03	0.00	0.02	0.01	0.02	0.03	0.00	0.03	0.00	0.04	0.00	0.00	0.01	0.03
Total	91.04	92.85	92.46	92.10	90.58	97.62	93.10	89.60	92.94	90.12	92.37	93.66	94.60	92.36	93.93	84.34
Fe2O3	30.97	41.97	68.09	40.78	55.89	2.72	31.40	49.95	37.23	49.09	37.42	25.79	30.05	33.60	25.63	61.07
FeO	44.31	40.00	30.93	37.15	33.64	59.93	45.07	34.36	39.12	34.56	42.44	47.46	46.47	44.00	47.64	28.43
Total	94.15	97.05	99.28	96.19	96.18	97.89	96.25	94.60	96.67	95.04	96.12	96.24	97.61	95.72	96.50	90.45

Point	32-7	33-7	34-7	35-7	36-7	37-7	38-7	39-7	40-7	41-7	42-7	43-7	44-7	45-7
SiO2	21.48	0.96	0.47	0.25	0.54	1.63	19.28	0.92	0.48	0.54	0.30	0.29	0.30	0.19
TiO2	23.33	24.25	18.74	15.57	13.85	16.18	22.63	17.20	15.60	5.75	21.46	16.45	11.62	23.60
Al2O3	2.47	1.28	0.80	1.22	0.82	1.27	1.83	1.39	1.41	1.26	0.70	0.62	2.86	0.84
FeO	30.41	62.39	73.44	75.01	77.24	69.92	34.62	71.80	75.64	84.01	72.72	77.32	78.47	69.85
MnO	0.14	3.41	0.54	0.44	0.36	0.65	0.12	0.67	0.79	0.12	0.45	0.24	0.58	0.25
MgO	0.07	0.18	0.21	0.00	0.01	0.32	0.55	0.00	0.09	0.00	0.19	0.15	0.61	0.29
CaO	18.68	0.07	0.24	0.20	0.42	0.77	15.55	0.59	0.19	0.22	0.14	0.06	0.06	0.07
Na2O	0.00	0.00	0.00	0.00	0.00	0.00	0.00	0.05	0.00	0.00	0.00	0.07	0.00	0.00
K2O	0.01	0.00	0.00	0.00	0.00	0.02	0.03	0.02	0.00	0.00	0.01	0.00	0.02	0.00
Total	96.59	92.54	94.45	92.70	93.24	90.74	94.60	92.63	94.20	91.90	95.96	95.19	94.51	95.07
Fe2O3	0.00	14.40	29.10	34.25	38.05	28.37	0.00	29.23	34.56	53.26	25.14	35.26	41.98	20.17
FeO	30.41	49.43	47.26	44.19	43.00	44.39	34.62	45.50	44.54	36.08	50.10	45.58	40.69	51.70
Total	96.59	93.98	97.36	96.13	97.05	93.59	94.60	95.56	97.66	97.24	98.48	98.73	98.71	97.09

J. Electron probe microanalysis of magnetite from the Moonzie Burn (MB) sediments.

Point	1-1	2-1	3-1	4-1	5-1	6-1	7-1	8-1	9-1	10-1	11-1	12-1	13-1	16-1	17-1	18-1
SiO2	8.01	2.87	1.21	3.02	0.37	0.65	0.44	3.44	0.40	0.82	0.28	0.22	0.25	2.18	0.38	0.28
TiO2	21.09	0.02	25.19	39.34	22.91	5.75	0.05	0.00	0.03	0.01	0.28	0.14	18.66	21.56	9.13	0.05
Al2O3	1.54	0.02	2.84	1.14	2.47	2.26	0.03	1.13	0.03	0.00	0.90	0.09	1.00	1.72	4.35	0.04
FeO	55.77	77.14	61.15	45.78	69.53	78.53	89.18	70.13	74.33	83.39	97.36	91.81	73.83	63.40	67.20	91.78
MnO	0.37	0.00	1.69	0.15	0.46	0.29	0.10	0.42	0.14	0.16	0.13	0.06	0.55	1.24	0.26	0.07
MgO	0.00	0.12	0.37	0.17	0.71	0.11	0.00	0.27	0.00	0.00	0.00	0.00	0.23	0.45	4.13	0.00
CaO	6.97	0.22	0.12	1.14	0.00	0.07	0.06	0.46	0.05	0.05	0.03	0.04	0.04	0.14	0.02	0.04
Na2O	0.00	0.00	0.00	0.00	0.00	0.00	0.00	0.56	0.00	0.00	0.00	0.00	0.00	0.10	0.00	0.00
K2O	0.01	0.00	0.00	0.04	0.00	0.00	0.01	0.06	0.00	0.01	0.01	0.00	0.00	0.00	0.04	0.00
Total	93.77	80.38	92.55	90.77	96.44	87.66	89.87	76.48	74.97	84.43	99.00	92.36	94.57	90.79	85.51	92.26
Fe2O3	5.14	52.40	9.98	0.00	20.32	48.63	65.37	48.97	54.47	60.50	70.96	67.47	29.61	15.57	40.46	67.51
FeO	51.15	29.99	52.17	45.78	51.24	34.77	30.36	26.06	25.32	28.95	33.51	31.09	47.19	49.39	30.80	31.04
Total	94.28	85.63	93.55	90.77	98.47	92.53	96.42	81.38	80.43	90.49	106.10	99.12	97.53	92.34	89.57	99.02

Point	19-1	20-1	21-1	22-1	23-1	24-1	25-1	26-1	27-1	28-1	29-1	30-1	33-1	34-1	35-1	41-1
SiO2	2.00	0.27	0.71	0.79	0.67	8.21	0.25	0.14	0.56	0.18	0.84	0.95	3.10	0.42	0.29	2.75
TiO2	0.06	0.00	17.36	17.97	24.09	25.63	14.16	50.75	23.79	0.00	0.00	18.79	0.02	25.32	16.37	20.93
Al2O3	0.18	0.00	2.82	0.87	1.07	1.41	1.10	0.04	1.20	0.06	0.02	2.08	1.04	2.67	0.92	1.14
FeO	72.09	69.36	66.16	71.02	66.22	51.95	78.80	48.94	67.41	80.50	84.50	67.68	77.56	63.75	75.24	66.35
MnO	0.20	1.79	1.75	1.33	0.72	0.49	0.40	0.64	0.58	0.21	0.51	0.43	0.26	0.87	0.35	0.52
MgO	0.06	17.61	0.79	0.11	0.63	0.26	0.21	0.40	0.46	0.00	0.15	0.00	0.03	0.14	0.79	0.16
CaO	0.29	0.66	0.13	0.10	0.32	5.76	0.00	0.05	0.03	4.39	0.55	0.51	0.36	0.10	0.06	2.07
Na2O	0.00	0.00	0.00	0.00	0.00	0.00	0.00	0.00	0.00	0.00	0.00	0.00	0.06	0.00	0.00	0.00
K2O	0.00	0.00	0.02	0.02	0.00	0.00	0.02	0.00	0.00	0.02	0.02	0.02	0.00	0.00	0.00	0.00
Total	74.88	89.69	89.74	92.23	93.72	93.70	94.93	100.96	94.03	85.35	86.58	90.45	82.43	93.25	94.02	93.90
Fe2O3	50.21	76.13	25.68	28.11	16.88	0.00	39.10	0.00	17.69	63.64	62.28	23.20	52.24	12.29	34.29	18.36
FeO	26.90	0.85	43.06	45.73	51.03	51.95	43.61	48.94	51.49	23.23	28.46	46.80	30.55	52.68	44.38	49.82
Total	79.90	97.32	92.31	95.04	95.41	93.70	98.84	100.95	95.80	91.72	92.82	92.78	87.66	94.49	97.45	95.74

Point	42-1	1-4	2-4	3-4	4-4	5-4	6-4	7-4	12-4	13-4	14-4	15-4	16-4	17-4	18-4	19-4
SiO2	0.91	0.37	0.25	0.47	3.70	18.14	1.04	0.33	0.39	0.54	0.40	5.34	0.35	0.50	0.22	1.70
TiO2	21.92	7.10	51.82	10.07	19.65	17.13	19.64	0.06	0.07	27.65	8.10	21.29	0.00	0.07	17.69	3.06
Al2O3	2.34	2.75	0.10	2.67	1.09	2.58	0.46	0.03	0.29	1.19	0.66	1.67	0.00	2.34	1.73	0.56
FeO	67.38	81.50	41.77	75.09	59.89	38.86	65.91	90.55	89.73	61.05	79.69	59.56	91.67	88.68	70.86	82.03
MnO	0.37	0.30	1.25	0.48	4.23	0.41	2.06	0.12	0.12	1.16	0.08	0.20	0.16	0.64	0.72	0.00
MgO	0.00	1.07	3.38	1.26	0.00	0.06	0.20	0.00	0.00	0.00	0.00	1.19	0.00	0.46	0.05	0.00
CaO	0.65	0.02	0.11	0.22	3.96	14.13	0.09	0.00	0.07	0.03	0.04	0.41	0.00	0.09	0.10	0.28
Na2O	0.00	0.00	0.04	0.13	0.02	0.00	0.00	0.18	0.00	0.00	0.00	0.01	0.00	0.00	0.00	0.00
K2O	0.01	0.00	0.00	0.03	0.01	0.07	0.02	0.01	0.01	0.00	0.03	0.07	0.00	0.00	0.00	0.04
Total	93.58	93.12	98.72	90.42	92.54	91.38	89.43	91.28	90.67	91.61	88.99	89.74	92.18	92.77	91.37	87.67
Fe2O3	18.77	50.49	0.00	42.84	18.11	0.00	22.52	67.28	65.75	7.71	47.36	7.77	67.41	64.66	28.33	53.75
FeO	50.49	36.07	41.77	36.54	43.60	38.86	45.65	30.01	30.56	54.12	37.07	52.57	31.01	30.49	45.36	33.66
Total	95.46	98.18	98.72	94.71	94.35	91.38	91.68	98.02	97.26	92.38	93.73	90.52	98.93	99.25	94.21	93.05

J. (continuation)

Point	21-4	23-4	24-4	25-4	26-4	27-4	28-4	29-4	30-4	31-4	32-4	34-4	35-4	36-4	38-4
SiO2	1.33	0.60	0.43	1.49	11.19	2.72	0.78	0.45	2.02	2.21	1.15	13.47	7.02	0.65	0.37
TiO2	14.50	10.49	0.15	24.73	23.43	25.15	30.99	0.17	11.95	0.00	25.26	0.24	0.13	17.18	16.42
Al2O3	0.67	1.25	0.19	1.27	1.00	1.61	2.05	0.42	0.87	0.04	1.91	7.16	5.86	0.91	1.32
FeO	72.22	78.90	87.42	61.50	49.09	60.39	55.67	65.59	74.27	76.80	60.21	72.22	79.28	72.52	72.47
MnO	0.37	0.45	0.13	0.68	0.04	2.67	0.54	1.94	0.65	0.31	1.13	0.11	0.16	0.96	0.22
MgO	0.00	0.14	0.00	0.06	0.00	0.87	0.00	14.13	0.00	0.11	0.03	0.34	0.22	0.13	0.72
CaO	0.26	0.02	0.10	0.63	9.32	0.10	0.54	0.60	0.27	0.80	1.01	0.23	0.23	0.03	0.09
Na2O	0.00	0.00	0.00	0.00	0.00	0.00	0.00	0.00	0.15	0.00	0.00	0.50	0.20	0.00	0.00
K2O	0.02	0.00	0.03	0.01	0.00	0.05	0.00	0.01	0.00	0.03	0.04	0.79	0.40	0.00	0.00
Total	89.36	91.85	88.45	90.37	94.08	93.54	90.57	83.29	90.18	80.30	90.72	95.06	93.50	92.38	91.60
Fe2O3	32.04	43.31	63.98	10.50	0.00	8.94	0.00	68.07	36.47	54.18	9.87	30.67	45.70	30.13	31.66
FeO	43.38	39.93	29.85	52.05	49.09	52.34	55.67	4.33	41.45	28.05	51.34	44.62	38.16	45.41	43.99
Total	92.57	96.19	94.86	91.42	94.08	94.43	90.57	90.10	93.83	85.72	91.71	98.13	98.08	95.40	94.77

Point	40-4	41-4	42-4	43-4	45-4
SiO2	0.82	0.42	0.42	0.31	4.00
TiO2	15.00	6.99	28.87	5.64	17.38
Al2O3	1.13	2.88	0.46	2.14	2.35
FeO	72.00	80.00	58.48	82.27	63.48
MnO	2.56	0.03	0.81	0.34	0.51
MgO	0.07	0.86	0.77	0.29	0.21
CaO	0.07	0.03	0.00	0.09	0.28
Na2O	0.00	0.09	0.06	0.03	0.13
K2O	0.01	0.02	0.01	0.00	0.03
Total	91.66	91.32	89.88	91.13	88.38
Fe2O3	33.40	49.30	5.76	52.62	17.14
FeO	41.94	35.64	53.30	34.92	48.06
Total	95.00	96.26	90.46	96.40	90.09

K. Electron probe microanalysis of magnetite from the Kilgour Burn (KB) sediments.

Point	1-1	2-1	3-1	4-1	5-1	6-1	7-1	8-1	9-1	10-1	11-1	12-1	13-1	14-1	15-1	16-1
SiO2	0.61	6.87	1.12	1.77	8.79	0.98	0.50	1.62	0.40	10.16	2.76	0.43	0.83	2.98	1.41	0.36
TiO2	20.92	19.95	20.89	18.27	11.75	17.63	19.39	16.49	16.88	22.28	18.38	8.57	30.20	8.42	16.17	18.29
Al2O3	1.00	1.15	0.99	0.87	3.02	1.52	1.30	1.42	1.93	0.81	1.02	1.98	0.70	0.80	1.77	1.39
FeO	65.90	65.68	65.27	66.47	61.69	70.42	70.61	71.54	71.22	54.08	63.18	81.40	59.95	76.02	64.35	71.14
MnO	1.27	1.15	1.73	0.22	0.59	2.48	0.72	0.55	3.43	0.53	1.19	0.25	2.54	0.77	0.78	1.69
MgO	0.04	0.30	0.23	0.00	0.49	0.00	0.00	0.22	0.02	0.13	0.00	0.20	0.19	0.07	0.06	0.00
CaO	0.21	0.71	0.18	0.61	4.75	0.30	0.12	0.11	0.03	5.77	4.98	0.03	0.59	1.92	0.62	0.07
Na2O	0.00	0.13	0.09	0.00	0.00	0.03	0.00	0.00	0.00	0.00	0.00	0.00	0.00	0.00	0.00	0.00
K2O	0.00	0.02	0.00	0.03	0.05	0.00	0.00	0.00	0.03	0.03	0.00	0.02	0.01	0.00	0.02	0.00
Total	89.95	95.95	90.50	88.24	91.14	93.35	92.64	91.93	93.92	93.80	91.51	92.88	95.01	91.00	85.17	92.95
Fe2O3	20.55	11.86	20.18	22.13	18.64	28.39	25.58	28.23	31.25	0.00	22.52	47.63	5.06	41.89	24.00	28.29
FeO	47.40	55.01	47.12	46.55	44.92	44.87	47.60	46.13	43.09	54.08	42.91	38.54	55.39	38.32	42.75	45.68
Total	92.01	97.13	92.52	90.45	93.01	96.19	95.20	94.76	97.05	93.80	93.77	97.65	95.51	95.19	87.57	95.78

Point	17-1	18-1	19-1	21-1	22-1	23-1	24-1	27-1	28-1	29-1	30-1	31-1	32-1	33-1	1-6	2-6
SiO2	0.33	1.00	15.77	0.57	5.68	3.07	0.50	4.73	7.57	0.47	1.13	0.38	5.49	10.75	0.45	2.82
TiO2	16.69	18.86	19.84	15.68	10.90	17.19	21.50	18.75	20.77	21.36	16.57	17.74	21.55	24.54	14.97	18.76
Al2O3	1.04	1.02	1.81	2.24	0.60	0.65	1.33	1.12	1.12	1.48	1.13	1.13	1.14	0.74	2.03	0.78
FeO	71.39	68.10	55.84	73.16	68.94	68.16	63.01	69.99	57.31	67.36	71.19	74.10	57.03	47.39	76.70	68.42
MnO	1.69	0.85	0.56	0.57	0.67	0.45	0.49	0.42	0.75	1.17	1.11	0.29	0.59	1.19	0.74	0.63
MgO	0.00	0.05	0.24	0.83	0.00	0.02	0.44	0.08	0.32	0.00	0.13	0.15	0.53	0.10	0.11	0.02
CaO	0.11	1.49	0.73	0.08	4.68	2.39	0.21	3.33	6.14	0.03	0.69	0.03	5.19	8.53	0.09	2.24
Na2O	0.00	0.00	0.01	0.00	0.00	0.00	0.00	0.00	0.00	0.04	0.09	0.00	0.00	0.00	0.00	0.00
K2O	0.00	0.00	0.08	0.00	0.02	0.00	0.01	0.00	0.01	0.00	0.03	0.01	0.00	0.06	0.00	0.02
Total	91.24	91.38	94.88	93.13	91.49	91.93	87.49	98.44	93.99	91.91	92.07	93.83	91.52	93.31	95.07	93.69
Fe2O3	30.90	25.14	0.00	32.71	31.17	24.43	17.61	21.47	7.62	20.92	30.22	30.47	9.27	0.00	35.80	22.95
FeO	43.58	45.48	55.84	43.72	40.90	46.18	47.16	50.67	50.45	48.54	44.00	46.68	48.69	47.39	44.48	47.77
Total	94.34	93.90	94.88	96.40	94.61	94.38	89.25	100.59	94.76	94.01	95.10	96.88	92.45	93.31	98.66	95.98

Point	3-6	4-6	5-6	6-6	7-6	8-6	9-6	10-6	11-6	12-6	16-6	17-6	18-6	19-6	20-6	22-6
SiO2	12.83	0.44	0.37	1.64	0.53	1.08	0.38	6.96	0.48	11.58	7.94	0.41	12.30	0.50	0.30	0.46
TiO2	22.77	21.46	21.84	3.97	0.00	0.00	10.67	2.89	24.26	28.33	0.06	19.00	30.49	2.77	23.09	22.93
Al2O3	1.17	1.05	2.27	0.71	0.00	0.16	2.11	4.11	2.33	2.00	1.64	1.48	1.70	0.39	2.99	2.86
FeO	47.32	66.89	66.62	82.78	85.86	73.56	73.95	62.31	63.62	33.50	65.97	70.48	31.85	83.31	65.37	64.56
MnO	0.72	0.22	0.78	0.24	0.13	0.34	0.97	0.57	2.02	0.79	0.51	2.52	0.12	0.23	1.46	1.45
MgO	0.06	0.13	0.00	0.00	0.00	0.00	0.00	3.13	0.00	0.71	0.59	0.00	0.30	0.03	0.00	0.00
CaO	10.56	0.05	0.09	1.02	0.07	0.18	0.02	0.46	0.04	3.49	2.50	0.11	10.08	0.22	0.08	0.05
Na2O	0.00	0.00	0.00	0.00	0.00	0.00	0.19	0.22	0.00	0.18	0.21	0.00	0.47	0.04	0.00	0.00
K2O	0.05	0.01	0.02	0.03	0.02	0.00	0.02	0.03	0.03	0.30	0.01	0.00	0.06	0.03	0.00	0.01
Total	95.50	90.26	91.98	90.38	86.61	75.33	88.31	80.69	92.79	80.90	79.43	93.99	87.36	87.52	93.28	92.31
Fe2O3	0.00	20.04	19.12	54.00	62.89	52.93	40.42	33.85	14.36	0.00	38.36	27.40	0.00	57.65	16.73	16.11
FeO	47.32	48.87	49.42	34.19	29.27	25.93	37.58	31.85	50.70	33.50	31.44	45.82	31.85	31.44	50.31	50.06
Total	95.50	92.27	93.90	95.79	92.90	80.63	92.36	84.08	94.23	80.90	83.27	96.73	87.36	93.29	94.96	93.92

K. (continuation)

Point	23-6	24-6	26-6	27-6	29-6	30-6	31-6	33-6	34-6	35-6	36-6	37-6	38-6	39-6	40-6	41-6
SiO2	3.11	1.63	10.50	1.36	0.18	0.32	0.33	0.96	1.10	0.82	0.36	0.43	4.16	0.39	0.27	0.41
TiO2	21.34	18.39	25.24	18.23	0.10	0.08	24.64	0.07	0.04	19.72	13.41	19.38	17.37	20.67	33.54	16.82
Al2O3	1.48	2.24	2.23	0.67	0.00	0.06	2.69	0.00	0.15	1.66	1.91	1.72	1.55	1.39	0.61	3.86
FeO	64.83	66.11	41.95	71.15	91.45	90.62	63.44	83.69	73.43	67.77	75.99	69.43	68.67	71.01	56.86	65.24
MnO	1.80	2.29	0.87	0.68	0.04	0.18	1.99	0.45	0.41	1.59	0.76	1.87	0.47	0.81	0.24	3.64
MgO	1.41	0.57	0.30	0.00	0.00	0.00	0.00	0.00	0.00	0.04	0.03	0.35	0.55	0.62	3.55	0.08
CaO	0.10	0.27	8.68	0.40	0.03	0.01	0.00	0.19	0.37	0.24	0.15	0.09	3.04	0.02	0.02	0.08
Na2O	0.00	0.00	0.00	0.00	0.00	0.00	0.00	0.05	0.42	0.00	0.00	0.00	0.00	0.00	0.00	0.03
K2O	0.03	0.00	0.02	0.00	0.00	0.00	0.01	0.03	0.00	0.00	0.01	0.00	0.00	0.01	0.00	0.04
Total	94.10	91.49	89.79	92.49	91.80	91.27	93.10	85.44	75.92	91.85	92.62	93.27	95.79	94.91	95.09	90.22
Fe2O3	16.69	23.15	0.00	26.54	67.36	66.58	13.68	61.03	54.77	23.08	37.56	25.89	23.50	25.11	1.52	26.36
FeO	49.81	45.28	41.95	47.27	30.84	30.70	51.13	28.77	24.14	47.00	42.20	46.13	47.52	48.41	55.49	41.53
Total	95.77	93.81	89.79	95.14	98.54	97.94	94.47	91.55	81.41	94.16	96.38	95.86	98.15	97.43	95.24	92.86

Point	42-6	43-6	44-6	45-6
SiO2	0.29	0.28	0.28	1.70
TiO2	20.18	19.68	18.08	10.29
Al2O3	2.20	1.44	1.26	0.86
FeO	70.69	69.97	72.00	77.37
MnO	0.75	1.50	1.77	0.14
MgO	0.55	0.00	0.00	0.00
CaO	0.03	0.06	0.06	0.93
Na2O	0.00	0.00	0.00	0.00
K2O	0.00	0.00	0.01	0.00
Total	94.70	92.92	93.45	91.29
Fe2O3	25.14	25.55	29.51	41.13
FeO	48.07	46.98	45.44	40.36
Total	97.22	95.48	96.40	95.41

L. Electron probe microanalysis of magnetite from the Moonzie Burn (CB) sediments.

Point	1-1	2-1	4-1	5-1	6-1	7-1	8-1	9-1	10-1	11-1	12-1	13-1	14-1	15-1	16-1	17-1
SiO2	6.88	6.85	0.26	4.70	8.39	6.66	3.32	4.07	5.21	3.37	0.37	5.66	0.52	11.14	0.49	1.28
TiO2	21.17	25.27	18.05	17.78	18.74	19.76	12.48	16.09	14.88	16.77	19.68	22.20	16.07	15.43	17.81	22.10
Al2O3	1.06	1.65	1.26	1.30	1.10	0.60	0.77	0.72	0.75	0.65	0.96	0.99	0.80	0.81	0.94	1.23
FeO	56.06	52.52	66.81	64.51	58.94	61.58	71.32	68.45	67.53	68.70	69.39	57.77	74.25	57.20	72.95	63.12
MnO	0.21	0.06	1.39	0.44	0.13	0.27	0.46	0.20	0.23	0.21	2.85	0.46	1.63	0.15	0.85	0.13
MgO	0.24	0.09	0.00	0.36	0.09	0.07	0.00	0.00	0.01	0.01	0.12	0.13	0.04	0.02	0.00	0.11
CaO	6.23	5.85	0.24	3.28	7.07	4.66	1.78	3.17	4.11	2.52	0.05	4.65	0.51	9.22	0.25	0.20
Na2O	0.00	0.16	0.00	0.00	0.00	0.00	0.05	0.09	0.05	0.00	0.00	0.00	0.00	0.00	0.00	0.26
K2O	0.00	0.01	0.03	0.00	0.02	0.00	0.00	0.03	0.00	0.01	0.01	0.00	0.00	0.03	0.00	0.00
Total	91.85	92.46	88.03	92.37	94.47	93.59	90.16	92.80	92.78	92.23	93.43	91.87	93.83	94.00	93.30	88.42
Fe2O3	6.97	0.00	25.70	19.01	10.25	11.90	32.17	25.29	24.88	24.83	26.40	7.60	34.02	10.64	29.83	15.95
FeO	49.79	52.52	43.68	47.41	49.71	50.87	42.37	45.69	45.14	46.36	45.63	50.93	43.64	47.63	46.11	48.77
Total	92.55	92.46	90.60	94.27	95.50	94.79	93.38	95.34	95.27	94.71	96.08	92.63	97.24	95.07	96.28	90.02

Point	18-1	19-1	20-1	21-1	22-1	23-1	24-1	25-1	26-1	27-1	28-1	29-1	30-1	31-1	32-1	33-1
SiO2	0.93	3.07	3.37	9.70	0.45	12.64	9.89	7.24	0.54	14.87	9.73	2.27	11.44	3.04	3.76	1.05
TiO2	22.98	19.98	20.54	22.77	17.44	15.54	14.95	16.15	13.69	19.75	23.83	18.68	21.86	22.55	21.23	15.60
Al2O3	0.86	2.20	1.79	1.36	0.99	0.91	1.33	0.86	1.09	2.01	0.61	1.04	0.82	0.97	1.56	1.05
FeO	67.09	64.41	64.11	51.73	70.17	54.55	46.01	56.48	67.67	44.67	53.00	66.91	46.53	65.23	61.50	72.60
MnO	2.38	0.25	1.46	0.40	1.04	0.18	0.09	0.11	1.14	0.69	0.21	1.70	0.12	0.49	0.26	2.07
MgO	0.38	0.00	0.22	0.16	0.05	0.00	0.00	0.07	0.00	0.21	0.01	0.08	0.02	0.10	0.16	0.17
CaO	0.35	0.55	1.27	7.15	0.17	10.55	2.00	2.49	0.19	11.19	7.39	2.07	10.43	2.25	1.94	0.31
Na2O	0.00	0.81	0.00	0.00	0.00	0.00	0.55	0.36	0.00	0.26	0.22	0.00	0.00	0.00	0.15	0.00
K2O	0.01	0.10	0.01	0.03	0.00	0.00	0.43	0.55	0.07	0.09	0.00	0.00	0.02	0.03	0.02	0.02
Total	94.97	91.35	92.77	93.29	90.31	94.37	75.25	84.31	84.38	93.74	94.99	92.74	91.24	94.65	90.57	92.85
Fe2O3	19.64	18.96	15.83	0.00	28.45	6.99	1.48	12.66	31.59	0.00	0.00	23.46	0.00	15.08	12.74	32.70
FeO	49.42	47.34	49.87	51.73	44.57	48.27	44.67	45.09	39.24	44.67	53.00	45.80	46.53	51.65	50.04	43.17
Total	96.93	93.24	94.35	93.29	93.16	95.07	75.39	85.58	87.55	93.74	94.99	95.09	91.24	96.16	91.84	96.13

Point	35-1	36-1	37-1	39-1	40-1	41-1	42-1	47-1	50-1	1-5	2-5	5-5	6-5	7-5	8-5	9-5
SiO2	4.13	0.85	3.03	11.24	0.37	10.68	0.22	2.59	2.22	1.24	1.22	6.05	4.30	12.09	11.91	15.97
TiO2	25.12	16.42	20.52	19.98	12.56	11.99	18.52	23.71	17.25	16.72	15.24	20.05	20.16	19.15	21.59	16.77
Al2O3	0.59	1.34	2.08	1.08	1.15	0.64	1.04	1.52	1.05	1.05	1.38	1.07	1.21	0.76	1.02	0.85
FeO	61.61	69.40	59.86	53.69	78.25	60.41	73.64	57.79	68.22	72.83	72.61	61.21	60.99	51.83	50.67	48.22
MnO	0.50	0.52	0.16	0.15	0.85	0.17	0.47	0.26	1.09	0.37	0.66	0.30	0.29	0.14	0.09	0.07
MgO	0.17	0.00	0.03	0.01	0.00	0.00	0.14	0.09	0.00	0.42	0.40	0.16	0.31	0.00	0.00	0.00
CaO	3.17	0.27	1.48	10.02	0.19	9.07	0.06	0.72	1.81	0.14	0.24	4.86	3.61	10.33	10.27	13.51
Na2O	0.00	0.00	0.70	0.00	0.00	0.00	0.00	0.29	0.00	0.00	0.00	0.07	0.00	0.00	0.00	0.01
K2O	0.00	0.02	0.04	0.02	0.01	0.00	0.00	0.20	0.00	0.00	0.00	0.00	0.02	0.03	0.00	0.00
Total	95.29	88.80	87.91	96.19	93.39	92.96	94.09	87.15	91.64	92.78	91.74	93.76	90.89	94.34	95.56	95.39
Fe2O3	8.13	28.02	15.24	2.36	40.83	18.26	29.53	8.63	25.61	29.89	31.85	12.69	14.19	1.06	0.00	0.00
FeO	54.29	44.18	46.15	51.56	41.51	43.98	47.06	50.03	45.17	45.94	43.94	49.79	48.22	50.88	50.67	48.22
Total	96.10	91.61	89.44	96.42	97.48	94.79	97.05	88.02	94.21	95.78	94.93	95.03	92.31	94.45	95.56	95.39

L. (continuation)

Point	10-5	13-5	18-5	20-5	21-5	22-5	23-5	24-5	25-5	27-5	28-5	29-5	33-5	34-5	35-5	38-5
SiO2	0.22	0.16	0.23	5.30	1.55	11.11	3.26	3.90	0.32	0.12	0.23	0.47	0.18	0.67	0.37	0.29
TiO2	11.00	19.61	19.05	13.11	16.37	13.97	20.51	20.65	4.45	5.05	4.84	16.22	4.24	2.65	11.62	21.61
Al2O3	2.36	1.40	1.34	1.26	1.47	1.07	1.85	1.08	1.07	2.06	2.58	4.93	2.85	3.30	1.73	1.48
FeO	79.03	71.52	71.13	68.51	72.00	60.57	65.57	63.63	83.79	85.55	85.12	66.09	85.02	82.76	79.07	65.68
MnO	0.26	2.75	1.45	0.46	0.50	0.07	0.94	0.69	0.05	0.25	0.35	0.93	0.21	0.06	0.75	2.98
MgO	0.05	0.00	0.00	0.46	0.27	0.42	0.01	0.00	0.00	0.15	0.15	2.33	0.07	0.17	0.00	0.00
CaO	0.00	0.03	0.00	0.92	0.09	2.27	2.61	3.26	0.03	0.03	0.03	0.00	0.00	0.03	0.17	0.05
Na2O	0.00	0.00	0.07	0.14	0.04	0.00	0.02	0.17	0.00	0.00	0.00	0.00	0.00	0.00	0.00	0.00
K2O	0.00	0.03	0.00	0.15	0.04	0.56	0.01	0.03	0.00	0.02	0.01	0.00	0.00	0.01	0.00	0.00
Total	92.91	95.50	93.25	90.31	92.33	90.04	94.77	93.40	89.69	93.23	93.32	90.96	92.58	89.63	93.71	92.10
Fe2O3	42.53	27.99	27.59	26.08	29.10	10.36	17.82	16.56	55.09	55.85	55.37	27.73	55.78	55.19	42.26	20.86
FeO	40.76	46.33	46.30	45.05	45.81	51.25	49.53	48.73	34.22	35.30	35.30	41.14	34.82	33.10	41.04	46.92
Total	97.17	98.30	96.02	92.92	95.24	91.08	96.55	95.06	95.21	98.82	98.86	93.73	98.17	95.16	97.94	94.18

Point	39-5	41-5	42-5	44-5	45-5	46-5	47-5	48-5	49-5	50-5	51-5	52-5	53-5	54-5	55-5	56-5
SiO2	12.23	5.11	8.82	4.72	4.44	12.46	10.89	9.20	0.17	9.65	0.41	0.15	0.19	7.39	4.38	10.98
TiO2	9.79	14.12	4.93	16.48	16.96	21.30	2.94	23.90	20.37	16.75	17.31	17.67	18.35	20.63	14.54	25.13
Al2O3	1.70	0.74	1.61	1.28	0.64	1.48	3.20	1.14	1.57	2.40	2.39	1.75	1.03	0.60	1.02	1.28
FeO	63.48	70.07	70.08	63.81	67.09	56.86	69.95	52.06	68.94	56.99	71.65	70.14	74.21	59.10	68.01	48.14
MnO	0.13	0.42	0.26	0.23	0.16	0.20	0.13	0.45	3.06	0.52	2.30	3.30	0.32	1.01	0.62	0.31
MgO	1.51	0.00	1.40	0.65	0.02	0.03	3.27	0.05	0.00	0.57	0.07	0.00	0.13	0.00	0.03	0.13
CaO	1.63	3.00	0.65	3.09	2.73	9.29	0.34	6.95	0.07	7.61	0.11	0.22	0.00	6.00	4.00	9.94
Na2O	0.00	0.09	0.67	0.10	0.00	0.00	0.48	0.04	0.00	0.02	0.00	0.05	0.00	0.00	0.00	0.07
K2O	0.46	0.00	0.28	0.00	0.00	0.01	0.09	0.01	0.00	0.01	0.00	0.00	0.00	0.00	0.00	0.00
Total	90.92	93.54	88.69	90.36	92.05	101.63	91.28	93.80	94.16	94.51	94.25	93.28	94.21	94.74	92.60	95.99
Fe2O3	16.36	27.20	35.21	20.67	21.64	0.00	33.95	0.00	25.17	10.03	29.99	30.13	30.06	9.34	27.00	0.00
FeO	48.76	45.59	38.40	45.21	47.62	56.86	39.40	52.06	46.28	47.96	44.67	43.03	47.16	50.70	43.71	48.14
Total	92.56	96.26	92.22	92.43	94.22	101.63	94.68	93.80	96.68	95.51	97.25	96.30	97.22	95.67	95.30	95.99

Point	1-6	2-6	3-6	6-6	7-6	9-6	10-6	12-6	14-6	15-6	16-6	17-6	18-6	19-6	20-6	21-6
SiO2	0.22	6.00	12.45	8.99	0.47	8.66	8.62	6.11	0.33	0.14	10.38	5.52	7.87	2.41	7.57	0.28
TiO2	23.05	17.56	5.59	10.45	26.77	11.14	11.85	14.99	18.86	18.48	19.06	15.36	17.83	22.28	18.21	18.06
Al2O3	1.04	0.91	5.98	2.57	1.55	1.21	1.01	1.27	1.16	1.00	0.91	1.90	1.08	1.10	1.16	1.03
FeO	70.13	63.85	63.35	67.62	62.12	65.85	65.39	65.07	72.07	72.21	55.08	61.78	58.24	62.48	60.02	72.65
MnO	0.40	0.20	0.17	0.12	1.75	0.18	0.26	0.93	0.42	0.87	0.20	0.34	0.99	1.81	0.25	2.85
MgO	0.19	0.00	2.88	1.87	0.00	0.28	0.10	0.33	0.00	0.00	0.00	1.42	0.14	0.02	0.22	0.00
CaO	0.04	5.85	0.21	0.35	0.04	1.73	2.03	3.85	0.06	0.00	8.85	0.15	4.51	1.45	4.93	0.04
Na2O	0.00	0.00	0.17	0.33	0.29	0.09	0.34	0.06	0.00	0.24	0.00	0.00	0.00	0.00	0.00	0.00
K2O	0.00	0.01	0.05	0.13	0.02	0.79	0.83	0.04	0.00	0.06	0.00	0.01	0.01	0.00	0.00	0.03
Total	95.07	94.36	90.84	92.42	93.00	89.93	90.44	92.65	92.89	93.02	94.48	86.48	90.68	91.55	92.37	94.93
Fe2O3	20.89	18.52	19.27	23.58	11.36	22.72	22.93	21.92	27.44	29.98	5.11	16.83	10.12	14.51	11.32	30.98
FeO	51.34	47.18	46.01	46.40	51.90	45.40	44.76	45.35	47.37	45.23	50.49	46.64	49.14	49.42	49.84	44.77
Total	97.16	96.21	92.77	94.78	94.14	92.21	92.73	94.85	95.64	96.02	95.00	88.16	91.69	93.00	93.50	98.03

L. (continuation)

Point	22-6	23-6	24-6	25-6	26-6	31-6	32-6	33-6	34-6	35-6	36-6	37-6	38-6	39-6	40-6	41-6
SiO2	9.85	3.37	9.03	13.30	8.00	1.56	3.03	16.03	19.04	17.06	13.56	1.57	0.23	0.32	13.78	3.79
TiO2	26.61	18.67	15.40	23.57	24.10	20.76	11.98	23.57	19.13	19.82	26.43	19.91	19.57	22.06	25.22	3.25
Al2O3	1.75	0.58	1.05	2.03	2.14	0.60	0.45	1.15	3.19	2.75	2.30	1.06	5.84	1.29	1.22	1.37
FeO	46.67	62.43	51.29	45.51	52.01	61.98	68.57	38.97	41.40	52.79	46.24	69.04	67.71	69.12	43.11	79.01
MnO	2.04	0.29	0.21	0.19	0.33	0.10	0.02	0.22	0.20	0.16	0.12	1.01	0.74	1.86	0.19	0.27
MgO	0.11	0.07	0.04	0.43	0.51	0.05	0.00	0.04	2.07	1.01	0.82	0.46	2.67	0.00	0.05	1.04
CaO	8.04	3.03	7.53	8.94	5.70	0.59	0.92	11.58	3.01	3.10	2.69	0.38	0.02	0.10	11.66	0.27
Na2O	0.00	0.27	1.33	0.26	0.00	0.42	0.50	0.70	0.38	0.31	0.31	0.11	0.00	0.00	0.00	0.33
K2O	0.00	0.02	0.09	0.08	0.03	0.02	0.10	0.01	1.00	1.03	0.73	0.00	0.03	0.03	0.02	0.02
Total	95.07	88.73	85.96	94.32	92.80	86.09	85.57	92.26	89.41	98.04	93.20	93.55	96.80	94.79	95.26	89.33
Fe2O3	0.00	19.51	14.25	0.00	0.00	17.77	32.54	0.00	0.00	0.00	0.00	23.48	24.81	22.14	0.00	50.08
FeO	46.67	44.88	38.47	45.51	52.01	45.99	39.29	38.97	41.40	52.79	46.24	47.92	45.39	49.20	43.11	33.94
Total	95.07	90.68	87.39	94.32	92.80	87.87	88.83	92.26	89.41	98.04	93.20	95.90	99.29	97.01	95.26	94.35

Point	42-6
SiO2	1.17
TiO2	27.76
Al2O3	0.32
FeO	62.12
MnO	0.34
MgO	0.00
CaO	0.30
Na2O	0.00
K2O	0.02
Total	92.03
Fe2O3	7.36
FeO	55.50
Total	92.76

M. Electron probe microanalysis of magnetite from the Eden River (RE) sediments.

Point	4-1	7-1	10-1	12-1	13-1	14-1	15-1	16-1	17-1	18-1	19-1	20-1	23-1	27-1	28-1	29-1
SiO2	6.37	1.14	0.37	0.43	0.25	3.96	0.30	3.24	1.99	0.41	8.67	0.44	0.38	0.53	1.04	0.39
TiO2	23.57	4.27	4.70	20.17	18.15	16.71	17.96	1.63	1.63	19.28	20.91	3.10	3.40	0.07	16.32	9.24
Al2O3	2.35	0.55	1.76	1.03	1.24	1.52	1.89	1.13	0.62	2.00	2.06	0.98	1.17	0.02	0.36	2.32
FeO	57.73	86.97	81.45	72.73	71.95	66.60	73.92	82.47	84.73	69.43	54.23	85.64	86.56	88.72	74.42	82.54
MnO	0.17	0.39	0.49	0.34	1.17	0.47	0.80	0.02	0.10	0.98	0.08	0.23	0.19	0.03	0.29	0.46
MgO	0.84	0.00	0.00	0.21	0.00	0.99	0.59	0.13	0.00	0.00	0.06	0.15	0.21	0.00	0.00	0.12
CaO	1.81	0.59	0.11	0.02	0.00	0.19	0.03	0.18	0.05	0.04	6.07	0.00	0.07	0.38	0.36	0.04
Na2O	0.00	0.00	0.00	0.00	0.00	0.02	0.00	0.00	0.07	0.00	0.30	0.00	0.00	0.00	0.00	0.00
K2O	0.05	0.00	0.00	0.00	0.01	0.00	0.04	0.19	0.07	0.01	0.04	0.04	0.05	0.00	0.00	0.00
Total	92.86	93.91	88.88	94.93	92.77	90.47	95.53	88.99	89.27	92.15	92.43	90.57	92.03	89.76	92.79	95.11
Fe2O3	1.93	57.30	52.97	26.26	28.93	21.18	30.82	53.48	57.37	24.77	3.19	58.50	58.96	65.06	31.91	47.48
FeO	55.99	35.41	33.78	49.10	45.92	47.54	46.18	34.35	33.11	47.14	51.36	32.99	33.51	30.17	45.70	39.81
Total	93.06	99.65	94.19	97.56	95.67	92.59	98.62	94.35	95.01	94.63	92.75	96.43	97.94	96.28	95.99	99.86

Point	31-1	32-1	33-1	34-1	35-1	36-1	38-1	39-1	40-1	41-1	42-1	45-1	2-2	3-2	4-2	5-2
SiO2	0.31	9.10	1.00	1.40	0.40	0.24	0.37	0.31	2.97	0.42	1.89	0.18	0.97	0.24	0.26	0.33
TiO2	18.67	11.10	19.17	9.33	23.25	17.03	19.19	19.63	19.51	4.96	5.99	17.77	0.05	27.29	19.69	6.23
Al2O3	2.15	2.49	0.89	2.32	0.99	1.66	1.15	1.18	1.66	1.92	0.57	1.62	1.76	1.95	2.36	1.60
FeO	69.65	62.67	70.84	76.94	70.67	72.38	69.71	71.30	66.45	87.06	81.52	74.59	91.02	63.55	70.67	84.36
MnO	2.34	0.21	0.96	0.79	0.67	1.40	1.03	2.05	1.50	0.23	0.66	0.45	0.07	0.43	0.36	0.36
MgO	0.00	0.83	0.12	0.66	0.06	0.00	0.00	0.00	0.34	0.08	0.00	0.10	0.00	1.85	1.09	0.16
CaO	0.05	2.22	0.38	0.09	0.03	0.04	0.08	0.01	1.44	0.03	0.49	0.01	0.01	0.02	0.01	0.06
Na2O	0.00	0.00	0.00	0.00	0.00	0.00	0.03	0.00	0.10	0.02	0.27	0.01	0.00	0.00	0.00	0.00
K2O	0.05	0.53	0.06	0.00	0.03	0.02	0.00	0.02	0.00	0.01	0.03	0.01	0.00	0.01	0.02	0.01
Total	93.22	89.17	93.41	91.54	96.09	92.76	91.55	94.50	93.97	94.72	91.43	94.73	93.88	95.33	94.47	93.11
Fe2O3	26.98	19.08	26.11	42.42	20.85	30.78	25.79	27.08	20.48	56.52	50.98	30.95	64.78	12.06	26.20	53.33
FeO	45.37	45.51	47.34	38.77	51.91	44.69	46.51	46.93	48.02	36.20	35.65	46.74	32.73	52.69	47.09	36.37
Total	95.92	91.08	96.02	95.78	98.17	95.84	94.13	97.22	96.02	100.38	96.53	97.83	100.37	96.53	97.09	98.45

Point	6-2	7-2	8-2	9-2	10-2	11-2	12-2	13-2	14-2	15-2	17-2	18-2	19-2	20-2	21-2	22-2
SiO2	0.34	0.35	0.25	0.84	0.63	0.77	1.39	1.41	0.44	0.28	0.34	0.79	0.40	5.88	11.06	0.41
TiO2	24.88	0.00	3.71	31.32	26.88	0.06	0.18	17.84	6.89	5.77	13.88	15.10	16.74	30.92	12.90	19.74
Al2O3	0.71	0.00	2.08	0.39	1.01	2.92	5.34	1.60	2.10	0.89	1.10	1.43	2.81	1.11	1.82	2.29
FeO	68.52	91.27	87.97	52.56	62.55	90.50	87.48	71.20	83.57	87.18	78.42	74.65	74.53	52.23	60.65	72.63
MnO	0.63	0.16	0.36	5.58	3.26	0.09	0.19	0.38	0.33	0.29	0.48	0.77	0.79	0.15	0.16	0.85
MgO	0.33	0.00	0.14	0.29	0.11	0.00	0.00	0.81	0.12	0.02	0.42	0.00	0.39	0.13	0.71	0.86
CaO	0.01	0.06	0.00	0.20	0.03	0.05	0.06	0.29	0.00	0.05	0.03	0.25	0.05	1.56	2.11	0.02
Na2O	0.00	0.00	0.00	0.11	0.00	0.00	0.00	0.00	0.00	0.00	0.05	0.00	0.05	0.00	0.00	0.00
K2O	0.02	0.00	0.00	0.00	0.03	0.01	0.00	0.00	0.00	0.00	0.02	0.00	0.00	0.29	0.62	0.00
Total	95.43	91.85	94.51	91.28	94.50	94.40	94.64	93.53	93.45	94.49	94.72	92.98	95.74	92.27	90.04	96.81
Fe2O3	17.60	67.18	59.16	0.72	11.60	64.24	59.52	27.28	51.26	56.22	39.60	33.84	32.09	0.00	11.99	27.38
FeO	52.68	30.82	34.73	51.92	52.12	32.69	33.93	46.65	37.45	36.59	42.78	44.20	45.65	52.23	49.86	48.00
Total	97.19	98.57	100.44	91.35	95.66	100.83	100.60	96.26	98.58	100.12	98.69	96.37	98.96	92.27	91.24	99.55

M. (continuation)

Point	23-2	25-2	26-2	27-2	30-2	33-2	34-2	37-2	38-2	40-2	41-2	43-2	45-2	1-3	5-3
SiO2	0.39	0.82	2.37	0.41	1.23	3.23	0.23	0.39	0.37	0.38	0.52	0.47	0.38	0.87	0.28
TiO2	18.83	12.42	11.67	19.57	0.16	14.16	16.04	25.70	0.08	10.34	0.12	13.33	11.61	16.78	12.76
Al2O3	2.52	1.57	1.24	2.17	5.97	1.55	1.44	0.57	0.74	1.49	0.06	0.98	1.92	0.71	0.89
FeO	72.28	75.13	70.63	72.34	86.54	70.96	77.78	62.81	91.02	81.75	91.44	74.39	80.03	72.19	77.24
MnO	0.65	1.23	0.46	0.54	0.01	0.30	0.46	2.05	0.17	0.36	0.00	0.26	0.49	0.06	0.31
MgO	0.28	0.00	0.04	0.72	0.44	0.01	0.31	0.81	0.00	0.05	0.00	0.00	0.12	0.00	0.22
CaO	0.04	0.32	2.05	0.03	0.55	1.71	0.02	0.05	0.03	0.00	0.03	0.28	0.02	0.14	0.07
Na2O	0.04	0.00	0.22	0.00	0.00	0.00	0.00	0.00	0.00	0.00	0.00	0.01	0.00	0.00	0.00
K2O	0.00	0.00	0.07	0.03	0.00	0.02	0.00	0.02	0.00	0.00	0.00	0.02	0.02	0.01	0.00
Total	95.02	91.50	88.73	95.82	94.90	91.93	96.27	92.38	92.41	94.37	92.17	89.73	94.58	90.76	91.76
Fe2O3	27.50	38.06	35.40	27.12	59.71	29.11	35.85	13.99	66.44	45.67	66.66	36.56	42.73	29.43	39.84
FeO	47.53	40.88	38.77	47.94	32.81	44.77	45.52	50.22	31.24	40.65	31.46	41.49	41.58	45.71	41.39
Total	97.78	95.31	92.28	98.53	100.88	94.85	99.86	93.78	99.06	98.95	98.85	93.39	98.86	93.70	95.75

Point	6-3	7-3	8-3	9-3	11-3	12-3	13-3	14-3	15-3	16-3	17-3	19-3	20-3	21-3	22-3
SiO2	7.54	0.45	1.01	0.68	0.23	0.10	8.98	17.03	0.40	7.99	0.30	3.62	5.83	14.07	0.45
TiO2	7.79	0.05	17.47	14.54	19.97	0.25	17.17	19.75	21.10	24.21	11.89	21.17	21.08	18.57	16.99
Al2O3	1.68	0.28	0.86	2.64	7.00	0.08	0.92	2.36	2.80	1.77	1.87	1.27	0.91	1.98	1.28
FeO	63.67	80.66	70.94	72.60	66.00	91.90	59.08	39.20	67.51	52.59	76.63	63.14	59.48	45.61	71.52
MnO	0.20	0.28	0.82	0.26	0.66	0.00	0.17	0.07	1.31	0.26	2.75	0.86	0.41	0.06	1.19
MgO	1.21	0.04	0.18	0.00	3.62	0.00	0.02	0.08	0.00	0.12	0.20	0.00	0.00	0.04	0.00
CaO	3.05	0.56	0.44	0.10	0.08	0.01	8.18	15.43	0.18	5.33	0.04	2.93	4.68	12.27	0.11
Na2O	0.03	0.29	0.06	0.00	0.00	0.00	0.00	0.05	0.00	0.00	0.00	0.00	0.00	0.13	0.00
K2O	0.14	0.01	0.00	0.00	0.00	0.00	0.02	0.02	0.00	0.01	0.03	0.00	0.01	0.01	0.03
Total	85.30	82.62	91.78	90.82	97.56	92.34	94.54	93.98	93.29	92.28	93.71	92.99	92.38	92.73	91.56
Fe2O3	27.70	60.81	28.56	32.11	23.57	67.54	12.45	0.00	20.89	0.00	41.87	14.93	9.94	0.00	29.96
FeO	38.74	25.94	45.24	43.71	44.78	31.12	47.88	39.20	48.71	52.59	38.96	49.71	50.53	45.61	44.56
Total	88.07	88.71	94.64	94.03	99.92	99.10	95.78	93.98	95.39	92.28	97.90	94.48	93.38	92.73	94.56

Point	23-3	24-3	25-3	27-3	28-3	29-3	32-3	33-3	35-3	38-3	40-3	41-3	42-3	43-3	45-3
SiO2	7.63	2.52	0.33	11.21	7.47	6.39	9.28	14.12	4.28	2.48	15.49	0.30	1.15	1.98	0.26
TiO2	14.14	23.17	20.34	21.41	16.67	19.48	11.52	15.22	22.58	14.92	19.98	0.01	12.61	13.00	3.30
Al2O3	1.06	1.56	1.36	1.47	1.68	0.88	0.63	1.28	1.35	0.81	1.15	0.06	1.22	2.08	1.37
FeO	63.97	62.72	69.11	51.05	60.25	59.96	63.83	50.50	54.85	71.19	49.91	90.73	72.75	70.31	86.86
MnO	0.32	0.70	2.89	0.23	0.11	0.41	0.20	0.18	0.19	0.12	0.31	0.04	0.41	0.38	0.16
MgO	0.02	0.46	0.00	0.31	0.00	0.03	0.00	0.00	0.09	0.04	0.31	0.00	0.00	0.17	0.00
CaO	5.60	0.17	0.08	9.56	2.06	5.87	8.06	12.44	3.33	1.81	3.51	0.00	0.39	0.31	0.07
Na2O	0.00	0.00	0.00	0.00	0.17	0.00	0.00	0.00	0.45	0.00	0.00	0.00	0.00	0.15	0.03
K2O	0.02	0.03	0.01	0.00	0.74	0.01	0.00	0.00	0.10	0.00	0.51	0.00	0.00	0.01	0.01
Total	92.76	91.32	94.12	95.24	89.15	93.03	93.51	93.74	87.23	91.36	91.16	91.13	88.53	88.40	92.03
Fe2O3	20.10	11.69	25.07	0.00	13.14	12.63	22.98	3.37	7.93	29.90	0.00	66.69	35.09	31.62	59.11
FeO	45.88	52.20	46.55	51.05	48.43	48.60	43.16	47.46	47.72	44.28	49.91	30.72	41.17	41.85	33.66
Total	94.77	92.49	96.63	95.24	90.46	94.29	95.82	94.08	88.02	94.36	91.16	97.81	92.04	91.57	97.95

M. (continuation)

Point	2-4	3-4	4-4	5-4	6-4	7-4	8-4	9-4	13-4	14-4	16-4	18-4	20-4	21-4	22-4	23-4
SiO2	0.44	0.36	0.35	0.31	0.33	0.26	26.50	0.50	0.30	0.28	5.70	9.66	0.32	8.10	1.69	0.29
TiO2	22.02	19.39	19.04	19.07	14.43	14.77	2.51	21.05	10.59	15.27	23.46	7.41	20.77	30.51	29.40	16.48
Al2O3	3.66	2.39	1.47	1.82	1.02	0.92	6.87	1.92	1.09	0.61	0.82	1.51	2.07	3.09	0.40	1.02
FeO	65.40	73.16	69.60	74.24	74.99	77.99	42.39	67.20	79.69	77.69	60.31	66.91	68.78	46.42	59.10	74.46
MnO	0.42	0.44	1.17	0.22	0.21	0.16	0.16	1.52	0.33	0.29	0.62	0.26	1.64	0.24	0.25	0.92
MgO	0.60	1.42	0.00	0.07	0.00	0.00	10.22	0.00	0.74	0.58	0.05	0.76	0.00	0.09	0.00	0.00
CaO	0.18	0.00	0.24	0.00	0.12	0.02	1.87	0.04	0.00	0.02	4.44	4.56	0.04	3.20	0.51	0.03
Na2O	0.00	0.00	0.10	0.00	0.00	0.00	0.09	0.00	0.00	0.00	0.00	0.00	0.00	0.00	0.00	0.00
K2O	0.02	0.02	0.00	0.01	0.00	0.01	0.04	0.01	0.00	0.00	0.00	0.14	0.00	0.26	0.01	0.00
Total	92.73	97.18	91.97	95.73	91.09	94.14	90.64	92.22	92.75	94.73	95.42	91.21	93.61	91.90	91.35	93.20
Fe2O3	17.76	28.72	26.33	28.37	35.49	37.32	0.00	21.06	45.05	37.40	7.63	27.72	22.90	0.00	2.09	32.86
FeO	49.42	47.31	45.91	48.71	43.05	44.41	42.39	48.25	39.15	44.03	53.45	41.97	48.17	46.42	57.22	44.89
Total	94.51	100.05	94.61	98.57	94.65	97.88	90.64	94.33	97.26	98.48	96.18	93.99	95.90	91.90	91.56	96.49

Point	25-4	27-4	28-4	29-4	30-4	32-4	33-4	34-4	36-4	37-4	38-4	39-4	40-4	41-4	42-4	43-4
SiO2	12.12	7.14	1.47	7.91	0.53	6.33	12.65	0.56	0.25	0.87	16.11	26.12	0.31	17.05	11.17	0.30
TiO2	23.28	21.09	20.62	16.40	16.17	20.16	19.40	17.55	0.22	16.43	18.36	32.18	23.36	11.15	16.19	16.70
Al2O3	0.84	0.77	0.72	0.77	1.01	1.75	0.94	1.05	0.78	0.33	1.77	2.92	1.77	4.39	0.80	1.24
FeO	48.27	58.44	68.79	63.65	73.39	59.11	51.23	72.50	81.85	74.01	43.68	11.32	65.99	48.77	56.71	73.41
MnO	0.23	0.43	0.37	0.36	1.14	0.30	0.14	0.48	0.91	0.31	0.11	0.06	1.87	0.22	0.08	1.99
MgO	0.03	0.01	0.00	1.52	0.26	0.70	0.04	0.21	3.36	0.00	0.00	0.91	0.00	2.59	0.00	0.00
CaO	10.17	4.44	0.21	0.76	0.16	4.80	10.99	0.08	0.08	0.72	14.21	22.86	0.03	3.15	8.88	0.10
Na2O	0.00	0.00	0.00	0.02	0.00	0.10	0.07	0.00	0.00	0.00	0.00	0.03	0.00	0.00	0.00	0.00
K2O	0.03	0.08	0.03	0.13	0.00	0.00	0.01	0.00	0.01	0.06	0.00	0.09	0.00	0.84	0.03	0.02
Total	94.97	92.40	92.19	91.50	92.66	93.25	95.45	92.43	87.45	92.73	94.26	96.48	93.33	88.13	93.86	93.75
Fe2O3	0.00	6.90	21.06	14.30	32.71	10.91	0.09	29.51	64.73	32.33	0.00	0.00	17.71	0.00	8.80	32.61
FeO	48.27	52.23	49.84	50.78	43.96	49.30	51.15	45.95	23.60	44.93	43.68	11.32	50.06	48.77	48.79	44.06
Total	94.97	93.09	94.30	92.94	95.93	94.34	95.46	95.38	93.93	95.97	94.26	96.48	95.10	88.13	94.74	97.02

Point	44-4	45-4	1-5	2-5	3-5	5-5	6-5	7-5	8-5	9-5	10-5	13-5	14-5	15-5	16-5	17-5
SiO2	0.32	0.33	5.21	12.23	5.55	0.34	11.11	0.20	20.54	0.30	14.07	0.30	0.92	7.99	0.41	0.31
TiO2	20.03	6.03	18.46	15.82	37.46	22.18	10.16	19.09	20.12	0.07	9.79	0.25	16.77	19.94	15.87	12.18
Al2O3	1.18	1.89	1.15	0.90	1.50	1.80	2.08	1.15	3.50	0.08	2.27	0.27	0.95	0.92	1.64	1.85
FeO	72.05	85.30	63.53	53.78	44.09	67.59	60.90	72.51	39.55	92.93	53.99	90.41	73.80	57.60	70.81	79.43
MnO	2.40	0.23	0.50	0.18	0.18	3.06	0.58	0.72	0.16	0.04	0.22	0.00	0.27	0.60	1.70	0.42
MgO	0.00	0.28	0.01	0.00	1.28	0.00	2.74	0.00	1.51	0.00	3.46	0.00	0.20	0.00	0.00	0.19
CaO	0.05	0.02	4.04	10.05	1.50	0.00	1.53	0.33	4.27	0.00	2.64	0.01	0.58	6.43	0.06	0.06
Na2O	0.00	0.00	0.00	0.04	0.20	0.00	0.08	0.00	0.10	0.00	0.32	0.00	0.09	0.00	0.00	0.00
K2O	0.00	0.00	0.00	0.04	0.13	0.03	0.39	0.00	0.49	0.00	0.61	0.01	0.00	0.04	0.00	0.02
Total	96.02	94.08	92.90	93.03	91.89	95.00	89.57	93.99	90.24	93.43	87.36	91.25	93.57	93.51	90.49	94.44
Fe2O3	27.37	54.13	16.84	6.58	0.00	21.35	17.75	28.17	0.00	68.21	11.16	66.02	31.61	8.14	31.05	41.76
FeO	47.43	36.59	48.37	47.85	44.09	48.38	44.93	47.16	39.55	31.56	43.95	31.00	45.35	50.28	42.86	41.86
Total	98.76	99.50	94.59	93.68	91.89	97.13	91.34	96.81	90.24	100.26	88.48	97.86	96.74	94.33	93.60	98.63

M. (continuation)

Point	19-5	23-5	24-5	25-5	26-5	27-5	29-5	30-5	32-5	33-5	35-5	36-5	37-5	39-5	40-5
SiO2	4.95	5.24	5.31	23.78	3.35	0.37	0.27	0.28	0.29	0.84	0.29	1.10	0.20	2.03	9.25
TiO2	16.61	22.47	16.15	25.18	19.00	17.40	4.10	11.37	17 38	17.87	0.03	21.46	0.24	24.27	8.00
Al2O3	1.33	0.67	0.69	1.56	1.12	1.28	2.33	1.07	1.24	1.01	0.02	1.37	0.00	0.81	2.38
FeO	63.76	58.36	66.87	23.75	63.26	73.25	83.61	81.70	73.09	72.19	92.94	68.53	91.43	64.28	68.34
MnO	1.16	0.41	0.27	0.06	0.77	0.84	0.81	0.51	2.55	0.40	0.07	0.68	0.03	1.64	0.19
MgO	0.19	0.00	0.00	0.26	0.00	0.11	1.12	0.15	0.19	0.00	0.00	0.49	0.00	0.59	4.02
CaO	4.10	3.80	4.85	19.94	3.17	0.04	0.01	0.04	0.08	0.15	0.00	0 12	0.02	0.23	1.09
Na2O	0.00	0.00	0.07	0.00	0.06	0.00	0.00	0.00	0.00	0.00	0.00	0.00	0.00	0.00	0.00
K2O	0.00	0.01	0.00	0.00	0.03	0.01	0.01	0.00	0.00	0.00	0.00	0.03	0.04	0.04	0.03
Total	92.09	90.95	94.20	94.54	90.75	93.29	92.25	95.11	94.82	92.46	93.36	93.77	91.96	93.88	93.29
Fe2O3	20.64	7.62	23.33	0.00	18.94	30.59	56.91	44.95	32.07	28.09	68.36	20.85	67.21	13.58	28.87
FeO	45.18	51.51	45.88	23.75	46.21	45.73	32.40	41.25	44.23	46.91	31.42	49.77	30.95	52.05	42 36
Total	94.16	91.71	96.54	94.54	92.65	96.35	97.95	99.61	98.04	95.27	100.21	95.86	98.69	95.24	96.18

Point	41-5	46-5	1-6	2-6	3-6	4-6	5-6	6-6	7-6	8-6	9-6	10-6	11-6	12-6	13-6
SiO2	1.34	0.66	2 38	7.77	2.09	11.12	0.42	0.30	1.86	3.45	1.26	7.86	0.55	0 45	7.50
TiO2	14.91	50.58	20.32	19.60	23.12	12.74	10.12	27.97	23.01	28.46	18.93	21.87	22.58	12.14	18.46
Al2O3	1.03	0.25	0.73	0.89	0.61	1.83	1.59	0.73	0.47	0.50	1.81	1.77	2.06	2.25	1.60
FeO	71.80	44.14	67.86	57.39	64.64	54.63	81.56	65.94	64.65	58.02	67.31	54.06	64.17	76.89	60.47
MnO	2.27	3.47	0.78	0.30	1.09	0.19	0.44	0.67	0.54	0.18	2.11	0.27	2 52	0.81	0.26
MgO	0.00	0.17	0.06	0.00	0.06	0 02	0.23	0.43	0.00	0.00	0.00	0.46	0.00	0.00	0.06
CaO	0.10	0.70	1.85	6.07	1.80	9.37	0.02	0.01	0.41	1.51	1.15	6.30	0.26	0.18	5.36
Na2O	0.10	0.00	0.00	0.00	0.00	0.11	0.00	0.00	0.00	0.03	0.00	0 00	0.00	0.00	0.00
K2O	0.00	0.00	0.00	0.00	0.01	0.00	0.03	0.01	0.02	0.01	0.02	0 03	0.01	0.00	0.02
Total	91.55	99.96	93.97	92.01	93.39	90.02	94.41	96.07	90.96	92.15	92.59	92.63	92.15	92.72	93.72
Fe2O3	32.62	0.00	21.02	8.15	15.68	12.38	46.12	11.79	14.54	0.37	24.20	2.94	17.57	39.59	11.49
FeO	42.45	44.14	48.95	50.06	50.53	43.50	40.05	55.33	51.57	57.69	45.53	51.42	48.36	41.26	50.13
Total	94.82	99.96	96.07	92.83	94.96	91.26	99.03	97.25	92.41	92.19	95.02	92.93	93.90	96.68	94.87

Point	14-6	16-6	17-6	18-6	19-6	21-6	22-6	25-6	27-6	29-6	31-6	34-6	35-6	36-6	37-6
SiO2	1.44	1.85	0.67	0.86	1.24	6.77	0.34	0.94	3.15	1.14	0.33	1.43	0.24	4.74	0.80
TiO2	23.74	14.94	20.24	20.98	33.61	16.15	20.33	12.43	12.73	0.16	9.72	18.46	16.49	6.59	11.68
Al2O3	0.63	0.44	0.40	0.93	0.35	1.14	1.09	0.62	0.68	0.04	0.99	0.77	1.81	0.56	0.83
FeO	63.20	73.40	68.44	66.11	55.36	60.94	70.26	76.64	70.40	82.66	81.08	70.44	72.08	75.64	76.34
MnO	0.23	0.13	0.16	0.17	0.17	0.31	0.22	0.24	0.45	0.22	0.73	0.30	1.83	0.21	0.44
MgO	0.09	0.07	0.00	0.00	0.00	0.05	0.00	0.00	0.02	0.00	0.00	0.00	0.00	0.00	0.00
CaO	0.30	0.29	0.11	0.22	0.27	5.47	0.03	0.09	0.46	0.29	0.00	0.15	0.05	4.07	0.16
Na2O	0.00	0.00	0.00	0.01	0.00	0.00	0.00	0.00	0.00	0.00	0.00	0.00	0.00	0.00	0.00
K2O	0.01	0.01	0.01	0.00	0.00	0.00	0.00	0.02	0.10	0.02	0.00	0.00	0.01	0.00	0.02
Total	89.63	91.13	90.04	89.27	91.01	90.83	92.26	90.98	87.98	84.53	92.84	91.55	92.50	91.81	90.27
Fe2O3	12.89	31.45	22.60	19.38	0.00	16.53	23.97	38.53	30.34	59.48	46.58	25.01	31.50	42.59	39.67
FeO	51.60	45.10	48.11	48.67	55.36	46.07	48.68	41.96	43.10	29.13	39.17	47.93	43.73	37.31	40.65
Total	90.92	94.28	92.30	91.22	91.01	92.49	94.66	94.84	91.01	90.48	97.51	94 05	95.66	96.07	94.24

M. (continuation)

Point	38-6	39-6	40-6	41-6	43-6	44-6	45-6	49-6	51-6	52-6	54-6	46-6	47-6	48-6
SiO2	1.24	0.36	4.88	0.31	15.63	0.35	2.51	0.24	0.30	0.37	9.05	4.35	16.98	0.24
TiO2	12.01	14.83	0.31	29.13	12.86	19.05	17.93	18.89	18.12	22.97	23.58	24.12	18.42	18.95
Al2O3	0.91	2.63	8.99	1.95	2.17	0.75	0.74	3.20	3.84	2.27	1.84	0.56	1.36	0.89
FeO	72.21	75.85	79.87	58.81	54.27	71.36	67.31	68.57	69.34	65.06	51.05	60.85	43.02	71.21
MnO	0.53	0.19	0.00	1.98	0.18	1.15	0.52	2.91	2.57	0.70	0.26	0.20	0.13	0.60
MgO	0.00	0.00	0.09	0.01	1.48	0.00	0.00	0.36	0.24	0.00	0.00	0.04	0.01	0.02
CaO	0.11	0.01	0.22	0.05	2.70	0.81	2.07	0.03	0.06	0.01	7.68	2.30	14.43	0.08
Na2O	0.00	0.00	0.00	0.00	0.00	0.00	0.00	0.04	0.00	0.00	0.00	0.00	0.00	0.00
K2O	0.02	0.00	0.04	0.01	0.43	0.00	0.01	0.01	0.00	0.00	0.02	0.03	0.06	0.02
Total	87.02	93.89	94.40	92.24	89.72	93.47	91.09	94.27	94.46	91.38	93.47	92.45	94.40	92.01
Fe2O3	35.38	34.58	45.86	4.76	0.10	28.11	23.53	26.40	26.99	16.29	0.00	7.38	0.00	27.20
FeO	40.37	44.74	38.61	54.53	54.19	46.06	46.14	44.81	45.05	50.40	51.05	54.21	43.02	46.73
Total	90.56	97.35	98.99	92.72	89.73	96.29	93.44	96.91	97.16	93.01	93.47	93.19	94.40	94.73

N. Electron probe microanalysis of ilmenite from the Barroway Burn (BB) sediments.

Point	1-3	7-3	18-3	35-3	45-3	46-3	47-3	15-6L	9-6	14-6	18-6	21-6	35-6	43-6	4-7	26-7
SiO2	0.41	0.21	0.31	0.31	0.20	0.17	3.56	7.27	0.36	0.45	3.56	0.22	6.32	0.23	0.34	0.18
TiO2	52.19	52.67	51.91	54.31	49.64	51.76	49.13	62.47	51.75	49.57	50.82	49.11	47.85	51.38	50.41	51.08
Al2O3	0.10	0.00	0.03	0.06	0.09	0.06	3.35	6.63	0.19	0.35	1.58	0.06	0.94	0.06	0.06	0.07
FeO	42.99	47.45	46.98	40.69	47.61	48.42	39.42	11.53	43.04	46.21	32.22	47.17	31.82	41.46	47.53	46.69
MnO	0.82	0.50	0.58	1.37	0.55	0.44	0.09	0.12	1.20	1.31	1.89	0.75	4.44	4.53	0.79	0.61
MgO	0.89	0.13	0.80	1.59	1.33	1.29	1.09	0.42	1.21	1.23	1.43	1.04	0.16	0.25	0.43	0.93
CaO	0.37	0.05	0.10	0.21	0.06	0.02	1.63	3.37	0.30	0.21	0.31	0.03	5.22	0.07	0.04	0.07
Na2O	0.02	0.10	0.00	0.00	0.00	0.00	0.75	0.00	0.00	0.00	0.00	0.00	0.05	0.00	0.00	0.00
K2O	0.00	0.00	0.00	0.04	0.00	0.00	0.05	0.01	0.01	0.02	0.01	0.00	0.00	0.02	0.01	0.00
Total	97.78	101.12	100.71	98.59	99.48	102.16	99.07	91.82	98.05	99.35	91.82	98.36	96.79	98.00	99.60	99.63
Fe2O3	0.00	1.24	2.30	0.00	6.35	4.93	0.00	0.00	0.00	5.49	0.00	5.97	0.00	0.17	3.79	3.23
FeO	42.99	46.33	44.91	40.69	41.89	43.98	39.42	11.53	43.04	41.27	32.22	41.80	31.82	41.30	44.12	43.79
Total	97.78	101.24	100.94	98.59	100.11	102.65	99.07	91.82	98.05	99.90	91.82	98.96	96.79	98.01	99.98	99.95

O. Electron probe microanalysis of ilmenite from the Moonzie Burn (MB) sediments.

Point	14-1	15-1	32-1	36-1	37-1	39-1	40-1	8-4	10-4	20-4	22-4	39-4	44-4
SiO2	0.21	0.16	0.23	0.20	0.18	0.16	0.43	2.87	1.71	0.20	0.39	0.34	0.94
TiO2	49.29	52.52	56.14	53.82	47.58	45.96	45.86	44.25	37.13	47.94	49.87	52.14	47.76
Al2O3	0.00	0.00	0.18	0.05	0.05	0.21	0.31	1.11	0.78	0.02	0.08	0.08	0.12
FeO	47.46	44.80	32.61	40.39	45.82	48.33	36.66	45.37	52.59	48.62	44.51	38.82	44.09
MnO	1.13	0.43	0.38	0.65	0.44	0.72	0.26	0.30	0.28	0.71	1.98	1.58	1.72
MgO	0.20	0.51	1.19	1.83	0.47	1.52	0.49	0.55	0.19	1.42	0.29	2.42	1.12
CaO	0.05	0.04	0.04	0.05	0.16	0.04	3.41	0.33	0.37	0.00	0.10	0.08	0.08
Na2O	0.00	0.00	0.00	0.00	0.00	0.03	0.06	0.00	0.09	0.00	0.00	0.00	0.00
K2O	0.01	0.00	0.02	0.04	0.00	0.02	0.01	0.00	0.01	0.00	0.00	0.00	0.04
Total	98.33	98.45	90.77	97.02	94.68	97.00	87.47	94.78	93.14	98.92	97.23	95.47	95.86
Fe2O3	4.96	0.00	0.00	0.00	4.77	11.67	0.74	4.28	20.73	9.46	2.05	0.00	4.39
FeO	42.99	44.80	32.61	40.39	41.53	37.83	35.99	41.52	33.93	40.11	42.67	38.82	40.13
Total	98.83	98.45	90.77	97.02	95.16	98.16	87.55	95.20	95.21	99.86	97.43	95.47	96.30

P. Electron probe microanalysis of ilmenite from the Kilgour Burn (KB) sediments.

Point	20-1	25-1	26-1	13-6	14-6	28-6	32-6	46-6
SiO2	0.36	0.55	0.17	0.16	0.50	0.83	0.40	0.89
TiO2	53.11	43.56	52.74	51.71	47.61	47.43	48.13	47.20
Al2O3	0.09	2.49	0.00	0.02	0.13	0.32	0.26	0.27
FeO	42.06	28.39	47.68	41.10	39.27	44.31	48.38	41.93
MnO	2.73	3.01	0.41	0.80	11.29	2.83	0.48	4.05
MgO	1.23	0.33	0.27	2.11	0.09	0.72	0.06	0.53
CaO	0.11	0.19	0.05	0.00	0.26	0.32	0.08	0.37
Na2O	0.06	0.07	0.00	0.00	0.09	0.11	0.05	0.24
K2O	0.06	0.00	0.00	0.02	0.05	0.00	0.03	0.02
Total	99.82	78.59	101.34	95.92	99.28	96.87	97.87	95.48
Fe2O3	0.00	0.00	1.12	0.00	9.27	6.37	6.22	5.68
FeO	42.06	28.39	46.67	41.10	30.93	38.58	42.79	36.81
Total	99.82	78.59	101.45	95.92	100.20	97.51	98.49	96.05

Q. Electron probe microanalysis of ilmenite from the Coalpit Burn (CB) sediments.

Point	3-1	34-1	45-1	46-1	48-1	3-5	4-5	11-5	12-5	14-5	15-5	16-5	17-5	19-5	26-5
SiO2	10.35	2.67	2.29	1.00	11.18	3.99	2.37	0.72	0.18	4.63	0.18	0.12	0.20	0.31	0.69
TiO2	32.97	41.75	30.12	31.98	33.74	32.45	33.13	50.34	53.29	29.16	50.88	50.72	50.82	29.86	51.03
Al2O3	1.32	0.93	0.59	0.37	3.57	0.91	0.89	0.00	0.06	1.10	0.01	0.00	0.04	0.89	0.13
FeO	34.19	48.89	54.99	58.54	37.12	51.09	57.17	45.02	42.07	55.68	45.89	46.92	46.49	61.86	45.30
MnO	0.11	1.75	0.07	0.44	1.42	1.78	1.70	2.83	3.23	0.39	0.93	0.85	0.74	1.43	2.78
MgO	0.14	0.62	0.14	0.58	3.06	0.47	0.16	0.36	0.76	0.10	0.47	0.51	0.47	0.22	0.00
CaO	9.42	1.30	0.53	0.19	0.49	3.17	1.47	0.02	0.04	3.18	0.00	0.10	0.03	0.07	0.65
Na2O	0.77	0.06	0.15	0.03	0.23	0.00	0.00	0.00	0.00	0.00	0.00	0.00	0.00	0.00	0.00
K2O	0.06	0.00	0.09	0.00	0.12	0.03	0.00	0.03	0.01	0.00	0.01	0.00	0.00	0.07	0.00
Total	89.33	97.96	88.96	93.13	90.91	93.89	96.88	99.32	99.64	94.24	98.35	99.23	98.79	94.71	100.58
Fe2O3	9.26	14.43	30.15	33.84	2.60	26.57	31.60	2.80	0.00	31.76	1.90	3.40	2.40	40.87	2.48
FeO	25.86	35.91	27.86	28.09	34.78	27.18	28.73	42.50	42.07	27.10	44.18	43.87	44.33	25.08	43.07
Total	90.26	99.41	91.98	96.51	91.17	96.55	100.04	99.60	99.64	97.42	98.54	99.57	99.03	98.80	100.83

Point	30-5	31-5	36-5	37-5	40-5	43-5	4-6	5-6	8-6	11-6	27-6	28-6	29-6	30-6	43-6
SiO2	0.14	0.34	0.14	1.82	0.21	0.16	4.50	1.88	1.28	0.27	0.14	0.14	0.04	0.07	0.13
TiO2	51.68	50.83	50.95	40.48	52.58	50.72	39.78	31.60	29.23	53.43	52.99	51.33	46.57	46.33	50.58
Al2O3	0.06	0.08	0.05	0.27	0.00	0.02	2.09	0.67	1.26	0.05	0.05	0.07	0.00	0.05	0.08
FeO	47.46	46.29	47.28	50.53	46.16	47.21	48.77	57.88	61.51	47.08	40.01	47.38	46.91	46.15	48.00
MnO	0.34	0.37	0.54	0.23	0.96	0.65	0.06	0.09	1.75	0.55	0.85	0.64	0.58	0.63	0.95
MgO	0.14	0.10	0.22	0.00	0.78	1.09	1.03	0.00	0.00	0.27	0.47	1.30	0.16	0.49	0.27
CaO	0.04	0.09	0.09	0.27	0.02	0.07	0.29	0.32	0.11	0.06	0.07	0.00	0.03	0.01	0.02
Na2O	0.00	0.00	0.00	0.00	0.00	0.00	0.24	0.02	0.20	0.00	0.09	0.00	0.00	0.18	0.00
K2O	0.00	0.00	0.00	0.01	0.00	0.00	0.02	0.03	0.02	0.02	0.03	0.00	0.03	0.01	0.00
Total	99.85	98.10	99.28	93.61	100.70	99.92	96.76	92.50	95.35	101.72	94.70	100.85	94.32	93.93	100.02
Fe2O3	1.62	0.94	2.60	13.94	1.11	4.55	12.25	31.03	40.67	0.00	0.00	4.46	6.66	7.52	4.23
FeO	46.00	45.45	44.93	37.98	45.16	43.12	37.75	29.97	24.91	47.08	40.01	43.36	40.91	39.39	44.19
Total	100.01	98.19	99.54	95.01	100.82	100.38	97.99	95.60	99.42	101.72	94.70	101.30	94.99	94.68	100.44

R. Electron probe microanalysis of ilmenite from the River Eden (RE) sediments.

Point	1-1	2-1	5-1	6-1	8-1	11-1	21-1	22-1	24-1	26-1	30-1	37-1	43-1	44-1	28-2
SiO2	0.30	0.32	1.38	0.60	0.28	0.25	0.36	0.31	0.36	0.41	0.28	0.22	0.25	3.67	0.50
TiO2	48.90	31.72	50.94	48.56	50.95	52.43	49.19	50.86	48.97	53.12	48.47	52.64	50.13	36.99	49.66
Al2O3	0.00	0.08	1.09	0.18	0.00	0.09	0.03	0.09	0.00	0.09	0.23	0.03	0.16	1.18	0.42
FeO	43.66	31.53	33.77	42.24	46.75	41.50	46.57	43.52	47.39	43.61	48.52	47.25	47.45	48.95	45.78
MnO	0.73	0.23	0.14	4.82	1.82	4.87	1.79	1.69	1.63	1.09	1.10	0.74	0.39	1.21	1.88
MgO	1.14	0.69	0.28	0.13	0.18	1.15	0.49	1.24	0.77	0.32	0.56	0.75	1.53	0.69	0.86
CaO	0.05	0.03	1.00	0.26	0.02	0.02	0.00	0.13	0.10	0.27	0.00	0.01	0.01	2.01	0.06
Na2O	0.00	0.00	0.51	0.10	0.00	0.00	0.00	0.00	0.02	0.00	0.00	0.00	0.00	0.09	0.00
K2O	0.01	0.00	0.05	0.03	0.00	0.00	0.06	0.02	0.02	0.02	0.01	0.03	0.03	0.03	0.00
Total	94.78	64.58	89.16	96.91	100.00	100.30	98.49	97.85	99.27	98.92	99.16	101.66	99.94	94.81	99.17
Fe2O3	2.42	4.55	0.00	4.26	3.08	1.16	5.28	1.71	6.91	0.00	7.48	2.01	5.86	18.69	4.47
FeO	41.48	27.43	33.77	38.40	43.98	40.46	41.82	41.98	41.18	43.61	41.78	45.44	42.17	32.14	41.76
Total	95.02	65.04	89.16	97.33	100.31	100.42	99.02	98.02	99.96	98.92	99.91	101.86	100.53	96.68	99.62

Point	42-2	44-2	2-3	10-3	18-3	34-3	36-3	37-3	39-3	10-4	11-4	26-4	35-4	46-4	11-5
SiO2	0.39	1.10	0.36	0.24	0.13	0.17	0.30	0.22	0.98	0.23	0.19	0.29	0.25	0.12	0.19
TiO2	49.08	40.15	52.70	53.92	57.59	52.56	52.60	49.85	42.61	49.33	49.17	51.69	50.40	50.59	50.56
Al2O3	0.01	0.58	0.04	0.03	0.10	0.09	0.01	0.07	0.27	0.06	0.04	0.07	0.07	0.04	0.08
FeO	47.40	51.27	45.72	46.80	31.97	46.81	43.45	45.92	48.73	46.83	47.19	45.10	48.32	46.92	48.20
MnO	2.87	2.96	1.15	0.32	1.12	0.84	3.83	0.57	4.91	0.46	0.52	0.41	0.61	1.83	0.60
MgO	0.00	0.69	0.91	0.13	1.91	0.22	0.11	1.97	0.18	0.23	0.65	0.35	0.88	0.79	0.73
CaO	0.04	0.20	0.19	0.13	0.03	0.01	0.06	0.00	0.54	0.18	0.05	0.07	0.06	0.05	0.03
Na2O	0.00	0.00	0.00	0.00	0.00	0.00	0.00	0.00	0.00	0.00	0.00	0.01	0.00	0.00	0.00
K2O	0.02	0.04	0.00	0.02	0.01	0.02	0.00	0.00	0.00	0.02	0.03	0.00	0.01	0.01	0.00
Total	99.81	96.97	101.07	101.59	92.84	100.72	100.36	98.60	98.21	97.34	97.83	97.98	100.60	100.36	100.38
Fe2O3	6.47	20.47	1.03	0.00	0.00	0.71	0.00	5.47	16.92	3.71	5.08	0.00	5.54	5.15	4.93
FeO	41.58	32.85	44.79	46.80	31.97	46.17	43.45	41.01	33.51	43.49	42.62	45.10	43.33	42.29	43.76
Total	100.46	99.02	101.18	101.59	92.84	100.79	100.36	99.15	99.91	97.71	98.34	97.98	101.15	100.87	100.88

Point	18-5	21-5	28-5	31-5	38-5	44-5	15-6	23-6	26-6	28-6	32-6	33-6	42-6	50-6	53-6
SiO2	0.14	0.09	0.53	0.38	0.16	1.33	0.18	0.19	0.22	0.21	0.21	0.28	2.55	0.24	0.63
TiO2	52.69	50.66	49.02	50.77	55.45	56.37	53.84	51.74	51.47	52.02	51.30	50.24	46.89	53.87	35.80
Al2O3	0.01	0.00	0.10	0.08	0.02	0.33	0.00	0.07	0.04	0.01	0.03	0.07	0.23	0.08	1.24
FeO	46.94	45.79	46.80	46.21	40.04	49.03	44.46	46.06	47.58	48.10	44.58	48.16	43.21	45.03	56.81
MnO	1.23	0.59	1.19	1.69	0.26	1.12	1.06	0.65	0.76	0.74	0.69	0.72	0.16	0.59	2.64
MgO	0.37	2.04	0.37	0.44	0.00	0.23	1.04	1.40	1.16	0.49	0.17	0.96	0.03	2.35	0.20
CaO	0.09	0.02	0.08	0.27	0.04	0.34	0.05	0.05	0.05	0.03	0.03	0.00	0.43	0.03	0.49
Na2O	0.08	0.00	0.02	0.00	0.00	0.04	0.00	0.00	0.00	0.00	0.00	0.00	0.00	0.00	0.00
K2O	0.00	0.03	0.02	0.00	0.00	0.04	0.00	0.00	0.01	0.04	0.00	0.00	0.05	0.02	0.01
Total	101.54	99.21	98.12	99.84	95.97	108.83	100.63	100.16	101.29	101.64	97.02	100.44	93.54	102.20	97.80
Fe2O3	1.94	4.95	4.64	3.25	0.00	0.00	0.00	2.78	4.41	3.14	0.00	5.64	0.00	1.29	30.59
FeO	45.19	41.33	42.62	43.28	40.04	49.03	44.46	43.55	43.61	45.27	44.58	43.08	43.21	43.87	29.28
Total	101.74	99.71	98.58	100.16	95.97	108.83	100.63	100.44	101.73	101.95	97.02	101.00	93.54	102.33	100.87

S. Magnetic properties of the Barroway Burn (BB) and the Moonzie Burn (MB) sediments.

Sample	wt (g)	X_{lf}(-8) (m^3/kg)	X_{hf}(-8) (m^3/kg)	X_{fd} %	Xarm(-5) (m^3/kg)	IRM_{20}(-5) (Am^2/Kg)	IRM_{40}(-5) (Am^2/Kg)	IRM_{100}(-5) (Am^2/Kg)	IRM_{300}(-5) (Am^2/Kg)	IRM_{500}(-5) (Am^2/Kg)	SIRM(-5) (Am^2/Kg)	IRM_{-20}(-5) (Am^2/Kg)	IRM_{-40}(-5) (Am^2/Kg)	IRM_{-100}(-5) (Am^2/Kg)	IRM_{-300}(-5) (Am^2/Kg)
BB1((-1)-0 Φ)	10.69	404.23	397.68	1.62	1.99	751.69	2740.43	7123.98	9677.83	10009.92	10130.63	6676.62	2165.06	-5215.36	-9482.36
0-1 Φ	10.32	387.52	380.74	1.75	1.89	804.40	2965.41	7560.36	10003.58	10287.25	10417.75	6652.01	1893.53	-5772.47	-9713.82
1-2 Φ	11.40	201.75	200.00	0.87	0.95	428.51	1559.47	3934.12	4998.51	5110.09	5182.19	3338.68	809.54	-3021.28	-4805.03
2-3 Φ	11.98	126.00	125.17	0.66	0.63	280.52	966.68	2239.79	2732.28	2794.90	2814.37	1455.30	303.15	-1480.93	-2242.57
>3 Φ	12.72	123.42	121.85	1.27	0.67	252.44	814.56	1807.21	2261.58	2322.52	2354.12	1227.36	276.92	-1124.98	-1830.92
BB2(Bulk)	9.88	207.84	203.95	1.87	1.33	479.65	1649.33	4338.97	6018.07	6298.51	6531.29	4560.10	1928.87	-2774.45	-5487.01
(-1)-0 Φ	9.67	240.90	235.73	2.15	1.34	454.72	1649.81	4160.77	5613.32	5790.84	5947.37	3700.99	1491.63	-2654.84	-5088.68
0-1 Φ	10.16	247.07	243.13	1.59	1.44	483.36	1768.97	4258.29	5726.94	5892.41	6047.64	3769.86	1444.93	-2804.72	-5224.77
1-2 Φ	8.86	122.98	119.60	2.75	0.72	258.74	843.89	2145.89	2970.33	3099.51	3191.92	2111.93	729.45	-1370.60	-2755.13
2-3 Φ	9.18	92.60	90.42	2.35	0.52	188.65	621.19	1492.21	2028.43	2149.47	2229.11	1434.25	450.81	-964.95	-1830.17
>3 Φ	4.63	94.97	94.97	0.00	0.65	196.24	658.54	1388.69	2065.77	2153.81	2270.02	1438.38	446.06	-880.14	-1848.13
BB3(Bulk)	9.57	249.84	243.57	2.51	1.50	498.54	1685.97	4225.70	5966.65	6282.04	6403.93	4326.57	1553.42	-2914.74	-5855.82
(-1)-0 Φ	8.81	308.81	299.73	2.94	1.99	658.23	2147.82	5223.55	7499.55	7741.71	7871.71	5398.05	1940.51	-3656.69	-7215.54
0-1 Φ	10.11	299.58	290.69	2.97	1.76	619.73	2028.67	4776.45	6866.32	7106.68	7248.37	4823.31	1624.09	-3317.07	-6586.97
1-2 Φ	10.12	178.78	174.83	2.21	1.09	402.06	1289.11	3063.02	4259.28	4298.99	4660.51	2719.97	1016.30	-2018.71	-3855.43
2-3 Φ	8.82	106.55	104.28	2.13	0.68	257.37	815.09	1902.74	2627.41	2642.94	2900.25	1671.96	568.40	-1240.61	-2346.79
>3 Φ	9.54	118.44	115.29	2.65	0.79	276.81	845.88	1916.05	2638.82	2662.93	2924.96	1628.55	541.71	-1251.15	-2356.37
BB4(Bulk)	9.34	142.97	139.78	2.65	1.11	213.24	1117.30	3074.33	4593.82	4776.89	4939.92	3528.16	1710.97	-1800.12	-4158.24
(-1)-0 Φ	10.21	322.17	313.36	2.74	1.82	636.27	2150.90	5435.57	8027.61	8116.14	8508.42	5286.33	2321.19	-3411.88	-7247.92
0-1 Φ	10.36	234.51	228.72	2.47	1.33	441.60	1507.33	3750.24	5460.72	5544.10	5830.63	3667.05	1609.25	-2310.75	-4842.68
1-2 Φ	10.86	111.43	107.74	3.31	0.70	207.83	801.97	1959.11	2806.52	2958.74	2948.06	1887.93	773.92	-1207.39	-2491.85
2-3 Φ	10.68	76.78	74.91	2.44	0.49	144.83	568.25	1372.94	1948.60	2061.14	2065.36	1319.57	537.69	-836.99	-1722.62
>3 Φ	8.82	87.29	85.02	2.60	0.57	159.05	603.04	1439.86	2084.80	2233.99	2268.00	1440.77	619.17	-821.27	-1812.50
BB5(Bulk)	10.47	179.88	176.09	2.60	1.01	291.92	1408.47	3743.26	5295.53	5469.87	5568.85	3648.52	1405.05	-2597.80	-4987.50
(-1)-0 Φ	9.42	270.64	264.28	2.35	1.33	500.02	1836.45	5064.21	7646.36	8122.69	8118.02	5887.07	2779.03	-3060.90	-7092.59
0-1 Φ	9.13	235.56	232.28	1.40	1.16	453.13	1693.66	4389.72	6143.20	6487.24	6601.29	4599.10	1739.56	-2754.55	-5643.45
1-2 Φ	10.70	142.03	139.23	1.97	0.66	308.60	1121.01	2695.85	3630.16	3851.06	3927.40	2529.15	769.55	-1806.64	-3319.25
2-3 Φ	11.02	112.50	109.78	2.42	0.48	236.91	853.05	2052.80	2699.60	2874.07	2958.08	1866.90	510.08	-1358.51	-2448.88
>3 Φ	8.62	117.13	112.49	3.96	0.57	235.85	796.72	1865.71	2508.18	2760.87	2826.39	1722.37	442.55	-1231.95	-2304.22
BB6(Bulk)	11.67	266.50	260.50	2.25	1.35	575.23	1931.45	4748.67	7060.07	7230.68	7381.23	4757.84	1615.85	-3471.11	-6817.34
(-1)-0 Φ	9.46	296.05	289.70	2.14	1.75	554.92	2054.66	5723.09	8695.39	8896.17	9181.65	6329.67	3144.64	-3409.37	-8120.81

S. (continuation)

Sample	$IRM_{-1000}(-5)$ (Am^2/Kg)	$HIRM_{20}(-5)$ (Am^2/Kg)	$HIRM_{40}(-5)$ (Am^2/Kg)	$HIRM_{100}(-5)$ (Am^2/Kg)	$HIRM_{300}(-5)$ (Am^2/Kg)	$HIRM_{500}(-5)$ (Am^2/Kg)	$HIRM_{-20}(-5)$ (Am^2/Kg)	$HIRM_{-40}(-5)$ (Am^2/Kg)	$HIRM_{-100}(-5)$ (Am^2/Kg)	$HIRM_{-300}(-5)$ (Am^2/Kg)	$(Bo)_{cr}$ (mT)	Rev.Sat. (mT)
BB1((-1)-0 Φ)	-10422.85	9378.94	7390.19	3006.64	452.79	120.71	3454.01	7965.57	15345.98	19612.99	-54	-380
0-1 Φ	-10652.10	9613.35	7452.33	2857.39	414.16	130.50	3765.74	8524.22	16190.22	20131.56	-50	-450
1-2 Φ	-5328.32	4753.68	3622.72	1248.07	183.68	72.11	1843.51	4372.66	8203.47	9987.22	-48	-420
2-3 Φ	-2559.80	2533.85	1847.69	574.57	82.09	19.47	1359.07	2511.21	4295.30	5056.93	-47	-1000
>3 Φ	-2143.22	2101.67	1539.56	546.91	92.54	31.59	1126.76	2077.20	3479.10	4185.03	-45	-1000
BB2(Bulk)	-6336.22	6051.63	4881.96	2192.32	513.21	232.77	1971.18	4602.42	9305.74	12018.29	-60	-1000
(-1)-0 Φ	-5885.88	5492.65	4297.56	1786.60	334.06	156.53	2246.38	4455.75	8602.21	11036.05	-58	-1000
0-1 Φ	-6025.07	5564.28	4278.67	1789.35	320.70	155.23	2277.78	4602.72	8852.37	11272.41	-56	-1000
1-2 Φ	-3274.72	2933.18	2348.03	1046.03	221.60	92.41	1080.00	2462.47	4562.52	5947.05	-56	-550
2-3 Φ	-2266.72	2040.46	1607.92	736.90	200.68	79.64	794.86	1778.30	3194.06	4059.28	-54	-720
>3 Φ	-2339.02	2073.78	1611.48	881.33	204.25	116.21	831.64	1823.96	3150.16	4118.15	-55	-670
BB3(Bulk)	-6603.61	5905.39	4717.96	2178.24	437.28	121.89	2077.36	4850.51	9318.67	12259.75	-56	-430
(-1)-0 Φ	-8086.42	7213.48	5723.89	2648.16	372.16	130.00	2473.66	5931.20	11528.39	15087.25	-56	-420
0-1 Φ	-7454.86	6628.64	5219.70	2471.92	382.04	141.68	2425.05	5624.28	10565.43	13835.34	-54	-430
1-2 Φ	-4421.56	4258.45	3371.39	1597.49	401.22	361.52	1940.54	3644.21	6679.22	8515.94	-56	-1000
2-3 Φ	-2728.49	2642.88	2085.16	997.51	272.84	257.31	1228.29	2331.85	4140.86	5247.04	-54	-1000
>3 Φ	-2741.02	2648.15	2079.08	1008.91	286.13	262.03	1296.40	2383.24	4176.10	5281.32	-54	-1000
BB4(Bulk)	-4789.47	4726.68	3822.62	1865.60	346.10	163.04	1411.76	3228.95	6740.04	9098.16	-66	-1000
(-1)-0 Φ	-8061.56	7872.15	6357.52	3072.86	480.81	392.28	3222.09	6187.23	11920.30	15756.35	-60	-1000
0-1 Φ	-5523.82	5389.03	4323.30	2080.39	369.91	286.53	2163.58	4221.39	8141.38	10673.31	-62	-1000
1-2 Φ	-2927.13	2740.23	2146.09	988.95	141.54	-10.68	1060.13	2174.14	4155.45	5439.91	-60	-1000
2-3 Φ	-2055.67	1920.52	1497.11	692.42	116.76	4.21	745.79	1527.67	2902.34	3787.98	-59	-1000
>3 Φ	-2219.07	2108.94	1664.96	828.14	183.20	34.01	827.23	1648.83	3089.26	4080.50	-62	-1000
BB5(Bulk)	-5430.72	5276.93	4160.39	1825.59	273.32	98.98	1920.33	4163.80	8166.65	10556.35	-56	-1000
(-1)-0 Φ	-7746.92	7618.00	6281.58	3053.81	471.66	-4.67	2230.95	5338.99	11178.92	15210.61	-64	-1000
0-1 Φ	-6409.39	6148.16	4907.64	2211.57	458.09	114.06	2002.19	4861.73	9355.85	12244.75	-58	-1000
1-2 Φ	-3820.03	3618.80	2806.39	1231.55	297.23	76.34	1398.24	3157.85	5734.04	7246.65	-55	-1000
2-3 Φ	-2861.15	2721.18	2105.04	905.28	258.48	84.01	1091.18	2448.00	4316.59	5406.97	-51	-1000
>3 Φ	-2789.03	2590.55	2029.68	960.69	318.22	65.52	1104.02	2383.85	4058.34	5130.62	-51	-1000
BB6(Bulk)	-7592.43	6806.01	5449.79	2632.56	321.17	150.56	2623.39	5765.38	10852.34	14198.58	-54	-420
(-1)-0 Φ	-9044.35	8626.73	7126.98	3458.55	486.26	285.47	2851.98	6037.01	12591.01	17302.45	-66	-1000

S. (continuation)

Sample	wt (g)	X_{lf}(-8) (m^3/kg)	X_{hf}(-8) (m^3/kg)	X_{fd} %	Xarm(-5) (m^3/kg)	IRM_{20}(-5) (Am^2/Kg)	IRM_{40}(-5) (Am^2/Kg)	IRM_{100}(-5) (Am^2/Kg)	IRM_{300}(-5) (Am^2/Kg)	IRM_{500}(-5) (Am^2/Kg)	SIRM(-5) (Am^2/Kg)	IRM_{-20}(-5) (Am^2/Kg)	IRM_{-40}(-5) (Am^2/Kg)	IRM_{-100}(-5) (Am^2/Kg)	IRM_{-300}(-5) (Am^2/Kg)
0-1 Φ	10.36	247.22	242.39	1.95	1.37	464.25	1660.07	4338.87	6375.57	6506.81	6731.24	4505.26	1902.37	-2715.63	-5955.14
1-2 Φ	9.75	150.75	146.65	2.72	0.83	307.40	1090.97	2859.30	4097.22	4193.21	4346.12	2817.76	1092.30	-1787.50	-3719.31
2-3 Φ	11.19	119.76	117.97	1.49	0.54	246.46	884.23	2205.83	2971.04	3036.11	3156.05	1923.23	543.83	-1516.40	-2735.37
>3 Φ	11.27	142.84	140.18	1.86	0.65	260.40	913.58	2266.35	3160.23	3245.94	3439.27	2092.09	704.64	-1494.14	-2644.53
BB7(Bulk)	10.36	210.71	205.60	1.86	1.38	343.01	1784.41	4738.73	6680.76	6923.99	7050.48	4871.75	2082.66	-3143.60	-6262.41
(-1)-0 Φ	9.93	312.25	304.19	2.58	1.85	597.72	2137.39	5756.75	8652.40	9190.77	9224.01	6535.76	3004.33	-3397.94	-8126.56
0-1 Φ	10.13	268.59	261.68	2.57	1.45	528.22	1825.52	4739.61	6800.04	7283.40	7397.45	5147.63	2113.66	-2888.79	-6203.81
1-2 Φ	10.77	164.28	160.57	2.26	0.91	334.00	1181.92	2929.09	4218.02	4475.96	4552.35	3135.14	1203.92	-1764.31	-3822.35
2-3 Φ	9.39	113.98	110.78	2.80	0.61	241.48	867.84	2116.21	2906.05	3108.54	3191.52	2076.05	719.35	-1338.44	-2623.81
>3 Φ	10.51	135.06	130.30	3.52	0.67	273.05	923.54	2123.45	2920.20	3133.82	3199.16	1985.26	597.10	-1345.23	-2601.10
MB1(Bulk)	10.52	87.75	85.76	3.52	0.50	159.72	669.44	1325.79	1600.43	1671.98	1744.43	872.83	-6.63	-1023.95	-1462.82
(-1)-0 Φ	9.61	152.00	149.92	1.37	0.68	288.38	913.64	1833.63	2377.10	2421.45	2495.78	1452.68	192.22	-1357.63	-2182.90
0-1 Φ	11.03	142.39	138.76	2.55	0.65	304.84	913.57	1798.29	2244.33	2278.89	2358.24	1292.13	55.25	-1406.66	-2103.93
1-2 Φ	10.47	66.84	65.89	1.43	0.35	142.36	448.28	893.72	1121.18	1144.39	1188.98	679.79	53.42	-637.94	-997.61
2-3 Φ	11.00	48.18	47.27	1.89	0.25	101.82	313.41	595.16	753.10	782.90	814.63	441.34	24.69	-434.47	-670.01
>3 Φ	10.33	55.16	53.23	3.51	0.27	103.06	330.68	627.38	794.41	831.46	890.00	463.76	39.06	-449.11	-703.34
MB2(Bulk)	10.92	238.81	233.32	3.51	0.98	392.65	1683.64	3817.46	4766.19	4863.23	4992.10	2789.46	394.92	-300.49	-4442.20
(-1)-0 Φ	10.80	302.89	295.48	2.45	1.12	665.09	2029.83	4226.01	4905.61	4949.70	4961.47	2164.41	-141.16	-2957.91	-5085.76
0-1 Φ	10.80	253.82	248.26	2.19	0.97	528.46	1629.92	3493.38	4242.33	4249.65	4251.97	1996.85	170.14	-2429.18	-4327.17
1-2 Φ	8.75	166.80	163.37	2.05	0.64	414.57	1225.52	2628.93	2997.94	3109.68	3190.91	1349.37	201.73	-1827.35	-3164.85
2-3 Φ	10.83	131.07	129.22	1.41	0.46	277.82	866.43	1849.27	2197.71	2201.77	2206.02	1000.18	72.79	-1286.60	-2210.96
>3 Φ	9.87	102.37	94.26	7.92	0.46	210.78	659.79	1403.91	1676.46	1719.85	1793.84	833.77	139.02	-918.22	-1667.06
MB3(Bulk)	9.84	125.56	122.32	7.92	0.71	209.58	914.00	1998.88	2576.86	2682.22	2786.05	1633.40	352.04	-1442.23	-2326.03
(-1)-0 Φ	9.88	190.28	184.21	3.19	0.94	403.56	1416.80	3180.26	4022.87	4078.74	4099.19	2155.06	458.71	-2001.72	-4055.11
0-1 Φ	10.00	184.94	179.95	2.70	0.92	409.89	1352.49	2892.63	3559.03	3616.12	3618.91	1854.54	216.32	-1847.93	-3519.61
1-2 Φ	11.21	108.82	107.93	0.82	0.52	244.21	744.35	1579.79	1934.26	1971.28	2026.85	1004.82	151.24	-960.43	-1851.95
2-3 Φ	10.64	117.50	114.68	2.40	0.43	233.90	746.79	1578.59	1886.16	1922.54	1973.59	916.91	129.16	-1037.42	-1829.95
>3 Φ	10.36	140.98	138.08	2.05	0.48	265.08	798.75	1620.51	1950.17	1994.98	2048.38	895.99	123.91	-1042.33	-1847.18
MB4(Bulk)	12.13	206.12	201.17	2.40	0.90	322.43	1100.54	2414.25	3083.21	3138.21	3300.13	1697.63	84.02	-1796.22	-2837.36
(-1)-0 Φ	10.98	266.97	261.50	2.05	1.12	426.73	1561.31	3272.85	4193.65	4262.73	4362.44	2290.51	90.73	-2483.66	-3776.77
0-1 Φ	11.42	230.40	224.27	2.66	0.91	361.97	1317.35	2811.31	3597.84	3672.34	3814.18	1993.21	128.52	-2111.41	-3232.63
1-2 Φ	11.43	137.35	135.60	1.27	0.54	236.39	847.48	1801.20	2277.45	2339.97	2429.87	1265.71	100.92	-1327.29	-2012.39
2-3 Φ	10.79	91.75	88.97	3.03	0.29	135.78	581.76	1183.49	1483.96	1531.49	1588.21	836.00	-93.61	-851.56	-1323.73
>3 Φ	7.92	102.25	97.20	4.94	0.55	175.60	603.67	1283.97	1580.89	1680.18	1712.35	856.62	-48.28	-919.78	-1427.83

S. (continuation)

Sample	$IRM_{-1000}(-5)$ (Am^2/Kg)	$HIRM_{20}(-5)$ (Am^2/Kg)	$HIRM_{40}(-5)$ (Am^2/Kg)	$HIRM_{100}(-5)$ (Am^2/Kg)	$HIRM_{300}(-5)$ (Am^2/Kg)	$HIRM_{500}(-5)$ (Am^2/Kg)	$HIRM_{-20}(-5)$ (Am^2/Kg)	$HIRM_{-40}(-5)$ (Am^2/Kg)	$HIRM_{-100}(-5)$ (Am^2/Kg)	$HIRM_{-300}(-5)$ (Am^2/Kg)	$(Bo)_{cr}$ (mT)	Rev.Sat. (mT)
				2392.37								
0-1 Φ	-6564.38	6266.99	5071.17		355.67	224.43	2225.98	4828.87	9446.87	12686.38	-60	-1000
1-2 Φ	-4304.33	4038.71	3255.15	1486.82	248.90	152.91	1528.36	3253.82	6133.62	8065.43	-58	-1000
2-3 Φ	-3119.64	2909.59	2271.81	950.22	185.00	119.94	1232.82	2612.22	4672.45	5891.41	-51	-1000
>3 Φ	-3379.70	3178.87	2525.69	1172.92	279.03	193.33	1347.17	2734.63	4933.40	6083.80	-54	-1000
BB7(Bulk)	-6940.90	6707.47	5266.07	2311.76	369.72	126.50	2178.74	4967.82	10194.08	13312.90	-60	-1000
(-1)-0 Φ	-9100.88	8626.29	7086.62	3467.26	571.62	33.24	2688.26	6219.68	12621.95	17350.57	-65	-1000
0-1 Φ	-7163.27	6869.23	5571.94	2657.85	597.41	114.05	2249.83	5283.80	10286.24	13601.26	-61	-1000
1-2 Φ	-4398.65	4218.35	3370.43	1623.26	334.32	76.39	1417.21	3348.43	6316.66	8374.70	-59	-1000
2-3 Φ	-3113.30	2950.04	2323.68	1075.31	285.47	82.98	1115.47	2472.17	4529.96	5815.33	-55	-1000
>3 Φ	-3114.84	2926.12	2275.62	1075.71	278.96	65.34	1213.91	2602.06	4544.40	5800.27	-52	-1000
MB1(Bulk)	-1675.41	1584.71	1074.99	418.64	144.00	72.45	871.60	1751.06	2768.38	3207.25	-40	-1000
(-1)-0 Φ	-2571.23	2207.40	1582.14	662.16	118.69	74.34	1043.10	2303.56	3853.41	4678.69	-45	-590
0-1 Φ	-2504.21	2053.40	1444.68	559.95	113.91	79.36	1066.12	2302.99	3764.90	4462.17	-41	-500
1-2 Φ	-1252.37	1046.62	740.70	295.26	67.80	44.60	509.19	1135.56	1826.92	2186.59	-42	-600
2-3 Φ	-854.98	712.81	501.22	219.46	61.52	31.72	373.28	789.94	1249.10	1484.64	-42	-620
>3 Φ	-930.49	786.94	559.32	262.62	95.60	58.54	426.25	850.94	1339.12	1593.34	-43	-700
MB2(Bulk)	-4868.49	4599.45	3308.46	1174.64	225.91	128.87	2202.64	4597.18	5292.59	9434.30	-60	-1000
(-1)-0 Φ	-5619.63	4296.38	2931.64	735.46	55.85	11.76	2797.05	5102.63	7919.38	10047.23	-38	-280
0-1 Φ	-4811.72	3723.51	2622.05	758.59	9.63	2.32	2255.12	4081.82	6681.15	8579.14	-42	-290
1-2 Φ	-3450.34	2776.34	1965.38	561.98	192.96	81.23	1841.54	2989.18	5018.26	6355.75	-45	-300
2-3 Φ	-2500.16	1928.20	1339.59	356.75	8.31	4.25	1205.83	2133.23	3492.62	4416.97	-42	-300
>3 Φ	-1971.31	1583.05	1134.05	389.92	117.37	73.99	960.06	1654.81	2712.06	3460.90	-46	-360
MB3(Bulk)	-2714.43	2576.46	1872.04	787.16	209.19	103.83	1152.64	2434.00	4228.27	5112.07	-48	-1000
(-1)-0 Φ	-4710.16	3695.63	2682.39	918.93	76.32	20.45	1944.13	3640.48	6100.91	8154.30	-48	-300
0-1 Φ	-4073.61	3209.03	2266.42	726.28	59.88	2.80	1764.37	3402.60	5466.84	7138.53	-44	-310
1-2 Φ	-2259.50	1782.64	1282.50	447.06	92.59	55.57	1022.03	1875.60	2987.28	3878.80	-44	-380
2-3 Φ	-2203.68	1739.69	1226.80	395.00	87.42	51.04	1056.67	1844.43	3011.01	3803.53	-44	-360
>3 Φ	-2266.59	1783.29	1249.62	427.87	98.20	53.40	1152.39	1924.47	3090.71	3895.56	-44	-400
MB4(Bulk)	-3132.11	2977.71	2199.60	885.89	216.92	161.92	1602.50	3216.11	5096.35	6137.49	-41	-1000
(-1)-0 Φ	-4178.92	3935.71	2801.13	1089.59	168.79	99.71	2071.93	4271.71	6846.10	8139.22	-41	-1000
0-1 Φ	-3616.83	3452.21	2496.84	1002.87	216.35	141.84	1820.97	3685.67	5925.59	7046.82	-41	-1000
1-2 Φ	-2304.84	2193.48	1582.39	628.68	152.43	89.90	1164.17	2328.96	3757.17	4442.26	-42	-1000
2-3 Φ	-1510.29	1452.43	1006.45	404.72	104.25	56.72	752.22	1681.82	2439.77	2911.95	-36	-1000
>3 Φ	-1642.40	1536.75	1108.67	428.38	131.46	32.16	845.72	1760.63	2632.13	3140.18	-38	-1000

T. Magnetic properties of the Kilgour Burn (KB) and the Coalpit Burn (CB) sediments.

Sample	wt (g)	X_{lf}(-8) (m^3/kg)	X_{hf}(-8) (m^3/kg)	X_{fd} %	Xarm(-5) (m^3/kg)	IRM_{20}(-5) (Am^2/Kg)	IRM_{40}(-5) (Am^2/Kg)	IRM_{100}(-5) (Am^2/Kg)	IRM_{300}(-5) (Am^2/Kg)	IRM_{500}(-5) (Am^2/Kg)	SIRM(-5) (Am^2/Kg)	IRM_{-20}(-5) (Am^2/Kg)	IRM_{-40}(-5) (Am^2/Kg)	IRM_{-100}(-5) (Am^2/Kg)	IRM_{-300}(-5) (Am^2/Kg)
KB1 (Bulk)	8.58	45.46	44.29	2.56	0.29	111.28	466.24	906.21	993.79	1016.10	1039.17	452.16	-185.09	-737.56	-841.31
(-1)-0 Φ	8.54	35.14	32.79	6.67	0.28	64.09	254.43	566.42	714.55	762.60	811.65	466.69	-134.56	-308.97	-530.94
0-1 Φ	9.65	69.43	69.43	0.00	0.29	158.46	712.37	1350.18	1456.98	1493.19	1500.16	676.85	-245.95	-1112.04	-1221.92
1-2 Φ	8.17	53.89	53.89	0.00	0.30	135.42	623.54	1120.82	1173.45	1192.81	1197.70	483.44	-276.67	-962.12	-1003.03
2-3 Φ	8.77	22.82	21.67	5.00	0.20	61.08	250.33	396.79	430.56	438.41	448.33	197.98	-131.06	-296.86	-350.58
>3 Φ	8.26	24.23	24.23	0.00	0.23	59.95	229.27	337.31	398.58	413.64	428.41	203.42	-101.54	-265.91	-303.32
KB2 (Bulk)	10.46	82.02	81.21	0.99	0.30	196.16	840.05	1733.30	2002.26	2021.43	2024.65	1124.08	-133.64	-1618.99	-2046.59
(-1)-0 Φ	10.07	308.78	306.79	0.64	0.84	623.60	2177.42	4255.52	4872.01	4881.89	4884.83	2753.21	-480.08	-3705.20	-4724.76
0-1 Φ	7.93	212.81	210.20	1.23	0.80	567.97	2539.03	4769.55	5525.34	5546.23	5769.19	3013.31	-567.74	-4675.29	-5656.97
1-2 Φ	10.67	53.44	52.50	1.75	0.22	127.90	401.07	871.63	943.65	945.10	946.85	584.07	-142.92	-819.38	-928.90
2-3 Φ	10.54	17.08	17.08	0.00	0.12	24.32	140.90	285.17	330.48	333.13	335.22	163.61	-100.99	-240.72	-330.86
KB3 (Bulk)	11.58	123.51	121.78	1.40	0.42	253.39	1064.54	2155.16	2545.49	2619.62	2681.15	1116.36	-401.37	-2180.60	-2629.69
(-1)-0 Φ	10.57	460.83	457.99	0.62	1.27	979.44	4037.05	7790.55	9129.85	9668.90	9746.40	3809.94	-1940.37	-8148.10	-9531.62
0-1 Φ	12.30	416.43	413.18	0.78	0.96	833.68	3706.99	7415.97	8382.28	8563.16	8749.33	3541.90	-1698.41	-7616.27	-8670.04
1-2 Φ	12.95	74.93	74.93	0.00	0.25	145.51	703.30	1479.32	1709.74	1744.69	1786.05	762.68	-232.21	-1505.26	-1752.56
2-3 Φ	11.70	20.52	20.52	0.00	0.05	17.82	195.18	424.23	506.46	514.69	529.47	208.57	-60.69	-432.69	-520.28
>3 Φ	9.77	32.77	32.77	0.00	0.16	35.99	274.65	588.40	676.73	711.77	742.48	309.95	-55.56	-558.84	-689.80
KB4 (Bulk)	13.44	365.33	363.84	0.41	0.94	155.88	2770.61	5325.90	5689.62	5721.58	5721.73	3379.34	-1202.56	-4996.05	-5712.51
(-1)-0 Φ	10.40	360.61	358.69	0.53	1.02	465.98	2698.27	5352.78	5813.52	5838.07	6008.89	2762.14	-840.42	-4641.54	-5666.50
0-1 Φ	11.30	616.71	613.17	0.57	1.44	783.27	4825.79	9793.80	10139.92	10214.39	10421.58	4486.82	-2313.47	-8673.33	-10138.11
1-2 Φ	11.84	175.65	174.80	0.48	0.37	232.33	1381.24	2842.82	2894.96	2927.33	2976.14	1296.07	-657.25	-2518.00	-2890.68
2-3 Φ	12.98	36.98	36.98	0.00	0.19	51.65	283.49	640.09	659.35	667.95	677.94	307.82	-111.01	-523.04	-662.94
>3 Φ	10.65	47.91	47.91	0.00	0.27	87.84	343.94	722.93	784.69	815.66	821.04	367.96	-148.60	-601.46	-793.53
KB5 (Bulk)	11.78	171.51	170.66	0.50	0.48	97.49	1363.41	2793.06	3017.82	3036.74	3056.55	1817.53	-475.58	-2549.02	-3009.12
(-1)-0 Φ	10.71	238.03	238.03	0.00	0.88	427.26	1696.23	3588.57	4258.84	4273.40	4359.92	2346.72	-149.06	-2894.87	-4015.89
0-1 Φ	8.89	335.71	333.52	0.65	0.98	811.58	3924.80	7776.48	8657.05	8658.52	8666.44	4668.93	-1093.61	-7660.47	-8664.28
1-2 Φ	8.76	126.23	124.97	1.00	0.29	293.39	1546.47	3285.82	3533.17	3537.86	3652.24	1907.68	-497.24	-3239.54	-3608.55
2-3 Φ	11.99	40.04	40.04	0.00	0.20	102.74	323.55	697.01	727.60	733.83	749.30	340.68	-118.01	-628.11	-733.79
>3 Φ	9.52	45.19	45.19	0.00	0.28	111.82	318.32	668.04	713.82	732.96	758.13	392.12	-110.19	-546.45	-689.50
KB6 (Bulk)	12.23	226.51	224.06	1.08	0.70	139.01	736.49	3028.73	3467.96	3459.24	3543.72	2153.82	-312.95	-2557.87	-3394.27
(-1)-0 Φ	10.08	281.80	276.84	1.76	1.05	738.90	2036.82	4193.85	5229.96	5368.32	5483.42	2837.19	162.52	-3262.89	-4901.60

T. (continuation)

Sample	$IRM_{-1000}(-5)$ (Am^2/Kg)	$HIRM_{20}(-5)$ (Am^2/Kg)	$HIRM_{40}(-5)$ (Am^2/Kg)	$HIRM_{100}(-5)$ (Am^2/Kg)	$HIRM_{300}(-5)$ (Am^2/Kg)	$HIRM_{500}(-5)$ (Am^2/Kg)	$HIRM_{-20}(-5)$ (Am^2/Kg)	$HIRM_{-40}(-5)$ (Am^2/Kg)	$HIRM_{-100}(-5)$ (Am^2/Kg)	$HIRM_{-300}(-5)$ (Am^2/Kg)	$(Bo)_{cr}$ (mT)	Rev.Sat. (mT)
KB1 (Bulk)	-900.55	927.88	572.92	132.95	45.38	23.07	587.00	1201.19	1753.65	1857.41	-35	-1000
(-1)-0 Φ	-699.95	747.56	557.23	245.23	97.11	49.05	344.96	897.17	1071.57	1293.55	-36	-1000
0-1 Φ	-1307.65	1341.70	787.78	149.98	43.17	6.96	823.31	1739.14	2605.23	2715.11	-35	-1000
1-2 Φ	-1053.56	1062.28	574.16	76.88	24.25	4.89	714.26	1469.48	2154.93	2195.84	-32	-1000
2-3 Φ	-391.80	387.26	198.00	51.54	17.77	9.92	250.35	569.47	735.27	788.99	-31	-1000
>3 Φ	-363.05	368.46	199.14	90.60	29.82	14.77	224.99	515.18	679.55	716.96	-32	-1000
KB2 (Bulk)	-2117.40	1828.49	1184.61	291.36	22.39	3.22	900.57	2155.07	3640.42	4068.01	-41	-280
(-1)-0 Φ	-4972.63	4261.23	2707.41	629.31	12.82	2.94	2131.62	5361.97	8587.09	9606.65	-40	-380
0-1 Φ	-5895.37	5201.21	3230.16	999.63	243.85	222.95	2755.87	6113.97	10221.53	11203.21	-40	-360
1-2 Φ	-948.91	818.95	545.78	75.21	3.20	1.74	362.77	1088.02	1764.48	1874.00	-38	-1000
2-3 Φ	-340.52	310.90	194.32	50.05	4.73	2.09	171.60	434.12	573.85	663.99	-34	-310
KB3 (Bulk)	-2711.27	2427.75	1616.60	525.99	135.65	61.52	1564.79	3021.00	4800.22	5249.32	-35	-380
(-1)-0 Φ	-9911.74	8766.97	5709.36	1955.86	616.55	77.51	5936.47	11609.26	17816.99	19200.52	-32	-370
0-1 Φ	-8837.68	7915.65	5042.34	1333.36	367.05	186.17	5207.43	10261.57	16179.44	17233.21	-32	-340
1-2 Φ	-1795.82	1640.54	1082.75	306.73	76.31	41.36	1023.37	1976.90	3249.95	3497.25	-36	-390
2-3 Φ	-542.49	511.65	334.29	105.24	23.00	14.77	320.90	575.38	947.38	1034.97	-36	-360
>3 Φ	-746.13	706.49	467.82	154.08	65.75	30.71	432.52	767.32	1270.61	1401.57	-37	-1000
KB4 (Bulk)	-5863.63	5565.85	2951.12	395.83	32.11	0.15	2342.39	6924.14	10717.63	11434.08	-34	-300
(-1)-0 Φ	-5973.10	5542.91	3310.62	656.10	198.36	170.81	3246.74	6678.49	10479.61	11504.57	-35	-1000
0-1 Φ	-10423.71	9638.31	5595.79	627.78	281.66	207.19	5934.76	12527.85	18887.72	20352.50	-32	-1000
1-2 Φ	-2981.51	2743.81	1594.90	133.31	81.18	48.81	1680.06	3584.57	5445.32	5818.00	-32	-1000
2-3 Φ	-683.66	626.29	394.45	37.84	18.58	9.98	370.12	778.96	1190.99	1330.89	-34	-360
>3 Φ	-838.47	733.20	477.11	98.11	36.36	5.38	453.09	964.26	1417.12	1609.19	-33	-370
KB5 (Bulk)	-3062.28	2959.06	1693.14	263.48	38.72	19.81	1239.01	3512.32	5585.75	6045.86	-35	-1000
(-1)-0 Φ	-4318.57	3932.66	2663.69	771.34	101.08	86.52	2013.20	4422.46	7168.26	8289.28	-38	-1000
0-1 Φ	-8948.49	7854.85	4741.64	889.96	9.39	7.92	3997.50	9752.13	16318.99	17322.80	-35	-300
1-2 Φ	-3703.31	3358.85	2105.77	366.42	119.07	114.38	1744.55	4035.10	6777.40	7146.41	-36	-340
2-3 Φ	-752.92	646.57	425.75	52.29	21.71	15.48	408.63	851.84	1361.93	1467.62	-34	-1000
>3 Φ	-766.17	646.31	439.81	90.09	44.31	25.17	366.01	843.15	1279.41	1422.46	-35	-720
KB6 (Bulk)	-3616.92	3404.71	2807.23	514.99	75.75	84.48	1389.89	3772.19	6017.11	6853.50	-37	-400
(-1)-0 Φ	-5483.50	4744.52	3446.60	1289.57	253.46	115.10	2646.23	5205.79	8631.21	10269.91	-41	-1000

T. (continuation)

Sample	wt (g)	X_{lf}(-8) (m^3/kg)	X_{hf}(-8) (m^3/kg)	X_{fd} %	Xarm(-5) (m^3/kg)	IRM_{20}(-5) (Am^2/Kg)	IRM_{40}(-5) (Am^2/Kg)	IRM_{100}(-5) (Am^2/Kg)	IRM_{300}(-5) (Am^2/Kg)	IRM_{500}(-5) (Am^2/Kg)	SIRM(-5) (Am^2/Kg)	IRM_{-20}(-5) (Am^2/Kg)	IRM_{-40}(-5) (Am^2/Kg)	IRM_{-100}(-5) (Am^2/Kg)	IRM_{-300}(-5) (Am^2/Kg)
0-1 Φ	11.39	360.06	358.30	0.49	1.09	818.96	2673.74	5365.05	6071.16	6146.84	6215.18	2915.33	-609.76	-4605.95	-5727.76
1-2 Φ	11.65	123.56	122.70	0.69	0.33	247.43	963.88	1877.23	2033.47	2035.68	2060.55	893.05	-354.58	-1665.83	-1940.56
2-3 Φ	11.64	27.49	27.49	0.00	0.21	79.66	172.64	346.03	384.89	399.88	428.70	148.25	-111.18	-303.45	-351.04
>3 Φ	8.74	44.65	44.65	0.00	0.34	126.95	256.35	505.16	657.18	684.77	710.59	315.37	-100.80	-402.04	-576.22
CB1 (Bulk)	11.89	503.74	492.81	2.17	3.35	2290.08	12271.58	27615.11	29248.61	29474.99	29557.52	13522.90	-5404.17	-26913.69	-29239.72
(-1)-0 Φ	8.42	909.44	901.89	0.83	2.54	1530.22	10434.27	24712.09	26419.12	26799.28	26799.28	13895.25	-3662.99	-22999.76	-25959.38
0-1 Φ	7.20	1548.90	1534.70	0.92	4.30	2391.67	16894.73	41638.90	44583.08	45529.54	46020.64	20772.47	-7729.25	-43201.65	-45144.24
1-2 Φ	6.53	1810.04	1790.75	1.07	4.75	2982.03	20559.73	48511.05	51728.65	53004.15	53434.10	23555.64	-10277.15	-50429.51	-51496.14
2-3 Φ	9.31	468.11	464.50	0.77	1.24	895.29	5701.54	12064.63	12478.67	12594.70	12647.44	6155.65	-2802.51	-11472.38	-12406.36
>3 Φ	9.47	171.14	170.08	0.62	0.61	420.46	1921.79	3562.42	3813.35	3820.87	3842.21	1520.72	-1126.10	-3537.30	-3794.27
CB2 (Bulk)	11.01	928.08	925.35	0.29	2.56	1597.93	8165.04	17870.63	19002.58	19141.53	19218.13	7626.47	-3584.19	-16399.98	-17916.89
(-1)-0 Φ	7.65	587.30	578.78	1.45	1.75	1121.94	6413.67	14862.89	16216.19	16463.36	16465.56	8598.29	-1714.73	-13794.89	-16090.55
0-1 Φ	7.92	888.22	876.70	1.30	2.38	1521.14	9578.07	22689.78	24033.85	24303.63	24503.63	12667.15	-3128.87	-21022.34	-23983.55
1-2 Φ	8.05	1251.93	1239.75	0.97	2.37	2725.65	13314.78	32083.17	34221.99	35028.96	35497.84	16069.20	-5981.64	-32707.31	-34016.23
2-3 Φ	9.12	397.25	395.07	0.55	1.13	948.36	5067.90	10138.97	10576.06	10747.10	10783.05	5478.11	-2295.98	-9663.99	-10565.38
>3 Φ	8.03	183.16	180.51	1.45	0.73	456.72	2077.24	4324.74	4626.25	4741.40	4811.08	1988.77	-1177.67	-4427.90	-4671.48
CB3 (Bulk)	5.69	1123.73	1107.57	1.44	3.20	2115.43	12997.01	33086.66	35426.34	36135.25	36137.31	17468.26	-5710.54	-31204.73	-34752.67
(-1)-0 Φ	8.47	546.13	540.23	1.08	1.44	810.41	5751.75	13153.98	14239.71	14523.09	14552.60	7405.11	-1989.09	-12325.37	-14138.42
0-1 Φ	8.30	1162.28	1153.65	0.74	2.06	2245.39	11370.96	28465.65	30938.29	31468.38	32284.06	15057.13	-4068.74	-28717.89	-31284.42
1-2 Φ	5.54	1940.88	1924.43	0.85	5.25	3900.74	22986.38	58434.44	60606.95	62549.90	63123.06	31071.55	-9772.76	-56192.98	-60540.56
2-3 Φ	9.44	591.54	585.51	1.02	1.53	1120.18	6553.72	14803.81	15906.48	15919.17	15959.14	8107.04	-2362.62	-14061.26	-15515.43
>3 Φ	5.31	181.24	178.81	1.34	1.05	460.75	2356.12	4960.13	5406.05	5408.63	5465.88	2556.27	-1098.04	-4737.76	-5064.73
CB4 (Bulk)	12.49	1063.17	1053.56	0.90	2.63	2095.19	11087.17	23355.58	24918.32	24963.53	24996.01	13567.26	-5345.61	-27076.33	-29694.19
(-1)-0 Φ	9.07	814.70	806.32	1.03	2.23	1477.13	9051.64	20796.03	22531.55	22546.26	22739.22	11461.12	-3111.29	-19588.18	-21893.95
0-1 Φ	5.41	1205.97	1192.19	1.14	3.69	2253.05	14432.65	34071.55	38455.23	42564.32	47904.22	29028.51	-7852.90	-41804.00	-47142.19
1-2 Φ	4.00	1717.78	1701.33	0.96	6.53	4104.75	20914.93	48760.00	53041.70	53157.35	53364.50	27722.55	-4052.50	-47857.40	-52328.83
2-3 Φ	8.31	499.17	493.75	1.09	1.38	973.03	5924.77	13018.84	13932.82	13941.04	14092.13	7115.05	-2272.34	-12403.38	-13594.47
>3 Φ	8.98	167.06	163.72	2.00	0.65	510.51	2412.80	4541.81	4860.14	4865.26	5466.97	1689.93	-946.63	-3519.39	-3871.64
CB5 (Bulk)	7.86	602.56	598.17	0.73	1.70	1088.53	6533.05	14779.39	16445.45	16500.69	16691.75	7453.22	-2435.78	-14773.24	-16488.96
(-1)-0 Φ	7.29	352.51	350.19	0.66	1.10	714.87	3929.05	8910.10	9916.69	9973.30	10005.96	5112.79	-1268.99	-8483.24	-9750.93
0-1 Φ	7.40	712.83	707.25	0.78	2.00	1301.55	7979.15	18113.75	19858.89	19907.57	19913.48	9552.78	-2931.09	-17670.22	-19422.93

T. (continuation)

Sample	$IRM_{-1000}(-5)$ (Am^2/Kg)	$HIRM_{20}(-5)$ (Am^2/Kg)	$HIRM_{40}(-5)$ (Am^2/Kg)	$HIRM_{100}(-5)$ (Am^2/Kg)	$HIRM_{300}(-5)$ (Am^2/Kg)	$HIRM_{500}(-5)$ (Am^2/Kg)	$HIRM_{-20}(-5)$ (Am^2/Kg)	$HIRM_{-40}(-5)$ (Am^2/Kg)	$HIRM_{-100}(-5)$ (Am^2/Kg)	$HIRM_{-300}(-5)$ (Am^2/Kg)	$(Bo)_{cr}$ (mT)	Rev.Sat. (mT)
0-1 Φ	-6220.13	5396.21	3541.43	850.13	144.02	68.33	3299.84	6756.60	10752.79	11874.60	-36	-1000
1-2 Φ	-2062.71	1813.13	1096.68	183.33	27.08	24.88	1167.50	2390.26	3701.51	3976.24	-34	-1000
2-3 Φ	-430.87	349.03	256.05	82.66	43.81	28.82	280.45	511.06	703.33	750.92	-30	-940
>3 Φ	-689.14	583.64	454.24	205.43	53.41	25.82	395.21	785.58	1086.81	1261.00	-35	-1000
CB1 (Bulk)	-29498.55	27267.45	17285.94	1942.41	308.91	82.53	16034.62	34879.16	56388.68	58714.71	-33	-900
(-1)-0 Φ	-26041.04	25269.06	16365.01	2087.18	380.15	0.00	12904.03	30462.26	49799.04	52758.65	-35	-1000
0-1 Φ	-45429.16	43628.97	29125.92	4381.75	1437.56	491.10	25248.17	53258.79	88731.19	90673.78	-33	-1000
1-2 Φ	-52835.31	50452.07	32874.38	4923.05	1705.45	429.96	29878.46	63281.29	103433.66	104500.29	-32	-1000
2-3 Φ	-12469.01	11752.14	6945.90	582.81	168.77	52.73	6491.79	15397.22	24067.09	25001.06	-32	-1000
>3 Φ	-3868.29	3421.75	1920.42	279.79	28.86	21.34	2321.50	4946.98	7358.18	7615.15	-30	-360
CB2 (Bulk)	-17943.35	17620.20	11053.09	1347.49	215.55	76.60	11591.65	22725.72	35541.51	37058.42	-32	-1000
(-1)-0 Φ	-16190.37	15343.62	10051.89	1602.68	249.37	2.21	7867.28	18178.08	30258.25	32553.91	-37	-1000
0-1 Φ	-24044.06	22982.48	14925.55	1813.84	469.77	200.00	11836.48	27432.50	45325.97	48287.18	-36	-1000
1-2 Φ	-34904.61	32772.18	22183.06	3414.67	1275.85	468.88	19428.64	41010.60	67736.27	69045.19	-34	-1000
2-3 Φ	-10618.32	9834.69	5715.14	644.07	206.99	35.95	5304.93	13043.07	20411.09	21312.48	-33	-1000
>3 Φ	-4741.80	4354.37	2733.84	486.35	184.83	69.68	2822.32	5919.07	9169.30	9412.88	-31	-1000
CB3 (Bulk)	-35538.58	34021.88	23140.30	3050.65	710.97	2.06	18669.05	41845.80	67339.98	70887.93	-33	-1000
(-1)-0 Φ	-14296.14	13742.19	8800.85	1398.62	312.89	29.51	7147.49	16512.18	26848.45	28661.51	-34	-1000
0-1 Φ	-31480.35	30038.67	20913.10	3818.41	1345.77	815.68	17226.93	35537.12	60186.27	62752.80	-34	-1000
1-2 Φ	-62452.37	59222.32	40136.68	4688.62	2516.11	573.16	32051.51	72322.66	118742.88	123090.46	-34	-1000
2-3 Φ	-15524.24	14838.96	9405.42	1155.33	52.66	39.98	7852.11	18281.79	29980.43	31434.59	-34	-1000
>3 Φ	-5447.46	5005.13	3109.76	505.75	59.83	57.25	2909.61	6506.67	10146.39	10473.36	-32	-1000
CB4 (Bulk)	-30213.20	22900.82	13908.83	1640.42	77.69	32.47	11428.75	30309.14	52039.87	54657.72	-33	-1000
(-1)-0 Φ	-22128.32	21262.08	13687.57	1943.19	207.66	192.95	11278.09	25657.55	42134.44	44440.21	-34	-1000
0-1 Φ	-47642.62	45651.17	33471.57	13832.67	9448.98	5339.90	18875.71	50417.22	84368.31	89706.51	-35	-1000
1-2 Φ	-52792.58	49259.75	32449.58	4604.50	322.80	207.15	25641.95	57209.85	101014.75	105486.18	-37	-1000
2-3 Φ	-13637.21	13119.10	8167.36	1073.28	159.30	151.09	6977.07	16213.38	26344.42	27535.51	-34	-1000
>3 Φ	-3902.33	4956.45	3054.17	925.16	606.83	601.70	3777.04	5811.89	8384.65	8736.91	-32	-1000
CB5 (Bulk)	-16876.75	15603.22	10158.70	1912.35	246.30	191.06	9238.53	18936.47	31273.93	32989.65	-34	-350
(-1)-0 Φ	-9951.70	9291.09	6076.91	1095.85	89.27	32.66	4893.16	11242.29	18456.54	19724.23	-34	-1000
0-1 Φ	-19834.22	18611.92	11934.32	1799.73	54.59	5.91	10360.70	22838.66	37577.79	39330.50	-34	-1000

T. (continuation)

Sample	wt (g)	X_{lf}(-8) (m^3/kg)	X_{hf}(-8) (m^3/kg)	X_{fd} %	Xarm(-5) (m^3/kg)	IRM_{20}(-5) (Am^2/Kg)	IRM_{40}(-5) (Am^2/Kg)
1-2 Φ	6.77	797.34	790.21	0.89	2.21	1451.46	9195.39
2-3 Φ	7.23	493.85	490.54	0.67	1.42	950.23	6061.77
>3 Φ	7.84	331.05	328.18	0.87	1.01	634.94	4096.60
CB6 (Bulk)	13.42	2007.90	1992.99	0.74	4.67	3982.85	19686.43
(-1)-0 Φ	7.86	820.37	810.86	1.16	2.54	1497.25	8343.01
0-1 Φ	12.50	1782.17	1770.17	0.67	3.97	1899.54	17556.35
1-2 Φ	9.28	2930.29	2897.89	1.11	6.20	5457.55	30538.52
2-3 Φ	7.84	998.76	989.56	0.92	2.49	2937.99	10283.35
>3 Φ	9.77	163.83	161.79	1.25	0.51	224.73	1790.23
CB7 (Bulk)	6.36	919.07	907.87	1.22	2.61	1738.46	10336.09
(-1)-0 Φ	9.72	687.97	679.97	1.16	1.86	1169.75	7241.81
0-1 Φ	4.32	1129.99	1117.10	1.14	3.59	2028.48	13249.14
1-2 Φ	5.65	1334.80	1317.45	1.30	3.73	2500.44	14903.22
2-3 Φ	9.31	357.17	353.73	0.96	0.95	728.87	4409.48
>3 Φ	10.55	163.93	162.04	1.16	0.32	309.03	1453.63
CB8 (Bulk)	11.39	684.11	677.97	0.90	1.79	2047.18	8927.96
(-1)-0 Φ	9.93	607.19	603.16	0.66	1.99	2075.58	8479.54
0-1 Φ	9.70	765.11	762.01	0.40	2.05	2314.69	10510.35
1-2 Φ	10.30	942.11	941.14	0.10	2.27	2962.74	13960.63
2-3 Φ	11.16	363.00	361.21	0.49	0.85	1206.25	5467.66
>3 Φ	10.39	195.34	195.34	0.00	0.62	687.39	2587.95

$IRM_{100}(-5)$ (Am^2/Kg)	$IRM_{300}(-5)$ (Am^2/Kg)	$IRM_{500}(-5)$ (Am^2/Kg)	$SIRM(-5)$ (Am^2/Kg)	$IRM_{-20}(-5)$ (Am^2/Kg)	$IRM_{-40}(-5)$ (Am^2/Kg)	$IRM_{-100}(-5)$ (Am^2/Kg)	$IRM_{-300}(-5)$ (Am^2/Kg)
20879.29	22560.22	22610.27	22616.41	10750.98	-3709.06	-20365.20	-22430.47
13192.42	14233.10	14240.79	14251.71	7197.79	-2528.59	-12966.18	-14146.25
8687.30	9435.37	9458.02	9465.40	4791.89	-1425.45	-8512.99	-9388.73
42864.74	45762.16	45762.84	45811.75	18713.35	-7525.92	-40987.66	-44698.43
20452.51	23275.80	24721.85	28985.54	17541.45	-6020.18	-25520.46	-28505.32
37439.63	39538.56	39677.93	39836.99	16897.86	-6465.52	-35293.06	-38993.69
76233.96	81135.51	82552.31	83947.53	36945.29	-13488.96	-77665.67	-82511.84
26358.16	29962.83	33008.96	36988.03	22541.33	-5020.63	-33614.55	-36847.02
3632.21	3897.98	3905.48	3957.61	1604.97	-691.62	-3408.73	-3823.78
25390.22	26731.93	31699.80	36099.91	20832.39	-8190.83	-32489.63	-35363.14
16272.44	17835.14	17977.17	18210.60	9301.55	-2801.78	-15391.59	-17323.93
30548.75	35762.56	41714.76	47074.57	28377.07	-5894.86	-41374.71	-46060.64
37041.87	39530.89	46292.21	51513.44	30510.30	-9436.38	-46671.46	-51336.29
9368.65	9943.37	9986.46	10020.87	5078.37	-1865.88	-8953.38	-9730.05
2901.28	3067.20	3081.01	3107.00	1277.38	-887.33	-2593.05	-2879.20
17184.15	18464.88	18615.75	20989.79	6578.99	-3653.32	-13417.21	-14787.95
16996.04	18585.34	18724.86	21026.74	7220.28	-2438.61	-12845.96	-14821.74
20927.31	22373.02	22461.57	24921.35	7996.84	-4220.90	-16258.06	-17968.25
27628.58	28947.01	28985.62	32637.06	10389.45	-5535.06	-21569.06	-23221.51
10261.65	10730.97	10768.83	12098.93	3813.40	-2260.73	-8042.83	-8607.99
4718.69	5031.92	5058.52	5736.24	1599.80	-1181.25	-3656.79	-4011.10

T. (continuation)

Sample	IRM_{-1000}(-5) (Am^2/Kg)	$HIRM_{20}$(-5) (Am^2/Kg)	$HIRM_{40}$(-5) (Am^2/Kg)	$HIRM_{100}$(-5) (Am^2/Kg)	$HIRM_{300}$(-5) (Am^2/Kg)
1-2 Φ	-22559.57	21164.95	13421.02	1737.12	56.19
2-3 Φ	-14184.72	13301.48	8189.94	1059.28	18.61
>3 Φ	-9422.83	8830.46	5368.81	778.11	30.03
CB6 (Bulk)	-45019.84	41828.90	26125.33	2947.01	49.59
(-1)-0 Φ	-28751.80	27488.29	20642.53	8533.03	5709.74
0-1 Φ	-39183.93	37937.45	22280.63	2397.36	298.43
1-2 Φ	-82535.38	78489.98	53409.02	7713.57	2812.02
2-3 Φ	-36862.23	34050.04	26704.68	10629.87	7025.20
>3 Φ	-3851.58	3732.88	2167.38	325.39	59.63
CB7 (Bulk)	-36041.28	34361.44	25763.82	10709.69	9367.97
(-1)-0 Φ	-17533.80	17040.85	10968.79	1938.15	375.46
0-1 Φ	-46139.84	45046.09	33825.43	16525.82	11312.01
1-2 Φ	-52229.53	49012.99	36610.21	14471.57	11982.55
2-3 Φ	-9728.23	9291.99	5611.39	652.21	77.50
>3 Φ	-2935.63	2797.97	1653.37	205.72	39.80
CB8 (Bulk)	-15064.94	18942.61	12061.82	3805.64	2524.91
(-1)-0 Φ	-15103.66	18951.16	12547.21	4030.70	2441.41
0-1 Φ	-18146.05	22606.66	14411.00	3994.04	2548.34
1-2 Φ	-23362.44	29674.32	18676.44	5008.48	3690.05
2-3 Φ	-8667.68	10892.69	6631.27	1837.29	1367.97
>3 Φ	-4098.14	5048.85	3148.29	1017.55	704.32

$HIRM_{500}(-5)$ (Am^2/Kg)	$HIRM_{-20}(-5)$ (Am^2/Kg)	$HIRM_{-40}(-5)$ (Am^2/Kg)	$HIRM_{-100}(-5)$ (Am^2/Kg)	$HIRM_{-300}(-5)$ (Am^2/Kg)	$(Bo)_{cr}$ (mT)	Rev.Sat. (mT)
6.13	11865.42	26319.33	42975.48	45040.74	-34	-1000
10.92	7053.92	16769.38	27206.97	28387.03	-34	-1000
7.38	4673.51	10883.47	17971.02	18846.75	-34	-1000
48.92	27098.41	53288.76	86750.50	90461.27	-54	-1000
4263.69	11444.09	30742.03	50242.31	53227.17	-59	-1000
159.06	22939.12	46143.45	74970.99	78671.62	-55	-1000
1395.23	47002.24	96041.26	160217.98	165064.14	-51	-1000
3979.07	14446.70	38029.59	66623.51	69855.98	-51	-1000
52.13	2352.64	4597.10	7314.21	7729.25	-52	-1000
4400.11	15267.52	39890.62	64189.43	67062.94	-33	-1000
233.42	8909.04	20778.95	33368.76	35301.10	-35	-1000
5359.81	18697.50	47609.63	83089.47	87775.40	-37	-1000
5221.22	21003.13	55728.59	92963.67	97628.50	-35	-300
34.41	4942.50	11852.34	18939.85	19716.51	-33	-1000
25.99	1829.62	3968.34	5674.06	5960.21	-30	-1000
2374.03	14410.79	22269.07	32032.97	33403.71	-32	-1000
2301.88	13806.46	21163.47	31570.82	33546.60	-34	-1000
2459.79	16924.51	26682.47	38719.63	40429.82	-32	-1000
3651.45	22247.61	34520.68	50554.67	52207.13	-32	-1000
1330.11	8285.53	13029.56	18811.66	19376.82	-32	-1000
677.72	4136.44	6239.76	8715.31	9069.62	-30	-1000

U. Magnetic properties of the River Eden (RE) sediments.

Sample	wt (g)	X_{lf}(-8) (m^3/kg)	X_{hf}(-8) (m^3/kg)	X_{fd} %	Xarm(-5) (m^3/kg)	IRM_{20}(-5) (Am^2/Kg)	IRM_{40}(-5) (Am^2/Kg)	IRM_{100}(-5) (Am^2/Kg)	IRM_{300}(-5) (Am^2/Kg)	IRM_{500}(-5) (Am^2/Kg)	SIRM(-5) (Am^2/Kg)	IRM_{-20}(-5) (Am^2/Kg)	IRM_{-40}(-5) (Am^2/Kg)	IRM_{-100}(-5) (Am^2/Kg)	IRM_{-300}(-5) (Am^2/Kg)
RE1(Bulk)	7.05	36.56	35.67	2.44	0.26	100.04	220.31	746.22	1016.81	1082.65	1142.80	725.80	223.30	-480.26	-937.29
(-1)-0 Φ	8.23	194.71	189.77	2.54	1.14	454.67	1009.15	3288.24	4753.21	4981.26	5181.59	3400.16	1342.28	-2022.80	-4450.66
0-1 Φ	7.81	124.20	121.00	2.58	0.90	285.90	743.04	2328.41	3272.04	3467.29	3596.34	2311.04	757.34	-1519.83	-3061.86
1-2 Φ	9.26	43.63	42.49	2.60	0.38	121.12	361.11	837.05	1116.79	1172.30	1207.58	676.24	184.82	-546.30	-1008.03
2-3 Φ	9.30	19.44	19.09	1.83	0.19	54.49	192.26	373.84	493.49	515.60	528.71	253.69	80.45	-249.73	-438.44
>3 Φ	10.32	19.52	19.12	2.08	0.19	50.16	178.67	365.50	472.39	488.86	511.19	240.73	79.30	-232.18	-422.38
RE2(Bulk)	9.27	261.90	255.40	2.48	1.05	633.99	1861.92	4582.42	6166.48	6402.83	6597.41	3777.83	1172.96	-3215.06	-5826.12
(-1)-0 Φ	9.17	241.20	236.83	1.81	1.28	621.68	1800.07	4419.61	5977.77	6200.04	6340.32	3649.39	1172.22	-3054.73	-5648.17
0-1 Φ	9.62	212.03	207.45	2.16	1.13	652.95	1755.08	3876.99	5027.60	5176.70	5308.95	2633.91	365.92	-2891.17	-4695.01
1-2 Φ	10.73	146.27	144.44	1.26	0.60	410.59	1265.67	2686.30	3154.65	3232.77	3292.67	1261.58	-350.62	-2300.36	-2986.98
2-3 Φ	10.78	116.52	115.36	1.00	0.37	276.56	955.68	2036.41	2303.41	2350.96	2402.68	886.87	-211.41	-1739.05	-2166.27
>3 Φ	9.66	109.91	108.20	1.55	0.48	238.88	763.76	1693.53	2105.32	2207.20	2299.35	1081.19	102.89	-1273.36	-1876.62
RE3(Bulk)	9.47	25.37	24.73	2.50	0.15	82.35	216.55	484.53	598.85	624.54	662.97	373.80	17.90	-365.85	-556.46
1-2 Φ	10.26	34.54	33.69	2.45	0.21	100.73	275.92	630.07	806.17	842.90	888.04	518.14	77.38	-448.96	-745.15
2-3 Φ	11.22	22.80	22.28	2.27	0.12	64.55	174.98	432.81	508.20	525.18	551.83	292.80	-15.02	-342.30	-473.05
>3 Φ	11.37	23.08	22.52	2.40	0.14	61.76	129.06	385.09	485.25	507.57	538.22	293.34	-22.72	-302.80	-449.49
RE4(Bulk)	9.80	92.03	90.37	1.80	0.53	222.80	900.90	1889.15	2396.57	2482.74	2537.89	1395.64	180.25	-1524.72	-2276.90
(-1)-0 Φ	8.56	210.32	205.44	2.32	1.26	481.90	1895.60	4107.28	5512.94	5720.77	5842.29	3469.05	976.80	-3042.42	-5237.58
0-1 Φ	10.58	156.78	154.13	1.69	0.80	364.02	1338.13	2791.17	3650.53	3791.07	3882.24	2106.16	424.43	-2174.23	-3459.23
1-2 Φ	9.25	50.42	49.58	1.67	0.24	102.26	520.94	1063.66	1280.40	1324.95	1347.10	688.01	14.74	-912.57	-1226.42
2-3 Φ	9.52	47.46	47.07	0.82	0.16	147.13	473.56	1012.99	1120.53	1137.49	1169.10	583.49	-151.69	-930.90	-1089.53
>3 Φ	10.17	70.44	69.58	1.23	0.22	185.28	647.39	1336.84	1502.68	1540.79	1595.42	784.26	-166.41	-1225.68	-1443.54
RE5(Bulk)	7.42	65.77	64.51	1.93	0.50	169.37	462.59	1019.07	1237.77	1276.22	1306.78	621.14	-20.95	-857.80	-1158.95
(-1)-0 Φ	5.14	175.75	173.05	1.54	0.86	649.54	1615.60	3219.26	3813.20	3909.19	4003.41	1603.70	-167.93	-2714.18	-3589.87
0-1 Φ	5.33	153.41	150.84	1.67	0.64	443.78	1192.88	2568.90	3031.74	3074.73	3139.43	1623.68	99.40	-2208.51	-2841.79
1-2 Φ	6.24	60.85	59.71	1.87	0.35	173.44	473.85	1058.51	1253.57	1287.75	1316.37	625.99	-44.33	-862.44	-1193.11
2-3 Φ	8.39	34.47	33.68	2.28	0.20	82.04	267.47	545.21	634.91	657.11	682.15	297.32	-46.15	-437.28	-601.31
>3 Φ	7.24	59.00	57.76	2.11	0.33	134.99	404.17	905.15	1086.86	1125.23	1169.13	590.85	100.40	-699.12	-1003.98
RE6(Bulk)	9.58	99.21	97.21	2.01	0.45	290.76	958.46	1889.15	2160.43	2205.70	2255.92	971.86	-246.10	-1667.51	-2081.18
(-1)-0 Φ	6.26	204.82	200.53	2.10	1.07	621.23	1723.90	3481.18	4275.32	4400.06	4558.10	2280.34	197.17	-2685.35	-4002.25
0-1 Φ	9.19	173.12	169.94	1.84	0.86	603.68	1677.25	3221.43	3877.77	3973.69	4060.89	1872.66	-551.70	-2677.25	-3706.06
1-2 Φ	9.84	89.26	87.94	1.48	0.47	254.31	919.80	1798.12	2018.53	2061.45	2091.46	936.79	-257.44	-1632.57	-1958.48
2-3 Φ	10.37	85.82	85.13	0.81	0.32	231.37	838.52	1639.55	1789.87	1814.29	1819.09	752.08	-310.07	-1556.10	-1764.77
>3 Φ	8.54	124.74	121.81	2.35	0.48	317.38	1095.15	2172.32	2472.49	2520.27	2570.63	1113.41	-279.16	-1969.73	-2393.47

U. (continuation)

Sample	$IRM_{-1000}(-5)$ (Am^2/Kg)	$HIRM_{20}(-5)$ (Am^2/Kg)	$HIRM_{40}(-5)$ (Am^2/Kg)	$HIRM_{100}(-5)$ (Am^2/Kg)	$HIRM_{300}(-5)$ (Am^2/Kg)	$HIRM_{500}(-5)$ (Am^2/Kg)	$HIRM_{-20}(-5)$ (Am^2/Kg)	$HIRM_{-40}(-5)$ (Am^2/Kg)	$HIRM_{-100}(-5)$ (Am^2/Kg)	$HIRM_{-300}(-5)$ (Am^2/Kg)	$(Bo)_{cr}$ (mT)	Rev.Sat. (mT)
RE1(Bulk)	-1131.60	1042.76	922.49	396.58	126.00	60.15	417.00	919.50	1623.06	2080.09	-54	-1000
(-1)-0 Φ	-5140.44	4726.92	4172.44	1893.35	428.38	200.33	1781.43	3839.31	7204.39	9632.25	-59	-1000
0-1 Φ	-3535.62	3310.43	2853.30	1267.93	324.30	129.05	1285.30	2839.00	5116.17	6658.20	-55	-1000
1-2 Φ	-1174.50	1086.46	846.46	370.53	90.79	35.28	531.34	1022.76	1753.88	2215.61	-51	-1000
2-3 Φ	-525.73	474.22	336.46	154.88	35.22	13.11	275.02	448.26	778.44	967.16	-50	-1000
>3 Φ	-497.36	461.03	332.52	145.69	38.80	22.33	270.46	431.89	743.37	933.57	-52	-1000
RE2(Bulk)	-6411.77	5963.42	4735.49	2014.99	430.94	194.59	2819.58	5424.45	9812.47	12423.54	-51	-1000
(-1)-0 Φ	-6215.23	5718.64	4540.26	1920.71	362.55	140.28	2690.93	5168.10	9395.05	11988.49	-51	-1000
0-1 Φ	-5183.88	4656.00	3553.87	1431.96	281.35	132.25	2675.04	4943.03	8200.12	10003.96	-44	-1000
1-2 Φ	-3222.21	2882.08	2027.00	606.37	138.01	59.90	2031.09	3643.28	5593.03	6279.65	-35	-1000
2-3 Φ	-2358.93	2126.12	1447.00	366.27	99.27	51.72	1515.81	2614.09	4141.73	4568.95	-36	-1000
>3 Φ	-2260.16	2060.47	1535.58	605.82	194.03	92.15	1218.16	2196.46	3572.71	4175.97	-42	-1000
RE3(Bulk)	-641.29	580.62	446.42	178.44	64.12	38.43	289.17	645.07	1028.82	1219.43	-40	-1000
1-2 Φ	-876.89	787.31	612.12	257.98	81.88	45.14	369.90	810.67	1337.01	1633.20	-46	-1000
2-3 Φ	-542.94	487.28	376.85	119.02	43.63	26.66	259.03	566.85	894.14	1024.88	-39	-1000
>3 Φ	-530.60	476.47	409.17	153.14	52.98	30.66	244.88	560.95	841.02	987.71	-38	-1000
RE4(Bulk)	-2512.62	2315.10	1636.99	648.74	141.32	55.16	1142.25	2357.65	4062.62	4814.79	-43	-1000
(-1)-0 Φ	-5807.01	5360.39	3946.69	1735.01	329.35	121.52	2373.24	4865.49	8884.71	11079.87	-50	-1000
0-1 Φ	-3845.57	3518.22	2544.11	1091.07	231.71	91.17	1776.08	3457.81	6056.48	7341.47	-48	-1000
1-2 Φ	-1342.88	1244.85	826.16	283.44	66.71	22.15	659.10	1332.36	2259.67	2573.52	-40	-1000
2-3 Φ	-1159.44	1021.96	695.54	156.10	48.57	31.61	585.61	1320.79	2100.00	2258.62	-35	-1000
>3 Φ	-1570.41	1410.13	948.03	258.58	92.74	54.62	811.16	1761.83	2821.10	3038.96	-36	-1000
RE5(Bulk)	-1302.98	1137.41	844.19	287.71	69.01	30.56	685.64	1327.73	2164.57	2465.73	-39	-1000
(-1)-0 Φ	-3862.92	3353.87	2387.81	784.15	190.20	94.22	2399.71	4171.33	6717.59	7593.28	-37	-1000
0-1 Φ	-3015.19	2695.65	1946.55	570.53	107.69	64.70	1515.75	3040.03	5347.94	5981.21	-41	-1000
1-2 Φ	-1315.29	1142.93	842.51	257.86	62.79	28.61	690.38	1360.69	2178.81	2509.47	-38	-1000
2-3 Φ	-679.92	600.11	414.68	136.94	47.24	25.04	384.83	728.31	1119.43	1283.46	-36	-1000
>3 Φ	-1186.49	1034.14	764.96	263.98	82.27	43.90	578.28	1068.73	1868.25	2173.11	-45	-780
RE6(Bulk)	-2257.15	1965.16	1297.45	366.76	95.49	50.21	1284.06	2502.02	3923.42	4337.10	-35	-920
(-1)-0 Φ	-4547.06	3936.87	2834.20	1076.92	282.78	158.04	2277.76	4360.93	7243.45	8560.35	-41	-1000
0-1 Φ	-4076.17	3457.21	2383.64	839.45	183.12	87.20	2188.22	4612.58	6738.13	7766.95	-35	-1000
1-2 Φ	-2088.83	1837.14	1171.65	293.34	72.92	30.00	1154.67	2348.90	3724.03	4049.93	-35	-1000
2-3 Φ	-1840.14	1587.72	980.57	179.55	29.22	4.80	1067.01	2129.16	3375.20	3583.87	-33	-490
>3 Φ	-2575.89	2253.26	1475.48	398.31	98.14	50.36	1457.22	2849.79	4540.36	4964.10	-34	-880

Appendix 5

In this appendix all statistical results obtained from performing Spearman's rank correlation coefficients and analysis of variance (Mood's median test and one-way ANOVA) (see Chapter 3 for explanation) of all chemical and magnetic data obtained in this study (Appendix 4) are presented. These statistical analyses include:

A. Spearman's rank correlation coefficients for all major and trace elements concentrations measured in 24 rock samples from the River Eden catchment.

B. One-way analysis of variance (ANOVA) for all major and trace elements concentrations measured in 24 rock samples from the River Eden catchment in order to distinguish 4 groups: (1) basalts, (2) basaltic andesites, (3) andesites, and (4) dacite-ryholites.

C. Spearman's rank correlation coefficients for the 8 main elements analysed in 547 magnetite grains from igneous rocks and glacial till samples collected in the River Eden catchment.

D. Mood's median test for the 8 main elements measured in magnetite grains from samples of the 5 potential sources of magnetic minerals in the River Eden catchment: (1) basalts, (2) basaltic andesites, (3) andesites, (4) dacite-rhyolites, and (5) glacial till.

E. One-way analysis of variance (ANOVA) for magnetite mean composition values for each sample of the 5 potential sources of magnetic minerals in the River Eden catchment: (1) basalts, (2) basaltic andesites, (3) andesites, (4) dacite-rhyolites, and (5) glacial till.

F. Spearman's rank correlation coefficients for the 28 main magnetic parameters measured in 26 rock samples and 14 glacial till samples from the River Eden catchment.

G. One-way analysis of variance (ANOVA) for the 28 main magnetic parameters measured in 39 samples of the 6 potential sources of stream sediments in the River Eden catchment: (1) basalts, (2) basaltic andesites, (3) andesites, (4) dacite-rhyolites, (5) sedimentary rocks, and (6) glacial till.

A. Spearman's rank correlation coefficients for all major and trace elements concentrations measured in 24 rock samples from the River Eden catchment. $r_s \geq 0.521$ is significant at a 0.01 level.

	SiO_2	TiO_2	Al_2O_3	Fe_2O_3	MnO	MgO	CaO	Na_2O	K_2O	P_2O_5	Nb	Zr	Y	Sr	U	Rb	Th	Pb	Ga	Zn	Cu	Ni	Cr	Ce	Sc	V	Ba	La
SiO_2	1.000																											
TiO_2	-0.916	1.000																										
Al_2O_3	0.448	-0.429	1.000																									
Fe_2O_3	-0.896	0.953	-0.351	1.000																								
MnO	-0.858	0.826	-0.475	0.835	1.000																							
MgO	-0.863	0.835	-0.507	0.755	0.747	1.000																						
CaO	-0.905	0.867	-0.476	0.860	0.861	0.811	1.000																					
Na_2O	0.304	-0.253	0.704	-0.213	-0.405	-0.300	-0.257	1.000																				
K_2O	0.868	-0.850	0.389	-0.908	-0.791	-0.702	-0.892	0.096	1.000																			
P_2O_5	-0.090	0.125	0.660	0.189	-0.013	0.060	0.129	0.571	-0.132	1.000																		
Nb	0.019	-0.046	-0.195	-0.123	-0.191	0.164	0.107	0.094	-0.028	-0.026	1.000																	
Zr	0.596	-0.488	0.748	-0.454	-0.666	-0.511	-0.591	0.440	0.598	0.496	-0.161	1.000																
Y	-0.256	0.412	0.188	0.548	0.421	0.190	.385	0.145	-0.414	0.613	-0.229	0.145	1.000															
Sr	-0.250	0.235	0.407	0.232	0.222	0.073	0.354	0.525	-0.359	0.617	-0.226	0.098	0.328	1.000														
U	0.494	-0.483	0.329	-0.525	-0.726	-0.358	-0.578	0.363	0.487	-0.042	0.082	0.503	-0.423	-0.128	1.000													
Rb	0.916	-0.841	0.356	-0.878	-0.839	-0.765	-0.942	0.125	0.945	-0.153	-0.016	0.574	-0.379	-0.405	0.559	1.000												
Th	0.843	-0.801	0.381	-0.791	-0.852	-0.849	-0.824	0.286	0.723	-0.100	0.070	0.499	-0.391	-0.184	0.521	0.819	1.000											
Pb	0.772	-0.734	0.491	-0.735	-0.738	-0.817	-0.731	0.486	0.704	0.024	-0.133	0.522	-0.270	0.088	0.401	0.680	0.813	1.000										
Ga	-0.400	0.498	-0.115	0.636	0.344	0.309	0.430	-0.204	-0.493	0.305	-0.113	0.044	0.706	-0.052	-0.322	-0.432	-0.382	-0.448	1.000									
Zn	-0.694	0.800	-0.245	0.824	0.593	0.580	0.619	0.078	-0.750	0.073	-0.024	-0.430	0.340	0.100	-0.262	-0.667	-0.572	-0.514	0.416	1.000								
Cu	-0.463	0.478	-0.573	0.388	0.240	0.431	0.309	-0.580	-0.286	-0.531	0.050	-0.303	-0.325	-0.400	0.032	-0.290	-0.333	-0.443	0.187	0.368	1.000							
Ni	-0.707	0.704	-0.623	0.571	0.535	0.731	0.651	-0.362	-0.601	-0.331	0.198	-0.609	-0.275	-0.022	-0.203	-0.588	-0.506	-0.610	0.042	0.581	0.681	1.000						
Cr	-0.680	0.625	-0.576	0.508	0.448	0.674	0.614	-0.300	-0.547	-0.305	0.243	-0.592	-0.353	-0.021	-0.199	-0.572	-0.413	-0.474	0.000	0.541	0.632	0.932	1.000					
Ce	0.356	-0.274	0.704	-0.271	-0.448	-0.358	-0.291	0.576	0.340	0.748	-0.185	0.790	0.281	0.543	0.281	0.288	0.328	0.521	-0.012	-0.316	-0.475	-0.530	-0.455	1.000				
Sc	-0.940	0.963	-0.496	0.925	0.888	0.826	0.918	-0.275	-0.869	0.044	-0.057	-0.596	0.362	0.272	-0.559	-0.894	-0.838	-0.714	0.427	0.764	0.439	0.694	0.659	-0.333	1.000			
V	-0.914	942.000	-0.505	0.904	0.830	0.794	0.857	-0.280	-0.839	-0.040	-0.061	-0.592	0.253	0.178	-0.455	-0.833	-0.730	-0.685	0.389	0.835	0.516	0.770	0.748	-0.393	0.963	1.000		
Ba	0.783	-0.708	0.360	-0.798	-0.773	-0.619	-0.782	0.290	0.842	0.000	0.146	0.424	-0.352	-0.219	0.438	0.836	0.675	0.710	-0.453	-0.528	-0.367	-0.511	-0.451	0.366	-0.752	-0.738	1.000	
La	0.496	-0.446	0.705	-0.462	-0.623	-0.478	-0.460	0.604	0.455	0.613	-0.057	0.790	0.049	0.435	0.343	0.429	0.443	0.547	-0.131	-0.433	-0.454	-0.500	-0.474	0.878	-0.513	-0.568	0.508	1.000

B. Mood's median test for all major and trace elements concentrations measured in 24 rock samples from the River Eden catchment in order to distinguish 4 groups:(1) basalts, (2) basaltic andesites, (3) andesites, and (4) dacite-rhyolites.
Critical value of chi-square with 3 degrees of freedom is 11.30 at the 99% confidence level.

```
MTB > Mood 'SiO2' '4 Groups'.

Mood median test of SiO2

Chisquare = 17.14   df = 3   p = 0.001

                                          Individual 95.0% CI's
4 Groups   N<=    N>   Median    Q3-Q1   --+---------+---------+---------+----
       1    8     0     48.8      1.7    (+-)
       2    4     3     56.6      0.8              (+)
       3    0     5     59.5      1.7                (--+)
       4    0     4     66.1      5.8                             (+---------)
                                         --+---------+---------+---------+----
                                        49.0      56.0      63.0      70.0
Overall median = 56.6
* NOTE * Levels with < 6 obs. have confidence < 95.0%

MTB > Mood 'TiO2' '4 Groups'.

Mood median test of TiO2

Chisquare = 10.44   df = 3   p = 0.015

                                          Individual 95.0% CI's
4 Groups   N<=    N>   Median    Q3-Q1   ---------+---------+---------+-------
       1    1     7     2.16     0 97                          (----+--------)
       2    3     4     1.08     0.11              (+)
       3    4     1     0.73     0.20         +----)
       4    4     0     0.51     0.31   (----+)
                                         ---------+---------+---------+-------
                                              0.80      1.60      2.40
Overall median = 1.08
* NOTE * Levels with < 6 obs. have confidence < 95.0%

MTB > Mood 'Al2O3' '4 Groups'.

Mood median test of Al2O3

Chisquare = 17.57   df = 3   p = 0.001

                                          Individual 95.0% CI's
4 Groups   N<=    N>   Median    Q3-Q1   ----+---------+---------+---------+--
       1    8     0    13.99     1.15   (------+-)
       2    1     6    17.95     1.67                        (-----------+)
       3    0     5    17.83     0.73                              (----+--)
       4    3     1    15.93     1.94        (--------------+)
                                         ----+---------+---------+---------+--
                                           13.5      15.0      16.5      18.0
Overall median = 16.10
* NOTE * Levels with < 6 obs. have confidence < 95.0%

MTB > Mood 'Fe2O3' '4 Groups'.

Mood median test of Fe2O3

Chisquare = 10.44   df = 3   p = 0.015

                                          Individual 95.0% CI's
4 Groups   N<=    N>   Median    Q3-Q1   --------+---------+---------+---------
       1    1     7     12.6      3.6                         (-+-------)
       2    3     4      7.0      0.8             (-+
       3    4     1      5.5      1.0             +--)
       4    4     0      3.7      2.2   (----+)
                                         --------+---------+---------+---------
                                               5.0      10.0      15.0
Overall median = 6.9
* NOTE * Levels with < 6 obs. have confidence < 95.0%
```

B. (continuation)

```
MTB > Mood 'MnO' '4 Groups'.

Mood median test of MnO

Chisquare = 15.02   df = 3   p = 0.002

                                                  Individual 95.0% CI's
4 Groups   N<=   N>   Median    Q3-Q1  --+---------+---------+---------+----
       1    0    8    0.170    0.037                                 +-------)
       2    5    2    0.120    0.040            (------+--)
       3    4    1    0.080    0.045         (-+-------------)
       4    4    0    0.050    0.050   (-+---------)
                                       --+---------+---------+---------+----
                                      0.050     0.100     0.150     0.200
Overall median = 0.120
* NOTE * Levels with < 6 obs. have confidence < 95.0%

MTB > Mood 'MgO' '4 Groups'.

Mood median test of MgO

Chisquare = 13.49   df = 3   p = 0.004

                                                  Individual 95.0% CI's
4 Groups   N<=   N>   Median    Q3-Q1  ---------+---------+---------+------
       1    0    8      6.51     2.04                          (---+-----)
       2    5    2      2.20     0.64           (+--)
       3    3    2      2.23     1.04            +----)
       4    4    0      0.74     0.74   (-+-)
                                       ---------+---------+---------+------
                                              2.5       5.0       7.5
Overall median = 2.43
* NOTE * Levels with < 6 obs. have confidence < 95.0%

MTB > Mood 'CaO' '4 Groups'.

Mood median test of CaO

Chisquare = 13.94   df = 3   p = 0.003

                                                  Individual 95.0% CI's
4 Groups   N<=   N>   Median    Q3-Q1  ---------+---------+---------+-------
       1    0    8      8.31     0.51                                   +-)
       2    4    3      5.24     2.24             (---------+--)
       3    4    1      3.08     2.86      (-------+--------)
       4    4    0      0.98     1.60   (-+-----)
                                       ---------+---------+---------+-------
                                             2.5       5.0       7.5
Overall median = 5.26
* NOTE * Levels with < 6 obs. have confidence < 95.0%

MTB > Mood 'Na2O' '4 Groups'.

Mood median test of Na2O

Chisquare = 17.80   df = 3   p = 0.001

                                                  Individual 95.0% CI's
4 Groups   N<=   N>   Median    Q3-Q1  ---+---------+---------+---------+---
       1    8    0      2.95     1.23      (-------+-----)
       2    0    7      4.78     0.90                          (-------+---)
       3    1    4      4.77     0.72                       (----------+)
       4    3    1      2.37     2.69   (-----+-------------------------)
                                       ---+---------+---------+---------+---
                                        2.0       3.0       4.0       5.0
Overall median = 3.85
* NOTE * Levels with < 6 obs. have confidence < 95.0%
```

B. (continuation)

```
MTB > Mood 'K2O' '4 Groups'.

Mood median test of K2O

Chisquare = 10.44   df = 3   p = 0.015

                                                Individual 95.0% CI's
4 Groups   N<=    N>   Median    Q3-Q1  ----+---------+---------+---------+---
       1    7     1     1.09     0.31  (+-)
       2    4     3     1.91     1.16        +-------)
       3    1     4     3.83     2.97        (-------------+------------)
       4    0     4     5.30     2.93             (------------------+----)
                                       ----+---------+---------+---------+---
                                         1.5       3.0       4.5       6.0
Overall median = 2.03
* NOTE * Levels with < 6 obs. have confidence < 95.0%

MTB > Mood 'P2O5' '4 Groups'.

Mood median test of P2O5

Chisquare = 12.29   df = 3   p = 0.007

                                                Individual 95.0% CI's
4 Groups   N<=    N>   Median    Q3-Q1  ------+---------+---------+---------+
       1    6     2    0.275     0.120            (--+-------)
       2    2     5    0.610     0.340               (----------------------+
       3    0     5    0.420     0.110                         (+-----------)
       4    4     0    0.215     0.123   (---------+)
                                       ------+---------+---------+---------+
                                          0.15      0.30      0.45      0.60
Overall median = 0.340
* NOTE * Levels with < 6 obs. have confidence < 95.0%

MTB > Mood 'Nb' '4 Groups'.

Mood median test of Nb

Chisquare = 1.87   df = 3   p = 0.600

                                                Individual 95.0% CI's
4 Groups   N<=    N>   Median    Q3-Q1  ---------+---------+---------+-------
       1    4     4     13.5     13.8   (----+---------------------------------)
       2    5     2     13.0      3.0   (---+---)
       3    2     3     14.0      1.0       (-+
       4    3     1     13.0      5.3       +-------------)
                                       ---------+---------+---------+-------
                                              15.0      20.0      25.0
Overall median = 13.0
* NOTE * Levels with < 6 obs. have confidence < 95.0%

MTB > Mood 'Zr' '4 Groups'.

Mood median test of Zr

Chisquare = 14.29   df = 3   p = 0.003

                                                Individual 95.0% CI's
4 Groups   N<=    N>   Median    Q3-Q1  --+---------+---------+---------+----
       1    8     0      165       40       (----+--)
       2    2     5      285       45                        (-------+)
       3    0     5      303       16                                 (--+
       4    2     2      264      155  (--------------------------+-----)
                                       --+---------+---------+---------+----
                                         120       180       240       300
Overall median = 256
* NOTE * Levels with < 6 obs. have confidence < 95.0%
```

B. (continuation)

```
MTB > Mood 'Y' '4 Groups'.

Mood median test of Y

Chisquare = 5.94   df = 3   p = 0.115

                                                Individual 95.0% CI's
4 Groups   N<=   N>   Median    Q3-Q1  ----+---------+---------+---------+---
       1    4    4     26.5      8.4             (----+----------)
       2    3    4     33.0     14.5    (-----------------------+---)
       3    1    4     28.0      4.5                (---+----------)
       4    4    0     19.0      5.3  (-+-----------)
                                       ----+---------+---------+---------+---
                                        20.0      25.0      30.0      35.0
Overall median = 27.0
* NOTE * Levels with < 6 obs. have confidence < 95.0%

MTB > Mood 'Sr' '4 Groups'.

Mood median test of Sr

Chisquare = 6.77   df = 3   p = 0.080

                                                Individual 95.0% CI's
4 Groups   N<=   N>   Median    Q3-Q1  --------+---------+---------+---------
       1    6    2      400      109                (--+---)
       2    1    6      605      208                  (----------+--)
       3    2    3      424      294         (----------+--------)
       4    3    1      108      352   (-+-------------------)
                                       --------+---------+---------+---------
                                             200       400       600
Overall median = 414
* NOTE * Levels with < 6 obs. have confidence < 95.0%

MTB > Mood 'U' '4 Groups'.

Mood median test of U

Chisquare = 5.32   df = 3   p = 0.150

                                                Individual 95.0% CI's
4 Groups   N<=   N>   Median    Q3-Q1  +---------+---------+---------+------
       1    7    1     0.00     0.38  +--------)
       2    4    3     0.50     1.50  (------+---------------)
       3    2    3     1.00     1.25         (-------+----------------------)
       4    1    3     1.50     1.75  (---------------------+--------)
                                       +---------+---------+---------+------
                                     0.00      0.70      1.40      2.10
Overall median = 0.50
* NOTE * Levels with < 6 obs. have confidence < 95.0%

MTB > Mood 'Rb' '4 Groups'.

Mood median test of Rb

Chisquare = 13.87   df = 3   p = 0.003

                                                Individual 95.0% CI's
4 Groups   N<=   N>   Median    Q3-Q1  ------+---------+---------+---------+
       1    8    0       26       11  (--+)
       2    4    3       41       10       (+---)
       3    1    4       57       27        (---+--------)
       4    0    4      127       78              (-----------------+----)
                                       ------+---------+---------+---------+
                                            40        80       120       160
Overall median = 42
* NOTE * Levels with < 6 obs. have confidence < 95.0%
```

B. (continuation)

```
MTB > Mood 'Th' '4 Groups'.

Mood median test of Th

Chisquare = 13.94   df = 3   p = 0.003

                                                  Individual 95.0% CI's
4 Groups   N<=    N>   Median    Q3-Q1  ------+---------+---------+---------+
       1    8     0      2.0      2.0  (-+-----)
       2    3     4      6.0      2.0          (--+----)
       3    1     4      6.5      2.2        (-------+---)
       4    0     4     13.0      0.8                                  +--)
                                        ------+---------+---------+---------+
                                            3.5       7.0      10.5      14.0
Overall median = 5.7
* NOTE * Levels with < 6 obs. have confidence < 95.0%

MTB > Mood 'Pb' '4 Groups'.

Mood median test of Pb

Chisquare = 13.49   df = 3   p = 0.004

                                                  Individual 95.0% CI's
4 Groups   N<=    N>   Median    Q3-Q1  +---------+---------+---------+------
       1    8     0      0.8      2.6  (+---)
       2    2     5     13.0      6.0              (-----+--------)
       3    2     3     12.5     14.3             (-----+----------)
       4    0     4     14.0      8.3                   (+----------)
                                        +---------+---------+---------+------
                                      0.0       7.0      14.0      21.0
Overall median = 10.0
* NOTE * Levels with < 6 obs. have confidence < 95.0%

MTB > Mood 'Ga' '4 Groups'.

Mood median test of Ga

Chisquare = 5.94   df = 3   p = 0.115

                                                  Individual 95.0% CI's
4 Groups   N<=    N>   Median    Q3-Q1  ------+---------+---------+---------+-
       1    3     5    21.00     3.50                (----+----------)
       2    3     4    21.00     4.50  (-----------------+---)
       3    4     1    20.00     3.00        (--------+-------)
       4    4     0    19.00     2.75     (-------+---)
                                        -----+---------+---------+---------+-
                                          17.5      20.0      22.5      25.0
Overall median = 20.00
* NOTE * Levels with < 6 obs. have confidence < 95.0%

MTB > Mood 'Zn' '4 Groups'.

Mood median test of Zn

Chisquare = 10.44   df = 3   p = 0.015

                                                  Individual 95.0% CI's
4 Groups   N<=    N>   Median    Q3-Q1  -------+---------+---------+---------
       1    1     7       98       22                    (-+-----)
       2    3     4       83       19                (--+----------------)
       3    4     1       60       13              +-----)
       4    4     0       22       45  (-+-------------)
                                        -------+---------+---------+---------
                                              40        80       120
Overall median = 81
* NOTE * Levels with < 6 obs. have confidence < 95.0%
```

B. (continuation)

```
MTB > Mood 'Cu' '4 Groups'.

Mood median test of Cu

Chisquare = 9.64   df = 3   p = 0.022

                                          Individual 95.0% CI's
4 Groups   N<=    N>   Median    Q3-Q1  ----------+---------+---------+------
       1    1     7       61       31                  (---+---------)
       2    4     3        9       16    (+-----)
       3    5     0        7        5    +-)
       4    2     2       45       96   (-------------+-------------------)
                                         ----------+---------+---------+------
                                                  30        60        90

Overall median = 13
* NOTE * Levels with < 6 obs. have confidence < 95.0%

MTB > Mood 'Ni' '4 Groups'.

Mood median test of Ni

Chisquare = 14.14   df = 3   p = 0.003

                                          Individual 95.0% CI's
4 Groups   N<=    N>   Median    Q3-Q1  ----------+---------+---------+------
       1    0     8       60      100          (----+-----------------)
       2    4     3        5       34   +---------)
       3    5     0        3        4  (+
       4    3     1       13       10  (--+
                                         ----------+---------+---------+------
                                                  50        100       150

Overall median = 13
* NOTE * Levels with < 6 obs. have confidence < 95.0%

MTB > Mood 'Cr' '4 Groups'.

Mood median test of Cr

Chisquare = 14.14   df = 3   p = 0.003

                                          Individual 95.0% CI's
4 Groups   N<=    N>   Median    Q3-Q1  ----------+---------+---------+------
       1    0     8      126      223     (------------+--------------------)
       2    4     3        7       65   +-----------)
       3    5     0        4        4   +
       4    3     1        8       15  (+-)
                                         ----------+---------+---------+------
                                                  80        160       240

Overall median = 16
* NOTE * Levels with < 6 obs. have confidence < 95.0%

MTB > Mood 'Ce' '4 Groups'.

Mood median test of Ce

Chisquare = 17.57   df = 3   p = 0.001

                                          Individual 95.0% CI's
4 Groups   N<=    N>   Median    Q3-Q1  ----+---------+---------+---------+--
       1    8     0     48.5      9.6            (---+--)
       2    1     6     74.5     15.0                        (-------+----)
       3    0     5     76.5      7.5                          (-+--)
       4    3     1     62.5     30.8   (----------------------+--)
                                         ----+---------+---------+---------+--
                                           32        48        64        80

Overall median = 65.5
* NOTE * Levels with < 6 obs. have confidence < 95.0%
```

B. (continuation)

```
MTB > Mood 'Sc' '4 Groups'.

Mood median test of Sc

Chisquare = 17.14   df = 3   p = 0.001

                                                Individual 95.0% CI's
4 Groups   N<=    N>   Median    Q3-Q1  ---------+---------+---------+-------
       1    0     8     26.0     10.9                        (----+--------)
       2    3     4     12.0      3.5             (-+-)
       3    5     0      6.0      3.3      (-+----)
       4    4     0      2.5      2.5  (-+)
                                        ---------+---------+---------+-------
                                                10        20        30

Overall median = 11.2
* NOTE * Levels with < 6 obs. have confidence < 95.0%

MTB > Mood 'V' '4 Groups'.

Mood median test of V

Chisquare = 17.14   df = 3   p = 0.001

                                                Individual 95.0% CI's
4 Groups   N<=    N>   Median    Q3-Q1  +---------+---------+---------+-------
       1    0     8      328      292                  (--------+-----------)
       2    3     4       68       48       (+--)
       3    5     0       47       15      +)
       4    4     0       41       36  (--+
                                        +---------+---------+---------+-------
                                        0        150       300       450

Overall median = 67
* NOTE * Levels with < 6 obs. have confidence < 95.0%

MTB > Mood 'Ba' '4 Groups'.

Mood median test of Ba

Chisquare = 13.94   df = 3   p = 0.003

                                                Individual 95.0% CI's
4 Groups   N<=    N>   Median    Q3-Q1  -------+---------+---------+---------
       1    8     0      314       48  (--+
       2    3     4      508      254             (+-------------)
       3    1     4      578      215            (------+--------)
       4    0     4      647      261                    (-+---------------)
                                        -------+---------+---------+---------
                                             400       600       800

Overall median = 498
* NOTE * Levels with < 6 obs. have confidence < 95.0%

MTB > Mood 'La' '4 Groups'.

Mood median test of La

Chisquare = 14.14   df = 3   p = 0.003

                                                Individual 95.0% CI's
4 Groups   N<=    N>   Median    Q3-Q1  -----+---------+---------+---------+-
       1    8     0     20.0      2.5  (---+)
       2    3     4     34.0     10.5                    (------+--------)
       3    0     5     32.0      3.0                      (-+---)
       4    1     3     32.0     10.2      (----------------+)
                                        -----+---------+---------+---------+-
                                          21.0      28.0      35.0      42.0

Overall median = 30.8
* NOTE * Levels with < 6 obs. have confidence < 95.0%
```

C. Spearman's rank correlation coefficients for the 8 main elements analysed in 547 magnetite grains from igneous rocks and glacial till samples collected in the River Eden catchment.
$r_s \geq 0.521$ is significant at a 0.01 level.

	SiO_2	TiO_2	Al_2O_3	Fe_2O_3	FeO	MnO	MgO	CaO
SiO_2	1.000							
TiO_2	-0.158	1.000						
Al_2O_3	-0.033	0.003	1.000					
Fe_2O_3	-0.023	-0.954	-0.042	1.000				
FeO	0.003	0.937	-0.033	-0.916	1.000			
MnO	-0.191	0.469	0.171	-0.409	0.345	1.000		
MgO	-0.141	0.007	0.354	-0.008	-0.129	-0.051	1.000	
CaO	0.482	0.004	-0.216	-0.113	0.126	-0.207	-0.296	1.000

D. Mood's median test for the 8 main elements measured in magnetite grains from samples of the 5 potential sources of magnetic minerals in the River Eden catchment: (1) basalts, (2) basaltic andesites, (3) andesites, (4) dacite-rhyolites, and (5) glacial till.
Critical value of chi-square with 4 degrees of freedom is13.3at the 99% confidence level.

```
MTB > Mood 'SiO2' 'Group 5'.

Mood median test of SiO2

Chisquare = 55.42   df = 4   p = 0.000

                                                Individual 95.0% CI's
Group 5   N<=   N>   Median   Q3-Q1   ---------+---------+---------+---------
      1    68   66     0.40    0.77     +)
      2   137   67     0.33    0.31    +
      3    21   70     1.04    1.54          (--+---)
      4    35   36     0.41    0.38     +)
      5     8   20     0.93    3.12     (-------+-------------------------)
                                        ---------+---------+---------+---------
                                            0.80      1.60      2.40

Overall median = 0.40

MTB > Mood 'TiO2' 'Group 5'.

Mood median test of TiO2

Chisquare = 188.38   df = 4   p = 0.000

                                                Individual 95.0% CI's
Group 5   N<=   N>   Median   Q3-Q1   ------+---------+---------+---------+-
      1    15  119     17.0     7.7                                  (-+--)
      2    91  113     13.3     8.5                            (--+--)
      3    84    7      3.4     4.0   (-+)
      4    62    9      5.5     5.2       (-+--)
      5    12   16     14.4    12.2                       (-----+-------)
                                        ------+---------+---------+---------+-
                                             5.0      10.0      15.0      20.0

Overall median = 12.3

MTB > Mood 'Al2O3' 'Group 5'.

Mood median test of Al2O3

Chisquare = 9.10   df = 4   p = 0.059

                                                Individual 95.0% CI's
Group 5   N<=   N>   Median   Q3-Q1   ----------+---------+---------+------
      1    67   67    0.910   0.783            (---------+---)
      2    92  112    0.965   0.612                  (--+---)
      3    53   38    0.785   0.827    (--------+--------)
      4    42   29    0.833   0.819          (-----+----)
      5    10   18    1.148   0.858              (-----------------+------)
                                        ----------+---------+---------+------
                                             0.80      1.00      1.20

Overall median = 0.913

MTB > Mood 'Fe2O3' 'Group 5'.

Mood median test of Fe2O3

Chisquare = 179.18   df = 4   p = 0.000

                                                Individual 95.0% CI's
Group 5   N<=   N>   Median   Q3-Q1   ------+---------+---------+---------+
      1   117   17     26.9    12.0    (-+-)
      2   109   95     37.3    16.1             (--+--)
      3     8   83     54.3    12.1                                (--+-)
      4    10   61     49.5    11.4                           (-+---)
      5    20    8     30.8    31.6   (------+----)
                                        ------+---------+---------+---------+
                                            30        40        50        60

Overall median = 38.6
```

D. (continuation)

```
MTB > Mood 'FeO' 'Group 5'.

Mood median test of FeO

Chisquare = 175.89   df = 4   p = 0.000

                                                Individual 95.0% CI's
Group 5   N<=    N>   Median    Q3-Q1  ---------+---------+---------+---------
      1    19   115     45.4      6.0                                  (-+--)
      2    91   113     40.4      7.7                       (-+-)
      3    82     9     33.8      3.9   (-+-)
      4    63     8     33.9     12.2  (--+-)
      5     9    19     43.0      9.8                         (------+------)
                                        ---------+---------+---------+---------
                                              36.0      40.0      44.0

Overall median = 39.9

MTB > Mood 'MnO' 'Group 5'.

Mood median test of MnO

Chisquare = 32.24   df = 4   p = 0.000

                                                Individual 95.0% CI's
Group 5   N<=    N>   Median    Q3-Q1  ---+---------+---------+---------+---
      1    53    81     0.73     0.94          (--+--)
      2    92   112     0.65     1.31        (-+--)
      3    69    22     0.41     0.37   (-+)
      4    36    35     0.58     5.86  (-------+-------------------------)
      5    15    13     0.54     1.02      (-+-----------)
                                        ---+---------+---------+---------+---
                                        0.40      0.80      1.20      1.60

Overall median = 0.58

MTB > Mood 'MgO' 'Group 5'.

Mood median test of MgO

Chisquare = 40.62   df = 4   p = 0.000

                                                Individual 95.0% CI's
Group 5   N<=    N>   Median    Q3-Q1  +---------+---------+---------+------
      1    93    41    0.005    0.235  +--)
      2    71   133    0.405    0.993                        (-------+------)
      3    51    40    0.070    0.350  (----+----------)
      4    34    37    0.190    1.000        (------+-------------)
      5    15    13    0.146    0.336     (-----+------)
                                        +---------+---------+---------+------
                                      0.00      0.15      0.30      0.45

Overall median = 0.157

MTB > Mood 'CaO' 'Group 5'.

Mood median test of CaO

Chisquare = 84.87   df = 4   p = 0.000

                                                Individual 95.0% CI's
Group 5   N<=    N>   Median    Q3-Q1  ------+---------+---------+---------+
      1    42    92    0.160    0.303              (----+----)
      2   144    60    0.060    0.070    (+-)
      3    28    63    0.130    0.180          (---+---)
      4    51    20    0.060    0.090   (-+--)
      5     8    20    0.204    0.475           (----------+----------)
                                        ------+---------+---------+---------+
                                          0.080     0.160     0.240     0.320

Overall median = 0.090
```

E. One-way analysis of variance (ANOVA) for magnetite mean composition values for each sample of the 5 potential sources of magnetic minerals in the River Eden catchment: (1) basalts, (2) basaltic andesites, (3) andesites, (4) dacite-rhyolites, and (5) glacial till.
Critical value of F with 4 and 22 degrees of freedom is 4.31 at the 99% confidence level.

```
MTB > Oneway 'SiO2' '5 groups'.

ANALYSIS OF VARIANCE ON SiO2
SOURCE      DF         SS         MS         F         p
5 groups     4      2.114      0.528      2.78     0.052
ERROR       22      4.181      0.190
TOTAL       26      6.294

                                        INDIVIDUAL 95 PCT CI'S FOR MEAN
                                        BASED ON POOLED STDEV
 LEVEL       N       MEAN      STDEV  -+---------+---------+---------+-----
     1       7     0.9124     0.7236               (------*------)
     2       7     0.3709     0.0950     (-----*------)
     3       8     0.9913     0.3630                 (------*-----)
     4       3     0.4819     0.1761  (----------*---------)
     5       2     1.1000     0.0000             (------------*------------)
                                       -+---------+---------+---------+-----
POOLED STDEV =    0.4359              0.00      0.50      1.00      1.50
MTB > Oneway 'TiO2' '5 groups'.

ANALYSIS OF VARIANCE ON TiO2
SOURCE      DF         SS         MS         F         p
5 groups     4      500.2      125.1      3.71     0.019
ERROR       22      742.0       33.7
TOTAL       26     1242.2

                                        INDIVIDUAL 95 PCT CI'S FOR MEAN
                                        BASED ON POOLED STDEV
 LEVEL       N       MEAN      STDEV  -+---------+---------+---------+-----
     1       7     16.872      8.147                    (-----*------)
     2       7     14.808      5.914                  (-----*------)
     3       8      7.070      4.080       (-----*-----)
     4       3      6.872      2.946     (----------*---------)
     5       2     13.700      0.000           (------------*-----------)
                                       -+---------+---------+---------+-----
POOLED STDEV =     5.808              0.0       7.0      14.0      21.0
MTB > Oneway 'Al2O3' '5 groups'.

ANALYSIS OF VARIANCE ON Al2O3
SOURCE      DF         SS         MS         F         p
5 groups     4      1.007      0.252      1.00     0.428
ERROR       22      5.527      0.251
TOTAL       26      6.534

                                        INDIVIDUAL 95 PCT CI'S FOR MEAN
                                        BASED ON POOLED STDEV
 LEVEL       N       MEAN      STDEV  ----+---------+---------+---------+--
     1       7     0.9297     0.5615        . (---------*---------)
     2       7     0.9308     0.4403          (---------*---------)
     3       8     1.3621     0.5193                    (--------*--------)
     4       3     0.9530     0.5407      (--------------*--------------)
     5       2     1.0000     0.0000    (-----------------*-----------------)
                                       ----+---------+---------+---------+--
POOLED STDEV =    0.5012               0.40      0.80      1.20      1.60
MTB > Oneway 'Fe2O3' '5 groups'.

ANALYSIS OF VARIANCE ON Fe2O3
SOURCE      DF         SS         MS         F         p
5 groups     4       1459        365      3.24     0.031
ERROR       22       2476        113
TOTAL       26       3935

                                        INDIVIDUAL 95 PCT CI'S FOR MEAN
                                        BASED ON POOLED STDEV
 LEVEL       N       MEAN      STDEV  ------+---------+---------+---------+
     1       7      28.86      13.19     (------*------)
     2       7      34.85      11.39           (------*------)
     3       8      46.22       8.76                   (------*-----)
     4       3      46.58       7.64                (----------*---------)
     5       2      33.30       0.00   (------------*------------)
                                       ------+---------+---------+---------+
POOLED STDEV =     10.61               24        36        48        60
```

E. (continuation)

```
MTB > Oneway 'FeO' '5 groups'.

ANALYSIS OF VARIANCE ON FeO
SOURCE      DF         SS          MS          F         p
5 groups     4      503.0       125.8       4.94     0.005
ERROR       22      560.4        25.5
TOTAL       26     1063.4

                                                INDIVIDUAL 95 PCT CI'S FOR MEAN
                                                BASED ON POOLED STDEV
 LEVEL       N       MEAN      STDEV  ---+---------+---------+---------+---
     1       7     44.745      5.663                        (-----*-----)
     2       7     41.777      6.194                   (-----*-----)
     3       8     35.796      2.353            (----*----)
     4       3     32.508      7.039   (--------*--------)
     5       2     42.690      0.000                (-----------*-----------)
                                       ---+---------+---------+---------+---
POOLED STDEV =     5.047               28.0       35.0       42.0       49.0
MTB > Oneway 'MnO' '5 groups'.

ANALYSIS OF VARIANCE ON MnO
SOURCE      DF         SS          MS          F         p
5 groups     4       7.24        1.81       1.36     0.279
ERROR       22      29.25        1.33
TOTAL       26      36.49

                                                INDIVIDUAL 95 PCT CI'S FOR MEAN
                                                BASED ON POOLED STDEV
 LEVEL       N       MEAN      STDEV  --------+---------+---------+---------
     1       7      0.855      0.491           (-----*-----)
     2       7      0.892      0.710           (-----*-----)
     3       8      0.586      0.401         (-----*-----)
     4       3      2.347      3.439                  (---------*---------)
     5       2      0.600      0.000   (-----------*-----------)
                                       --------+---------+---------+---------
POOLED STDEV =     1.153               0.0        1.5        3.0
MTB > Oneway 'MgO' '5 groups'.

ANALYSIS OF VARIANCE ON MgO
SOURCE      DF         SS          MS          F         p
5 groups     4      0.791       0.198       0.58     0.681
ERROR       22      7.507       0.341
TOTAL       26      8.297

                                                INDIVIDUAL 95 PCT CI'S FOR MEAN
                                                BASED ON POOLED STDEV
 LEVEL       N       MEAN      STDEV  --+---------+---------+---------+----
     1       7     0.3043     0.4271            (--------*--------)
     2       7     0.6987     0.8874                     (--------*--------)
     3       8     0.5119     0.3668                  (--------*--------)
     4       3     0.4974     0.6105            (-----------*-----------)
     5       2     0.1400     0.0000  (-------------*-------------)
                                       --+---------+---------+---------+----
POOLED STDEV =     0.5841            -0.60       0.00       0.60       1.20
MTB > Oneway 'CaO' '5 groups'.

ANALYSIS OF VARIANCE ON CaO
SOURCE      DF         SS          MS          F         p
5 groups     4      0.1691      0.0423      3.50     0.023
ERROR       22      0.2657      0.0121
TOTAL       26      0.4348

                                                INDIVIDUAL 95 PCT CI'S FOR MEAN
                                                BASED ON POOLED STDEV
 LEVEL       N       MEAN      STDEV  -----+---------+---------+---------+--
     1       7     0.2404     0.1921                   (-----*-----)
     2       7     0.0712     0.0230       (-----*----)
     3       8     0.1194     0.0738          (----*----)
     4       3     0.0635     0.0382  (---------*---------)
     5       2     0.2900     0.0000                (---------*----------)
                                       -----+---------+---------+---------+--
POOLED STDEV =     0.1099              0.00       0.15       0.30       0.45
```

F. Spearman's rank correlation coefficients for main magnetic parameters measured in 26 rock and 14 glacial till samples from the River Eden catchment. $r_s \geq 0.405$ is significant at a 0.01 level.

	X_{lf}	$Xf_{d\%}$	X_{ARM}	IRM_{20}	IRM_{40}	IRM_{100}	IRM_{300}	IRM_{500}	SIRM	IRM_{-20}	IRM_{-40}	IRM_{-100}	IRM_{-300}
X_{lf}	1.000												
$Xf_{d\%}$	-0.701	1.000											
X_{ARM}	0.954	-0.630	1.000										
IRM_{20}	0.969	-0.674	0.970	1.000									
RM_{40}	0.977	-0.682	0.983	0.986	1.000								
IRM_{100}	0.967	-0.672	0.968	0.953	0.984	1.000							
IRM_{300}	0.958	-0.665	0.958	0.943	0.977	0.996	1.000						
IRM_{500}	0.959	-0.665	0.959	0.943	0.977	0.995	1.000	1.000					
SIRM	0.951	-0.669	0.923	0.922	0.956	0.970	0.974	0.974	1.000				
IRM_{-20}	0.718	-0.429	0.705	0.659	0.737	0.792	0.812	0.813	0.813	1.000			
IRM_{-40}	-0.602	0.381	-0.577	-0.579	-0.605	-0.592	-0.559	-0.556	-0.545	-0.240	1.000		
IRM_{-100}	-0.962	0.663	-0.957	-0.952	-0.980	-0.987	-0.980	-0.980	-0.946	-0.755	0.642	1.000	
IRM_{-300}	-0.947	0.660	-0.938	-0.929	-0.963	-0.980	-0.986	-0.986	-0.949	-0.788	0.581	0.985	1.000
IRM_{-1000}	-0.953	0.695	-0.949	-0.932	-0.969	-0.988	-0.995	-0.995	-0.973	-0.824	0.536	0.971	0.985
$HIRM_{20}$	0.947	-0.660	0.947	0.925	0.966	0.989	0.995	0.995	0.979	0.849	-0.519	-0.966	-0.978
$HIRM_{40}$	0.901	-0.612	0.909	0.874	0.927	0.961	0.973	0.973	0.957	0.906	-0.445	-0.929	-0.950
$HIRM_{100}$	0.661	-0.478	0.638	0.588	0.666	0.727	0.758	0.759	0.781	0.923	-0.115	-0.671	-0.731
$HIRM_{300}$	0.264	-0.187	0.268	0.204	0.259	0.295	0.321	0.324	0.349	0.583	0.262	-0.207	-0.264
$HIRM_{500}$	0.251	-0.180	0.268	0.185	0.235	0.260	0.280	0.283	0.303	0.503	0.267	-0.170	-0.217
$HIRM_{-20}$	0.979	-0.668	0.968	0.981	0.992	0.980	0.973	0.973	0.963	0.720	-0.616	-0.977	-0.959
$HIRM_{-40}$	0.967	-0.668	0.965	0.951	0.985	0.996	0.993	0.993	0.970	0.782	-0.614	-0.988	-0.980
$HIRM_{-100}$	0.965	-0.681	0.965	0.950	0.983	0.998	0.998	0.998	0.973	0.802	-0.573	-0.985	-0.984
$HIRM_{-300}$	0.959	-0.675	0.954	0.940	0.974	0.992	0.998	0.998	0.974	0.814	-0.550	-0.977	-0.989
IRM_{20}/ARM	0.914	-0.752	0.856	0.940	0.911	0.874	0.866	0.865	0.847	0.534	-0.584	-0.886	-0.868
$(Bo)_{CR}$	0.865	-0.651	0.847	9.842	0.860	0.837	0.810	0.810	0.791	0.462	-0.773	-0.859	-0.809
SIRM/X_{lf}	-0.330	0.290	-0.222	-0.289	-0.239	-0.177	-0.144	-0.145	-0.126	0.013	0.295	0.253	0.190
X_{ARM}/X_{lf}	-0.636	0.522	-0.496	-0.544	-0.560	-0.573	-0.571	-0.571	-0.570	-0.450	0.496	0.585	0.584
D	-0.854	0.628	-0.833	-0.828	-0.848	-0.828	-0.802	-0.801	-0.785	-0.454	0.780	0.850	0.801

	IRM_{-1000}	$HIRM_{20}$	$HIRM_{40}$	$HIRM_{100}$	$HIRM_{300}$	$HIRM_{500}$	$HIRM_{-20}$	$HIRM_{-40}$	$HIRM_{-100}$	$HIRM_{-300}$
IRM_{-1000}	1.000									
$HIRM_{20}$	-0.995	1.000								
$HIRM_{40}$	-0.976	0.987	1.000							
$HIRM_{100}$	-0.781	0.802	0.867	1.000						
$HIRM_{300}$	-0.364	0.381	0.459	0.670	1.000					
$HIRM_{500}$	-0.319	0.336	0.411	0.607	0.890	1.000				
$HIRM_{-20}$	-0.962	0.959	0.914	0.657	0.233	0.211	1.000			
$HIRM_{-40}$	-0.985	0.984	0.953	0.720	0.284	0.247	0.983	1.000		
$HIRM_{-100}$	-0.994	0.993	0.967	0.744	0.317	0.279	0.978	0.995	1.000	
$HIRM_{-300}$	-0.997	0.995	0.973	0.765	0.328	0.285	0.970	0.990	0.996	1.000
IRM_{20}/ARM	-0.859	0.834	0.765	0.478	0.072	0.013	0.916	0.876	0.872	0.867
$(Bo)_{CR}$	-0.789	0.777	0.701	0.392	0.027	-0.015	0.862	0.857	0.825	0.803
SIRM/X_{lf}	0.133	-0.114	-0.060	0.030	0.172	0.161	-0.247	-0.182	-0.165	-0.144
X_{ARM}/X_{lf}	0.584	-0.566	-0.530	-0.404	-0.158	-0.157	-0.568	-0.574	-0.579	-0.578
D	0.780	-0.768	-0.693	-0.383	-0.021	0.020	-0.854	-0.850	-0.816	-0.795

	IRM_{20}/ARM	$(Bo)_{CR}$	SIRM/X_{lf}	X_{ARM}/X_{lf}	D
IRM_{20}/ARM	1.000				
$(Bo)_{CR}$	0.810	1.000			
SIRM/X_{lf}	-0.363	-0.380	1.000		
X_{ARM}/X_{lf}	-0.603	-0.439	0.451	1.000	
D	-0.799	-0.995	0.380	0.431	1.000

G. One-way analysis of variance (ANOVA) for the 28 main magnetic parameters measured in 39 samples of the 6 potential sources of stream sediment in the River Eden catchment: (1) basalts, (2) basaltic andesites, (3) andesites, (4) dacite-rhyolites, (5) sedimentary rocks, and (6) glacial till. Critical value of Fwith 5 and 33 degrees of freedom is 3.64 at the 99% confidence level.

```
MTB > Oneway 'Xlf' '6Groups'.

ANALYSIS OF VARIANCE ON Xlf
SOURCE      DF         SS          MS          F          p
6Groups      5   12521402     2504280      11.41      0.000
ERROR       33    7241830      219449
TOTAL       38   19763232

                                          INDIVIDUAL 95 PCT CI'S FOR MEAN
                                          BASED ON POOLED STDEV
 LEVEL       N       MEAN      STDEV      --------+---------+---------+--------
     1       7     1600.5      972.4                                  (----*----)
     2       7      709.0      500.5                        (----*----)
     3       5      398.4      103.7                  (-----*-----)
     4       3        4.9        2.0      (--------*--------)
     5       3        0.0        0.2      (--------*--------)
     6      14      103.5       41.6             (--*---)
                                          --------+---------+---------+--------
POOLED STDEV =     468.5                          0        700       1400
MTB > Oneway 'Xfd' '6Groups'.

ANALYSIS OF VARIANCE ON Xfd
SOURCE      DF         SS          MS          F          p
6Groups      5     92.634      18.527      30.04      0.000
ERROR       33     20.354       0.617
TOTAL       38    112.988

                                          INDIVIDUAL 95 PCT CI'S FOR MEAN
                                          BASED ON POOLED STDEV
 LEVEL       N       MEAN      STDEV      -+---------+---------+---------+-----
     1       7     0.5729     0.4047       (-*--)
     2       7     1.1269     0.7469         (--*-)
     3       5     0.4947     0.0984      (--*--)
     4       3     3.0869     0.7434                (--*---)
     5       3     6.4696     1.6967                          (---*---)
     6      14     1.8615     0.8377              (*-)
                                          -+---------+---------+---------+-----
POOLED STDEV =     0.7854                0.0       2.5       5.0       7.5
MTB > Oneway 'Xarm' '6Groups'.

ANALYSIS OF VARIANCE ON Xarm
SOURCE      DF         SS          MS          F          p
6Groups      5     65.900      13.180      14.66      0.000
ERROR       33     29.669       0.899
TOTAL       38     95.569

                                          INDIVIDUAL 95 PCT CI'S FOR MEAN
                                          BASED ON POOLED STDEV
 LEVEL       N       MEAN      STDEV      -------+---------+---------+---------
     1       7     3.9360     2.1341                                  (----*---)
     2       7     1.6074     0.5160                      (----*----)
     3       5     1.0720     0.2183                   (-----*----)
     4       3     0.0172     0.0057      (------*------)
     5       3     0.0070     0.0028      (------*------)
     6      14     0.6181     0.2065              (--*--)
                                          -------+---------+---------+---------
POOLED STDEV =     0.9482                     0.0       1.6       3.2
MTB > Oneway 'IRM20' '6Groups'.

ANALYSIS OF VARIANCE ON IRM20
SOURCE      DF         SS          MS          F          p
6Groups      5   71426128    14285226      23.67      0.000
ERROR       33   19917442      603559
TOTAL       38   91343568

                                          INDIVIDUAL 95 PCT CI'S FOR MEAN
                                          BASED ON POOLED STDEV
 LEVEL       N       MEAN      STDEV      -------+---------+---------+---------
     1       7     3808.0     1637.9                                  (---*---)
     2       7     1130.8      783.4                        (---*---)
     3       5      472.4       86.4                  (----*----)
     4       3        3.3        1.7      (-----*-----)
     5       3        0.4        0.2      (-----*-----)
     6      14      208.9       91.8             (-*--)
                                          -------+---------+---------+---------
POOLED STDEV =     776.9                        0       1500       3000
```

G. (continuation)

```
MTB > Oneway 'IRM40' '6Groups'.

ANALYSIS OF VARIANCE ON IRM40
SOURCE      DF         SS         MS        F        p
6Groups      5 958608832 191721760     8.70    0.000
ERROR       33 727379200  22041794
TOTAL       38 1.686E+09

                                                 INDIVIDUAL 95 PCT CI'S FOR MEAN
                                                 BASED ON POOLED STDEV
 LEVEL       N       MEAN      STDEV  ---------+---------+---------+--------
     1       7      13886      10499                              (----*----)
     2       7       4504       3281                    (----*-----)
     3       5       1652        178               (------*------)
     4       3         11          6          (--------*--------)
     5       3          1          1          (--------*--------)
     6      14        710        318               (---*---)
                                                 ---------+---------+---------+--------
POOLED STDEV =      4695                                 0       7000      14000
MTB > Oneway 'IRM100' '6Groups'.

ANALYSIS OF VARIANCE ON IRM100
SOURCE      DF         SS         MS        F        p
6Groups      5 3.610E+09 722089216     6.30    0.000
ERROR       33 3.780E+09 114542584
TOTAL       38 7.390E+09

                                                 INDIVIDUAL 95 PCT CI'S FOR MEAN
                                                 BASED ON POOLED STDEV
 LEVEL       N       MEAN      STDEV  ---------+---------+---------+--------
     1       7      26936      23881                              (-----*----)
     2       7      11094       7580                    (----*-----)
     3       5       4053       1345               (------*------)
     4       3         52         44          (--------*--------)
     5       3          2          2          (--------*--------)
     6      14       1595        687               (---*---)
                                                 ---------+---------+---------+--------
POOLED STDEV =     10702                                 0      15000      30000
MTB > Oneway 'IRM300' '6Groups'.

ANALYSIS OF VARIANCE ON IRM300
SOURCE      DF         SS         MS        F        p
6Groups      5 3.960E+09 792064448     6.32    0.000
ERROR       33 4.139E+09 125413264
TOTAL       38 8.099E+09

                                                 INDIVIDUAL 95 PCT CI'S FOR MEAN
                                                 BASED ON POOLED STDEV
 LEVEL       N       MEAN      STDEV  ---------+---------+---------+--------
     1       7      28302      24702                              (-----*-----)
     2       7      13365       8610                    (-----*-----)
     3       5       5047       2251               (------*------)
     4       3        102         67          (---------*---------)
     5       3          2          2          (---------*---------)
     6      14       2129        973               (---*---)
                                                 ---------+---------+---------+--------
POOLED STDEV =     11199                                 0      15000      30000
MTB > Oneway 'IRM500' '6Groups'.

ANALYSIS OF VARIANCE ON IRM500
SOURCE      DF         SS         MS        F        p
6Groups      5 3.966E+09 793188992     6.33    0.000
ERROR       33 4.134E+09 125276232
TOTAL       38 8.100E+09

                                                 INDIVIDUAL 95 PCT CI'S FOR MEAN
                                                 BASED ON POOLED STDEV
 LEVEL       N       MEAN      STDEV  ---------+---------+---------+--------
     1       7      28364      24711                              (-----*-----)
     2       7      13522       8532                    (-----*-----)
     3       5       5186       2291               (------*------)
     4       3        146         85          (---------*---------)
     5       3          3          2          (---------*---------)
     6      14       2201        983               (---*----)
                                                 ---------+---------+---------+--------
POOLED STDEV =     11193                                 0      15000      30000
```

G. (continuation)

```
MTB > Oneway 'SIRM' '6Groups'.

ANALYSIS OF VARIANCE ON SIRM
SOURCE      DF         SS         MS        F        p
6Groups      5 3.952E+09  790444480     6.24    0.000
ERROR       33 4.182E+09  126735832
TOTAL       38 8.135E+09

                                        INDIVIDUAL 95 PCT CI'S FOR MEAN
                                        BASED ON POOLED STDEV
 LEVEL       N       MEAN      STDEV  ---------+---------+---------+-------
     1       7      28452      24755                          (-----*-----)
     2       7      13397       8855                (-----*-----)
     3       5       5436       2309          (------*-----)
     4       3        257        125  (---------*---------)
     5       3          3          2  (---------*---------)
     6      14       2278       1021          (----*---)
                                        ---------+---------+---------+-------
POOLED STDEV =     11258                       0     15000     30000
MTB > Oneway 'IRM-20' '6Groups'.

ANALYSIS OF VARIANCE ON IRM-20
SOURCE      DF         SS         MS        F        p
6Groups      5 485535840   97107168     3.10    0.021
ERROR       33 1.035E+09   31367382
TOTAL       38 1.521E+09

                                        INDIVIDUAL 95 PCT CI'S FOR MEAN
                                        BASED ON POOLED STDEV
 LEVEL       N       MEAN      STDEV  -+---------+---------+---------+------
     1       7       9832      12498                        (------*-------)
     2       7       6703       3549                   (------*------)
     3       5       3000       2037            (-------*-------)
     4       3        239        113  (-----------*-----------)
     5       3          2          2  (-----------*-----------)
     6      14       1302        666            (----*----)
                                        -+---------+---------+---------+------
POOLED STDEV =      5601          -6000          0       6000      12000
MTB > Oneway 'IRM-40' '6Groups'.

ANALYSIS OF VARIANCE ON IRM-40
SOURCE      DF         SS         MS        F        p
6Groups      5 430001792   86000360    10.58    0.000
ERROR       33 268217264    8127796
TOTAL       38 698219072

                                        INDIVIDUAL 95 PCT CI'S FOR MEAN
                                        BASED ON POOLED STDEV
 LEVEL       N       MEAN      STDEV  -------+---------+---------+---------
     1       7      -8503       6341  (-----*-----)
     2       7      -1811       1731                  (-----*-----)
     3       5        458       1381                       (------*------)
     4       3        207         90                    (--------*--------)
     5       3          1          1                    (--------*--------)
     6      14        426        322                         (---*---)
                                        -------+---------+---------+---------
POOLED STDEV =      2851          -8000     -4000          0
MTB > Oneway 'IRM-100' '6Groups'.

ANALYSIS OF VARIANCE ON IRM-100
SOURCE      DF         SS         MS        F        p
6Groups      5 3.548E+09  709686144     6.14    0.000
ERROR       33 3.811E+09  115493072
TOTAL       38 7.360E+09

                                        INDIVIDUAL 95 PCT CI'S FOR MEAN
                                        BASED ON POOLED STDEV
 LEVEL       N       MEAN      STDEV  ----+---------+---------+---------+--
     1       7     -26329      24005    (----*-----)
     2       7     -10051       7609              (----*-----)
     3       5      -3206        906                 (------*-----)
     4       3        140         49                  (--------*--------)
     5       3         -1          1                  (--------*--------)
     6      14      -1027        491                    (---*---)
                                        ----+---------+---------+---------+--
POOLED STDEV =     10747          -30000    -15000          0      15000
```

G. (continuation)

```
MTB > Oneway 'IRM-300' '6Groups'.

ANALYSIS OF VARIANCE ON IRM-300
SOURCE      DF          SS          MS        F        p
6Groups      5 3.944E+09 788889664     6.21    0.000
ERROR       33 4.195E+09 127115248
TOTAL       38 8.139E+09

                                          INDIVIDUAL 95 PCT CI'S FOR MEAN
                                          BASED ON POOLED STDEV
 LEVEL       N       MEAN      STDEV      -----+---------+---------+---------+-
     1       7     -28174      24910      (-----*-----)
     2       7     -12935       8516            (----*-----)
     3       5      -4674       2243                 (------*------)
     4       3         56         46                  (--------*--------)
     5       3         -2          2                  (--------*--------)
     6      14      -2012       1127                      (---*---)
                                          -----+---------+---------+---------+-
POOLED STDEV =      11275                 -30000     -15000          0      15000
MTB > Oneway 'IRM-1000' '6Groups'.

ANALYSIS OF VARIANCE ON IRM-1000
SOURCE      DF          SS          MS        F        p
6Groups      5 3.923E+09 784602304     6.19    0.000
ERROR       33 4.186E+09 126837872
TOTAL       38 8.109E+09

                                          INDIVIDUAL 95 PCT CI'S FOR MEAN
                                          BASED ON POOLED STDEV
 LEVEL       N       MEAN      STDEV      -----+---------+---------+---------+-
     1       7     -28307      24943      (-----*-----)
     2       7     -13464       8282            (-----*-----)
     3       5      -5361       2331                 (------*------)
     4       3       -220        117                  (--------*--------)
     5       3         -3          2                  (--------*--------)
     6      14      -2271       1222                     (---*----)
                                          -----+---------+---------+---------+-
POOLED STDEV =      11262                 -30000     -15000          0      15000
MTB > Oneway 'HIRM20' '6Groups'.

ANALYSIS OF VARIANCE ON HIRM20
SOURCE      DF          SS          MS        F        p
6Groups      5 2.993E+09 598571520     5.32    0.001
ERROR       33 3.711E+09 112453336
TOTAL       38 6.704E+09

                                          INDIVIDUAL 95 PCT CI'S FOR MEAN
                                          BASED ON POOLED STDEV
 LEVEL       N       MEAN      STDEV      ---------+---------+---------+-------
     1       7      24644      23511                        (----*-----)
     2       7      12526       7758                  (----*-----)
     3       5       4963       2337            (------*------)
     4       3        253        123      (-------*-------)
     5       3          3          2      (-------*-------)
     6      14       2069        932             (--*---)
                                          ---------+---------+---------+-------
POOLED STDEV =      10604                         0      15000      30000
MTB > Oneway 'HIRM40' '6Groups'.

ANALYSIS OF VARIANCE ON HIRM40
SOURCE      DF          SS          MS        F        p
6Groups      5 1.072E+09 214454496     4.69    0.002
ERROR       33 1.509E+09  45719172
TOTAL       38 2.581E+09

                                          INDIVIDUAL 95 PCT CI'S FOR MEAN
                                          BASED ON POOLED STDEV
 LEVEL       N       MEAN      STDEV      ---------+---------+---------+-------
     1       7      14566      14753                          (------*------)
     2       7       9153       5410                  (------*------)
     3       5       3783       2266            (-------*------)
     4       3        246        119      (---------*---------)
     5       3          2          2      (---------*---------)
     6      14       1568        715             (----*----)
                                          ---------+---------+---------+-------
POOLED STDEV =       6762                         0       8000      16000
```

G. (continuation)

```
MTB > Oneway 'HIRM100' '6Groups'.

ANALYSIS OF VARIANCE ON HIRM100
SOURCE      DF         SS         MS        F        p
6Groups      5   24860542    4972108     6.39    0.000
ERROR       33   25683124     778277
TOTAL       38   50543664

                                                 INDIVIDUAL 95 PCT CI'S FOR MEAN
                                                 BASED ON POOLED STDEV
 LEVEL       N       MEAN      STDEV  ---------+---------+---------+-------
     1       7     1516.2     1294.8                  (-----*----)
     2       7     2563.1     1275.5                             (----*-----)
     3       5     1382.7      980.9                (------*-----)
     4       3      205.0       88.2    (---------*--------)
     5       3        1.0        0.9  (---------*---------)
     6      14      683.2      392.1             (---*---)
                                                 ---------+---------+---------+-------
POOLED STDEV =      882.2                              0       1200       2400
MTB > Oneway 'HIRM300' '6Groups'.

ANALYSIS OF VARIANCE ON HIRM300
SOURCE      DF         SS         MS        F        p
6Groups      5     414402      82880     5.77    0.001
ERROR       33     473983      14363
TOTAL       38     888386

                                                 INDIVIDUAL 95 PCT CI'S FOR MEAN
                                                 BASED ON POOLED STDEV
 LEVEL       N       MEAN      STDEV  --------+---------+---------+---------
     1       7      150.6      103.9             (----*---)
     2       7      291.7      212.6                   (----*---)
     3       5      388.6      131.4                      (----*-----)
     4       3      154.5       63.3          (------*------)
     5       3        0.4        0.4   (------*------)
     6      14      149.3       68.5             (--*---)
                                                 --------+---------+---------+---------
POOLED STDEV =      119.8                             0        200        400
MTB > Oneway 'HIRM500' '6Groups'.

ANALYSIS OF VARIANCE ON HIRM500
SOURCE      DF         SS         MS        F        p
6Groups      5     156256      31251     5.90    0.001
ERROR       33     174939       5301
TOTAL       38     331195

                                                 INDIVIDUAL 95 PCT CI'S FOR MEAN
                                                 BASED ON POOLED STDEV
 LEVEL       N       MEAN      STDEV  --------+---------+---------+---------
     1       7      87.68      87.68             (---*----)
     2       7     134.61      92.75                 (---*----)
     3       5     249.49      83.30                        (-----*----)
     4       3     110.70      47.21          (------*------)
     5       3       0.20       0.23   (------*------)
     6      14      77.04      58.82             (--*---)
                                                 --------+---------+---------+---------
POOLED STDEV =      72.81                             0        120        240
MTB > Oneway 'HIRM-20' '6Groups'.

ANALYSIS OF VARIANCE ON HIRM-20
SOURCE      DF         SS         MS        F        p
6Groups      5 1.732E+09  346342848     9.90    0.000
ERROR       33 1.154E+09   34971588
TOTAL       38 2.886E+09

                                                 INDIVIDUAL 95 PCT CI'S FOR MEAN
                                                 BASED ON POOLED STDEV
 LEVEL       N       MEAN      STDEV  -------+---------+---------+---------
     1       7      18620      12811                       (----*---)
     2       7       6954       5272            (----*----)
     3       5       2435        383       (----*-----)
     4       3         18         12   (------*------)
     5       3          1          1   (------*------)
     6      14        976        387         (--*--)
                                                 -------+---------+---------+---------
POOLED STDEV =       5914                            0     10000     20000
```

G. (continuation)

```
MTB > Oneway 'HIRM-40' '6Groups'.

ANALYSIS OF VARIANCE ON HIRM-40
SOURCE      DF         SS         MS        F        p
6Groups      5 6.928E+09 1.386E+09     7.63    0.000
ERROR       33 5.994E+09 181633104
TOTAL       38 1.292E+10

                                        INDIVIDUAL 95 PCT CI'S FOR MEAN
                                        BASED ON POOLED STDEV
 LEVEL       N       MEAN      STDEV    --------+---------+---------+--------
     1       7      36955      30146                        (----*-----)
     2       7      15468       9389                 (----*----)
     3       5       4977       1002       (------*------)
     4       3         49         38   (--------*-------)
     5       3          2          2   (--------*-------)
     6      14       1852        790         (---*---)
                                        --------+---------+---------+--------
POOLED STDEV =     13477                       0      20000     40000
MTB > Oneway 'HIRM-100' '6Groups'.

ANALYSIS OF VARIANCE ON HIRM-100
SOURCE      DF         SS         MS        F        p
6Groups      5 1.499E+10 2.998E+09     6.24    0.000
ERROR       33 1.586E+10 480507264
TOTAL       38 3.085E+10

                                        INDIVIDUAL 95 PCT CI'S FOR MEAN
                                        BASED ON POOLED STDEV
 LEVEL       N       MEAN      STDEV    ---------+---------+---------+-------
     1       7      54782      48729                        (----*-----)
     2       7      23708      16021                 (-----*-----)
     3       5       8641       3201          (------*------)
     4       3        117         91   (---------*---------)
     5       3          4          3   (---------*---------)
     6      14       3305       1487          (---*---)
                                        ---------+---------+---------+-------
POOLED STDEV =     21920                       0      30000     60000
MTB > Oneway 'HIRM-300' '6Groups'.

ANALYSIS OF VARIANCE ON HIRM-300
SOURCE      DF         SS         MS        F        p
6Groups      5 1.582E+10 3.165E+09     6.26    0.000
ERROR       33 1.667E+10 505168160
TOTAL       38 3.249E+10

                                        INDIVIDUAL 95 PCT CI'S FOR MEAN
                                        BASED ON POOLED STDEV
 LEVEL       N       MEAN      STDEV    ---------+---------+---------+-------
     1       7      56626      49664                        (-----*-----)
     2       7      26592      16979                  (-----*-----)
     3       5      10110       4548          (------*------)
     4       3        201        138   (---------*---------)
     5       3          5          4   (---------*---------)
     6      14       4290       2134          (---*----)
                                        ---------+---------+---------+-------
POOLED STDEV =     22476                       0      30000     60000
MTB > Oneway 'Bo' '6Groups'.

ANALYSIS OF VARIANCE ON Bo
SOURCE      DF         SS         MS        F        p
6Groups      5     507852     101570    69.82    0.000
ERROR       33      48004       1455
TOTAL       38     555856

                                        INDIVIDUAL 95 PCT CI'S FOR MEAN
                                        BASED ON POOLED STDEV
 LEVEL       N       MEAN      STDEV    -----+---------+---------+---------+-
     1       7     -26.43       6.70                                   (-*-)
     2       7     -39.29      13.90                                 (-*-)
     3       5     -42.60      10.09                                 (-*-)
     4       3    -470.00     147.31   (--*--)
     5       3     -90.33      34.36                          (--*--)
     6      14     -49.93       5.59                              (-*)
                                        -----+---------+---------+---------+-
POOLED STDEV =     38.14                  -450       -300       -150          0
```

G. (continuation)

```
MTB > Oneway 'IRM20/AR' '6Groups'.

ANALYSIS OF VARIANCE ON IRM20/AR
SOURCE      DF         SS          MS        F        p
6Groups      5     3444.5       688.9    14.74    0.000
ERROR       33     1542.1        46.7
TOTAL       38     4986.7

                                          INDIVIDUAL 95 PCT CI'S FOR MEAN
                                          BASED ON POOLED STDEV
 LEVEL       N       MEAN      STDEV      -----+---------+---------+---------+-
     1       7     32.734     10.312                              (---*--)
     2       7     19.883     11.891                    (--*---)
     3       5     14.042      2.458          (---*-----)
     4       3      5.933      1.359      (-----*-----)
     5       3      1.564      0.445   (-----*-----)
     6      14     10.407      1.456           (--*-)
                                          -----+---------+---------+---------+-
POOLED STDEV =     6.836                      0        15        30        45
MTB > Oneway 'SIRM/X' '6Groups'.

ANALYSIS OF VARIANCE ON SIRM/X
SOURCE      DF         SS          MS        F        p
6Groups      5     2911.2       582.2     6.01    0.000
ERROR       33     3195.1        96.8
TOTAL       38     6106.3

                                          INDIVIDUAL 95 PCT CI'S FOR MEAN
                                          BASED ON POOLED STDEV
 LEVEL       N       MEAN      STDEV      -------+---------+---------+---------
     1       7     19.059      8.514      (-----*-----)
     2       7     25.766     15.743           (-----*-----)
     3       5     14.390      7.272   (------*------)
     4       3     50.827      9.695                          (-------*-------)
     5       3     19.730     20.526     (-------*-------)
     6      14     21.702      1.542          (---*---)
                                          -------+---------+---------+---------
POOLED STDEV =     9.840                     16        32        48
MTB > Oneway 'Xarm/X' '6Groups'.

ANALYSIS OF VARIANCE ON Xarm/X
SOURCE      DF         SS          MS        F        p
6Groups      5       2616         523     3.80    0.008
ERROR       33       4538         138
TOTAL       38       7154

                                          INDIVIDUAL 95 PCT CI'S FOR MEAN
                                          BASED ON POOLED STDEV
 LEVEL       N       MEAN      STDEV      -------+---------+---------+---------
     1       7       3.06       1.72       (------*------)
     2       7       4.38       4.66       (------*------)
     3       5       2.73       0.28     (-------*-------)
     4       3       3.61       0.37   (---------*---------)
     5       3      34.83      46.81                          (---------*---------)
     6      14       6.10       0.78          (---*---)
                                          -------+---------+---------+---------
POOLED STDEV =    11.73                      0        16        32
MTB > Oneway 'D' '6Groups'.

ANALYSIS OF VARIANCE ON D
SOURCE      DF         SS          MS        F        p
6Groups      5    18.4241      3.6848    41.87    0.000
ERROR       33     2.9040      0.0880
TOTAL       38    21.3281

                                          INDIVIDUAL 95 PCT CI'S FOR MEAN
                                          BASED ON POOLED STDEV
 LEVEL       N       MEAN      STDEV      -------+---------+---------+---------
     1       7    -0.3815     0.2154     (-*-)
     2       7    -0.1039     0.3170       (-*-)
     3       5     0.0291     0.1810        (-*--)
     4       3     2.4342     0.9217                                (--*---)
     5       3     0.5144     0.1856            (--*---)
     6      14     0.1956     0.0976          (-*-)
                                          -------+---------+---------+---------
POOLED STDEV =     0.2967                   0.0       1.0       2.0
```

Appendix 6

In this appendix the results of the test of linearity performed for the 25 main magnetic parameters measurement in all glacial till and stream sediment samples collected along 4 selected River Eden tributaries: the Barroway Burn (BB), the Moonzie Burn (MB), the Kilgour Burn (KB) and the Coalpit Burn (CB), as well as along the River Eden are displayed. The predicted value of each magnetic variable for each bulk sample, which is obtained by applying Equation 3.1 to each of the particle size fraction subsamples, are compared to the analytical magnetic results by using the equation:

$$\text{Error \%} = \frac{(\text{Predicted value} - \text{Measured value})}{\text{Measured value}} * 100$$

The total Error% or deviation from linear additivity of each magnetic parameter is also given.

A. Test of the linear additivity of magnetic parameters.

Sample	X_{lf}(-8) (m^3/kg)	X_{hf}(-8) (m^3/kg)	X_{fd} %	Xarm(-5) (m^3/kg)	IRM_{20}(-5) (Am^2/Kg)	IRM_{40}(-5) (Am^2/Kg)	IRM_{100}(-5) (Am^2/Kg)	IRM_{300}(-5) (Am^2/Kg)	IRM_{500}(-5) (Am^2/Kg)	SIRM(-5) (Am^2/Kg)	IRM_{-20}(-5) (Am^2/Kg)	IRM_{-40}(-5) (Am^2/Kg)	IRM_{-100}(-5) (Am^2/Kg)	IRM_{-300}(-5) (Am^2/Kg)
BB2(Bulk)	207.84	203.95	1.87	1.33	479.65	1649.33	4338.97	6018.07	6298.51	6531.29	4560.10	1928.87	-2774.45	-5487.01
Predicted	204.66	200.89	1.79	1.18	398.04	1428.91	3499.48	4746.81	4901.18	5041.11	3159.38	1211.05	-2263.60	-4318.68
Error %	-1.53	-1.50	-4.73	-11.25	-17.01	-13.36	-19.35	-21.12	-22.19	-22.82	-30.72	-37.21	-18.41	-21.29
BB3(Bulk)	249.84	243.57	2.51	1.50	498.54	1685.97	4225.70	5966.65	6282.04	6403.93	4326.57	1553.42	-2914.74	-5855.82
Predicted	256.81	249.56	2.75	1.57	546.73	1776.91	4227.17	6031.26	6205.98	6404.83	4189.63	1464.31	-2911.33	-5723.17
Error %	2.79	2.46	9.46	4.59	9.67	6.39	0.03	1.08	-1.21	0.01	-3.17	-5.74	-0.12	-2.27
BB4(Bulk)	142.97	139.78	2.65	1.11	213.24	1117.30	3074.33	4593.82	4776.89	4939.92	3528.16	1710.97	-1800.12	-4158.24
Predicted	190.80	185.59	2.80	1.11	364.83	1280.57	3185.19	4643.73	4757.79	4931.25	3100.40	1339.37	-1970.43	-4144.37
Error %	33.45	32.77	5.54	-0.12	71.09	14.61	3.61	1.09	-0.40	-0.18	-12.12	-21.72	9.46	-0.33
BB5(Bulk)	179.88	176.09	2.60	1.01	291.92	1408.47	3743.26	5295.53	5469.87	5568.85	3648.52	1405.05	-2597.80	-4987.50
Predicted	185.66	181.71	2.23	0.89	367.03	1340.24	3436.35	4860.88	5165.92	5231.45	3581.20	1375.63	-2180.61	-4472.63
Error %	3.21	3.19	-14.26	-11.63	25.73	-4.84	-8.20	-8.21	-5.56	-6.06	-1.85	-2.09	-16.06	-10.32
BB6(Bulk)	266.50	260.50	2.25	1.35	575.23	1931.45	4748.67	7060.07	7230.68	7381.23	4757.84	1615.85	-3471.11	-6817.34
Predicted	208.41	203.95	2.15	1.16	401.35	1452.28	3874.91	5693.15	5821.16	6023.77	4018.41	1750.01	-2401.47	-5268.86
Error %	-21.79	-21.71	-4.56	-13.98	-30.23	-24.81	-18.40	-19.36	-19.49	-18.39	-15.54	8.30	-30.82	-22.71
BB7(Bulk)	210.71	205.60	1.86	1.38	343.01	1784.41	4738.73	6680.76	6923.99	7050.48	4871.75	2082.66	-3143.60	-6262.41
Predicted	241.99	235.60	2.70	1.36	473.71	1665.43	4334.59	6330.71	6750.08	6822.43	4739.74	2010.28	-2612.10	-5844.77
Error %	14.84	14.59	44.80	-1.83	38.10	-6.67	-8.53	-5.24	-2.51	-3.23	-2.71	-3.48	-16.91	-6.67
MB1(Bulk)	87.75	85.76	3.52	0.50	159.72	669.44	1325.79	1600.43	1671.98	1744.43	872.83	-6.63	-1023.95	-1462.82
Predicted	75.95	74.40	2.09	0.37	155.55	483.48	946.57	1197.20	1228.60	1278.52	710.38	55.12	-698.74	-1084.14
Error %	-13.45	-13.25	-40.67	-25.91	-2.61	-27.78	-28.60	-25.19	-26.52	-26.71	-18.61	-931.60	-31.76	-25.89
MB2(Bulk)	238.81	233.32	3.51	0.98	392.65	1683.64	3817.46	4766.19	4863.23	4992.10	2789.46	394.92	-300.49	-4442.20
Predicted	237.53	231.84	2.51	0.90	520.91	1589.52	3358.50	3949.18	3992.31	4017.45	1791.38	47.65	-2339.52	-4075.19
Error %	-0.54	-0.63	-28.49	-8.70	32.67	-5.59	-12.02	-17.14	-17.91	-19.52	-35.78	-87.93	678.56	-8.26
MB3(Bulk)	125.56	122.32	7.92	0.71	209.58	914.00	1998.88	2576.86	2682.22	2786.05	1633.40	352.04	-1442.23	-2326.03
Predicted	129.69	127.18	1.79	0.58	276.47	879.31	1874.96	2291.77	2333.20	2377.73	1169.88	174.43	-1183.10	-2229.69
Error %	3.29	3.97	-77.46	-19.40	31.92	-3.80	-6.20	-11.06	-13.01	-14.66	-28.38	-50.45	-17.97	-4.14

A. (continuation)

Sample	$IRM_{-1000}(-5)$ (Am^2/Kg)	$HIRM_{20}(-5)$ (Am^2/Kg)	$HIRM_{40}(-5)$ (Am^2/Kg)	$HIRM_{100}(-5)$ (Am^2/Kg)	$HIRM_{300}(-5)$ (Am^2/Kg)	$HIRM_{500}(-5)$ (Am^2/Kg)	$HIRM_{-20}(-5)$ (Am^2/Kg)	$HIRM_{-40}(-5)$ (Am^2/Kg)	$HIRM_{-100}(-5)$ (Am^2/Kg)	$HIRM_{-300}(-5)$ (Am^2/Kg)	$(Bo)_{cr}$ (mT)
BB2(Bulk)	-6336.22	6051.63	4881.96	2192.32	513.21	232.77	1971.18	4602.42	9305.74	12018.29	-60.00
Predicted	-5030.31	4643.07	3612.19	1541.62	294.29	139.93	1881.73	3830.05	7304.71	9359.79	-56.51
Error %	-20.61	-23.28	-26.01	-29.68	-42.66	-39.89	-4.54	-16.78	-21.50	-22.12	-5.81
BB3(Bulk)	-6603.61	5905.39	4717.96	2178.24	437.28	121.89	2077.36	4850.51	9318.67	12259.75	-56.00
Predicted	-6476.72	5858.10	4627.92	2177.66	373.57	198.85	2215.19	4940.52	9316.16	12127.99	-54.96
Error %	-1.92	-0.80	-1.91	-0.03	-14.57	63.14	6.64	1.86	-0.03	-1.07	-1.86
BB4(Bulk)	-4789.47	4726.68	3822.62	1865.60	346.10	163.04	1411.76	3228.95	6740.04	9098.16	-66.00
Predicted	-4727.84	4566.42	3650.68	1746.06	287.52	173.46	1830.85	3591.88	6901.68	9075.62	-60.69
Error %	-1.29	-3.39	-4.50	-6.41	-16.93	6.39	29.69	11.24	2.40	-0.25	-8.04
BB5(Bulk)	-5430.72	5276.93	4160.39	1825.59	273.32	98.98	1920.33	4163.80	8166.65	10556.35	-56.00
Predicted	-5054.27	4864.42	3891.21	1795.10	370.57	65.53	1650.25	3855.82	7412.06	9704.08	-56.77
Error %	-6.93	-7.82	-6.47	-1.67	35.58	-33.79	-14.06	-7.40	-9.24	-8.07	1.37
BB6(Bulk)	-7592.43	6806.01	5449.79	2632.56	321.17	150.56	2623.39	5765.38	10852.34	14198.58	-54.00
Predicted	-5926.44	5622.43	4571.50	2148.86	330.62	202.61	2005.37	4273.76	8425.24	11292.63	-59.41
Error %	-21.94	-17.39	-16.12	-18.37	2.94	34.57	-23.56	-25.87	-22.36	-20.47	10.01
BB7(Bulk)	-6940.90	6707.47	5266.07	2311.76	369.72	126.50	2178.74	4967.82	10194.08	13312.90	-60.00
Predicted	-6669.96	6348.72	5157.00	2487.84	491.72	72.35	2082.69	4812.16	9434.53	12667.21	-60.45
Error %	-3.90	-5.35	-2.07	7.62	33.00	-42.81	-4.41	-3.13	-7.45	-4.85	0.75
MB1(Bulk)	-1675.41	1584.71	1074.99	418.64	144.00	72.45	871.60	1751.06	2768.38	3207.25	-40.00
Predicted	-1341.10	1122.97	795.03	331.95	81.31	49.92	568.13	1223.40	1977.25	2362.65	-42.36
Error %	-19.95	-29.14	-26.04	-20.71	-43.53	-31.10	-34.82	-30.13	-28.58	-26.33	5.90
MB2(Bulk)	-4868.49	4599.45	3308.46	1174.64	225.91	128.87	2202.64	4597.18	5292.59	9434.30	-60.00
Predicted	-4514.48	3496.54	2427.93	658.95	68.26	25.14	2226.07	3969.79	6356.97	8092.64	-41.27
Error %	-7.27	-23.98	-26.61	-43.90	-69.78	-80.49	1.06	-13.65	20.11	-14.22	-31.22
MB3(Bulk)	-2714.43	2576.46	1872.04	787.16	209.19	103.83	1152.64	2434.00	4228.27	5112.07	-48.00
Predicted	-2666.12	2101.25	1498.42	502.77	85.96	44.52	1207.85	2203.30	3560.83	4607.42	-44.30
Error %	-1.78	-18.44	-19.96	-36.13	-58.91	-57.12	4.79	-9.48	-15.79	-9.87	-7.71

A. (continuation)

Sample	X_{lf}(-8) (m^3/kg)	X_{hf}(-8) (m^3/kg)	X_{fd} %	Xarm(-5) (m^3/kg)	IRM_{20}(-5) (Am^2/Kg)	IRM_{40}(-5) (Am^2/Kg)	IRM_{100}(-5) (Am^2/Kg)	IRM_{300}(-5) (Am^2/Kg)	IRM_{500}(-5) (Am^2/Kg)	SIRM(-5) (Am^2/Kg)	IRM_{-20}(-5) (Am^2/Kg)	IRM_{-40}(-5) (Am^2/Kg)	IRM_{-100}(-5) (Am^2/Kg)	IRM_{-300}(-5) (Am^2/Kg)
MB4(Bulk)	20.61	20.12	2.05	0.90	322.43	1100.54	2414.25	3083.21	3138.21	3300.13	1697.63	84.02	-1796.22	-2837.36
Predicted	19.12	18.70	2.05	0.76	307.47	1127.28	2382.12	3036.18	3103.31	3206.34	1676.88	78.45	-1781.86	-2719.41
Error %	-7.22	-7.06	0.00	-14.85	-4.64	2.43	-1.33	-1.53	-1.11	-2.84	-1.22	-6.64	-0.80	-4.16
KB1(Bulk)	45.46	44.29	2.56	0.29	111.28	466.24	906.21	993.79	1016.10	1039.17	452.16	-185.09	-737.56	-841.31
Predicted	51.38	51.06	1.14	0.29	124.63	563.13	1026.69	1094.69	1117.97	1127.21	481.79	-240.03	-853.15	-922.68
Error %	13.02	15.28	-55.55	-1.07	12.00	20.78	13.29	10.15	10.03	8.47	6.55	29.68	15.67	9.67
KB3(Bulk)	123.51	121.78	1.40	0.42	253.39	1064.54	2155.16	2545.49	2619.62	2681.15	1116.36	-401.37	-2180.60	-2629.69
Predicted	130.51	129.86	0.15	0.35	255.28	1174.57	2367.18	2729.04	2816.82	2869.62	1164.15	-497.21	-2435.70	-2822.43
Error %	5.67	6.63	-89.22	-15.13	0.74	10.34	9.84	7.21	7.53	7.03	4.28	23.88	11.70	7.33
KB4(Bulk)	365.33	363.84	0.41	0.94	155.88	2770.61	5325.90	5689.62	5721.58	5721.73	3379.34	-1202.56	-4996.05	-5712.51
Predicted	210.11	209.07	0.34	0.53	273.99	1631.05	3333.98	3460.52	3490.74	3561.17	1563.30	-723.73	-2927.80	-3444.24
Error %	-42.49	-42.54	-16.81	-43.52	75.77	-41.13	-37.40	-39.18	-38.99	-37.76	-53.74	-39.82	-41.40	-39.71
KB5(Bulk)	171.51	170.66	0.50	0.48	97.49	1363.41	2793.06	3017.82	3036.74	3056.55	1817.53	-475.58	-2549.02	-3009.12
Predicted	160.74	160.02	0.38	0.52	352.37	1591.82	3283.84	3669.67	3677.46	3735.44	1978.38	-394.03	-3062.85	-3634.13
Error %	-6.28	-6.23	-23.47	8.50	261.45	16.75	17.57	21.60	21.10	22.21	8.85	-17.15	20.16	20.77
KB6(Bulk)	226.51	224.06	1.08	0.70	139.01	736.49	3028.73	3467.96	3459.24	3543.72	2153.82	-312.95	-2557.87	-3394.27
Predicted	176.28	174.74	0.64	0.59	412.69	1303.47	2615.71	3018.57	3064.99	3116.32	1471.67	-248.23	-2203.30	-2844.55
Error %	-22.18	-22.01	-40.56	-15.68	196.89	76.99	-13.64	-12.96	-11.40	-12.06	-31.67	-20.68	-13.86	-16.20
CB1(Bulk)	503.74	492.81	2.17	3.35	2290.08	12271.58	27615.11	29248.61	29474.99	29557.52	13522.90	-5404.17	-26913.69	-29239.72
Predicted	1149.13	1138.39	0.88	3.13	1889.55	12962.19	30771.44	32806.10	33459.52	33696.76	15639.98	-5873.42	-31038.47	-32773.94
Error %	128.12	131.00	-59.42	-6.63	-17.49	5.63	11.43	12.16	13.52	14.00	15.66	8.68	15.33	12.09
CB2(Bulk)	928.08	925.35	0.29	2.56	1597.93	8165.04	17870.63	19002.58	19141.53	19218.13	7626.47	-3584.19	-16399.98	-17916.89
Predicted	709.94	702.16	1.08	1.77	1446.99	7842.89	18091.94	19269.68	19609.56	19773.56	9672.00	-3054.61	-17521.33	-19191.19
Error %	-23.50	-24.12	268.25	-30.93	-9.45	-3.95	1.24	1.41	2.45	2.89	26.82	-14.78	6.84	7.11
CB3(Bulk)	1123.73	1107.57	1.44	3.20	2115.43	12997.01	33086.66	35426.34	36135.25	36137.31	17468.26	-5710.54	-31204.73	-34752.67
Predicted	962.65	954.20	0.95	2.33	1818.71	10485.92	25709.89	27333.58	27938.76	28286.05	13808.48	-4051.38	-24950.82	-27292.30
Error %	-14.33	-13.85	-33.66	-26.99	-14.03	-19.32	-22.30	-22.84	-22.68	-21.73	-20.95	-29.05	-20.04	-21.47

A. (continuation)

Sample	$IRM_{-1000}(-5)$ (Am^2/Kg)	$HIRM_{20}(-5)$ (Am^2/Kg)	$HIRM_{40}(-5)$ (Am^2/Kg)	$HIRM_{100}(-5)$ (Am^2/Kg)	$HIRM_{300}(-5)$ (Am^2/Kg)	$HIRM_{500}(-5)$ (Am^2/Kg)	$HIRM_{-20}(-5)$ (Am^2/Kg)	$HIRM_{-40}(-5)$ (Am^2/Kg)	$HIRM_{-100}(-5)$ (Am^2/Kg)	$HIRM_{-300}(-5)$ (Am^2/Kg)	$(Bo)_{cr}$ (mT)
MB4(Bulk)	-3132.11	2977.71	2199.60	885.89	216.92	161.92	1602.50	3216.11	5096.35	6137.49	-41.00
Predicted	-3051.75	2898.86	2079.05	824.22	170.16	103.02	1529.46	3127.89	4988.19	5925.75	-40.57
Error %	-2.57	-2.65	-5.48	-6.96	-21.56	-36.37	-4.56	-2.74	-2.12	-3.45	-1.06
KB1(Bulk)	-900.55	927.88	572.92	132.95	45.38	23.07	587.00	1201.19	1753.65	1857.41	-35.00
Predicted	-987.71	1002.58	564.08	100.52	32.52	9.24	645.41	1358.00	1971.12	2040.65	-32.76
Error %	9.68	8.05	-1.54	-24.39	-28.33	-59.96	9.95	13.05	12.40	9.87	-6.40
KB3(Bulk)	-2711.27	2427.75	1616.60	525.99	135.65	61.52	1564.79	3021.00	4800.22	5249.32	-35.00
Predicted	-2903.66	2614.34	1695.05	502.44	140.58	52.80	1705.47	3314.03	5252.52	5639.25	-35.19
Error %	7.10	7.69	4.85	-4.48	3.63	-14.18	8.99	9.70	9.42	7.43	0.54
KB4(Bulk)	-5863.63	5565.85	2951.12	395.83	32.11	0.15	2342.39	6924.14	10717.63	11434.08	-34.00
Predicted	-3562.27	3287.19	1930.13	227.20	100.65	70.44	1997.88	4214.47	6418.54	6934.97	-32.95
Error %	-39.25	-40.94	-34.60	-42.60	213.50	47234.69	-14.71	-39.13	-40.11	-39.35	-3.09
KB5(Bulk)	-3062.28	2959.06	1693.14	263.48	38.72	19.81	1239.01	3512.32	5585.75	6045.86	-35.00
Predicted	-3789.35	3383.08	2143.62	451.60	65.77	57.98	1757.06	4071.49	6740.31	7311.60	-35.71
Error %	23.74	14.33	26.61	71.40	69.85	192.71	41.81	15.92	20.67	20.94	2.03
KB6(Bulk)	-3616.92	3404.71	2807.23	514.99	75.75	84.48	1389.89	3772.19	6017.11	6853.50	-37.00
Predicted	-3117.80	2703.63	1812.85	500.61	97.75	51.33	1644.65	3313.22	5268.29	5909.54	-34.74
Error %	-13.80	-20.59	-35.42	-2.79	29.04	-39.24	18.33	-12.17	-12.44	-13.77	-6.10
CB1(Bulk)	-29498.55	27267.45	17285.94	1942.41	308.91	82.53	16034.62	34879.16	56388.68	58714.71	-33.00
Predicted	-33174.24	31807.22	20734.58	2925.32	890.66	237.25	18056.78	39332.94	64497.98	66233.45	-32.95
Error %	12.46	16.65	19.95	50.60	188.32	187.46	12.61	12.77	14.38	12.81	-0.14
CB2(Bulk)	-17943.35	17620.20	11053.09	1347.49	215.55	76.60	11591.65	22725.72	35541.51	37058.42	-32.00
Predicted	-19436.62	18326.57	11930.67	1681.62	503.88	164.00	10101.56	22664.17	37130.89	38800.75	-34.48
Error %	8.32	4.01	7.94	24.80	133.77	114.10	-12.85	-0.27	4.47	4.70	7.76
CB3(Bulk)	-35538.58	34021.88	23140.30	3050.65	710.97	2.06	18669.05	41845.80	67339.98	70887.93	-33.00
Predicted	-27790.02	26467.34	17800.14	2576.16	952.47	347.29	14477.57	31990.13	52889.58	55231.06	-33.86
Error %	-21.80	-22.20	-23.08	-15.55	33.97	16789.76	-22.45	-23.55	-21.46	-22.09	2.62

A. (continuation)

Sample	X_{lf}(-8) (m^3/kg)	X_{hf}(-8) (m^3/kg)	X_{fd} %	Xarm(-5) (m^3/kg)	IRM_{20}(-5) (Am^2/Kg)	IRM_{40}(-5) (Am^2/Kg)	IRM_{100}(-5) (Am^2/Kg)	IRM_{300}(-5) (Am^2/Kg)	IRM_{500}(-5) (Am^2/Kg)	SIRM(-5) (Am^2/Kg)	IRM_{-20}(-5) (Am^2/Kg)	IRM_{-40}(-5) (Am^2/Kg)	IRM_{-100}(-5) (Am^2/Kg)	IRM_{-300}(-5) (Am^2/Kg)
CB4(Bulk)	1063.17	1053.56	0.90	2.63	2095.19	11087.17	23355.58	24918.32	24963.53	24996.01	13567.26	-5345.61	-27076.33	-29694.19
Predicted	1020.40	1009.62	1.11	3.26	2077.01	12060.93	27970.42	30757.47	31959.21	33639.60	18454.07	-4415.87	-29466.52	-32792.87
Error %	-4.02	-4.17	22.29	23.85	-0.87	8.78	19.76	23.43	28.02	34.58	36.02	-17.39	8.83	10.44
CB5(Bulk)	602.56	598.17	0.73	1.70	1088.53	6533.05	14779.39	16445.45	16500.69	16691.75	7453.22	-2435.78	-14773.24	-16488.96
Predicted	535.95	531.63	0.79	1.55	1006.19	6189.38	13863.36	15121.20	15163.06	15176.45	7421.55	-2310.45	-13486.94	-14942.02
Error %	-11.05	-11.12	8.34	-8.85	-7.56	-5.26	-6.20	-8.05	-8.11	-9.08	-0.42	-5.15	-8.71	-9.38
CB6(Bulk)	2007.90	1992.99	0.74	4.67	3982.85	19686.43	42864.74	45762.16	45762.84	45811.75	18713.35	-7525.92	-40987.66	-44698.43
Predicted	1579.99	1564.60	0.99	3.69	2754.50	16140.93	38668.36	41811.81	43104.50	45332.95	22140.69	-7529.05	-41079.44	-44598.70
Error %	-21.31	-21.49	33.57	-21.09	-30.84	-18.01	-9.79	-8.63	-5.81	-1.05	18.31	0.04	0.22	-0.22
CB7(Bulk)	919.07	907.87	1.22	2.61	1738.46	10336.09	25390.22	26731.93	31699.80	36099.91	20832.39	-8190.83	-32489.63	-35363.14
Predicted	846.50	836.42	1.14	2.43	1551.91	9577.45	22441.73	24788.16	27917.36	30543.23	17640.54	-4854.90	-27078.79	-29978.63
Error %	-7.90	-7.87	-6.05	-6.74	-10.73	-7.34	-11.61	-7.27	-11.93	-15.39	-15.32	-40.73	-16.65	-15.23
CB8(Bulk)	684.11	677.97	0.90	1.79	2047.18	8927.96	17184.15	18464.88	18615.75	20989.79	6578.99	-3653.32	-13417.21	-14787.95
Predicted	665.05	662.77	0.37	1.77	2120.42	9534.84	18809.66	19986.94	20058.88	22475.41	7261.99	-3627.02	-14579.87	-16018.97
Error %	-2.79	-2.24	-58.34	-1.35	3.58	6.80	9.46	8.24	7.75	7.08	10.38	-0.72	8.67	8.32
RE1(Bulk)	36.56	35.67	2.44	0.26	100.04	220.31	746.22	1016.81	1082.65	1142.80	725.80	223.30	-480.26	-937.29
Predicted	36.83	35.94	2.29	0.32	97.80	298.62	699.80	938.89	984.91	1017.53	566.40	169.29	-455.86	-851.34
Error %	0.75	0.76	-6.35	25.69	-2.24	35.54	-6.22	-7.66	-9.03	-10.96	-21.96	-24.19	-5.08	-9.17
RE2(Bulk)	261.90	255.40	2.48	1.05	633.99	1861.92	4582.42	6166.48	6402.83	6597.41	3777.83	1172.96	-3215.06	-5826.12
Predicted	198.17	194.57	1.75	0.99	554.58	1586.63	3618.22	4671.06	4819.44	4931.41	2502.41	419.70	-2703.52	-4392.70
Error %	-24.33	-23.82	-29.64	-5.51	-12.52	-14.79	-21.04	-24.25	-24.73	-25.25	-33.76	-64.22	-15.91	-24.60
RE3(Bulk)	25.37	24.73	2.50	0.15	82.35	216.55	484.53	598.85	624.54	662.97	373.80	17.90	-365.85	-556.46
Predicted	26.46	25.82	2.39	0.16	73.79	179.19	464.30	584.42	610.44	644.92	361.11	9.29	-350.93	-541.12
Error %	4.31	4.41	-4.20	10.68	-10.39	-17.25	-4.18	-2.41	-2.26	-2.72	-3.39	-48.09	-4.08	-2.76
RE4(Bulk)	92.03	90.37	1.80	0.53	222.80	900.90	1889.15	2396.57	2482.74	2537.89	1395.64	180.25	-1524.72	-2276.90
Predicted	75.93	74.67	1.55	0.37	173.84	719.33	1498.06	1860.01	1923.75	1964.66	1044.54	97.26	-1237.58	-1776.09
Error %	-17.49	-17.38	-13.50	-30.55	-21.97	-20.15	-20.70	-22.39	-22.52	-22.59	-25.16	-46.04	-18.83	-22.00

A. (continuation)

Sample	$IRM_{-1000}(-5)$ (Am^2/Kg)	$HIRM_{20}(-5)$ (Am^2/Kg)	$HIRM_{40}(-5)$ (Am^2/Kg)	$HIRM_{100}(-5)$ (Am^2/Kg)	$HIRM_{300}(-5)$ (Am^2/Kg)	$HIRM_{500}(-5)$ (Am^2/Kg)	$HIRM_{-20}(-5)$ (Am^2/Kg)	$HIRM_{-40}(-5)$ (Am^2/Kg)	$HIRM_{-100}(-5)$ (Am^2/Kg)	$HIRM_{-300}(-5)$ (Am^2/Kg)	$(Bo)_{cr}$ (mT)
CB4(Bulk)	-30213.20	22900.82	13908.83	1640.42	77.69	32.47	11428.75	30309.14	52039.87	54657.72	-33.00
Predicted	-33109.40	31562.59	21578.67	5669.18	2882.13	1680.39	15185.53	36375.08	61425.73	64752.08	-34.75
Error %	9.59	37.82	55.14	245.59	3609.89	5075.00	32.87	20.01	18.04	18.47	5.31
CB5(Bulk)	-16876.75	15603.22	10158.70	1912.35	246.30	191.06	9238.53	18936.47	31273.93	32989.65	-34.00
Predicted	-15118.27	14170.27	8987.07	1313.09	55.25	13.39	7754.91	17473.51	28650.00	30105.08	-34.00
Error %	-10.42	-9.18	-11.53	-31.34	-77.57	-92.99	-16.06	-7.73	-8.39	-8.74	0.00
CB6(Bulk)	-45019.84	41828.90	26125.33	2947.01	49.59	48.92	27098.41	53288.76	86750.50	90461.27	-54.00
Predicted	-44724.22	42578.45	29192.02	6664.59	3521.14	2228.45	23192.26	50633.55	84183.94	87703.20	-54.27
Error %	-0.66	1.79	11.74	126.15	6999.96	4455.71	-14.41	-4.98	-2.96	-3.05	0.49
CB7(Bulk)	-36041.28	34361.44	25763.82	10709.69	9367.97	4400.11	15267.52	39890.62	64189.43	67062.94	-33.00
Predicted	-30269.64	28991.33	20965.79	8101.50	5755.07	2625.88	12902.69	32772.25	54996.15	57895.99	-34.72
Error %	-16.01	-15.63	-18.62	-24.35	-38.57	-40.32	-15.49	-17.84	-14.32	-13.67	5.22
CB8(Bulk)	-15064.94	18942.61	12061.82	3805.64	2524.91	2374.03	14410.79	22269.07	32032.97	33403.71	-32.00
Predicted	-16179.32	20354.99	12940.57	3665.75	2488.47	2416.53	15213.42	23685.90	34638.74	36077.85	-32.31
Error %	7.40	7.46	7.29	-3.68	-1.44	1.79	5.57	6.36	8.13	8.01	0.98
RE1(Bulk)	-1131.60	1042.76	922.49	396.58	126.00	60.15	417.00	919.50	1623.06	2080.09	-54.00
Predicted	-994.75	919.73	718.92	317.74	78.64	32.62	451.13	848.25	1473.40	1868.87	-51.28
Error %	-12.09	-11.80	-22.07	-19.88	-37.59	-45.76	8.18	-7.75	-9.22	-10.15	-5.03
RE2(Bulk)	-6411.77	5963.42	4735.49	2014.99	430.94	194.59	2819.58	5424.45	9812.47	12423.54	-51.00
Predicted	-4825.85	4376.82	3344.78	1313.19	260.35	111.97	2429.00	4511.70	7634.93	9324.11	-43.61
Error %	-24.73	-26.61	-29.37	-34.83	-39.58	-42.46	-13.85	-16.83	-22.19	-24.95	-14.48
RE3(Bulk)	-641.29	580.62	446.42	178.44	64.12	38.43	289.17	645.07	1028.82	1219.43	-40.00
Predicted	-636.08	571.14	465.73	180.63	60.51	34.49	283.82	635.64	995.86	1186.04	-40.37
Error %	-0.81	-1.63	4.33	1.23	-5.64	-10.24	-1.85	-1.46	-3.20	-2.74	0.92
RE4(Bulk)	-2512.62	2315.10	1636.99	648.74	141.32	55.16	1142.25	2357.65	4062.62	4814.79	-43.00
Predicted	-1952.07	1790.82	1245.33	466.60	104.65	40.91	920.12	1867.40	3202.24	3740.75	-40.88
Error %	-22.31	-22.65	-23.93	-28.08	-25.95	-25.82	-19.45	-20.79	-21.18	-22.31	-4.93

A. (continuation)

Sample	X_{lf}(-8) (m^3/kg)	X_{hf}(-8) (m^3/kg)	X_{fd} %	Xarm(-5) (m^3/kg)	IRM_{20}(-5) (Am^2/Kg)	IRM_{40}(-5) (Am^2/Kg)	IRM_{100}(-5) (Am^2/Kg)	IRM_{300}(-5) (Am^2/Kg)	IRM_{500}(-5) (Am^2/Kg)	SIRM(-5) (Am^2/Kg)	IRM_{-20}(-5) (Am^2/Kg)	IRM_{-40}(-5) (Am^2/Kg)	IRM_{-100}(-5) (Am^2/Kg)	IRM_{-300}(-5) (Am^2/Kg)
RE5(Bulk)	65.77	64.51	1.93	0.50	169.37	462.59	1019.07	1237.77	1276.22	1306.78	621.14	-20.95	-857.80	-1158.95
Predicted	61.81	60.62	2.08	0.33	170.98	483.72	1026.37	1213.21	1247.25	1284.17	596.48	-10.64	-838.12	-1141.09
Error %	-6.02	-6.03	7.94	-35.38	0.95	4.57	0.72	-1.98	-2.27	-1.73	-3.97	-49.20	-2.29	-1.54
RE6(Bulk)	99.21	97.21	2.01	0.45	290.76	958.46	1889.15	2160.43	2205.70	2255.92	971.86	-246.10	-1667.51	-2081.18
Predicted	99.59	98.22	1.29	0.44	284.89	975.12	1905.10	2146.09	2186.67	2213.49	967.00	-305.08	-1732.72	-2087.94
Error %	0.39	1.04	-35.98	-0.39	-2.02	1.74	0.84	-0.66	-0.86	-1.88	-0.50	23.97	3.91	0.32
Till BB1(Bulk)	95.30	92.86	2.56	0.53	171.16	574.98	1471.38	2033.36	2136.04	2143.46	1275.94	537.25	-765.09	-1691.97
Predicted	97.36	95.94	1.21	0.53	174.00	600.15	1308.31	1933.32	2012.43	2133.52	1338.63	592.66	-812.84	-2087.81
Error %	2.16	3.32	-52.68	0.22	1.66	4.38	-11.08	-4.92	-5.79	-0.46	4.91	10.31	6.24	23.40
Till BB4(Bulk)	94.55	92.12	2.56	0.60	196.17	635.27	1478.35	1799.66	1893.13	1917.04	989.04	197.82	-952.40	-1463.07
Predicted	93.79	91.52	2.30	0.65	194.54	667.73	1556.67	1906.36	1955.50	2021.22	1024.29	243.85	-968.79	-1521.25
Error %	-0.80	-0.65	-10.31	8.07	-0.83	5.11	5.30	5.93	3.29	5.43	3.56	23.27	1.72	3.98
Total Error %	-37.02	-28.25	-305.72	-275.88	566.78	-14.21	-173.70	-179.77	-182.59	-175.35	-225.59	-1435.91	507.60	-164.89

A. (continuation)

Sample	$IRM_{-1000}(-5)$ (Am^2/Kg)	$HIRM_{20}(-5)$ (Am^2/Kg)	$HIRM_{40}(-5)$ (Am^2/Kg)	$HIRM_{100}(-5)$ (Am^2/Kg)	$HIRM_{300}(-5)$ (Am^2/Kg)	$HIRM_{500}(-5)$ (Am^2/Kg)	$HIRM_{-20}(-5)$ (Am^2/Kg)	$HIRM_{-40}(-5)$ (Am^2/Kg)	$HIRM_{-100}(-5)$ (Am^2/Kg)	$HIRM_{-300}(-5)$ (Am^2/Kg)	$(Bo)_{cr}$ (mT)
RE5(Bulk)	-1302.98	1137.41	844.19	287.71	69.01	30.56	685.64	1327.73	2164.57	2465.73	-39.00
Predicted	-1269.57	1113.19	800.45	257.80	70.97	36.92	687.69	1294.82	2122.29	2425.26	-38.79
Error %	-2.56	-2.13	-5.18	-10.40	2.84	20.81	0.30	-2.48	-1.95	-1.64	-0.55
RE6(Bulk)	-2257.15	1965.16	1297.45	366.76	95.49	50.21	1284.06	2502.02	3923.42	4337.10	-35.00
Predicted	-2223.88	1928.59	1238.37	308.39	67.40	26.82	1246.48	2518.57	3946.21	4301.43	-34.07
Error %	-1.47	-1.86	-4.55	-15.92	-29.42	-46.60	-2.93	0.66	0.58	-0.82	-2.67
Till BB1(Bulk)	-1963.45	1972.31	1568.49	672.09	110.11	7.42	867.52	1606.21	2908.55	3835.43	-50.00
Predicted	-2288.60	1959.52	1533.37	825.21	200.20	121.09	794.89	1540.86	2946.36	4221.33	-53.90
Error %	16.56	-0.65	-2.24	22.78	81.82	1531.80	-8.37	-4.07	1.30	10.06	7.81
Till BB4(Bulk)	-1727.31	1720.87	1281.77	438.69	117.38	23.92	928.00	1719.22	2869.44	3380.11	-45.00
Predicted	-1792.78	1826.68	1353.49	464.56	114.86	65.72	996.93	1777.37	2990.02	3542.47	-47.39
Error %	3.79	6.15	5.60	5.90	-2.14	174.82	7.43	3.38	4.20	4.80	5.31
Total Error %	-155.46	-204.16	-203.86	133.92	10883.95	75143.62	-40.15	-173.28	-148.40	-176.92	-42.06

Appendix 7

GEOGACETA, 20 (3), 1996

Relationship between magnetite chemistry and magnetic susceptibility of igneous rocks: Implications for sedimentary provenance studies

Relación entre composición química de la magnetita y susceptibilidad magnética en rocas ígneas: Implicaciones en estudios de procedencia de sedimentos

E. Martínez Monasterio

Department of Geology, University of St Andrews St Andrews, Fife KY16 9ST Scotland, UK

ABSTRACT

A direct relationship between magnetite chemistry and rock magnetic susceptibility has been found. Electron probe microanalysis of titanomagnetites from various igneous rocks has shown them to be enriched in either the ulvospinel phase (Fe_2TiO_4) or in the magnetite phase (Fe_3O_4). It has been found that the greater the enrichment in the magnetite phase of the titanomagnetites, the higher the magnetic susceptibility value for chemically similar rocks. Both magnetic and chemical data may be used to characterise the rocks (potential sources of sediments) which has important implications for sedimentary provenance studies.

Key words: *magnetite, ulvospinel, magnetic susceptibility, sedimentary provenance.*

RESUMEN

Una relación directa entre la composición química de la magnetita y la susceptibilidad magnética de las rocas que la contienen ha sido encontrada. El análisis mediante microsonda electrónica de titanomagnetitas de varias rocas ígneas ha mostrado un enriquecimiento de dichas titanomagnetitas, bien en término ulvospinela (Fe_2TiO_4) o bien en término magnetita (Fe_3O_4). Se ha observado que rocas químicamente similares presentan valores de susceptibilidad magnética más altos cuanto mayor es el enriquecimiento en término magnetita de sus titanomagnetitas. Tanto los datos químicos como los de susceptibilidad magnética permiten una precisa caracterización de las rocas fuentes (potenciales de sedimentos), hecho este que tiene importantes implicaciones en estudios de procedencia de sedimentos.

Geogaceta, 20 (3) (1996), 660-661
ISSN:0213683X

Introduction

In recent years, the study of Fe-Ti oxides has received increasing interest in terms of both chemistry and the magnetic properties of these minerals (Lindsley, 1991). However, hitherto these two lines of investigation have essentially followed different paths. In this paper, the importance of the relationship between magnetite chemistry and whole rock magnetic susceptibility is explored by a study of the igneous rock formations in the catchment of the River Eden, eastern Scotland. In this area three main rock types are present which exert a control on the topography (Fig. 1). The northern, upland part is characterised by andesites and volcanoclastic deposits of Lower Devonian age whereas the hills of the southern part are composed mainly of dolerite sills of Upper Carboniferous age. The intervening valley of Stratheden is underlain by relatively soft sandstones of Upper Devonian age (Armstrong, 1985).

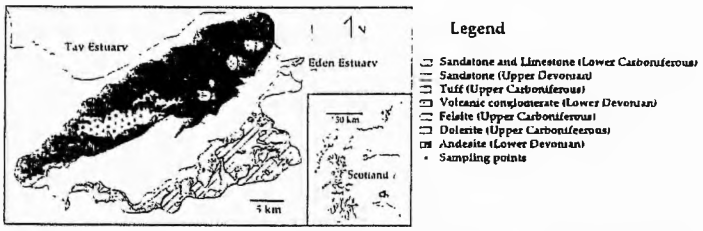

Fig.1.-Mapa geológico simplificado de la cuenca hidrográfica del río Eden mostrando los puntos de recogida de muestras.
Fig.1.-Simplified geological map of the catchment of the River Eden showing the sample locations.

Methology

Sampling: Samples of the principal bedrock lithologies of the River Eden catchment were collected at points shown in Fig. 1. In total, 18 samples were collected in 13 locations.

Geochemical analysis: For each sample the whole rock chemistry was analysed in terms of 10 major elements (Si, Al, Ti, Fe^{3+}, Ca, Na, K, Mg, Mn, P) as oxides and 18 trace elements by means of X-ray fluorescence (XRF) techniques. In addition, electron probe microanalysis was carried out for nine elements (Si, Ti, Al, Fe, Mn, Mg, Ca, Na, K) as oxides on approximately 15 grains of magnetite in a thin section of each sample. All mineral Fe was analysed as FeO and recalculated to weight percent Fe_2O_3 and FeO following the procedure of Droop (1987).

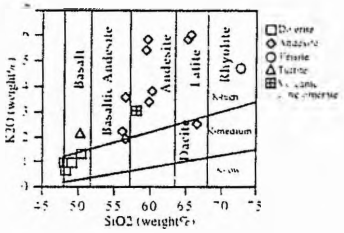

Fig. 2.-Diagrama SiO_2 frente a K_2O. Campos según Peccerillo & Taylor (1976).

Fig.2.-K_2O versus SiO_2 diagram. Fields according to Peccerillo & Taylor (1976).

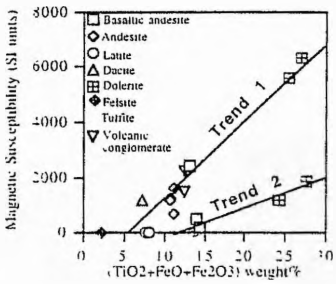

Fig. 4.-Diagrama de la susceptibilidad magnética frente al tanto por ciento en peso de (TiO_2+FeO+Fe_2O_3) de la roca (ver texto).

Fig.4.-Magnetic susceptibility versus whole rock weight percentage of (TiO_2+FeO+Fe_2O_3) diagram (see text).

Magnetic measurements: Whole rock magnetic susceptibility was measured for a core of 10 cubic centimeter from each sample using a Bartington MS2B single sample, dual frequency sensor which creates a weak magnetic field from an alternating current and detects the magnetization of the material lying within it which is roughly proportional to the concentration of ferrimagnetic minerals within the sample. The measurements were made at low frequency and displayed in SI units.

Results

Whole rock chemistry: The Upper Carboniferous dolerites are very similar in chemical composition within the River Eden catchment. The Lower Devonian andesites, however, show differences in their chemistry regionally and can be classified as basaltic andesites, andesites, latites, and dacites, on the basis of a K_2O versus SiO_2 diagram (Fig. 2).

Magnetite chemistry: The electron microprobe data are presented in the form of a TiO_2-FeO-Fe_2O_3 ternary diagram (Fig. 3). By

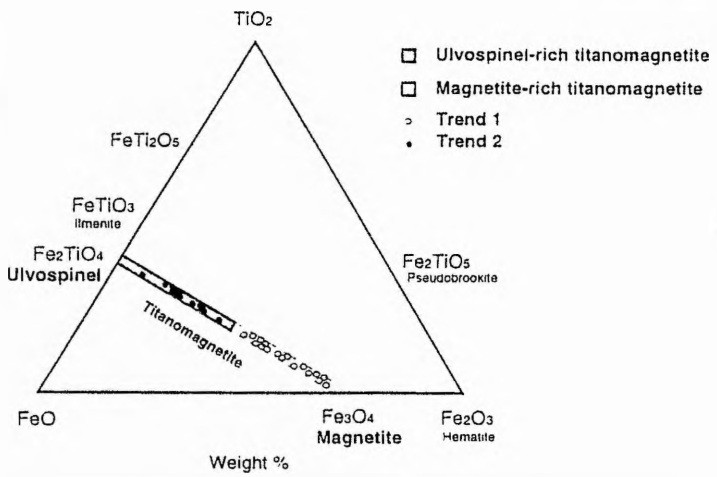

Fig. 3.- 30 análisis representativos de los 270 análisis de magnetita realizados, representados en el sistema FeO-Fe_2O_3-TiO_2 mostrando las principales soluciones sólidas magnetita-ulvospinela, hematite-ilmenita y pseudobrokita-$FeTi_2O_5$ (ver texto).

Fig. 3.- 30 Representative magnetite analysis from a dataset of 270 analyses plotted in the system FeO-Fe_2O_3-TiO_2 showing the major solid solution series magnetite-ulvospinel, hematite-ilmenite, and pseudobrookite-$FeTi_2O_5$ (see text).

this means, all of the magnetites analysed are classified as titanomagnetites. Within each individual sample the magnetite grains analysed are chemically very similar (approximately the same weight percentage of TiO_2, FeO, and Fe_2O_3). However, the magnetite grains show differences in their chemistries between samples. In 6 samples the titanomagnetites are enriched in the ulvospinel phase (Fe_2TiO_4) while in the other 12 samples they are enriched in the magnetite phase (Fe_3O_4).

Discussion and conclusions

When magnetic susceptibility is plotted versus whole rock weight percentage of (TiO_2+FeO+Fe_2O_3) (Fig. 4) two different trends can be distinguished. Each shows a direct relationship between magnetic susceptibility values and whole rock chemistry: the higher the weight percentage of (TiO_2+FeO+Fe_2O_3) in the rock, the higher the magnetic susceptibility value. However, the two trends are differentiated on the basis of magnetite chemistry. The titanomagnetites of all the rocks in trend 1 are those enriched in the magnetite phase, whereas those in trend 2 are all enriched in the ulvospinel phase (Fig. 3).

This study has shown that there is a clear, direct relationship between magnetite chemistry and whole rock magnetic susceptibility. It has enabled the characterisation of igneous rocks so that chemically and magnetically similar materials can be differentiated on the basis of their magnetite chemistry. The implications for sedimentary provenance studies are important. Since the above analytical methods applied to the study of rocks, which are potential sources of sediments can also be applied to sediments, the comparison of "source" and "sediment" dataset should allow a precise determination of sediment provenance and permit quantification of the relative contribution of source lithologies. Further work on these aspects is in progress.

Acknowledgements

Special thanks go to Dr. W. E. Stephens and Dr. R.W. Duck for their continuous support. Thanks are extended to Angus Calder, Donnie Herd and Andy Mackie for their technical assistance. This research was supported by a grant from the program "Programa de Formación de Investigadores del Departamento de Educación, Universidades e Investigación" from the Basque Government, which is gratefully acknowledged.

References

Armstrong, M., Paterson, I.B. & Browne, M.A.E. (1985): *B.G.S.*, 108 pp.

Dearing, J. (1994): *The Bartington MS2 System Manual*, 104 pp.

Droop, G.T.R. (1987): *Mineralogical Magazine*, 51, 431-435.

Lindsley, D.H. (1991): *Reviews in Mineralogy*, 25, 509 pp.

Peccerillo, A. & Taylor, D.R. (1976): *Contrib. Mineral. Petrol.*, 58, 63-81